

Characterisation of the host immune response to biofilm-related infections

Maria Paula Sarmiento Mempin

Master of Research (Advanced Medicine)

Bachelor of Medical Sciences (Biomedical)

A Thesis in the Field of Biomedical Sciences, Faculty of Medicine and Health Sciences,

Macquarie University, submitted in fulfilment of the requirements

for the Degree of Doctor of Philosophy

Principal Supervisor: A/Prof. Karen Vickery

Associate Supervisors: Prof. Anand Deva, Prof. Helen Rizos

Co-Supervisor: Dr. Honghua Hu



MACQUARIE
University
SYDNEY • AUSTRALIA

January 2019

Table of Contents

Table of Contents	ii
Abstract.....	xvi
Declaration of Originality	xviii
Publications and Communications.....	xix
Acknowledgements	xxii
List of Figures.....	xxiv
List of Tables	xxxiv
List of Symbols and Abbreviations	xxxvii
Chapter I. Literature Review	1
1.1. Breast implants for cosmetic and reconstructive augmentation	1
1.1.1. Types of breast implants.....	2
Silicone breast implants	2
Saline breast implants	5
Smooth breast implants.....	6
Textured breast implants.....	6
Round breast implants.....	8
Anatomic breast implants	8
1.2. Capsular formation and contracture after breast augmentation and reconstruction, and the role of bacterial biofilm.....	9
1.2.1. Contracture of the peri-prosthetic capsule	11
1.2.2. Factors that can influence the development of capsular contracture	13
1.2.3. Bacterial colonisation and capsular contracture	17
1.2.4. Subclinical infection theory	20

1.2.5.	Influence of breast implant surface texture on biofilm formation and subsequent contracture.....	25
1.2.6.	T-cell response to chronic biofilm infection around breast implants	29
1.3.	Bacterial biofilm, breast implants and anaplastic large-cell lymphoma.....	31
1.3.1.	Clinical features and subforms of ALCL.....	33
	Primary cutaneous-ALCL.....	34
	Secondary ALCL	34
	ALK-positive ALCL.....	35
	ALK-negative ALCL	35
	Breast implant associated-ALCL.....	36
	Structure and pathogenic role of the NPM-ALK gene	39
1.3.2.	The role of bacterial biofilm in breast implant associated-ALCL	40
	Bacterial infection in other lymphomas	41
1.3.3.	Immune environment in breast implant associated-ALCL.....	42
	Multifactorial pathway to malignancy	43
	Peri-prosthetic inflammation.....	44
	T-cell infiltrate in breast implant associated-ALCL	46
	Th1/Th17 phenotype of breast implant associated-ALCL tumour cells..	49
1.4.	Bacterial biofilms.....	51
1.4.1	Process of biofilm formation	52
	Reversible and irreversible attachment.....	53
	Growth and differentiation.....	55
	Biofilm dissemination.....	56
1.4.2.	Signalling in biofilm formation	56
1.4.3.	Host immune response against biofilm.....	58
1.4.4.	Surface factors influencing bacterial attachment.....	60
	Irregular/random surface structures	61
	Patterned surfaces	63

MT-4 cells	79
Peripheral blood mononuclear cells	79
2.5.2. Preparation of non-specific mitogens	80
2.5.3. Subculturing of tumour cells/cell lines	81
2.5.4. Cell counts and viability	81
2.5.5. Freezing of cells for long-term storage	82
2.5.6. Thawing a frozen cell stock	82
2.6. Optimisation of <i>in vitro</i> bacterial attachment assays to breast implants.....	83
2.6.1. Optimisation methods	84
2.6.1.1. Preparation of breast implants.....	84
2.6.1.2. Bacterial strains and culture conditions	85
2.6.1.3. Breast implant textures	85
2.6.1.4. Experiment 1: <i>In vitro</i> bacterial attachment assay	85
2.6.1.5. Statistical analysis	89
2.6.2. Results.....	90
2.6.3. Experiment 2: Optimisation of removal of residual silicone from the inner surface of smooth implants	91
Results.....	91
2.6.4. Experiment 3: Comparison of <i>S. epidermidis</i> attachment to Mentor smooth and Mentor Siltex following removal of silicone from the inner surface of implants.....	92
Results.....	93
2.6.5. Testing bacterial attachment and growth <i>in vitro</i> on breast implants with different surface morphology.....	93
Results.....	94
2.6.6. Comparison of immediate floating and prewetting of breast implants prior to bacterial attachment assay	95

Results.....	96
2.7. Established <i>in vitro</i> bacterial attachment assay	97
Results.....	97
Chapter III. The functional influence of breast implant outer shell morphology on bacterial attachment and growth	101
Abstract.....	102
Introduction.....	103
Methods	104
Implant surfaces tested.....	104
Implant surfaces imaging.....	105
Scanning electron microscopy	105
Micro CT scan.....	105
Surface area determination	106
Surface roughness determination.....	107
<i>In vitro</i> bacterial attachment assay.....	107
Statistical analysis.....	108
Results.....	108
Scanning electron microscopy	108
Surface area determination	112
Surface roughness determination.....	119
<i>In vitro</i> bacterial attachment assay.....	120
<i>S. epidermidis</i>	120
<i>S. aureus</i>	123
<i>P. aeruginosa</i>	123
<i>R. pickettii</i>	123
Combined categories.....	124

Discussion	125
Conclusion	127
Acknowledgements.....	128
References.....	128
Chapter IV. The influence of implant surface on biofilm formation in an <i>in vivo</i> porcine model	
.....	131
4.1. Introduction.....	131
4.2. Materials and Methods.....	132
4.2.1. Breast implant surfaces tested.....	132
4.2.2. Subjects	133
4.2.3. Preparation of contaminating inoculum.....	133
4.2.4. Surgical procedure	133
4.2.5. Baker grading.....	135
4.2.6. Explant surgery	135
4.2.7. Biofilm analysis	137
Bacterial load in capsules and attached to implants by qPCR	137
Calculation of microbial load attached to the different implants	138
<i>Staphylococcus epidermidis</i> specific PCR.....	138
Lymphocyte number in capsules and implants by qPCR	138
Scanning electron microscopy	139
4.2.8. Micro computed tomography scanning of breast implant and surface analysis.....	139
4.2.9. Statistical analysis.....	139
4.3. Results.....	140
4.3.1. Baker grading.....	140
4.3.2. Weight of tissue attached to implants	141

4.3.3.	Control implants and capsules	142
4.3.4.	Presence of <i>Staphylococcus epidermidis</i> in explanted samples.....	143
4.3.5.	Total microbial load attached to type A and type B implants	144
4.3.6.	Total microbial load in capsules surrounding type A and type B implants..	146
4.3.7.	Total lymphocyte number on the surface of implant types A and B and in surrounding capsules.....	147
	Implants.....	147
	Capsules	151
4.3.8.	Scanning electron microscopy	153
4.3.9.	Surface area and surface roughness determinations	159
4.4.	Discussion	160

Chapter V. Analysis of bacterial biofilm and host response in new cases of Breast Implant-associated Anaplastic Large-cell Lymphoma..... 165

5.1.	Introduction.....	165
5.2.	Materials and Methods.....	166
5.2.1.	Patients.....	166
5.2.2.	Processing of implant and capsule samples	167
5.2.3.	DNA extraction.....	167
5.2.4.	Total bacterial load and lymphocyte number in capsules and attached to implants by qPCR	167
5.2.5.	Scanning electron microscope	168
5.2.6.	Statistical analysis.....	168
5.3.	Results.....	169
5.3.1.	Clinical features	169
5.3.2.	BIA-ALCL implants and capsules.....	172

5.3.3.	Total microbial load attached to implants.....	173
5.3.4.	Total microbial load in capsules	176
5.3.5.	Lymphocyte number in capsules	179
5.3.6.	Scanning electron microscopy	186
5.4.	Discussion	188
Chapter VI. Differential mitogenic response of Breast Implant-associated Anaplastic Large-cell Lymphoma to Gram-negative lipopolysaccharide.....		192
6.1.	Introduction.....	192
6.2.	Part A: Optimisation of <i>in vitro</i> cell proliferation assays	193
6.2.1.	Optimisation Methods.....	193
6.2.1.1.	Preparation of cell lines/tumour cells.....	193
6.2.1.2.	Preparation of non-specific mitogens	194
6.2.1.3.	MTT colourimetric assay to determine cell proliferation	194
6.2.1.4.	Statistical analysis	195
6.2.2A.	Optimisation of MTT assay	195
	Stimulation of MT-4 cells with PHA.....	196
	Results.....	196
6.2.2B.	Determining the optimum incubation time for MTT	198
	Stimulation of MT-4 cells with PHA.....	198
	Results.....	198
6.2.2C.	Stimulating lymphocytes with PHA and LPS to determine optimum cell concentration and MTT incubation time.....	199
	Results.....	200
6.2.2D.	Stimulating cells with PHA to confirm optimum cell concentration...	200
	Results.....	200
6.3.	Established <i>in vitro</i> cell proliferation assay	201

6.4.	Part B: Response of patient-derived tumour cells and peripheral blood mononuclear cells to mitogenic stimulation.....	207
6.4.1.	Introduction.....	207
6.4.2.	Materials and Methods.....	207
6.4.2.1.	Tumour cells/peripheral blood mononuclear cells/cell lines	207
6.4.2.2.	<i>In vitro</i> cell proliferation assay	208
6.4.2.3.	Statistical analysis	208
6.4.3.	Results.....	209
6.4.3.1.	Clinical features	209
6.4.3.2.	Cell proliferation response following mitogenic stimulation ...	210
6.5.	Discussion	224
Chapter VII. Differential mitogenic response of Breast Implant-associated Anaplastic Large-cell Lymphoma to staphylococcal superantigens.....		228
7.1.	Introduction.....	228
7.2.	Materials and Methods.....	229
7.2.1.	Tumour cells/cell lines.....	229
7.2.2.	Preparation of staphylococcal superantigens	230
7.2.3.	<i>In vitro</i> cell proliferation assay	230
7.2.4.	Testing the effects of 1% penicillin/streptomycin	230
7.2.5.	Statistical analysis.....	231
7.3.	Results.....	231
7.3.1.	Cell proliferation response following staphylococcal superantigen stimulation	231
7.3.2.	Differential response to SEA, TSST-1, PHA and LPS.....	244
7.3.3.	Effects of penicillin/streptomycin antibiotics	246
7.4.	Discussion	249

Chapter VIII. The development of a co-culture system of mammalian cells and biofilm composed of different bacterial species	253
8.1. Introduction.....	253
8.2. Part A: Optimisation of bacterial biofilm formation assays	254
8.2.1. Optimisation methods	254
8.2.1.1. Bacterial strains and culture conditions	254
8.2.1.2. Biofilm formation assays	254
8.2.1.3. Biofilm quantification	256
8.2.1.4. Statistical analysis	256
8.2.2. Testing the growth of bacteria in cell culture media and biofilm formation in a cell culture plate	256
Results.....	256
8.2.3. Growing <i>S. aureus</i> biofilm over five days, changing the media every 24 hr	258
Results.....	259
8.2.4. <i>S. aureus</i> biofilm formation on polycarbonate coupons and transfer to tissue culture plates	261
Biofilm formation assays	261
Results.....	262
8.2.5. Growing <i>S. aureus</i> biofilm on breast implants over seven days.....	262
Preparation of breast implants.....	263
Biofilm formation assays	263
Results.....	264
8.2.6. Growing <i>S. epidermidis</i> , <i>P. aeruginosa</i> and <i>R. pickettii</i> biofilm on breast implants over seven days	266
Bacterial strains and culture conditions	266
Results.....	266

8.3.	Established bacterial biofilm formation assay	269
8.4.	Part B: Optimisation of mammalian cells and bacterial biofilm co-culture assays	270
8.4.1.	Optimisation methods	270
8.4.1.1.	Biofilm formation assays	270
8.4.1.2.	Preparation of tumour cells	271
8.4.1.3.	Tumour cells and biofilm co-culture.....	271
8.4.1.4.	MTT colourimetric assay to determine cell proliferation response to biofilm.....	271
8.4.1.5.	Biofilm quantification	271
8.4.2.	Co-culture of BIA-ALCL tumour cells with <i>P. aeruginosa</i> biofilm Results.....	271 272
8.4.3.	Co-culture of BIA-ALCL tumour cells with <i>S. epidermidis</i> and <i>R. pickettii</i> biofilms	274
	Results.....	274
8.4.4.	Testing the culture medium to determine if bacteria detach from biofilm formed on implants	276
	Results.....	277
8.5.	Part C: Co-culture of BIA-ALCL tumour cells and biofilm composed of different bacterial species	279
8.5.1.	Introduction.....	279
8.5.2.	Materials and Methods.....	280
8.5.2.1.	Preparation of breast implants.....	280
8.5.2.2.	Bacterial strains and culture conditions	280
8.5.2.3.	Biofilm formation assays	280
8.5.2.4.	Preparation of tumour cells	280
8.5.2.5.	Co-culture of BIA-ALCL tumour cells with bacterial biofilm	281

8.5.2.6. MTT colourimetric assay to determine cell proliferation response to biofilm.....	281
8.5.2.7. Biofilm quantification.....	281
8.5.3. Results.....	282
8.5.3.1. Cell proliferation response following bacterial biofilm infection	282
8.5.3.2. Bacterial numbers attached to the implant before and after co-culture and in the co-culture supernatant	283
8.6. Discussion.....	286
Chapter IX. Effect of TLR4 on LPS stimulation of BIA-ALCL tumour cells.....	290
9.1. Introduction.....	290
9.2. Optimisation of TLR4 inhibitor peptide	292
9.2.1. Preparation of TLR4 inhibitory peptide.....	292
9.2.2. TLR4 inhibition assay on BIA-ALCL tumour cells.....	292
9.2.3. MTT assay to determine inhibition of LPS-induced TLR4 activation ...	293
Results.....	293
9.3. Materials and Methods.....	294
9.3.1. Tumour cells/cell lines.....	294
BIA-ALCL tumour cells	294
Plasma	295
9.3.2. TLR4 inhibition assays	295
9.3.3. Enzyme-linked immunosorbent assay for TNF- α	295
9.3.4. <i>In vitro</i> cell proliferation assay	296
9.3.5. Statistical analysis.....	296
9.4. Results.....	296
9.4.1. Clinical features	296
9.4.2. Standard curve for TNF- α ELISA.....	297

9.4.3. TLR4 inhibition	298
TNF- α ELISA	298
Cell proliferation response following stimulation, inhibition and no stimulation.....	300
9.5. Discussion	301
Chapter X. General Discussion.....	303
Conclusion	312
Appendices.....	314
Appendix 1. Human ethics approval	315
Appendix 2. Participant information and consent forms.....	318
Appendix 3. BIA-ALCL proforma.....	322
Appendix 4. Animal ethics approval	324
Appendix 5. Animal ethics approval letter	328
Appendix 6. Permission for reproduction of material from Oxford University Press .	329
References.....	333

Abstract

Breast implant-associated anaplastic large-cell lymphoma (BIA-ALCL) is a recently diagnosed, rare non-Hodgkin T-cell lymphoma in tissue around a breast implant. Since 2000, its detection and incidence has risen worldwide due to the increase use of breast implants in breast surgery. Although the aetiopathogenesis is unclear, it is postulated that the cancer results from chronic bacterial antigen stimulation and sustained T-cell proliferation that potentially leads to malignant transformation. This is in conjunction with implant properties, implant exposure time and host predisposition or genetic factors. The experiments described in this thesis explore the influence of implant surface texture, bacterial load and host response in patient specimens, and initiating and potentiating factors to malignancy.

The majority of BIA-ALCL cases have occurred in patients with textured implants, which have been shown to support a higher bacterial load. The work described in Chapter III of this thesis describes the development of an *in vitro* bacterial attachment assay to further characterise the surface texture of implants and their capacity to support bacterial growth *in vitro*. We describe a significant relationship between the measurement of available surface area, surface roughness and potentiation of bacterial growth for both Gram-positive and Gram-negative bacteria. In Chapter IV, we examine the influence of implant texture *in vivo* using a well-established porcine model. We describe the association between textured implant surfaces with bacterial attachment, biofilm formation, development of capsular contracture and host response following artificial bacterial contamination of breast implants in pigs.

The role of bacteria in BIA-ALCL has recently been supported by the discovery of high levels of bacterial contamination within BIA-ALCL specimens. In Chapter V, we compare the

bacterial load and host response in fresh implants and capsules from new cases of BIA-ALCL to non-tumour specimens.

In Chapter VI, we utilise previous findings of a significantly higher proportion of Gram-negative pathogens present in the microbiome of BIA-ALCL specimens when compared to the microbiome surrounding non-tumour implant capsules. We interrogate BIA-ALCL cell lines derived from fresh tumour with antigens including lipopolysaccharide from Gram-negative bacterial cell wall. We demonstrate a unique response to lipopolysaccharide in BIA-ALCL cells compared to other tumour and non-tumour cell lines. In Chapter VII, we also interrogate these cell lines with staphylococcal superantigens since their potential to restrict T-cell receptor expression has recently been reported. We describe a differential response to Gram-positive bacterially derived antigens, providing support to the hypothesis of a Gram-negative antigenic trigger to malignancy.

We further investigated the potentiation of BIA-ALCL tumour cell growth this time to bacterial biofilm infection composed of different pathogen species. In Chapter VIII, we develop a co-culture system of biofilm and mammalian cells and describe the differential responses of BIA-ALCL cells when challenged with biofilm consisting of Gram-negative or Gram-positive bacteria.

The work described in Chapter IX, examines whether the stimulation by lipopolysaccharide is through Toll-like receptor 4 (TLR4), which positively impacts T-cell priming. We demonstrate a dampening of responses to lipopolysaccharide in BIA-ALCL cells following inhibition of TLR4 signalling.

The data from this thesis provides important new insights into the aetiopathogenesis of this newly characterised neoplasm.

Declaration of Originality

I hereby declare that the work presented in this thesis entitled “Characterisation of the host immune response to biofilm-related infections” has not previously been submitted for a degree nor has it been submitted as part of requirements for a degree to any other university or institution other than Macquarie University. I also declare that the thesis is an original piece of research and contains no material previously published or written by another person, except where due reference is stated otherwise. Any help and assistance that I have received in my research work and the preparation of the thesis itself is explicitly acknowledged.

The research presented in this thesis was approved by the Macquarie University Human Research Ethics Committee, Human Ethics Approval: 5201600427 – August 2016 and the University of Sydney Animal Ethics Committee, Animal Ethics Approval: 2017/1193 – June 2017.

Maria Paula Sarmiento Mempin

Department of Biomedical Sciences

Faculty of Medicine and Health Sciences

Macquarie University

22 January 2019

Publications and Communications

Publications arising from this thesis

Jones, P., **Mempin, M.**, Hu, H., Chowdhury, D., Foley, M., Cooter, R., Adams Jr, W. P., Vickery, K., Deva, A. K. The functional influence of breast implant outer shell morphology on bacterial attachment and growth. *Plastic and Reconstructive Surgery*; October 2018; Accepted 31 March 2018.

Mempin, M., Hu, H., Chowdhury, D., Deva, A. K., Vickery, K. The A, B and C's of silicone breast implants: Anaplastic large-cell lymphoma, biofilm and capsular contracture. *Materials*; November 2018; Accepted 28 November 2018.

Manuscript in preparation

Mempin, M., Vickery, K., Kadin, M. E., Prince, H. M., Hu, H., Kouttab, N., Adams Jr, W. P., Deva, A. K. Gram-negative lipopolysaccharide and breast implant-associated anaplastic large-cell lymphoma – implications for pathogenesis.

Conference presentations

Poster presentations

Mempin, M., Orozco, J. L., Hu, H., Deva, A. K., Vickery, K. (2017). Characterisation of the host immune response to biofilm infections. American Society of Microbiology (ASM) Microbe, New Orleans, USA.

Mempin, M., Orozco, J. L., Hu, H., Deva, A. K., Vickery, K. (2017). Characterisation of the host immune response to biofilm infections. Cell Symposia: Cancer, Inflammation, and Immunity, San Diego, USA.

Vickery, K., **Mempin, M.**, Hu, H., Deva, A. K. (2017). Biofilm and Breast Implant-Associated Anaplastic Large-Cell Lymphoma. Presented by A/Prof. Vickery at Eurobiofilms, 5th European Congress on Microbial Biofilms, Amsterdam, Netherlands.

Oral presentations by Prof. Anand Deva of the work presented in this thesis

Deva, A. K. (2016). Biofilm, breast implants and ALCL. American Society for Aesthetic Plastic Surgery (ASAPS) Annual Meeting, Las Vegas, USA.

Deva, A. K., Kadin, M. E. (2016). Biomarkers provide early clues on the genesis of ALCL. ASAPS Annual Meeting, Las Vegas, USA.

Deva, A. K. (2016). Incidence and risk factors for BIA-ALCL in ANZ population. American Society of Plastic Surgeons Plastic Surgery The Meeting, Los Angeles, USA.

Deva, A. K. (2016). Biofilm, breast implants and ALCL – the unifying theory. 39th Annual Australasian Society of Aesthetic Plastic Surgeons (ASAPS) Conference, Gold Coast, Australia.

Deva, A. K. (2017). Biofilm, breast implants and ALCL – the unifying theory. ASAPS The Aesthetic Meeting, San Diego, USA.

Deva, A. K. (2017). Biofilm, breast implants and ALCL. Johnson & Johnson Institute 5th Mentor Surgical Excellence Symposium, Hamburg, Germany.

Deva, A. K. (2017). Breast implant infection and relevance to breast surgery. Royal Australasian College of Surgeons (RACS) 86th Annual Scientific Congress, Adelaide, Australia.

Deva, A. K. (2017). Breast implants safety. ASAPS Plastic Surgery Congress, Gold Coast, Australia.

Deva, A. K. (2017). Breast implants and ALCL. Oncoplastic Reconstructive Breast Surgery Meeting 6th International Scientific Meeting, Nottingham, UK.

Deva, A. K. (2017). Biofilm, breast implants, ALCL, the unifying theory. British Association of Aesthetic Plastic Surgeons (BAAPS) Annual Scientific Meeting, London, UK.

Deva, A. K. (2017). Breast implants – research and Australian update. 40th Annual ASAPS Conference, Melbourne, Australia.

Deva, A. K. (2018). BIA-ALCL: Translational research update. ASAPS The Aesthetic Meeting, New York, USA.

Deva, A. K. (2018). Towards a generic classification of breast implants. ASAPS The Aesthetic Meeting, New York, USA.

Deva, A. K. (2018). BIA-ALCL: Update. RACS The Annual Scientific Congress, Sydney, Australia.

Deva, A. K. (2018). Update on BIA-ALCL. Beauty through Science (BTS) Meeting, Stockholm, Sweden.

Deva, A. K. (2018). ALCL round table. Therapeutic Goods Administration (TGA) Meeting, Melbourne, Australia.

Awards arising during candidature

2017 – American Society for Microbiology Student and Postdoctoral Travel Award

2017 – Skipper Foundation – Skipper Postgraduate Travel Award

2018 – Finalist Australian Society for Microbiology Student Travel Award

Acknowledgements

I would like to thank all the people without whom this project would never have been possible. First, many thanks to my supervisors, A/Prof. Karen Vickery, Prof. Anand Deva, Prof. Helen Rizos and Dr. Helen Hu for all the tremendous help and support. Karen, I feel extremely fortunate to have had the opportunity to learn and develop as a researcher under your supervision. Your patient guidance, encouragement, advice, and the care you showed in my work and in the production of this thesis, I am forever grateful. Helen, I express my deepest appreciation for your unreserved help, constant support, availability and good heart, not just in my work but also outside of work. Anand, thank you for your enthusiasm, ideas and the many insightful discussions and suggestions throughout my candidature.

A special thank you to Dr. Khalid Al Johani for helping me out with experiments, for providing a stimulating and fun environment in which to learn and grow, and most importantly for your friendship. I thank all the past and present members of the Surgical Infection Research Group: Arifur Rahman, Dr. Durdana Chowdhury, Dr. Dayane de Melo Costa, Dr. Phoebe Jones, Dr. Kaila Medina Alarcón, Dr. Shamaila Tahir, Dr. Lissandra Santos and Dr. Lillian Lopes. Thank you for the support and for keeping me accompanied along the way. I'll never forget the many wonderful lunches and memorable outings we've had together. I'm also glad to have worked with a wonderful undergraduate student volunteer, Jonathon Mifsud.

I also thank our collaborators, Prof. Miles Prince and his team down at Peter MacCallum Cancer Centre, and to Prof. Marshall Kadin and the team at Roger Williams Medical Centre, for their help, many interesting discussions, insights and paradoxes. To Marshall, Haiying, Donna and Dotti, thank you for being so welcoming and looking after me during my visit to your lab. It made my stay all the more enjoyable and one I will never forget.

My sincere thanks to all the plastic surgeons, clinical staff and patients for providing the samples to our project. Thank you to the scientific and technical assistance of Dr. Matthew Foley and the Australian Centre for Microscopy and Microanalysis at the University of Sydney. I also thank Prof. Andrew Dart, Dr. Eduardo Uquillas, Greg Macnamara, and the wonderful staff at the University of Sydney Veterinary Teaching Hospital.

I would like to thank the administrative staff members of the Department, particularly Laura Newey, Annie Clark and Viviana Bong, who have been kind enough to advise and help me in their respective roles throughout my candidature. I also thank the Faculty lab operations staff, Louise Marr, Lucy Lu, Tamara Leo and Mitchell Borton for always being so helpful and friendly.

I'm grateful to the funding bodies that have supported me throughout my candidature. In particular, the Macquarie University Research Training Program Scholarship, the Skipper Foundation Postgraduate Travel Award – thank you Jack and Lynette Skipper for your continual support of Macquarie University students, and the American Society of Microbiology Student and Postdoctoral Travel Award.

Finally, to my family, Mum and Dad, Mervin and Pilar, thank you for your unflagging love, unflinching support throughout my life and encouragement to pursue my interests: this work is simply impossible without you. Thank you Mum for all that you have done and continue to do for me, you have made a tremendous contribution in helping me reach this stage in my life. A special thanks to my beautiful sister Pilar for helping me out with the formatting and editing of this thesis, as well as everything else. I thank my beloved dog, Belle, wish you were still with us. I also wish to thank the newest and cutest addition to our family, my little nephew Marcus, for being a welcome distraction (most of the time) during the writing of this thesis.

List of Figures

Chapter I.

Figure 1.1. Subclinical infection theory.....	21
Figure 1.2. Validation of the subclinical infection hypothesis. Schematic depiction of the progression in smooth and textured breast implants from bacterial inoculation to established biofilm to contracture.....	28
Figure 1.3. Unifying hypothesis of breast implant-associated anaplastic large-cell lymphoma. ..	32
Figure 1.4. Differentiation of T-cell subsets.....	45
Figure 1.5. Hypothesis for progression of immune responding T-lymphocytes to BIA-ALCL. ..	50
Figure 1.6. The stages of the biofilm life cycle.	53
Figure 1.7. Factors that determine bacterial adhesion.	61

Chapter II.

Figure 2.1. Processing blood to separate peripheral blood mononuclear cells using the standard Ficoll method.	80
Figure 2.2. Preparation of smooth and textured breast implants for <i>in vitro</i> bacterial attachment assays.	85
Figure 2.3. <i>In vitro</i> bacterial attachment assay for breast implants.	89
Figure 2.4. The number of (A) <i>S. aureus</i> and (B) <i>S. epidermidis</i> attached to Mentor smooth and Mentor textured implants following incubation in 15 mL of 10^5 bacterial cells/mL at 2, 6 and 24 hr.	91
Figure 2.5. The number of <i>S. epidermidis</i> attached to Mentor smooth implants using different methods to remove silicone from their inner surface.....	92

Figure 2.6. The number of <i>S. epidermidis</i> attached to Mentor smooth and Mentor textured implants following silicone removal using a blunt knife.....	93
Figure 2.7. The number of <i>S. epidermidis</i> attached to breast implants with different surface morphology at the 24 hr time point.....	94
Figure 2.8. Effect of prewetting implants prior to incubation on the number of <i>S. epidermidis</i> attaching to Mentor textured implants.	96
Figure 2.9. The number of <i>S. epidermidis</i> attached to various breast implant surface types at the 2 hr time point utilising the optimised study.	98
Figure 2.10. The number of <i>S. epidermidis</i> attached to various breast implant surface types at the 6 hr time point utilising the optimised study.	98
Figure 2.11. The number of <i>S. epidermidis</i> attached to various breast implant surface types at the 24 hr time point utilising the optimised study.	99
 Chapter III.	
Figure 1 Supp: Algorithm for calculation of 3D area:2D ratio.....	106
Figure 1: Scanning electron micrographs of surface morphology of implants studied at 25X and 400X magnification.....	109
Figure 2: Samples of three-dimensional cross sections, extraction and greyscale reconstruction from micro CT analysis utilized for measurement of surface area/roughness.....	113
Figure 2 Supp: (a) Silimed Polyurethane and (b) Polytech Mesmo 3D extraction and 3D greyscale reconstruction.	117
Figure 3: 3D:2D ratios for various implant types studied.	118
Figure 3 Supp: Demonstration of “caves” (sequestered surface area) for Polytech Mesmo coloured red on 3D reconstruction.	119
Figure 4: Surface roughness for various implants studied.....	120

Figure 5: <i>S. epidermidis</i> attachment and growth on various implants shells measured at 0, 2, 6 and 24 hours.	121
Figure 6: (A) <i>S. epidermidis</i> , (B) <i>S. aureus</i> , (C) <i>P. aeruginosa</i> and (D) <i>R. pickettii</i> attachment and growth on various implant shells measured at 24 hours.	122
Figure 7: Implant surface classification relating manufacturing method, surface area, surface roughness.....	124
Chapter IV.	
Figure 4.1. Type A and type B textured surface implants tested. Average diameter of the implants is 3 cm.	132
Figure 4.2. Randomisation of implants.....	134
Figure 4.3. Implantation procedure in an <i>in vivo</i> porcine model.	136
Figure 4.4. Dissection during explant surgery.....	137
Figure 4.5. Explanted (A) type A and (B) type B implant with surrounding capsule intact.	142
Figure 4.6. Microbial load (16S rRNA copies) per mg of (A) implant and (B) capsular tissue present in type A control implants (non-inoculated) and implant types A and B inoculated with <i>S. epidermidis</i>	146
Figure 4.7. (A) CD3, (B) CD4, CD8a and CD79a copy number per mg of implant on the surface of type A and type B control implants and implants inoculated with <i>S. epidermidis</i>	150
Figure 4.8. CD3, CD4, CD8a, CD79a from pig implants versus total bacteria per milligram of implant sample.	150
Figure 4.9. (A) CD3, (B) CD4, CD8a and CD79a copy number per mg of capsular tissue surrounding type A and type B control implants and implants inoculated with <i>S. epidermidis</i>	152

Figure 4.10. CD3, CD4, CD8a, CD79a from pig capsules versus total bacteria per milligram of capsular sample.....	152
Figure 4.11. Scanning electron micrographs of <i>S. epidermidis</i> inoculated and non-inoculated control implant types A and B and the surrounding capsules.....	155
Figure 4.12. Three-dimensional cross sections and extractions from micro CT analysis used for measurement of surface area and roughness of (A) type A and (B) implants.	159
Chapter V.	
Figure 5.1. Number of bacteria per mg of implant explanted from eight BIA-ALCL patients and their contralateral (non-ALCL) normal breast ($n = 7$) as determined by qPCR.	174
Figure 5.2. Number of bacteria per mg of implant explanted from BIA-ALCL patients, their contralateral normal breast and contracture patients as determined by qPCR.....	175
Figure 5.3. Number of bacteria per mg in the different textured implants explanted from BIA-ALCL patients and their contralateral normal breast as determined by qPCR.	176
Figure 5.4. Number of bacteria per mg of capsule surrounding implants from BIA-ALCL patients, their contralateral normal breast and contracture patients as determined by qPCR.	178
Figure 5.5. Number of bacteria per mg of capsule surrounding Silimed PU and Allergan Biocell implants explanted from BIA-ALCL patients and their contralateral normal breast as determined by qPCR.	178
Figure 5.6. Total number of CD3+ T-cells and B-cells in capsules explanted from BIA-ALCL patients, their contralateral normal breast and contracture patients as determined by qPCR.	182
Figure 5.7. CD3, CD4, CD8a, CD79a from capsules versus total bacteria per mg of capsular sample in BIA-ALCL patients.	184
Figure 5.8. CD3, CD4, CD8a, CD79a from capsules versus total bacteria per mg of capsular sample in contracture patients.	185

Figure 5.9. CD3, CD4, CD8a, CD79a from capsules versus total bacteria per mg of capsular sample in the contralateral normal breast of BIA-ALCL patients.	186
Figure 5.10. Scanning electron micrographs showing bacterial biofilm present on capsules taken from three BIA-ALCL patients.....	187
Chapter VI.	
Figure 6.1. Metabolisation of MTT to formazan salt by viable cells.	194
Figure 6.2. Optimisation of cell and mitogen concentrations: absorbance and proliferative response of MT-4 cells to PHA stimulation.	197
Figure 6.3. Comparison of MTT labelling time of 4 hr, 8 hr and overnight to maximise detection of proliferative responses (SI) of MT-4 cells to PHA.....	199
Figure 6.4. Comparison of MTT labelling time of 6 hr or 8 hr to maximise detection of proliferative responses (SI) of MT-4 cells to PHA and LPS stimulation.	200
Figure 6.5. Comparison of MTT labelling time of 6 or 8 hr to maximise detection of proliferative responses (SI) of BIA-ALCL cells to PHA and LPS stimulation.....	201
Figure 6.6. Proliferative responses (SI) of MT-4 cells to PHA and LPS stimulation at MTT incubation of 6 hr.	202
Figure 6.7. Proliferative responses (SI) of BIA-ALCL cells to PHA and LPS stimulation at MTT incubation of 6 hr.	203
Figure 6.8. Proliferation response (SI) of (A) MT-4 cells and (B) BIA-ALCL cells to PHA.	201
Figure 6.9. Established MTT colourimetric assay to determine cell proliferation.	206
Figure 6.10. Proliferation response (SI) of the nine patient-derived BIA-ALCL tumour cells to (A) 5 and (B) 10 µg/mL of PHA and LPS.	210
Figure 6.11. Proliferation response (SI) of the three BIA-ALCL cell lines, TLBR-1, TLBR-2 and TLBR-3, to (A) 5 and (B) 10 µg/mL of PHA and LPS.	213

Figure 6.12. Proliferation response (SI) of the two cutaneous-ALCL cell lines, MAC-1 and MAC-2A, to (A) 5 and (B) 10 µg/mL of PHA and LPS.	214
Figure 6.13. Proliferation response (SI) of the MT-4 immortal T-cell line to (A) 5 and (B) 10 µg/mL of PHA and LPS.....	215
Figure 6.14. Proliferation response (SI) of the peripheral blood mononuclear cells purified from patients with capsular contracture to (A) 5 and (B) 10 µg/mL of PHA and LPS.	216
Figure 6.15. Proliferation response (SI) of the peripheral blood mononuclear cells purified from healthy patients undergoing primary breast augmentation to (A) 5 and (B) 10 µg/mL of PHA and LPS.....	217
Figure 6.16. Proliferation response (SI) of the peripheral blood mononuclear cells purified from BIA-ALCL patients to (A) 5 and (B) 10 µg/mL of PHA and LPS.....	218
Figure 6.17. Summary of the proliferative response (SI) of the different cell types to 5 and 10 µg/mL of LPS.	220
Figure 6.18. Summary of the proliferative response (SI) of the different cell types to 5 and 10 µg/mL of PHA.	221
Figure 6.19. Maximum significant SI of the individual cell types tested following PHA and LPS stimulation.....	222
Chapter VII.	
Figure 7.1. Proliferation response (SI) of the five patient-derived BIA-ALCL tumour cells to (A) 5 and (B) 10 µg/mL of SEA and TSST-1.	232
Figure 7.2. Proliferation response (SI) of the three BIA-ALCL cell lines, TLBR-1, TLBR-2 and TLBR-3, to (A) 5 and (B) 10 µg/mL of SEA and TSST-1.....	234
Figure 7.3. Proliferation response (SI) of the two cutaneous-ALCL cell lines, MAC-1 and MAC-2A, to (A) 5 and (B) 10 µg/mL of SEA and TSST-1.....	235

Figure 7.4. Proliferation response (SI) of the MT-4 immortal T-cell line to (A) 5 and (B) 10 µg/mL of SEA and TSST-1.	236
Figure 7.5. Proliferation response (SI) of the peripheral blood mononuclear cells purified from patients with capsular contracture to (A) 5 and (B) 10 µg/mL of SEA and TSST-1.	237
Figure 7.6. Proliferation response (SI) of the peripheral blood mononuclear cells purified from healthy patients undergoing primary breast augmentation to (A) 5 and (B) 10 µg/mL of SEA and TSST-1.	238
Figure 7.7. Proliferation response (SI) of the peripheral blood mononuclear cells purified from BIA-ALCL patients to (A) 5 and (B) 10 µg/mL of SEA and TSST-1.	239
Figure 7.8. Summary of the proliferative response (SI) of the different cell types to 5 and 10 µg/mL of SEA.....	241
Figure 7.9. Summary of the proliferative response (SI) of the different cell types to 5 and 10 µg/mL of TSST-1.....	242
Figure 7.10. Maximum significant SI of the individual cell types tested following SEA and TSST-1 stimulation.....	243
Figure 7.11. Mean maximum proliferative response (SI) of primary BIA-ALCL tumour cells (PHA/LPS, $n = 9$; SEA/TSST-1, $n = 5$), TLBR ($n = 3$), cutaneous-ALCL ($n = 2$) and MT-4 ($n = 1$) cell lines, and PBMC purified from patients with contracture ($n = 3$), primary augmentation ($n = 3$) and BIA-ALCL patients ($n = 5$), following stimulation with SEA, TSST-1, PHA and LPS.....	245
Figure 7.12. Comparison of the proliferation responses (SI) of BIA-ALCL tumour cells to non-specific mitogens at (A) 5 and (B) 10 µg/mL cultured in media with or without 1% penicillin/streptomycin.	247

Chapter VIII.

Figure 8.1. <i>S. aureus</i> biofilm formation in DMEM and RPMI 1640 medium for 24 hr.	255
Figure 8.2. Quantification of <i>S. aureus</i> biofilm biomass and viability after 24 and 48 hr culture in DMEM and RPMI.....	257
Figure 8.3. Mean absorbance of culture supernatant from triplicate <i>S. aureus</i> planktonic growth in DMEM and RPMI 1640 medium after 24 and 48 hr.	258
Figure 8.4. <i>S. aureus</i> biofilm (A) biomass and (B) viability after five days in culture with daily media changes or no change in media.	259
Figure 8.5. Mean absorbance of culture supernatant from (A) <i>S. aureus</i> planktonic growth and (B) DMEM only after five days in culture with daily media changes or no change in media.	260
Figure 8.6. Process for growing <i>S. aureus</i> biofilm on polycarbonate coupons in DMEM, 10% TSB or 20% TSB for 48 hr and then in DMEM with daily media changes for three days.	261
Figure 8.7. <i>S. aureus</i> biofilm formed in triplicate in DMEM, 10% TSB or 20% TSB on polycarbonate coupons for 48 hr and then transferred to DMEM with daily media changes for three days.....	262
Figure 8.8. Process for growing <i>S. aureus</i> biofilm on replicate Motiva SilkSurface and Motiva VelvetSurface textured implants in DMEM, 10% TSB or 20% TSB for 48 hr and then in DMEM with daily media changes for five days.	263
Figure 8.9. Quantification of <i>S. aureus</i> biofilm formed in DMEM, 10% TSB or 20% TSB on the surface of replicate textured breast implants for 48 hr and then transferred to DMEM with daily media changes for five days.....	264
Figure 8.10. Mean absorbance of culture supernatant from replicate <i>S. aureus</i> planktonic growth after five days in culture with daily media changes.....	265

Figure 8.11. (A) <i>S. epidermidis</i> (B) <i>P. aeruginosa</i> and (C) <i>R. pickettii</i> biofilm formed in DMEM, 10% TSB or 20% TSB on replicate textured breast implants for 48 hr and then transferred to DMEM with daily media changes for five days.....	267
Figure 8.12. Mean absorbance of culture supernatant from replicate (A) <i>S. epidermidis</i> , (B) <i>P. aeruginosa</i> and (C) <i>R. pickettii</i> planktonic growth after five days in culture with daily media changes.....	268
Figure 8.13. Established bacterial biofilm formation assay using textured breast implants.	270
Figure 8.14. Co-culture of BIA-ALCL tumour cells with <i>P. aeruginosa</i> biofilm.....	273
Figure 8.15. Viability of the biofilm formed on replicate implants after three days in culture...	273
Figure 8.16. Proliferation response of BIA-ALCL tumour cells to <i>S. epidermidis</i> biofilm, LPS stimulation and textured implants after three days in culture.	274
Figure 8.17. Proliferation response of BIA-ALCL tumour cells to <i>R. pickettii</i> biofilm, LPS stimulation and textured implants after three days in culture.	275
Figure 8.18. Testing the culture medium by standard plate culture to determine if bacteria detach from biofilm formed on implants.....	277
Figure 8.19. Stimulation index obtained by detached biofilm bacteria during three days of co-culture with BIA-ALCL cells as measured by MTT assay.....	278
Figure 8.20. Quantification of biofilm formed on triplicate implants before and after co-culture and in co-culture supernatant after three days in co-culture with BIA-ALCL tumour cells.	279
Figure 8.21. Proliferation response (SI) of BIA-ALCL tumour cells to biofilm composed of different bacterial species, LPS stimulation and textured implants.....	282
Figure 8.22. Stimulation index from co-culture of media only to biofilm composed of different bacterial species, LPS stimulation and textured implants.....	283

Figure 8.23. Biofilm bacterial numbers formed on six replicate implants before and after co-culture and in co-culture supernatant after three days in co-culture with BIA-ALCL tumour cells.	284
---	-----

Figure 8.24. Quantification of biofilm formed on six replicate implants before and after co-culture and in co-culture supernatant after three days in co-culture with media only.	285
--	-----

Chapter IX.

Figure 9.1. Overview of TLR4 signalling.....	291
--	-----

Figure 9.2. Titration assay to determine optimum TLR4 inhibitor concentration.....	294
--	-----

Figure 9.3. Standard curve generated for human TNF- α ELISA.	298
--	-----

Figure 9.4. Inhibitory effect of the TLR4 inhibitor peptide on LPS-mediated TLR4 activation in BIA-ALCL cells as measured by ELISA.....	299
---	-----

Figure 9.5. Inhibitory effect of the TLR4 inhibitor peptide on LPS-mediated TLR4 activation in BIA-ALCL cells as measured by MTT.	300
--	-----

List of Tables

Chapter I.

Table 1.1. The different types of breast implant devices for breast augmentation and reconstruction.	3
Table 1.2. Baker grade classification system of capsular contracture.	12
Table 1.3. Summary of studies investigating the role of implant filler, surgical technique and implant texture in the development of capsular contracture (CC).	15
Table 1.4. The different organisms identified in the implants and capsules of contracture patients.	18
Table 1.5. 14-point intraoperative plan listing the clinical recommendations for prevention of device-associated infection in breast prostheses.	29
Table 1.6. Summary of the immunophenotypic features of the different subforms of ALCL.	37

Chapter II.

Table 2.1. Primer sequences used for real-time PCR of microbial load and lymphocyte number in pig and human samples.	73
Table 2.2. Clinical summary of established T-cell lymphoma breast cell lines.	78
Table 2.3. Summary of the eleven breast implant surface types tested for bacterial attachment and growth <i>in vitro</i>	86

Chapter III.

Table 1: Manufacturing process for textured implants.	104
Table 2: Raw surface area calculation and 3D:2D ratio for each implant type.	112
Table 3: Surface roughness for each implant type.	120
Table 4: Proposed generic breast implant classification based on fill, surface, shape and size. .	124

Chapter IV.

Table 4.1. Baker grading results for pigs 1 and 2.....	141
Table 4.2. Amount (g) of host tissue remaining attached to implant.....	142
Table 4.3. Microorganisms cultured from control implants.	143
Table 4.4. Detection of <i>S. epidermidis</i> in inoculated and non-inoculated implant types A and B and the surrounding capsules.	143
Table 4.5. Number of bacteria as determined by 16S rRNA copies attached to a mg of implant..	145
Table 4.6. Number of bacteria as determined by 16S rRNA copies per mg of capsular tissue...	145
Table 4.7. Number of T-cells (CD3), helper T-cells (CD4), cytotoxic T-cells (CD8a) and B-cells (CD79a) on the surface of a mg of implant as determined by qPCR.....	148
Table 4.8. Number of T-cells (CD3), helper T-cells (CD4), cytotoxic T-cells (CD8a) and B-cells (CD79a) per mg of capsular tissue as determine by qPCR.	149
Table 4.9. Criteria used to determine the degree of biofilm.	153
Table 4.10. Bacterial load and SEM scoring for the amount of biofilm present on implant types A and B.	153
Table 4.11. Bacterial load and SEM scoring for the amount of biofilm present in capsules surrounding implant types A and B.....	154
Table 4.12. Raw surface area calculations and 3D:2D ratio for each implant type.....	159

Chapter V.

Table 5.1. Clinical summary of breast implant-associated ALCL patients.	170
Table 5.2. Microorganisms cultured from BIA-ALCL and contralateral non-ALCL specimens.	172
Table 5.3. Number of bacteria attached to a mg of implant as determined by qPCR.	173
Table 5.4. Number of bacteria attached to a mg of implant as determined by qPCR.	173

Table 5.5. Number of bacteria attached to a mg of capsular tissue as determined by qPCR.	176
Table 5.6. Number of bacteria attached to a mg of capsular tissue as determined by qPCR.	177
Table 5.7. Number of T-cells (CD3), helper T-cells (CD4), cytotoxic T-cells (CD8a) and B-cells (CD79a) per mg of capsular tissue as determined by qPCR.	180
Table 5.8. Number of T-cells (CD3), helper T-cells (CD4), cytotoxic T-cells (CD8a) and B-cells (CD79a) per mg of capsular tissue as determined by qPCR.	181
Table 5.9. Summary of the total number of CD3, CD4, CD8a and CD79a lymphocytes per mg of tissue in capsules from BIA-ALCL patients, their contralateral normal breast and CC patients as determined by qPCR.	182

Chapter IX.

Table 9.1. Titration assay to determine optimum TLR4 inhibitor concentration.	293
--	-----

List of Symbols and Abbreviations

°	degree
°C	degrees Celsius
%	percent
μA	microampere
μg	microgram
μL	microlitre
μM	micromolar
μm	micrometre
2D	two-dimensional
3D	three-dimensional
Agr	accessory gene regulator
AHL	acylated homoserine lactone
AIP	autoinducer peptide
ALK	anaplastic lymphoma kinase
ALK-	ALK-negative
ALK+	ALK-positive
ANOVA	Analysis of Variance
ASPS	American Society of Plastic Surgeons
ATCC	American Type Culture Collection
Bap	biofilm-associated protein
BIA-ALCL	breast implant-associated anaplastic large-cell lymphoma
BLAST	Basic Logical Alignment Search Tool
CC	capsular contracture
CD	cluster of differentiation
CFU	colony forming unit
CI	confidence interval
cm	centimetre
cm ²	square centimetre
CO ₂	carbon dioxide
CT	computed tomography
CV	crystal violet
dL	decilitre
DMEM	Dulbecco's Modified Eagle Medium
DMSO	dimethyl sulfoxide
DNA	deoxyribonucleic acid
ECACC	European Collection of Authenticated Cell Cultures
EDTA	ethylenediaminetetraacetic acid
e.g.	for example
ELISA	enzyme-linked immunosorbent assay
EPS	extracellular polymeric substance
FBS	foetal bovine serum
FDA	Food and Drug Administration

g	gram
HBA	horse blood agar
HLA-DR	human leukocyte antigen-antigen D related
hr	hour
i.e.	that is
IFN- β	interferon-beta
IFN- γ	interferon-gamma
IL	interleukin
JAK	Janus kinase
kD	kilo Dalton
kg	kilogram
kV	kilovolt
L	litre
LBP	lipopolysaccharide-binding protein
LPS	lipopolysaccharide
LyP	lymphomatoid papulosis
MALT	mucosa-associated lymphoid tissue
MAPK	mitogen-activated protein kinase
MD-2	myeloid differentiation factor-2
mg	milligram
MHC	major histocompatibility complex
min	minute
mL	millilitre
mm	millimetre
mM	millimolar
mPNA	mitochondrial peptide nucleic acid
MRI	magnetic resonance imaging
MRSA	methicillin-resistant <i>Staphylococcus aureus</i>
MTT	3-(4,5-dimethylthiazol-2-yl)-2,5-diphenyl tetrazolium bromide
MyD88	myeloid differentiation factor 88
NF- κ B	nuclear factor kappa-light-chain enhancer of activated B-cells
ng	nanogram
NHL	non-Hodgkin lymphoma
nm	nanometre
NPM	nucleophosmin
nt	nucleotide collection
OD	optical density
PBMC	peripheral blood mononuclear cell
PBS	phosphate buffered saline
PHA	phytohemagglutinin
PIA	polysaccharide intercellular adhesin
PMN	polymorphonuclear neutrophil
PNAG	poly- β -1,6-N-acetylglucosamine
PU	polyurethane
qPCR	real-time quantitative polymerase chain reaction
QS	quorum sensing
R ²	R-squared
RCF	relative centrifugal force
rpm	revolutions per minute

RPMI	Roswell Park Memorial Institute
rRNA	ribosomal ribonucleic acid
RT	room temperature
SD	standard deviation
SEA	staphylococcal enterotoxin A
sec	second
SEM	scanning electron microscopy
SEM	standard error of the mean
SHP-1	tyrosine phosphatase
SI	stimulation index
SOCS3	suppressor of cytokine signalling 3
STAT3	signal transducer and activator of transcription 3
TCR	T-cell receptor
TCR-V β	T-cell receptor-V beta chain
TDA	toluenediamine
TGA	Therapeutic Goods Administration
TGF- β 1	transforming growth factor-beta 1
Th	T-helper
TIA-1	T-cell-restricted intracellular antigen-1
TIR	Toll/interleukin-1 receptor
TIRAP	TIR domain-containing adaptor protein
TLBR	T-cell breast lymphoma
TLR4	Toll-like receptor 4
TNF- α	tumour necrosis factor-alpha
TRAM	TIR domain-containing adaptor inducing IFN-beta-related adaptor molecule
Treg	T-regulatory
TRIF	TIR domain-containing adaptor inducing IFN-beta
TSB	tryptone soya broth
TSST-1	toxic shock syndrome toxin-1
U	Unit
US	United States
v/v	volume per volume
VIPER	viral inhibitor peptide of TLR4
X	times

Chapter I.

Literature Review

BIA-ALCL is a recently diagnosed, rare type of T-cell non-Hodgkin lymphoma for which the aetiopathogenesis and optimal treatment remain unknown. First described in 1997 (Keech and Creech, 1997), its detection and incidence has risen worldwide due to the increase use of breast implants in breast augmentation and reconstructive surgery. It is now defined by the World Health Organisation as a distinct new cancer (Swerdlow et al., 2016). A number of reported observations about BIA-ALCL point to an underlying biofilm infection as a potential cause. This review outlines the different breast implant types, complications associated with breast implants, the role of bacteria, and the implications for BIA-ALCL. This review will also discuss the interplay of host, implant and microbial factors, including the patient's genetic background, immune response, the textured implant surface, and bacterial phenotype that lead to the development of BIA-ALCL. Specifically, this review will discuss the potential role of chronic bacterial antigen stimulation in the pathogenesis of this newly characterised implant-associated neoplasm, which is the main subject of this thesis.

1.1. Breast implants for cosmetic and reconstructive augmentation

Breast implantation either for cosmetic or reconstructive purposes is one of the most common procedures performed in plastic surgery (Albornoz et al., 2013, Doren et al., 2017). The procedure usually involves the insertion of an implant within the breast pocket to alter the size and

shape of the breast. According to the American Society of Plastic Surgeons (ASPS), in 2015 alone, more than 280 000 women underwent breast enlargement surgery (with silicone or saline implants) in the United States (US), and an estimated 106 000 breast cancer patients underwent reconstruction after mastectomy, often with implants (ASPS, 2015). With the rise in implant-based augmentation surgery, it is not surprising that there are many different styles and features of breast implants commercially available. The diversity in implant choice is important for both surgeons and patients undergoing augmentation since the various implant characteristics can affect the feel and performance of the implant device.






1.1.1. Types of breast implants

The rise in implant-based augmentation over the last decade is in line with improvements in breast implant safety, quality, performance and manufacturing. In fact, in just the past few years, the Food and Drug Administration (FDA) has approved new implant styles, shapes and textures (O'Shaughnessy, 2015). Modern generation breast implants can be divided into categories based on implant filling, *silicone* or *saline*, surface texture, *textured* or *smooth*, and shape, *round* or *anatomic*, each of which have slightly different properties (Namnoum et al., 2013, Headon et al., 2015) (Table 1.1).

Silicone breast implants

Silicone breast implants were first introduced in the early 1960s (Cronin and Gerow, 1964) and over the past five decades since, have gone through a number of modifications that have ultimately led to major improvements. Today, silicone implants remain the most popular and accepted material for use in breast augmentation. They are designed in various anatomic dimensions that comprise of a silicone shell elastomer filled with silicone gel that has cohesive properties (O'Shaughnessy, 2015). Prior to 1991, there were several versions of silicone implants available in the US. These included double-lumen, reverse double-lumen, adjustable, smooth shell and textured

Table 1.1. The different types of breast implant devices for breast augmentation and reconstruction.

Implant filling	Surface texture	Shape
Silicone	Smooth	Round
		
Saline	Textured	Anatomic
		
		
	Polyurethane	

shell implants manufactured by Dow Corning, Surgitek, Bristol-Myers, McGhan Medical, Silimed and Mentor, among others (Spear et al., 2014). Following on from the US FDA voluntary moratorium in 1992 that effectively removed silicone implants from the US market, future silicone gel-filled implants needed to be designed and manufactured to meet substantial performance and safety benchmarks that would be significantly higher than earlier versions (i.e. first-, second- and third-generation silicone implants) (Maxwell and Gabriel, 2009, Spear et al., 2014, O'Shaughnessy, 2015). In 2006, the US FDA approved Mentor Worldwide LLC (Santa Barbara, California) and McGhan/Inamed Medical Corporation (now Allergan, Irvine, California) applications to market smooth and textured round silicone gel-filled implants (fourth-generation), which are currently available today (Calobrace and Capizzi, 2014). Fifth-generation implants include Sientra's (Silimed, Santa Barbara, California) round implant filled with high-strength cohesive gel, available in both smooth and TRUE texture surfacing, and MemoryShape (Mentor) and Natrelle 410 (Allergan) form-stable shaped and textured devices (Maxwell and Gabriel, 2009, Calobrace and Capizzi, 2014, O'Shaughnessy, 2015). These new gel devices are filled with a highly cohesive, more viscous and greater cross-linking gel than their predecessors (Brown et al., 2005). Increasing cross-linking and form stability correlate with better shape retention and firmness of the device, which makes them look and feel more like natural breast tissue.

In contrast to saline breast implants, a larger incision is needed for inserting a full-sized silicone implant, which increases the risk of scarring. If the silicone implant leaks, the high-viscosity, cohesive silicone gel may remain within the implant shell or escape into the breast implant pocket. A leaking implant filled with silicone gel will not collapse and hence will not affect the size of the breast, thereby making it difficult to identify the rupture (Maxwell and Gabriel, 2009, O'Shaughnessy, 2015). A ruptured silicone implant can only be detected through magnetic resonance imaging (MRI) screening, and thus patients are recommended to visit their surgeons regularly to assess the condition of their implants.

Saline breast implants

Inflatable saline-filled breast implants were first reported in 1965 (Arion, 1965) and comprise a silicone elastomer shell filled with sterile salt water. The push for the development of saline implants was to allow smaller incisions through which a non-inflated device could be inserted that was then inflated with liquid filler material (Walker et al., 2009). The volume of saline in the silicone shell determines the firmness of the implant, providing a uniform shape, size and feel. Unlike silicone-filled implants, should the implant shell leak or rupture, the saline-filled implant will collapse and the saline will be absorbed by the breast tissues and naturally expelled by the body. However, in under-filled devices surface wrinkles can be visible, while in over-filled devices the implant may feel and appear firm (Walker et al., 2009). For these reasons, saline implants generally perform better under thicker tissue, and surgeons usually fill implants to the recommended volume. Moreover, on a volumetric basis, saline implants tend to be heavier than silicone gel implants and over time may cause excessive stretch or thinning of patient tissues with inferior displacement of the implant (Maxwell and Gabriel, 2009). Alternatively, there are also structured saline implants, which contain an internal structure consisting of a series of nested shells that control fluid movement. The implant combines certain key features and benefits of saline and silicone gel implants that aims to make the implant feel and look more natural, a major drawback of saline implants (Nichter et al., 2018).

The silicone moratorium in 1992 led to widespread use of saline-filled implants for both breast augmentation and reconstruction. During which the US FDA determined saline-filled implants from both Mentor and McGhan were safe and did not cause any major disease (Cunningham et al., 2000, Rohrich, 2000). A study on the effect of saline versus silicone prosthetic breast reconstruction on patients' post-operative satisfaction has found higher satisfaction among patients with silicone implants compared to those with saline implants (McCarthy et al., 2010, Macadam et al., 2013).

Smooth breast implants

Smooth breast implants are the softest feeling implants. These devices can move within the breast pocket to give a more natural movement. Smooth surface implants are usually manufactured by repeatedly dipping mandrels in silicone and curing in a laminar flow oven (O'Shaughnessy, 2015). Smooth implants may have some palpable or visible rippling under the skin.

Textured breast implants

Textured breast implants were developed with the aim to produce better tissue incorporation between the implant and the human tissue. Following early attempts (from 1951 to 1962) at breast augmentation with polyurethane (PU) sponge proving unsuccessful, where within one year of augmentation breasts became very firm and lost over 25% of their volume (Peters, 2002). It was not until 1970 that favourable use of a silicone gel implant covered with a thin layer of PU foam was reported (Ashley, 1970, Peters, 2002). The PU surface produced aesthetically pleasing results, adhering to the surrounding tissues, which subsequently delaminated and created a relatively non-contractible capsule (Sinclair et al., 1993). The favourable clinical outcomes and commercial success of PU-covered silicone gel implants throughout the 1980s led to the development of textured silicone surfaces in the hope of achieving similar results. In 1986, McGhan/Allergan introduced Biocell textured implants and expanders, Mentor introduced Siltex textured implants, and Sientra, the TRUE texture (Xu and Siedlecki, 2012, O'Shaughnessy, 2015). Texturisation of the surface of implants has been shown to have biological benefits in enhancing biocompatibility and achieving optimal integration of living host and the implant (Xu and Siedlecki, 2012). These effects include enhancing tissue adhesion, growth and proliferation of host blood supply, enhancement of cellular migration and fibroblast adhesion (Danino et al., 2001, Dalby et al., 2002). Surface texture is an important characteristic for device stability as it prevents rotation in the breast pocket, or migration of implants and tissue expanders, which are inflatable implants often used in breast reconstruction to stretch the skin and muscle to make room for a future, more permanent

implant (Calobrace and Capizzi, 2014). It is postulated that the texture pore size correlates with tissue adherence and implant stability (Danino et al., 2001). In contrast to the manufacturing of smooth implants, in textured implants there is an intermediate step to allow texturing. Biocell is an aggressive open-pore textured silicone surface that is composed of irregular pores with an average diameter of 600 to 800 μm and depth of 150 to 200 μm (Danino et al., 2001). The Biocell surface is manufactured by a “salt-loss” technique that involves adding salt crystals to the dipped silicone mandrel before curing, which is then washed from the surface leaving behind a pitted appearance with randomly arranged pores (Barr and Bayat, 2011). As a result, these interconnected pores promote adherence to the surrounding tissue, and thus developing capsule through an adhesive effect (Danino et al., 2001, Dalby et al., 2002). Although tissue adherence is clinically similar to that seen with the PU foam surface, Biocell differs in that there is no delamination of the texture as occurs with PU (Maxwell and Gabriel, 2014). Moreover, like the PU implants, Biocell implants have a high friction coefficient around the device, which makes them relatively immobile (Maxwell and Gabriel, 2014). Siltex is a less aggressive textured silicone surface created by pressing the dipped silicone mandrel into PU foam, a process termed negative contact imprinting. The resulting texture pore size, has an average diameter of 70 to 150 μm and depth of 60 to 275 μm , and is meant to mimic the PU foam (Danino et al., 2001). In contrast to PU and Biocell, Siltex does not adhere to the surrounding tissue and are not immobile (Danino et al., 2001). Despite the lack of tissue in-growth, these form-stable devices instead move within their surrounding pocket in a similar way to smooth-walled implants to maintain proper position (Calobrace and Hammond, 2014). TRUE texture is a hybrid of the other textures, more aggressive than Siltex but less aggressive than Biocell. It is designed to promote tissue in-growth and is created neither by salt-loss, sugar, soak/scrub or imprinting, but a proprietary process that leaves behind a novel “nano” texture containing smooth hollow pores with thin cell webbing that reduces particle formation (Sforza et al., 2017). Other textured surfaces include the micro textured implant (pore size of an average 100

to 150 µm diameter) manufactured by Polytech Mesmo through a gas diffusion process that coats the surface of the uncured implant with ammonium carbonate (Barr et al., 2009, Henderson et al., 2015). There is also the micro structured implant with pillar-structured texture previously manufactured by Dow Corning (Batra et al., 1995) and the PU foam-covered implant manufactured in Brazil by Silimed (Heden et al., 2001).

Round breast implants

Round breast implants have a tendency to make breasts appear fuller and provide a softer, more natural breast feel than form-stable implants. Patients will have movement of the implant within the breast pocket and are more likely to visualise and palpate wrinkling of the device (Caplin, 2014, Nahabedian, 2014). Thus, the round devices are a good choice for women who have adequate upper pole tissue and who desire a soft, natural feeling breast (Caplin, 2014, Nahabedian, 2014). Moreover, since rotation is not an issue, round implants may be more appropriate in difficult revision cases where many variables can affect the size and shape of the breast pocket (O'Shaughnessy, 2015).

Anatomic breast implants

Anatomically-shaped, silicone-filled breast implants have only been on the US market for a few years (from 2012) and so few studies have evaluated their long-term performance and patient satisfaction (Macadam et al., 2013, Caplin, 2014, Nahabedian, 2014). Anatomically-shaped devices have complication profiles similar to those of round implants and also have low rates of rotation in both aesthetic and reconstructive breast surgery (Nahabedian, 2014).

Anatomic or form-stable breast implants were created to provide immobility with softness (Burkhardt and Demas, 1994, Heden et al., 2001, Spear and Mardini, 2001). In the 1980s, popular early generation anatomic-shaped implants included the PU Optimum and Replicon devices, which are no longer available today (Ashley, 1972, Capozzi and Pennisi, 1981). Anatomic implants maintain their shape even when the implant shell is broken as the silicone gel inside the implant is

thicker than traditional silicone gel implants (Maxwell and Gabriel, 2014). These implants are also firmer than traditional implants and usually have more projection at the bottom of the implant and are tapered towards the top. Unlike round implants, if an anatomic implant rotates, it may lead to an unusual appearance of the breast that may require a separate procedure to correct (Maxwell and Gabriel, 2014).

Several companies have released a variety of anatomic-shaped implants. For example, the tissue adherence observed in tissue expanders with the Biocell surface led McGhan to develop anatomically-shaped expanders (Hester and Cukic, 1990, Barone et al., 1992). Favourable clinical experience led to the development of a matrix of variable height-to-width ratio anatomic expanders and implants (Heden et al., 2001, Bronz, 2002), which are used in aesthetic surgery worldwide. Silimed manufacture PU-covered cohesive silicone gel implants in anatomic shapes (Hester et al., 2001), which are also popular worldwide. Mentor introduced a mid-height Siltex textured anatomic-shaped tissue expander in 1997 and other height options in 2003. However, because tissue adherence does not generally occur in Siltex, the pocket must be exact and only minimally larger than the implant device to minimise the possibility of implant rotation (Baeke, 2002). In the US, virtually all tissue expanders marketed for breast reconstruction are textured and anatomically-shaped (Maxwell and Gabriel, 2014).

1.2. Capsular formation and contracture after breast augmentation and reconstruction, and the role of bacterial biofilm

Despite the popularity of implant-based breast augmentation or reconstruction, as with any form of surgery, the procedure has been associated with a number of complications. These include hematoma, seroma, infection, altered nipple sensation, asymmetry, scarring, swelling, rupture, leakage and capsular contracture (CC) (Adams Jr, 2009, Araco et al., 2009). Such complications can often lead to reoperation and removal of the breast implants. In fact, in 2015, as many as 43

000 implant removal procedures were reported (ASPS, 2015). While the FDA reports that between 20 to 40% of augmentation patients and 40 to 70% of reconstruction patients had reoperations during the first eight to ten years after receiving their implants (FDA, 2013). Of particular concern to both the patient and surgeon is contracture of the peri-prosthetic capsule. The pathologic process of CC occurs in response to the implantation of the breast implants, and is characterised by the tightening and hardening of the tissue capsule around the implant (Adams Jr et al., 2006b, McLaughlin et al., 2007). The condition can distort the shape and cause pain in the augmented breast. Individual studies have reported incidence rates of CC ranging from 1.3 to 45% of patients (Ersek and Salisbury, 1997, Barnsley et al., 2006, Araco et al., 2009, Rieger et al., 2013). The wide range of heterogeneity can be attributed to differences in follow-up times and a lack of standardisation in the type of implants and surgical techniques used, which can affect CC development rates (Headon et al., 2015). Despite the diversity in incidence rates reported, it is widely accepted that CC is the most common complication following implant-based breast augmentation and reconstructive surgery, and is one of the most common causes of reoperation following implantation (Barone et al., 1992, Barnsley et al., 2006, Adams Jr, 2009, Jacombs et al., 2014).



The aetiopathogenesis of CC remains unclear but is likely multifactorial. Of the possible aetiologies that have been studied, including filler material, placement of the implant (submuscular versus subglandular) etc., however, there is now wide acceptance that bacterial biofilm infection on the surface of breast implants is associated with the development of CC (Virden et al., 1992, Ahn et al., 1996, Deva and Chang, 1999, Pajkos et al., 2003, Pittet et al., 2005, Tamboto et al., 2010, Chang and Lee, 2011, Codner et al., 2011, Silvestri et al., 2011, Jacombs et al., 2012, Rieger et al., 2013, Jacombs et al., 2014, Hu et al., 2015).

1.2.1. Contracture of the peri-prosthetic capsule

First reported in the early 1970s, CC remains the most significant clinical complication associated with breast implants and the predominant cause for patient dissatisfaction after breast augmentation or reconstruction (Barone et al., 1992, Cash et al., 2002, Barnsley et al., 2006, Adams Jr, 2009, Barr et al., 2009, Jacombs et al., 2014). It results from an exaggerated scar response around the foreign prosthetic material. When an implant is inserted, as part of the physiologic response to a “foreign body”, the body forms a capsule of scar tissue around the implant, which is too large to be phagocytised and too inert to produce a toxic reaction (Nemecek and Young, 1993). This fibrotic reaction helps to maintain the position of the implant with little or no effect on the appearance of the breast. All surgical implants undergo some degree of encapsulation. However, clinical problems arise when this scar formation becomes excessive, causing the capsule to tighten or contract. This can alter the breast contours and produce a range of symptoms varying from local tenderness to hardening of the breast, excessive firmness, pain, sensitivity to touch, deformity of the breast, implant distortion, and movement or displacement of the implant (Barone et al., 1992, Adams Jr, 2009, Araco et al., 2009, Headon et al., 2015). Furthermore, patients with severe contracture of the peri-prosthetic capsule often require additional operations, resulting in additional costs to the patient, potential for suboptimal results, and increase likelihood of repeated CC (Barnsley et al., 2006).

In 1975, Baker proposed a clinical classification system of CC (Baker, 1975) that remains the most popular and practical method of assessing clinical firmness of the breast after augmentation surgery. The Baker classification system is a subjective grading system based not only on the appearance of the breast but also the perception of the breast by the patient and the surgeon (Baker, 1975, Spear and Baker, 1995). The system is divided into four grades as outlined in Table 1.2. Grade I and II are not clinically significant, such that grade I describes a breast that looks and feels absolutely natural, and grade II describes a breast with minimal contracture where

Table 1.2. Baker grade classification system of capsular contracture.

Grade	Description	References		
I	Breast absolutely natural, no one could tell breast was augmented			
II	Minimal contracture; surgeon can tell surgery was performed but patient has no complaint			
III	Moderate contracture; patient feels some firmness			
IV	Severe contracture; obvious just from observation	<p><i>Example 1.</i></p> 	<p>Appearance of inflamed and contracted left breast before removal of implant.</p>	<p>Deva and Chang (1999)</p>
		<p><i>Example 2.</i></p> 	<p>Left breast is noticeably higher and there is noticeable skin puckering along the medial side. The nipple is higher relative to the right side.</p>	<p>Headon et al. (2015)</p>

**Table (adapted) from Baker, J. Augmentation mammoplasty. In J. W. Owsley, Jr. (Ed.), Symposium on Aesthetic Surgery of the Breast: Proceedings of the Symposium of the Educational Foundation of the American Society of Plastic and Reconstructive Surgeons, and the American Society for Aesthetic Plastic Surgery, in Scottsdale, Arizona, November 23 – 26, 1975. Mosby, St. Louis; 1978: 256-263. Modified to include illustrations of grade IV capsular contracture from Deva and Chang (1999) and Headon et al. (2015).*

the surgeon can tell surgery has been performed but there are no symptoms. Grade III and IV are considered to be clinically significant and symptomatic, where grade III describes moderate contracture with some firmness felt by the patient, and grade IV describes severe contracture that is obvious from observation and symptomatic in the patient (Spear and Baker, 1995).

The genesis of CC appears to be multifactorial, and as such the management of this condition has remained a difficult challenge to clinicians. Management strategies attempting to prevent CC have included alternative implant placement (subglandular versus submuscular) (Vazquez et al., 1987, Barnsley et al., 2006, Barr et al., 2009), low bleed silicone elastomer shells (Chang et al., 1992), under filling implants, use of double-lumen implants or saline-filled implants (Spear et al., 2000, Heydarkhan-Hagvall et al., 2007, Barr et al., 2009), administration of intraluminal steroids into the breast pocket (Ceravolo and del Vescovo, 1993, Lemperle and Exner, 1993), systemic antibiotics (Freedman and Jackson, 1989), antibiotic washes to reduce bacterial colonisation of the implant (Burkhardt and Demas, 1994, Burkhardt and Eades, 1995, Barnsley et al., 2006, Barr et al., 2009), and surface texturisation of the implant (Barnsley et al., 2006, Wong et al., 2006).

1.2.2. Factors that can influence the development of capsular contracture

Much attention has been given to the role of implant filler, surgical technique and implant texture in the development of CC. Indeed, the evolution of breast augmentation surgery has been driven by the need to prevent capsule formation and contracture. As mentioned earlier, since the late 1960s, there have been five generations of silicone gel implants, each generation reflected changes in the manufacturing process and implant design (Adams Jr, 2009). With each generation, there has been a corresponding decrease in the incidence of CC, although it is unclear if this correlation is entirely due to implant design (Danino et al., 2001, Bengtson et al., 2007, Cunningham, 2007, Hester Jr et al., 2012). Historically, the type of fill was thought to influence

the development of CC (Table 1.3). Older generation silicone gel devices were characterised by higher gel bleeds and rupture rates compared to current generation implants (Maxwell and Gabriel, 2009, Berry et al., 2010, O'Shaughnessy, 2015). The rates of CC were six-fold higher with these older devices than with devices containing low-bleed silicone gel fillings (Chang et al., 1992, Berry et al., 2010, Stevens et al., 2010), while the fifth-generation form-stable cohesive silicone gel-filled implants also had lower rates of CC (Bogetti et al., 2000, Brown et al., 2005, Bengtson et al., 2007, El-Sheikh et al., 2008, Calobrace and Capizzi, 2014).

Studies have also investigated the role of surgical technique (Table 1.3), with some finding that textured implant surfaces are associated with reduced contracture following subglandular placement of saline and silicone gel-filled implants (Pollock, 1993, Henriksen et al., 2005). In contrast, these implant surfaces showed no beneficial effect when other techniques of implant placement were used, including submuscular placement (Collis et al., 2000, Barnsley et al., 2006).

Surface textures were developed to mimic the surface of PU foam-covered implants, which were thought to reduce the incidence of CC since collagen fibrils are hindered from arranging in a parallel formation and instead arrange randomly (Danino et al., 2001, Adams Jr, 2009). The next generation of surface texturing was introduced in the late 1980s, using a number of techniques to modify the external silicone shell (Tarpila et al., 1997b, Fagrell et al., 2001). There have been numerous studies to determine whether surface texture of the implant reduces the risk of CC but have shown mixed findings (Table 1.3). While some studies have found textured implants have lesser rates of clinically significant CC compared to smooth surface implants (Hakelius and Ohlsén, 1992, Asplund et al., 1996), others have also shown smooth implants are more likely to develop CC (Wong et al., 2006, Stevens et al., 2013, Liu et al., 2015). However, more recent studies have found no difference in contracture rates between both implant surface types (Schreml et al., 2007, Jacombs et al., 2014, Spear et al., 2014).

Table 1.3. Summary of studies investigating the role of implant filler, surgical technique and implant texture in the development of capsular contracture (CC).

Study	Study design (n)	Results	References
Role of implant filler	Breast augmentation surgery (14 patients)	Reduced incidence of CC with cohesive silicone gel-filled implants after 2 year follow-up.	Bogetti et al. (2000)
	Prospective clinical study (10 patients)	Biocell and Siltex textured implants have a significantly lower incidence of CC compared with smooth surface implants, irrespective of whether they were filled with silicone gel or saline.	Danino et al. (2001)
	Retrospective study (117 patients, 235 implants)	Reduced CC rates in cohesive silicone gel-filled implants.	Brown et al. (2005)
	Prospective, non-randomised study (492 primary augmentation, 225 breast reconstruction and 224 breast revision patients)	Cohesive silicone gel-filled implants had lower CC rates.	Bengtson et al. (2007)
	Meta-analysis (4 prospective studies, 8 retrospective studies)	Pooled odds ratio = 2.25 for silicone implants developing CC.	El-Sheikh et al. (2008)
	Systemic review (16 studies)	Unable to draw conclusions based on available data.	Schaub et al. (2010)
Role of surgical technique	Retrospective study (98 patients with smooth surface implants and 99 patients with texture surface implants)	Textured implant surfaces are associated with reduced contracture following subglandular placement of saline and silicone gel-filled implants.	Pollock (1993)
	Prospective randomised controlled trial (40 patients)	No difference in contracture rates when submuscular placement used.	Collis et al. (2000)
	Meta-analysis (11 randomised controlled trials)	No difference in contracture rates when submuscular placement used.	Barnsley et al. (2006)
	Prospective comparative study (2277 patients)	Subglandular placement are associated with decreased CC.	Henriksen et al. (2005)

Table 1.3. Continued.

Study	Study design (n)	Results	References
Role of implant texture	Randomised controlled trials	Textured implants showed lesser rates of clinically significant CC compared to smooth surface implants.	Hakelius and Ohlsén (1992), Asplund et al. (1996).
	Inserting one smooth and one textured implant in the same patient.	Reduced contracture rates with textured implants. No difference in contracture rates.	Burkhardt and Eades (1995) Tarpila et al. (1997b), Fagrell et al. (2001).
	Systemic review (6 randomised controlled trials, 235 patients)	Smooth implants more likely to undergo CC at 1, 3 and 7 years.	Wong et al. (2006)
	Case-control (45 patients)	Culture only, no difference in CC rates between textures; no follow-up time recorded.	Schreml et al. (2007)
	Sientra's prospective comparative study (2560 patients, 5109 implants)	Smooth implants more likely to undergo CC; 5 year study.	Stevens et al. (2013)
	Allergan Core, 410 and 410 Continued Access prospective comparative study (4412 patients, 8811 implants)	Smooth implants more likely to undergo CC; mean follow-up 37 months.	Namnoum et al. (2013)
	Allergan Core study (715 patients)	Smooth and textured implants had similar rates of CC over 10 year follow-up.	Spear et al. (2014)
	Meta-Analysis (16 randomised controlled trials, 2 case-control studies; 4486 patients, 8867 implants)	Smooth implants more likely to undergo CC; follow-up range 1 to 5 years.	Liu et al. (2015)

CC most often occurs and is readily evident during the first year after implantation (Coleman et al., 1991, Hakelius and Ohlsen, 1997, Tarpila et al., 1997a, Kjølner et al., 2002, McLaughlin et al., 2007, Stevens et al., 2013). However, it can also occur 10 years after implantation (Handel et al., 2006, Adams Jr, 2009). Indeed, in both augmentation and reconstruction, the longer an implant remains in the body, the greater the cumulative risk of contracture (El-Sheikh et al., 2008, Stevens et al., 2013). The reasons for the delayed development of CC remains unclear, however, the presence of bacteria at the time of breast implant surgery resulting in an intra-capsular inoculum have been implicated. It is thought potentiation of CC is a result of bacterial contamination of the breast pocket, which stimulates inflammation and fibroblast growth, and leads to collagen deposition and contracture of the breast (Kamel et al., 2001, Adams Jr et al., 2006b).

1.2.3. Bacterial colonisation and capsular contracture

There is growing evidence of a significant association between the presence of bacteria on breast implants and CC. In the absence of sepsis, *Staphylococcus epidermidis* has been the most commonly isolated organism from bacteriologic cultures of contracted capsules (Burkhardt et al., 1981, Shah et al., 1981, Virden et al., 1992, Pajkos et al., 2003, Netscher, 2004). *S. epidermidis* is part of the microflora of the skin (Kloos and Musselwhite, 1975) and the endogenous flora of the breast (Thornton et al., 1988), and has been cultured from breast milk and nipple secretions, and biopsied from breast parenchyma (Courtiss et al., 1979, Burkhardt, 1988). However, other bacteria have also been implicated in the formation of CC and is summarised in Table 1.4 (Dobke et al., 1995, Ahn et al., 1996, Adams Jr, 2009).

Table 1.4. The different organisms identified in the implants and capsules of contracture patients.

Bacteria	References
<i>Bacillus cereus</i>	Virden et al. (1992), Pajkos et al. (2003)
Capnocytophaga	Edmiston et al. (2015)
<i>Corynebacterium</i>	Virden et al. (1992), Young et al. (1997), Del Pozo et al. (2009)
Diphtheroids	Netscher et al. (1995), Young et al. (1997)
<i>Enterobacter cloacae</i>	Young et al. (1997), Mukhtar et al. (2009)
<i>Escherichia coli</i>	Virden et al. (1992), Ahn et al. (1996), Young et al. (1997), Pajkos et al. (2003)
Group D Enterococcus	Thornton et al. (1988)
<i>Klebsiella pneumoniae</i>	Virden et al. (1992), Young et al. (1997), Pajkos et al. (2003)
Micrococcus	Ransjö et al. (1985), Thornton et al. (1988)
Peptococcus	Gang et al. (2012)
<i>Propionibacterium acnes</i>	Virden et al. (1992), Ahn et al. (1996), Pajkos et al. (2003), Del Pozo et al. (2009), Rieger et al. (2013)
<i>Propionibacterium avidum</i>	Levin et al. (2008), Del Pozo et al. (2009), Kritikos et al. (2015)
<i>Propionibacterium granulosum</i>	Del Pozo et al. (2009)
<i>Proteus mirabilis</i>	Olsen et al. (2008), Lapid (2011)
<i>Pseudomonas</i>	Young et al. (1997), Olsen et al. (2008), Wixtrom et al. (2012)
<i>Staphylococcus aureus</i>	Virden et al. (1992), Young et al. (1997), Rieger et al. (2013), Nahabedian (2014)
<i>Staphylococcus epidermidis</i>	Virden et al. (1992), Dobke et al. (1994), Netscher et al. (1995), Ahn et al. (1996), Pajkos et al. (2003), Del Pozo et al. (2009), Rieger et al. (2013)

A study by Virden et al. (1992), which cultured 55 silicone devices (38 implants, 17 tissue expanders) from 40 patients, detected bacteria on 56% of implants removed from breasts with symptomatic contracture and 18% of devices without contracture. *S. epidermidis* was the predominant isolate identified and other organisms isolated included *Corynebacterium* species, *Propionibacterium acnes*, *Bacillus* species, *Klebsiella pneumonia* and *Escherichia coli* (Virden et al., 1992). Similarly, Dobke et al. (1994) took bacterial cultures of 150 implants explanted from 86 patients, 47 of whom underwent explant surgery due to CC and/or systemic complaints. Bacteria was detected on 76% of implants surrounded with CC and 28% of those without CC, with *S. epidermidis* the predominant isolate (Dobke et al., 1994). While Netscher et al. (1995) found positive bacterial cultures in 23.5% of contracted and 6% of non-contracted capsules that

surrounded 389 implants. Most of the organisms isolated were coagulase-negative staphylococci and anaerobic diphtheroids, and significantly correlated with Baker grade IV contracture (Netscher et al., 1995). A prospective study by Ahn et al. (1996) found a 47% culture positive rate for *S. epidermidis* and *P. acnes* in patients with symptomatic breast prostheses and 13% of implants without contracture. In another prospective study of capsules and implants following breast augmentation surgery, Pajkos et al. (2003) found a significant association with the presence of coagulase-negative staphylococci and CC, mainly isolating *S. epidermidis* in 83% of samples from women with significantly contracted breasts but isolating bacteria from only one of eight prosthesis collected from clinically normal breasts. While Del Pozo et al. (2009) took cultures of explanted breast implants processed using a vortexing/sonication procedure and found that of the 27 out of 45 contracted cases, *Propionibacterium* species, coagulase-negative staphylococci and *Corynebacterium* species was detected on 33% of cases. While of the 18 non-contracted cases only 5% of cases had positive culture that also included different organisms (Del Pozo et al., 2009). Thus, in some cases more than one type of organism can grow on the surface of implants and in capsules.

A number of studies have also shown that the presence of *S. epidermidis* accelerates contracture development in animal models (Shah et al., 1981, Marques et al., 2011). Shah and colleagues (1981) implanted two miniature silicone implants into the flanks of 16 female rabbits and inoculated each rabbit with both *S. epidermidis* and saline. They found considerably thicker capsules that were graded III and IV in all the contaminated implants, with capsule thickness proportionate to the level of staphylococcal inoculation. In contrast, the control implants were much thinner and graded I or II (Shah et al., 1981). In a more recent study, Marques et al. (2011) implanted 31 female rabbits each with one tissue expander and two implants. The rabbits received implants and expanders inoculated with either *S. epidermidis*, fibrin or left untreated. The presence of *S. epidermidis* on implants was associated with increased polymorph-type inflammatory cells,

capsule pressure and capsule thickness that had an increased density of collagen and increased angiogenesis (Marques et al., 2011), which are all hallmarks of CC (Kamel et al., 2001, Adams Jr et al., 2006a). In contrast, fibrin treatment significantly decreased intra-capsular pressure, produced thinner capsules, denser connective tissue and negative/mild angiogenesis (Marques et al., 2011).

The observation from human (Virden et al., 1992, Dobke et al., 1994, Netscher et al., 1995, Ahn et al., 1996, Pajkos et al., 2003, Del Pozo et al., 2009) and animal (Shah et al., 1981, Marques et al., 2011) studies that the fibrous tissue that forms around breast implants due to natural healing can be further stimulated by the presence of bacterial aggregates, provides support to the role of subclinical infection in potentiating CC.

1.2.4. Subclinical infection theory

The subclinical infection hypothesis to explain CC was first proposed by Burkhardt et al. (1981). Since then, with advances in our understanding of bacteria and their propensity to form biofilm, defined as bacteria encased within their own polymeric matrix that adheres to medical devices, the subclinical infection theory has accumulated a plethora of supporting data and several lines of evidence now suggest a role of subclinical infection in CC pathogenesis (Virden et al., 1992, Dobke et al., 1994, Dobke et al., 1995).

S. epidermidis has been increasingly associated with infections, particularly those involving prosthetic devices. The pathogenicity of *S. epidermidis* is derived primarily from its ability to form biofilms on the surfaces of indwelling medical devices, such as catheters, cardiac valves, orthopaedic prostheses, vascular grafts and contact lenses (Donlan, 2001, O'gara and Humphreys, 2001, Costerton, 2005, Vinh and Embil, 2005, Tunney et al., 2007, Francolini and Donelli, 2010). The detection of a *S. epidermidis* biofilm in a patient with recurrent CC led to the hypothesis that biofilm formation may have an aetiologic role in the establishment and recurrence of peri-prosthetic CC (Deva and Chang, 1999). The theory suggests that when a breast implant is inserted

into a patient, it induces a foreign body reaction that is essentially an excessive fibrotic response. Local skin flora or those within the breast ducts, such as coagulase-negative staphylococci, or bacteria present at time of surgery, may gain access to the implant during or following placement. Once in contact with the prosthetic surface of the implant, they will form a biofilm. This biofilm will continue to proliferate and expand, causing ongoing low-grade chronic inflammation and subsequent capsular fibrosis, leading to accelerated contracture (Figure 1.1) (Virden et al., 1992, Dobke et al., 1994, Deva and Chang, 1999, Pajkos et al., 2003, Netscher, 2004, Tamboto et al., 2010, Hu et al., 2015).

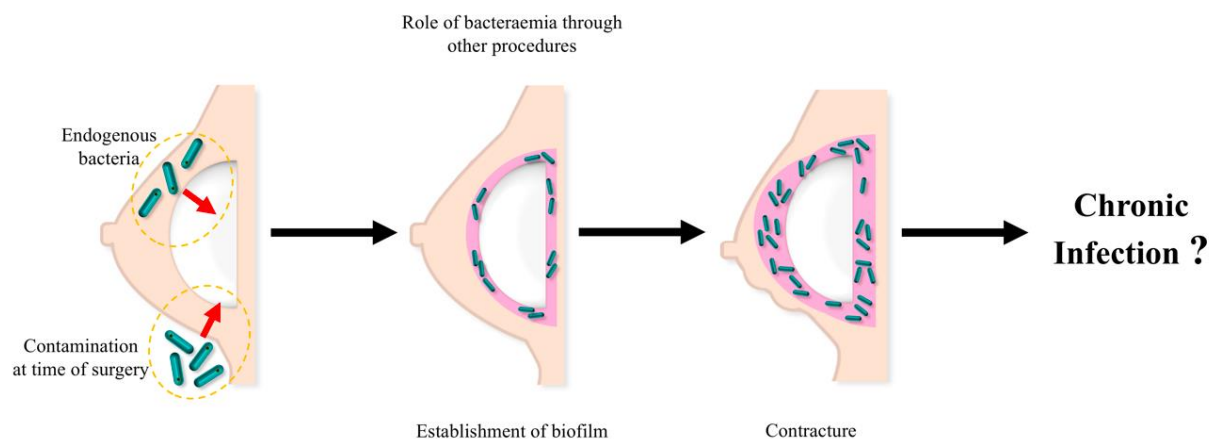


Figure 1.1. Subclinical infection theory.

Biofilm hypothesis showing progression from bacterial contamination, formation of biofilm, and eventual formation of capsular contracture.

Evidence from clinical studies (Virden et al., 1992, Ahn et al., 1996, Deva and Chang, 1999, Pajkos et al., 2003, Pittet et al., 2005, Chang and Lee, 2011, Codner et al., 2011, Silvestri et al., 2011) and from *in vivo* porcine models of CC (Tamboto et al., 2010, Jacombs et al., 2012) supports the hypothesis that the majority of CC is due to subclinical infection around breast implants caused by bacterial biofilm. Pajkos et al. (2003) identified a strong correlation between the presence of

biofilm and significant grade III/IV CC, with *S. epidermidis* being the principal bacteria implicated in biofilm formation. Using culture with visual confirmation of biofilm presence by scanning electron microscopy, bacterial biofilms were identified on 54% of implants from significantly contracted breasts (Pajkos et al., 2003). In contrast, implants from breasts without significant contracted capsules were free of such deposits. Moreover, organisms were observed as either biofilm or microcolonies on 57.9% of significantly contracted capsules and on 12.5% of breasts with minimal or no capsule (Pajkos et al., 2003). A recent clinical study by Rieger et al. (2013) of 121 implants explanted over a five year period confirmed that the degree of Baker grade CC directly correlates with the number of bacteria identified by sonication and culture. The most frequent organisms were *P. acnes* and coagulase-negative staphylococci (Rieger et al., 2013). In animal studies, Tamboto et al. (2010) developed an *in vivo* porcine model to investigate the relationship between subclinical infection with *S. epidermidis* and CC following breast implantation. Briefly, six adult female pigs underwent breast augmentation surgery using miniature textured, silicone gel-filled breast implants. Prior to implant insertion, the breast pockets were inoculated randomly with either a known dose of *S. epidermidis* (total of 36 infected teats) or an equal volume of sterile phosphate buffered saline (total of 15 non-inoculated control teats). Implants were then inserted aseptically into the submammary pocket and left *in situ* for an average of 13 weeks (Tamboto et al., 2010). After which, clinical assessment of the capsule using the Baker score (Baker, 1975, Spear and Baker, 1995) was performed, and the implants and capsules removed and analysed to detect biofilm (Tamboto et al., 2010). The authors were able to show that breast pocket inoculation of *S. epidermidis* led to biofilm development and biofilm presence was significantly associated with CC. 72.2% of implants inoculated with *S. epidermidis* resulted in biofilm production, with pocket inoculation significantly associated with biofilm formation (Tamboto et al., 2010). Moreover, 80.6% of biofilm-positive implants developed thick, contracted capsules and the presence of biofilm was significantly associated with CC development compared

with the non-inoculated pockets. Biofilm formation was associated with a four-fold increased risk of developing contracture (odds ratio = 4.1667) (Tamboto et al., 2010). However, the authors still found incidences of CC in non-inoculated groups. Five of the fifteen non-inoculated pockets developed contracture with biofilm-positive growth (Tamboto et al., 2010). Although it is likely that implant contamination (either from pig skin flora or endogenous breast flora) during insertion was sufficient to elicit biofilm formation and the subsequent CC, there was still a statistically significant difference between the contracture rates of inoculated and uninoculated implant pockets (Tamboto et al., 2010).

These findings reinforce the subclinical infection hypothesis that bacteria were able to form biofilms on the polymer surface of the breast implant subsequent to contact and stimulate CC formation. Therefore, any measures to reduce implant contamination could potentially prevent biofilm formation and subsequent contracture. Jacombs et al. (2012) investigated this using the established porcine model (Tamboto et al., 2010) by testing whether the placement of antibiotic-impregnated mesh at the time of implant insertion would prevent biofilm formation and subsequent contracture. Briefly, miniature breast implants were randomly selected to be inserted either alone (13 untreated controls) or with a circular disk of antibiotic-impregnated polypropylene mesh (14 treated) placed directly beneath the implant during surgery (Jacombs et al., 2012). The mesh was coated with a resorbable polymer carrying minocycline and rifampicin (TYRX, Inc, Monmouth Junction, New Jersey), which have been shown to be effective against *S. epidermidis* (Jacombs et al., 2012). All implants were inoculated with *S. epidermidis* and were left *in situ* for 16 weeks and then assessed for contracture by Baker grading, and the implants and capsules removed for biofilm analysis (Jacombs et al., 2012). The capsule tissues surrounding the 13 untreated control implants were all found to be contracted with Baker grade III/IV. In contrast, the 14 implants treated with antibiotic-impregnated mesh remained non-contracted with Baker grade I/II, and this difference was highly significant (Jacombs et al., 2012). Bacterial biofilm was detected on implant surfaces

and capsules obtained from both untreated and treated breasts. However, in the untreated implants and surrounding capsules, the biofilm detected was multi-layered, whereas in the antibiotic-treated implants and capsules, the biofilm was generally single-layered or composed of isolated bacterial cells (Jacombs et al., 2012). Therefore, the presence of an antibiotic-impregnated mesh at the time of implant insertion had a protective effect against bacterial attachment to breast implants, protecting against subclinical infection and significantly reducing both the numbers of bacteria and the incidence of CC (Jacombs et al., 2012). These findings are in line with studies that showed antibiotic coating of breast implants *in vitro* (van Heerden et al., 2009), use of antibiotic solution (Adams Jr et al., 2006b) and betadine solute (Wiener, 2007) in the implant pocket of aesthetic and reconstructive breast implant patients significantly reduces biofilm formation on the implants, and the subsequent risk of infection and contracture. Thus, the findings that antibacterial strategies can reduce the risk of implant infection further strengthens the subclinical infection hypothesis as a stimulus of CC following breast augmentation surgery (Figure 1.1).

Further evidence to support the subclinical infection theory include the lower incidence of contracture observed with subpectoral implants, which can be attributed to the difficulty of breast flora accessing the implant through the natural musculofascial barrier (Jacombs et al., 2012). In addition, from the numerous studies on the role of biofilms in CC and their propensity to attach to the silicone elastomer, it is evident that multiple bacterial strains may cause the development of CC (Table 4) (Virden et al., 1992, Dobke et al., 1994, Netscher et al., 1995, Ahn et al., 1996, Pajkos et al., 2003, Del Pozo et al., 2009). Furthermore, the occurrence of unilateral contracture following bilateral insertion of identical breast implants means that systemic or implant material-related causes are unlikely, which provides further support to the hypothesis that infection may lead to capsular fibrosis and contracture (Rieger et al., 2013). Thus, although contracture remains poorly understood, it is likely to be multifactorial in origin, and of all the theories on the potential aetiology of CC, the subclinical infection hypothesis remains the leading theory.

1.2.5. Influence of breast implant surface texture on biofilm formation and subsequent contracture

Textured breast implants confer better tissue incorporation and potentially less contracture. However, studies remain evenly divided as to whether texturisation of the implant surface shows any benefit (Hakelius and Ohlsén, 1992, Burkhardt and Eades, 1995, Asplund et al., 1996, Malata et al., 1997, Collis et al., 2000, Barnsley et al., 2006) or confers no difference (Tarpila et al., 1997b, Deva and Chang, 1999, Fagrell et al., 2001, Poepl et al., 2007, Schreml et al., 2007, Spear et al., 2014) (Table 3). A recent study by Jacombs et al. (2014) using the well-established *in vivo* porcine model (Tamboto et al., 2010) investigated whether a smooth or textured outer surface implant provided any advantage in preventing the development of CC in deliberately inoculated pockets of pigs. Briefly, 16 adult female pigs had 121 miniature implants inserted into the submammary pockets. 66 implants, consisting of 23 smooth and 43 textured, were inoculated with *S. epidermidis*. The implants were left *in situ* for an average of 19 weeks, after which they were assessed for contracture, and the implants and capsules removed for biofilm analysis (Jacombs et al., 2014). The authors found no significant differences between smooth surface and textured surface implants in the rate of CC following deliberate inoculation with 83.7% of the capsules around textured implants and 82.6% of the capsules around smooth implants developing contracture (Baker grade III/IV) (Jacombs et al., 2014). Furthermore, contracted breast capsules were found to have 250% more bacteria compared with non-contracted breast capsules, with no significant difference in total bacterial numbers in capsule tissue around smooth and textured implants. Interestingly, there were significantly more bacteria (20-fold) attached to the textured implants compared with smooth implants (Jacombs et al., 2014).

Jacombs et al. (2014) also conducted an *in vitro* attachment assay to determine the influence of implant surface on the growth and attachment of bacterial biofilm. Briefly, 14 miniature textured and 14 miniature smooth implants, each with a 2 cm diameter, were incubated in 10% tryptone soya broth containing a clinical strain of *S. epidermidis* obtained from a contracted human breast

(Jacombs et al., 2014). At 2 hours, the mean number of bacteria attached to the textured implants was 11-fold higher, by 6 hours, 43-fold and at 24 hours 72-fold more bacteria were attached to textured implants when compared with the smooth implants ($P < 0.001$) (Jacombs et al., 2014). These findings suggest that breast implants with a textured outer shell support a higher bacterial load compared to smooth surfaced implants. This is because a textured surface would offer a significantly greater surface-area-to-volume ratio for bacteria to colonise.

In a separate study by Hu et al. (2015), *S. epidermidis* biofilm-infected implants (12 textured and 12 smooth implants) were inserted into three adult pigs and left *in situ* for a mean period of 8.75 months, three times longer than previous studies. All explanted capsule and implant samples were positive for bacterial biofilm. In addition, bacterial culture and real-time quantitative polymerase chain reaction (qPCR) findings showed a significant increase in the number of bacteria for increasing Baker grade of CC, and significantly more bacteria were attached to textured implants (4.2×10^5 bacteria/mg of implant) compared with smooth implants (1.52×10^3 bacteria/mg of implant) (Hu et al., 2015). The authors also prospectively examined human peri-prosthetic capsules and implants from 34 patients with Baker grade IV CC undergoing revision surgery to generate comparative findings. All explanted implants were textured (Biocell (Allergan), Siltex (Mentor Worldwide), Poly Implant Prothèse and PU (Silimed)), which reflects the greater use of textured implants by Australian surgeons. All capsules were positive for bacterial biofilm, with a mean of 2.52×10^7 bacteria/mg of capsule. Furthermore, analysis of bacterial number versus texture implant surface type showed that PU implants had significantly more bacteria compared with other textured implants (Hu et al., 2015).

These findings from human and pig studies of increasing numbers of bacteria for increasing Baker grade (Tamboto et al., 2010, Jacombs et al., 2014, Hu et al., 2015) further validate the subclinical infection theory, reinforcing the pathway from initial contamination of breast implants with bacteria progressing to established biofilm and subsequent contracture. Moreover, Jacombs et

al. (2014) suggest that there is a threshold of biofilm load, which, once surpassed, host responses are triggered that can lead to significant potentiation of contracture (Figure 1.2). If implants are contaminated with only low numbers of bacteria, the host can contain the biofilm to a level that does not produce further inflammation. Although not all bacteria are removed, the host immunity is able to restrict the inflammatory response (Hu et al., 2015). However, once a critical load is reached, bacteria overwhelm the host response, continue to proliferate, and trigger an inflammatory response, leading to subsequent fibrosis and CC. It is likely this threshold will vary depending on host immunity, bacterial pathogenicity and the type of implant surface (Hu et al., 2015). Moreover, this threshold appears to be independent of whether the implant surface is smooth or textured, since both implant surface types will readily form biofilm under experimental conditions using deliberate inoculation with *S. epidermidis* (Jacombs et al., 2014). The finding that the presence of a textured outer shell on breast implants encourages higher numbers of bacteria (20-fold *in vivo* and 72-fold *in vitro*) (Jacombs et al., 2014) are also consistent with the subclinical infection hypothesis, since additional bacteria above the biofilm load threshold leads to the same outcome, development of CC (Figure 1.2). Moreover, the finding that textured surface implants significantly potentiate biofilm formation *in vivo* and *in vitro* compared with smooth surface implants has important implications.

Clinically, the use of textured breast implants should be especially combined with stringent intraoperative strategies to prevent bacterial contamination of the implant at the time of surgical implantation (Jacombs et al., 2014). Recommended strategies for reducing the risk of bacterial contamination at the time of surgical breast implantation include, nipple shields (Wixtrom et al., 2012), pocket irrigation (Wiener, 2007, Adams Jr, 2009), no-touch insertion (Bell and McKee, 2009), peri-operative antibiotic prophylaxis (Mirzabeigi et al., 2011) and avoiding the transareolar incision (Wiener, 2008). Thus, the biological benefits of texture such as better tissue integration, need to be balanced by the higher risk of bacterial contamination. Surgeons should be aware of the

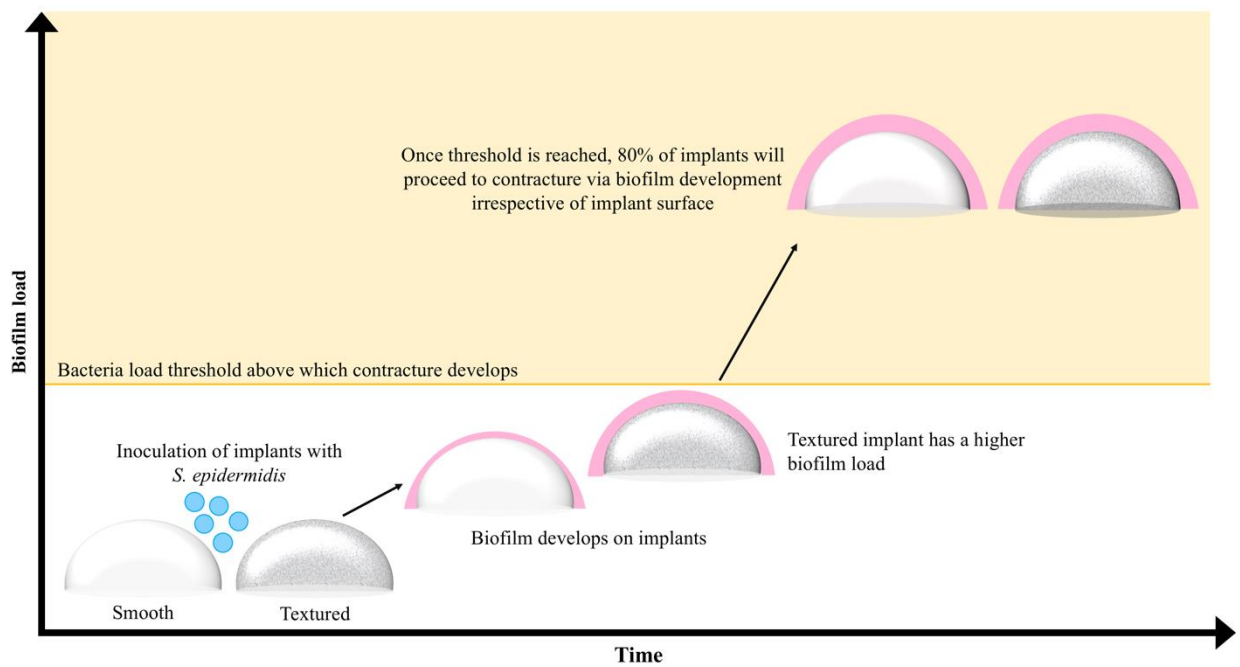


Figure 1.2. Validation of the subclinical infection hypothesis. Schematic depiction of the progression in smooth and textured breast implants from bacterial inoculation to established biofilm to contracture.

risk and modify their intraoperative strategy to limit bacterial contamination of breast implants and in turn reduce the risk of biofilm formation and subsequent contracture (Jacombs et al., 2014).

On the basis of increasing evidence that bacterial access at the time of breast implant insertion is the leading cause of CC, a 14-point intraoperative plan has been developed for surgeons to help reduce the risk of implant contamination at the time of insertion with the aim of ultimately reducing contracture (Table 1.5) (Deva et al., 2013).

Table 1.5. 14-point intraoperative plan listing the clinical recommendations for prevention of device-associated infection in breast prostheses.

14-point plan	Clinical recommendations
1.	Use intravenous antibiotic prophylaxis at the time of anaesthetic induction.
2.	Avoid periareolar incisions; these have been shown in both laboratory and clinical studies to lead to a higher rate of contracture as the pocket dissection is contaminated directly by bacteria within the breast tissue (Wiener, 2008, Bartsich et al., 2011, Wiener, 2012).
3.	Use nipple shields to prevent spillage of bacteria into the pocket (Wiener, 2008, Bartsich et al., 2011, Wixtrom et al., 2012).
4.	Perform careful atraumatic dissection to minimise devascularised tissue.
5.	Perform careful haemostasis.
6.	Avoid dissection into the breast parenchyma. The use of a dual-plane, subfascial pocket has anatomic advantages.
7.	Perform pocket irrigation with triple antibiotic solution or betadine (Adams Jr et al., 2000, Adams Jr et al., 2001, Adams Jr et al., 2006b).
8.	Use an introduction sleeve (Mladick, 1993). The use of a cut-off surgical glove to minimise skin contact.
9.	Use new instruments and drapes, and change surgical gloves prior to handling the implant.
10.	Minimise the time of implant opening.
11.	Minimise the repositioning and replacement of the implant.
12.	Use a layered closure.
13.	Avoid using a drainage tube, which can be a potential site of entry for bacteria.
14.	Use antibiotic prophylaxis to cover subsequent procedures that breach the skin or mucosa.

1.2.6. T-cell response to chronic biofilm infection around breast implants

Since the late 1970s, silicone breast implants have been suspected to be linked with systemic disease and malignancy (Angell, 1996, Brinton and Brown, 1997, Gabriel et al., 1997, Janowsky et al., 2000, de Jong et al., 2008). Although no health risk had been proven, the US FDA banned the use of silicone-filled breast implants in 1992, although saline-filled, silicone-covered implants remained on the market. In addition, CC and rupture are frequent events in silicone-filled implants, and interference with breast cancer detection may also be a problem (de Jong et al., 2008). There have been several cases of non-Hodgkin lymphoma (NHL) in women with breast implants reported (Cook et al., 1995, Duvic et al., 1995, Keech and Creech, 1997, Gaudet et al., 2002,

Kraemer et al., 2003, Sahoo et al., 2003, de Jong et al., 2008, Fritzsche et al., 2006, Newman et al., 2008, Roden et al., 2008, FDA, 2011, George et al., 2013, Taylor et al., 2013). Of these, the majority have been anaplastic large-cell lymphoma (ALCL).

Hu et al. (2015) investigated the possible link between bacterial biofilm and T-cell hyperplasia given reports of breast implant-associated ALCL (BIA-ALCL) (Cook et al., 1995, Duvic et al., 1995, Said et al., 1996, Keech and Creech, 1997, Gaudet et al., 2002, Kraemer et al., 2003, Sahoo et al., 2003, Fritzsche et al., 2006, de Jong et al., 2008, Newman et al., 2008, Roden et al., 2008, FDA, 2011, George et al., 2013, Taylor et al., 2013). They prospectively collected 57 capsules around textured implants from patients undergoing total capsulectomy and removal of implants for Baker grade IV contracture over a four year period. Human capsules, as well as explanted capsules around *S. epidermidis* infected implants from the *in vivo* pig model were subjected to qPCR to determine the number of lymphocytes, their cluster of differentiation (CD) status and the total number of bacteria (Hu et al., 2015). In the human capsules, they found significantly more T-cells (CD4, CD8a) compared with B-cells (CD79a). There was a significant linear correlation between the number of lymphocytes (CD3, CD4, CD8a, CD79a) and the number of bacteria per milligram of capsular tissue, with CD4 showing the most significant correlation ($r = 0.83$) with increasing bacterial numbers (Hu et al., 2015). Similarly, analysis of the lymphocytic infiltrate in the *in vivo* pig model showed breast implant capsules had a significant predominance of T-cells (CD3) compared with B-cells (CD79a). While analysis of lymphocytes on implants showed that textured implants had a significantly higher number of both T-cells and B-cells on their surface (8.23×10^5 lymphocytes/mg of implant) compared with smooth implants (1.3×10^4 lymphocytes/mg of implant), a 63-fold increase for textured implants (Hu et al., 2015). Like in the human data, the majority of the lymphocytes associated with the surface of implants contaminated with biofilm were T-cells (Hu et al., 2015).

1.3. Bacterial biofilm, breast implants and anaplastic large-cell lymphoma

The findings from animal and human studies that bacterial infection significantly potentiates CC (Virden et al., 1992, Ahn et al., 1996, Deva and Chang, 1999, Pajkos et al., 2003, Pittet et al., 2005, Tamboto et al., 2010, Chang and Lee, 2011, Codner et al., 2011, Silvestri et al., 2011, Jacombs et al., 2012, Rieger et al., 2013, Jacombs et al., 2014, Hu et al., 2015) has important implications for BIA-ALCL, a recently diagnosed disease. In 2016, the World Health Organisation recognised BIA-ALCL as a rare type of T-cell NHL that can develop in tissue around a breast implant (FDA, 2018). The association between breast implants and ALCL was first reported in 1997, where a patient developed an anaplastic T-cell lymphoma that was surface marker CD30 positive and occurred in proximity to a saline-filled breast implant (Keech and Creech, 1997). There are now over 500 cases reported worldwide and recent epidemiological analysis from both the US (Doren et al., 2017) and Australia and New Zealand (Knight et al., 2016, Loch-Wilkinson et al., 2017) have signalled a significant rise in the number of new cases. In Australia, there is a high incidence rate with the Australian Therapeutic Goods Administration (TGA) reporting 70 confirmed cases of BIA-ALCL, including four deaths (Loch-Wilkinson et al., 2017, TGA, 2018). The TGA estimates the risk of developing BIA-ALCL to be between 1:1 000 and 1:10 000 women with breast implants (Loch-Wilkinson et al., 2017, TGA, 2018). In the US, the FDA have received 359 medical device reports of BIA-ALCL, including nine deaths (Doren et al., 2017, FDA, 2018). While in Brazil, which has the second highest rate of breast augmentation surgery in the world, behind the US (ISAPS, 2018), there have been two reported cases (Gualco et al., 2009, Pastorello et al., 2018). However, the true incidence of BIA-ALCL is likely to be higher due to under reporting and the lack of awareness of this condition, and hence patient seroma fluid, late seroma being the most common clinical presentation, is not being sent for detailed pathological analysis.

Given the extreme rarity of BIA-ALCL, it remains unclear why a presumed aetiologic factor of chronic irritation or inflammation in the breast implant milieu results in ALCL. However,

a growing number of reported observations about BIA-ALCL point to an underlying biofilm infection as a potential cause (Baumgaertner et al., 2009, Bertoni et al., 2011, Jacombs et al., 2014, Hu et al., 2015, Loch-Wilkinson et al., 2017). It is hypothesised that subclinical infection of implant surfaces is common. Once a critical mass of the responsible organism is reached, bacterial antigens activate T-lymphocytes and trigger polyclonal proliferation. In some cases this will lead to monoclonal proliferation and, in a subset of those, the development of ALCL (Figure 1.3). This is in combination with host, implant and microbial factors, such as the patient's genetic background, immune response, the textured implant surface and bacterial phenotype (Loch-Wilkinson et al., 2017). Thus, ALCL arising in close proximity to breast implants appears to be a new, distinct entity with a multifactorial cause. This section will discuss the characteristics of BIA-ALCL and the growing evidence that bacterial biofilm has a significant role in malignancy.

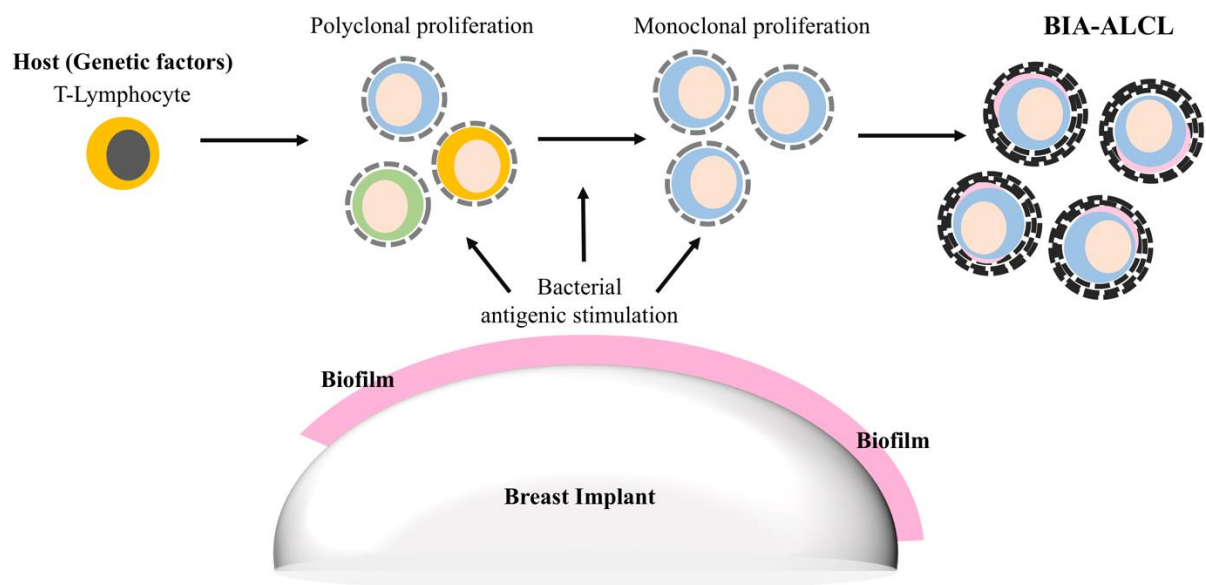


Figure 1.3. Unifying hypothesis of breast implant-associated anaplastic large-cell lymphoma.

The combination of factors including implant properties, bacterial infection, endogenous patient-specific factors and implant exposure time contribute to the transformation of inflammatory T-cells into malignant lymphoma in BIA-ALCL.

1.3.1. Clinical features and subforms of ALCL

ALCL was first described by Stein et al. (1985) as a rare T- or null-cell NHL characterised by large, anaplastic, lymphoid cells with strong, uniform expression of CD30, a 120 kD transmembrane cytokine receptor of the tumour necrosis factor receptor family (Smith et al., 1993). Indeed, T-cell lymphoma is a rare type of NHL in itself, representing approximately 12 to 15% of all NHL diagnosed in Western countries (Savage et al., 2004, Morton et al., 2006, Alexander et al., 2007) whilst ALCL constitutes less than 3% of all NHL diagnosed worldwide (Kellogg et al., 2014). Malignant lymphomas involving the breast is the least common type and may present as a primary or secondary tumour (Roden et al., 2008, Wong et al., 2008, Bishara et al., 2009). They comprise less than 0.5 to 1% of all breast malignancies and 0.7% of all NHL (FDA, 2011, Jewell et al., 2011, Lazzeri et al., 2011, Weathers et al., 2013) and 1.7% to 2.2% of extranodal lymphomas (Cohen and Brooks, 1991). Most lymphomas of the breast have a B-cell phenotype (90%) comprising the subtypes of marginal zone lymphoma, follicular lymphoma and diffuse large B-cell lymphoma (Roden et al., 2008, Wong et al., 2008, Bishara et al., 2009, Brody et al., 2010), with only rare cases of breast lymphoma showing the T-cell phenotype (10%) (Keech and Creech, 1997, Gaudet et al., 2002, Sahoo et al., 2003, Roden et al., 2008). In recent years, there has been an unexpectedly high frequency of ALCL cases of the T-cell phenotype reported in association with silicone-shelled breast implants, prompting the FDA to release an official advisory warning of the potential causal relationship between the two (FDA, 2011). However, the low incidence of BIA-ALCL continues to present a challenge to conducting meaningful epidemiologic studies, and thus the pathogenesis of T-cell lymphoma in the breast remains poorly understood.

ALCL has been clinically subdivided into a primary (*de novo*) and secondary form (anaplastic transformation from another lymphoma). Primary ALCL can present with systemic disease or disease limited to the skin in primary cutaneous-ALCL (Kempf, 2006, Swerdlow, 2008, Falini and Martelli, 2009). Systemic ALCL is an aggressive NHL typically presenting with

advanced-stage disease, systemic symptoms and frequent extranodal disease (Kempf, 2006, Swerdlow, 2008, Falini and Martelli, 2009). Systemic ALCL can be subdivided based on the tissue expression of the tyrosine kinase protein, anaplastic lymphoma kinase (ALK) into ALK-positive (ALK+) and ALK-negative (ALK-) phenotypes (Galkin et al., 2007). To address BIA-ALCL, Roden et al. (2008) proposed seroma-associated-ALCL, which shares morphologic features of both primary systemic ALK- ALCL and primary-ALCL but has no evidence of skin involvement and is distinct in its presentation, with localised late malignant seroma fluid occurring adjacent to breast implants and varied clinical progression (indolent to aggressive) (Roden et al., 2008).

Primary cutaneous-ALCL

Primary cutaneous-ALCL arises *de novo* in the skin and differs from the systemic form in its site of origin, its clinical features, and its absence of the ALK protein (ALK- ALCL) (Swerdlow, 2008, Falini and Martelli, 2009, Jewell et al., 2011, Talagas et al., 2014). This lymphoma affects older patients with a median age of approximately 60 years and accounts for approximately 9% of cutaneous lymphomas (Willemze et al., 1997, Diamantidis et al., 2009). The lesion typically presents as a solitary or localised, asymptomatic, cutaneous or subcutaneous reddish-violet tumour, with treatment usually including surgical excision with or without radiotherapy (Willemze et al., 1997, Diamantidis et al., 2009). Primary cutaneous-ALCL is associated with long-term survival and has a more favourable prognosis, with five year survival beyond 90% compared to systemic ALCL, which may secondarily involve the skin.

Secondary ALCL

Secondary neoplasms are usually ALK- (Pulford et al., 1997, Vergier et al., 1998) and may arise in the progression of other lymphomas, most commonly during the course of mycosis fungoides, peripheral T-cell lymphomas, Hodgkin disease, or lymphomatoid papulosis (Kinney and Jones, 2007). Such tumours mainly occur in older adults and have a poor prognosis, indicating that the

appearance of CD30 expression in a previously CD30- lymphoma (most frequently being primary-cutaneous T-cell lymphomas) is an unfavourable prognostic sign (Kinney and Jones, 2007).

ALK-positive ALCL

ALK+ ALCL, including systemic and secondary ALCL, frequently express ALK (t(2;5)(p23;q35) translocation), and are characterised by an aggressive clinical course (Fritzsche et al., 2006, Kempf, 2006, Rosen and Querfeld, 2006, Falini and Martelli, 2009, Ferreri et al., 2012). This lymphoma frequently presents as an aggressive stage III to IV disease, usually associated with systemic symptoms (75% of cases), and especially high fever (Falini et al., 1999). Extranodal involvement is frequent (60% of cases), with approximately 40% of patients showing two or more extranodal sites of the disease. The frequency of extranodal sites of lymphoma involvement include skin (21%), bone (solitary or multiple lesions) (17%), soft tissues (17%), lung (11%) and liver (8%), whilst involvement of the gut and central nervous system is rare (Falini et al., 1999). ALK+ disease is more common in younger patients and appears to benefit from chemotherapy more than ALK- forms of systemic ALCL. ALK+ also has a more favourable prognosis with five year survival rates of 70% to 90% in comparison with 40% to 60% for ALK- (Savage et al., 2008, Sibon et al., 2012).

ALK-negative ALCL

ALK- ALCL, including primary cutaneous- and seroma-associated-ALCL, are indolent malignancies that rarely carry the t(2;5) translocation (Bishara et al., 2009). Most cases of CD30+ ALK-, primary cutaneous- or seroma-associated-ALCL present as solitary or regional nodules and/or tumours showing ulceration, with extracutaneous or regional lymph node involvement seen in only 10% of patients (Bishara et al., 2009). ALK- systemic ALCL occurs in older individuals and is associated with a lower incidence of stage III to IV disease and extranodal involvement has been reported in one study (Falini et al., 1999). The preferred treatment for primary cutaneous- or seroma-associated-ALCL is localised radiation or surgical incision, with systemic chemotherapy reserved for cases with large tumour burden and extracutaneous involvement (Brody et al., 2010).

ALK- systemic ALCL is aggressive, with a five year overall survival rate of only 49%, compared with ALK+ ALCL (70%) and primary cutaneous-ALCL (90%) (Savage et al., 2008).

Other features reported in ALK- ALCL include a T-cell immunophenotype, cytotoxic phenotype activation (with expression of perforin, granzyme B and T-cell-restricted intracellular antigen-1 (TIA-1)), antigen-presentation antigens (e.g. CD25, human leukocyte antigen-antigen D related (HLA-DR), CD80, CD86, CD56), and transferrin receptor CD71 (Table 1.6) (Foss et al., 1996, Krenacs et al., 1997, Felgar et al., 1999, Kempf, 2006, de Jong et al., 2008, Lechner et al., 2011). T-cell neoplasms usually demonstrate monoclonal rearrangements of the T-cell receptor (TCR) genes, TCR γ and TCR β , but up to 10% of ALCL neoplasms also show rearrangement of the immunoglobulin heavy-chain gene (Alobeid et al., 2009, Lechner et al., 2012). Aberrant expression of cell-cycle genes and embryonic transcription factor Notch1 can contribute to malignant transformation in lymphoma, as well as overexpression of T-cell specific genes, T-cell acute lymphocytic leukaemia protein 1, homeobox protein HOX-11, lymphoblastic leukaemia-derived sequence 1 and LIM domain only 1/2 (Jundt et al., 2002, Ferrando and Look, 2003). Because of the very limited clinical follow-up available, the natural history of this disease remains unknown.

Breast implant associated-ALCL

ALCL arising in close proximity to breast implants is a recently recognised distinct clinical and pathological entity. Although the vast majority of primary breast lymphomas are of B-cell origin (Roden et al., 2008, Joks et al., 2011, George et al., 2013), the opposite is seen in BIA-ALCL. Where of the more than 31 reported cases of primary breast lymphoma in close proximity to breast implants, only three are of a B-cell phenotype and the remainder are overwhelmingly of a T-cell origin (Roden et al., 2008). It is the least common type of lymphoma involving the breast and is generally ALK-, occurring in the peri-prosthetic capsule (Swerdlow, 2008, Jewell et al., 2011, Talagas et al., 2014). In recent years, BIA-ALCL has garnered much attention given the rarity with which ALCL, especially ALK-, involves this anatomic site. Indeed primary lymphomas of the

Table 1.6. Summary of the immunophenotypic features of the different subforms of ALCL.

Subforms of ALCL	Immunophenotype	References
ALK-positive ALCL	CD30+, CD5+, Granzyme B, TIA-1. EMA positive CD2, CD3, CD7, CD4, CD8, CD20 and CD79a negative staining. EBV negative	Suzuki et al. (2000), Muzzafar et al. (2009), Cao et al. (2016)
Primary cutaneous-ALCL	ALK-, CD30+, CD4+, expression of cytotoxic proteins – Granzyme B, TIA-1, perforin. Antigen presentation antigens – CD25, HLA-DR. CD8+ T-cell phenotype and co-expression of CD56 and CD30 are extremely rare.	Foss et al. (1996), Krenacs et al. (1997), Felgar et al. (1999), Kempf (2006), de Jong et al. (2008), Roden et al. (2008), Diamantidis and Myrou (2011), Lechner et al. (2011), Clemens and Miranda (2015), Clemens et al. (2016)
BIA-ALCL	ALK-, CD30+, CD2+, CD3+, CD4+, CD43+, CD5+, CD7+, CD45+, TIA-1+, cytotoxic granules. Antigen presentation antigens – CD25, CD122, HLA-DR, CD80, CD86, CD56. Transferrin receptor CD71 EBV negative	Epstein and Kaplan (1979), Foss et al. (1996), Krenacs et al. (1997), Pawson et al. (1997), Felgar et al. (1999), Venard et al. (2000), Kempf (2006), de Jong et al. (2008), Roden et al. (2008), Lechner et al. (2011), Aladily et al. (2012), Lechner et al. (2012), Clemens and Miranda (2015), Clemens et al. (2016)

ALK, anaplastic lymphoma kinase; TIA-1, T-cell restricted intracellular antigen-1; HLA-DR, human leukocyte antigen-antigen D related; EBV, Epstein-Barr; EMA, epithelial membrane antigen.

breast occurs in less than 1% of all breast neoplasms (FDA, 2011, Jewell et al., 2011, Lazzeri et al., 2011, Weathers et al., 2013). The disease is characterised by abnormal growth of lymphocytes with a strong expression of CD30 that arises within the breast capsule. The clinical presentation of BIA-ALCL is commonly as a localised late peri-implant seroma containing malignant cells and less commonly as a tumour mass attached to the scar capsule with potential to metastasise, occurring an average of seven to ten years after implant placement but can range from 0.4 to 20 years (Stein et al., 2000, Thompson et al., 2010, Rupani et al., 2015, Loch-Wilkinson et al., 2017).

Most cases are indolent, with early stage disease curable by removal of the implant and capsulectomy surgery with local adjuvant chemotherapy and radiation therapy (five year disease-free survival rates of 55% to 65%) (Ryan et al., 2007, Jeanneret-Sozzi et al., 2008). Mass disease carries a worse prognosis with chemotherapy having limited effectiveness, 10% of cases present with metastasis and 5% of cases are fatal (Stein et al., 2000, Brody et al., 2010).

BIA-ALCL rarely occurs in the breast in the absence of breast implants, which suggests a possible aetiologic relationship between BIA-ALCL and breast implants. A case series by Brody et al. (2010) provided the first conclusive report that textured breast implants using the salt-loss method may pose an increased risk for BIA-ALCL. Of the 40 BIA-ALCL cases identified, all were classified as T-cell, anaplastic, primary, breast NHL, an exceedingly rare diagnosis (Brody et al., 2010). The average age of the patients was 44.7 years (range, 33 to 87 years) and the initial presentation was late peri-implant seroma, severe CC, or peri-capsular tumour mass, with an average time from implant of 5.8 years (range, one to 20 years) (Brody et al., 2010). The clinical course of the malignancy was typically benign. Treatment included capsulectomy, chemotherapy and/or radiotherapy, and all except for one patient remained disease free (Brody et al., 2010). Data on the type of implant was available for 25 of the 40 patients; of these, 23 shared a common salt-loss method of the textured shell with both silicone gel and saline-filled implants involved (Brody et al., 2010). Although previous reports have not conclusively shown an increased risk of primary breast NHL with silicone gel or saline-filled implants (de Jong et al., 2008), this case series arising from textured salt-loss breast implants found a subset of patients with an increased risk of malignancy (Brody et al., 2010).

In a recent report, Loch-Wilkinson and colleagues (2017) described 55 cases of BIA-ALCL in Australia and New Zealand (38 having cosmetic implants and 17 having reconstructive surgery). They identified five clusters of two to six cases throughout Australia. The mean age of patients was 47.1 years and the mean time of implant exposure was 7.46 years (Loch-Wilkinson et al., 2017).

Four deaths were reported related to mass and/or metastatic presentation. All patients were exposed to textured implants with 85% of cases associated with implants with a high surface area (Loch-Wilkinson et al., 2017).

Analysis of the effusion aspirate isolated from BIA-ALCL patients has shown aggressive cytological features similar to those of systemic ALCL. The effusion is composed of large, pleomorphic cells with hallmark horseshoe-shaped nuclei and immunophenotypically show positivity for CD30 and a range of immune markers, including T-cell markers, such as CD3, CD4, CD43, cytotoxic granules and antigen presentation molecules (Table 1.6) (Epstein and Kaplan, 1979, Pawson et al., 1997, Venard et al., 2000, Roden et al., 2008, Aladily et al., 2012). Moreover, like other T-cell neoplasms (Epstein and Kaplan, 1979, Pawson et al., 1997), BIA-ALCL show clonal TCR gene arrangement and/or the demonstration of phenotypic aberrancy, including CD4 and CD8 co-expression (Venard et al., 2000, Roden et al., 2008).

Structure and pathogenic role of the NPM-ALK gene

A subset of ALCL are associated with a 2;5 chromosomal translocation, which causes the nucleophosmin (NPM) gene located at 5q35 to fuse with a gene at 2p23 encoding the receptor tyrosine kinase ALK (Kempf, 2006, Rosen and Querfeld, 2006, Falini and Martelli, 2009, Ferreri et al., 2012). The NPM-ALK protein can form either homodimers, by cross-linking with other NPM-ALK molecules, or heterodimers, by cross-linking with wild-type NPM. The formation of homodimers results in the constitutive activation of the catalytic ALK domain contained in the NPM-ALK fusion protein (Drexler et al., 2000, Ferreri et al., 2012, Mussolin et al., 2013), and this activated ALK domain has been shown to bind growth factor receptor-bound protein 2 (Riera et al., 2010) and the Src homology 2 domains of phospholipase C- γ (Azarova et al., 2011). These interactions have been shown to induce mitogenic activity and are likely to be involved in neoplastic transformation (Hallberg and Palmer, 2013, Crescenzo et al., 2015). Further support for the oncogenic property of ALK fusion proteins have come from studies that have shown the NPM-

ALK fusion protein when transfected with murine hematopoietic cells can induce transplantable lymphoid tumours (Kuefer et al., 1997, Pearson et al., 2012, Hallberg and Palmer, 2013) and can also transform rat fibroblasts *in vitro* (Wellmann et al., 1997, Hallberg and Palmer, 2013).

1.3.2. The role of bacterial biofilm in breast implant associated-ALCL

The strongest support for the role of bacterial biofilm in BIA-ALCL was in a study by Hu et al. (2016), which provided the first evidence of the presence of bacterial biofilm in BIA-ALCL. The authors analysed 26 samples obtained from 22 BIA-ALCL patients, as well as three samples obtained from the contralateral normal breast capsule for the presence of biofilm. Non-tumour capsule samples from 62 patients undergoing revision surgery for high-grade CC collected over a five year period were also included for comparative analysis (Hu et al., 2016). The presence of bacterial contamination was determined using qPCR, the bacterial species involved by next-generation sequencing, and the presence of biofilm was visually confirmed using fluorescent *in situ* hybridisation and scanning electron microscopy (Hu et al., 2016). They found high mean numbers of bacteria in both the BIA-ALCL (4.7×10^6 bacteria/mg of tissue) and non-tumour capsule (4.9×10^6 bacteria/mg of tissue) samples. The three samples taken from the contralateral breast of BIA-ALCL patients yielded 7.6×10^5 bacteria/mg of tissue, which was significantly less than that detected in BIA-ALCL tissue (Hu et al., 2016). Analysis of the microbiome (bacterial community profile) in BIA-ALCL specimens showed a significantly greater proportion of Gram-negative *Ralstonia* spp. present in BIA-ALCL specimens compared with non-tumour capsule specimens, suggesting that different bacterial species may preferentially trigger lymphocyte activation (Hu et al., 2016). Interestingly, analysis of the capsules from the contralateral breast in BIA-ALCL patients showed a similar microbiome to that surrounding the tumour specimens but with significantly fewer bacteria. This is in line with the authors previous findings of a linear correlation between the number of activated lymphocytes and the number of bacteria (Hu et al.,

2015, Hu et al., 2016). The authors concluded that it is likely that the threshold for inflammation and/or lymphocyte proliferation is determined not only by the number of infecting biofilm bacteria but also by the species of infecting biofilm bacteria (Hu et al., 2016). In contrast, significantly more Gram-positive *Staphylococcus* spp. were found associated with non-tumour capsule specimens compared with BIA-ALCL specimens (Hu et al., 2016). Fluorescent *in situ* hybridisation and pyrosequencing confirmed the presence of *Ralstonia* spp. in five of ten BIA-ALCL samples analysed. Moreover, scanning electron microscopy demonstrated transformed lymphocytes and the presence of bacterial biofilm in all seven BIA-ALCL samples analysed (Hu et al., 2016).

The novel findings of *Ralstonia* spp. present in BIA-ALCL specimens is interesting. Although *Ralstonia* spp. are non-fermenting Gram-negative bacilli commonly found in soil and water (Ryan and Adley, 2013), they have been reported in nosocomial infections resulting from the contamination of medical solutions (Ryan and Adley, 2013, Wee et al., 2013, Ryan and Adley, 2014). Moreover, they are being increasingly recognised as a pathogen causing serious soft-tissue and implant-related infections (Ryan and Adley, 2013, Wee et al., 2013, Ryan and Adley, 2014). Thus, further studies are needed to elucidate the role of Gram-negative bacteria in BIA-ALCL to determine if they have a role in promoting malignancy. More importantly, the potential for Gram-negative bacteria to trigger lymphocyte proliferation and/or malignant transformation reinforces the need to develop and disseminate strategies to prevent bacterial infection of breast implants.

Bacterial infection in other lymphomas

The concept of chronic viral and bacterial infections promoting malignant transformation, resulting in other lymphomas is well established (Parsonnet et al., 1994, Ishitsuka and Tamura, 2014, Paydas, 2015, Vockerodt et al., 2015). *Helicobacter pylori*, a non-fermenting Gram-negative bacillus like *Ralstonia* spp., has been implicated in causing gastric lymphoma and produces a number of virulence factors, including flagella, lipopolysaccharide, vacuolating cytotoxin and cytotoxin-associated gene pathogenicity island that have relevance to lymphomagenesis (Parsonnet et al.,

1994, Yamaoka, 2010, Wang et al., 2013). Secondary to infection *H. pylori* targets different cellular proteins and thus modulates the host inflammatory response and initiate multiple insults, including oxidative stress and environmental toxins that interact together on the gastric mucosa, resulting in chronic gastritis and peptic ulceration (Wang et al., 2014a). Among the long-term consequences of *H. pylori* infection is gastric malignancies, particularly the progression of lymphoma from gastric mucosa-associated lymphoid tissue (MALT) (Wang et al., 2014a). More recently, virulence factors from *H. pylori*, such as the cytotoxin-associated gene A protein have been shown to deregulate intracellular signalling pathways and promote lymphomagenesis (Wang et al., 2013).

Therefore, the reported observations about BIA-ALCL that point to an underlying biofilm infection as a potential cause, the microbiome of BIA-ALCL specimens containing significantly more Gram-negative bacteria than the microbiome surrounding non-tumour capsule specimens (Hu et al., 2016), and the known association between *H. pylori* infection and MALT gastric lymphoma establishes a pathway from bacterial infection, inflammation and subsequent lymphomagenesis.

1.3.3. Immune environment in breast implant associated-ALCL

The exact aetiology and pathogenesis of BIA-ALCL remains unknown. In particular, why BIA-ALCL is a T-cell derived cancer, since lymphomas of the breast arising from *H. pylori* infection are of B-cell origin (Kuo and Cheng, 2013). Interestingly, CD4⁺ T-cells have the highest correlation ($r = 0.83$) (Hu et al., 2015) and are the predominant phenotype of tumour cells in BIA-ALCL (Lechner et al., 2011, Lechner et al., 2012). Thus, the underlying mechanism could be a sustained T-cell immune response related to chronic bacterial antigen stimulation coating breast implants and the CD4⁺ T-cells undergo malignant transformation, which lead to the development of BIA-ALCL.

Multifactorial pathway to malignancy

The development of BIA-ALCL is likely to be a complex process resulting from an interplay of host, implant and microbial factors, including the patient's genetic background, immune response, the textured implant surface, and bacterial phenotype that lead to neoplastic lymphoid tissue progression. This could account for why some patients with biofilm infection around breast implants proceed to contracture and why others, although less common, proceed to lymphocytic hyperplasia and BIA-ALCL (Hu et al., 2016). Age-related immune changes may play a role in the genesis of BIA-ALCL. In Hu et al. (2016), the mean age of BIA-ALCL presentation was 52.7 years (range, 29 to 77 years), which was older than the mean age of patients with non-tumour capsules but comparable to previous studies (Gidengil et al., 2015, Rupani et al., 2015).

It is also important to note that 30% of women with BIA-ALCL develop this malignancy following breast implant reconstruction for breast cancer, pointing to a possible additional genetic risk for carcinogenesis (Loch-Wilkinson et al., 2017). It has been proposed that genetic instability might be pivotal to the pathogenesis of BIA-ALCL, especially in susceptible individuals (George et al., 2013). Indeed, consistent with the development of other malignancies, such as CD30+ primary cutaneous-ALCL, it is likely that there are earlier benign precursors to BIA-ALCL on the pathway to malignant transformation (Kadin et al., 2016). BIA-ALCL shares some similarities with primary cutaneous-ALCL, including anaplastic morphology, CD30+, HLA-DR+, TIA-1+, ALK-immunophenotype, usual absence of clinical symptoms, localised lesions in most cases, infrequent spread to regional lymph nodes, and excellent prognosis (Table 1.6) (Foss et al., 1996, Krenacs et al., 1997, Felgar et al., 1999, Kempf, 2006, de Jong et al., 2008, Roden et al., 2008, Lechner et al., 2011, Clemens and Miranda, 2015, Clemens et al., 2016). In some patients, primary cutaneous-ALCL is preceded by lymphomatoid papulosis (LyP), which is characterised by spontaneously regressing skin lesions (Kempf et al., 2011). Progression of lymphomatoid papulosis to primary cutaneous-ALCL, which are clonally related (Chott et al., 1996), is associated with accumulating

genetic abnormalities resulting in activation of signal transducer and activator of transcription 3 (STAT3) and suppressor of cytokine signaling 3 (SOCS3), among other transcription factors characteristic of ALCL (Ehrentraut et al., 2013). Thus, given the similarities in the gene expression pattern of BIA-ALCL and primary cutaneous-ALCL cell lines, the identification of genetic events during progression of LyP to primary cutaneous-ALCL may provide clues to the pathogenesis of BIA-ALCL (Kadin et al., 2016).

Peri-prosthetic inflammation

Chronic inflammation is considered to be a precursor of many cancers (Talmadge et al., 2007) and is hypothesised to initiate BIA-ALCL (Figure 1.3). In BIA-ALCL specimens, the interleukin (IL)-6 signalling pathway, a primary regulator of both acute and chronic inflammation has been detected and histological examination of excised peri-prosthetic capsule tissues showed chronic inflammation, including fibrosis, plasma cell hyperplasia and lymphocyte infiltrates (Lechner et al., 2012). In contracted specimens, phenotypic analysis of the intra-capsular T-cells has shown the presence of CD4 and CD8 T-cells, with a predominance of the T-helper (Th) cell type 1 phenotype (Wolfram et al., 2012). Moreover, the cytokine profile of intra-capsular T-cells were IL-6, IL-8, IL-17, interferon-gamma (IFN- γ), IL-1 beta (IL-1 β), tumour necrosis factor-alpha (TNF- α) and transforming growth factor-beta 1 (TGF- β 1), which corresponds to a Th1/Th17-weighted local immune response in peri-implants with capsular fibrosis (Wolfram et al., 2012).

Th17 cells represent a more recently discovered subset of CD4 T-effector cells, identified by their ability to produce IL-17A, IL-17F, TNF and IL-22 (Figure 1.4) (Yao et al., 1995, Yang et al., 2008, Crome et al., 2010). Stimulation of Th17 differentiation by IL-6 and TGF- β 1, a profibrotic cytokine, places them in close association to T-regulatory (Treg) cells, as TGF- β 1 also induces the differentiation of naïve T-cells into Treg cells (Awasthi et al., 2008, Korn et al., 2009, Erdman et al., 2010, Passos et al., 2010). Treg cells are essential for maintaining peripheral tolerance because they can suppress activation and effector functions of autoreactive T-cells (Figure 1.4) (Jonuleit et

al., 2001, Pfoertner et al., 2006, Chowdary Venigalla et al., 2008, Wilczynski et al., 2008, Suen et al., 2009). A number of studies have now established that subclinical (biofilm) infection on the surface of breast implants is the principal pathogenic pathway to peri-prosthetic inflammation and contracture (Ahn et al., 1996, Deva and Chang, 1999, Pajkos et al., 2003, Adams Jr, 2009, Vasilev et al., 2009, Tamboto et al., 2010). During an inflammatory response, IL-6 is produced, which inhibits the generation of Treg cells in the periphery and induces the development of Th17 cells from naïve CD4 T-cells. In cases of subclinical infection, the immune system is also activated, therefore, Treg cell generation in the periphery is suppressed. In concert with IL-17 and IFN- γ , both responsible for the Th1/Th17-weighted immune response (Figure 1.4), IL-6 and IL-8 were the most prominent cytokines in the supernatant of the intra-capsular T-cells (Wolfram et al., 2012).

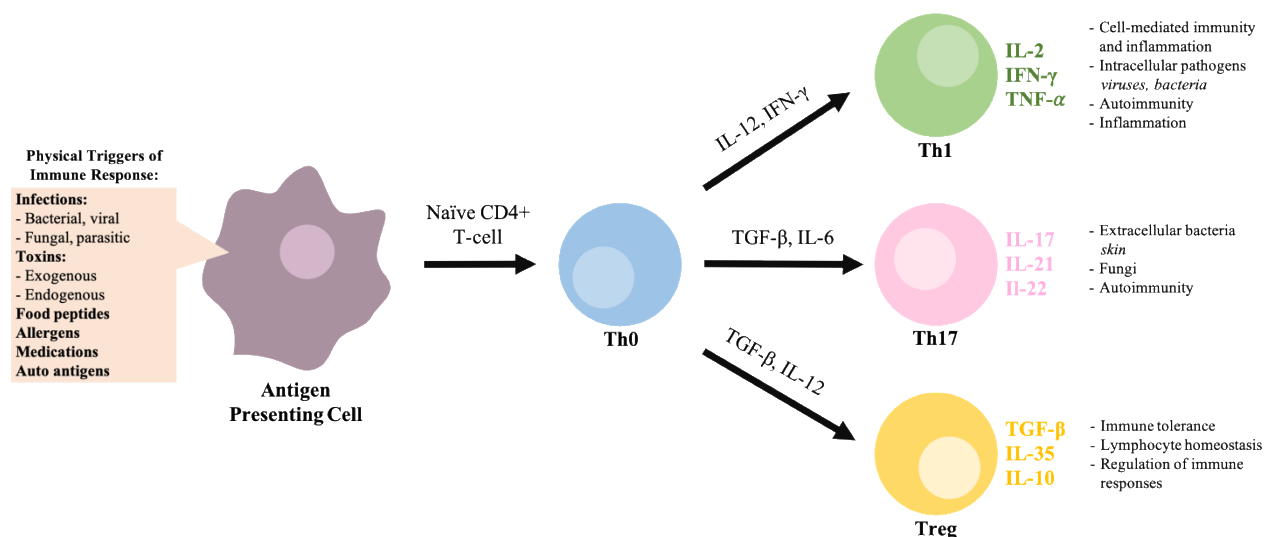


Figure 1.4. Differentiation of T-cell subsets.

Upon activation by antigen-presenting cells, naïve CD4+ T-cells can be polarised into different effector T-cell subsets: Th1, Th17 or Treg cells directed by the local inflammatory milieu. IL-2 induce Th1 cell polarisation characterised by the production of IL-2, IFN- γ and TNF- α , which are involved in cell-mediated immunity against intracellular viruses and bacteria. The combination of TGF- β and proinflammatory cytokines including IL-6, drives polarisation into IL-17-producing Th17 cells. Th17 cells play a critical role in host protection against extracellular pathogens and in inflammatory autoimmune diseases. In addition, TGF- β can induce Treg cell polarisation, which produce TGF- β and IL-10 and act as modulators of immune responses. Th, T-helper; Treg, T-regulatory; IL, interleukin; IFN- γ , interferon-gamma; TNF- α , tumour necrosis factor-alpha.

Thus, these results strongly argue for an antigen-driven T-cell proliferation within the contracted capsule tissue. BIA-ALCL could be potentially associated with prolonged inflammatory states, similar to the theoretical pathogenesis of CC. It is likely that possible triggers of BIA-ALCL, including textured breast implants and bacterial antigens, produce a specific antigen-driven local immune response of activated Th1/Th17 cells with subsequent fibrosis promoted by production of pro-fibrotic cytokines. Furthermore, there are likely to be two pathways of inflammation dependent on the bacteria. In Gram-positive bacteria, a pathway toward inflammation and fibrosis leading to contracture; while in Gram-negative bacteria (e.g. *Ralstonia* spp.), a pathway toward lymphocyte stimulation and/or malignant transformation (Hu et al., 2016). Thus, more studies on the relationship between bacterial biofilm, lymphocytes, and the local breast environment are needed to elucidate the possible pathways from bacterial biofilm infection to the development of BIA-ALCL.

T-cell infiltrate in breast implant associated-ALCL

Three CD30+, ALK-, IL-2-dependent T-cell BIA-ALCL cell lines, T-cell breast lymphoma (TLBR)-1, -2, -3, from patients' primary tumour biopsies with textured (salt-loss produced) breast implants have recently been established (Lechner et al., 2011, Lechner et al., 2012). Morphologic and cytogenetic studies confirmed the ALK- T-cell lymphoma classification of the BIA-ALCL TLBR cell lines with the absence of the NPM-ALK (2;5) translocation (Lechner et al., 2011, Lechner et al., 2012). In addition, characterisation of the phenotype and functional features of these tumours to identify mechanisms of cell survival and potential therapeutic targets showed strong positivity for CD30, CD71, T-cell CD2, CD5, CD7, and antigen presentation markers (HLA-DR, CD80, CD86), and IL-2 (CD25, CD122) and IL-6 receptors (Table 1.6) (Lechner et al., 2011, Lechner et al., 2012). While functional studies of the TLBR cell lines identified high production of T-cell-associated cytokines, IL-6 and IL-10 along with IFN- γ and TNF- α , and strong activation of the Janus kinase (JAK)/STAT3 signalling pathways likely related to autocrine production of IL-6,

which promotes tumour cell survival and decreased protein tyrosine phosphatase, non-receptor type 6 (SHP-1) (Lechner et al., 2011, Lechner et al., 2012). As well as strong expression of transcription factors associated with Th1 cells whose main transcription factor is T-bet (a T-box transcription factor) and signature cytokine is IFN- γ (Kadin et al., 2016), and Treg cell lineages (Lechner et al., 2011, Lechner et al., 2012). Inhibition of STAT3, either directly or by recovery of SHP-1, and chemotherapy reagents consisting of cyclophosphamide, adriamycin, vincristine, prednisone, were shown to effectively kill cells of all three TLBR cell lines *in vitro*, and hence may be pursued as therapies for patients with BIA-ALCL (Lechner et al., 2011, Lechner et al., 2012). Moreover, TLBR-2 and TLBR-3 cell lines were found to have a Treg-like suppressive function manifested by transcription factor forkhead box P3 and secretion of suppressive cytokines, IL-10 and TGF- β (Lechner et al., 2012). This suggests that BIA-ALCL is capable of suppressing the local immune response.

It is postulated that a milieu rich in immune stimulatory cytokines which promotes rapid division of host lymphocytes may cause the initial tumorigenic changes that lead to BIA-ALCL in some patients. Autocrine production of IL-6 has been identified as a driver of tumorigenesis in some diffuse large B-cell lymphomas, as well as solid tumours, including breast, lung and ovarian carcinomas (Grivennikov and Karin, 2008, Lam et al., 2008, Scuto et al., 2011). The cytokine profile of BIA-ALCL cell lines, specifically IL-6, TGF- β and IL-10, has also been shown to induce immune suppressor cell populations (Treg and myeloid-derived suppressor cells), which may inhibit host anti-tumour immunity and facilitate cancer development (Lechner et al., 2010, Stewart and Smyth, 2011). Texturing of the breast implant surface shell is one of the recurring features in BIA-ALCL cases, and promotes higher numbers of bacteria, with more aggressive texture having more bacteria (Jacombs et al., 2014, Hu et al., 2015). Whether this inflammatory stimulus is increased in textured implants and may play a role in the development of BIA-ALCL requires

further investigation. Regardless, the prominent role of IL-6 found in the TLBR cell lines suggests that immune reactions are important to the progression of this disease.

Activated Notch1 was also found to be overexpressed in the TLBR cell lines. Interestingly the highest levels were observed in TLBR-2 cell line, derived from a treatment-resistant, fatal case of BIA-ALCL (Lechner et al., 2012). Thus, Notch1 activation may be a marker of more aggressive diseases, and studies to evaluate Notch1 levels in tumour specimens from patients with BIA-ALCL may be used as a potential therapeutic target for primary breast lymphomas as well as other T-cell ALCL.

In a separate study characterising the transcription factor and cytokine profiles of tumour cells and surrounding lymphocytes in BIA-ALCL and primary cutaneous-ALCL cell lines, Kadin et al. (2016) found a common expression of transcription factors, SOCS3, JunB, SATB Homeobox 1 (SATB1), and a cytokine profile suggestive of a Th1 phenotype. SOCS proteins inhibit cytokine signalling, and in Hodgkin lymphoma SOCS3 is expressed at relatively low levels and is characterised by numerous tumour-derived cytokines and abundant inflammatory cells (Skinnider and Mak, 2002). Kadin et al. (2016) suggest the high expression of SOCS3 by BIA-ALCL tumour cells could explain the lower inflammatory cells and usual absence of clinical symptoms of BIA-ALCL patients. Similarly, JunB nuclear activity is increased in BIA-ALCL and primary-ALCL cell lines and clinical samples (Kadin et al., 2016). JunB is a transcription factor involved in regulating gene activity following the primary growth factor response (Watanabe et al., 2005). Overexpression of JunB is associated with neoplastic transformation, with high levels of JunB and CD30 a hallmark of malignant cells in Hodgkin lymphoma and ALK+ ALCL (Mathas et al., 2002). Because JunB regulates the CD30 promoter (Watanabe et al., 2005), silencing JunB leads to decreased CD30 activity and suppresses ALCL growth (Kadin et al., 2016). Moreover, JunB is also expressed in LyP. This is consistent with a role of JunB in the progression of LyP to ALCL (Mao et al., 2003). Thus, the high levels of JunB in BIA-ALCL is consistent with malignant

transformation. SATB1 is a thymocyte specific chromatin organiser that is overexpressed in lymphoma cells in CD30+ cutaneous lymphoproliferative disorder, with its expression up-regulated during disease progression (Wang et al., 2014b). SATB1 promotes proliferation of CD30+ lymphoma cells by direct transcriptional repression of cell cycle inhibitor p21 (Kadin et al., 2016). SATB1 is overexpressed in LyP and is also expressed by BIA-ALCL tumour cells. However, its role in progression from activated T-cells to BIA-ALCL remains unclear.

Th1/Th17 phenotype of breast implant associated-ALCL tumour cells

The findings from contracted specimens that the cytokine profile of the intra-capsular T-cells correspond to a Th1/Th17-weighted local immune response (Figure 1.4) suggest a similar phenotype may also exist in BIA-ALCL tumour cells. Naïve T-cells which polarise towards Th17 have a high capacity for self-renewal and persistence. In contrast, Th1 cells have a relatively limited capacity for self-renewal and typically undergo senescence, which could explain the typical slow development of BIA-ALCL (Muranski et al., 2011, Clemens and Miranda, 2015, Clemens et al., 2016). Th17 cells can polarise towards Th1 cells with intermediate Th17/Th1-like cells observed. If antigen activated T-cell precursors of BIA-ALCL cells mimic polarisation and maturation of non-malignant Th memory T-cells, their phenotype may determine the time required to initiate BIA-ALCL, that is, a longer time for Th1 polarised cells than for Th17 cells (Muranski et al., 2011). The observation that BIA-ALCL onset occurs an average of seven to ten years after initial implantation (Stein et al., 2000, Thompson et al., 2010, Rupani et al., 2015) is consistent with these findings.

H. pylori infection has been shown to initiate and contribute to the progression of a B-cell lymphoma from gastric MALT (Wang et al., 2013). Increasing evidence shows that eradication of *H. pylori* with antibiotic therapy can lead to regression of gastric MALT lymphoma and can result in a ten year sustained remission (Wündisch et al., 2012). The similarities between BIA-ALCL and primary cutaneous-ALCL support the hypothesis that bacterial antigens are linked to the

pathogenesis of BIA-ALCL. Staphylococcal superantigen endotoxins colonising the skin and nares have been implicated in the pathogenesis of cutaneous T-cell lymphomas (Willerslev-Olsen et al., 2016). Eradication of staphylococci from the skin with antibiotic treatment was associated with clinical improvement (Talpur et al., 2008). Superantigens of *S. aureus* are particularly efficient in stimulating IL-17 production and the cytokines produced are from memory T-cells (Islander et al., 2010). Studies on malignant T-cell lines established from patients with cutaneous T-cell lymphoma have found that these cells spontaneously secrete IL-17F (Krejsgaard et al., 2013). However, it has been shown that inhibitors of JAK and STAT3 are able to block this secretion (Lechner et al., 2012), which suggests that IL-17 cytokines and their receptors may serve as therapeutic targets for BIA-ALCL. Figure 1.5 summarises the hypothesis for the progression of immune responding T-lymphocytes to BIA-ALCL (Kadin et al., 2016).

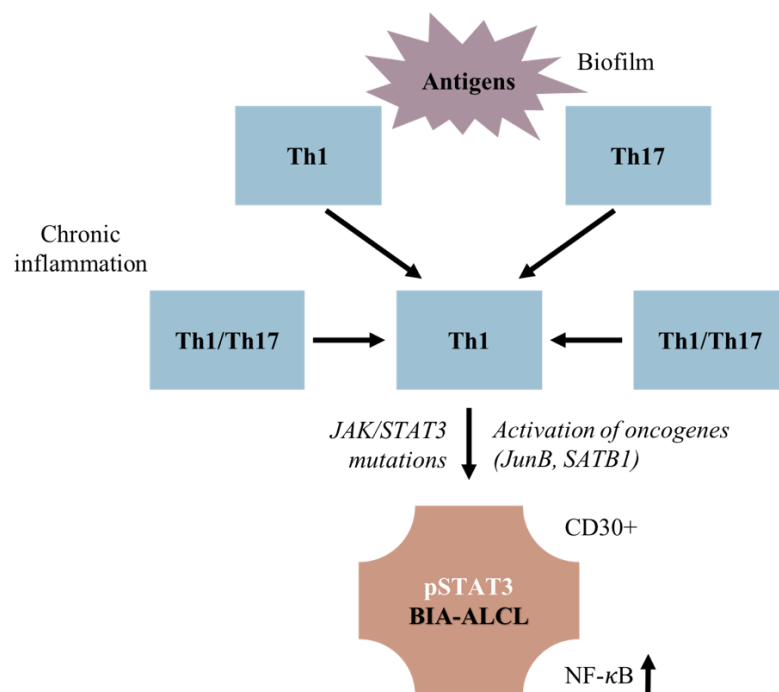


Figure 1.5. Hypothesis for progression of immune responding T-lymphocytes to BIA-ALCL.

BIA-ALCL cells may be derived from Th1/Th17 cells (antigen driven memory T-cells) in capsular tissues and surrounding seromas. This is consistent with the hypothesis that BIA-ALCL results from chronic bacterial antigen stimulation, sustained T-cell proliferation, and subsequent genetic events. Further studies are needed to determine whether select biomarkers (JunB, SATB1) will identify non-malignant precursors to BIA-ALCL.

1.4. Bacterial biofilms

A biofilm is a community of microorganisms that can attach to each other and/or to a surface (living and non-living) because of a self-produced extracellular protective and adhesive matrix of a polymeric substance (EPS) (Hall-Stoodley et al., 2004). Within this glycoprotein matrix, a number of survival advantages are conferred upon the bacteria, including an inherent tolerance and resistance to antimicrobial therapies, and protection against host immune defences (Mah and O'Toole, 2001, Matz and Kjelleberg, 2005, Anderson and O'toole, 2008, Deva et al., 2013).

In recent years, they have received a lot of attention in human medicine due to the number of post-operative surgical site infections occurring after implantation of medical devices, which in up to 80% of cases may contain biofilms (Veerachamy et al., 2014). Bacteria can colonise the surfaces of both tissues and implantable medical devices, including orthopaedic implants, joint prostheses, prosthetic valves, cardiac pacemakers, intravenous and urinary catheters, peritoneal dialysis catheters, endoscopes, in dermatological situations such as dermal fillers and cheek implants, and pertinent to this thesis, breast implants (Darouiche, 1998, Parsek and Singh, 2003, Parsek and Fuqua, 2004, Deva et al., 2013, Veerachamy et al., 2014).

The biological behaviour of medical implants, such as tissue integration and antibacterial activity, essentially depends on both the chemical composition and the morphology of their surface. For a successful implant, tissue integration should occur prior to significant bacterial adhesion, thereby preventing bacterial colonisation of the implant. The factors influencing bacterial attachment and subsequent biofilm formation on an implant surface include chemical composition of the material, surface charge, hydrophobicity, surface roughness or physical configuration (Katsikogianni and Missirlis, 2004, Crawford et al., 2012, Ribeiro et al., 2012). Biofilm infections on the surface of implantable medical devices constitute a number of clinical challenges, including serious illness, disease, chronic inflammation, impaired wound healing, rapidly acquired antibiotic

resistance, tissue destruction, systemic dissemination of the pathogen, dysfunction of the device, and in some cases even death (Hall-Stoodley et al., 2004, Veerachamy et al., 2014). Implant-related infections occur despite many preventative measures and intervention with antibiotics are often ineffective due to their poor penetration through the biofilm matrix. In cases where the infection is not treatable using conventional antibiotic treatment, the most effective means of treatment and often the only feasible solution, is to remove the infected medical device. Therefore, novel approaches in the surface treatment of implantable medical devices by various physical and chemical techniques are emerging to improve their surface properties so as to facilitate bio-integration and prevent bacterial adhesion and subsequent biofilm formation.

1.4.1 Process of biofilm formation

The introduction of an implant into the body is invariably associated with the risk of microbial infection. Sources of infectious bacteria include the surgical theatre, surgical equipment, contaminated disinfectants, resident bacteria on the patient's skin and bacteria residing in the patient's body, e.g. *S. epidermidis*, part of the skin microflora and breast endogenous flora (Ribeiro et al., 2012). It has been reported that many bacteria can cause implant-related infections, including *S. aureus*, methicillin-resistant *S. aureus*, *S. epidermidis*, *P. acnes*, *Pseudomonas aeruginosa*, *Haemophilus influenzae*, *Providencia*, *Enterococcus faecalis*, *Streptococcus viridans*, *E. coli*, *Lactobacillus*, *Acinetobacter*, *Serratia marcescens*, *K. pneumoniae*, *Corynebacterium* and *P. mirabilis* (Donlan and Costerton, 2002, Veerachamy et al., 2014, Franci et al., 2015).

Most bacterial species in nature exist in two different forms, a planktonic or free-floating form and a sessile biofilm form. The formation of bacterial biofilms begins with planktonic cells adhering to the implant surface. Upon strong adhesion, the bacterium begins to secrete and collect proteins, polysaccharides and deoxyribonucleic acid (DNA) to formulate a biofilm (Donlan and Costerton, 2002, Francolini and Donelli, 2010). The process occurs in four stages, (i) reversible

attachment, (ii) irreversible attachment, (iii) growth and differentiation, and (iv) dissemination (Figure 1.6), and each stage is regulated by a number of specific genes (Parsek and Singh, 2003, Hall-Stoodley et al., 2004, Francolini and Donelli, 2010, Deva et al., 2013, Veerachamy et al., 2014).

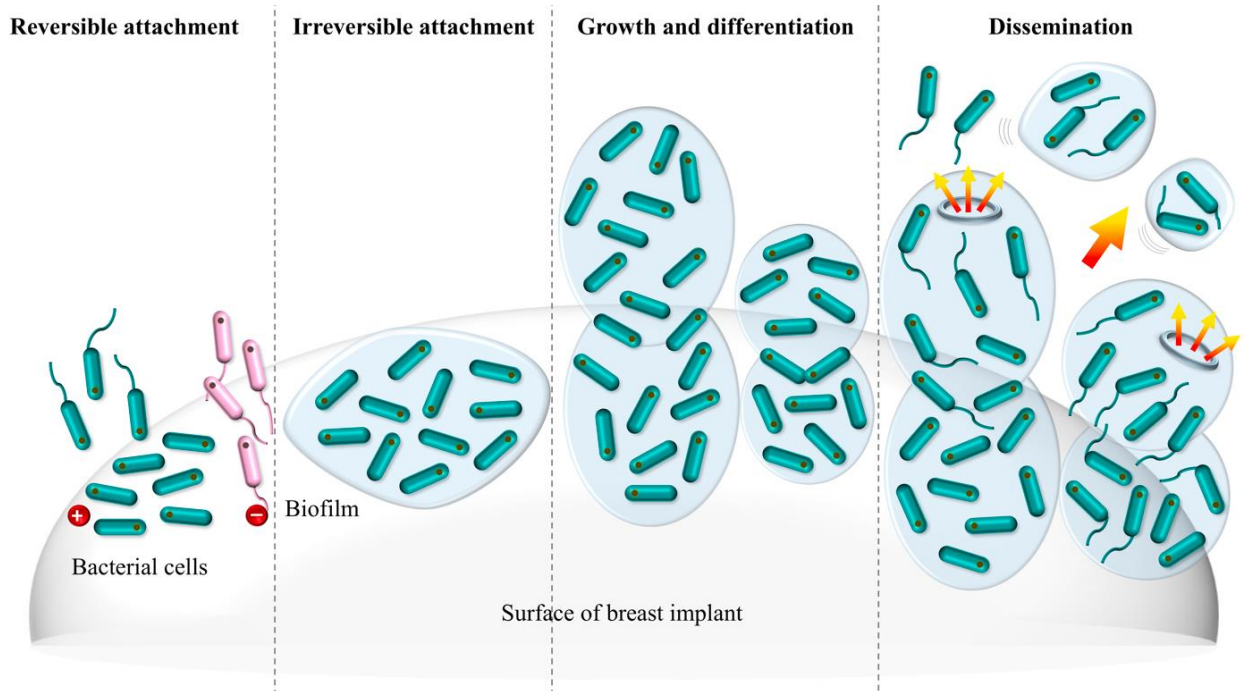


Figure 1.6. The stages of the biofilm life cycle.

Reversible attachment: planktonic (free-floating) bacteria adhere to the surface of the breast implant. Irreversible attachment: bacterial cells aggregate, form microcolonies and excrete extracellular polymeric substances. The attachment becomes irreversible and a biofilm is formed. Growth and differentiation: three-dimensional growth and further maturation of the biofilm occurs, providing protection against host defence mechanisms and antibiotics. Dissemination: the biofilm reaches a critical mass and disperses planktonic bacteria, ready to colonise other surfaces.

Reversible and irreversible attachment

Bacterial attachment to human tissue and implanted medical device surfaces is an important step in the pathogenesis of infection, whereby the bacteria can divide and colonise the surface (Puckett et al., 2010, Hori and Matsumoto, 2010, Costa et al., 2011). Bacteria move to the material surface through physical forces, such as Brownian movement, Van der Waals attraction forces, gravitational forces, surface electrostatic charges and hydrophobic interactions (Cerca et al., 2005,

Harris and Richards, 2006). Chemotaxis is also involved in this process occurring in almost all microbes, which modulate their growth on the surface by regulating cellular adhesion components and preparing the cells for cell to cell and cell to surface interactions (Cerca et al., 2005, Harris and Richards, 2006).

When planktonic bacteria initially attach to a surface they are reversibly bound and are susceptible to antibiotic treatment, gentle rinsing or changes in conditions. The rate and extent of bacterial attachment is dependent not only on the properties of the bacteria, but of the material surface and the immediate surroundings. Generally, attachment is more likely on surfaces that are hydrophobic, rougher or coated by a conditioning film (Pasmore et al., 2001, Simoes et al., 2010). Once in contact, the interactions with the implant surface are then reinforced by host and tissue-specific adhesions and ultimately result in the irreversible attachment of the planktonic cells. The bacteria then undergo a phenotypic switch from planktonic to the biofilm state. The extracellular polymeric slime (EPS) is produced at this stage and comprises of polysaccharides, proteins, lipids and extracellular DNA. EPS is responsible for the binding and cell adhesion to the surface, stabilising the biofilm architecture (Costerton et al., 1999, Sutherland, 2001, Donlan and Costerton, 2002, Allison, 2003, Flemming and Wingender, 2010).

Different organisms adopt different mechanisms for the formation and stabilisation of the biofilm. For example, in Gram-negative bacteria, *P. aeruginosa* makes biofilm by producing three distinct exopolysaccharides: alginate, Pel and Psl (Ryder et al., 2007, Tart and Wozniak, 2008, Colvin et al., 2012). In Gram-positive bacteria, *S. aureus* use a polysaccharide intercellular adhesin (PIA) to form biofilms (O'Gara, 2007, Rohde et al., 2010). This polymer is synthesised by the *ica* operon, which is not carried by all strains of *S. aureus*. However, deletion of the operon in strains that do carry it does not impair their ability to make biofilm due to an *ica*-independent mechanism (O'Gara, 2007, Otto, 2008). This alternative mechanism relies on the ability of *S. aureus* to express a variety of adhesion proteins, which enable cells to attach and colonise a large number of different surfaces

(Lasa and Penadés, 2006, Rohde et al., 2010). *S. aureus* and *S. epidermidis* extracellular matrices harbour biofilm-associated proteins (Bap) that are required for biofilm formation (Lasa and Penadés, 2006, Sugimoto et al., 2013). These proteins are found anchored to their cell wall and serve to hold cells together within the biofilm, likely by interacting with other proteins on the surface of neighbouring cells. *P. aeruginosa* also has many surface proteins that contribute to biofilm formation. These include matrix-associated lectin-binding proteins, Lec A and Lec B, which recognise and bind carbohydrate moieties that facilitate cell to matrix or cell to cell interactions within the biofilm (Tielker et al., 2005, Flemming and Wingender, 2010). *P. aeruginosa* and *S. aureus* biofilms also contain extracellular DNA in their matrix, which provides structural integrity to the biofilm (Whitchurch et al., 2002, Rice et al., 2009, Flemming and Wingender, 2010). Thus, the variation between matrices of different bacterial species is one of the reasons why biofilm control remains a challenge.

Growth and differentiation

In the growth stage, bacterial cells aggregate to form stable microcolonies, whereby either the organism multiplies without releasing progeny cells or primary colonisers recruit and co-aggregate members of the same or different species onto the implant surface (Allison, 2003). Microcolonies further develop into macrocolonies and are enclosed by EPS. EPS confers a number of survival advantages upon the bacteria. It helps in the colonisation of the implant surface, storage of nutrients, protection against phagocytosis, interference with the cellular immune response and decreasing antibiotic susceptibility by providing a relative buffer against diffusion of antibiotics (Mah and O'Toole, 2001, Jefferson, 2004, Moscoso et al., 2006, Flemming and Wingender, 2010, López et al., 2010). Other advantages include cooperative metabolism based on complex intercellular signalling (Williams and Cámara, 2009) and the ability to use horizontal gene transfer to protect against unexpected environmental challenges (Del Pozo and Patel, 2007, Ehrlich et al.,

2010). Bacterial persister cells, which are metabolically inactive and highly resistant to anti-infective agents, have been shown to exist within mature biofilms (Lewis, 2010).

As the biofilm continues to grow, it becomes highly differentiated and complex. The microenvironment within the biofilm is also heterogeneous, with significant variation in pH, oxygen concentration, nutrient availability and cell density (von Ohle et al., 2010). Thus, the wide heterogeneity in metabolic activity among cells in different locations within the colony, make it difficult to target the entire biofilm with one type of therapy (Fux et al., 2004, Chambless and Stewart, 2007, Pamp et al., 2008).

Over time, the biofilm reaches a critical mass and generates planktonic bacteria. These free-floating organisms escape the biofilm and colonise on other surfaces. The planktonic cells become inactive or die due to the lack of nutrients, decrease in pH or accumulation of toxic metabolic by-products (Tunney et al., 2007). In this stage, matured biofilm is formed and the planktonic cells are ready for the disruption from the surface.

Biofilm dissemination

In the dissemination stage, planktonic cells detach from biofilm to colonise new surfaces. As with the other stages, a number of environmental signals, bacterial signal transduction pathways and their effectors are involved in the detachment process (Guilhen et al., 2017). The release of planktonic cells facilitates bacterial survival and disease transmission (Smith and Iglewski, 2003, Karatan and Watnick, 2009).

1.4.2. Signalling in biofilm formation

Bacteria within biofilm can produce and secrete signal or autoinducer molecules. Autoinducers accumulate extracellularly and their concentration is correlated with the bacterial population density. At high concentrations, autoinducers trigger signal transduction cascades that lead to multicellular responses between cells of either the same or different species, benefitting the

population and the biofilm as a whole. This mechanism of cell to cell communication is known as quorum sensing (QS). QS controls a large number of developmental processes including those related to biofilm infection (Camilli and Bassler, 2006, Rutherford and Bassler, 2012).

Microorganisms use QS to coordinate their communal behaviour, such as surface attachment, biofilm formation, motility, EPS production, the detachment or the release of planktonic cells and the expression of virulence factors (Rutherford and Bassler, 2012, Kalia, 2013). Both Gram-positive and Gram-negative bacteria have QS systems. In *P. aeruginosa* and other Gram-negative bacteria, QS systems respond to acylated homoserine lactone (AHL) autoinducers. *P. aeruginosa* has two AHL QS systems, *las* and *rhl*, and each system has its own AHL synthase (LasI and RhlI) and its own transcriptional regulator (LasR and RhlR) (De Kievit, 2009). The role of these systems in biofilm formation varies between strains (Stapper et al., 2004, De Kievit, 2009). For example, in *P. aeruginosa* PAO1, both Las and Rhl systems are important for extracellular DNA release, which plays a role in biofilm matrix and structure (Allesen-Holm et al., 2006). While in PA14, the Las system is essential for biofilm architecture, possibly by controlling Pel EPS production (Sauer et al., 2002, Sakuragi and Kolter, 2007, Yang et al., 2007). In Gram-positive *S. aureus*, QS systems utilise the autoinducer peptide (AIP) derived from the product of the accessory gene regulator (Agr) D gene (López et al., 2010). It is secreted and detected by AgrC, which activates the regulator AgrA. AgrA in turn positively regulates the transcription of genes including those that code for several extracellular proteases, which are involved in biofilm dispersal (Yarwood et al., 2004, O'Gara, 2007, Periasamy et al., 2012). Thus, QS negatively regulates biofilm formation in *S. aureus*. Such that, adhesion of *S. aureus* to a surface is favoured only when the Agr QS system is inhibited (Boles and Horswill, 2008). In *S. epidermidis*, initial attachment to a polymer surface may be mediated by autolysin ATIE, a surface-associated autolysin (Fey and Olson, 2010). Once attached, bacteria accumulate forming a complex architecture that involves the production of PNAG (poly- β -1,6-N-acetylglucosamine) or PIA

EPS. In addition, clumping factors, proteins and teichoic acid also contribute to the generation of biofilm (Cerca et al., 2005, Chokr et al., 2006, Rohde et al., 2007).

In addition to QS molecules, other molecules can also induce biofilm formation that are independent of QS. These include secondary metabolites, such as antibiotics, pigments and siderophores (Rutherford and Bassler, 2012).

1.4.3. Host immune response against biofilm

The host immune response against biofilm infections remain unknown. Specifically, it is unclear why the inflammatory response fails in removing biofilms. It has been suggested that biofilms are able to sense and manipulate host immune responses (Smith and Iglewski, 2003, Tateda et al., 2003, Wu et al., 2005).

In Gram-positive bacteria, human polymorphonuclear leukocytes have been shown to effectively penetrate *S. aureus* biofilms, likely through the nutrient channels that exist in mature biofilms (Flemming and Wingender, 2010, Periasamy et al., 2012). However, these leukocytes showed impaired phagocytosis and a decreased ability to kill the bacteria (Høiby et al., 2010). While subsequent studies have shown that polymorphonuclear neutrophils (PMN) are able to clear staphylococci biofilms by phagocytosis (Meyle et al., 2010, Arciola et al., 2012, Hanke and Kielian, 2012). Moreover, immature staphylococci biofilms were more sensitive to phagocytosis compared to mature biofilms, although the latter are not completely immune to PMN attack (Günther et al., 2009). In contrast, macrophages were not capable of phagocytising *S. aureus* biofilms but were capable of engulfing disrupted biofilm, which suggests that the size and/or physical complexity of the biofilm architecture are responsible for their resistance to phagocytosis (Arciola et al., 2012). It has been postulated that evasion of host immunity and persistence of *S. aureus* biofilms could be attributed to their ability to skew the immune response to favour anti-inflammatory and pro-fibrotic pathways (Hanke and Kielian, 2012). Hence, targeting

proinflammatory activity represents a novel therapeutic strategy to overcome the local immune inhibitory environment created during a biofilm infection (Hanke et al., 2013).

In Gram-negative bacteria, *P. aeruginosa* biofilms have been shown to activate the oxidative burst response of polymorphonuclear leukocytes, which is crucial for the destruction of invading microorganisms by phagocytes (Alhede et al., 2009). However, this response was 25% lower compared to planktonic cells (Alhede et al., 2009). *In vitro* microscopic studies suggest that *P. aeruginosa* biofilms disrupt the normal migratory behaviour of phagocytes. Such that, the host innate cells are able to settle into the biofilm but cannot migrate from the point of contact even though they appear to mount an oxidative burst, degranulate and retain their phagocytic and secretory activity (Jesaitis et al., 2003). The mechanism(s) through which the biofilms immobilise polymorphonuclear leukocytes, which are still capable of phagocytosing bacteria, remain unknown. It has been suggested that exotoxins or other components produced by *P. aeruginosa* and immune cells, respectively, may be involved (Jesaitis et al., 2003, Gellatly and Hancock, 2013). While others suggest that *P. aeruginosa* biofilm tolerance to PMN is QS-dependent (Bjarnsholt et al., 2005).

The biofilm matrix plays an important role in the protection of biofilm bacteria from host defences. For example, *S. aureus* containing knockout mutations for PIA, the major matrix component in staphylococcal biofilms, were phagocytosed and killed by polymorphonuclear leukocytes (Vuong et al., 2004). These mutants were also more susceptible to killing by major antibacterial peptides of human skin, e.g cathelicidins (Vuong et al., 2004, Boles et al., 2010). In *P. aeruginosa* biofilm, the exopolysaccharide alginate protects the bacteria from leukocyte phagocytosis (Pier et al., 2001, Leid et al., 2005). *In vitro* studies have shown that in the presence of the potent leukocyte activator IFN- γ , human phagocytes kill *P. aeruginosa* bacteria lacking the ability to produce the alginate exopolysaccharide (Leid et al., 2005). However, the inability of innate cells to eliminate biofilms is negated as soon as the biofilm is mechanically disrupted into

individual cells (Leid et al., 2005, Jensen et al., 2010). The matrix may also trigger a more intense inflammatory response, which may further provide advantage to the biofilm by promoting host cell lysis and subsequent release of nutrients for bacteria (Flemming and Wingender, 2010).

1.4.4. Surface factors influencing bacterial attachment

Implantable medical devices must satisfy certain performance criteria, including biocompatibility and long-term stability (Pavithra and Doble, 2008). Biocompatibility is the ability of the implant to perform its intended function without inducing uncontrolled activation of cellular or plasma protein cascades when placed inside the body. Factors that contribute to the degree of biocompatibility of any given implant include the type of material, genetic inheritance of the patient, site of implantation and contact duration. While factors that depend on the implant include shape, size, surface chemistry and roughness, design, morphology and porosity, composition, sterility issues and nature of degradation (Pavithra and Doble, 2008). These factors may be responsible for variations in the intensity and the duration of the tissue reaction.

All medical implants, including breast implants, are susceptible to bacterial colonisation and biofilm formation (Costerton et al., 1999, Castelli et al., 2006, Bryers, 2008, Veerachamy et al., 2014). The majority of these infections are not controllable with antibiotics and it may become necessary to remove the implanted medical device from the patient. The initial stage in the pathogenesis of the infection is bacterial adhesion on the implant surface. Three key factors influence bacterial adhesion on an implant surface. These include the type of organism, the properties of the material and the nature of the environment, and each factor is in turn affected by other factors (Figure 1.7). The different types of surface patterning or topographies of the implant can also influence bacterial attachment and these can be grouped into three general patterns: (i) irregular or 'random', (ii) regularly patterned and (iii) hierarchical surface structures.

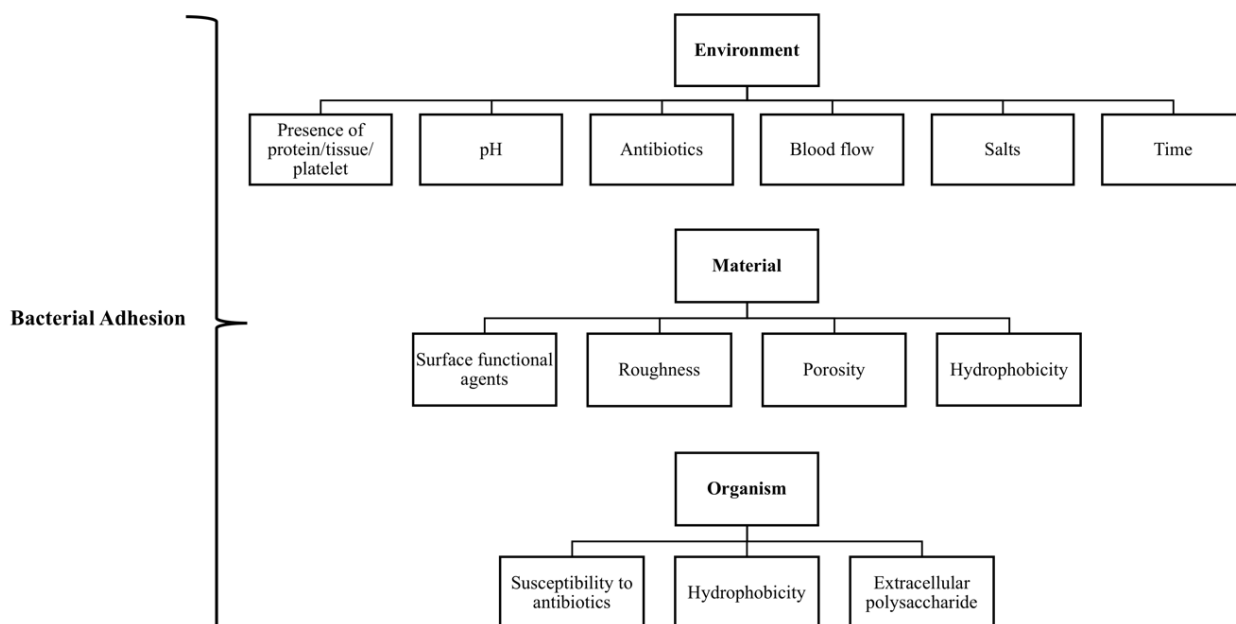


Figure 1.7. Factors that determine bacterial adhesion.

The three primary factors that influence bacterial adhesion on a polymeric surface are the nature of the environment, the properties of the material and the type of microorganism, and each one of these factors is in turn affected by several other parameters.

Irregular/random surface structures

Surface irregularities or roughness is known to affect bacterial attachment and biofilm formation (Crawford et al., 2012). However, attempts to characterise the effect of these surfaces in bacterial attachment have shown mixed findings. For example, studies of surface topographies with sub-micron features have shown stainless steel surfaces with an average roughness of 0.16 μm measured over 50 μm x 50 μm scan areas have minimal bacterial attachment compared to more rougher surfaces, which exhibit greater degrees of bacterial attachment (Medilanski et al., 2002). Moreover, bacterial adhesion occurred more along the sub-micrometric grooves (Medilanski et al., 2002). Similarly, analysis of roughness, density and area of 50 μm x 50 μm sections of titanium surfaces showed that bacterial attachment was higher on titanium surfaces exhibiting greater surface area and average roughness (Fröjd et al., 2011). While an average roughness of 10 to 15 nm over scanning areas of 10 μm x 10 μm has been shown to be inversely correlated with the

number of *S. aureus*, *P. aeruginosa* and *E. coli* cells adhering to the surface of titanium (Truong et al., 2009, Truong et al., 2010b). The surface nanostructure was also found to stimulate the metabolic activity of the bacteria and the amount of EPS produced was higher on the smoother titanium surfaces (Truong et al., 2009, Truong et al., 2010b). In addition, nano-etched glass surfaces with an average roughness of 1.3 nm was found to attract more bacteria than surfaces with an average roughness of 2.1 nm (Mitik-Dineva et al., 2009).

More comprehensive roughness analysis correlating the cellular interactions with surface microtopography have shown surface features with an average roughness below 1.5 nm influence the adhesive behaviours and EPS production levels of *S. aureus* and *P. aeruginosa* (Truong et al., 2010a). Whereby cell attachment and EPS production for both organisms were enhanced for titanium thin film substrata containing higher average roughness, whereas on polished bulk titanium surfaces decreasing roughness was found to enhance the adhesive behaviour of only *P. aeruginosa*, with *S. aureus* exhibiting a reduced propensity for adhesion. In addition, molecularly smooth titanium films on silicone containing an average roughness below 0.5 nm have been shown to enhance the adhesive behaviour and EPS production of *S. aureus*, but not for *P. aeruginosa* (Truong et al., 2010a). It is likely that the differences in the attachment of both bacteria on molecularly smooth films were due to variations in cell deformability arising from their morphologies (Crawford et al., 2012).

In breast implants there have been limited studies conducted examining the influence of surface roughness in bacterial adhesion. All breast implant outer surface shells are known to show irregularity on microscopic scales (Ajdic et al., 2016). Thus, given biofilm formation is favoured when the average roughness of a surface is greater than 0.2 μm (Teughels et al., 2006), the surfaces of both smooth and textured breast implant outer shells will provide enough roughness for biofilm formation.

Patterned surfaces

Bacterial adhesion on regularly patterned surfaces has received less attention compared to irregular surface topographies. Several patterns, such as etched grooves, pits, squared-features and shark-skin inspired surfaces have been developed for the purpose of developing anti-biofouling surfaces and directing bacterial attachment (Rowan et al., 2002, Whitehead et al., 2005, Rozhok et al., 2006, Chung et al., 2007). For example, polydimethylsiloxane surfaces fabricated with regularly spaced arrays of square protrusions with controlled dimensions were tested for their ability to control *E. coli* attachment and biofilm formation (Hou et al., 2011). The surface dimensions were systematically varied, with side lengths of the protrusions ranging between 2 and 100 μm , with the distance between adjacent features ranging between 5 and 20 μm . *E. coli* was found to preferentially adhere to, and form biofilms on the valleys between the square features of all the dimensions tested, suggesting that square-shaped microsurface patterns can promote bacterial adhesion and subsequent biofilm formation (Hou et al., 2011).

Microscale-patterned surfaces, such as grooved and pitted surfaces highlight the importance of ‘shelter’ from external forces (e.g. hydrodynamic turbulence), which may otherwise dislodge adhering cells. Flow experiments using *P. aeruginosa* and *Pseudomonas fluorescens* cultures across rectangular-grooved silicone surfaces of various dimensions have showed preferential attachment of bacteria to the downstream edges of the grooves, where they could become lodged and could not be easily removed (Scheuerman et al., 1998). Similarly, the attachment behaviour of *S. aureus* and *P. aeruginosa* was studied on surfaces with 0.2 to 2 μm diameter etched pits and showed that the larger diameter pits provided better shelter to cells, with the smaller, coccus-shaped *S. aureus* retained in larger numbers than the larger, rod-shaped *P. aeruginosa* (Whitehead et al., 2005). However, there are also inconsistent findings in the relationship between patterned surfaces and bacterial adhesion. For example, pits with diameters of 2.5 μm etched into an optical fibre

surface were found to prevent bacterial attachment, relative to control non-fabricated control optical fibre surfaces (Mitik-Dineva et al., 2010).

Textured breast implants that are manufactured using a salt-loss technique contain randomly arranged pores that vary in diameter and depth depending on the level of texture on the surface (Section 1.1.1.) (Barr and Bayat, 2011). The aggressive textured Biocell implant contains pores measuring 600 to 800 μm in diameter (Danino et al., 2001). In contrast, smooth implants manufactured by Allergan contain parallel surface grooves measuring 5 μm (Barr et al., 2009). Studies have shown that parallel grooves measuring 5 μm or less facilitate fibroblast migration and organised collagen disposition (Den Braber et al., 1998). Thus, the better tissue ingrowth seen in textured implants is presumably related to pore size which permits the entry and growth of breast tissue cells (Barr et al., 2017). However, such biological benefits need to be balanced by the higher risk of bacterial contamination associated with these surfaces. As with irregular surfaces, more research into the relationship between bacterial attachment and regularly patterned microscale surfaces is needed.

Hierarchical surfaces

Most of the studies on hierarchical surface patterns have come from natural surfaces (Babu et al., 2010, Salta et al., 2010, Boreyko et al., 2011, Yan et al., 2011). These surfaces are superhydrophobic and possess self-cleaning ability. Thus, studies on bacterial attachment on superhydrophobic, hierarchical surfaces have focused on a better understanding of these surfaces to potentially minimise or prevent bacterial colonisation (Crick et al., 2011, Ma et al., 2011). Studies on natural hierarchical surfaces, such as taro leaves and artificial superhydrophobic elastomeric silicone surfaces have found that structures on these surfaces resist bacterial attachment (Crick et al., 2011, Ma et al., 2011). It is postulated that the air trapped between the dual-scale surface features present on these surfaces limits the available contact area for bacteria (Ma et al., 2011). The extent of bacterial attachment has also been investigated on titanium samples modified

to mimic the dual-scale features of the surface of the lotus (*Nelumbo nucifera*) leaf (Fadeeva et al., 2011). *S. aureus* and *P. aeruginosa* cultures were tested on the surface that consisted of microscale, grain-like, convex ‘bumps’ that varied from 10 to 20 µm covered with nanoscale undulations of 200 nm or less. *P. aeruginosa* were found to be unable to colonise the surface, but *S. aureus* could colonise the surface (Fadeeva et al., 2011). Thus, self-cleaning properties of some surfaces may not be sufficient to prevent bacterial attachment and more research on bacterial attachment on hierarchical surfaces is needed.

1.4.5. Conclusion

Biofilms are particularly durable and persistent, and as such the most effective course of action to limit their impacts is to prevent their initial formation rather than remediation. This can be achieved by inhibiting the initial colonisation stage in the biofilm lifecycle (Figure 1.6). The prevention of biofilm formation in implantable medical devices may potentially be controlled using new emerging strategies, including QS quenchers, polymer/device coatings, antimicrobial coatings, enzyme-mediated approaches, phage therapy, immunotherapy, nanostructured coatings, surface modifications and biosurfactants (Campoccia et al., 2006, López et al., 2010, Veerachamy et al., 2014). Promising bioactive coatings have been developed to reduce the bacterial adhesion and to prevent biofilm formation in medical implants using natural and synthetic materials. These include antibiotic-hydroxyapatite-based coatings, antiseptic-based coatings, nano-silver coatings, photoactive-based coatings, nanostructured coatings and treatment with nanoparticles (Veerachamy et al., 2014, Zhang et al., 2014, Cloutier et al., 2015).

The 14-point plan (Table 1.5) for reducing the risk of infection and BIA-ALCL is now well established (Deva et al., 2013). However, given the lag time in disease onset, cases in Australia are predicted to peak in about 12 years. Therefore, it should be a matter of priority that all surgeons adopt these strategies into their routine practice. Moreover, all patients with breast implants should

be enlisted into a program of ongoing surveillance, and new technologies that protect and prevent breast (and other) implants from infection should be the focus of ongoing research.

1.5. Aims and scope of research project

Due to the worldwide, growing popularity of implant-based breast augmentation surgery, it is of great diagnostic and clinical importance to better understand the molecular mechanisms behind the development of BIA-ALCL. As outlined in this review, a number of reported observations about BIA-ALCL point to an underlying biofilm infection as a potential cause. These include:

- All BIA-ALCL cases have occurred in patients with textured surface implants (Brody, 2012, Hu et al., 2016, Loch-Wilkinson et al., 2017), which is consistent with findings that textured implants support a higher bacterial load, both *in vitro* and *in vivo* (Jacombs et al., 2014, Hu et al., 2015).
- A linear increase in T-cell activation proportionate to bacterial infection of breast implants in both a pig model and in human specimens collected from patients with chronic implant infection (Hu et al., 2015).
- The late onset of BIA-ALCL following insertion of breast implants allowing underlying inflammation from bacteria to stimulate lymphoproliferation (Brody et al., 2010, Hu et al., 2016).
- Late seroma, the commonest clinical presentation of BIA-ALCL is associated with both textured implants and biofilm infection (Hu et al., 2016).
- High bacterial load, present as a biofilm, in BIA-ALCL samples with a significant predominance of Gram-negative *Ralstonia* spp. compared with non-tumour capsule specimens, where significantly more Gram-positive *Staphylococcus* spp. were found (Hu et al., 2016).

- The biologically proven pathway from bacterial infection with *H. pylori* to MALT gastric lymphoma establishes a pathway from bacterial infection, inflammation and subsequent lymphomagenesis (Baumgaertner et al., 2009, Bertonni et al., 2011).

1.5.1 Project hypotheses

We hypothesise that:

- The increased surface area of textured implant increases bacterial attachment sites.
- BIA-ALCL development is stimulated by chronic bacterial (biofilm), particularly Gram-negative, antigen stimulation, resulting in sustained T-cell proliferation that potentiates malignant transformation.
- The trigger for both reactive lymphoproliferation and potential malignant transformation is underlying chronic bacterial biofilm infection of breast implants.

1.5.2 Project objectives

- To measure the surface area and surface roughness of eleven available commercial implant types using surface and three-dimensional scanning and to use this information to correlate surface area with *in vitro* bacterial attachment.
- To compare bacterial attachment, biofilm formation, development of contracture and host response following artificial bacterial contamination of breast implants composed of test surfaces type A and type B in an *in vivo* porcine model.
- To determine the bacterial load and host lymphocytic response found attached to fresh implants and capsules from new cases of BIA-ALCL and compare this to bacterial load and host lymphocytic response found attached to fresh implants and in capsules obtained from non-tumour contracted capsule specimens.

- To measure the cell proliferation of primary BIA-ALCL tumour cells and BIA-ALCL cell lines in response to non-specific mitogens, phytohaemagglutinin, lipopolysaccharide and staphylococcal superantigens – staphylococcal enterotoxin A and toxic shock syndrome-1, and compare these responses to peripheral blood mononuclear cells (PBMC) obtained from patients with BIA-ALCL, cutaneous-ALCL cell lines, an immortal T-cell line, and PBMC purified from healthy control patients.
- To develop co-culture of biofilm and mammalian cells and measure the cell proliferation response of BIA-ALCL tumour cells to biofilm infection composed of different bacterial species, *S. epidermidis*, methicillin-resistant *S. aureus*, *P. aeruginosa* and *R. picketii*.
- To investigate whether LPS stimulation is mediated by TLR4 in BIA-ALCL tumour cells.

Chapter II.

Materials and Methods

2.1. Bacterial strains and culture conditions

2.1.1. Maintenance of bacterial strains

All bacterial strains were obtained from the American Type Culture Collection (ATCC, Manassas, Virginia, USA) and included *Staphylococcus aureus* ATCC 25923, *Staphylococcus epidermidis* ATCC 35984, *Pseudomonas aeruginosa* ATCC 25619, *Ralstonia pickettii* ATCC 27511 and methicillin-resistant *S. aureus* (MRSA) ATCC 43300. Each of the strains were routinely cultured on Columbia horse blood agar (HBA) (Micromedia Laboratories, Moe, Victoria, Australia) and incubated aerobically at 37°C for 24 hr.

Long-term storage of organisms was accomplished by inoculating three to four colonies from a fresh overnight culture into 20 mL of 100% tryptone soya broth (TSB) (Oxoid; Thermo Fisher Scientific, Scoresby, Victoria, Australia) at 37°C for 4 hr under vigorous shaking at a constant speed of 120 rpm in an Innova 42 incubator shaker (New Brunswick™; Eppendorf South Pacific Pty. Ltd., North Ryde, New South Wales, Australia). After which, 850 µL of bacterial culture was transferred to a sterile 1.5 mL microcentrifuge tube (Axygen; Fisher Biotech, Wembley, Western Australia, Australia) containing 150 µL of sterile glycerol (Sigma-Aldrich, Castle Hill, NSW, Australia), mixed thoroughly and stored at -70°C.

2.1.2. Preparation of bacterial cultures

Representative colonies were picked from a streaked HBA plate, inoculated into 100 mL of 100% TSB and grown overnight under vigorous shaking at a constant speed of 120 rpm at 37°C in an incubator shaker. The overnight bacteria culture was diluted with 100% TSB to an optical density of 0.3 at 600 nm wavelength (V-1200 Spectrophotometer; VWR™ International, Leicestershire, England), which equated to approximately 10^8 bacterial cells/mL.

2.2. Bacterial enumeration

2.2.1. Quantification of the number of bacteria attached to breast implants

Breast implant shells with a diameter of 5 mm were subjected to an *in vitro* bacterial attachment assay (Sections 2.6. to 2.7. and Chapter III) and a bacterial biofilm and mammalian cells co-culture assay (Chapter VIII). The number of bacteria attached to the 5 mm implants was quantified by viability counts (CFU). Four implants sections were transferred into a 1.5 mL microcentrifuge tube containing 500 µL of phosphate buffered saline (PBS) (Thermo Fisher Scientific). The tubes were then placed in an ultrasonic bath (Soniclean, Thebarton, South Australia, Australia) that had been filled with 2 L of distilled water and degassed for 5 min. The tubes were sonicated for 15 min at 80% (medium level) power at 20°C to detach the bacteria bound to the implants. Followed by vortexing for one minute. Viable counts on the sonicated implants were then performed by preparing serial ten-fold dilutions. Serial dilutions were made in 1.5 mL microcentrifuge tubes by transferring 100 µL of neat sonicated sample to 900 µL of PBS in a fresh tube, and vortexed for 10 sec. This procedure was repeated until the desired number of dilutions were made. For each dilution, 100 µL was spread onto HBA and incubated overnight at 37°C. The number of colonies formed on each plate were then counted and the concentration of bacteria in

the neat bacterial culture was calculated by CFU counts by the dilution factor for plates with CFU counts between 30 and 300.

2.2.2. Biofilm quantification: crystal violet assay and colony-forming unit counts

Biofilm biomass quantification

To fix the biofilm from our biofilm/mammalian cells co-culture assay (Chapter VIII), 1 mL of 100% ethanol (Chem-Supply, Gillman, South Australia, Australia) was added to the wells of a 12-well cell culture plate (Corning; Sigma-Aldrich) and allowed to stand for 15 min at RT, after which the ethanol was removed and the plates air-dried. Once dry, 1 mL of 0.3% (v/v, volume per volume) crystal violet (CV) (Sigma-Aldrich) was added to the wells and incubated for 10 min at RT. The excess CV was then removed and the plates washed under running distilled water until the water ran clear. The plates were inverted and vigorously tapped on paper towels to remove any excess water and then air-dried. The CV in stained wells was solubilised by adding 1 mL of 33% (v/v) glacial acetic acid (Chem-Supply) and incubated for 10 min at RT. The contents of the wells were then briefly mixed by pipetting the solution up-and-down. Relative biofilm formation was assessed by measuring absorbance at OD 600 nm using a plate reader, with 33% (v/v) glacial acetic acid used as a blank.

Biofilm viability quantification

A disadvantage of the CV assay is that CV stains not only cells but also any material adhering to the surface of the plate, including matrix components. Additionally, any dead biofilm that is attached to the plate will also be stained with CV. As a result, CV staining may overestimate the number of adherent bacteria. Therefore, we also quantified the number of bacteria attached to the wells by CFU counts (Chapter VIII). To do this, 1 mL of sterile PBS was added to the wells and the plate sonicated. The lid of the plate was sealed to its base with autoclave tape to prevent fluid loss and entry of water during sonication. The ultrasonic bath was filled with 2 L of distilled water,

degassed for 5 min, and the plate sonicated for 15 min at 80% (medium level) power at 20°C to detach the bacteria bound to the wells. Viable counts on the sonicated suspensions were then performed by serial ten-fold dilutions and plate count as described above.

2.3. qPCR to determine bacterial load attached to breast implants and in breast capsules

2.3.1. Pig samples

Between 50 and 100 mg of pig capsule and implant samples explanted from an *in vivo* porcine model (Tamboto et al., 2010) (Chapter IV) were digested by placing the sample into a sterile 1.5 mL microcentrifuge tube containing 180 µL of tissue lysis buffer (Sigma-Aldrich) and 20 µL of 20 mg/mL proteinase kinase (Sigma-Aldrich). This was incubated overnight at 56°C and resulted in complete digestion of the tissue. The proteinase kinase was then inactivated by incubation at 95°C for 5 min. After which, 20 µL of 10 mg/mL lysozyme (Sigma-Aldrich) was added and the sample incubated at 56°C for 1 hr to release the bacterial genomic DNA.

Following digestion, genomic DNA was extracted using the Roche high pure PCR template preparation kit (Roche; Sigma-Aldrich) or the QIAamp DNA mini kit (Qiagen, Chadstone, Victoria, Australia), following the manufacturer's instructions.

Each extracted DNA sample was subjected to real-time quantitative PCR (qPCR), in duplicate, using universal eubacterial 16S ribosomal ribonucleic acid (rRNA) 341F 5'-CCTACGGGAGGCAGCAG-3' and 16S rRNA 534R 5'-ATTACCGCGGCTGCTGG-3' to amplify a 194-base pair amplicon of 16S rRNA gene of all bacteria (Table 2.1).

To compare the number of bacteria between capsular samples, the extracted DNA was subjected to amplification of the pig 18S rRNA gene, which was used as a reference gene to normalise the amount of pig tissue used in DNA extraction. The primer pair used in 18S rRNA

Table 2.1. Primer sequences used for real-time PCR of microbial load and lymphocyte number in pig and human samples.

Gene	GenBank accession number	Amplicon size (base pair)	Primer	Sequence (5' to 3')	Direction	References
16S rRNA (<i>Eubacteria</i>)		194	341F 534R	CCTACGGGAGGCAGCAG ATTACCGCGGCTGCTGG	Forward Reverse	Jacombs et al. (2012), Jacombs et al. (2014)
18S rRNA	AY265350.1 NR_003286.2	122	756F 877R	GGTGGTGCCCTTCCGTCA CGATGCGGCGGCGTTATT	Forward Reverse	In-house
<i>icaA</i>		124		GGAAGTTCTGATAATACTGCTG GATGCTTGTTTGATTCCCTC	Forward Reverse	Nuryastuti et al. (2011)
<i>Sus scrofa</i> CD3	AY323829.1	125	718F 824R	TCCCTGGGCAAATCTTGGAC AATATCCTTGGGCTGGGTG	Forward Reverse	Hu et al. (2015)
<i>Sus scrofa</i> CD4	NM_001001908.1	61	1807F 1848R	CGCGTGGGACTGGACCTG ACCATGACTGCCCTGTGCTT	Forward Reverse	Hu et al. (2015)
<i>Sus scrofa</i> CD8a	AY590798.1	114	679F 773R	AACGCAGACCCGAGGAAG GCGGTGGCAGATGATGGTGA	Forward Reverse	Hu et al. (2015)
<i>Sus scrofa</i> CD79a	NM_001135962.1	181	466F 607R	TGCTGATCTGTGCCGTGGTG TCCTGGTAGGTGCCCTGGAG	Forward Reverse	Hu et al. (2015)
<i>Homo sapiens</i> CD3	NM_000733.3	66	690F 740R	TGCTGCTGGTTTACTACTGG CCGCTCCTCGTGTCAC	Forward Reverse	Hu et al. (2015)
<i>Homo sapiens</i> CD4	BT019811.1	74	1231F 1286R	TTCATTGGGCTAGGCATC ATCTGAGACATCCGCTCTG	Forward Reverse	Hu et al. (2015)
<i>Homo sapiens</i> CD8a	NM_001768.6 NM_171827.3	71	1148F 1199R	CAGCGGTTCTCGGGCAAGA TCGTTCTCTCGGCGGAAGTC	Forward Reverse	Hu et al. (2015)
<i>Homo sapiens</i> CD79a	NM_001783.3 NM_021601.3	54	337F 372R	ACTTCCAATGCCCCGCACAAT CGCGCCACCAGGTGACGTT	Forward Reverse	Hu et al. (2015)

gene real-time PCR was 18S rRNA 756F 5'-GGTGGTGGCCTTCCGTCA-3' and 18S rRNA 877R 5'-CGATGCGGCGGCGTTATT-3' to amplify a 122-base pair amplicon based on the pig (*Sus scrofa*) 18S rRNA gene sequence (GenBank accession no. AY265350.1) (Table 2.1). The 18S rRNA gene qPCR forward and reverse primers were checked by BLASTn (Basic Logical Alignment Search Tool) search against non-redundant nucleotide collection (nt) database. No match with any bacterial genomic DNA was found.

Real-time PCR was carried out in 25 μ L reaction mix containing 1X Brilliant II SYBR Green qPCR Master Mix (Agilent Technologies, Santa Clara, California, USA), 400 nM forward and reverse primers, 1 μ M of mitochondrial peptide nucleic acid (mPNA) PCR blocker (PNA Bio, Newbury Park, California, USA) and 100 ng of DNA template, and was performed in ViiA 7 Real-time PCR System (Applied Biosystems; Thermo Fisher Scientific) with the following cycling conditions: activation of Taq polymerase at 95°C for 10 min, followed by 40 cycles of denaturation at 95°C for 15 sec, annealing at 60°C for 1 min. mPNA was used to block the amplification of pig mitochondrial DNA by the eubacterial 16S rRNA gene (Ørum et al., 1993, Lundberg et al., 2013). Each qPCR was run with standard samples of known concentrations (copies/ μ L). Ten-fold serial dilutions of the quantified 16S rRNA gene and 18S rRNA gene PCR amplicon solutions were kept in aliquots at -20°C and used as external standards of known concentration (copies/ μ L) in real-time PCR reaction. The standard samples were ranged 10^2 to 10^8 copies/ μ L, which were used to construct a standard curve for each qPCR run. The calibration curve was created by plotting the cycle threshold (Ct) corresponding to each standard versus the value of their corresponding gene concentration (copies/ μ L). The Ct value is defined as the point at which the fluorescence rises above the background fluorescence (Pfaffl et al., 2002). Microbial DNA-free water (Qiagen) was used as a negative control. Copy number of total bacteria 16S rRNA gene was normalised against copy number of pig 18S rRNA gene in each pig capsule.

2.3.2. Human samples

Genomic DNA from fresh capsule and implant samples explanted from BIA-ALCL and non-tumour contracture patients (Chapter V) was extracted using the DNeasy PowerBiofilm kit (Qiagen) following the manufacturer's instructions. Between 0.05 to 0.20 g of sample was transferred to a PowerBiofilm bead tube containing 350 μ L of solution BF1 (inhibitor removal) and 100 μ L of solution BF2 (contains a chaotropic agent that aids in lysis, and also stabilises and protects DNA integrity), and briefly vortexed. The tube was incubated at 65°C for 5 min to activate the lysis components, which aids in the breakdown of EPS. The sample was then homogenised using the FastPrep®⁻²⁴ Homogeniser (MP Biomedicals, Santa Ana, California, USA) at 3200 rpm for 30 sec and centrifuged for 1 min at relative centrifugal force (RCF) 13000 x g. The supernatant was collected and transferred to a fresh 2 mL tube containing 100 μ L of solution BF3, briefly vortexed and incubated at 4°C for 5 min. This removed any additional non-DNA organic and inorganic material, including humic acid, cell debris, polyphenolics, polysaccharides and proteins. The tube was then centrifuged for 1 min at 13000 x g, RT. The supernatant was transferred to a fresh 2 mL tube containing 900 μ L of solution BF4 and briefly vortexed. This is a highly-concentrated salt solution that adjusts the DNA solution salt concentration to promote DNA binding, but not the binding of non-DNA organic and inorganic material, which may still be present at low levels. The mixture was then loaded onto a spin filter and centrifuged for 1 min at 13000 x g and the flow through discarded. This was repeated until all the mixture had been loaded onto the spin filter. The spin filter was then placed into a fresh 2 mL tube and 650 μ L of solution BF5 was added and centrifuged for 1 min at 13000 x g at RT. This is an alcohol-based wash solution that further cleans the DNA bound to the silica membrane in the spin filter, and also removes residual salt and other contaminants while the DNA stays bound to the silica membrane. The flow-through was discarded and centrifuged again for 2 min at 13000 x g to remove residual wash. The spin filter was inserted into a fresh 2 mL tube and 100 μ L of solution BF7 (elution buffer) was added to the

centre of the filter membrane and centrifuged for 1 min at 13000 x g. The extracted DNA was collected and stored at -20°C until molecular analysis.

Real-time PCR was performed in ViiA 7 Real-time PCR System in 25 µL of reaction mix as detailed in Section 2.3.1. with the following cycling conditions: 95°C for 10 min, followed by 40 cycles of 95°C for 15 sec, 56°C for 30 sec and 72°C for 20 sec. mPNA was used to block the amplification of human mitochondrial DNA by the eubacterial 16S rRNA gene (Ørum et al., 1993, Lundberg et al., 2013). Each qPCR was run with standard samples of known concentrations ranging from 10² to 10⁸ copies per µL as per Section 2.3.1.

2.4. Imaging of breast implant surfaces

2.4.1. Scanning electron microscopy

Scanning electron microscopy (SEM) imaging of breast implant and capsule specimens (Chapter III to V) was performed by Dr. Khalid Al Johani. Breast implants and capsules with dimensions up to 1 cm² were fixed in 3% glutaraldehyde solution (Sigma-Aldrich) and stored overnight at 4°C. Samples were rinsed three times with 0.1 M PBS, pH 7.4, for 10 min each rinse and dehydrated through a graded ethanol series (Sigma-Aldrich), 30%, 50%, 70%, 80%, 90% and 100%, for 10 min at each concentration. Implants were then immersed in 100% hexamethyldisilazane (Polysciences Inc., Warrington, Pennsylvania, USA) three times for 10 min each before being aspirated dry and allowed to evaporate overnight. Samples were mounted onto aluminum SEM stubs (ProSciTech, Thuringowa, Queensland, Australia) using carbon tabs (ProSciTech) and sputter coated with 20 nm of gold film in the Emitech K550 gold coater (West Sussex, England). The gold coated implants were then visualised using a JEOL 6480LA SEM (JEOL Ltd., Tokyo, Japan) with the following imaging parameter settings: 10 kV beam accelerating voltage, spot size 30, 15 mm working distance, and magnifications ranging from 300X to 23,500X.

2.4.2. Micro computed tomography scanning and analysis

Micro computed tomography (CT) micro-characterisations of the breast implant surfaces (Chapter V) was performed at the Australian Centre for Microscopy and Microanalysis, University of Sydney, Australia. The implants were mounted horizontally with adhesive on a metal pin before loading into a pin vice holder. These were then scanned using a Zeiss Xradia MicroXCT-400 system operating in absorption mode with peak source energy of 50 kV and beam current of 200 μ A (Carl Zeiss, Oberkochen, Baden-Württemberg, Germany). The implants were mounted in low-density polystyrene to prevent movement during their 180° total rotation with projections collected at 0.25° intervals, with an exposure time of 3 sec and saved as 16-bit images in a proprietary file format. The projections were reconstructed using XMReconstructor v7.0.2817 (Xradia; Carl Zeiss).

From this model, surface area and roughness measurements were taken to calculate the various required implant material properties. Analysis was performed with Avizo 9.3 (FEI Visualisation Sciences Group, Hillsboro, Oregon, USA) and FIJI (Schindelin et al., 2012), where a binarised model of the implant was produced by thresholding after noise-reduction filtering of the reconstructed slices.

2.5. Establishment and maintenance of cell lines

2.5.1. Tumour cells/peripheral blood mononuclear cells/cell lines

Patient-derived BIA-ALCL tumour cells, BIA-ALCL cell lines, cutaneous-ALCL cell lines, an immortal T-cell line (MT-4 cells), and peripheral blood mononuclear cells (PBMC) from BIA-ALCL, capsular contracture and primary augmentation patients were studied (Chapters VI to IX).

BIA-ALCL tumour cells

BIA-ALCL patients from centres around Australia and New Zealand, presenting with a unilateral malignant effusion or tumour mass participated in this study. The diagnosis of seroma was made clinically when a collection was detected around the breast cavity. The seroma fluid was collected by puncture and aspiration under sterile conditions. The aspirate was kept on ice during transport to the laboratory for immediate analysis.

BIA-ALCL tumour cells were recovered fresh from the seroma fluid and/or tumour mass by centrifugation at 753 x g for 5 min at 22°C (Heraeus XR3 Multifuge; Thermo Fisher Scientific). The supernatant was transferred to a new 15 mL centrifuge tube (Corning; Sigma-Aldrich), stored at -20°C and the cell pellet resuspended in Dulbecco's Modified Eagle Medium (DMEM) containing 4500 mg/L glucose, 2 mM L-glutamine, sodium pyruvate, sodium bicarbonate (Sigma-Aldrich), supplemented with 10% heat-inactivated foetal bovine serum (FBS) (Sigma-Aldrich) and 100 U/mL penicillin and 100 µg/mL streptomycin (1% penicillin/streptomycin solution) (Thermo Fisher Scientific).

Three newly established BIA-ALCL cell lines, T-cell breast lymphoma (TLBR)-1, -2 and -3, were kindly provided by Dr. Alan Epstein (Lechner et al., 2012). Table 2.2 lists the clinical features of patients from whom the tumour cell lines were derived (Lechner et al., 2012).

Table 2.2. Clinical summary of established T-cell lymphoma breast cell lines.

Cell line	Age at diagnosis	Implant type	Clinical presentation	Treatment
TLBR-1	42	Nagor	Seroma	Surgery/Radiation therapy
TLBR-2	43	Allergan Biocell	Seroma	Surgery/Chemotherapy and radiation therapy – patient had recurrence and deceased
TLBR-3	45	Allergan Biocell	Seroma	Surgery and radiation therapy

Cutaneous-ALCL cell lines

Two cutaneous-ALCL cell lines, MAC-1 and MAC-2A, were obtained from Prof. Marshall Kadin. MAC-1 and MAC-2A are clonally related cell lines derived from two successive steps of progression of lymphomatoid papulosis to ALCL (Kadin et al., 1994).

MT-4 cells

The MT-4 cell line was obtained from the European Collection of Authenticated Cell Cultures (ECACC), catalogue number 08081402 (ECACC, Salisbury, Wiltshire, United Kingdom). MT-4 are non-adherent cells derived from a 50-year-old Japanese male with adult T-cell leukaemia by co-culture of his peripheral leukocytes with male umbilical cord lymphocytes. The cells carry human T-lymphotrophic virus-1 and support the growth of human immunodeficiency virus (Miyoshi, 1982, Schoggins et al., 2011).

Peripheral blood mononuclear cells

A 10 mL volume of blood was collected fresh in EDTA (ethylenediaminetetraacetic acid) tubes (BD Biosciences, North Ryde, NSW, Australia) and sent directly to the laboratory for immediate processing. PBMC were isolated from blood using the Ficoll paque method (Figure 2.1).

First, the plasma was separated from the blood cells by centrifugation at 423 x g for 15 min at RT. Approximately 2 to 3 mL of plasma was removed and transferred in aliquots to 1.5 mL microcentrifuge tubes and centrifuged again (1579 x g for 10 min at RT) to remove cellular debris. The plasma was then transferred in aliquots to 600 µL tubes and stored at -80°C. The remaining blood was transferred into a 15 mL centrifuge tube and an equal volume of prewarmed PBS was then added and mixed well by inverting the tube five times. The diluted blood was then carefully overlaid onto Ficoll (GE Healthcare Life Sciences, Piscataway, New Jersey, USA), 3 mL of Ficoll was used per 10 mL of diluted blood (Figure 2.1). The tube was then centrifuged at 753 x g for 20 min at 22°C with settings: acceleration, 9 and deceleration, 2 (Heraeus XR3 Multifuge). The buffy coat containing the mononuclear layer of blood cells was then collected into 2 mL microcentrifuge

tubes (Axygen; Fisher Biotech) using a syringe and cannula (BD Biosciences). The tubes were made up to 1.5 mL with pre-warmed PBS and centrifuged at $135 \times g$ for 10 min at RT to wash the PBMC. The supernatant was discarded and the cell pellet resuspended in prewarmed RPMI 1640 medium.

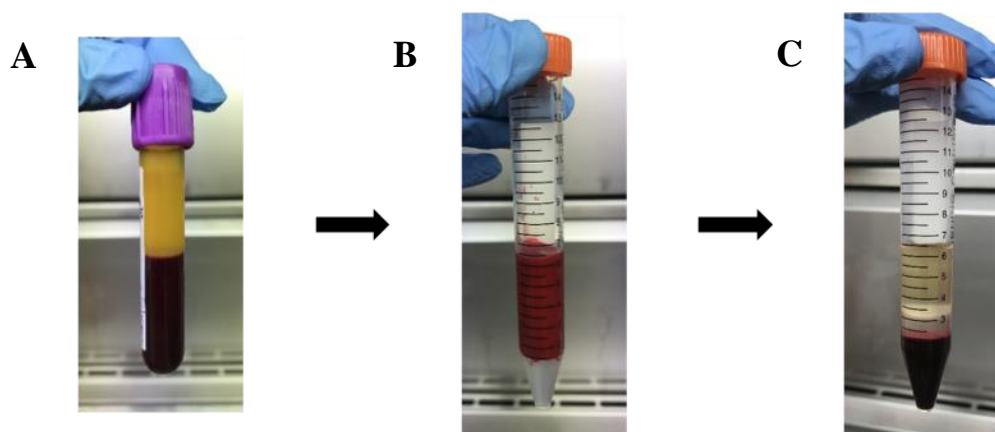


Figure 2.1. Processing blood to separate peripheral blood mononuclear cells using the standard Ficoll method.

(A) Patient blood collected in an EDTA tube was centrifuged ($423 \times g$ for 15 min at RT) to separate the plasma. (B) PBS diluted blood sample was overlaid onto Ficoll solution and centrifuged at $753 \times g$ for 20 min at 22°C . (C) After centrifugation, the PBMC layers (found at the interface between the plasma and the Ficoll solution) were collected.

2.5.2. Preparation of non-specific mitogens

Phytohaemagglutinin (PHA) (Roche; Sigma-Aldrich), lipopolysaccharide (LPS) (Sigma-Aldrich), staphylococcal enterotoxin A (SEA) (Sigma-Aldrich) and toxic shock syndrome-1 (TSST-1) (Sigma-Aldrich) were reconstituted in RPMI 1640 medium and made up at eleven times the desired final concentration, filter sterilised (Millex; Merck Millipore Ltd., Carrigtwohill, County Cork, Ireland) and stored in aliquots at -20°C as described previously by Vickery et al. (1995). Concentrations of 5 and $10 \mu\text{g/mL}$ of each mitogen prepared in RPMI 1640 medium were used to stimulate cell proliferation.

2.5.3. Subculturing of tumour cells/cell lines

ALCL cells were grown in DMEM supplemented with 10% heat-inactivated FBS and 1% penicillin/streptomycin solution as detailed above.

MT-4 cells were grown in Roswell Park Memorial Institute (RPMI) 1640 medium, containing 2 mM L-glutamine (Gibco; Thermo Fisher Scientific) and supplemented with 10% heat-inactivated FBS and 1% penicillin/streptomycin solution.

Cells were maintained at a volume of 10 mL in 25 cm² cell culture flasks (Falcon; In Vitro Technologies, Noble Park, Victoria, Australia) at 37°C in a 5% carbon dioxide (CO₂) cell culture incubator and a relative humidity of 95% (Sanyo Electric Medical System Co., Tokyo, Japan). Cells were observed under a phase-contrast microscope (Nikon Diaphot 300, Melville, New York, USA), and split at three- to four-day intervals for ALCL cells and every three days for MT-4 cells.

2.5.4. Cell counts and viability

Cell counts were determined with a Neubauer haemocytometer (Marienfeld, Lauda-Königshofen, Germany) and viability was assessed by trypan blue dye exclusion. Cells (10 µL) were transferred to a 600 µL microcentrifuge tube (Axygen; Fisher Biotech) containing 10 µL of 0.3% trypan blue solution (Sigma-Aldrich), mixed and allowed to stand for one minute. The cell suspension (10 µL) was then transferred to the edge of the haemocytometer cell chamber and allowed to flow into the chamber by capillary action until filled. The number of viable cells (do not take up the trypan blue stain) were counted on a light microscope and viability was determined by the following:

$$\text{Cell viability (\% viability)} = \frac{\text{Total cells} - \text{Dead cells}}{\text{Total cells}} \times 100$$

Concentration (viable cells/mL)

$$= \frac{\text{Number of viable cells}}{\text{Number of squares counted}} \times \text{Dilution factor} \times 10^4$$

2.5.5. Freezing of cells for long-term storage

Culture flasks were removed from the 5% CO₂ incubator and 10 mL of cells were transferred to a 15 mL centrifuge tube. The tube was centrifuged at 753 x g for 5 min at RT and the supernatant was removed and discarded. Cells were suspended at 1 x 10⁶ cells/mL in 10% dimethyl sulfoxide (DMSO) (Sigma-Aldrich), 20% FBS, 70% culture medium for ALCL and MT-4 cells or in 10% DMSO, 20% RPMI 1640 medium, 70% FBS for PBMC, and frozen in 1 mL aliquots in a 2 mL cryogenic vial (Corning; Sigma-Aldrich). The vial was transferred into a “Mr. Frosty” container (Thermo Fisher Scientific) and put through the following series of freezing temperatures: 2 hr at 20°C, overnight at -80°C and then to vapour phase liquid nitrogen for long-term storage.

2.5.6. Thawing a frozen cell stock

Cryogenic vials were removed from vapour phase liquid nitrogen storage and thawed immediately in a 37°C water bath (Thermoline Scientific, Wetherill Park, NSW, Australia). The cells were thawed until about half of the sample had melted and the 1 mL of cells was then transferred to a 15 mL centrifuge tube containing 9 mL of pre-warmed DMEM. The tube was centrifuged at 753 x g for 5 min at RT to remove the DMSO and the supernatant discarded. Cells were resuspended in 1 mL of growth media (Section 2.5.3.) and transferred to a 25 cm² culture flask containing 9 mL of growth media and incubated at 37°C in a 5% CO₂ incubator.

2.6. Optimisation of *in vitro* bacterial attachment assays to breast implants

Since the inception of the first breast implant at least 240 styles and 8300 models have been reported and manufactured (Barr et al., 2017). Texturing of the outer surface shell was introduced in an attempt to produce better tissue ingrowth and reduce the incidence of capsular contracture. Currently available textured implants are manufactured using four techniques: salt-loss, gas diffusion and imprinting as well as a more recently released surface which claims a novel “nano” texture remains proprietary (Section 1.1.1.). These techniques came from the need to produce texture on the outer silicone shell in the face of the changing breast implant market and the belief that texture is beneficial (Barr et al., 2017).

To date, all cases of BIA-ALCL have occurred in women with textured implants and implants with a higher surface area texture carry a 14 times higher risk of causing BIA-ALCL compared with low surface area textured implants (Loch-Wilkinson et al., 2017, de Boer et al., 2018). It is hypothesised that BIA-ALCL results from chronic bacterial antigenic stimulation and sustained proliferation that potentially leads to malignant transformation. The lymphocytic response has been shown in both the pig and human, to be positively associated with the number of contaminating bacteria (Hu et al., 2015). Therefore, it is expected that more bacteria could attach to textured implants as they have a larger surface area and hence attachment sites when compared with smooth implants.

Textured implants have been shown to support higher rates of bacterial adhesion and biofilm development *in vitro*, utilising miniature textured and smooth implants (Jacombs et al., 2014). Similarly, in a prospective clinical study involving implants removed from patients with Baker grade IV contracture, Hu et al. (2015) showed significantly more bacteria were attached to textured implants than smooth implants. However, the miniature implants tested in Jacombs et al.’s (2014) study were specifically made for a pig study and hence were experimental and may have had slightly different surface physiochemical properties when compared with clinical implants. In

any case, the miniature implants were obtained from only one manufacturer and may not have been representative of implants obtained from other manufacturers. In contrast, Hu et al.'s (2015) study utilised clinical implants but the study included very low numbers of some types of implants. In addition, as these implants were obtained clinically, the individual host response to bacterial contamination and biofilm formation may have varied from individual to individual, whilst the time from implantation to explantation and the species/strain of bacteria detected varied from patient to patient.

A series of experiments were performed to optimise an *in vitro* attachment assay, using *Staphylococcus* species, since these bacterial species are associated with 70% of contracted breasts and are frequently implicated in causing implant-related infections (Arciola et al., 2012, Ribeiro et al., 2012, Deva et al., 2013).

2.6.1. Optimisation methods

2.6.1.1. Preparation of breast implants

Breast implants were prepared by removing the silicone gel using the blunt edge of a knife. A strip of implant shell was then cut from the whole implant (Figure 2.2A). Using a 5 mm biopsy punch (Kai Industries Co., Ltd., Solingen, Germany), 5 mm diameter sections were then cut from the implant shell (Figure 2.2B).

Each 5 mm implant was carefully transferred with the outer surface down to a 100 mm x 15 mm glass petri dish (Pyrex; Corning Inc., Corning, New York, USA) and dry heat sterilised at 115°C for 39 hr, which is the standard procedure used by manufacturers in the sterilisation of breast implants (Davila, Research and Development, Mentor Worldwide LLC, personal communication, June 8, 2015). The number of bacteria attaching at 2, 6 and 24 hr was determined using three biological replicates. Each replicate consisted of four 5 mm sections of implant.

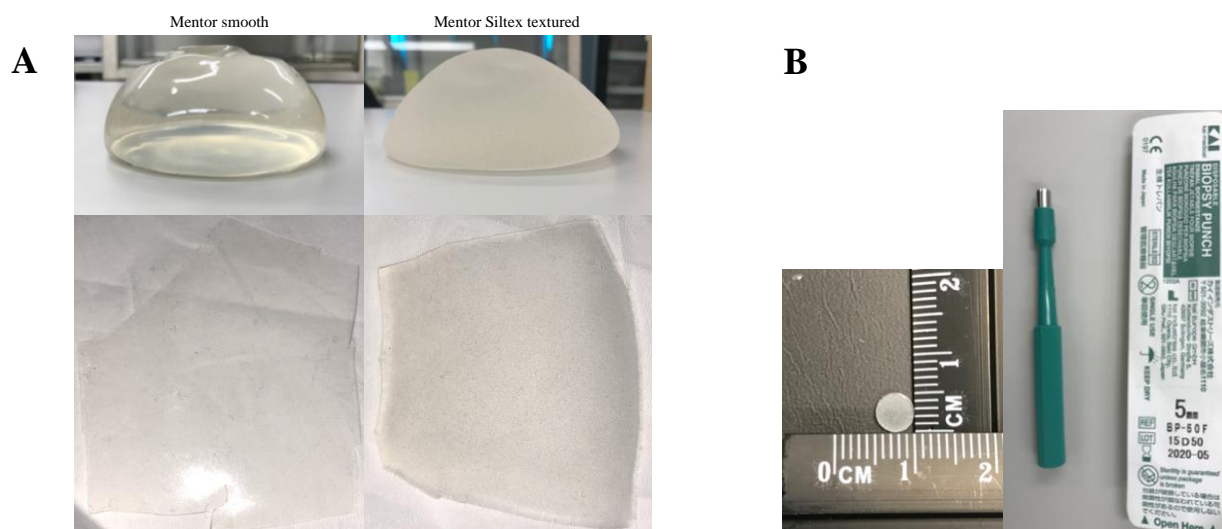


Figure 2.2. Preparation of smooth and textured breast implants for *in vitro* bacterial attachment assays.

(A) Smooth and textured breast implants were prepared by removing the silicone gel and then cutting a strip of implant shell from the whole implant. (B) 5 mm diameter sections were cut from the breast implant shell using a biopsy punch and carefully transferred with the outer surface down to a glass petri dish and dry heat sterilised at 115 °C for 39 hr.

2.6.1.2. Bacterial strains and culture conditions

S. aureus strain ATCC 25923 and *S. epidermidis* strain ATCC 35984 were used for optimisation of the *in vitro* attachment assays and prepared as detailed in Section 2.1.2.

2.6.1.3. Breast implant textures

Table 2.3 describes the different implant surface types utilised for the *in vitro* bacterial attachment assays.

2.6.1.4. Experiment 1: *In vitro* bacterial attachment assay

Approximately 10^8 bacterial cells/mL were diluted 1:10 in PBS to give roughly 10^7 cells/mL. For the *in vitro* attachment assays, this concentration was further diluted 1:100 in 10% TSB to give approximately 10^5 cells/mL. Fifteen mL of which was added to the petri dish containing the 5 mm implants and incubated at 37°C for either 2, 6 or 24 hr (Figure 2.3). At the end of each incubation

Table 2.3. Summary of the eleven breast implant surface types tested for bacterial attachment and growth *in vitro*.





Implant type		Surface type	Manufacturing type	Manufacturer
Allergan Biocell		Texture	Salt-loss	Allergan, Dublin, Ireland
Allergan Natrelle		Smooth	Dipping a mandrel into liquid silicone creating multi layers. The surface is then cured in a laminar flow oven.	Allergan, Dublin, Ireland
Eurosilicone		Texture	Salt-loss	Eurosilicone, Cedex, France
Mentor Siltex		Texture	Imprinting	Mentor Worldwide LLC, Irvine, California, USA

Table 2.3. Continued.






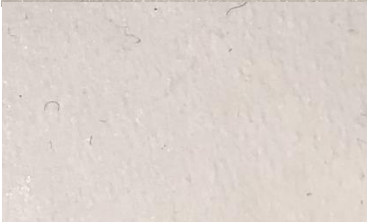
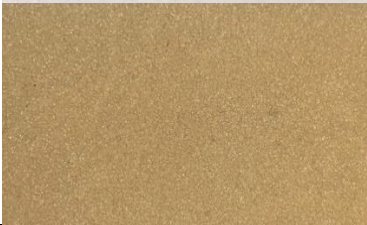
Implant type		Surface type	Manufacturing type	Manufacturer
Mentor Smooth		Smooth	Dipping a mandrel into liquid silicone creating multi layers. The surface is then cured in a laminar flow oven.	Mentor Worldwide LLC, Irvine, California, USA
Motiva SilkSurface		Texture	Unknown	Motiva, Alajuela, Costa Rica
Motiva VelvetSurface		Texture	Unknown	Motiva, Alajuela, Costa Rica
Nagor Nagotex		Texture	Salt-loss	Nagor Ltd., Glasgow, UK

Table 2.3. Continued.

Implant type		Surface type	Manufacturing type	Manufacturer
Polytech Mesmo		Texture	Gas diffusion (ammonium carbonate)	Polytech health and aesthetics, Dieburg, Hesse, Germany
Sientra		Smooth	Dipping a mandrel into liquid silicone creating multi layers. The surface is then cured in a laminar flow oven.	Sientra, Santa Barbara, California, USA
Silimed Polyurethane		Texture	Polyurethane bonded foam	Sientra, Dallas, Texas, USA

time, the bacterial culture was carefully removed using a pipette and discarded. Fifteen mL of PBS was added to the petri dish and the implants were washed by gently swirling the dish around to remove loosely adhered bacteria. The PBS was removed and discarded. This was repeated three times. The number of bacteria attached to implant sections was determined as per Section 2.2.1.

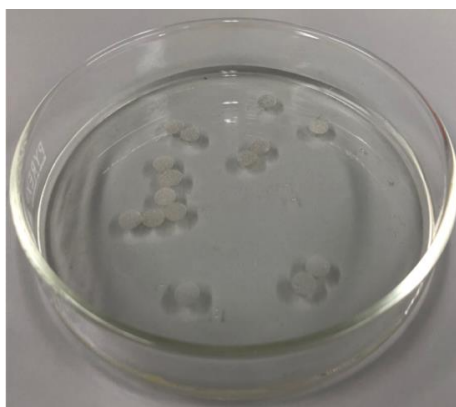


Figure 2.3. *In vitro* bacterial attachment assay for breast implants.

15 mL of 10^5 bacterial cells/mL was carefully added to the petri dish containing the sterilised 5 mm diameter implants and incubated at 37 °C for either 2, 6 or 24 hr.

2.6.1.5. Statistical analysis

All statistical analyses were performed with GraphPad Prism 7.0 (GraphPad Software Inc., San Diego, California, USA). The data were tested for normality of distribution by the D'Agostino and Pearson or Shapiro-Wilk normality test. To determine the number of bacteria attached to the different implant surface types tested after 2, 6 and 24 hr incubation, we used one-way analysis of variance (ANOVA) with Tukey's multiple comparisons or two-way ANOVA with Sidak's multiple comparisons post-hoc tests for normally distributed data. For data that were not normally distributed, Kruskal-Wallis non-parametric ANOVA followed by Dunn's pairwise multiple comparisons was utilised. *P* values less than or equal to 0.05 were considered statistically significant. Values are expressed as the mean number of bacteria attached to the implant per cm² implant \pm standard deviation (SD).

2.6.2. Results

We found no significant difference between smooth and textured surface implants in the number of *S. aureus* (Figure 2.4A) or *S. epidermidis* (Figure 2.4B) attached after 2, 6 or 24 hr ($P > 0.05$). Although, greater bacterial attachment was observed in the smooth implant (*S. aureus*/cm² implant: 2.26×10^5 (2 hr), 2.90×10^6 (24 hr); *S. epidermidis*: 1.19×10^6 (2 hr), 3.17×10^6 (6 hr), 2.97×10^6 (24 hr)) than in the textured implant (*S. aureus*: 8.97×10^4 (2 hr), 2.68×10^6 (24 hr); *S. epidermidis*: 3.93×10^5 (2 hr), 1.14×10^6 (6 hr), 8.63×10^5 (24 hr)). This was unexpected, since textured implants have been shown to support a higher bacterial load *in vivo* and in an *in vitro* assay where whole miniature implants were used (Jacombs et al., 2014, Hu et al., 2015). We attributed this to the difficulty we had in removing the silicone, which adhered firmly to the inner surface side of the smooth implant. In contrast, we did not have this issue with the textured implant, where the silicone separated quite easily from the inner shell. It was important to remove the residual silicone since its adhesive properties could encourage greater bacterial attachment to the implant and lead to false-positive results and account for high numbers of bacteria attached to the smooth implant (Figure 2.4B).

We found from 6 to 24 hr incubation with *S. aureus*, there was only a three-fold increase in the number of bacteria attached to the implants (Figure 2.4A). While incubation with *S. epidermidis* resulted in a decrease in attachment from 6 to 24 hr (Figure 2.4B). This is somewhat surprising since *S. aureus* and *S. epidermidis* are not fastidious organisms and will grow readily on commonly used media and under a variety of conditions (Rowlinson et al., 2006). It is likely the issues we encountered in removing the silicone residue from the inner implant shell could have affected attachment in this initial optimisation experiment. Therefore, in the next experiment we tested different methods to completely remove residual silicone from the inner surface of implants.

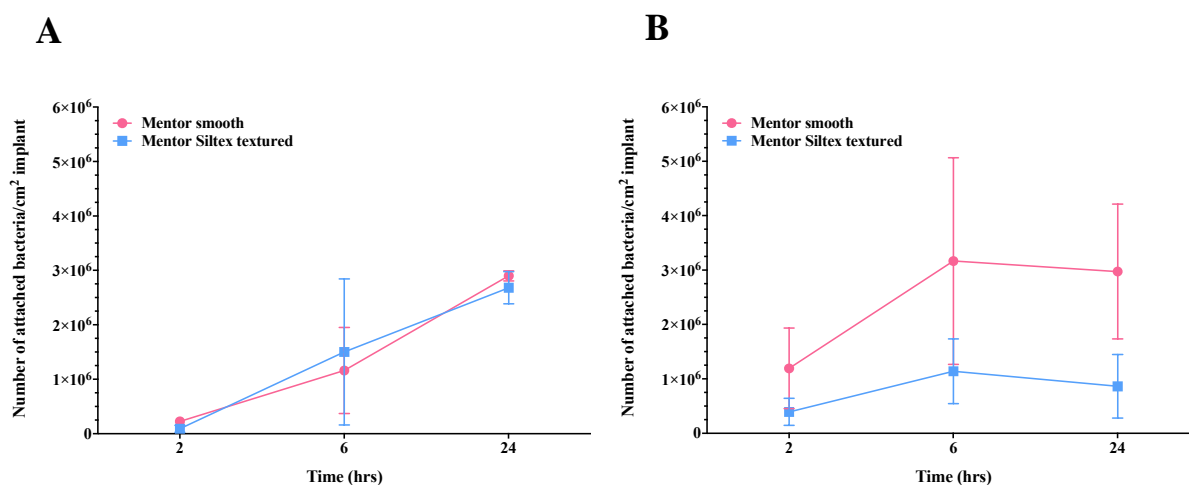


Figure 2.4. The number of (A) *S. aureus* and (B) *S. epidermidis* attached to Mentor smooth and Mentor textured implants following incubation in 15 mL of 10^5 bacterial cells/mL at 2, 6 and 24 hr. Values are the means \pm SD of three biological replicates.

2.6.3. Experiment 2: Optimisation of removal of residual silicone from the inner surface of smooth implants

The aim of this experiment was to remove the residual silicone from the inner surface side of the implant by testing three different methods: (i) using the blunt edge of a knife, (ii) using the blunt edge of a knife wrapped in gauze (Multigate Medical Products Pty. Ltd., Villawood, NSW, Australia) and (iii) using the blunt edge of a knife wrapped in gauze that had been soaked with detergent. Five mm diameter sections were then cut from the implant shell, dry heat sterilised and the attachment of *S. epidermidis* to Mentor smooth implants determined following 2, 6 and 24 hr incubation in triplicate as described in Sections 2.6.1.1. to 2.6.1.4.

Results

We found no significant difference among the three different methods tested in the number of bacteria attached to smooth implants after 2 (method i, 2.00×10^3 ; ii, 1.65×10^3 ; iii, 2.57×10^3), 6 (i, 1.90×10^4 ; ii, 7.93×10^4 ; iii, 6.60×10^4) or 24 hr (i, 7.97×10^5 ; ii, 1.07×10^6 ; iii, 2.95×10^5), *P*

> 0.05 (Figure 2.5). In this experiment, there was a ten-fold increase in *S. epidermidis* attachment from 6 to 24 hr, which was higher than the numbers found in the previous experiment (Section 2.6.2.). Although no significant differences were found, in practice, we found using the blunt edge of a knife alone was the most easy and effective in removing the residual silicone compared to the other methods tested. It also avoided possible bias of results from microfibrils of gauze or residual detergent being left on the implant. Therefore, in all subsequent experiments performed, we used this method to scrape away any residual silicone from the inner surface of implants we tested.

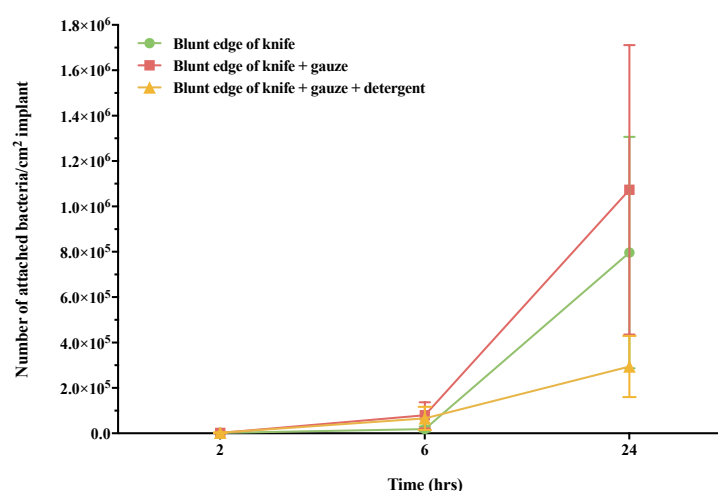


Figure 2.5. The number of *S. epidermidis* attached to Mentor smooth implants using different methods to remove silicone from their inner surface. Values are the means \pm SD of three biological replicates.

2.6.4. Experiment 3: Comparison of *S. epidermidis* attachment to Mentor smooth and Mentor Siltex following removal of silicone from the inner surface of implants

The aim of this experiment was to remove the silicone from the inner surface of the implants using the blunt edge of a knife and to repeat the experiment outlined in Section 2.6.2.

Results

We found Mentor Siltex textured implants (8.56×10^5) had higher numbers of bacteria attached after 24 hr compared to Mentor smooth surface implants (1.53×10^5), although this was not significant ($P > 0.05$) with a high standard deviation in CFU/mL among the triplicate samples tested (Figure 2.6). Nevertheless, these findings are in line with our hypothesis and the wider literature that textured surface implants support a higher bacterial load (Jacombs et al., 2014, Hu et al., 2015).

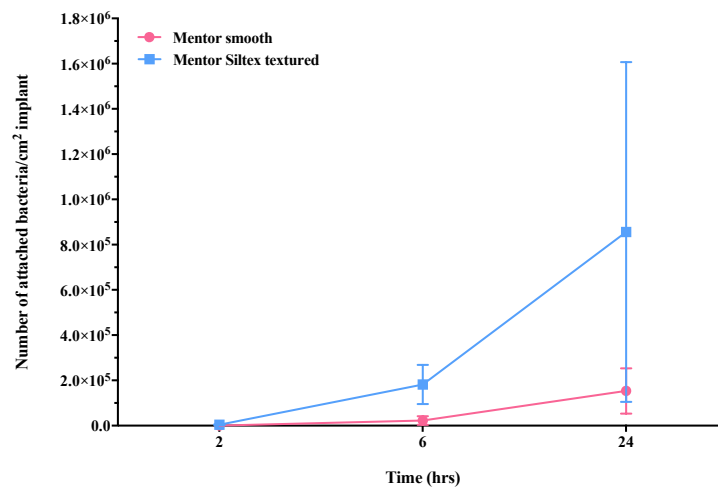


Figure 2.6. The number of *S. epidermidis* attached to Mentor smooth and Mentor textured implants following silicone removal using a blunt knife. Values are the means \pm SD of three biological replicates.

2.6.5. Testing bacterial attachment and growth *in vitro* on breast implants with different surface morphology

The aim of this experiment was to measure bacterial attachment to the surface of smooth and differently textured breast implants.

Eight implant surface types were tested, including textured implants, Allergan Biocell, Eurosilicone, McGhan, Mentor Siltex, Polytech Mesmo, Silimed Polyurethane (PU), Nagor

Nagotex and Mentor smooth implants, as described in Table 2.3, Section 2.6.1.3. The residual silicone was removed with the blunt edge of a knife. The attachment assay was conducted using *S. epidermidis* (Section 2.6.1.2.), and numbers of attached bacteria determined at 2, 6 and 24 hr incubation in triplicate.

Results

Silimed PU textured implants had a significantly higher number of bacteria attached compared to Mentor smooth implants after 2 (Silimed PU, 6.37×10^4 ; Mentor smooth, 2.57×10^2), 6 (Silimed PU, 4.32×10^5 ; Mentor smooth, 9.33×10^2) and 24 hr (Silimed PU, 4.69×10^7 ; Mentor smooth, 6.57×10^4), $P < 0.05$. This was predicted since Silimed PU implants appear to be more textured compared to the other implants tested. However, we also found inconsistencies with the number of bacteria attached among the different textured implant types. For example, at 24 hr Mentor Siltex (1.04×10^7) had higher bacterial attachment compared to McGhan (9.37×10^6), Eurosilicone (7.93×10^6) and Polytech Mesmo (3.11×10^6) textured implants, even though the latter types appear to have more textured outer surfaces, although not significant, $P > 0.05$ (Table 2.3 and Figure 2.7).

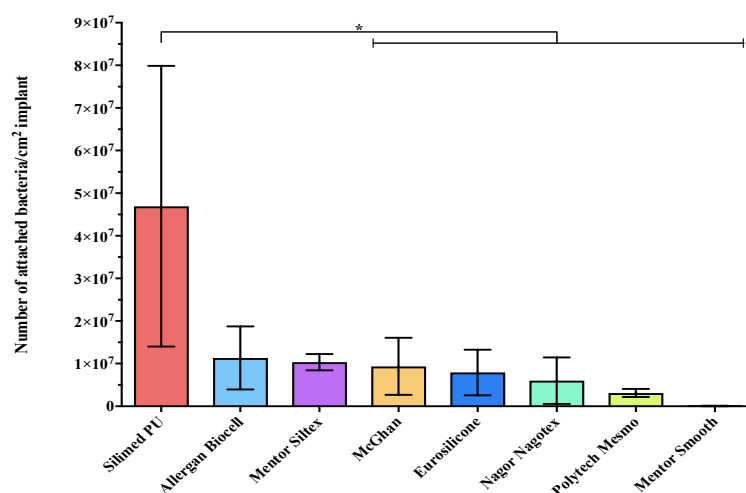


Figure 2.7. The number of *S. epidermidis* attached to breast implants with different surface morphology at the 24 hr time point. Values are the means \pm SD of three biological replicates. Significantly different at $*P \leq 0.05$.

We attributed this to a number of issues we encountered during this experiment.

1. Firstly, when we added the bacterial culture to the petri dish containing the implants, some implants would flip over onto their inner surface thus the wrong surface was in contact with the culture. Although we flipped these implants back, the inner surface was wet with the inoculum and hence bacteria present would be able to attach to the inner surface.
2. Preliminary microscopy analysis of the different textured implant types showed wide variation in their inner surfaces in regard to texture and hence we did not want this to affect bacterial attachment.
3. It was possible that air or dead space existed between the floating outer surface of the implants and the surface of the bacterial culture.

Therefore, to ensure experimental reproducibility it was important to (i) eliminate contact between the inner surface of the implant and the bacterial culture as much as possible and (ii) eliminate any air or dead space between the outer surface of the implant and the surface of the bacterial culture. In the next experiment, we tested whether initially floating the implants in sterile water would overcome this issue.

2.6.6. Comparison of immediate floating and prewetting of breast implants prior to bacterial attachment assay

The aim of this experiment was to test if pressing the implants outer surface down into sterile water to expel air and then allowing them to float to the surface of the water would prevent them from flipping over onto their inner surface and eliminate air/dead space when the bacterial inoculum is added. The number of bacteria attaching to Mentor Siltex textured breast implants was tested as outlined in Section 2.6.4. and compared to the new floating method where the implant surface was prewetted. Prewetting was achieved by adding 2 mL of sterile water to the petri dish

containing the sterile 5 mm implants and pressing the implants into the water to expel air. The implants were then allowed to float outer surface down and the bacterial inoculum carefully added to the petri dish and incubated at 37°C for either 2, 6 or 24 hr. Each condition contained three replicates.

Results

At the 24 hr time point more bacteria were attached to implants that had been subjected to prewetting (Prewetting, 1.88×10^7 ; Floating, 1.11×10^7), although this was not significant, $P > 0.05$ (Figure 2.8). However, prewetting of implants resulted in reduced numbers of implants flipping over with the majority of implants floating outer surface down thus limiting bacterial attachment to the inner surface of the implant. Extra implant sections were prepared so that any implants that did turn over were discarded and replaced. Therefore, in future experiments implants were prewetted.

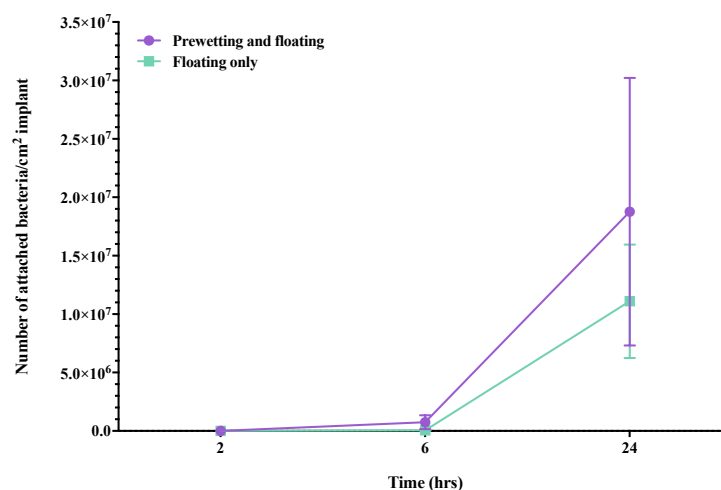


Figure 2.8. Effect of prewetting implants prior to incubation on the number of *S. epidermidis* attaching to Mentor textured implants. Values are the means \pm SD of three biological replicates.

2.7. Established *in vitro* bacterial attachment assay

Eight breast implant surface types were tested as shown in Table 2.3. Implants were prepared as detailed in Section 2.6.1.1., residual silicone was removed from the inner surface of implant shells using a blunt knife. Implant surfaces were prewetted with sterile water and then pressed into the water to expel air prior to adding the bacterial inoculum (Section 2.6.6.). The number of attached bacteria was determined following 2, 6 and 24 hr incubation with *S. epidermidis*. Each condition contained five replicates.

Results

We found the more textured the breast implant surface, the more bacteria there were attached after 2 and 24 hr (Figures 2.9 and 2.11). At the 2 hr time point, Silimed PU textured implants (2.12×10^4) had significantly higher numbers of bacteria attached compared to the surface of smooth (2.44×10^3) and differently textured breast implants, $P < 0.05$ (Figure 2.9). While McGhan textured implants (1.33×10^4) had significantly more bacteria attached when compared to Eurosilicone (4.42×10^3), Mentor Siltex (2.52×10^3) and Mentor smooth surface implants, $P < 0.01$ (Figure 2.9). At the 24 hr time point, significantly more bacteria were attached to Silimed PU implants (1.11×10^7) when compared to McGhan (6.76×10^6), salt-loss manufactured implants (Nagor, 5.30×10^6 ; Allergan Biocell, 2.55×10^6 ; Eurosilicone, 1.44×10^6), Mentor Siltex (5.66×10^5) and Mentor smooth implants (4.27×10^5), $P < 0.05$ (Figure 2.11). Additionally, McGhan, Polytech Mesmo (6.08×10^6) and Nagor textured implants had significantly higher numbers of bacteria attached after 24 hr compared to Mentor smooth implants, $P < 0.05$ (Figure 2.11).

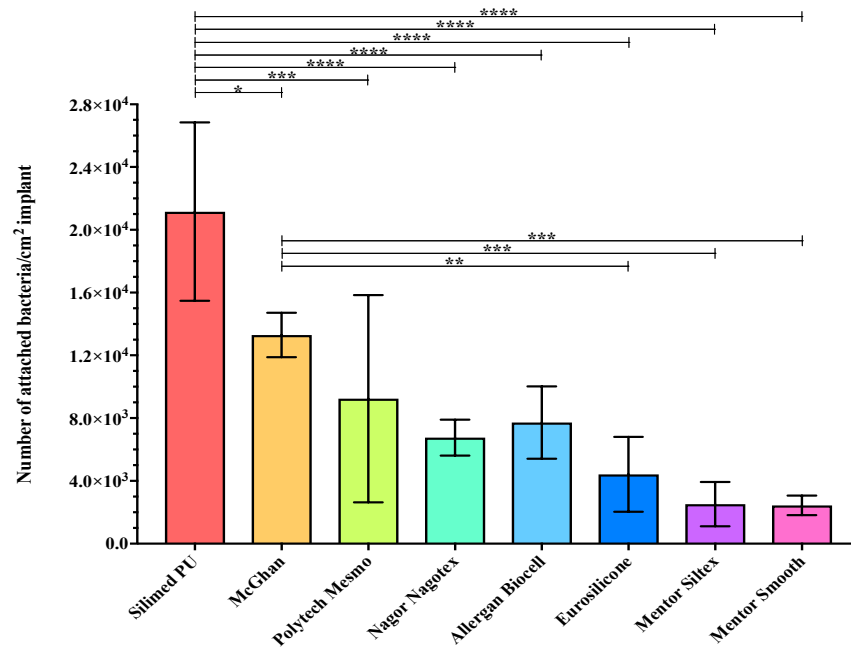


Figure 2.9. The number of *S. epidermidis* attached to various breast implant surface types at the 2 hr time point utilising the optimised study. Values are the means \pm SD of five biological replicates. Significantly different at $*P \leq 0.05$, $**P \leq 0.01$, $***P \leq 0.001$, $****P \leq 0.0001$.

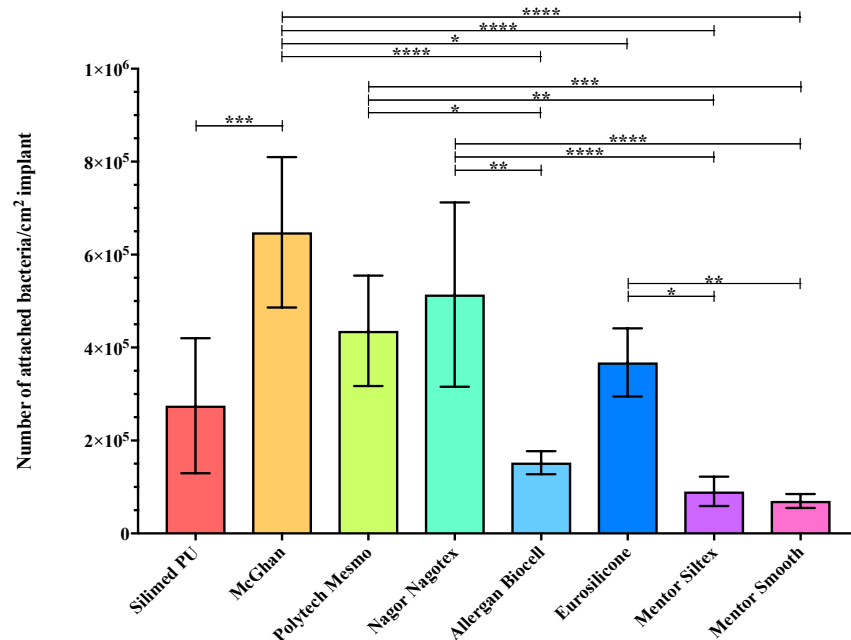


Figure 2.10. The number of *S. epidermidis* attached to various breast implant surface types at the 6 hr time point utilising the optimised study. Values are the means \pm SD of five biological replicates. Significantly different at $*P \leq 0.05$, $**P \leq 0.01$, $***P \leq 0.001$, $****P \leq 0.0001$.

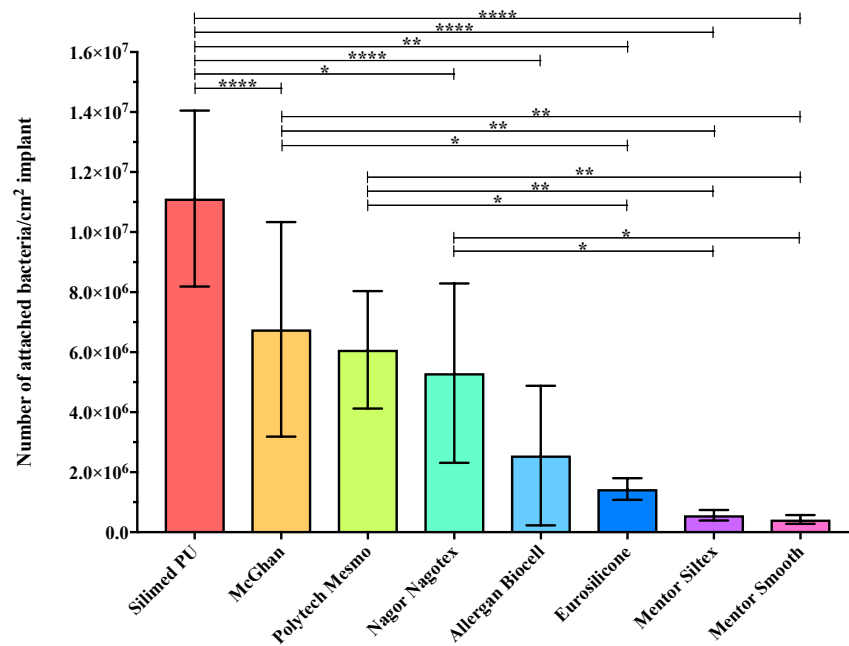


Figure 2.11. The number of *S. epidermidis* attached to various breast implant surface types at the 24 hr time point utilising the optimised study. Values are the means \pm SD of five biological replicates. Significantly different at $*P \leq 0.05$, $**P \leq 0.01$, $****P \leq 0.0001$.

At the 6 hr time point, McGhan textured implants (6.48×10^5) were found to have significantly more bacteria attached when compared to Silimed PU (2.75×10^5), Allergan Biocell (1.53×10^5), Eurosilicone (3.68×10^5), Mentor Siltex (9.06×10^4) and Mentor smooth implants (6.99×10^4), $P < 0.05$ (Figure 2.10). While Polytech Mesmo (4.36×10^5), Nagor (5.14×10^5) and Eurosilicone textured implants had significantly more bacteria attached compared to Mentor smooth implants, $P < 0.01$ (Figure 2.10). No significant difference was found in bacterial attachment between Silimed PU and Mentor smooth implants ($P > 0.05$) with a high standard deviation in the number of attached bacteria per cm^2 implant in Silimed PU implants (Figure 2.10). The differences in attachment to the Silimed PU, Polytech Mesmo and Allergan Biocell textured surfaces at 6 hr compared to the 2 and 24 hr time point could be because the bacteria were not well attached to the

implant surface. In contrast, at 2 hr, initial bacterial attachment is occurring and by the 24 hr time point, the bacteria have had more time to better attach to the implant.

Despite the variation in bacterial attachment among the different textured implants at the 6 hr time point, we still found more bacteria were attached to these surface types compared to smooth implants. Thus, these findings provide support to our hypothesis that a greater surface area, as occurs in textured breast implants, promotes higher bacterial attachment and subsequent growth.

In conclusion, we have established a protocol for determining the *in vitro* attachment of bacteria to the outer shell of breast implants. We used this newly optimised assay to investigate the *in vitro* attachment of bacterial pathogens, *S. aureus*, *P. aeruginosa* and *R. pickettii* on various breast implant surface types at the 24 hr time point only, as this time point resulted in greater variation among the differently textured implants.

Chapter III.

Candidate Contribution:

Dr. Phoebe Jones and the candidate developed and conducted the *in vitro* bacterial attachment experiments. Dr. Honghua Hu and Dr. Durdana Chowdhury performed the microscopy imaging. Dr. Matthew Foley performed the micro computed tomography scanning and surface area and surface roughness analysis. The candidate aided in result analysis and manuscript preparation.

Candidate overall contribution: 45%

The functional influence of breast implant outer shell morphology on bacterial attachment and growth

Jones P. *, **Mempin M.** *, Hu H. *, Chowdhury D. *, Foley M. **, Cooter R. ^, Adams Jr W. P. ‡, Vickery K. *, Deva A. K. *°

*Surgical Infection Research Group, Faculty of Medicine and Health Sciences, Macquarie University, Sydney, Australia

°Integrated Specialist Healthcare Education and Research Foundation, Australia

^Monash University, Melbourne, Australia

‡University of Texas Southwestern, USA

**Australian Centre for Microscopy & Microanalysis, University of Sydney, Sydney, Australia

All correspondence to

Anand K. Deva

Suite 301, 2 Technology Place, Macquarie Park NSW 2109

Email: Anand.deva@mq.edu.au

Declaration

Professor Deva is research coordinator and consultant to Allergan, Mentor (Johnson & Johnson), Sientra, Motiva and Acelity

Association Professor Vickery is research coordinator to Allergan, Mentor (Johnson & Johnson) and Acelity

Plastic and Reconstructive Surgery; October 2018; Accepted 31 March 2018

Abstract

Background: The introduction of texture to the outer shell of breast implants was aimed at increasing tissue incorporation and reducing capsular contracture. It has also been shown that textured surfaces promote a higher growth of bacteria and are linked to the development of breast implant-associated anaplastic large-cell lymphoma (BIA-ALCL).

Aims: We aimed to measure the surface area and surface roughness of 11 available implants. Additionally, we aimed to subject these implant shells to an *in vitro* bacterial attachment assay with four bacterial pathogens (*Staphylococcus epidermidis*, *S. aureus*, *Pseudomonas aeruginosa*, *Ralstonia pickettii*) and study the relationship between surface area, surface roughness and bacterial growth.

Results: Surface area measurement showed grouping of implants into high, intermediate, low and minimal. Surface roughness showed a correlation with surface area. The *in vitro* assay showed a significant linear relationship between surface area and bacterial attachment/growth. The high surface area/roughness implant texture grew significantly higher numbers of bacteria at 24 hours whilst the minimal surface area/roughness implant textures grew significantly less bacteria of all types at 24 hours. For intermediate and low surface area implants, some species differences were observed indicating possible affinity of specific bacterial species to surface morphology.

Conclusions: Implant shells should be reclassified using surface area/roughness into four categories (High/Intermediate/Low/Minimal). This classification is superior to the use of descriptive terms, such as macrotexture, microtexture and nanotexture, which are not well correlated with objective measurement and/or functional outcomes.

Introduction

The texturization of the outer shell of breast implants was first introduced in 1968 with the “Natural Y” implant which incorporated a 1.2 – 2 mm polyurethane foam coating on its outer surface (Ashley, 1972). It was proposed that this surface prevented organized alignment of myofibroblasts, reducing the risk of capsular contracture (Ashley, 1972). In 1991, a specific association between polyurethane and the carcinogen 2,4-toluenediamine (TDA) was reported (Chan et al., 1991b, Chan et al., 1991a). This led to voluntary withdrawal of polyurethane coated silicone implants in the USA, which is still in place. Alternative surface technologies to modify the outer silicone shell were introduced in an attempt to mimic the polyurethane surface. There are four processes for generating surface texture on the external silicone shell, salt-loss, gas diffusion and imprinting techniques (Henderson et al., 2015). A more recently released surface which claims a novel “nano” texture remains proprietary (Sforza et al., 2017).

The benefits of textured implants in reducing capsular contracture remains controversial. Systematic reviews of comparative clinical studies concluded texturization may reduce the incidence of early capsular contracture in subglandular augmentation (Barnsley et al., 2006, Wong et al., 2006). Many published reports lack adequate description of implant type, surgical technique and outcome assessment. Smaller comparative or split breast studies are evenly divided as to the benefit of texturization (Coleman et al., 1991, Hakelius and Ohlsen, 1992, Burkhardt and Demas, 1994, Burkhardt and Eades, 1995, Asplund et al., 1996, Malata et al., 1997, Tarpila et al., 1997a, Collis et al., 2000, Fagrell et al., 2001, Poepl et al., 2007, Stevens et al., 2013).

Previous published data has confirmed that textured implants are able to support higher rates of bacterial growth *in vitro* (Jacombs et al., 2014). Furthermore, there is a correlation between higher bacterial contamination and host response *in vivo* which suggests a threshold phenomenon where bacterial load triggers a host inflammatory response (Hu et al., 2015). More recently, bacterial

infection has been proposed as one of four factors that may play a role in the genesis of breast implant-associated anaplastic large-cell lymphoma (BIA-ALCL) (Loch-Wilkinson et al., 2017).

This study aimed to look at textures of varying morphology to study the relationship between surface area, roughness and capacity for bacterial attachment and growth *in vitro*.

Methods

Implant surfaces tested

Eleven implant surface types were subject to testing – Silimed Polyurethane (Sientra, Dallas, Texas), Polytech Mesmo (Polytech health and aesthetics, Dieburg, Germany), Mentor Siltex, Mentor Smooth (Mentor Worldwide LLC, Irvine, USA), Motiva SilkSurface and Motiva VelvetSurface (Motiva Alajuela, Costa Rica), Allergan Biocell (Allergan, Dublin, Ireland), Allergan Natrelle Smooth (Allergan, Dublin, Ireland), Nagor Nagotex (Nagor Ltd., Glasgow, UK), Sientra smooth (Santa Barbara, USA) and Eurosilicone textured (Eurosilicone Cedex, France).

Table 1 lists the manufacturing types for the various textured surfaces.

Table 1: Manufacturing process for textured implants.

Manufacturing type	Implant type
Polyurethane bonded foam	Silimed Polyurethane
Salt-loss	Allergan Biocell Eurosilicone texture Nagor Nagotex
Gas diffusion (ammonium carbonate)	Polytech Mesmo
Imprinting	Mentor Siltex
Unknown	Motiva SilkSurface Motiva VelvetSurface

Implant surfaces imaging

Scanning electron microscopy

Following fixation in 3% glutaraldehyde, samples (up to 1 cm²) were dehydrated in ethanol and immersion in hexamethyldisilazane (HMDS, Polysciences Inc., Warrington, PA, USA) for 3 minutes and the HMDS was allowed to evaporate overnight. Samples were mounted onto aluminium stubs (ProSciTech, Thuringowa, QLD, Australia) and sputter coated with 20 nm gold film in the Emitech K550 gold coater (West Sussex, England). The gold coated breast implant samples were visualized using a JEOL 6480LA scanning electron microscope (JEOL Ltd., Tokyo, Japan).

Micro CT scan

The specimens were mounted horizontally on a metal pin with adhesive before loading into a pin vice holder. These were then scanned in a Zeiss Xradia MicroXCT-400 system operating in absorption mode with peak source energy of 50 kV and beam current of 200 μ A (Carl Zeiss, Oberkochen, Germany). The projections were collected every 0.25 degrees over a total rotation of 180 degrees, with an exposure time of 3 seconds and saved as 16-bit images in a proprietary file format.

The projections were reconstructed using XMReconstructor v7.0.2817 (Zeiss Xradia) with consistent reconstruction parameters resulting in 2.2 μ m isotropic voxels.

Surface area and roughness measurements were taken from this model to calculate the various required material properties. Analysis was performed with Avizo 9.3 (FEI VSG) and FIJI (Schindelin et al., 2012), where a binarised model of the sample was produced by thresholding after noise-reduction filtering of the reconstructed slices.

Surface area determination

The 3D to 2D sample size surface area ratio was calculated by first measuring the surface area of the interface between the binarized sample and air (SA_{3D}) and then comparing it to the x-y dimensions of the sample itself (SA_{2D}) (Figure 1 Supplementary). All ratios were normalized to smooth implants.

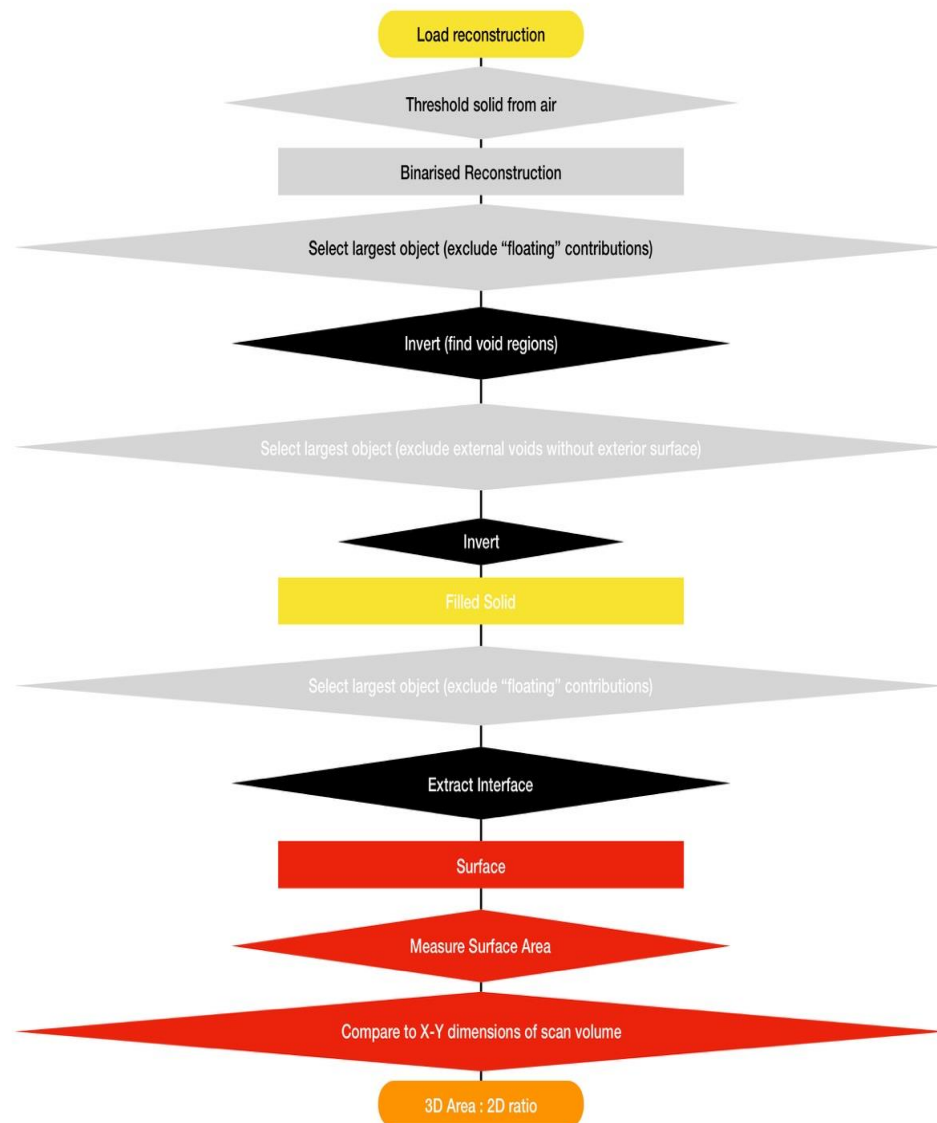


Figure 1 Supp: Algorithm for calculation of 3D area:2D ratio.

Surface roughness determination

To measure the roughness of the surface of each sample, it was necessary to first wrap the sample to avoid overhangs and cavities. To simplify things, a new surface was created by effectively dropping an infinitely thin probe towards the surface at each point. At the point of contact with the sample, the new surface was defined. The arithmetical mean deviation of the assessed profile (S_a) was calculated over this approximated surface via

$$S_a = \frac{1}{kn} \sum_{j=1}^k \sum_{i=1}^n |y_{ij} - \bar{y}|$$

where i and j represent column and row positions, y_{ij} is the surface height at (i, j) and \bar{y} is the mean surface height across the surface.

The roughness was expressed as a multiple of the value for smooth implants.

In vitro bacterial attachment assay

In vitro analysis was conducted on nine types of implants of varying morphology, against four bacterial types; *Staphylococcus epidermidis*, *S. aureus*, *Pseudomonas aeruginosa*, *Ralstonia pickettii*.

The implants were prepared by cutting a strip of implant shell from the whole implant and scraping away any residual silicone from the inner surface with the blunt edge of a knife. Sections of the implant shell were obtained using a 5 mm punch biopsy tool. The implant sections were placed outside surface down in a glass petri dish and sterilized under dry heat conditions at 115°C for 39 hours. Following sterilization, sterile water was added to each petri dish and the implants were pressed into the water and the air expelled. 10% tryptone soy broth containing 10^5 cells/ml of *S. epidermidis*, *S. aureus* and *R. pickettii* or 10^4 cells/ml of *P. aeruginosa* was then added to the petri dish and the implants were incubated at 37°C for up to 24 hours.

Implant samples were removed at 2, 6, and 24 hours for *S. epidermidis* and at 24 hours for *S. aureus*, *P. aeruginosa* and *R. pickettii* for colony-forming unit determination. The implant samples were washed three times in phosphate buffered saline. Four implant discs were placed in 0.5 mL of phosphate-buffered saline and subjected to sonication for 20 minutes followed by 1 minute of vortexing as described previously (Jacombs et al., 2014). Quantitative numbers of bacteria attached to the implant outer surface were determined by serial 10-fold dilutions and standard plate culture. Each condition was tested 5 times.

Statistical analysis

Statistical analysis was conducted using the statistical package Sigma Plot 13 (Systat Software, Inc., San Jose, California). For comparing different implant surfaces and bacterial attachment, the data was transformed and an Analysis of Variance (ANOVA) One-Way repeated measures analysis of variance was applied, and all pairwise multiple comparison procedures was performed using the Holm-Sidak method. If data was not normally distributed, the Kruskal-Wallis One-Way ANOVA on Ranks Test was performed, and all pairwise multiple comparison procedures conducted using Dunn's method. The relationship between implant 3D:2D surface area ratio and number of attached bacteria at 24 hours was tested using Pearson correlation if normally distributed or Spearman rank order correlation if non-normally distributed. $P < 0.05$ was set as significantly different.

Results

Scanning electron microscopy

Figures 1a-f demonstrate the surface morphology of some of the implants studied demonstrating a range of appearance from highly complex with many hidden surfaces to relatively featureless.

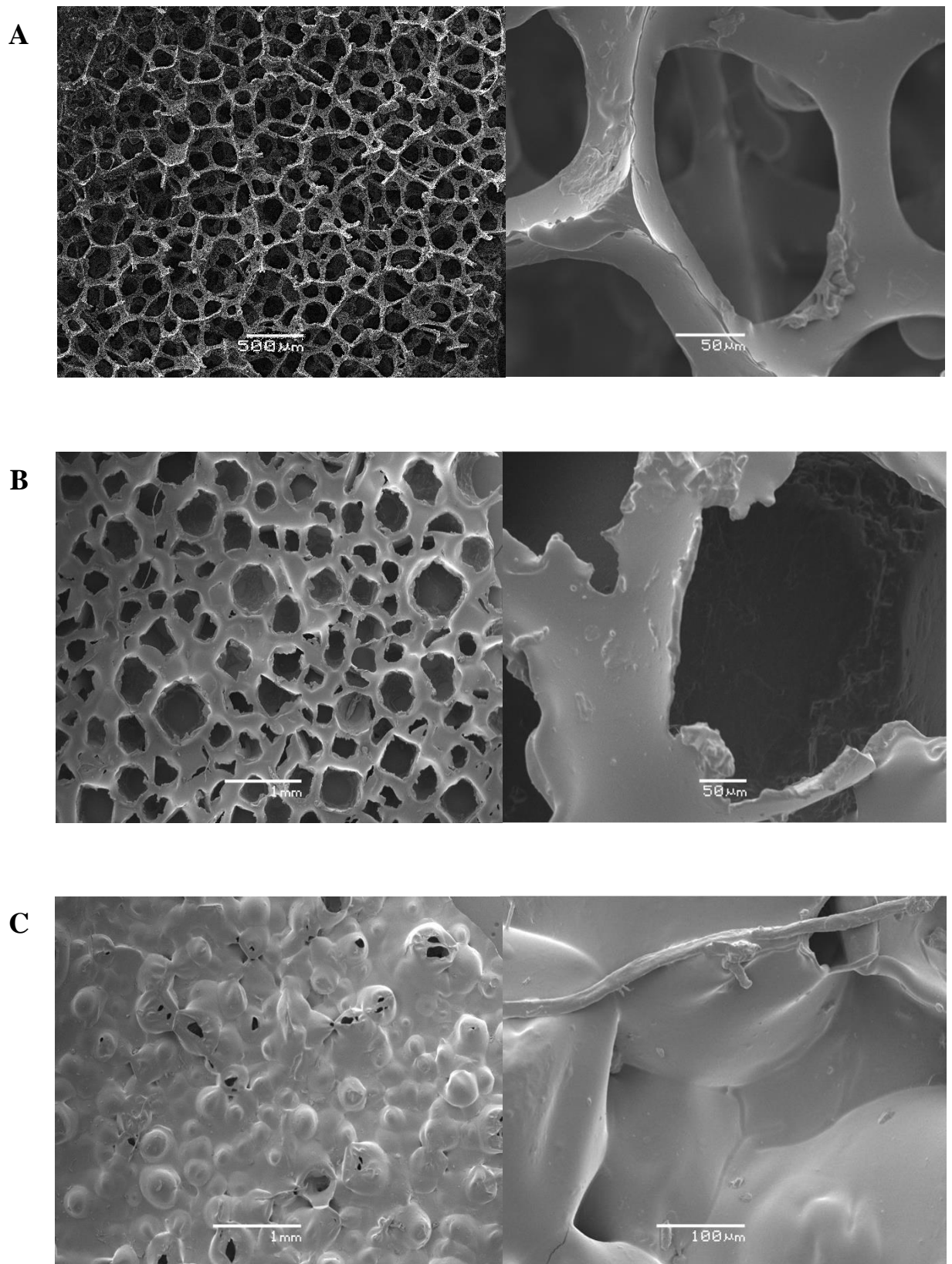


Figure 1: Scanning electron micrographs of surface morphology of implants studied at 25X and 400X magnification. (a) Silimed Polyurethane, (b) Eurosilicone, (c) Polytech Mesmo.

**Modified from published form to include additional scanning electron micrographs of implants.*

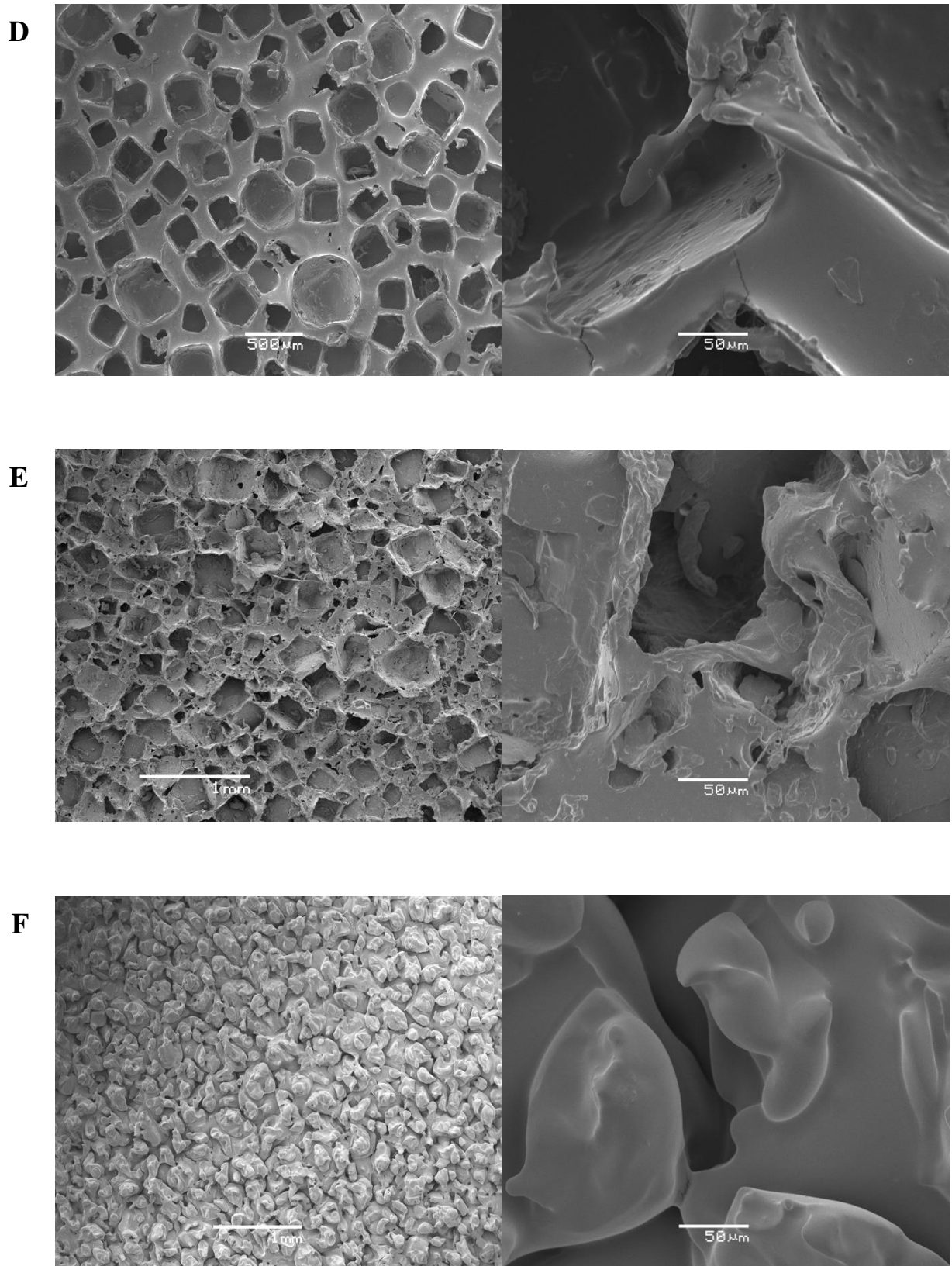


Figure 1: Continued. (d) Allergan Biocell, (e) Nagor Nagotex, (f) Mentor Siltex.

**Modified from published form to include additional scanning electron micrographs of implants.*

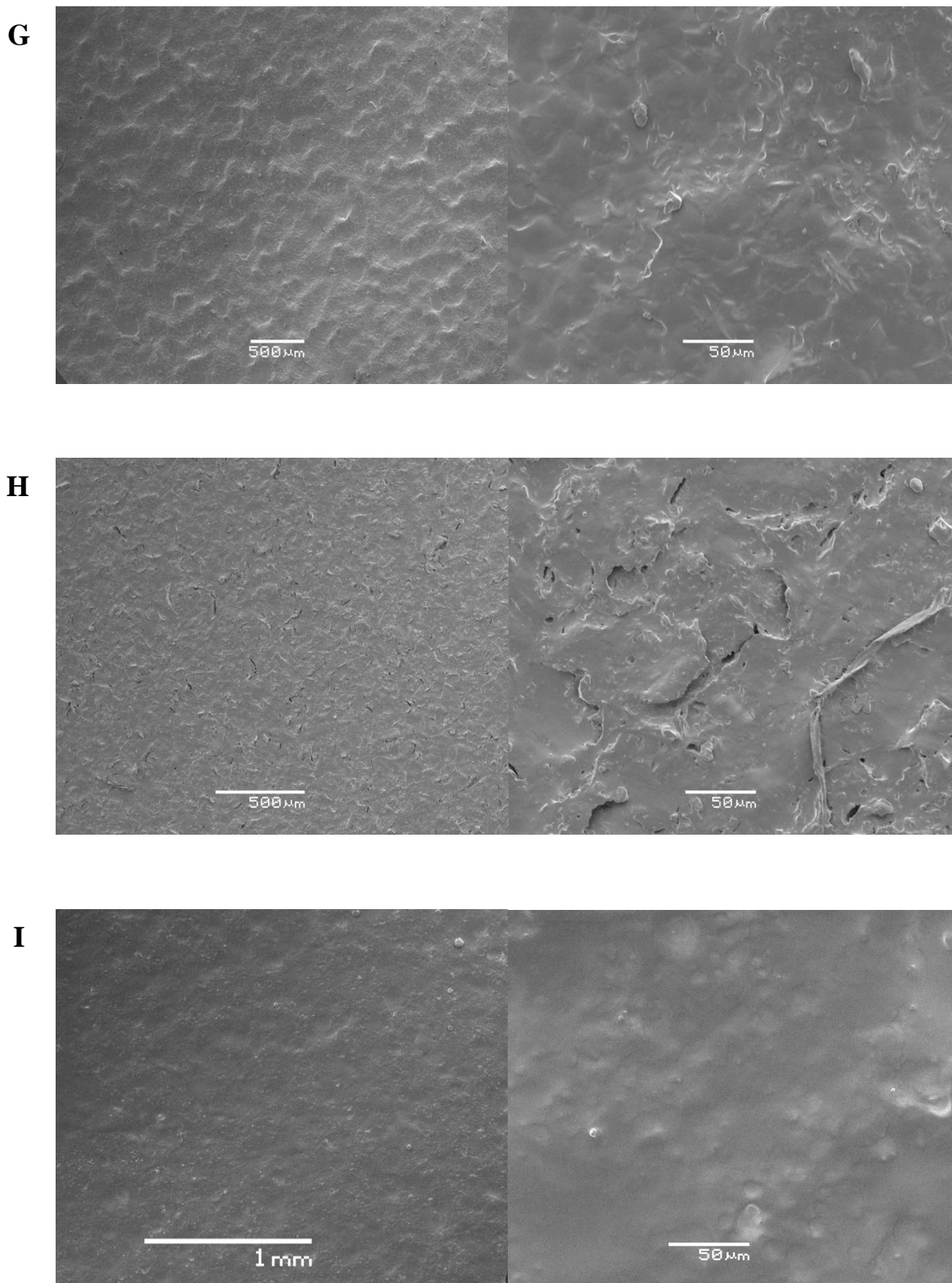


Figure 1: Continued. (g) Motiva VelvetSurface, (h) Motiva SilkSurface, (i) Mentor Smooth.

**Modified from published form to include additional scanning electron micrographs of implants.*

Surface area determination

Analysis using fine cut CT scans and confocal microscopy allowed visualization and calculation of surface area for each of the implant shells. Table 2 summarizes the findings.

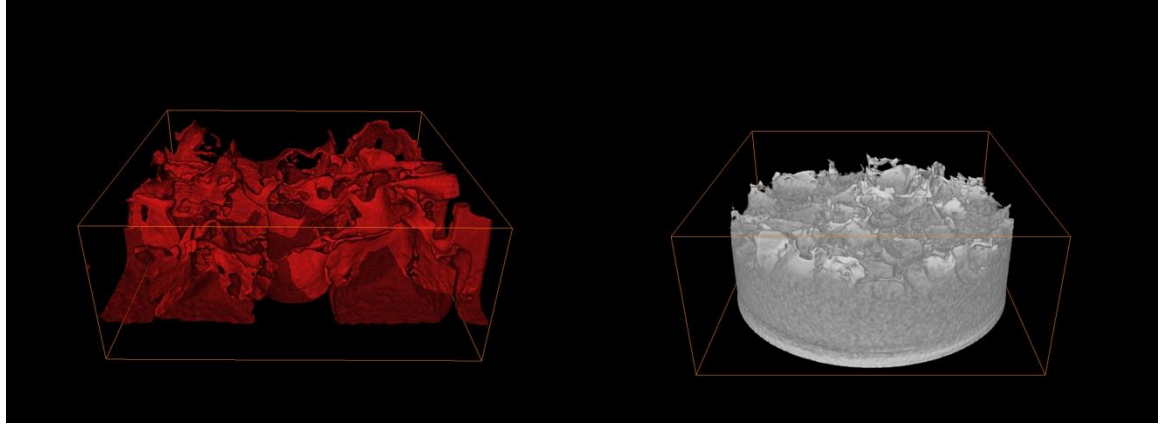
Table 2: Raw surface area calculation and 3D:2D ratio for each implant type.

Implant type	3D surface area (from 1.4 x 1.4 mm square)	3D:2D ratio [^]
Silimed Polyurethane	79 mm ²	20.8
Eurosilicone Textured	15 mm ²	3.9
Allergan Biocell	12 mm ²	3.2
Polytech Mesmo*	12 mm ²	3.2
Nagor Nagotex	10 mm ²	2.8
Mentor Siltex	8.1 mm ²	2.2
Motiva VelvetSurface	4.3 mm ²	1.2
Sientra Smooth	4.1 mm ²	1.1
Motiva SilkSurface	3.9 mm ²	1.1
Allergan Smooth	3.9 mm ²	1.0
Mentor Smooth	3.8 mm ²	1.0

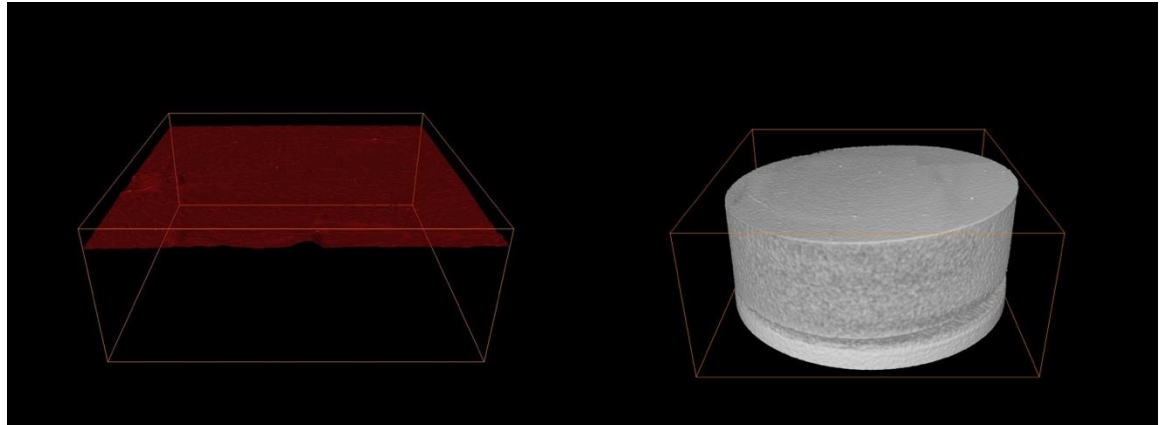
**Represents available surface area after exclusion of internal cavities, [^]normalized to Mentor Smooth*

Figures 2a-l show 3D surface area images, which were used for calculating the 3D:2D ratios for three of the implant surfaces. (See also Figures 2a-b Supplementary).

A



B



C

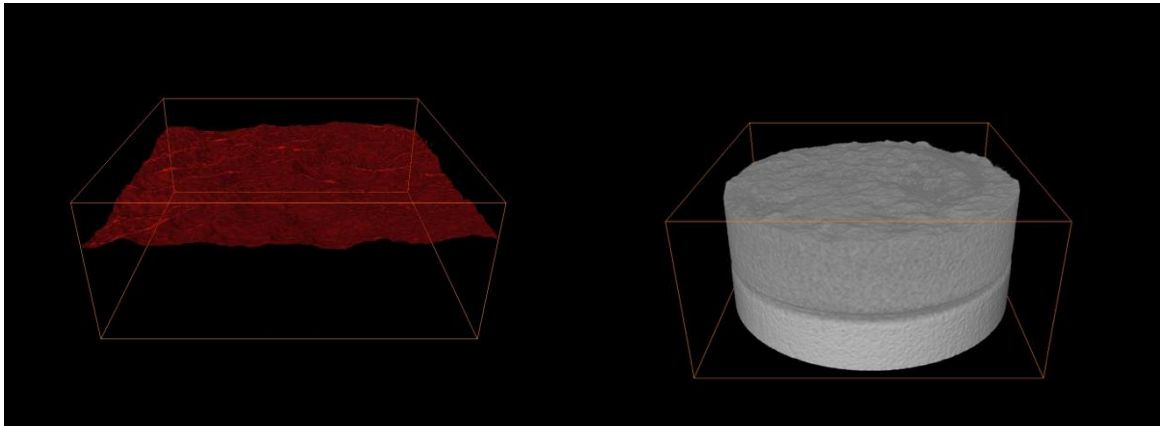
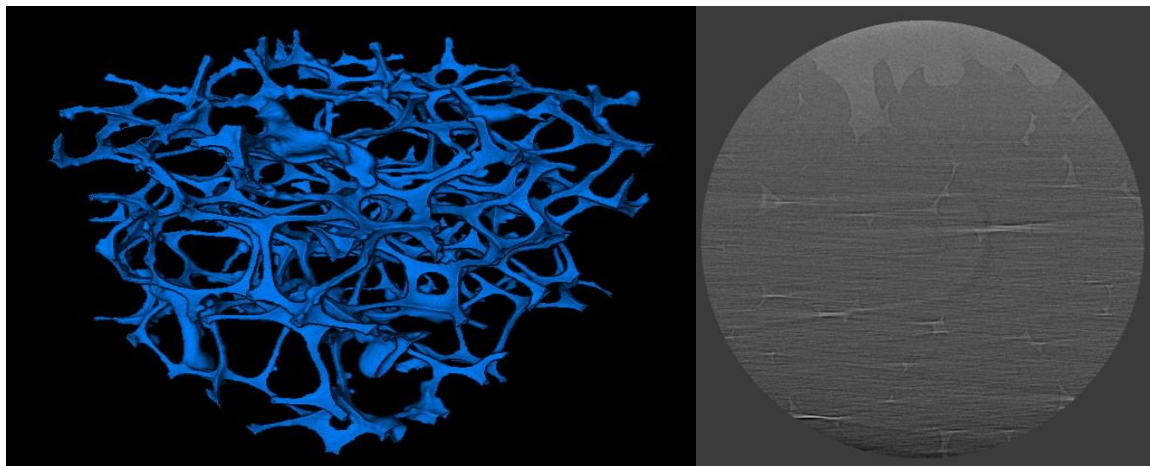


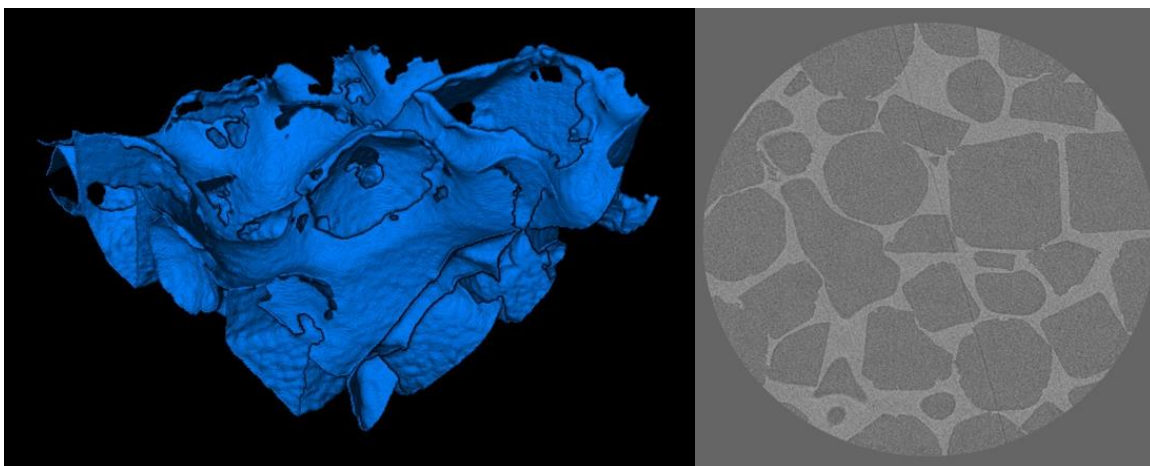
Figure 2: Samples of three-dimensional cross sections, extraction and greyscale reconstruction from micro CT analysis utilized for measurement of surface area/roughness. (a) Allergan Biocell, (b) Mentor Smooth, (c) Motiva VelvetSurface.

**Modified from published form to include additional three-dimensional cross sections, extraction and greyscale reconstructions.*

D



E



F

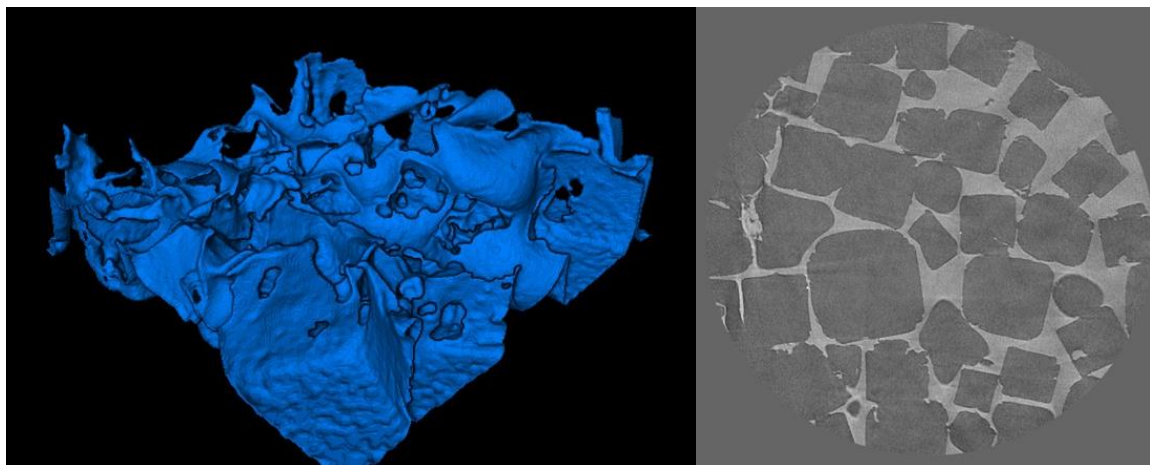


Figure 2: Continued. (d) Silimed Polyurethane, (e) Eurosilicone, (f) Allergan Biocell.

**Modified from published form to include additional three-dimensional cross sections, extraction and greyscale reconstructions.*

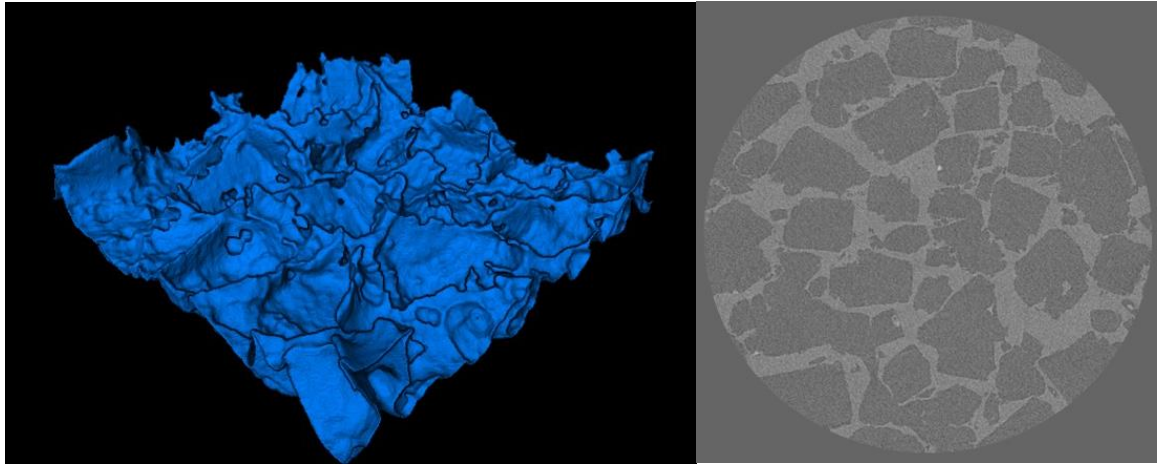
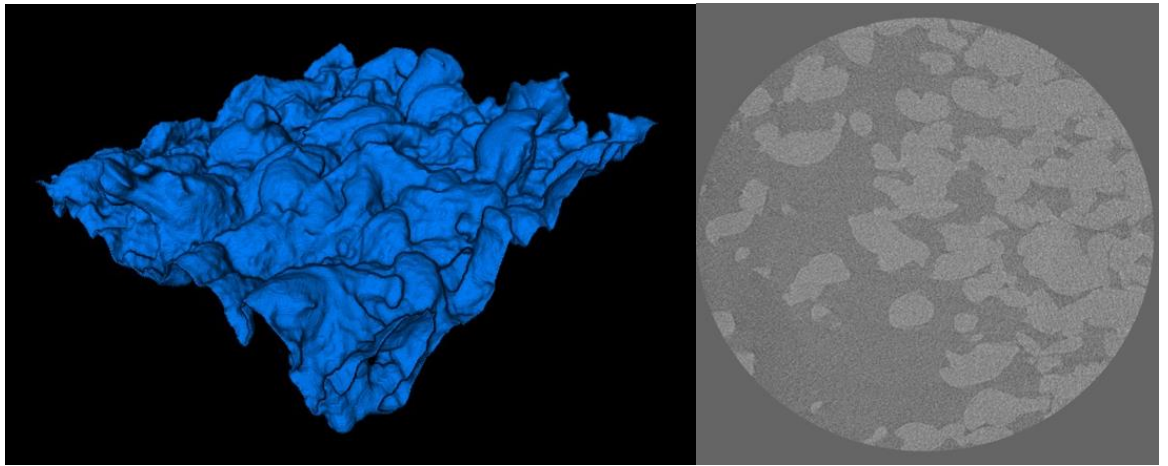
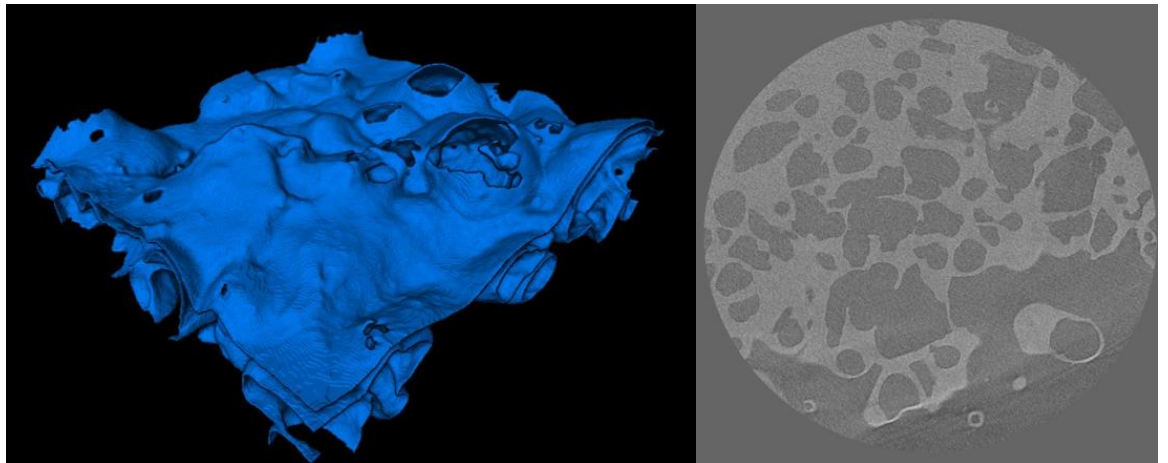
G**H****I**

Figure 2: Continued. (g) Nagor Nagotex, (h) Mentor Siltex, (i) Polytech Mesmo.

**Modified from published form to include additional three-dimensional cross sections, extraction and greyscale reconstructions.*

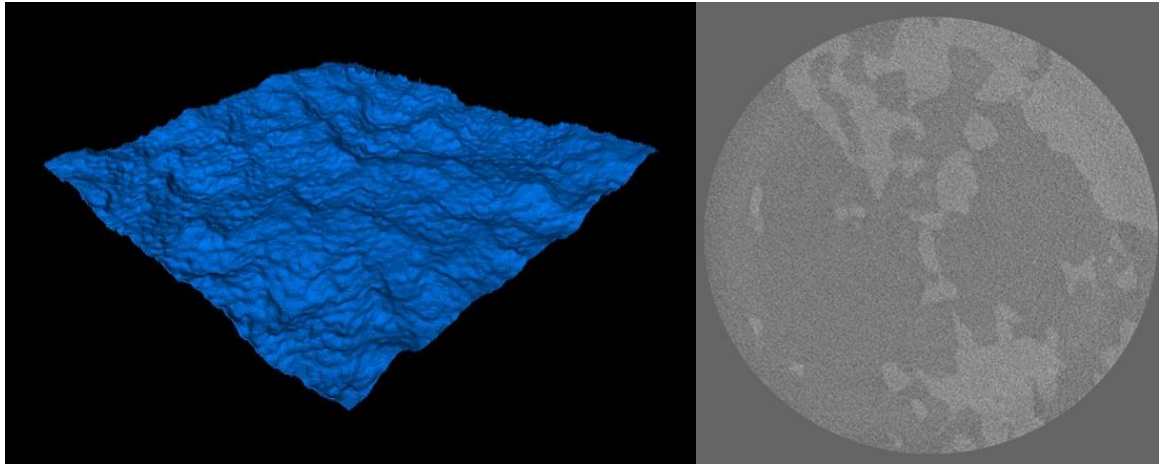
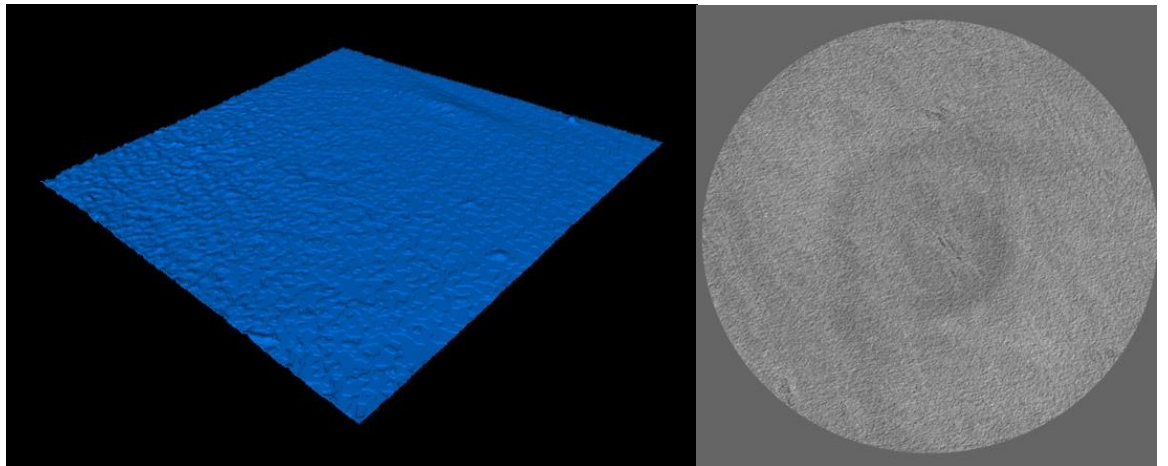
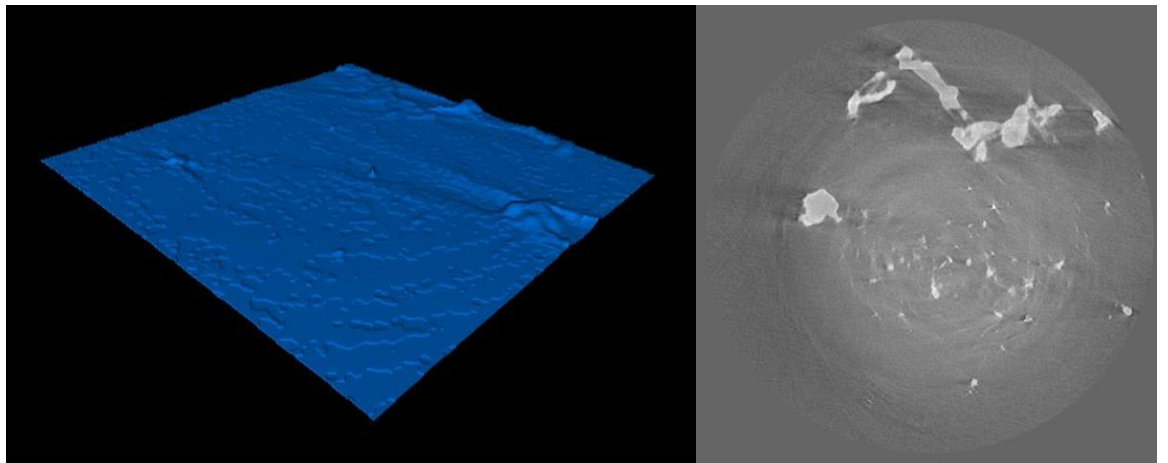
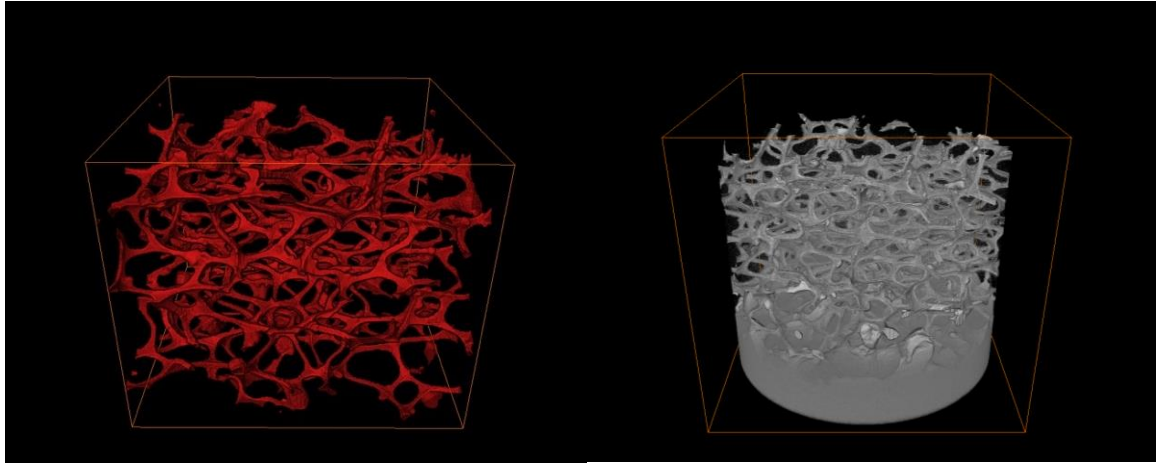
J**K****L**

Figure 2: Continued. (j) Motiva VelvetSurface, (k) Motiva SilkSurface, (l) Mentor Smooth.

**Modified from published form to include additional three-dimensional cross sections, extraction and greyscale reconstructions.*

A



B

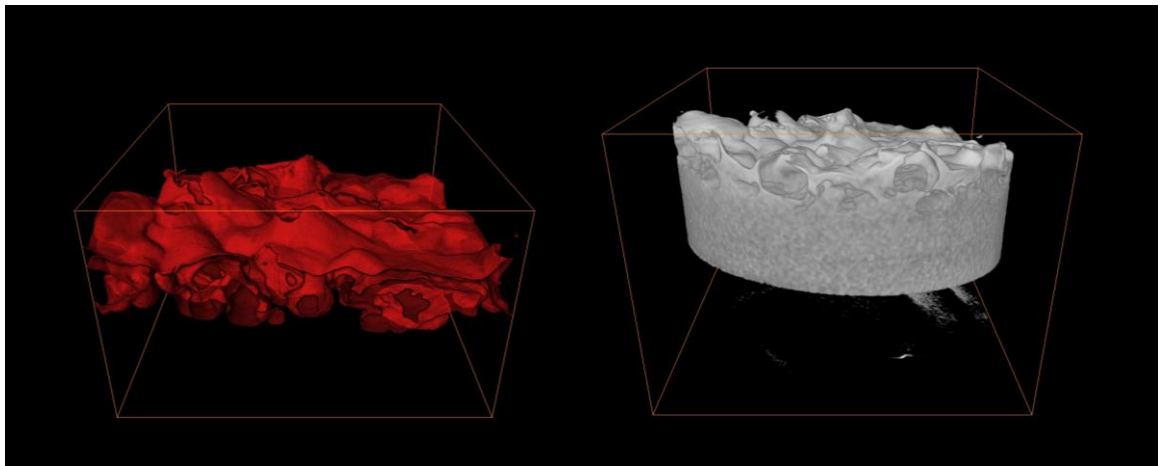


Figure 2 Supp: (a) Silimed Polyurethane and (b) Polytech Mesmo 3D extraction and 3D greyscale reconstruction.

Figure 3 is a graphical representation of the 3D:2D surface area ratio.

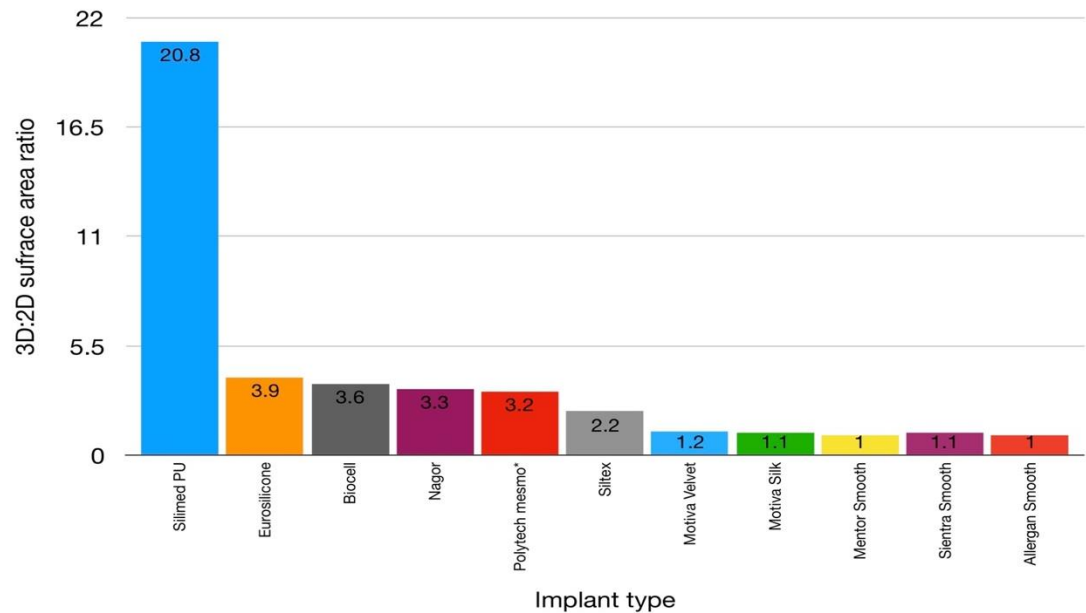


Figure 3: 3D:2D ratios for various implant types studied.

There were four groupings for surface area measurements according to 3D surface area vs. 2D surface area ratio. These were:

1. High > 5
2. Intermediate between 3 – 5
3. Low between 2 – 3
4. Minimal < 2

These categories corresponded generally to implant shell manufacturing processes with polyurethane open pore having the highest surface area, some salt-loss type and gas diffusion as intermediate, other salt-loss and imprinting type textures as low and smooth and “Nano” labelled surfaces as minimal. Salt-loss textures may vary in surface area dependent on the size of the crystals selected in the process. Interestingly, whilst the Polytech Mesmo had a high surface area reading

on first analysis, many of these surfaces were contained within the structure of the silicone outer shell and had no direct communication to the outer surface. An analysis of the choke zones (variation between 1 – 10 μm and hidden “caves” of sequestered internal surfaces) allowed an available surface area to be determined using subtractive analysis. The 3D surface area/3D:2D ratio for Polytech Mesmo was calculated assuming a mean choke size of 5 μm . (Figure 3 Supplementary).

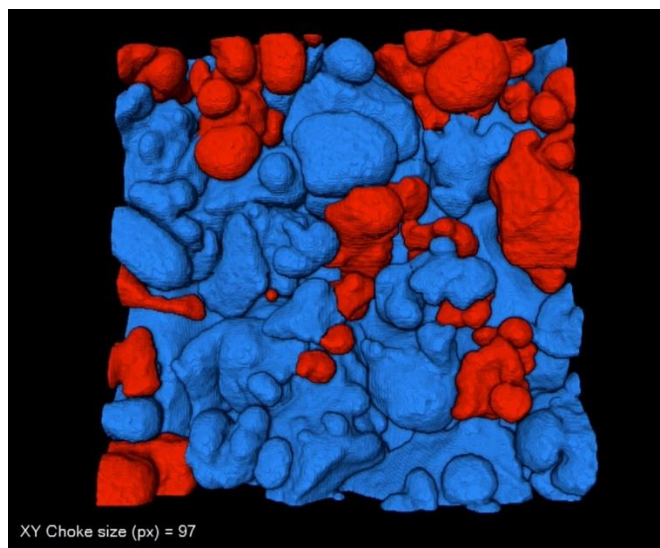


Figure 3 Supp: Demonstration of “caves” (sequestered surface area) for Polytech Mesmo coloured red on 3D reconstruction.

Surface roughness determination

There were four groupings for surface roughness measurements. These were:

1. High > 150
2. Intermediate between 75 – 150
3. Low between 25 – 75
4. Minimal < 25

Table 3 and Figure 4 summarise surface roughness findings.

Table 3: Surface roughness for each implant type.

Implant type	Surface roughness	Standard deviation
Silimed Polyurethane	277.6	32.5
Eurosilicone Textured	111.7	24.9
Allergan Biocell	91.7	13.9
Nagor Nagotex	60.9	12.3
Polytech Mesmo	58.8	19.2
Mentor Siltex	51.4	12.1
Motiva VelvetSurface	12.9	1.7
Motiva SilkSurface	20.1	0.3
Allergan Smooth	8.5	1.4
Sientra Smooth	8.1	0.8
Mentor Smooth	2.1	0.9

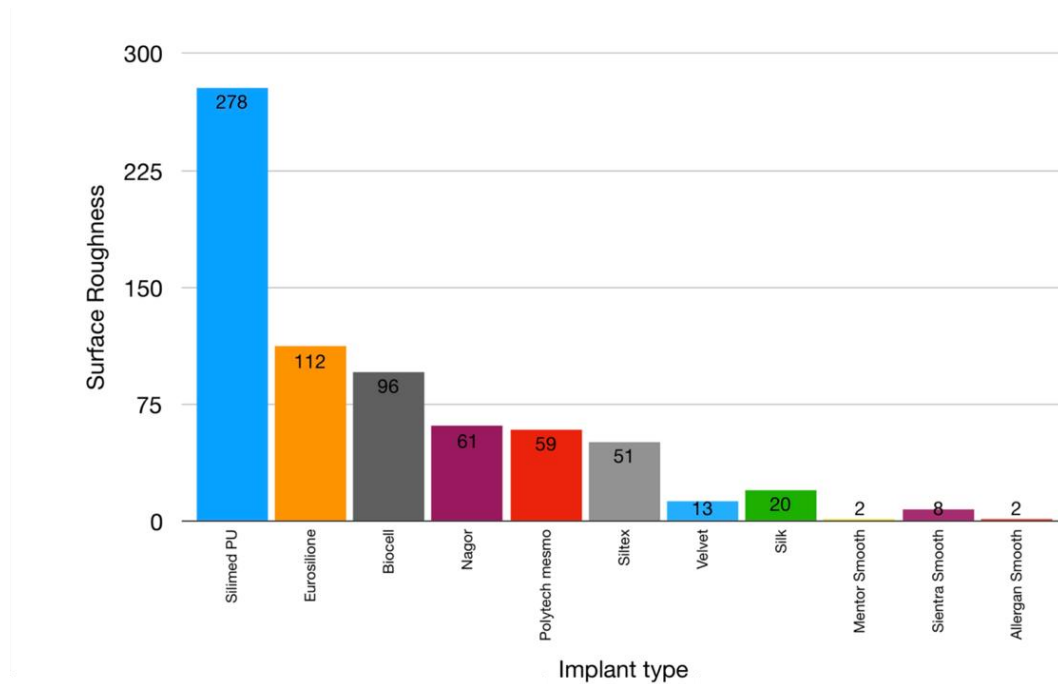


Figure 4: Surface roughness for various implants studied.

***In vitro* bacterial attachment assay**

S. epidermidis

Figure 5 shows the number of *S. epidermidis* attached to different types of implant outer shells at 2, 6 and 24 hours.

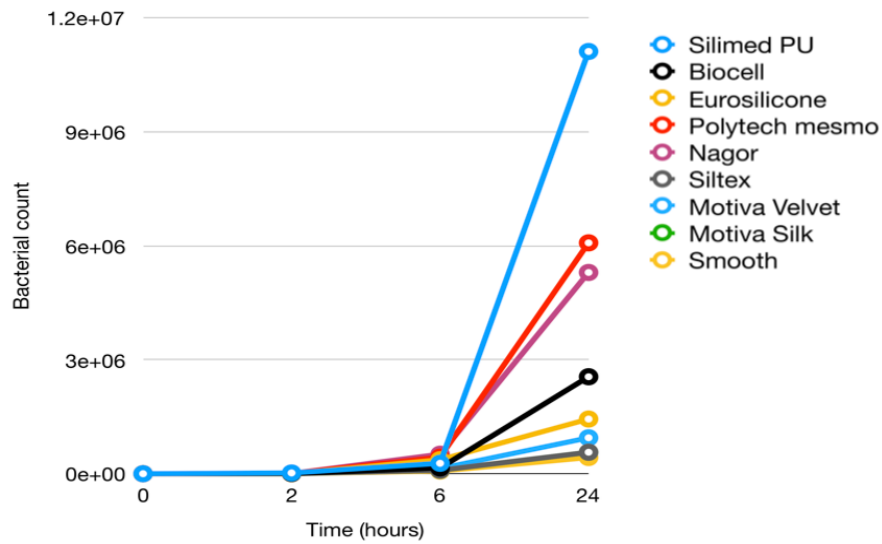


Figure 5: *S. epidermidis* attachment and growth on various implants shells measured at 0, 2, 6 and 24 hours.

Even by the 2 hours time point, the high surface area of textured Silimed Polyurethane implants had significantly larger number of bacteria attached to them than less textured implants with lower surface areas, such as Mentor Siltex, Smooth (Mentor, Sientra, Allergan), Motiva VelvetSurface and Motiva SilkSurface ($P < 0.001$). By 24 hours, implants with 3D:2D ratios of high or intermediate had significantly more bacteria attached to them than implants with low or minimal 3D:2D ratios ($P < 0.001$) and although Silimed Polyurethane implants had more bacteria attached to them, this was not significantly different from implants with intermediate profiles (Figure 6a). Within the salt-loss produced implants, roughly double the number of *S. epidermidis* attached to Nagor Nagotex implants ($P < 0.05$). At 24 hours the number of bacteria attached to the Smooth implant shell was no different to the number attached to implants with low or minimal profile ($P > 0.07$), however, it was significantly less than the number of bacteria attached to implants with intermediate to high profiles ($P < 0.001$). Over time, the number of bacteria attached to implants was positively correlated with the 3D:2D ratio, the higher the 3D:2D ratio the more bacteria were attached (correlation coefficient = 0.64, $P < 0.001$).

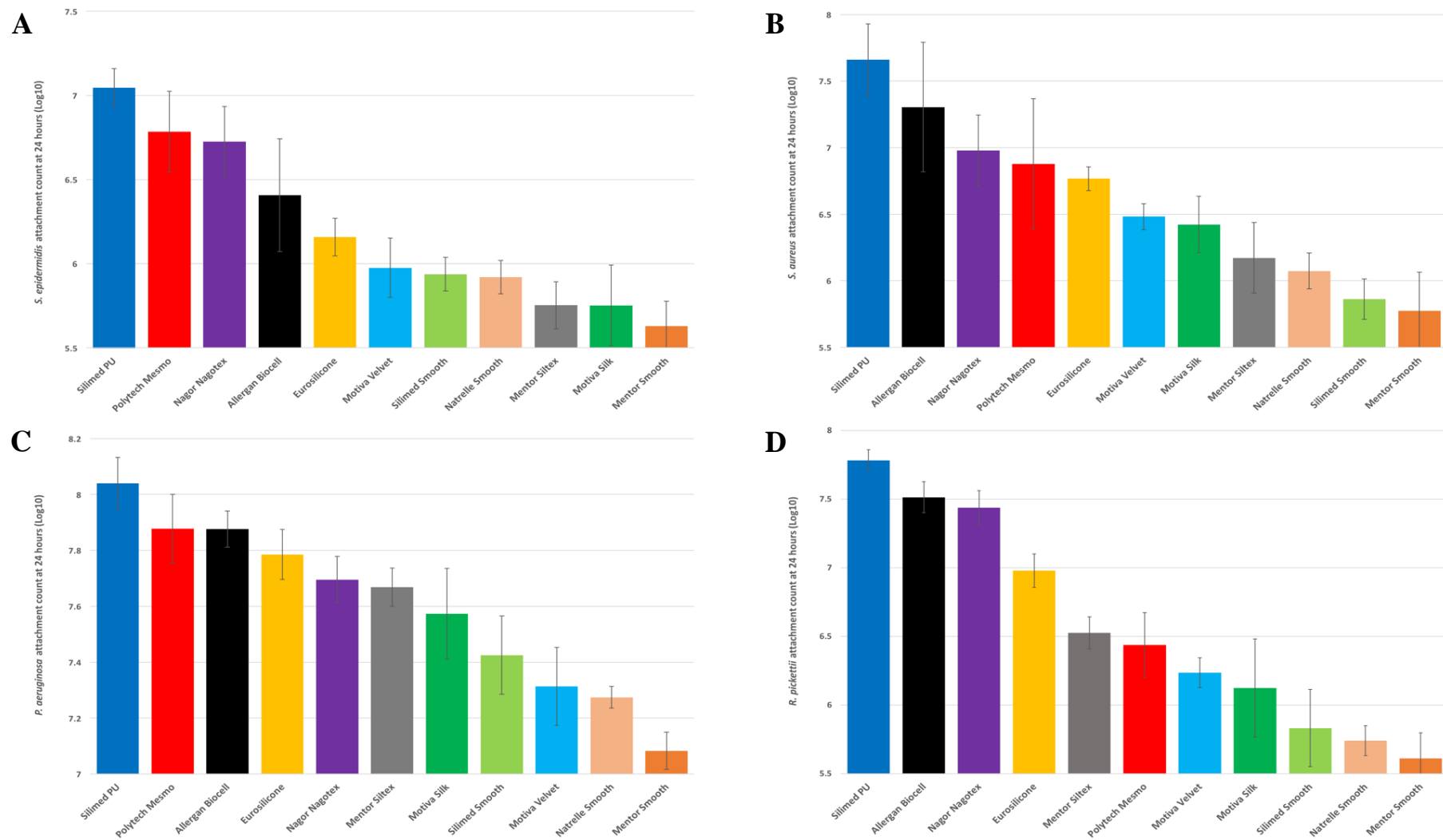


Figure 6: (A) *S. epidermidis*, (B) *S. aureus*, (C) *P. aeruginosa* and (D) *R. pickettii* attachment and growth on various implant shells measured at 24 hours. Error bars represent standard deviation.

S. aureus

Figure 6b shows the number of *S. aureus* attached to different types of silicone implant outer shells at 24 hours. Silimed polyurethane implants had significantly more bacteria attached to them than any other implant ($P < 0.05$) whilst Smooth implants (Mentor, Sientra, Allergan) had significantly less bacteria attached to them than any other implant ($P < 0.001$) except Mentor Siltex ($P = 0.4$). There was no significant difference in the number of bacteria that attached to the three salt-loss implants. The number of bacteria attached to implants was positively correlated with the 3D:2D ratio, the higher the 3D:2D ratio the more bacteria were attached (correlation coefficient = 0.75, $P < 0.001$).

P. aeruginosa

Figure 6c shows the number of *P. aeruginosa* attached to differing implant shells at 24 hours. The maximum number of bacteria attached to Silimed polyurethane implants, followed by Polytech Mesmo and the Biocell implant produced by salt-loss. The other two salt-loss implants Eurosilicone Textured and Nagor Nagotex had less bacteria attached at 24 hours but this was not significantly different from the numbers attached to the Biocell implant ($P > 0.09$). The number of bacteria attached to implants was positively correlated with the 3D:2D ratio, the higher the 3D:2D ratio the more bacteria were attached (correlation coefficient = 0.81, $P < 0.001$). Significantly fewer bacteria grew on Smooth implants when compared to all other implants ($P < 0.001$). In contrast, to the findings for staphylococcal species, significantly less bacteria attached to Motiva VelvetSurface implants compared to Motiva SilkSurface implants ($P = 0.008$) and was significantly less than all the other implants ($P < 0.001$).

R. pickettii

Figure 6d shows the number of *R. pickettii* attached to the different types of silicone outer shell at 24 hours. Only Silimed Polyurethane, Biocell and Nagor Nagotex had significantly more bacteria

attached than Smooth implants ($P < 0.001$). There was no significant difference in the number of bacteria attached to the three salt-loss produced implants. The number of bacteria attached to implants was positively correlated with the 3D:2D ratio, the higher the 3D:2D ratio the more bacteria were attached (correlation coefficient = 0.87, $P < 0.001$).

Combined categories

Figure 7 summarizes the proposed surface classification based on combining surface area with surface roughness. The surface grade can be then combined with a nomenclature to define fill, surface, shape and size of the implant. Table 4 summarizes the proposed classification. A Cohesive Gel 410 Allergan Biocell Anatomic 330cc implant, for example, would be classified as GF4A330, for example.



Process	Polyurethane foam	Salt Loss (Biocell/Eurosilicone)	Gas Diffusion	Salt Loss (Nagotex)	Imprinting	Smooth/Nano
Surface Area	High	Intermediate	Intermediate	Low	Low	Minimal
Roughness	High	Intermediate	Low	Low	Low	Minimal
SURFACE TYPE	4	3	3	2	2	1

Figure 7: Implant surface classification relating manufacturing method, surface area, surface roughness.

Table 4: Proposed generic breast implant classification based on fill, surface, shape and size.

Fill	Surface Area	Shape	Size
GF – gel filled	4 High	A – anatomic	In cc
S – saline filled	3 Intermediate	R – round	
A – part air filled	2 Low		
	1 Minimal		

Discussion

These findings support the use of a new classification system for implant outer shells based on measurable parameters of surface area and roughness, which correlate with bacterial growth. We now propose a classification of implant surfaces into four grades (high, intermediate, low and minimal) based on the direct measurement of their surface area and roughness.

Analysis of bacterial growth over varying implant surfaces showed a significant correlation with 3D:2D surface area demonstrating a linear relationship of bacterial attachment and growth as the surface area ratio increased. Figure 5 confirms the exponential growth rates for higher surface area textured implants for *S. epidermidis* we have reported previously (Jacombs et al., 2014). The Silimed polyurethane texture grew significantly higher numbers of bacteria for all species at 24 hours. Interestingly, the intermediate surface area implants showed good correlation and were no different to the high surface area implants for *S. epidermidis* and *P. aeruginosa*. These prolific biofilm formers may well overwhelm the surface area available and reach maximal growth capacity earlier than other species. These species and surface differences for intermediate/low texture require further investigation and may relate to the available surface area, specific bacterial cell size, motility and capacity to form biofilm together with environmental factors and availability of nutrition.

The Polytech Mesmo surface showed a high proportion of hidden surface area (“caves”) within the substance of the texture. These were either walled off entirely from the external environment or had very narrow choke zones to reduce the passage of bacteria and/or host cells. This may also explain higher growth for some species for this texture. Atlan et al. (2016) have utilized similar measurement techniques and demonstrated variation in texture morphology on different sites of the same implant. This was beyond the scope of this study but will be the subject of future bacterial attachment analysis.

Previously published morphological analysis of breast implant outer shells have utilized confocal microscopy (Barr et al., 2009, Valencia-Lazcano et al., 2013, Barr et al., 2017), scanning electron microscopy (Barr et al., 2017) and/or light microscopy (Barr et al., 2009) and wettability (Barr et al., 2017) to classify implant surfaces. We have previously utilized these techniques (Loch-Wilkinson et al., 2017) but found significant errors when examining higher thickness implant textures with loss of resolution in deeper zones. The use of the micro CT method has allowed a more accurate morphological assessment of the entire implant shell. These authors have also utilized fibroblast adhesion and/or macrophage activation as surrogate markers for predictors of tissue incorporation and reduction in capsular contracture (Barr et al., 2017). Whilst these *in vitro* factors may be important, they have yet to translate into proven clinical benefit and so their functional significance will need to be validated by clinical studies.

The presence of bacteria, by contrast, on the surface of implants has been shown to be a significant potentiator for the formation of capsular contracture in clinical and laboratory studies (Rieger et al., 2013, Jacombs et al., 2014, Chong and Deva, 2015). Clinical correlation has confirmed a significant correlation of bacterial contamination with increasing grade of capsular contracture (Rieger et al., 2014). In patients with high-grade capsular contracture, polyurethane texture was also shown to support a significantly higher load of bacteria as compared with other textured implants (Hu et al., 2015). Furthermore, translational research has now supported the use of anti-bacterial mitigation to reduce capsular contracture thus linking the surface area/bacterial growth relationship directly to a functional clinical outcome (Blount et al., 2013, Giordano et al., 2013).

We are not claiming that textured implants cause more contracture, as is often suggested in commentaries critiquing our previous findings. Surface texture provides a dual opportunity for better host tissue incorporation but also, unfortunately, for bacterial growth and proliferation. In the event that bacterial contamination is kept low, the advantages of a textured surface may well

promote better long-term results. High quality clinical comparative studies are still required to confirm this finding. It is also likely that factors other than implant texture alone have a suppressive effect on the development of biofilm and subsequent capsular contracture, including antibacterial pocket irrigation, prophylactic antibiotic use, avoidance of contamination, anatomical pocket location, and careful atraumatic dissection of the breast pocket (Adams Jr, 2009, Chong and Deva, 2015). Strategies to prevent contamination of the implant as it is placed help to reduce the numbers of bacteria and keep the contamination below threshold (Deva et al., 2013). This underscores the importance of overall bacterial load on breast implants that ultimately drives the clinical outcome.

More recently, an antigen driver for BIA-ALCL has been proposed. This, in combination with surface texture, patient genetics and time form the unifying hypothesis that explains both observed biology and epidemiology of BIA-ALCL (Loch-Wilkinson et al., 2017). The propensity for high and intermediate surface area textured implants to cause BIA-ALCL is 10x higher than for low surface area texture and is consistent with these data (Loch-Wilkinson et al., 2017). The need for a biological antigen to drive carcinogenesis indicates that it is likely that bacterial proteins rather than inert silicone particles that initiate the stimulation and transformation of T-cells (Kadin et al., 2016). The pathway from bacterial antigen stimulation to lymphoma has been proven for *Helicobacter pylori*, gastric MALT lymphoma and gastric cancer (Peek and Kuipers, 2012). Understanding the interaction between genes, the microbiome and immunity may well provide new approaches to both the treatment and prevention of cancer.

Conclusion

We support the use of a novel and functional classification of implant outer shells based on objective measurement into four degrees of surface texture: high, intermediate, low and minimal. The correlation of surface area/roughness with propensity for bacterial growth links this

classification to a functional outcome and strengthens its validity as a tool to help surgeons to select the optimal implant surface for both breast augmentation and reconstruction.

Acknowledgements

The authors acknowledge the facilities and the scientific and technical assistance of the Australian Microscopy & Microanalysis Research Facility at the Australian Centre for Microscopy & Microanalysis at the University of Sydney. The authors would like to thank implant manufacturers for supply of sample implant surfaces for the study.

References

- Adams WP, Jr. Capsular contracture: what is it? What causes it? How can it be prevented and managed? *Clin Plast Surg*. 2009;36(1):119-126, vii.
- Ashley FL. Further studies on the natural-Y breast prosthesis. *Plast Reconstr Surg*. 1972;49(4):414-419.
- Asplund O, Gylbert L, Jurell G, Ward C. Textured or smooth implants for submuscular breast augmentation: a controlled study. *Plast Reconstr Surg*. 1996;97(6):1200-1206.
- Atlan M, Bigerelle M, Larreta-garde V, Hindie M, Heden P. Characterization of Breast Implant Surfaces, Shapes, and Biomechanics: A Comparison of High Cohesive Anatomically Shaped Textured Silicone, Breast Implants from Three Different Manufacturers. *Aesthetic Plast Surg*. 2016;40(1):89-97.
- Barnsley GP, Sigurdson LJ, Barnsley SE. Textured surface breast implants in the prevention of capsular contracture among breast augmentation patients: a meta-analysis of randomized controlled trials. *Plast Reconstr Surg*. 2006;117(7):2182-2190.
- Barr S, Hill E, Bayat A. Current implant surface technology: an examination of their nanostructure and their influence on fibroblast alignment and biocompatibility. *Eplasty*. 2009;9:e22.
- Barr S, Hill EW, Bayat A. Functional biocompatibility testing of silicone breast implants and a novel classification system based on surface roughness. *J Mech Behav Biomed Mater*. 2017;75:75-81.
- Blount AL, Martin MD, Lineberry KD, Kettaneh N, Alfonso DR. Capsular contracture rate in a low-risk population after primary augmentation mammoplasty. *Aesthet Surg J*. 2013;33(4):516-521.

Burkhardt BR, Demas CP. The effect of Siltex texturing and povidone-iodine irrigation on capsular contracture around saline inflatable breast implants. *Plast Reconstr Surg.* 1994;93(1):123-128; discussion 129-130.

Burkhardt BR, Eades E. The effect of Biocell texturing and povidone-iodine irrigation on capsular contracture around saline-inflatable breast implants. *Plast Reconstr Surg.* 1995;96(6):1317-1325.

Chan SC, Birdsell DC, Gradeen CY. Urinary excretion of free toluenediamines in a patient with polyurethane-covered breast implants. *Clin Chem.* 1991;37(12):2143-2145.

Chan SC, Birdsell DC, Gradeen CY. Detection of toluenediamines in the urine of a patient with polyurethane-covered breast implants. *Clin Chem.* 1991;37(5):756-758.

Chong SJ, Deva AK. Understanding the Etiology and Prevention of Capsular Contracture: Translating Science into Practice. *Clin Plast Surg.* 2015;42(4):427-436.

Coleman DJ, Foo IT, Sharpe DT. Textured or smooth implants for breast augmentation? A prospective controlled trial. *Br J Plast Surg.* 1991;44(6):444-448.

Collis N, Coleman D, Foo IT, Sharpe DT. Ten-year review of a prospective randomized controlled trial of textured versus smooth subglandular silicone gel breast implants. *Plast Reconstr Surg.* 2000;106(4):786-791.

Deva AK, Adams WP, Jr., Vickery K. The role of bacterial biofilms in device-associated infection. *Plast Reconstr Surg.* 2013;132(5):1319-1328.

Fagrell D, Berggren A, Tarpila E. Capsular contracture around saline-filled fine textured and smooth mammary implants: a prospective 7.5-year follow-up. *Plast Reconstr Surg.* 2001;108(7):2108-2112; discussion 2113.

Giordano S, Peltoniemi H, Lilius P, Salmi A. Povidone-Iodine Combined With Antibiotic Topical Irrigation to Reduce Capsular Contracture in Cosmetic Breast Augmentation: A Comparative Study. *Aesthet Surg J.* 2013;33(5):675-680.

Hakelius L, Ohlson L. A clinical comparison of the tendency to capsular contracture between smooth and textured gel-filled silicone mammary implants. *Plast Reconstr Surg.* 1992;90(2):247-254.

Henderson PW, Nash D, Laskowski M, Grant RT. Objective Comparison of Commercially Available Breast Implant Devices. *Aesthetic Plast Surg.* 2015;39(5):724-732.

Hu H, Jacombs A, Vickery K, Merten SL, Pennington DG, Deva AK. Chronic biofilm infection in breast implants is associated with an increased T-cell lymphocytic infiltrate: implications for breast implant-associated lymphoma. *Plast Reconstr Surg.* 2015;135(2):319-329.

Jacombs A, Tahir S, Hu H, et al. In vitro and in vivo investigation of the influence of implant surface on the formation of bacterial biofilm in mammary implants. *Plast Reconstr Surg.* 2014;133(4):471e-480e.

- Kadin ME, Deva A, Xu H, et al. Biomarkers Provide Clues to Early Events in the Pathogenesis of Breast Implant-Associated Anaplastic Large Cell Lymphoma. *Aesthet Surg J*. 2016;36(7):773-781.
- Loch-Wilkinson A, Beath KJ, Knight RJW, et al. Breast Implant-Associated Anaplastic Large Cell Lymphoma in Australia and New Zealand: High-Surface-Area Textured Implants Are Associated with Increased Risk. *Plast Reconstr Surg*. 2017;140(4):645-654.
- Malata CM, Feldberg L, Coleman DJ, Foo IT, Sharpe DT. Textured or smooth implants for breast augmentation? Three year follow-up of a prospective randomised controlled trial. *Br J Plast Surg*. 1997;50(2):99-105.
- Peek RM, Jr., Kuipers EJ. Gained in translation: the importance of biologically relevant models of *Helicobacter pylori*-induced gastric cancer. *Gut*. 2012;61(1):2-3.
- Poepl N, Schreml S, Lichtenegger F, Lenich A, Eisenmann-Klein M, Prantl L. Does the surface structure of implants have an impact on the formation of a capsular contracture? *Aesthetic Plast Surg*. 2007;31(2):133-139.
- Rieger UM, Mesina J, Kalbermatten DF, et al. Bacterial biofilms and capsular contracture in patients with breast implants. *Br J Surg*. 2013;100(6):768-774.
- Rieger UM, Raschke GF, Frei R, Djedovic G, Pierer G, Trampuz A. Role of bacterial biofilms in patients after reconstructive and aesthetic breast implant surgery. *J Long Term Eff Med Implants*. 2014;24(2-3):131-138
- Schindelin J, Arganda-Carreras I, Frise E, et al. Fiji: an open-source platform for biological-image analysis. *Nat Methods*. 2012;9(7):676-682.
- Sforza M, Zaccheddu R, Alleruzzo A, et al. Preliminary 3-Year Evaluation of Experience With SilkSurface and VelvetSurface Motiva Silicone Breast Implants: A Single-Center Experience With 5813 Consecutive Breast Augmentation Cases. *Aesthet Surg J*. 2017.
- Stevens WG, Nahabedian MY, Calobrace MB, et al. Risk factor analysis for capsular contracture: a 5-year Sientra study analysis using round, smooth, and textured implants for breast augmentation. *Plast Reconstr Surg*. 2013;132(5):1115-1123.
- Tarpila E, Ghassemifar R, Fagrell D, Berggren A. Capsular contracture with textured versus smooth saline-filled implants for breast augmentation: a prospective clinical study. *Plast Reconstr Surg*. 1997;99(7):1934-1939.
- Valencia-Lazcano AA, Alonso-Rasgado T, Bayat A. Characterisation of breast implant surfaces and correlation with fibroblast adhesion. *J Mech Behav Biomed Mater*. 2013;21:133-148.
- Wong CH, Samuel M, Tan BK, Song C. Capsular contracture in subglandular breast augmentation with textured versus smooth breast implants: a systematic review. *Plast Reconstr Surg*. 2006;118(5):1224-1236.

Chapter IV.

The influence of implant surface on biofilm formation in an *in vivo* porcine model

4.1. Introduction

In Chapter III we identified a significant correlation between surface area and bacterial attachment/growth *in vitro*. Implant textures with high surface area/roughness grew significantly more bacteria in comparison to the minimal surface area/roughness implants, which grew significantly less bacteria of all types tested (*S. epidermidis*, *S. aureus*, *P. aeruginosa*, *R. pickettii*) at 24 hours.

In this Chapter, we investigated the influence of textured surface implants *in vivo* using the established porcine model (Tamboto et al., 2010). In this model, it has been shown that breast pocket inoculation of *S. epidermidis* leads to biofilm formation and the subsequent development of capsular contracture (CC) (Tamboto et al., 2010). Separate studies utilising this pig model have also shown no difference in contracture rates between smooth (82.6%) and textured (83.7%) implants after approximately 19 weeks following deliberate inoculation of pockets with *S. epidermidis* (Jacombs et al., 2014). Interestingly, initial bacterial attachment was 20-fold higher on textured implants compared to smooth implants (Jacombs et al., 2014). Moreover, there is a correlation between the quantity of bacterial biofilm load and the activation of lymphocytes in both the pig model and in human specimens recovered from patients with chronic implant infection (Hu et al., 2015).

For our *in vivo* study we tested two differently textured miniature implants, designated type A and type B. The type A implant had a new micro texture created through a proprietary process and the type B implant was manufactured using the salt-loss technique (commercial in confidence).

The aim of this Chapter was to compare bacterial attachment, biofilm formation, development of contracture and host response following artificial bacterial contamination of breast implants composed of test surfaces type A and type B in an *in vivo* porcine model.

4.2. Materials and Methods

4.2.1. Breast implant surfaces tested

Two round and textured surface implants, type A and type B, were tested (Figure 4.1). The type B implant had a slightly more textured surface compared to type A.

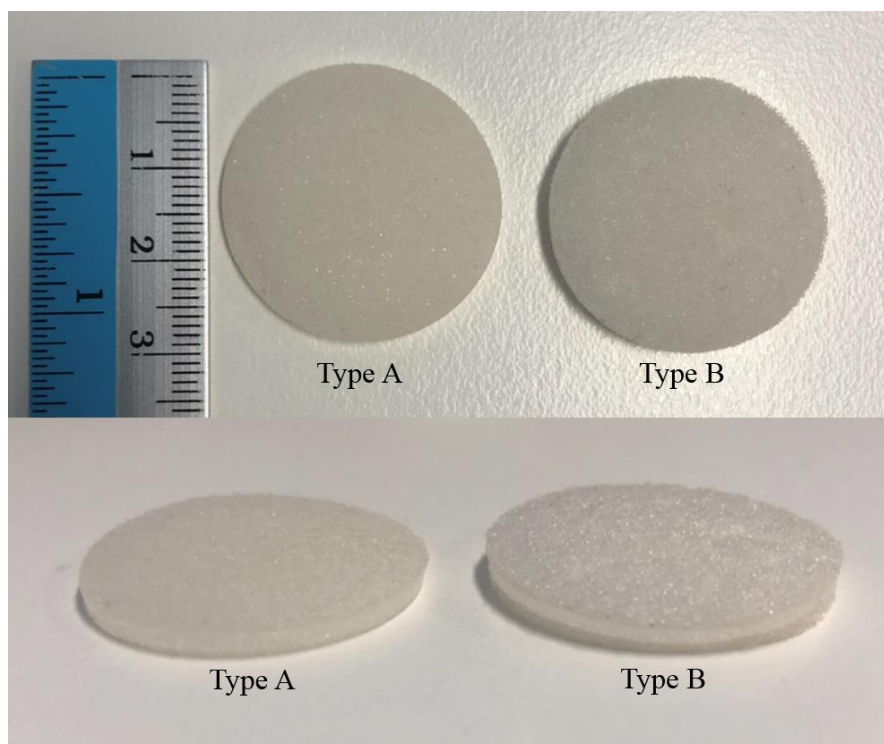


Figure 4.1. Type A and type B textured surface implants tested. Average diameter of the implants is 3 cm.

4.2.2. Subjects

Two adult, female, non-lactating, domestic Large White pigs (*Sus domesticus*) weighing approximately 200 kg received four type A implants and four type B implants each, as illustrated in Figure 4.2. Sample numbers were assigned to each of the test implants in pigs 1 (ear tag 35) and 2 (ear tag 33) (Figure 4.2).

4.2.3. Preparation of contaminating inoculum

A clinical isolate of *S. epidermidis* (strain number seven) originally isolated from a contracted breast in a human patient was used for the study (Tamboto et al., 2010). Bacteria were grown in TSB at 37°C overnight and then diluted in PBS to give an optical density of 0.3 at wavelength of 600 nm (equivalent to approximately 1×10^8 bacterial cells/mL). This culture was diluted again 1:100 with PBS to give approximately 2×10^6 cells/mL. The diluted bacteria were kept on ice and transported to the surgery site, University of Sydney Veterinary Teaching Hospital, Camden, Australia. The exact number of bacteria contained in the inoculum was determined by serial ten-fold dilution and standard plate culture and was found to be 2.04×10^6 cells/mL.

4.2.4. Surgical procedure

Pigs were fasted overnight before surgery. Anaesthesia was induced intramuscularly with xylocaine (250 mg/kg), ketamine (250 mg/kg) and Zoletil (250 mg/kg). Analgesia was given intravenously with meloxicam (0.4 mg/kg) and methadone (2 mL). The torso of the pig was prepared surgically using a 10% povidone-iodine wash (Orion, Welshpool, Western Australia, Australia) and a 70% alcohol rinse. Sterile surgical drapes were used to completely cover the pig while keeping the teats adequately exposed. An antimicrobial Ioban drape (3M Health Care, St. Paul, Minnesota, USA) was applied to cover all teats. Standard sterile operative techniques were used, including change of gloves and instruments with each implant placement, ensuring

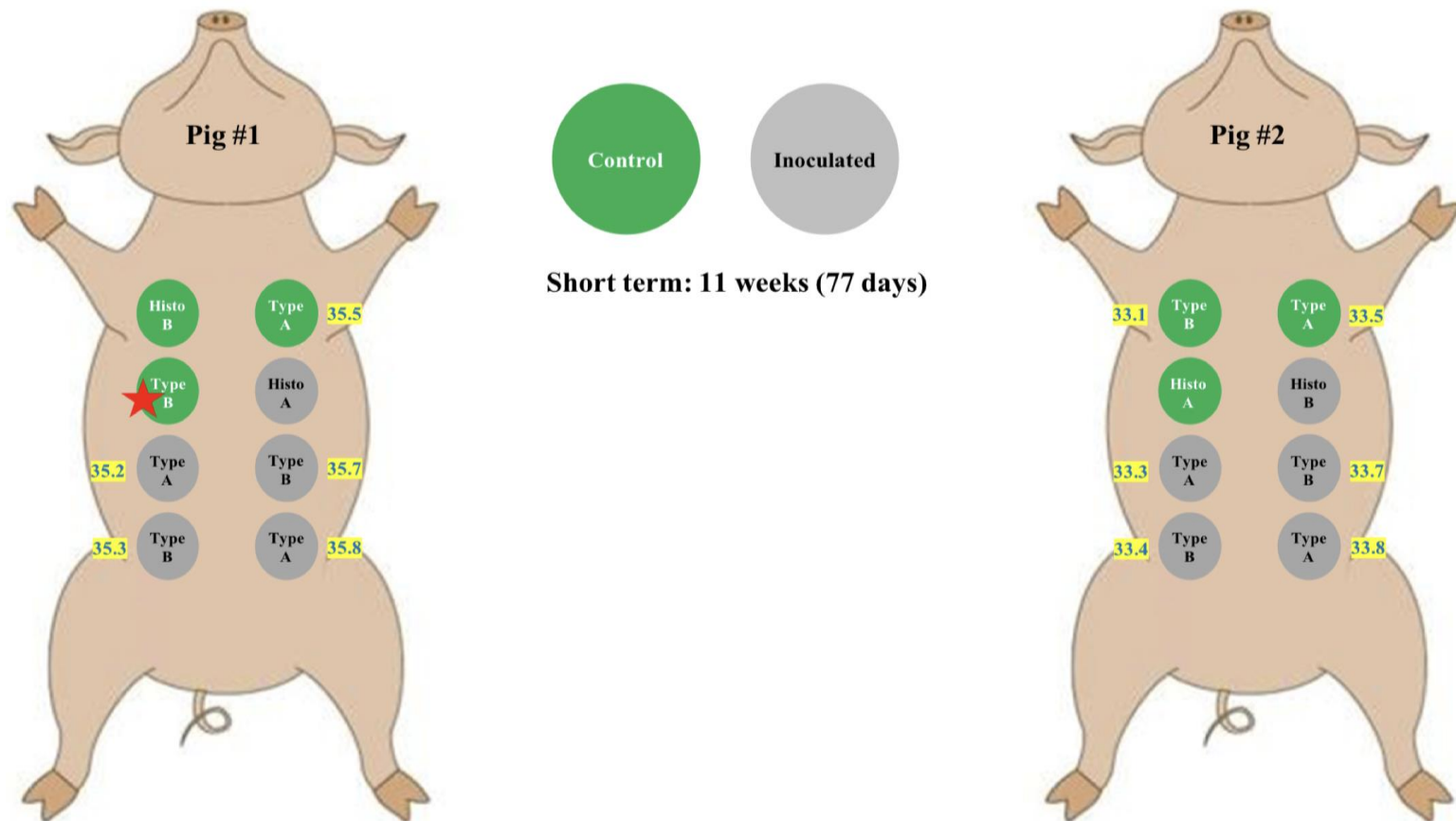


Figure 4.2. Randomisation of implants.

*Position of test implants, type A and type B in pigs 1 (ear tag 35) and 2 (ear tag 33). Each pig received four type A and four type B implants. Ten implants were inserted into *S. epidermidis* inoculated submammary pockets (grey) and six implants were inserted into non-inoculated (control) pockets (green) and left in situ for 11 weeks. Samples removed from teats labelled “Histo A” or “Histo B” were sent to the commercial partner in the USA for histology analysis. Numbers highlighted in yellow were the sample numbers assigned to each test implant.*

★ Denotes lost implant.

haemostasis prior to implant insertion, minimising implant handling and avoiding contact of the implant with skin as detailed by Tamboto et al. (2010).

The implants were inserted aseptically into the submammary pockets, which had been fashioned using blunt dissection. After implant insertion, submammary pockets were inoculated with 1 mL of PBS containing *S. epidermidis* test inoculum (for infection tests) or an equal volume of sterile PBS (for control tests). Each pig received eight implants, five implant pockets were *S. epidermidis* contaminated (Figure 4.2). Surgical wounds were closed using absorbable sutures, 4-0 undyed Monocryl (Ethicon Inc., Somerville, New Jersey, USA), and OpSite spray (Smith & Nephew, Hull, England) was applied over the operative wounds. Implants were left *in situ* for 11 weeks (77 days). Pigs were monitored daily for any sign of infection. Figure 4.3 illustrates the implantation procedure.

4.2.5. Baker grading

At the 11 week time point, the pigs were anaesthetised as detailed in Section 4.2.4. and contracture was assessed using the four-grade Baker scale (Spear and Baker, 1995) while the implants were *in situ*. Grade I indicating a relatively normal breast and Grade IV indicating severe CC.

4.2.6. Explant surgery

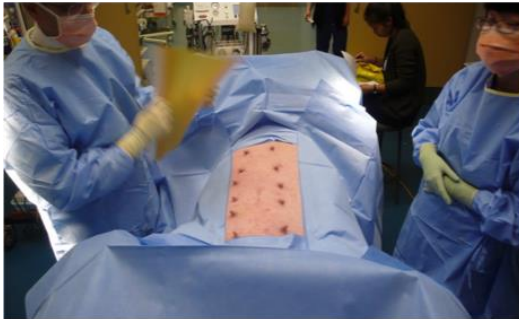
The pigs abdominal wall was surgically prepared as detailed in Section 4.2.4. Each implant was removed aseptically while keeping its surrounding capsule intact (Figure 4.4). Animals were euthanised following explant surgery. All samples were kept on ice during transport to the laboratory and processed using aseptic techniques in a class II biohazard cabinet.



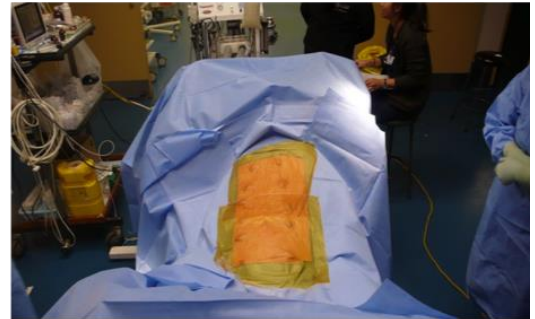
1. Surgical Preparation



2. Final adjustments to anaesthetic



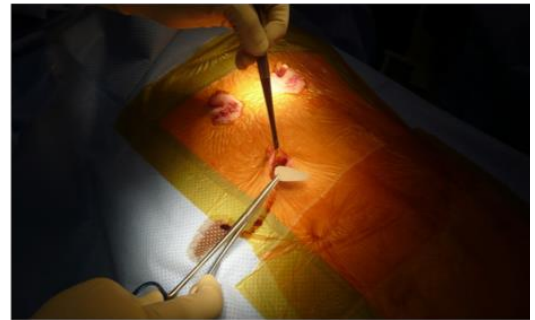
3. Addition of Ioban drape



4. Pig prepped and ready for implantation



5. Dissecting the pocket



6. Adding the implant



7. Post implantation

Figure 4.3. Implantation procedure in an *in vivo* porcine model.

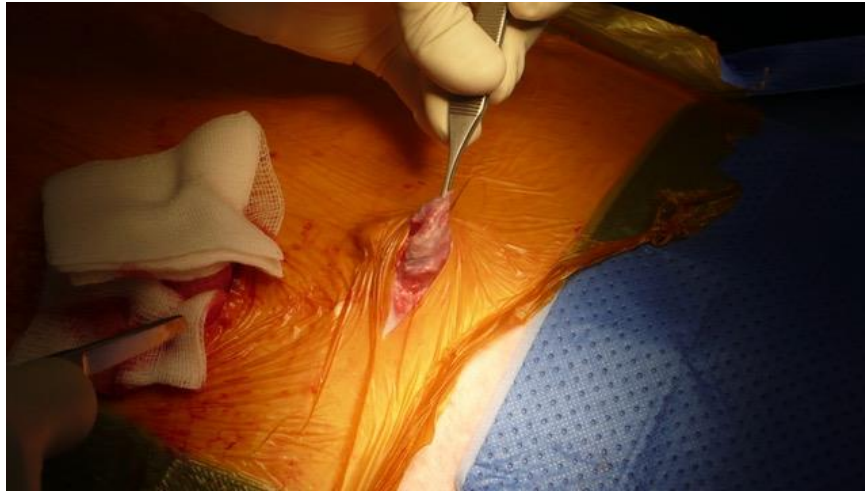


Figure 4.4. Dissection during explant surgery.

4.2.7. Biofilm analysis

The surrounding capsule was separated from the implant and both were sectioned for biofilm analysis by determining bacterial viability counts by culture, total bacterial counts by qPCR, and biofilm architecture by SEM.

Quantitative aerobic cultures, viability counts and bacterial identification were obtained by transferring sectioned samples into 10 mL of TSB followed by sonication for 15 min and standard plate culture (Section 2.2.1.).

Bacterial load in capsules and attached to implants by qPCR

The samples were aseptically sectioned from different parts of the capsule and implant. The total number of bacteria was estimated by qPCR. Genomic DNA was extracted from two separate biological samples of capsular tissue and implant using two different DNA extraction kits, Roche high pure PCR template preparation (Roche) for test 1 samples and the QIAamp DNA mini kit (Qiagen) for test 2 samples as detailed in Section 2.3.1. Extractions were performed on different days (test 1 and 2).

Each extracted DNA sample was subjected to real-time qPCR, in duplicate, using universal eubacterial 16S rRNA (Table 2.1, Section 2.3.1.). To compare the number of bacteria between capsular samples, the extracted DNA was subjected to amplification of the pig 18S rRNA gene, which was used as a reference gene to normalise the amount of pig tissue used in DNA extraction (Table 2.1, Section 2.3.1.).

Calculation of microbial load attached to the different implants

During extraction of DNA all the tissue attached to the implants was enzymatically removed leaving only the non-digestible implant. The implant was air-dried and its weight recorded. The number of bacteria in the tissue attached to the implant was based on the determination of the 18S rRNA and the number of bacteria in the capsule surrounding the implant. The total number of bacteria attached to the implant was determined by the following calculation:

$$\text{Bacterial load on implant (BI)} = T - C$$

where T equals total bacterial load in the implant sample including the bacteria in the tissue attached to the implant and C equals the number of bacteria present in the tissue that had remained attached to the implant. The bacterial load on the implant (BI) was then normalised against the weight of the implant (after the tissue had been removed) used for DNA extraction.

Staphylococcus epidermidis specific PCR

Each extracted DNA sample was subjected to *S. epidermidis* specific real-time PCR targeting the *icaA* gene (Table 2.1) (Nuryastuti et al., 2011) as detailed in Section 2.3.1.

Lymphocyte number in capsules and implants by qPCR

The number of T-cells and B-cells in capsular tissue and implant samples was quantified by qPCR of CD3 gene (total T-cell), CD4 gene (helper T-cell), CD8a gene (cytotoxic T-cell) and CD79a gene (total B-cell). Primers specific to these genes are listed in Table 2.1, Section 2.3.1. The total number of lymphocytes in samples was expressed per milligram (mg) of capsule/implant based on

the average number of copies of the 18S gene in a mg of pig tissue. qPCR was carried out as per Section 2.3.1.

Scanning electron microscopy

The presence of biofilm was confirmed visually using SEM. Sections, 2 to 3 mm², were obtained from two different areas of each capsule or implant. The samples were fixed in 3% glutaraldehyde solution and stored overnight at 4°C. Samples were prepared for SEM following the procedure detailed in Section 2.4.1. Samples were examined using a JEOL 6480LA SEM with the following imaging parameter settings: 10 kV beam accelerating voltage, spot size 30, 15 mm working distance, and magnifications ranging from 300X to approximately 23,500X. The two sections of each capsule or implant sample were examined on different days.

4.2.8. Micro computed tomography scanning of breast implant and surface analysis

Micro CT micro-characterisations of the type A implant was performed at the Australian Centre for Microscopy and Microanalysis, University of Sydney, Australia. The micro CT scanning, and surface area and surface roughness analysis were performed as described in Section 2.4.2., with the calculations normalised to smooth implants.

4.2.9. Statistical analysis

All statistical analyses were performed with the statistical package Sigma Plot 13 (Systat Software, Inc.). The Fisher's exact test was used to test for differences in Baker grading between control implants and implants contaminated with *S. epidermidis*, and between implant types A and B. To test normality of data distribution, the Shapiro-Wilk test was used. A Student's t-test was conducted to look for differences in outputs between type A and type B implants and between the two different DNA extraction kits tested, if results were normally distributed. If not normally distributed, the Mann-Whitney rank sum test was used. A Kruskal-Wallis one-way ANOVA by

ranks followed by Dunn's pairwise multiple comparison was conducted to measure for differences in the bacterial load and lymphocyte load in the capsules surrounding inoculated and control implants of implant types A and B. Linear regression analysis was used to test for association between qPCR results and lymphocyte numbers and between qPCR results and SEM scoring in implants and surrounding capsules (data transformed into log 10 values to ensure normality). *P* values less than or equal to 0.05 were considered statistically significant.

4.3. Results

Of the 16 implants, four were sent for histological analysis and one was lost during the course of the experiment, presumably because of exposure and subsequent extrusion, as has been previously reported (Hu et al., 2015). There were 11 capsular specimens surrounding inoculated and control implants of implant types A and B available for analysis. However, because the lost implant/capsule came from the control type B implant condition meant that there was only one sample in this condition for analysis. Thus, comparative statistical analysis of outcomes for the control type B implant was not possible.

4.3.1. Baker grading

Baker grading results for pigs 1 (ear tag 35) and 2 (ear tag 33) are shown in Table 4.1. Significantly more implants contaminated with *S. epidermidis* were graded as Baker grade III/IV (9 out of 10, 90%) than control implants (0 out of 5, 0%) (*P* = 0.002). While no significant difference in Baker grade score was found between implant types A and B (*P* = 0.6084).

Table 4.1. Baker grading results for pigs 1 and 2.

	Implant type	Treatment	Baker grade			
			I	II	III	IV
Pig 1	A	Control		X		
Ear tag 35	A	Inoculated			X	
	A	Inoculated				X
	A [#]	Inoculated		X		
	B*	Control				
	B	Inoculated				X
	B	Inoculated			X	
	B [#]	Control		X		
Pig 2	A	Control		X		
Ear tag 33	A	Inoculated			X	
	A	Inoculated			X	
	A [#]	Control	X			
	B	Control	X			
	B	Inoculated			X	
	B	Inoculated				X
	B [#]	Inoculated			X	

[#]Sent to the USA for histology analysis, *Lost implant

4.3.2. Weight of tissue attached to implants

Surrounding capsules were sectioned and the implant extruded. This required little force for type A implants, especially the control implants. In contrast, significant force was required to separate the type B implant from its surrounding capsule and visually it appeared that more tissue remained attached to the implant (Figure 4.5). As one measure of degree of tissue integration, the amount of pig tissue left on the implants during processing was determined (Table 4.2). There was significantly more tissue remaining attached to type B (1.602 g) when compared with the amount of tissue remaining attached to type A (0.243 g) ($P = 0.004$).

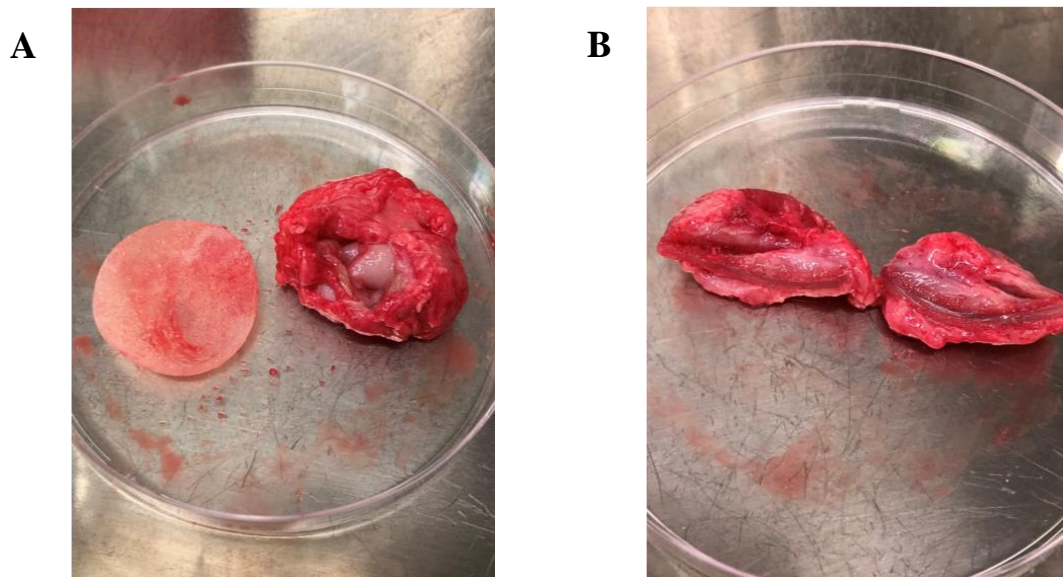


Figure 4.5. Explanted (A) type A and (B) type B implant with surrounding capsule intact.

Table 4.2. Amount (g) of host tissue remaining attached to implant.

	Type A	Type B
Pig 1	0.233	1.540
	0.183	1.860
	0.203	*Lost
Pig 2	0.253	1.210
	0.313	2.030
	0.273	1.370
Average	0.243 ± 0.05	1.602 ± 0.34

4.3.3. Control implants and capsules

Culture of explanted three non-inoculated control implants showed that these implants were contaminated probably via haematogenous spread (Coagulase-negative staphylococci) or ascending infection through the nipple (*S. aureus*, coagulase-negative staphylococci, *Enterococcus*) (Table 4.3). As the capsules around these implants were thinner, infection is likely to have been a more recent occurrence with minimal time for fibrous tissue formation.

Table 4.3. Microorganisms cultured from control implants.

	Sample number	Implant type	Organism
Pig 1	35.5	A	<i>S. aureus</i> , <i>Enterococcus</i>
		B	*Lost
Pig 2	33.5	A	Coagulase negative staphylococci
	33.1	B	<i>S. aureus</i>

4.3.4. Presence of *Staphylococcus epidermidis* in explanted samples

The individual cycle threshold (Ct) values of explanted implant and capsule specimens subjected to *S. epidermidis* specific PCR targeting the *icaA* gene are shown in Table 4.4. We arbitrarily considered Ct values less than 30 as *S. epidermidis* present in implant/capsule at high levels, Ct values 30 to 35 at moderate levels, and Ct values greater than 35 present at low levels.

Table 4.4. Detection of *S. epidermidis* in inoculated and control implant types A and B and the surrounding capsules. Individual real-time PCR cycle threshold (Ct) results for pigs 1 and 2.

	Sample number	Treatment	Implant type	<i>S. epidermidis</i> <i>icaA</i> PCR (Ct)	
				Implant	Capsule
Pig 1	35.5	Control	A	36.12	36.14
	35.2	Inoculated	A	36.05	36.14
	35.8	Inoculated	A	39.89	36.10
	35.3	Inoculated	B	39.01	36.15
	35.7	Inoculated	B	36.12	36.20
Pig 2	33.5	Control	A	36.20	36.15
	33.1	Control	B	36.13	No Ct
	33.3	Inoculated	A	No Ct	36.05
	33.8	Inoculated	A	36.06	36.10
	33.4	Inoculated	B	36.10	36.20
	33.7	Inoculated	B	36.11	No Ct

Low levels of *S. epidermidis* was detected using *S. epidermidis* specific PCR of the *icaA* gene in all inoculated and control implants (Ct > 35) except for type A implant 33.3 in pig 2 (No Ct), suggesting that the pigs' natural flora was taking over the induced biofilm. Similarly, low levels of *S. epidermidis* was detected in all capsules surrounding inoculated and control implants (Ct > 35) except for type B implants 33.1 and 33.7 in pig 2 (No Ct). A *S. epidermidis* positive control (ATCC 35984) had a Ct value of 15.78.

4.3.5. Total microbial load attached to type A and type B implants

Genomic DNA was extracted from implant and capsular tissue specimens using two different DNA extraction kits, Roche high pure PCR template preparation (Roche) (test 1) and the QIAamp DNA mini kit (Qiagen) (test 2). The individual total microbial load attached to type A and type B implants was determined after calculating the number of 16S rRNA copies present in the tissue attached to the implant (Table 4.5). Significantly higher numbers of 16S rRNA copies per mg implant were present on inoculated implants when DNA was extracted using test 1 (6566 ± 5560 SD) than compared to test 2 (2045 ± 1254), $P = 0.0416$. In non-inoculated control implants, the number of 16S rRNA copies were similar between test 1 (1382 ± 1532) and test 2 (1362 ± 1076), $P = 0.9861$. Overall, DNA extraction using the QIAamp DNA mini kit (test 2) consistently yielded DNA that produced less variability in 16S rRNA copy numbers when compared to test 1, which had inflated numbers for type B inoculated implants 35.3 (1.51×10^4) and 35.7 (1.01×10^4) in fig 1, and 33.4 (1.27×10^4) and 33.7 (7.36×10^3) in fig 2.

Although all implant pockets were inoculated with the same number of bacteria, there were significantly more bacteria attached to the inoculated type B implant (16S rRNA copy/mg implant, 7.03×10^3) when compared to the inoculated type A implant (1.58×10^3), as determined by qPCR ($P = 0.003$) (Figure 4.6A). In contrast, the mean number of 16S rRNA copies attached to the non-inoculated type A implant was 6.22×10^2 per mg implant, which was significantly less than the number attached to both type A and B inoculated implants ($P < 0.05$) (Figure 4.6A). No statistical comparisons were made to the non-inoculated (control) type B implant (33.1) given that there was only one result obtained from fig 2 as this implant was lost from fig 1. Although from this result, the type B control (2.87×10^3) appeared to have more bacteria attached to its surface when compared to the type A control, but in comparison to inoculated type B implants it had less bacteria attached.

Table 4.5. Number of bacteria as determined by 16S rRNA copies attached to a mg of implant. Individual results for pigs 1 and 2.

	Sample number	Treatment	Implant type	16S rRNA copy per mg implant		
				Test 1	Test 2	Average
Pig 1	35.5	Control	A	400.4	627.3	514
	35.2	Inoculated	A	2132.2	2643.8	2388
	35.8	Inoculated	A	1558.1	1114.5	1336
	35.3	Inoculated	B	15148.9	2552.5	8851
	35.7	Inoculated	B	10090.6	4452.2	7271
Pig 2	33.5	Control	A	599.2	862.0	731
	33.1	Control	B	3147.4	2597.6	2872
	33.3	Inoculated	A	870.3	841.6	856
	33.8	Inoculated	A	2680.7	820.6	1751
	33.4	Inoculated	B	12683.2	1349.1	7016
	33.7	Inoculated	B	7361.4	2587.8	4975

Table 4.6. Number of bacteria as determined by 16S rRNA copies per mg of capsular tissue. Individual results for pigs 1 and 2.

	Sample number	Treatment	Implant type	16S rRNA copy per mg capsule		
				Test 1	Test 2	Average
Pig 1	35.5	Control	A	2163.0	518.9	1341
	35.2	Inoculated	A	1715.3	1232.2	1474
	35.8	Inoculated	A	2997.4	1951.1	2474
	35.3	Inoculated	B	3411.5	1354.6	2383
	35.7	Inoculated	B	2744.0	1330.6	2037
Pig 2	33.5	Control	A	1965.1	628.0	1297
	33.1	Control	B	2982.0	687.9	1835
	33.3	Inoculated	A	3431.9	787.8	2110
	33.8	Inoculated	A	3159.5	1968.1	2564
	33.4	Inoculated	B	3764.4	1076.7	2421
	33.7	Inoculated	B	2822.0	1200.3	2011

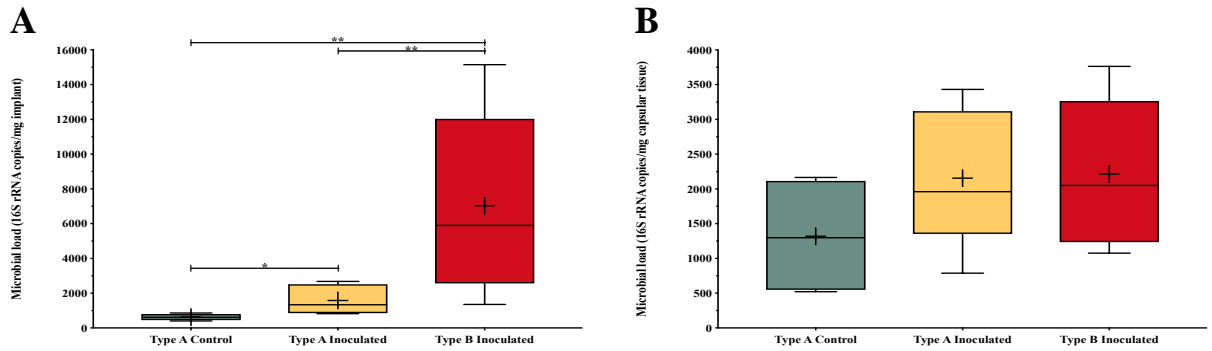


Figure 4.6. Microbial load (16S rRNA copies) per mg of (A) implant and (B) capsular tissue present in type A control implants (non-inoculated) and implant types A and B inoculated with *S. epidermidis*. Values are the medians \pm SD. Significantly different at $*P \leq 0.05$, $**P \leq 0.01$. ‘+’ denotes the mean.

4.3.6. Total microbial load in capsules surrounding type A and type B implants

Individual qPCR results on tissue obtained from two distinct areas of the capsule are shown in Table 4.6. As we found with the implants (Section 4.3.5.), DNA extracted using test 1 (Roche high pure PCR template preparation) produced higher numbers of 16S rRNA copies per mg tissue in capsules surrounding inoculated (3006 ± 623) and control implants (2370 ± 539) when compared to test 2 using the QIAamp DNA mini kit (inoculated, 1363 ± 409 ; control, 612 ± 86), $P < 0.01$. However, there was less variability in 16S rRNA copy numbers present in capsules when DNA was extracted using both test 1 (95% confidence interval (CI): 2485 to 3526 (inoculated), 1031 to 3709 (control)) and test 2 (95% CI: 1021 to 1704 (inoculated), 398.7 to 824.5 (control)).

While all inoculated implant pockets went on to develop CC and those not inoculated failed to do so. We still found no significant difference in the total number of bacteria (16S rRNA copies) in capsules surrounding inoculated implant types A (2.16×10^3) and B (2.21×10^3), as determined by qPCR ($P = 0.91$) (Figure 4.6B). In capsules surrounding type A implants, no significant difference was found in the microbial load present in inoculated and non-inoculated implants (1.32×10^3), $P = 0.171$ (Figure 4.7B). No statistical comparisons to the type B control implant were made given the one sample obtained in fig 2.

4.3.7. Total lymphocyte number on the surface of implant types A and B and in surrounding capsules

Implants

Individual qPCR results of the lymphocytic infiltrate on the surface of type A and type B implants are shown in Table 4.7. Among the inoculated implant types, there was a significant predominance of T-cells on their surface (CD3/mg of implant: type A, 3.15×10^4 ; type B, 7.67×10^4) than compared with B-cells (CD79a: type A, 93; type B, 2.86×10^2), $P < 0.01$ (Figure 4.7). In inoculated type B implants, there was an overwhelming high number of CD3+ T-cells obtained from pig 2 (1.27×10^5), which was ten-fold higher than those in pig 1 (2.63×10^4). Overall, there were higher lymphocyte numbers per milligram of implant on the surface of inoculated type B implants (CD3, 7.67×10^4 ; CD4, 4.79×10^3 ; CD8a, 8.89×10^2 ; CD79a, 2.86×10^2) than compared to inoculated type A implants (CD3, 3.15×10^4 ; CD4, 1.55×10^3 ; CD8a, 2.39×10^2 ; CD79a, 93), although no significant differences were found ($P > 0.05$) (Figure 4.7).

In type A implants, there was no difference in the number of both T-cells and B-cells on the surface of inoculated and control implants (CD3, 5.30×10^3 ; CD4, 1.20×10^2 ; CD8a, 35; CD79a, 39), $P > 0.9999$ (Figure 4.7). No statistical comparisons to the type B control implant were made due to insufficient sample numbers.

Linear regression analysis showed no association between the microbial load and the total number of T-cells attached to the implant (CD3: coefficient of determination, R-squared (R^2) = 0.342, $P = 0.059$) (Figure 4.8). A significant positive linear relationship was found between the number of bacteria attached to implant surfaces and the number of CD4 helper T-cells ($R^2 = 0.712$, $P = 0.001$), CD8a cytotoxic T-cells ($R^2 = 0.746$, $P < 0.001$) and CD79a B-cells ($R^2 = 0.786$, $P < 0.001$) attached to the implant (Figure 4.8).

Table 4.7. Number of T-cells (CD3), helper T-cells (CD4), cytotoxic T-cells (CD8a) and B-cells (CD79a) on the surface of a mg of implant as determined by qPCR. Individual results for pigs 1 and 2.

	Sample number	Treatment	Implant type	Lymphocyte copy number per mg implant			
				CD3	CD4	CD8a	CD79a
Pig 1	35.5	Control	A	5292	114	26	11
	35.2	Inoculated	A	14628	2276	436	109
	35.8	Inoculated	A	57646	1295	206	77
	35.3	Inoculated	B	22614	5853	1190	435
	35.7	Inoculated	B	29939	8077	1841	252
Pig 2	33.5	Control	A	5315	127	44	11
	33.1	Control	B	4789	793	264	72
	33.3	Inoculated	A	12476	1671	125	92
	33.8	Inoculated	A	41146	949	190	44
	33.4	Inoculated	B	139398	3549	217	351
	33.7	Inoculated	B	114742	1667	309	108

Table 4.8. Number of T-cells (CD3), helper T-cells (CD4), cytotoxic T-cells (CD8a) and B-cells (CD79a) per mg of capsular tissue as determined by qPCR. Individual results for pigs 1 and 2.

	Sample number	Treatment	Implant type	Lymphocyte copy number per mg capsule			
				CD3	CD4	CD8a	CD79a
Pig 1	35.5	Control	A	52737	8310	1480	44
	35.2	Inoculated	A	455125	76281	1342	388
	35.8	Inoculated	A	656403	12974	2011	463
	35.3	Inoculated	B	4313174	624478	12277	2855
	35.7	Inoculated	B	585491	83919	14825	3847
Pig 2	33.5	Control	A	24576	5891	142	26
	33.1	Control	B	717307	12377	6362	770
	33.3	Inoculated	A	60952	13364	3330	1341
	33.8	Inoculated	A	534060	37905	2358	826
	33.4	Inoculated	B	406303	65324	5182	3055
	33.7	Inoculated	B	2813887	129143	12651	2768

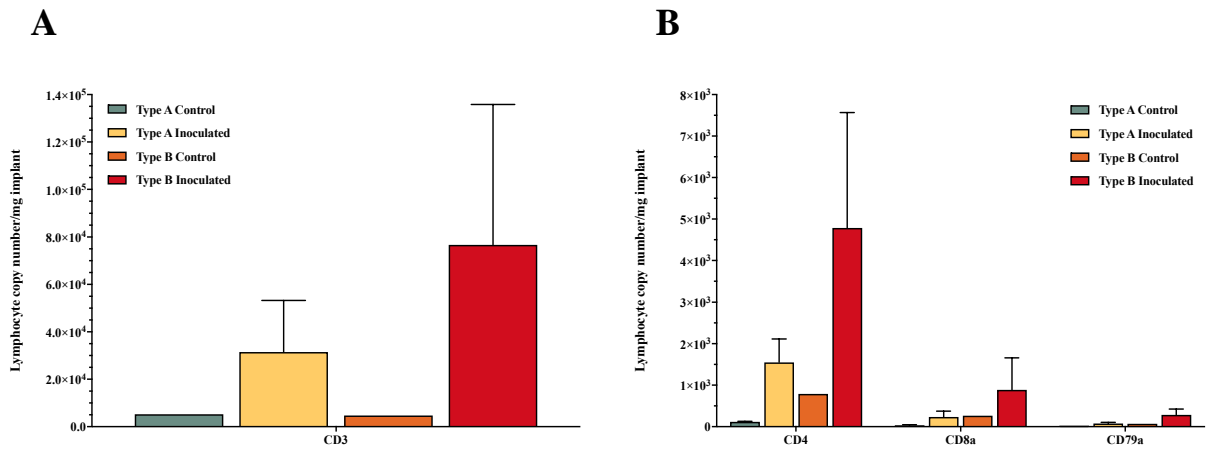


Figure 4.7. (A) CD3, (B) CD4, CD8a and CD79a copy number per mg of implant on the surface of type A and type B control implants and implants inoculated with *S. epidermidis*. Values are the means + SD.

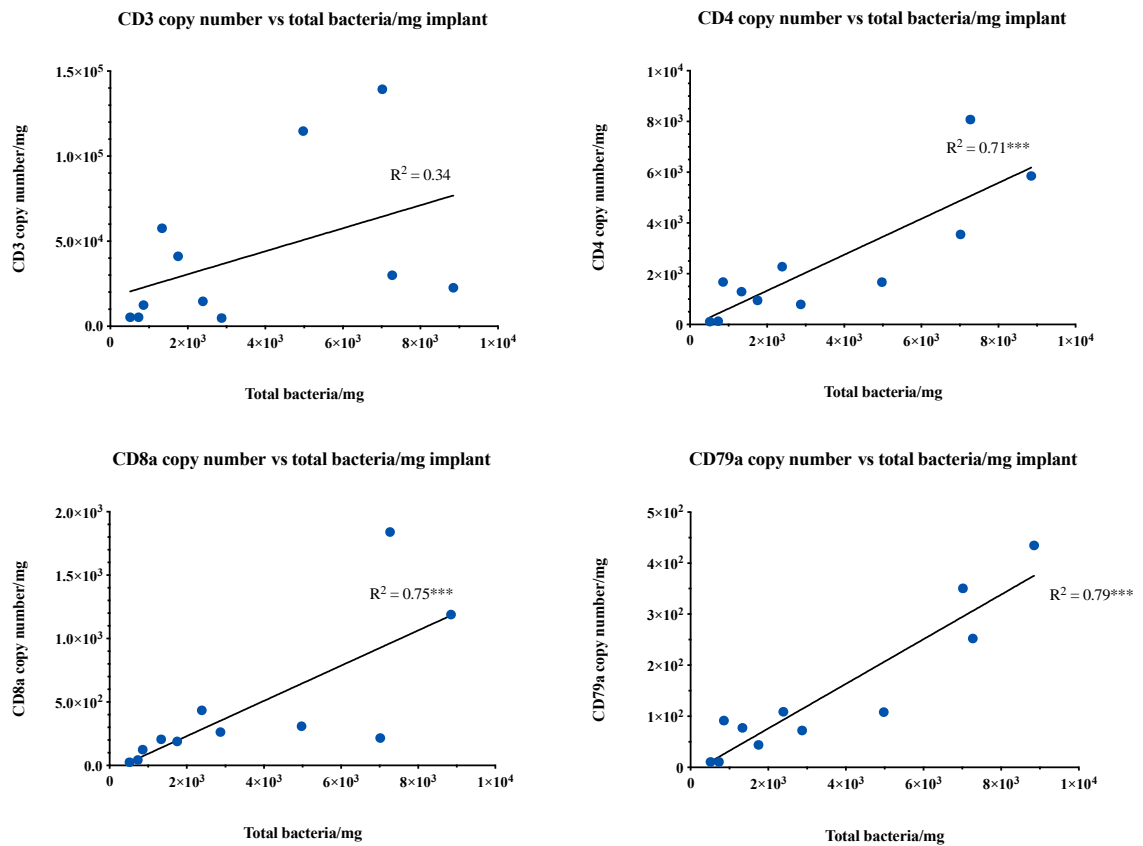


Figure 4.8. CD3, CD4, CD8a, CD79a from pig implants versus total bacteria per mg of implant sample. Significant correlation at $***P \leq 0.001$.

Capsules

qPCR analysis of lymphocytes in capsules surrounding implant types A and B are shown in Table 4.8. In capsules surrounding inoculated type A and type B implants, there was a significant predominance of CD3+ (type A, 4.27×10^5 ; type B, 2.03×10^6) and CD4+ T-cells (type A, 3.51×10^4 ; type B, 2.26×10^5) per mg of tissue compared with B-cells (type A, 7.54×10^2 ; type B, 3.13×10^3), $P < 0.05$ (Figure 4.9). In line with the lymphocytic infiltrate found in inoculated type B implants, the surrounding capsules had a higher number of CD3 (2.03×10^6), CD4 (2.26×10^5), CD8a (1.12×10^4) and CD79a cells (3.13×10^3) when compared to capsules surrounding inoculated type A implants (CD3, 4.27×10^5 ; CD4, 3.51×10^4 ; CD8a, 2.26×10^3 ; CD79a, 7.54×10^2), and this reached significance in CD8a+ T-cells and CD79a+ B-cells ($P = 0.0286$) (Figure 4.9). However, this result was likely due to inflated lymphocyte numbers for type B inoculated implants 35.3 (4.31×10^6) in pig 1 and 33.7 (2.81×10^6) in pig 2, which were ten-fold higher than the numbers obtained for the other inoculated implant types.

In capsules surrounding type A implants, no difference was found in the number of CD3, CD4 or CD8a T-cells and CD79a B-cells between inoculated and control implants (CD3, 3.87×10^4 ; CD4, 7.10×10^3 ; CD8a, 8.11×10^2 ; CD79a, 35), $P > 0.05$ (Figure 4.9). No statistical comparisons to the type B non-inoculated control implant were made due to the one sample.

There was a significant positive linear relationship between the number of bacteria and the total number of T-cells found in the capsular material (CD3: $R^2 = 0.373$, $P = 0.046$) but the power of this test (0.519) was below the recommended 0.8 (Figure 4.10). There was a similar positive relationship between the microbial load and CD8a+ T-cells ($R^2 = 0.377$, $P = 0.044$) and CD79a+ B-cells ($R^2 = 0.604$, $P = 0.005$) found in capsular material. No association was found between the microbial load and the number of CD4+ T-cells in capsular tissue ($R^2 = 0.211$, $P = 0.155$) (Figure 4.10).

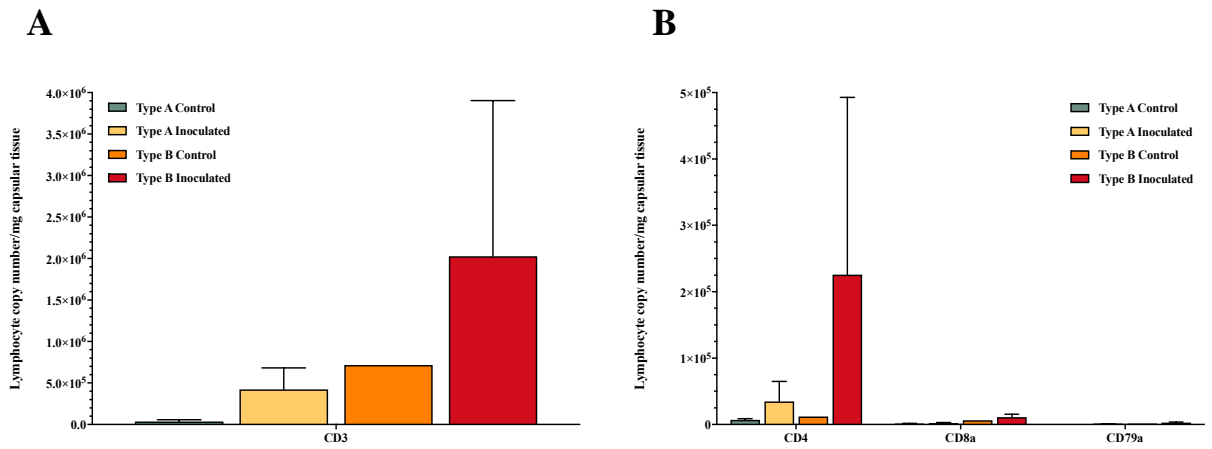


Figure 4.9. (A) CD3, (B) CD4, CD8a and CD79a copy number per mg of capsular tissue surrounding type A and type B control implants and implants inoculated with *S. epidermidis*. Values are the means + SD.

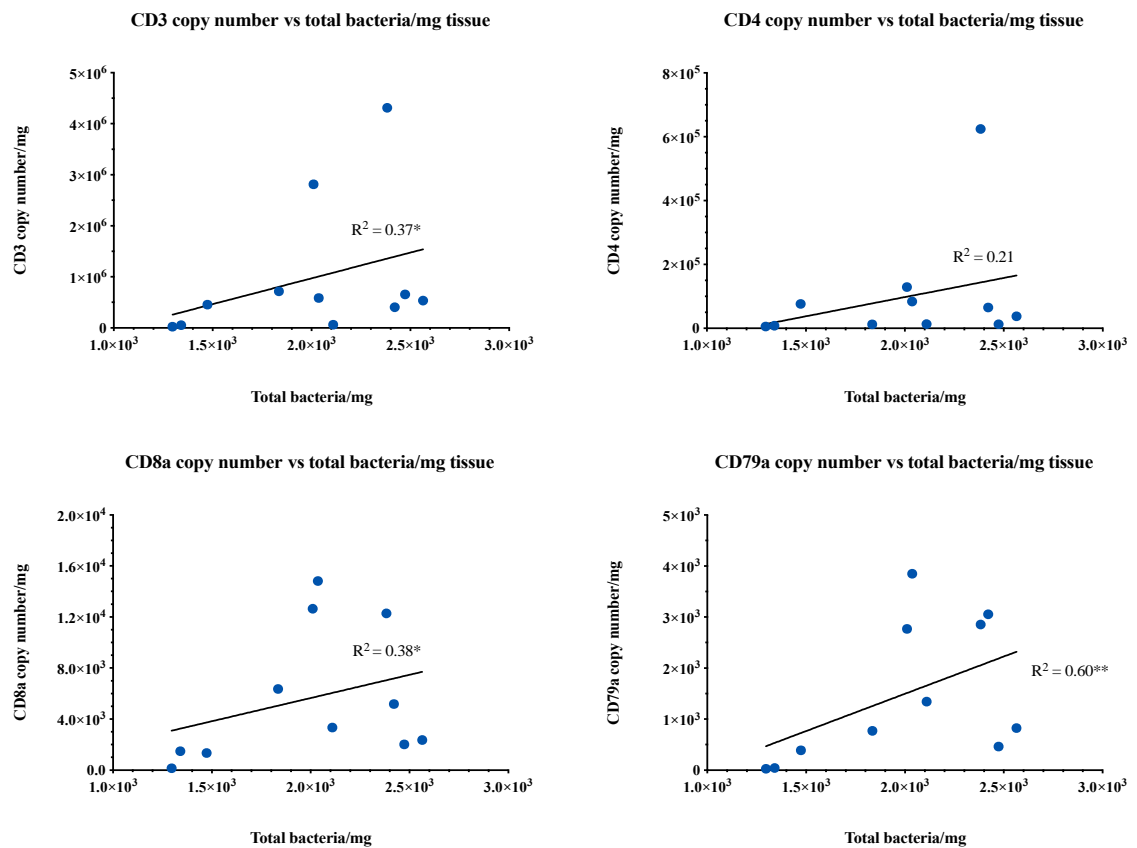


Figure 4.10. CD3, CD4, CD8a, CD79a from pig capsules versus total bacteria per mg of capsular sample. Significant correlation at * $P \leq 0.05$, ** $P \leq 0.01$.

4.3.8. Scanning electron microscopy

The whole SEM processed section of implants and capsules were viewed and the sample graded on the degree of bacterial biofilm using the criteria listed in Table 4.9.

Table 4.9. Criteria used to determine the degree of biofilm.

Score	Degree of biofilm
1	Low amount of biofilm – one to two areas with a few colonies covered with thick exopolymeric substances (EPS)
2	Medium amount of biofilm – three to five areas with larger colonies covered with thick EPS
3	High amount of biofilm – many colonies covered by thick EPS

Two separate pieces of implant or capsule from each implant or capsule were obtained at different time points and analysed at different time points by the one operator. Samples were scored blinded as to the implant type and whether or not it was inoculated (Tables 4.10 and 4.11). From Tables 4.10 and 4.11 differences in the subjective scoring can be seen between the two samples. This discrepancy probably reflects the patchy nature of biofilm infection in these samples. This was mirrored in the qPCR results for some of the samples, e.g. sample numbers 35.3 and 35.7 in pig 1 and 33.4 in pig 2.

Table 4.10. Bacterial load and SEM scoring for the amount of biofilm present on implant types A and B.

	Sample number	Treatment	Implant type	Implant		qPCR
				Sample 1	Sample 2	Average
Pig 1	35.5	Control	A	3	2	514
	35.2	Inoculated	A	3	3	2388
	35.8	Inoculated	A	3	2	1336
	35.3	Inoculated	B	2	2	8851
	35.7	Inoculated	B	3	1	7271
Pig 2	33.5	Control	A	3	1	731
	33.1	Control	B	3	1	2872
	33.3	Inoculated	A	2	2	856
	33.8	Inoculated	A	3	3	1751
	33.4	Inoculated	B	3	2	7016
	33.7	Inoculated	B	2	1	4975

Table 4.11. Bacterial load and SEM scoring for the amount of biofilm present in capsules surrounding implant types A and B.

	Sample number	Treatment	Implant type	Capsule		qPCR
				Sample 1	Sample 2	
Pig 1	35.5	Control	A	3	3	1341
	35.2	Inoculated	A	2	3	1474
	35.8	Inoculated	A	2	2	2474
	35.3	Inoculated	B	1	2	2383
	35.7	Inoculated	B	1	1	2037
Pig 2	33.5	Control	A	1	1	1297
	33.1	Control	B	3	3	1835
	33.3	Inoculated	A	3	1	2110
	33.8	Inoculated	A	3	Charging	2564
	33.4	Inoculated	B	2	1	2421
	33.7	Inoculated	B	2	3	2011

The charging effect occurred in the capsule surrounding type A inoculated implant 33.8 (Table 4.11). Charging is caused by the accumulation of static electric charges on the specimen surface, which results in unreliable evaluation of images due to unstable imaging conditions and a loss in resolution (Kim et al., 2010).

There was no significant relationship found between the SEM grading and the microbial load attached to the implants (type A: $R^2 = 0.259$, type B: $R^2 = 0.131$; $P > 0.05$) and capsules surrounding implants (type A: $R^2 = 0.163$, type B: $R^2 = 0.0162$; $P > 0.05$) demonstrating the patchy nature of biofilm.

Figure 4.11 shows the SEM images for inoculated and non-inoculated type A and type B implants and the surrounding capsules. SEM confirmed the presence of biofilm on the surface of implants and within the capsules surrounding implants from both inoculated and control implant types. At higher magnification, coccoid-shaped bacteria are readily evident, embedded in extracellular polymeric substance. The biofilm was generally multi-layered on inoculated and non-inoculated implant types A and B (Figure 4.11A, C, E, G) and the surrounding capsules (Figure 4.11B, F, H). Although in the capsular material surrounding inoculated type B implant, the biofilm was composed of isolated bacterial cells (Figure 4.11D).

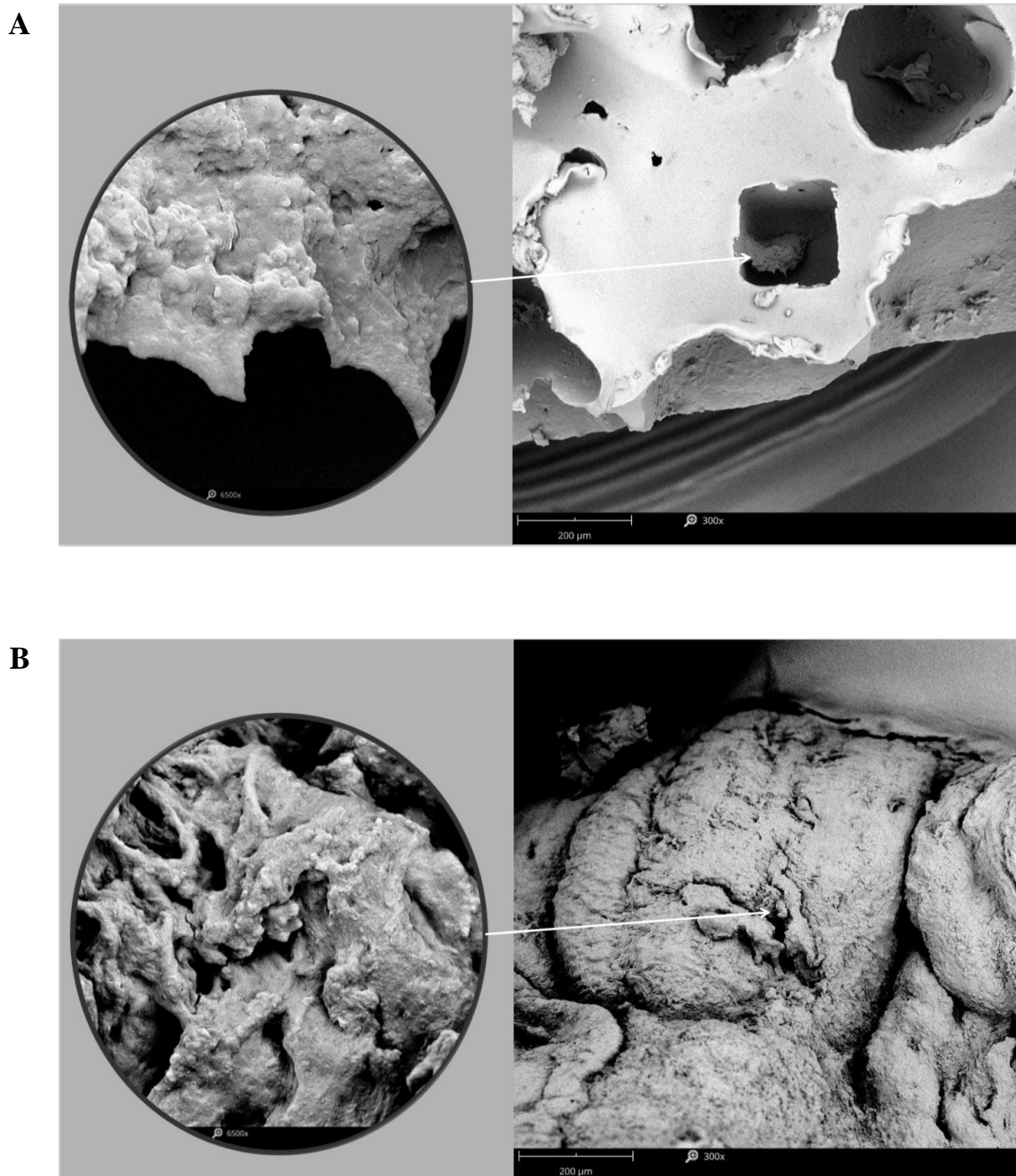
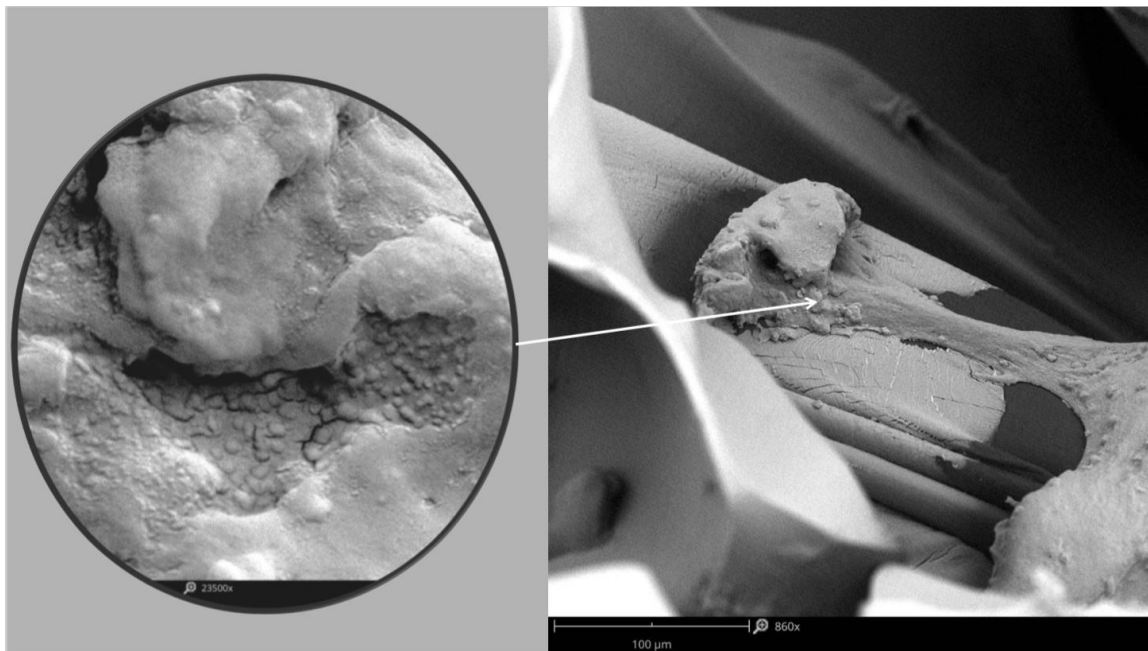


Figure 4.11. Scanning electron micrographs of *S. epidermidis* inoculated and non-inoculated control implant types A and B and the surrounding capsules. Bacterial biofilm was attached to the hidden surfaces of the implant and present within the capsules surrounding implants. Higher magnification shows clusters of coccoid bacterial cells encased in excreted polymeric substances intimately associated with the implant surface and capsule tissue.

(A) Inoculated type A implant and (B) surrounding capsule. Both magnified 300X and 6,500X.

C



D

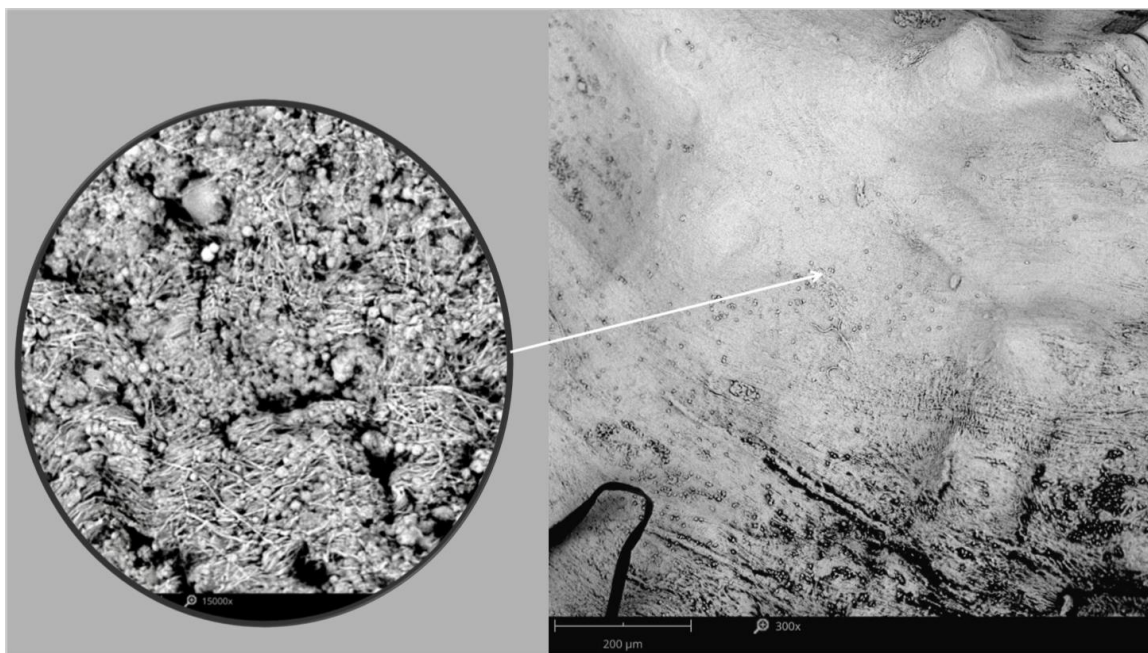
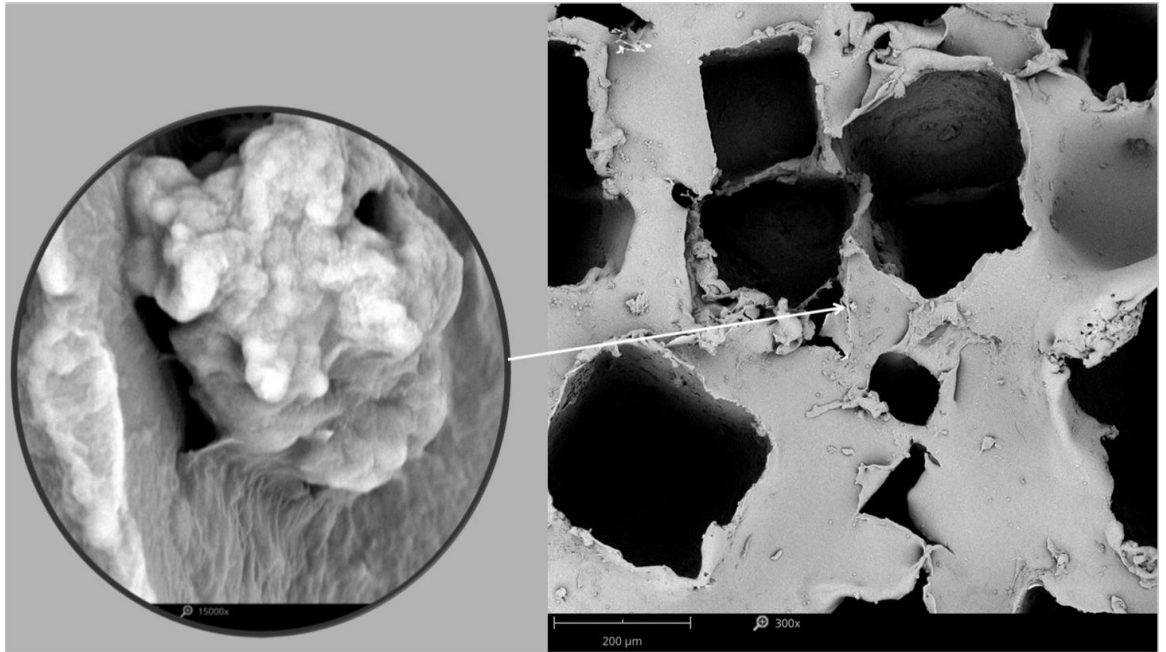


Figure 4.11. Continued.

(C) *Inoculated type B implant magnified 860X and 23,500X, and (D) surrounding capsule magnified 300X and 15,000X.*

E



F

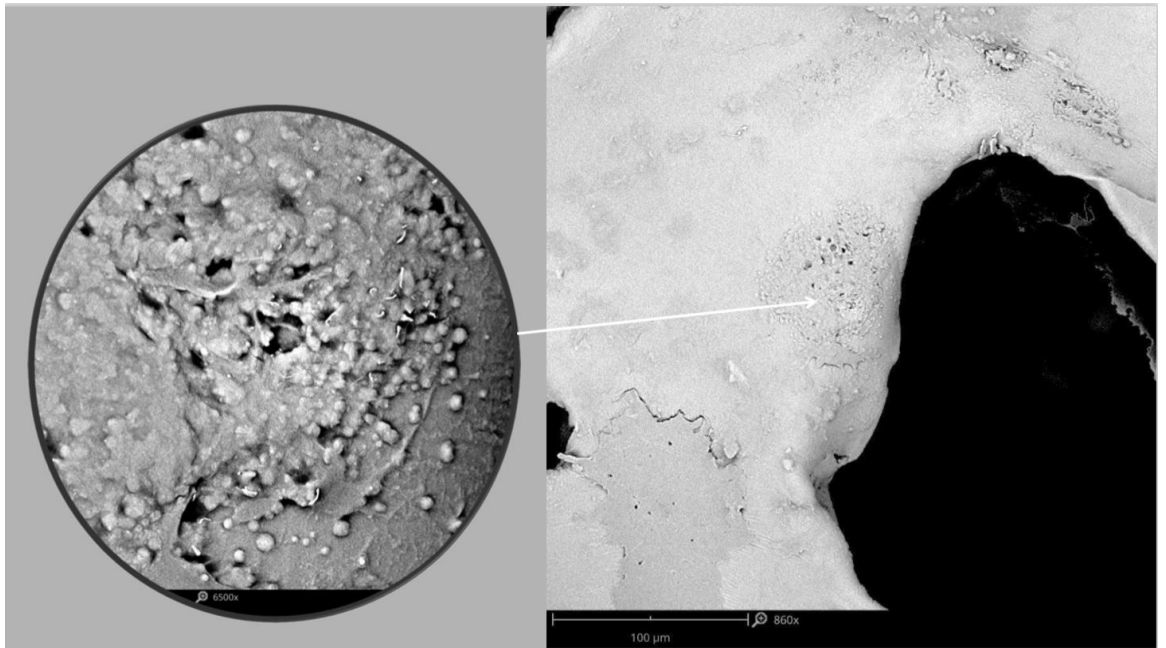


Figure 4.11. Continued.

(E) Non-inoculated type A implant magnified 300X and 15,000X, and (F) surrounding capsule magnified 860X and 6,500X.

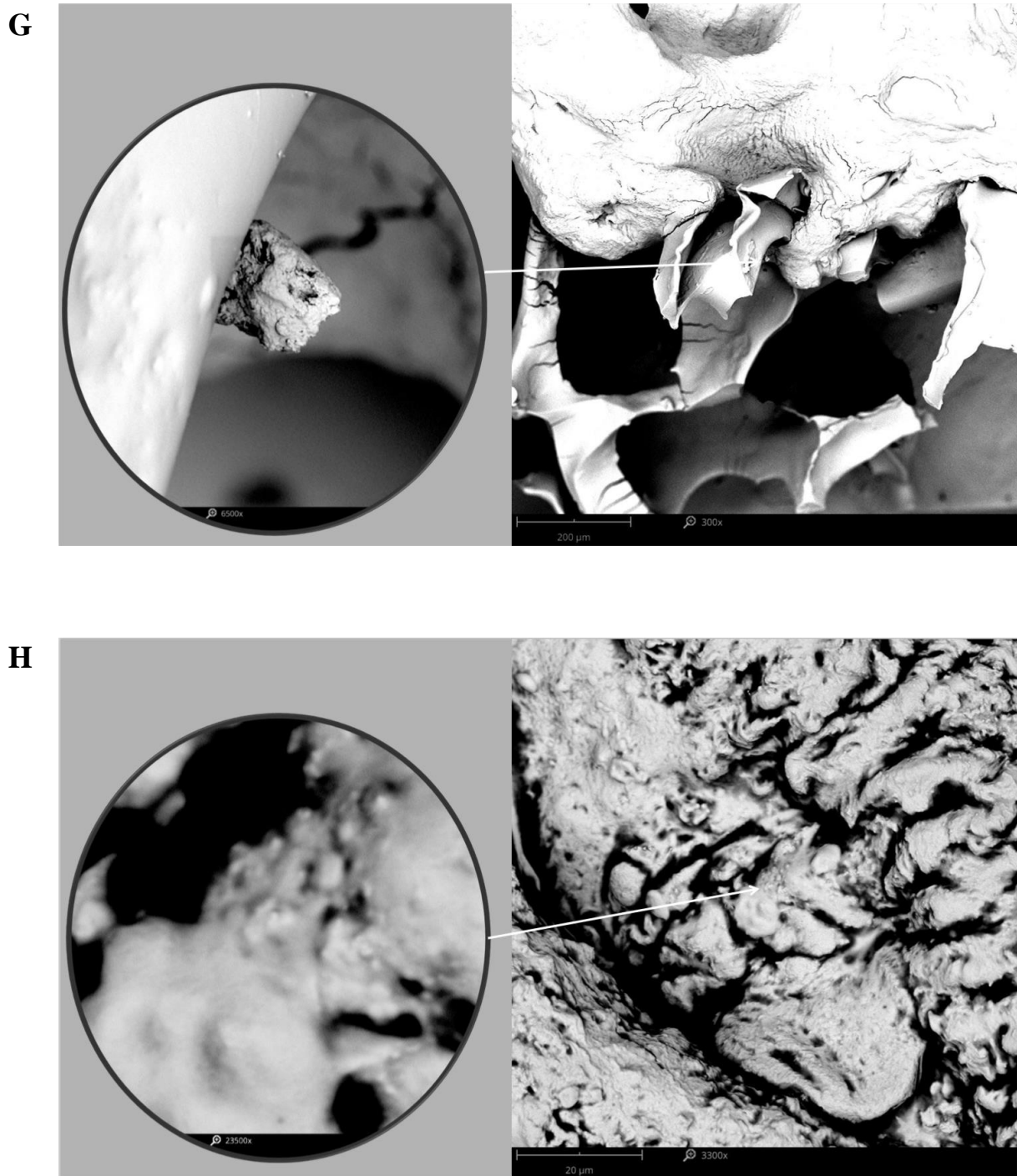


Figure 4.11. Continued.

(G) Non-inoculated type B implant magnified 300X and 6,500X, and (H) surrounding capsule magnified 3,300X and 23,500X.

4.3.9. Surface area and surface roughness determinations

Analysis using micro CT scans and confocal microscopy allowed visualisation and calculation of surface area for both implant types. Figure 4.12 shows the 3D surface area images of implant types A and B, which were used to calculate the 3D:2D ratio of its surface.

The calculated 3D:2D surface area ratio for type A was 1.70 and was classified as having minimal surface area and low roughness based on our proposed functional classification of implant outer shells (Table 4.12). While the salt-loss produced type B implant had a 3D:2D surface area ratio of 3.2 as determined in Chapter III. These measurements confirmed the type B texture had a higher surface area/roughness in comparison to type A, which could explain the higher microbial load observed in type B implants.

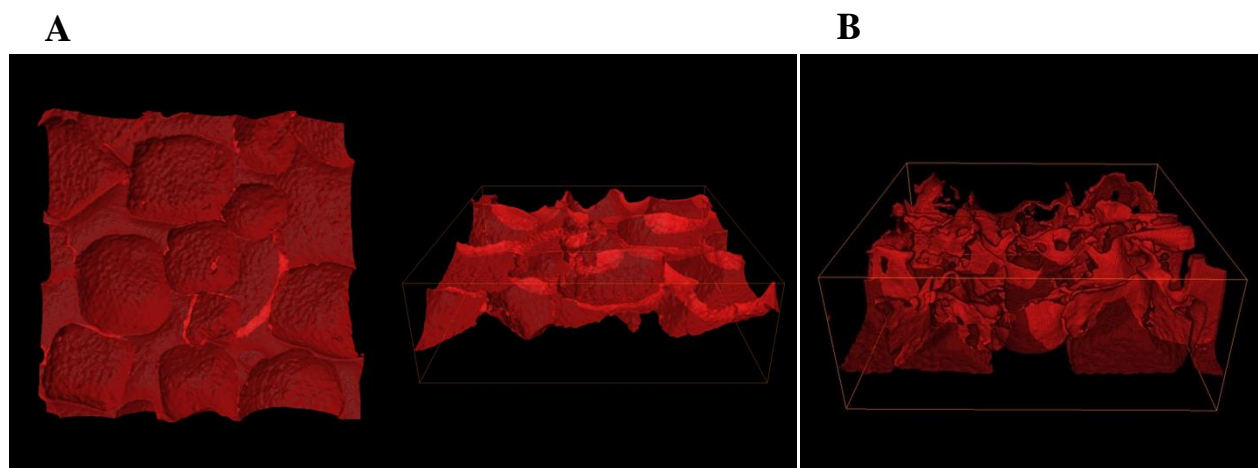


Figure 4.12. Three-dimensional cross sections and extractions from micro CT analysis used for measurement of surface area and roughness of (A) type A and (B) implants.

Table 4.12. Raw surface area calculations and 3D:2D ratio for each implant type.

Implant type	3D surface area (from 1.4 x 1.4 mm ²)	3D:2D ratio [^]	Surface area category (based on 3D:2D ratio)
Type B	12 mm ²	3.2	Intermediate
Type A	6.5 mm ²	1.7	Minimal

[^]Normalised to Mentor Smooth.

4.4. Discussion

In this Chapter we analysed the interactions among textured implants, biofilm load, CC and host response *in vivo*. We utilised the established porcine model previously described (Tamboto et al., 2010) but in our study biofilm-infected implants were left *in situ* for 11 weeks (77 days). Also, unlike previous studies we tested textured implants only since these surface types, with their greater surface area, support higher levels of bacterial growth (Chapter III).

Using this pig model, we found that artificial contamination of textured implants, type A and type B, with *S. epidermidis* led to the formation of biofilm and the development of CC. Of the 10 inoculated implants, nine (90%) resulted in significant contracture (Baker grade III or IV). By comparison, of the five control implants, none were found to have developed contracture. However, because the implants were composed of a sandwich of two implant surfaces (stacked one on top of the other) rather than a gel-filled implant, as occurs in human breast implants, Baker grading was less precise.

In all nine inoculated implants (types A and B), which all went on to develop contracture, there were significantly higher numbers of bacteria attached to their surface than non-inoculated type A implants. No statistical comparisons were made to the non-inoculated type B implant since only one result was obtained from pig 2 as this implant was lost from pig 1, but from this single result less bacteria were found attached when compared to type B inoculated implants. These findings are consistent with other animal studies (Shah et al., 1981, Marques et al., 2011, Tamboto et al., 2010, Jacombs et al., 2012, Jacombs et al., 2014) that have shown implants artificially contaminated with bacteria develop a significantly higher microbial load than implants which receive no inoculation. Furthermore, we have further validated the subclinical infection theory (Virden et al., 1992, Dobke et al., 1994, Deva and Chang, 1999, Pajkos et al., 2003, Netscher, 2004, Tamboto et al., 2010, Hu et al., 2015), with these findings reinforcing the pathway from initial

contamination of breast implants with bacteria progressing to established biofilm and subsequent contracture.

Both type A and type B implants retained different amounts of tissue during explantation. It was important to account for this retained tissue to precisely determine the levels of bacterial attachment to the two implant types. Thus, we devised a formula to separate (i) the bacteria attached to the implant and (ii) the bacteria in the tissue attached to the implant. Using this formula we found significantly more tissue incorporation with the type B implant than the type A implant. This is consistent with the findings of significantly higher numbers of bacteria attached to type B inoculated implants than type A inoculated implants. Moreover, micro CT analysis of implant surface area/roughness measurements showed the type B implant (salt-loss produced) had a greater surface area, classified as an “intermediate” surface area based on our proposed functional classification system (Chapter III), when compared to the “minimal” surface area type A implant. These findings are in line with our findings from Chapter III and previously published studies (Jacombs et al., 2014) that a more textured surface promotes a higher bacterial load. However, our results also show that, *in vivo*, once a threshold of biofilm forms on either type A or type B implant surfaces, there seems to be an equal propensity to progress to CC irrespective of surface type.

Despite finding that all inoculated implants went on to develop CC and those not inoculated failed to do so, we found no significant difference in the number of bacteria in capsules surrounding inoculated implant types A and B and non-inoculated type A implants. This has also been found previously reported by Jacombs et al. (2014), although in their study biofilm-infected implants were left *in situ* for an average of 19 weeks. Moreover, *S. epidermidis* specific PCR detected low levels of the bacteria in almost all inoculated implants and surrounding capsules, and endogenous porcine *Staphylococcus* was consistently cultured from explanted control implants. Therefore, it is likely contracture in inoculated implants resulted from contamination with endogenous bacteria, which have been shown to form biofilms around implants, subsequently leading to contracture

(Tamboto et al., 2010). Alternatively, the human *S. epidermidis* inoculum could initiate the development of a biofilm by overcoming local immunity. Endogenous porcine *Staphylococcus* species, which we found are present in high numbers, may then overcome the original inoculated human strain. Although we found these endogenous bacteria could not initiate contracture in non-inoculated implants.

SEM analysis showed the presence of coccoidal cells encased in a glycocalyx matrix within the capsules surrounding implants and attached to the implants. We observed no difference in the degree of biofilm development on implants between types A and B based on SEM evaluation, despite more bacteria being attached to implant type B. Moreover, there was no significant association between the SEM grading and the microbial load attached to the implants and capsules surrounding implants. The SEM grading we used in assessing the degree of biofilm formation was a subjective method of classification, which relied on non-specific determinants and the examiner's own biases. Although samples were analysed by the one operator, variability in the subjective scoring still occurred between replicate samples. This could be attributed to the patchy and inconsistent nature of biofilm rather than operator bias. Biofilms are not confluent on a surface and this was evident in our samples with some sites displaying large bacterial aggregations, while other regions were devoid of microorganisms. Thus, utilising high-powered microscopy on small samples (2 to 3 mm²) is likely to result in biofilm not being identified (Percival et al., 2015).

It was likely the biofilm-positive specimens visualised by SEM were composed mainly of natural pig flora given *S. epidermidis* specific PCR detected low levels of the bacteria in almost all inoculated implants. Nonetheless, we also found that both non-inoculated implants and capsules developed biofilms. This was most likely attributable to contamination of the implant with endogenous pig *Staphylococcus* by haematogenous spread or ascending infection through the nipple consistent with the culture positivity observed in explanted control implants. An alternative source of contamination could have been from endogenous breast flora deposited on the implant

surface by handling of the breast or disruption of its ducts during surgery. Although implant contamination was adequate to elicit biofilm formation, there was a statistically significant difference between the contracture rates of inoculated and non-inoculated implant pockets.

The analysis of lymphocytes on the surface of contaminated implants and in capsules surrounding contaminated implants showed that there is a strong T-cell response. Our findings are in agreement with previous studies, which have shown that the majority of inflammatory cells present in the implant capsule are T-cells (Wolfram et al., 2012, Hu et al., 2015). The higher bacterial load on contaminated implants may explain the observed higher lymphocyte numbers and predominantly T-cell hyperplasia. Indeed, we found an increased lymphocytic infiltrate in inoculated type B implants, which were found to have a more textured surface that promoted a higher bacterial load. Although, no significant difference was found in the T-cell response elicited between inoculated implant types A and B and the surrounding capsules, with each having a similar proportion of CD3+ T-cells. This response was likely to the presence of bacteria and not just the innate physiological defences since we found a significant linear relationship between the numbers of T-lymphocytes with increasing bacterial load. The proportion of helper and cytotoxic T-cells on implants and the proportion of CD3+ CD8a+ T-cells in capsules correlated with increasing bacterial load. In addition, there was a significant linear correlation between the number of B-cells and the number of detected bacteria. CD4+ helper T-cells will secrete cytokines to activate or regulate other cells in the immune system to trigger an immune response. While CD8a+ cytotoxic T-cells are involved in cell-mediated immunity (Britez et al., 2012). B cells are involved in the humoral response by producing circulating antibodies when they differentiate to plasma cells (Britez et al., 2012). Unfortunately, the relationship between B- and T-lymphocytes, as well as the different proportions of T-cell subtypes, has been infrequently reported in implants and capsular tissues. Nevertheless, we have further demonstrated a possible link between bacterial biofilm and T-cell hyperplasia, which is significant in light of BIA-ALCL.

The findings from this Chapter reinforce that textured implants support a higher bacterial load and whether implant inoculation was deliberate or by chance, *S. epidermidis* bacteria or the animal endogenous flora, were able to form biofilms on the polymer surface subsequent to contact. Moreover, chronic biofilm infection around breast implants was associated with a predominantly T-cell lymphocytic infiltrate, which is directly linked to the bacterial load attached to the implant. Due to the subjective nature of the Baker grading of CC and the SEM grading of degree of biofilm, as well as the limitations associated with utilising miniature implants we were not able to prove subclinical infection as a cause of CC. Although we do not assume that subclinical infection is the only cause of CC, our findings highlight that any measures to reduce the likelihood of bacterial contact with the implant surface at time of surgery may prevent or reduce its incidence. A further long-term study to investigate the correlation between the amount of biofilm load and degree of CC using the porcine model is currently underway.

Chapter V.

Analysis of bacterial biofilm and host response in new cases of Breast Implant-associated Anaplastic Large-cell Lymphoma

5.1. Introduction

In Chapters III and IV we showed that greater numbers of bacteria attach to textured implants, with their greater surface area, both *in vitro* (Chapter III) and *in vivo* (Chapter IV), in line with previously published studies (Jacombs et al., 2014, Hu et al., 2015). Moreover, chronic biofilm infection around breast implants in pigs produced a predominantly T-cell lymphocytic infiltrate, which was directly linked to the bacterial load attached to the implant (Chapter III). These findings are important in the context of BIA-ALCL, a rare T-cell lymphoma, with all cases having been exposed to textured implants.

Numerous hypotheses have been put forward to explain the genesis of BIA-ALCL. In a recent study, the association and risk of different textured implant surfaces with BIA-ALCL was investigated in 55 cases from Australia and New Zealand (Loch-Wilkinson et al., 2017). It found all patients in the series had prolonged exposure to textured implants, with Allergan Biocell salt-loss textures accounting for 58.7% of the implants followed by Silimed PU textures (18.7%). The risk of developing BIA-ALCL was significantly higher in Allergan Biocell (14.11 times) and Silimed PU (10.84 times) implants when compared to Mentor Siltex (imprinted texture) implants (Loch-Wilkinson et al., 2017). The use of Biocell textured implants has previously been implicated in late seroma and double capsule, which is a common presentation of BIA-ALCL (Park et al., 2014). Micro CT analysis has confirmed Silimed PU and Allergan Biocell implants have higher

surface area/roughness compared with Mentor Siltex implants (Chapter III). The authors attribute the higher risk for Allergan Biocell implants (intermediate surface area) compared to Silimed PU (high surface area) could be due to the shorter duration of use/exposure of Silimed PU in the Australian population (Loch-Wilkinson et al., 2017). PU implants have been shown to be associated with a significantly higher level of both bacterial contamination and lymphocyte activation in contracture patients (Hu et al., 2015).

The role of bacteria in BIA-ALCL is further supported by the finding of high levels of bacterial contamination within BIA-ALCL specimens (Hu et al., 2016). Interestingly, the microbiome of these specimens differed significantly from the microbiome surrounding non-tumour contracted capsule specimens (Hu et al., 2016). The presence of a higher proportion of Gram-negative bacteria in BIA-ALCL compared with Gram-positive bacteria, which predominate in non-tumour contracted capsules, may explain the pathway to proliferation and malignant transformation. However, in Hu et al.'s (2016) study a combination of fresh and fixed tissue was used. The fixation process can affect the quality and number of amplifiable DNA templates and may pose challenges to the sensitivity and specificity of molecular analyses if appropriate conditions of fixation and validation are not applied (Kumar et al., 2016).

Therefore, the aim of this Chapter was to compare the bacterial load and host response in fresh implants and capsules of patients with BIA-ALCL to non-tumour contracted capsule specimens.

5.2. Materials and Methods

5.2.1. Patients

Twenty breast implant-associated ALCL specimens were collected from centres around Australia and New Zealand from a total of 12 patients. In addition, 16 samples were obtained from

the contralateral normal breast in these patients. Non-tumour specimens from 14 patients undergoing revision surgery for CC collected over a two-year period from centres around Australia were included for comparative analysis. In most patients, both implant and capsule specimens were collected. However in some patients, either the implants or capsules were only collected.

5.2.2. Processing of implant and capsule samples

Fresh samples from patients with diagnosed BIA-ALCL ($n = 9$ implants, $n = 11$ capsules; contralateral breast, $n = 8$ implants, $n = 8$ capsules) and non-tumour samples ($n = 16$ implants, $n = 19$ capsules) from patients with CC were aseptically sectioned from different parts of the capsule and implant. Quantitative aerobic cultures, viability counts and bacterial identification were obtained by transferring sectioned samples (100 to 200 mg) to 10 mL of TSB followed by sonication for 15 min and standard plate culture (Section 2.2.1.). The remaining sectioned samples were then stored at -20°C until molecular analysis. Bacterial contamination was determined by bacterial viability counts utilising standard plate culture and total bacterial counts utilising real-time qPCR.

5.2.3. DNA extraction

The total number of bacteria was estimated by qPCR. For DNA extraction prior to qPCR, genomic DNA was extracted from biological samples of capsular tissue and implant using the DNeasy PowerBiofilm kit (Qiagen) as described in Section 2.3.2.

5.2.4. Total bacterial load and lymphocyte number in capsules and attached to implants by qPCR

Each extracted DNA sample was subjected to qPCR of the 16S rRNA gene using eubacterial universal primers (Table 2.1) as described in Section 2.3.2. The 18S rRNA gene was

used as a reference to normalise the amount of ALCL/non-tumour capsule tissue used in DNA extraction (Table 2.1, Section 2.3.2.).

The number of T-cells and B-cells in human capsular tissue was quantified by qPCR of CD3, CD4, CD8a and CD79a genes (Table 2.1) as per Section 2.3.2. The total number of bacteria and lymphocytes was expressed per milligram of capsule or implant based on the average number of copies of the 18S rRNA gene in human tissue.

5.2.5. Scanning electron microscope

The presence of bacterial biofilm was confirmed visually on capsules of three BIA-ALCL patients using SEM as described in Section 2.4.1.

5.2.6. Statistical analysis

All statistical analyses were performed with GraphPad Prism 7.0. The data were tested for normality of distribution by the Shapiro-Wilk normality test. The Mann-Whitney rank sum test was used to compare the age of patients and the time since implantation. A Kruskal-Wallis non-parametric ANOVA followed by Dunn's pairwise multiple comparisons was conducted to measure for differences in the bacterial load and lymphocyte number in explanted implant and capsule samples. The Wilcoxon matched-pairs signed rank test was used to look for differences in bacterial load between BIA-ALCL and contralateral non-ALCL samples when there was an equal number of pairs and/or more than three pairs in each group to allow sufficient comparison. Linear regression analysis, on log 10 transformed data, was used to determine the relationship between T-cells and the number of bacteria in capsules. *P* values less than or equal to 0.05 were considered statistically significant.

5.3. Results

5.3.1. Clinical features

Table 5.1 lists the clinical summary data from each of the 12 patients with BIA-ALCL included in the study (patients 1612, 1618, 1620, 1626, 1627, 1701, 1708, 1709, 1713, 1714, 1715, 1725). The mean patient age was 42.4 years (range, 24 to 58 years) and the mean duration of time between insertion of implants and diagnosis of BIA-ALCL was 7.55 years (range, 3 to 14 years). Of the 12 patients with a known indication, three had implants for postmastectomy reconstruction, whereas the remaining nine had implants for cosmetic augmentation. Eleven patients (91.7%) presented with a unilateral malignant effusion, whereas one patient (8.3%) presented with a tumour mass following infection (patient 1627). No clinical information was available as to whether the infection was caused by a Gram-negative or Gram-positive organism. In two patients the diagnosis of BIA-ALCL was an incidental finding after undergoing multiple implant exchange for CC. All of the implants removed upon diagnosis had a textured outer shell, with equal numbers of Biocell (Allergan) (41.7%) and Silimed PU (Sientra) (41.7%) implants, and two patients with Nagor (Nagor Ltd.) textured implants (16.7%). All BIA-ALCL patients were treated with capsulectomy and removal of implants.

Patients with non-tumour contracted capsules and implants had a mean age of 50.3 years (range, 28 to 71 years). There was no significant difference in the age of non-tumour contracture patients and BIA-ALCL patients ($P = 0.1220$). No clinical information on why CC patients had implants was available at the time of thesis writing. We speculate that implantation in these patients were perhaps less due to reconstruction rather than cosmetic.

Table 5.1. Clinical summary of breast implant-associated ALCL patients.

Patient number	State of location	Age at diagnosis (years)	Indication	Duration of implant (years)	Implant type	Presentation	Treatment	Experimental analysis conducted ⁺
1610	QLD	38	Cosmetic	13	Silimed PU	Seroma	Surgery	Cell proliferation (PHA, LPS), TLR4 inhibition
1612	ACT	45	Reconstructive	5	Silimed PU	Seroma	Surgery	qPCR, Cell proliferation (PHA, LPS)
1618	QLD	51	Cosmetic	14	Allergan Biocell	Seroma	Surgery	qPCR, Cell proliferation (PHA, LPS, SEA, TSST-1)
1620	WA	36	Reconstructive	5	Silimed PU	Seroma	Surgery	qPCR
1626	QLD	45	Cosmetic	10	Allergan Biocell	CC followed by seroma	Surgery	qPCR, Cell proliferation (PHA, LPS)
				1	Silimed PU			
				2	Nagor			
1627	NSW	41	Reconstructive	4	Allergan Biocell	Infection followed by revision and incidental mass	Surgery	qPCR, Cell proliferation (PHA, LPS, SEA, TSST-1), TLR4 inhibition
				0.5	Allergan Biocell			
1701	QLD	33	Cosmetic	5	Silimed PU	Seroma	Surgery	qPCR, Cell proliferation (PHA, LPS, SEA, TSST-1), TLR4 inhibition
1708	QLD	24	Cosmetic	3	Allergan Biocell	Seroma	Surgery	qPCR
1709	VIC	49	Cosmetic	7	Nagor	Seroma	Surgery	qPCR

⁺Experimental analyses conducted on patient specimens included real-time qPCR (Chapter V), cell proliferation assays (PHA, LPS, SEA, TSST-1) (Chapter VI to VII) and TLR4 inhibition assays (Chapter IX). QLD, Queensland; ACT, Australian Capital Territory; WA, Western Australia; NSW, New South Wales; VIC, Victoria; PU, polyurethane; CC, capsular contracture; qPCR, real-time quantitative PCR; PHA, phytohemagglutinin; LPS, lipopolysaccharide; SEA, staphylococcal enterotoxin A; TSST-1, toxic shock syndrome toxin-1; TLR4, Toll-like receptor 4.

Table 5.1. Continued.

Patient number	State of location	Age at diagnosis (years)	Indication	Duration of implant (years)	Implant type	Presentation	Treatment	Experimental analysis conducted ⁺
1713	VIC	58	Cosmetic	10	Allergan Biocell	Seroma	Surgery	qPCR, Cell proliferation (PHA, LPS, SEA, TSST-1), co-culture, TLR4 inhibition
1714	QLD	40	Cosmetic	0.1 4 6	PIP PIP Silimed PU	CC then seroma	Surgery	qPCR, Cell proliferation (PHA, LPS, SEA, TSST-), co-culture, TLR4 inhibition
1715	QLD	31	Cosmetic	5	Silimed PU	Seroma	Surgery	qPCR, Cell proliferation (PHA, LPS)
1725	NZ	56	Cosmetic	9	Allergan Biocell	Seroma	Surgery	qPCR
1802	WA	58	Reconstructive	1 2.5	Allergan Biocell Allergan Biocell*	Seroma	Surgery	TLR4 inhibition
1803	VIC	57	Reconstructive	4	Silimed PU	Seroma	Surgery	Cell proliferation (PHA, LPS, SEA, TSST-1)
1808	VIC	35	Cosmetic	8	Nagor	Seroma	Surgery	Cell proliferation (PHA, LPS, SEA, TSST-1)
1810	VIC	37	Cosmetic	7	Silimed PU	Seroma	Surgery	Cell proliferation (PHA, LPS, SEA, TSST-1)
1817	NSW	44	Reconstructive	4.5	Allergan Biocell	Seroma	Surgery	Cell proliferation (PHA, LPS, SEA, TSST-1)
1819	QLD	53	Reconstructive	5	Silimed PU	Seroma	Surgery	Cell proliferation (PHA, LPS, SEA, TSST-1)
1825	QLD	45	Cosmetic	9	Silimed PU	Seroma	Surgery	TLR4 inhibition

⁺Experimental analyses conducted on patient specimens included real-time qPCR (Chapter V), cell proliferation assays (PHA, LPS, SEA, TSST-1) (Chapter VI to VII), biofilm and mammalian cells co-culture assays (Chapter VIII) and TLR4 inhibition assays (Chapter IX). *Implant exchange for larger size. VIC, Victoria; QLD, Queensland; NZ, New Zealand; WA, Western Australia; PIP, Poly Implant Prothèse; PU, polyurethane; CC, capsular contracture; qPCR, real-time quantitative PCR; PHA, phytohemagglutinin; LPS, lipopolysaccharide; SEA, staphylococcal enterotoxin A; TSST-1, toxic shock syndrome toxin-1; TLR4, Toll-like receptor 4.

5.3.2. BIA-ALCL implants and capsules

Bacteria were cultured from samples obtained from the cancer affected breast of seven BIA-ALCL patients and in the contralateral breast of five of these patients (Table 5.2). The majority of the species isolated were staphylococcal. In patient 1701, *Micrococcus luteus* and *Pseudoclavibacter* spp. were isolated from both the implant and capsule. *Micrococcus* spp. are normal inhabitants of human skin and *Pseudoclavibacter* spp. have been identified in cutaneous and subcutaneous infections in humans (Lemaitre et al., 2011). In patient 1626, samples were contaminated likely during handling and/or processing following explanation surgery (Fungi) and was therefore excluded from qPCR analysis.

Table 5.2. Microorganisms cultured from BIA-ALCL and contralateral non-ALCL specimens.

Patient number	BIA-ALCL		Contralateral non-ALCL	
	Sample type	Organism	Sample type	Organism
1626	RI	Fungi		
1627	RI	<i>S. aureus</i>	LI	<i>S. aureus</i>
	RC	<i>S. aureus</i>		
1701	LI	<i>Micrococcus luteus</i> , <i>Pseudoclavibacter</i> spp.	RI	<i>Micrococcus luteus</i> , <i>Pseudoclavibacter</i> spp.
	LC	<i>Micrococcus luteus</i> , <i>Pseudoclavibacter</i> spp.	RC	<i>Micrococcus luteus</i> , <i>Pseudoclavibacter</i> spp.
1708	LI	<i>S. epidermidis</i>	RI	<i>S. epidermidis</i>
1709	LI	<i>S. aureus</i>	RI	<i>S. aureus</i>
1713	RC	<i>S. epidermidis</i>		
1714	RI	<i>S. epidermidis</i>		
	RC	<i>S. epidermidis</i>		

RI, right implant; RC, right capsule; LI, left implant; LC, left capsule.

5.3.3. Total microbial load attached to implants

The individual total microbial load attached to the implants explanted from BIA-ALCL patients and their contralateral normal non-ALCL breast (Table 5.3) and implants taken from non-tumour CC patients (Table 5.4) was determined by qPCR.

Table 5.3. Number of bacteria attached to a mg of implant as determined by qPCR. Individual results for BIA-ALCL patients ($n = 8$) and their contralateral non-ALCL breasts ($n = 7$).

Patient number	Implant type	BIA-ALCL	Contralateral non-ALCL
		Number of bacteria per mg implant	
1612	Silimed PU	6730	23364
1620	Silimed PU	12445	67112
1627	Allergan Biocell	47300	20485
1701	Silimed PU	656774	22765
1708	Allergan Biocell	990701	208920
1709	Nagor	36251	10734
1714	Silimed PU	26689	121391
1725	Allergan Biocell	82695	

Blank cells indicate no implant samples were collected.

Table 5.4. Number of bacteria attached to a mg of implant as determined by qPCR. Individual results for non-tumour contracture patients ($n = 16$).

Patient number	Capsular contracture	
	Left implant	Right implant
1613		37488
1614	19879	23142
1702	31280	12012
1711		712013
1716	13955	28218
1717	13275	
1726	21088	27351
1727		646880
1728	920306	726151
1729	614655	1121261

Blank cells indicate no implant samples were collected.

The mean total microbial load attached to explanted implants was 2.32×10^5 bacteria/mg of implant for BIA-ALCL implants ($n = 8$) and that to non-tumour implants ($n = 16$) was 3.11×10^5 bacteria/mg of implant. In contrast, the seven samples taken from the contralateral normal breast in patients with BIA-ALCL yielded a mean of 6.78×10^4 bacteria/mg of implant, which was lower than those detected attached to implants from their cancerous side, although this was not significant ($P = 0.5781$) (Figures 5.1 and 5.2). However, this result was likely inflated due to patients 1701 and 1708 having an overwhelming high number of bacteria in the BIA-ALCL breast when compared to the non-affected side (Figure 5.1). Overall, there was no significant difference in the number of bacteria attached to the implant between BIA-ALCL, contralateral normal breast and CC specimens ($P > 0.05$) (Figure 5.2). This result may be due to the wide variability in bacterial numbers within BIA-ALCL (CI: $- 8.23 \times 10^4$ to 5.47×10^5 bacteria/mg of implant) and contralateral normal breast specimens (CI: $- 17.22$ to 1.36×10^5) given the small sample sizes in comparison to CC specimens, which had less variability (CI: 9.75×10^4 to 5.24×10^5).

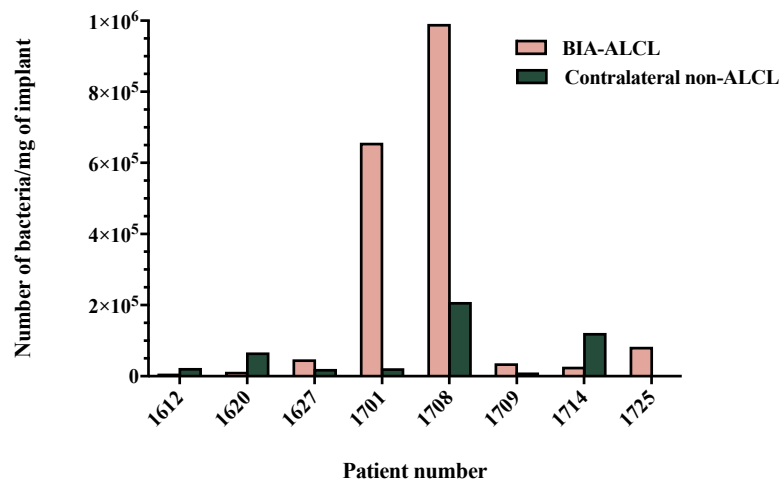


Figure 5.1. Number of bacteria per mg of implant explanted from eight BIA-ALCL patients and their contralateral (non-ALCL) normal breast ($n = 7$) as determined by qPCR. Values are the means.

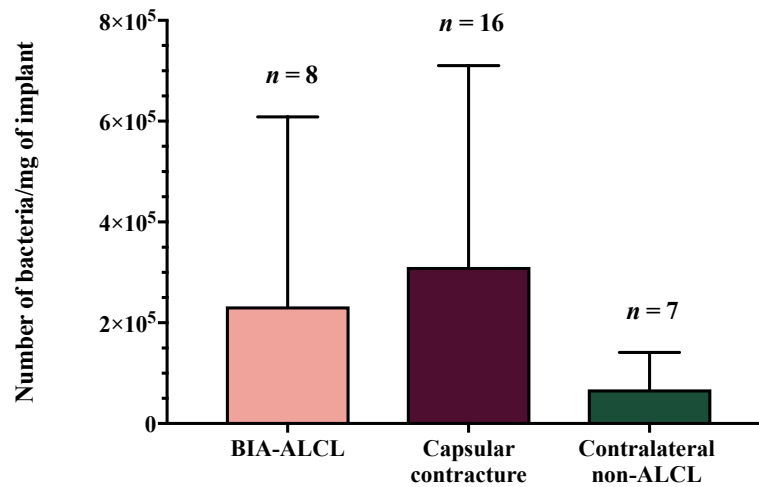


Figure 5.2. Number of bacteria per mg of implant explanted from BIA-ALCL patients, their contralateral normal breast and contracture patients as determined by qPCR. Values are the means + SD.

Analysis of the number of bacteria attached to the different textured implant types removed from BIA-ALCL patients showed no significant difference in bacterial load among Silimed PU (1.76×10^5 , $n = 4$), Allergan Biocell (3.74×10^5 , $n = 3$) and Nagor (3.63×10^4 , $n = 1$), $P > 0.05$ (Figure 5.3). Although there was only a single BIA-ALCL patient with Nagor implants for comparison (with patient 1626 excluded from qPCR analysis, Table 5.2), there was a ten-fold higher number of bacteria in Silimed PU and Allergan Biocell implants taken from BIA-ALCL patients (Figure 5.3), which we have shown have a high surface area/roughness (Chapter III). While no significant difference was found in the number of bacteria attached to Silimed PU implants taken from the BIA-ALCL affected breast and from the non-affected side ($P = 0.8750$), which suggests that the development of BIA-ALCL is not only limited to bacterial load but also the types of species present. No statistical tests for paired comparisons between BIA-ALCL and contralateral non-ALCL were performed for Allergan Biocell and Nagor implants given the unequal and/or small number of cases for these textures (Figure 5.3).

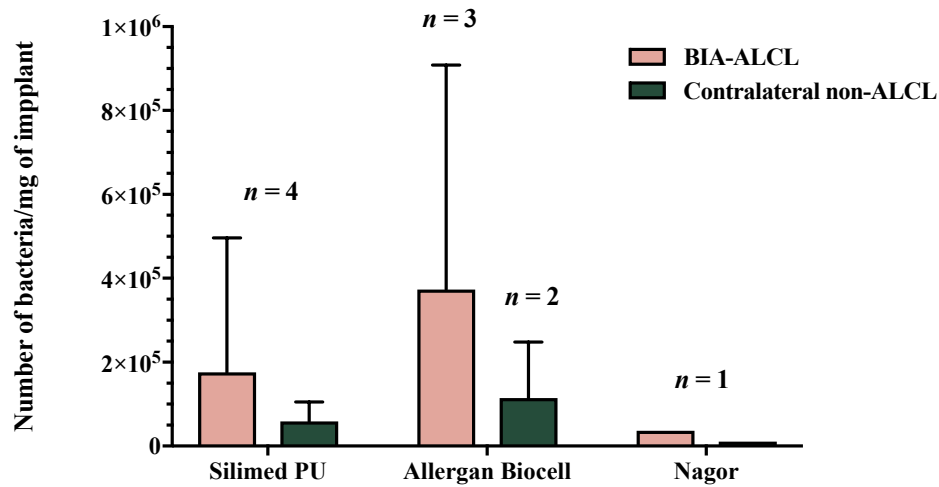


Figure 5.3. Number of bacteria per mg in the different textured implants explanted from BIA-ALCL patients and their contralateral normal breast as determined by qPCR. Values are the means + SD.

5.3.4. Total microbial load in capsules

Individual qPCR results of total microbial load in capsular tissue surrounding implants taken from BIA-ALCL patients and their contralateral non-ALCL breast are shown in Table 5.5 while implants taken from non-tumour CC patients are shown in Table 5.6.

Table 5.5. Number of bacteria attached to a mg of capsular tissue as determined by qPCR. Individual results for BIA-ALCL patients and their contralateral non-ALCL breasts.

Patient number	Implant type	BIA-ALCL	Contralateral non-ALCL
		Number of bacteria per mg capsule	
1612	Silimed PU	49366	18981
1618	Allergan Biocell	54254	50726
1620	Silimed PU	30426	
1627	Allergan Biocell	53729	30253
1701	Silimed PU	18714	23710
1708	Allergan Biocell	30077	19618
1713	Allergan Biocell	19010	26316
1714	Silimed PU	14340	12410
1715	Silimed PU	20565	
1725	Allergan Biocell	22425	

Blank cells indicate no capsule samples were collected.

Table 5.6. Number of bacteria attached to a mg of capsular tissue as determined by qPCR. Individual results for non-tumour contracture patients.

Patient number	Capsular contracture	
	Left capsule	Right capsule
1613	17337	102547
1614	12305	28737
1621	22531	34552
1702	100426	17985
1711	25562	
1716	24727	16098
1717	20134	
1719	29927	483371
1720	31682	23570
1722	39929	
1726	72065	28630

Blank cells indicate no capsule samples were collected.

There was no significant difference in the total number of bacteria in capsules surrounding implants as determined by qPCR (BIA-ALCL, 3.13×10^4 ; Contralateral non-ALCL, 2.60×10^4 ; CC, 5.96×10^4 ; $P > 0.05$) (Figure 5.4). Although more capsule specimens were obtained from CC patients ($n = 19$), these showed the most variability in bacterial numbers likely due to inflated numbers from patients 1613, 1702, 1719 and 1726 (Table 5.6). Unfortunately, no clinical information on CC patients including implant exposure time was available, but we can assume in these patients the high bacterial numbers came from the contracted breast. In addition, no difference was found in the number of bacteria in capsules surrounding BIA-ALCL textured implant types, Silimed PU (2.67×10^4) and Allergan Biocell (3.59×10^4) ($P = 0.3764$). No statistical tests for paired comparisons between BIA-ALCL and contralateral non-ALCL were performed for capsules surrounding Silimed PU and Allergan Biocell implants given the unequal number of cases in each group (Figure 5.5).

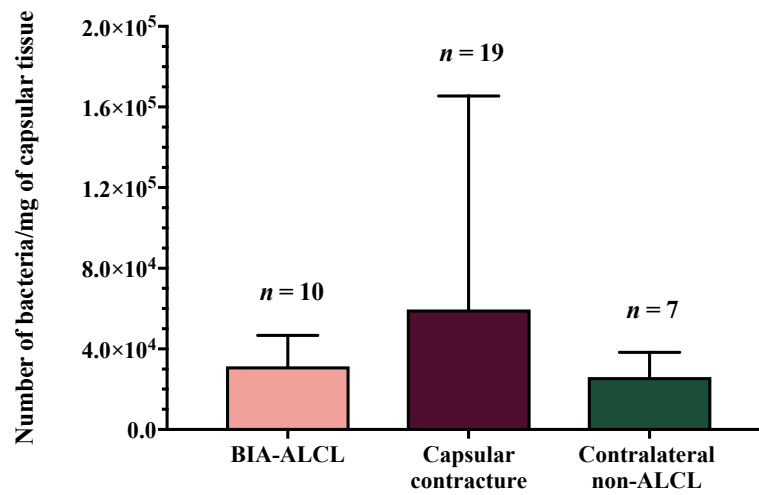


Figure 5.4. Number of bacteria per mg of capsule surrounding implants from BIA-ALCL patients, their contralateral normal breast and contracture patients as determined by qPCR. Values are the means + SD.

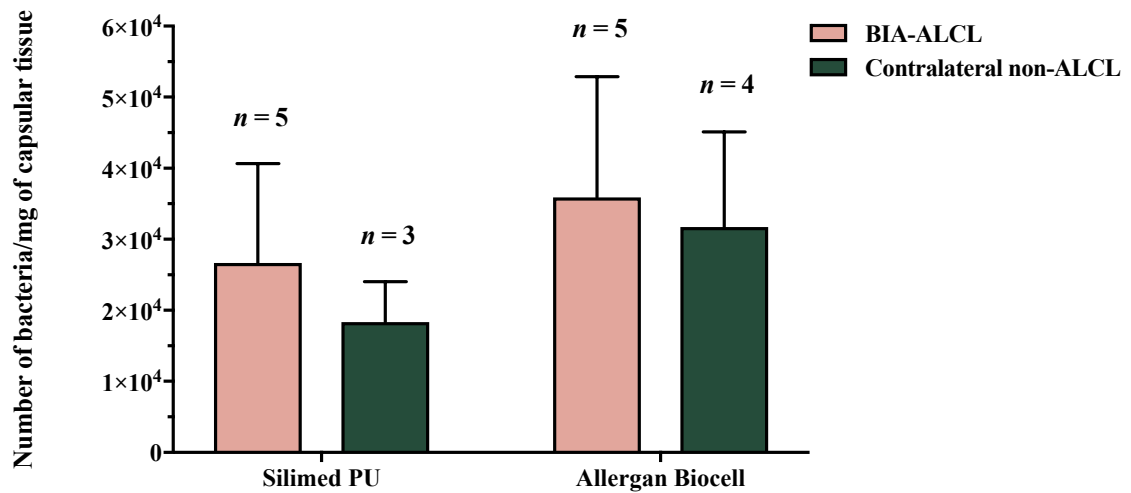


Figure 5.5. Number of bacteria per mg of capsule surrounding Silimed PU and Allergan Biocell implants explanted from BIA-ALCL patients and their contralateral normal breast as determined by qPCR. Values are the means + SD.

5.3.5. Lymphocyte number in capsules

The individual lymphocyte number in capsules explanted from BIA-ALCL patients and their contralateral non-ALCL normal breast (Table 5.7) and capsules taken from non-tumour contracture patients (Table 5.8) was determined by qPCR. Table 5.9 summarises the number of T-cells and B-cells for these samples.

As expected, there were significantly more CD3+ T-cells in BIA-ALCL capsules ($5.98 \times 10^6/\text{mg}$ tissue) when compared with the number of B-cells (CD79a, 1.33×10^4) ($P < 0.0001$). A similar pattern was observed in tissue taken from the contralateral normal breast of BIA-ALCL patients, with significantly higher numbers of CD3+ T-cells (6.04×10^6) than B-cells (4.09×10^3) ($P = 0.0002$). In non-tumour contracted capsules, there were significantly more CD3+ (1.12×10^7) and CD4+ T-cells (4.19×10^6) compared with B-cells (5.06×10^4) ($P < 0.0001$). It is the CD4 helper T-cells that are involved in the ongoing low-grade chronic inflammation seen in CC. Overall, the total lymphocyte counts (CD3+ T-cells and B-cells) in capsules from CC patients was almost double that of capsules taken from BIA-ALCL patients and their non-affected side, although not significant ($P > 0.05$) (Figure 5.6). This is unlikely to be a true representation of the total lymphocyte counts in capsules from BIA-ALCL patients given the smaller sample sizes and hence wide variability in the total number of CD3+ T-cells and B-cells (95% CI: 9.20×10^5 to $5.07 \times 10^6/\text{mg}$ of implant (BIA-ALCL), 2.21×10^5 to 5.82×10^6 (Contralateral non-ALCL)). While the number of CD3+ T-cells in capsules from BIA-ALCL, contralateral non-ALCL and non-tumour capsules were also no different ($P > 0.05$).

Table 5.7. Number of T-cells (CD3), helper T-cells (CD4), cytotoxic T-cells (CD8a) and B-cells (CD79a) per mg of capsular tissue as determined by qPCR. Individual results for BIA-ALCL patients and their contralateral non-ALCL breasts.

Patient number	BIA-ALCL				Contralateral non-ALCL			
	CD3	CD4	CD8a	CD79a	CD3	CD4	CD8a	CD79a
1612	2985872	82630	4470	3012	2981158	No Ct	4860	2078
1618	5896378	4370	5830	3316	15894390	62910	19330	10350
1620	5633577	1860	6730	3789				
1627	16760194	4695780	126021	102941	11568139	1820	13771	6942
1701	5487064	57390	5701	3875	4069143	14310	4770	2796
1708	10601285	28650	10311	6985	2972575	9730	3000	2148
1713	3031421	157340	2971	2760	3344744	211310	3390	2827
1714	1130277	280	2050	1077	1458848	19030	1850	1514
1715	1918203	1160820	5441	3347				
1725	6341937	42851	4600	2377				

Blank cells indicate no capsule samples were collected.

Table 5.8. Number of T-cells (CD3), helper T-cells (CD4), cytotoxic T-cells (CD8a) and B-cells (CD79a) per mg of capsular tissue as determined by qPCR. Individual results for non-tumour contracture patients.

Patient number	Left capsule				Right capsule			
	CD3	CD4	CD8a	CD79a	CD3	CD4	CD8a	CD79a
1613	8629720	4992834	773032	35582	23462546	1415553	183860	11463
1614	5801733	5325763	486298	13138	7434672	540863	518040	27006
1621	4930580	2405886	489279	25997	9783761	46751532	787997	536125
1702	10630855	496257	306462	12227	1535755	1800461	34793	27257
1711	10394326	1381992	104194	26753				
1716	1373151	181311	28918	20881	1546121	2974852	23489	20485
1717	3426453	1490722	23328	22127				
1719	2704124	971337	41086	22913	39791107	2697879	69813	14861
1720	13214551	459099	27285	14707	29080963	112815	46786	21613
1722					19757272	3789725	41703	40868
1726	2349927	111459	62892	46486	16541905	1673083	334327	20413

Blank cells indicate no capsule samples were collected.

Table 5.9. Summary of the total number of CD3, CD4, CD8a and CD79a lymphocytes per mg of tissue in capsules from BIA-ALCL patients, their contralateral normal breast and CC patients as determined by qPCR.

	CD3	CD4	CD8a	CD79a
<u>BIA-ALCL (<i>n</i> = 10)</u>				
Mean	5,978,621	623,197	17,413	13,348
Range				
Minimum	1,130,277	280	2,050	1,077
Maximum	16,760,194	4,695,780	126,021	102,941
<u>Non-tumour capsular contracture (<i>n</i> = 19)</u>				
Mean	11,178,396	4,188,075	230,715	50,574
Range				
Minimum	1,373,151	111,459	23,328	11,463
Maximum	39,791,107	46,751,532	787,997	536,125
<u>Contralateral non-ALCL (<i>n</i> = 7)</u>				
Mean	6,041,285	53,185	7,282	4,094
Range				
Minimum	1,458,848	1,820	1,850	1,514
Maximum	15,894,390	211,310	19,330	10,350

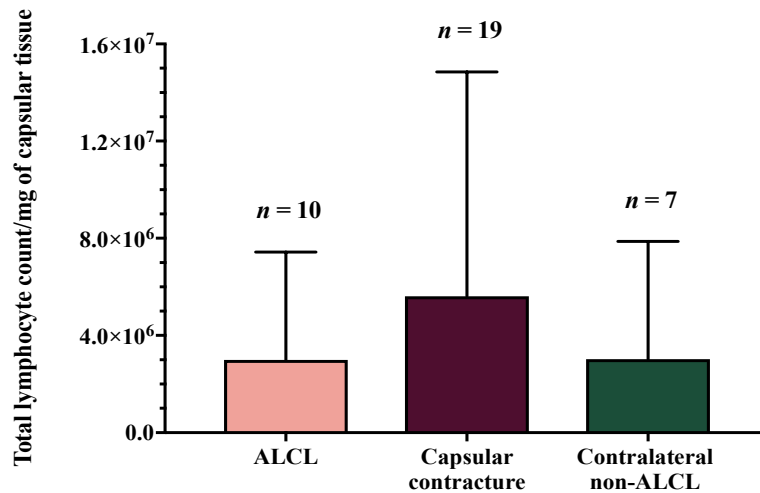


Figure 5.6. Total number of CD3+ T-cells and B-cells in capsules explanted from BIA-ALCL patients, their contralateral normal breast and contracture patients as determined by qPCR. Values are the means + SD.

It was predicted that there would be a greater number of CD4+ T-cells in BIA-ALCL capsules when compared to capsules taken from their non-ALCL breast, since it is the predominant phenotype of BIA-ALCL tumour cells. Indeed, there were higher CD4 (6.23×10^5), as well as CD8a (1.74×10^4) and CD79a lymphocyte numbers in BIA-ALCL capsules (Table 5.9) but this was likely due to inflated numbers from patients 1627 and 1715 (Table 5.7). As a result of this variability, no difference in CD4, CD8a and CD79a lymphocyte numbers was found between BIA-ALCL capsules and capsules taken from their contralateral normal side ($P > 0.05$). Interestingly, however, in BIA-ALCL patient 1627 who was the only patient that presented with a tumour mass, there was a much higher CD4+ T-cell count in their cancerous breast (4.70×10^6) when compared to the contralateral non-affected side (1.82×10^3) (Table 5.7). While their total lymphocyte count (CD3+ T-cells and B-cells) was similar between both sides (BIA-ALCL, 1.69×10^7 ; Contralateral non-ALCL, 1.16×10^7).

No correlation was found between the number of lymphocytes (CD3, $R^2 = 0.284$; CD4, $R^2 = 0.199$; CD8a, $R^2 = 0.274$; CD79a, $R^2 = 0.268$) and the number of bacteria per milligram of tissue in capsules from BIA-ALCL patients ($P > 0.05$) (Figure 5.7).

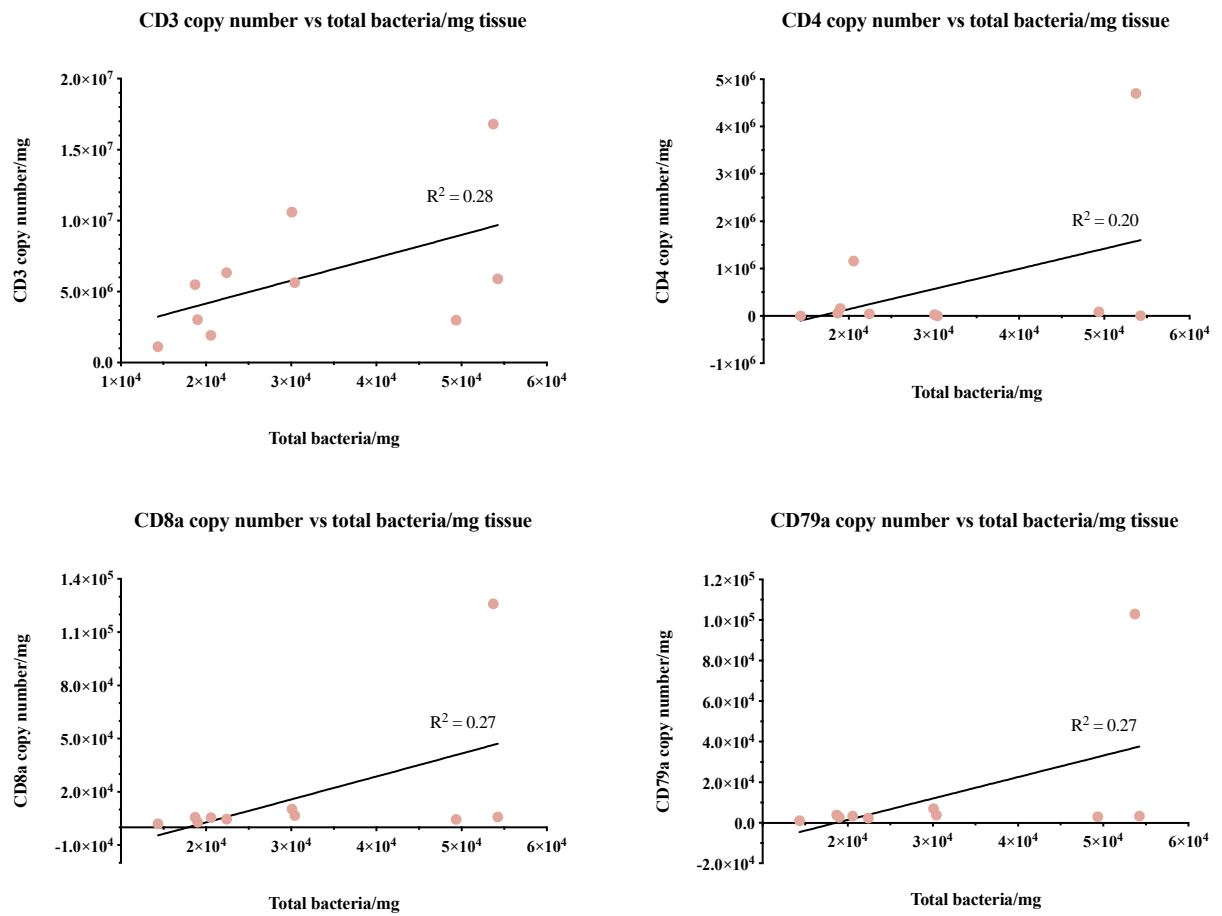


Figure 5.7. CD3, CD4, CD8a, CD79a from capsules versus total bacteria per mg of capsular sample in BIA-ALCL patients.

A significant relationship was found between the number of CD3+ T-cells and bacterial load in non-tumour contracted capsules ($R^2 = 0.488$, $P = 0.0009$) (Figure 5.8). While no correlation was found between the number of CD4 ($R^2 = 0.003$), CD8a ($R^2 = 0.027$), CD79a ($R^2 = 0.006$) lymphocytes and the number of bacteria per milligram of capsular tissue ($P > 0.05$).

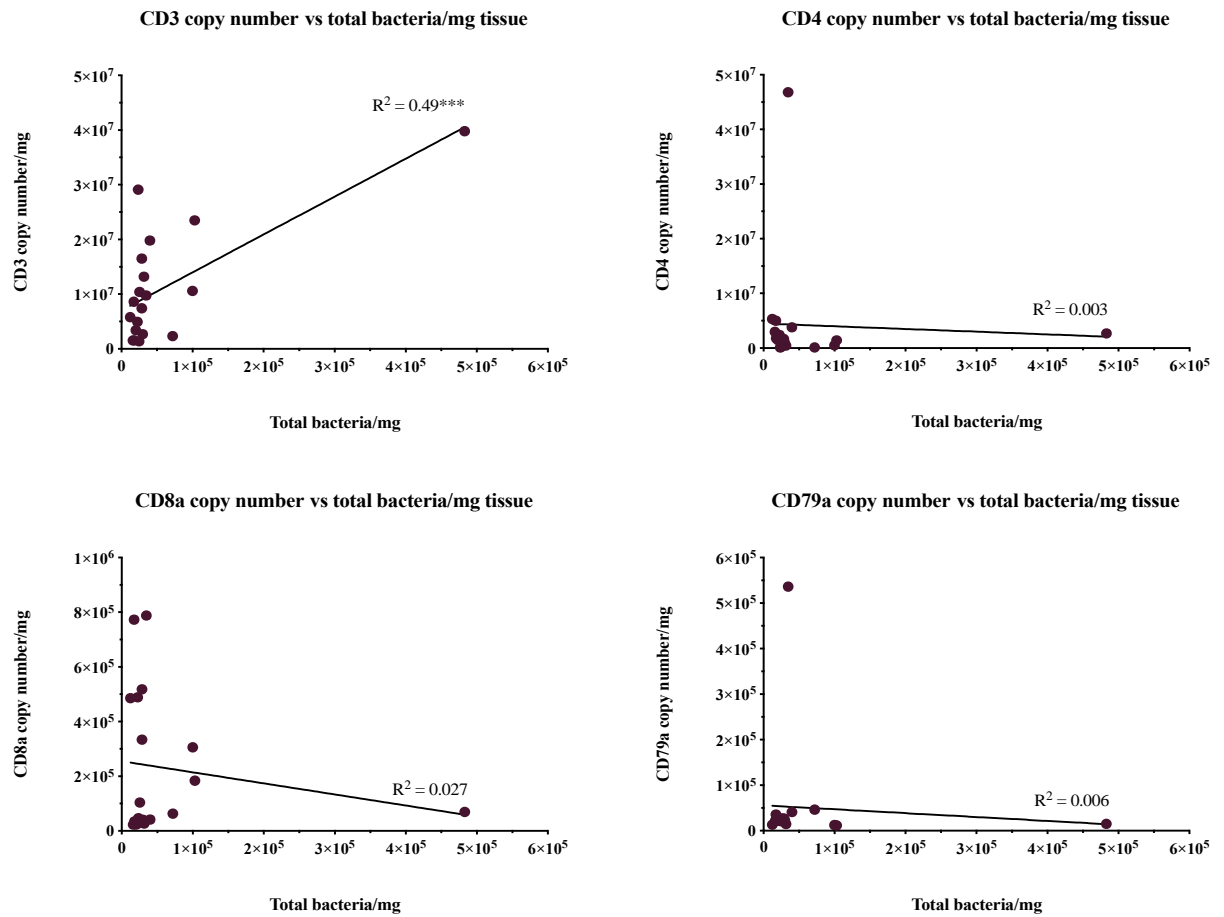


Figure 5.8. CD3, CD4, CD8a, CD79a from capsules versus total bacteria per mg of capsular sample in contracture patients. Significant correlation at $***P \leq 0.001$.

Interestingly, in contralateral non-ALCL capsules, the number of CD3, CD8a and CD79a lymphocytes correlated with the number of bacteria (CD3, $R^2 = 0.861$; CD8a, $R^2 = 0.840$; CD79a, $R^2 = 0.903$; $P < 0.01$) (Figure 5.9). While no relationship was found between the number of CD4+ T-cells and bacterial load ($R^2 = 0.052$, $P > 0.05$).

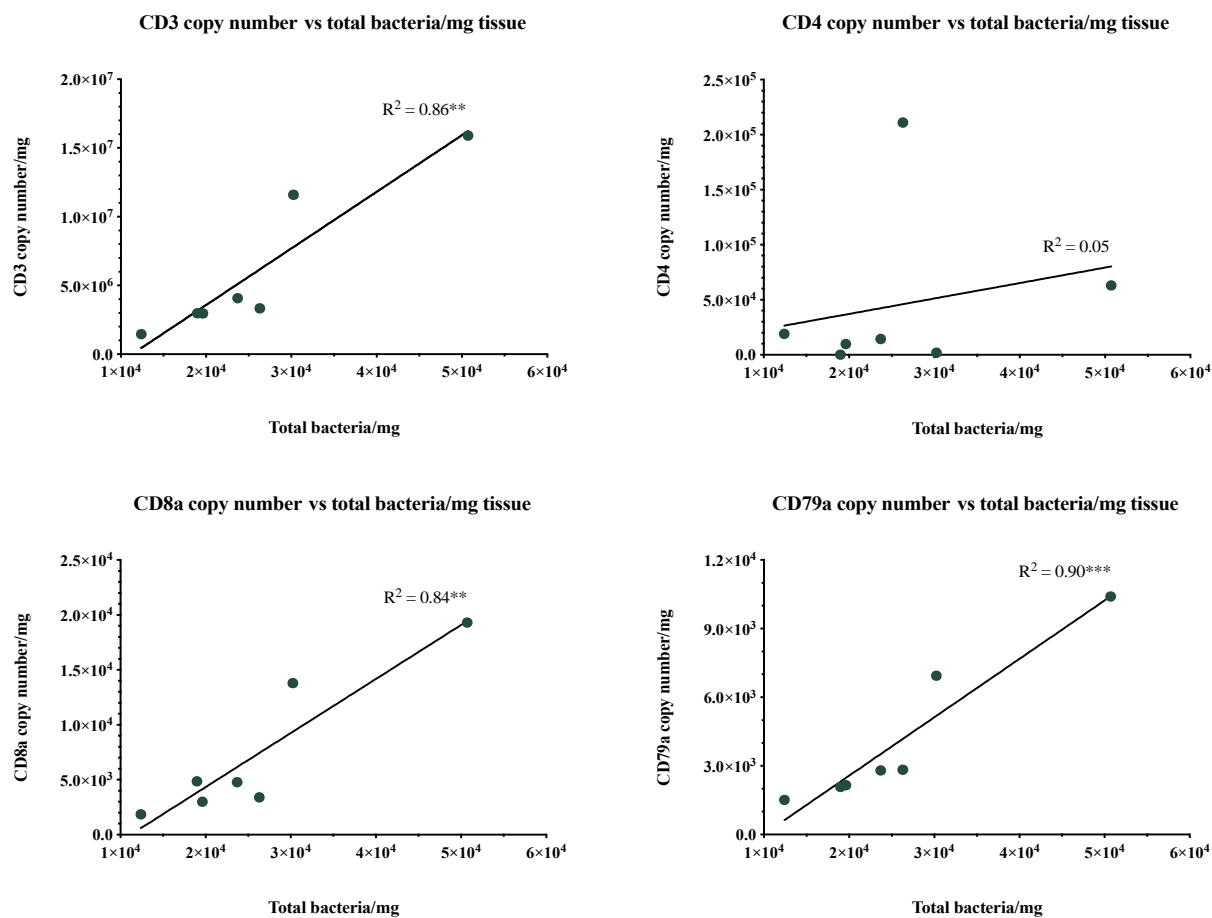


Figure 5.9. CD3, CD4, CD8a, CD79a from capsules versus total bacteria per mg of capsular sample in the contralateral normal breast of BIA-ALCL patients. Significant correlation at $^{**}P \leq 0.01$, $^{***}P \leq 0.001$.

5.3.6. Scanning electron microscopy

Three BIA-ALCL capsule samples with adequate material were subjected to SEM. All samples demonstrated bacterial biofilm consisting of coccoid bacteria and minimal amounts of excreted polymeric substances (EPS) (Figure 5.10).

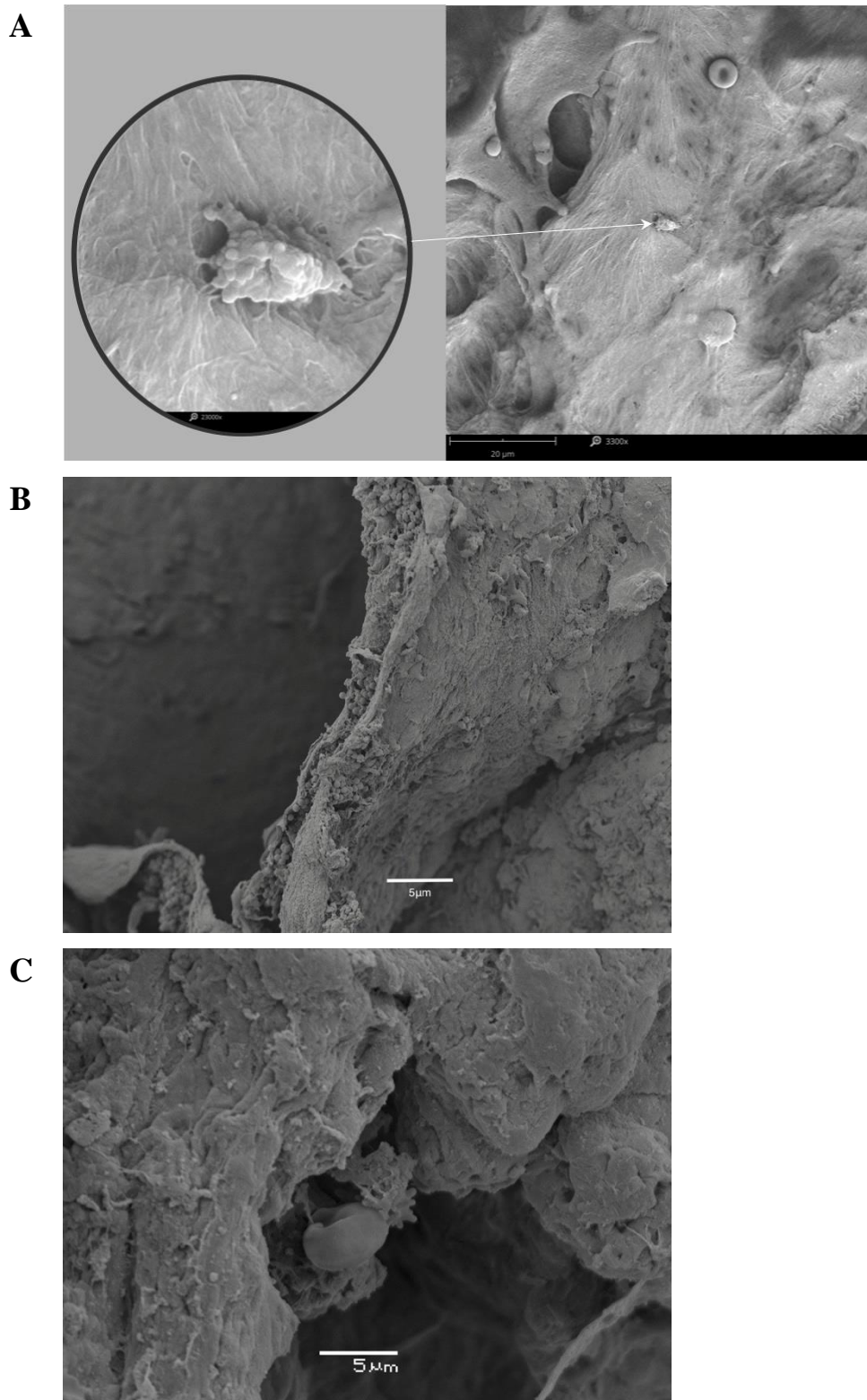


Figure 5.10. Scanning electron micrographs showing bacterial biofilm present on capsules taken from three BIA-ALCL patients.

(A) Capsule showing clusters of coccoid-shaped bacteria encased in EPS, magnified 23,500X. (B) and (C) Capsules showing a few individual cocci and little EPS, magnified 4,000X.

5.4. Discussion

In this Chapter we analysed the bacterial load and the number of lymphocytes on fresh implants and capsules collected prospectively from patients diagnosed with BIA-ALCL and compared the results to samples obtained from the contralateral non-ALCL breast of these patients and from non-tumour patients who have had surgery for implant-related complications. Bacterial detection was performed using sonication and broth culture, qPCR and the presence of biofilm confirmed using SEM.

Recently, bacterial infection was identified as one of the factors that may play a role in the development of BIA-ALCL (Loch-Wilkinson et al., 2017). In this study, we identified a high bacterial load, present as a biofilm, in BIA-ALCL samples. However, the number of bacteria present was not significantly different from those present in samples taken from the contralateral non-ALCL breast of BIA-ALCL patients and non-tumour contracture patients. Moreover, although the number of bacteria detected in these cohort of patient samples is ten-fold lower than previously reported (Hu et al., 2016), the numbers are still considerably high. It is believed that there is a threshold of bacterial load, which, once reached, causes ongoing immune activation and transformation in susceptible hosts (Kadin et al., 2016, Loch-Wilkinson et al., 2017). Indeed, the development of BIA-ALCL is a complex multifactorial process and it is likely that this threshold will vary depending on an interplay of microbial, implant and host factors.

The frequencies of the different implant types associated with BIA-ALCL showed all patients were exposed to textured implants, which reflects the greater use of textured implants by surgeons. Allergan Biocell and Silimed PU accounted for more than 80% of the implants, which is consistent with findings that have shown that both textures carry a significantly higher risk of developing BIA-ALCL (Loch-Wilkinson et al., 2017). Analysis of microbial load attached to these textures showed there was no difference in the number of bacteria attached to Allergan Biocell,

Silimed PU and Nagor implants removed from BIA-ALCL patients. Moreover, there was no difference in the bacterial load on these textures between implants obtained from BIA-ALCL patients and those taken from their contralateral non-ALCL breast. Nevertheless, these findings highlight the greater propensity of these higher surface area textures to increase the risk of BIA-ALCL, which need to be balanced against the clinical advantages of using textured implants and the need to combine textured implants with proven strategies to reduce the risk of bacterial contamination at the time of implant insertion (Loch-Wilkinson et al., 2017).

Culture-positivity was detected in less than half of BIA-ALCL and contralateral non-ALCL samples. The majority of bacteria cultured were *Staphylococcal* spp. which are most commonly associated with implant-related infections (Arciola et al., 2012, Ribeiro et al., 2012, Deva et al., 2013). A failure to obtain positive cultures may reflect the difficulty associated with culturing bacteria encased in biofilm, fastidious organisms or non-culturable bacteria of human origin. Additionally, these findings highlight the limitations that are associated with using traditional culture techniques. The use of culture-independent techniques, including PCR identification of total bacterial 16S RNA gene combined with SEM, provides an alternative to traditional culture techniques as a means of detecting biofilm (Høgdaal et al., 2010). Indeed, molecular testing of samples yielded high microbial load in samples that were found to be culture negative using traditional culture-based methods. The use of PCR with imaging of bacterial biofilm, therefore, provides an increased sensitivity and specificity for diagnosis and in the detection of pathogens.

Analysis of lymphocytes in capsules of BIA-ALCL patients, their contralateral non-ALCL breasts and capsules from contracture patients showed a predominance of T-cells. We found no relationship between the number of lymphocytes and bacterial load in BIA-ALCL capsules. However, there was a significant correlation between the total lymphocyte number and bacterial load in the contralateral normal breast of these patients, with cytotoxic CD8a T-cells and B-cells increasing as bacteria numbers increased. Moreover, there were significantly lower numbers of

CD4+ (T-helper) cells in BIA-ALCL and contralateral non-ALCL capsules compared to non-tumour capsules, with no difference in T-helper cell numbers in capsules from BIA-ALCL patients and their contralateral normal breast. In BIA-ALCL capsules, there was also no correlation in the number of CD4+ T-cells with the number of bacteria. It is these cells that undergo malignant transformation in BIA-ALCL, however in this cohort of patients we detected lower numbers of these cells compared to non-tumour capsules. Nevertheless, the commonest presentation of BIA-ALCL is late seroma – fluid swelling around the breast implant in the space between the implant and breast implant capsule. On removal of the entire capsule there is no evidence of tumour invasion into the capsule with the malignant cells restricted to the seroma (Clemens et al., 2016). Conversely, if the BIA-ALCL invades the surrounding tissue, termed “infiltrative” or “mass-associated”, the prognosis is poorer. This could explain the low CD4+ T-cell count we obtained in BIA-ALCL capsules, since we were not actually sampling the tumour. In contrast, in the single patient who presented with a tumour mass (patient 1627), we found an overwhelmingly high number of CD4+ T-cells compared to the contralateral normal breast. Thus, future studies measuring the T- and B-lymphocytes in the seroma fluid of BIA-ALCL patients could provide a more accurate analysis.

The detection of bacteria and lymphocytes in our cohort of samples was subject to a number of limitations. Given the rarity of this condition along with the possibility that there are other unidentified cases of BIA-ALCL through missed clinical and/or pathologic diagnosis, we therefore had small comparative numbers of both BIA-ALCL and contralateral non-ALCL samples compared with non-tumour samples. As a consequence, our statistical analysis was limited with reduced statistical power to detect differences in bacterial load and lymphocyte number among the patient cases, and whether an association exists between the presence of bacteria and lymphocyte activation. This was evident with the wide confidence intervals we obtained in our data set. In addition, the qPCR results showed that the sum of CD4+ and CD8+ T-cells in breast capsules did

not correspond to the total number of T-cells as defined by CD3. The CD4+ and CD8+ T-cells detected in the capsules are likely mature T-lymphocytes and the disparity in their numbers could be due to the presence of null T-cells, which were not quantified. T-cell activation is critical for the initiation and regulation of the immune response, and is initiated by complex interactions involving both T-cell receptor signalling and CD28 costimulation (Diehn et al., 2002). Further qPCR analysis measuring the number of CD28 (null) T-cells would confirm this. Another drawback of this study was that a limited portion of the capsule was subjected to biofilm analysis, increasing the risk of sampling error. The findings of a high bacterial load in all BIA-ALCL samples could, therefore, be an underrepresentation of the true numbers of bacteria present in the tumour capsule.

In this Chapter, we confirmed there are high levels of bacterial contamination of textured implants with a higher surface area in BIA-ALCL specimens, and whether this leads to chronic antigen stimulation and transformation of T-cells into BIA-ALCL requires further study. Indeed, the development of BIA-ALCL is not only limited to bacterial load but also the types of species present, which could be responsible for the enhanced cellular proliferation leading to tumour formation. However, other factors such as increased secretion of pro-angiogenic and/or inflammatory molecules from immune cells could promote transformation and malignancy. Thus, future studies should include a greater sample number to determine the microbiome in BIA-ALCL and non-tumour contracture cases to shed more light on which bacterial strains could be driving cancer development.

The findings from this Chapter further reinforce the importance of applying known and effective intraoperative studies (Table 1.5, Chapter I) to reduce the bacterial load so that biofilm infection remains below the threshold for host response.

Chapter VI.

Differential mitogenic response of Breast Implant-associated Anaplastic Large-cell Lymphoma to Gram-negative lipopolysaccharide

6.1. Introduction

The presence of a higher proportion of Gram-negative bacteria in BIA-ALCL specimens suggest that their associated antigens may provide differential activation of lymphocytes as compared with Gram-positive bacteria which predominate in non-tumour contracted capsules (Hu et al., 2016). We hypothesise that antigens associated with Gram-negative bacteria is the inflammatory trigger that leads to malignant transformation to BIA-ALCL. Given the Gram-negative shift in the microbiome of BIA-ALCL, in this Chapter we tested the response of BIA-ALCL tumour cells to Gram-negative bacterially derived antigens and predict that BIA-ALCL cells will respond more to lipopolysaccharide (LPS) which is bacterially derived when compared to phytohemagglutinin (PHA), a plant lectin.

PHA is a lectin extract from the red kidney bean (*Phaseolus Vulgaris*) and contains potent, cell agglutinating and mitogenic activities (Gerfen and Sawchenko, 1984, Zhang et al., 2008). The subunits of PHA are of two different types, designated leukocyte reactive (L) and erythrocyte reactive (E). L has a high affinity for lymphocyte surface receptors but low for receptors of erythrocytes and is responsible for the mitogenic properties of the isolectins. The E is responsible for the erythrocyte agglutinating properties (Gerfen and Sawchenko, 1984, Zhang et al., 2008). PHA activate T-cells by binding to cell membrane glycoproteins, including the T-cell receptor (TCR)-CD3 complex (Trickett and Kwan, 2003).

LPS is a characteristic component of the outer cell wall of Gram-negative bacteria. LPS and its lipid A moiety stimulate host cells via the Toll-like receptor 4 (TLR4), a member of the TLR protein family, which recognises common pathogen-associated molecular patterns (Akira et al., 2001, Nagai et al., 2002, Yamamoto et al., 2003, McAleer and Vella, 2008). Stimulation by LPS results in the generation of various proinflammatory cytokines, such as tumour necrosis factor- α (TNF- α), interleukin (IL)-1 and IL-6 (Akira et al., 2001, Nagai et al., 2002, Yamamoto et al., 2003, McAleer and Vella, 2008).

The aim of this Chapter was therefore to measure the cell proliferation of primary BIA-ALCL tumour cells to non-specific mitogens, PHA/LPS and compare BIA-ALCL cells response to peripheral blood mononuclear cells (PBMC) collected from BIA-ALCL patients, cutaneous-ALCL cell lines, an immortal T-cell line, and normal PBMC.

6.2. Part A: Optimisation of *in vitro* cell proliferation assays

The optimum cell concentrations, mitogen concentrations and incubation time of the reagents for detection of cell proliferation using the MTT cell proliferation kit (Roche; Sigma-Aldrich) were determined in a series of experiments initially with an immortalised cell line (MT-4 cells) and patient-derived BIA-ALCL tumour cells, both of T-cell origin.

6.2.1. Optimisation Methods

6.2.1.1. Preparation of cell lines/tumour cells

MT-4 cells (ECACC 0808140) were grown in RPMI 1640 medium and BIA-ALCL cells in DMEM. Both media were supplemented with 10% heat-inactivated FBS and 1% penicillin/streptomycin solution and cells were incubated in 5% CO₂ atmosphere at 37°C as detailed in Section 2.5.3.

6.2.1.2. Preparation of non-specific mitogens

PHA and LPS were prepared as described in Section 2.5.2. For the cell proliferation assays, we cultured 200 μL of cells in a 96-well flat bottom cell culture plate (Corning; Sigma-Aldrich) and stimulated them with 20 μL of mitogens to give final concentrations of 1, 5 and 10 $\mu\text{g/mL}$.

6.2.1.3. MTT colourimetric assay to determine cell proliferation

Cell proliferation was measured using a non-radioactive MTT assay kit, following the manufacturer's instructions. The MTT (3-(4,5-dimethylthiazol-2-yl)-2,5-diphenyl tetrazolium bromide) assay is based on the cleavage of the yellow tetrazolium salt MTT to purple formazan crystals by metabolically active cells (Figure 6.1) (Berridge et al., 2005, Pannecouque et al., 2008). When cells die they lose the ability to convert MTT into formazan, thus colour formation serves as a useful and convenient marker of only viable cells. The exact mechanism of MTT reduction into formazan is not well understood, but likely involves reaction with NADH or similar reducing molecules that transfer electrons to MTT (Figure 6.1) (Berridge et al., 2005).

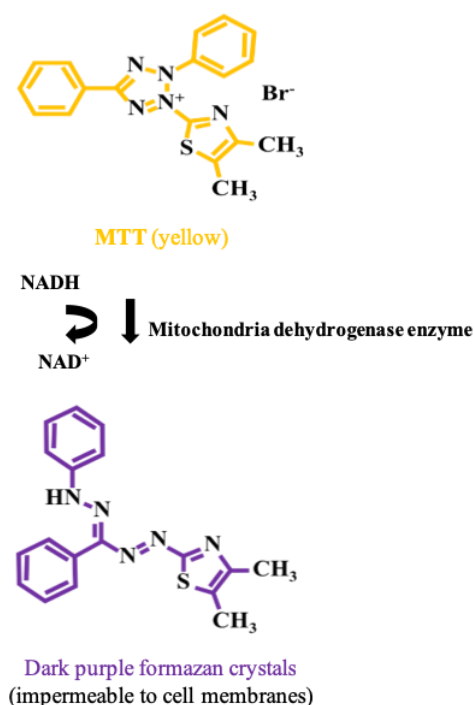


Figure 6.1. Metabolisation of MTT to formazan salt by viable cells.

A 20 µL aliquot of MTT labelling reagent (5 mg/mL in PBS) was added to all wells and incubated in 5% CO₂ for 4 to 8 hr at 37°C. After which, any purple formazan crystals that formed at the bottom of the wells, as observed under phase-contrast microscopy, was solubilised by adding 200 µL of solubilisation solution (10% sodium dodecyl sulfate in 0.01 M hydrochloric acid). The plate was incubated overnight in 5% CO₂ at 37°C to allow for complete solubilisation of the purple formazan crystals. The amount of MTT formazan produced was then measured using a PHERAstar microplate reader (BMG LABTECH, Mornington, Victoria, Australia) at a test wavelength of 570 nm minus the background optical density (OD) measured at 650 nm wavelength. Culture medium plus MTT was used as a blank. Cell proliferation results are based on the OD at the wavelength of 570 nm (OD_{570 nm}) and expressed as a stimulation index (SI), which was calculated by dividing cells stimulated with mitogens by those not stimulated as follows:

$$\text{Stimulation Index (SI)} = \frac{\text{OD}_{570 \text{ nm}} \text{ of stimulated cells}}{\text{OD}_{570 \text{ nm}} \text{ of unstimulated cells}}$$

6.2.1.4. Statistical analysis

All statistical analyses were performed with GraphPad Prism 7.0. The data were tested for normality of distribution by the Shapiro-Wilk normality test. To evaluate proliferation responses of cancerous and normal cells after mitogenic stimulation, we used two-way ANOVA with Tukey's or Sidak's multiple comparisons post-hoc test. *P* values less than or equal to 0.05 were considered statistically significant.

6.2.2A. Optimisation of MTT assay

The aim of this experiment was to determine the optimum concentration of MT-4 cells and PHA to use for the cell proliferation assays. MT-4 cells and PHA were prepared as outlined in Sections 6.2.1.1. and 6.2.1.2., respectively.

Stimulation of MT-4 cells with PHA

MT-4 cells were harvested by centrifugation at $753 \times g$ for 5 min at 22°C and resuspended in complete RPMI 1640 medium at a concentration of 10^8 cells/mL. This concentration was determined from viable cell counts using the Trypan blue dye exclusion test (Section 2.5.4.). To determine the optimum cell number, 10^8 MT-4 cells/mL was diluted ten-fold with RPMI to obtain 10^8 , 10^7 , 10^6 , 10^5 , 10^4 and 10^3 cells/mL. Cells were seeded at these concentrations into triplicate wells of a 96-well plate. MT-4 cells were then stimulated to proliferate non-specifically with 1, 5 or $10 \mu\text{g/mL}$ of PHA while control or unstimulated wells, received $20 \mu\text{L}$ of complete medium. Cells were incubated for 72 hr at 37°C in a 5% CO_2 incubator and cell proliferation measured using the MTT assay kit (Section 6.2.1.3.) by adding $20 \mu\text{L}$ of MTT labelling reagent (5 mg/mL in PBS) to all wells and incubating in 5% CO_2 for 4 hr at 37°C .

Results

Overall, we found low proliferative responses to PHA at all cell and mitogen concentrations tested (Figure 6.2C). Although stronger proliferative responses to PHA were observed at 10^5 and 10^6 cells/mL following stimulation with 5 and $10 \mu\text{g/mL}$, these responses were still lower than expected given the high concentration of cells and PHA tested.

Interpretation: It was likely that a longer incubation time with the MTT labelling reagent was needed since cells that were viable showed no purple colour when viewed under microscope (Figure 6.2A). Moreover, the decline in cell proliferation at 10^7 and 10^8 cells/mL could be attributed to the 72 hr incubation with PHA. This could have caused the MT-4 cells (already at a high concentration) to overwhelm the limited nutrients available, and hence the cells could not be stimulated or just died. Moreover, we could not determine the optimum cell concentration in this experiment because the linear portion of the absorbance curves generated produced absorbance values that were below the range of 0.75 to 1.25 ($\text{OD}_{570 \text{ nm}}$) (Figure 6.2B), which is the manufacturer's recommended guide for determining optimal cell concentrations in MTT-based

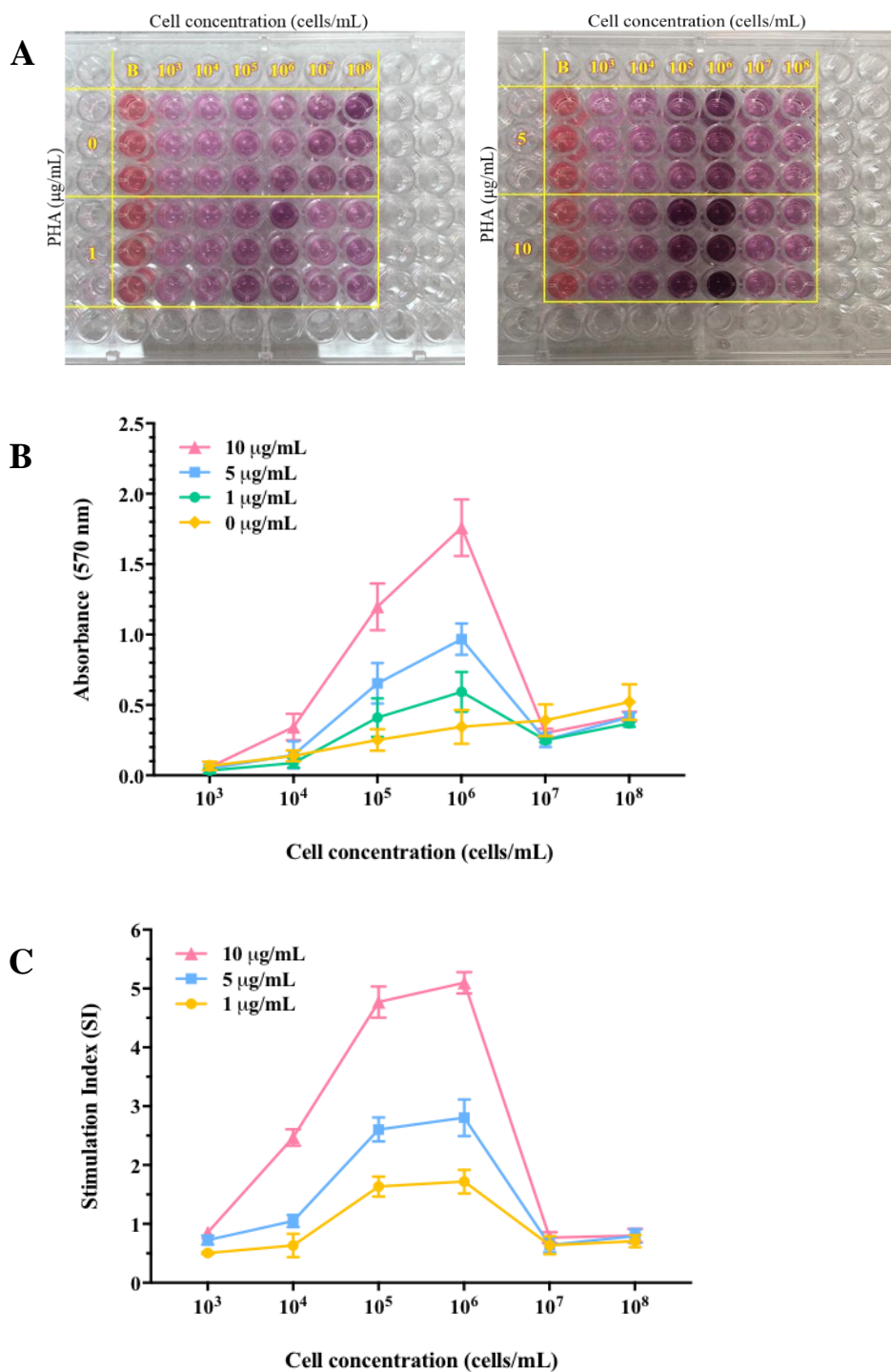


Figure 6.2. Optimisation of cell and mitogen concentrations: absorbance and proliferative response of MT-4 cells to PHA stimulation.

(A) Proliferation response was quantified using a MTT colourimetric assay. (B) The amount of MTT formazan produced was measured as an absorbance at 570 nm and (C) cell proliferation was calculated as a stimulation index (SI). Values are the means \pm SD of three technical replicates.

proliferation assays (Roche). Therefore, in the next experiment we tested MT-4 concentrations up to 10^6 cells/mL and whether leaving the MTT labelling reagent for longer than the manufacturer's specified 4 hr could enhance proliferation responses. We did not test PHA at higher concentrations because the manufacturer's recommended working concentration is between 2 to 10 $\mu\text{g/mL}$ (Roche).

6.2.2B. Determining the optimum incubation time for MTT

The aim of this experiment was to determine the optimum incubation time for the MTT labelling reagent since we attributed the low proliferation responses in Section 6.2.2A. to the short incubation time given for the purple formazan crystals to form. In this experiment, we tested 4 hr, 8 hr or overnight incubation with the MTT labelling reagent.

Stimulation of MT-4 cells with PHA

Cells were seeded at 10^6 , 10^5 , 10^4 and 10^3 cells/mL in triplicate wells of a 96-well plate and stimulated with 5 or 10 $\mu\text{g/mL}$ of PHA while control, unstimulated wells received 20 μL of RPMI for 72 hr, prior to addition of 20 μL of MTT labelling reagent to all wells and incubating for 4 hr, 8 hr or overnight (approximately 20 hr).

Results

We found leaving the MTT labelling reagent on for 8 hr resulted in significantly higher proliferative responses to PHA at both 5 and 10 $\mu\text{g/mL}$ compared to 4 hr and overnight incubation, $P < 0.05$ (Figure 6.3). While no significant difference in proliferation responses between 4 hr and overnight incubation with MTT was found ($P > 0.05$), with both having lower SI (Figure 6.3).

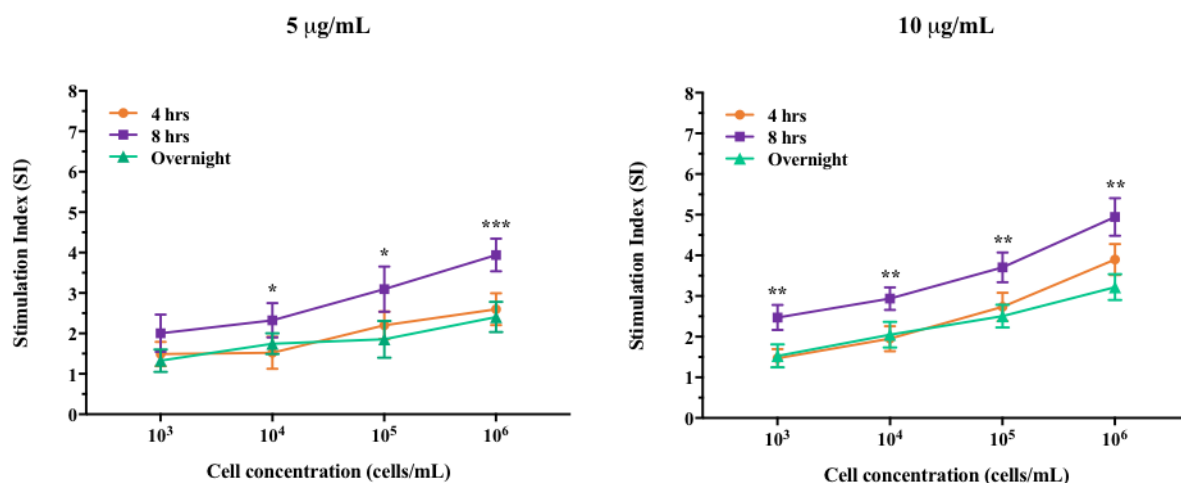


Figure 6.3. Comparison of MTT labelling time of 4 hr, 8 hr and overnight to maximise detection of proliferative responses (SI) of MT-4 cells to PHA. Values are the means \pm SD of three technical replicates. Significantly different at * $P \leq 0.05$, ** $P \leq 0.01$, *** $P \leq 0.001$.

6.2.2C. Stimulating lymphocytes with PHA and LPS to determine optimum cell concentration and MTT incubation time

In the previous section we showed that detection of proliferative responses was significantly greater when the MTT labelling reagent was left on for 8 hr, which is double that of the manufacturer's instructions. The aims of this experiment were to determine:

1. the optimum cell concentration of MT-4 cells and BIA-ALCL tumour cells for maximum proliferation to PHA and LPS, and
2. incubation time for the MTT labelling reagent.

MT-4 cells and BIA-ALCL cells were seeded at 10⁶, 10⁵, 10⁴ and 10³ cells/mL in triplicate wells and stimulated with 5 and 10 µg/mL of PHA and LPS as outlined in Section 6.2.2B., but with the MTT labelling reagent left on for either 6 hr or 8 hr.

Results

An MTT incubation of 6 hr detected cellular proliferation better than an incubation of 8 hours for both cell types in the majority of cases. For MT-4 cells, significantly higher SI were obtained for higher cell concentrations and higher mitogen concentrations, $P < 0.05$ (Figure 6.4).

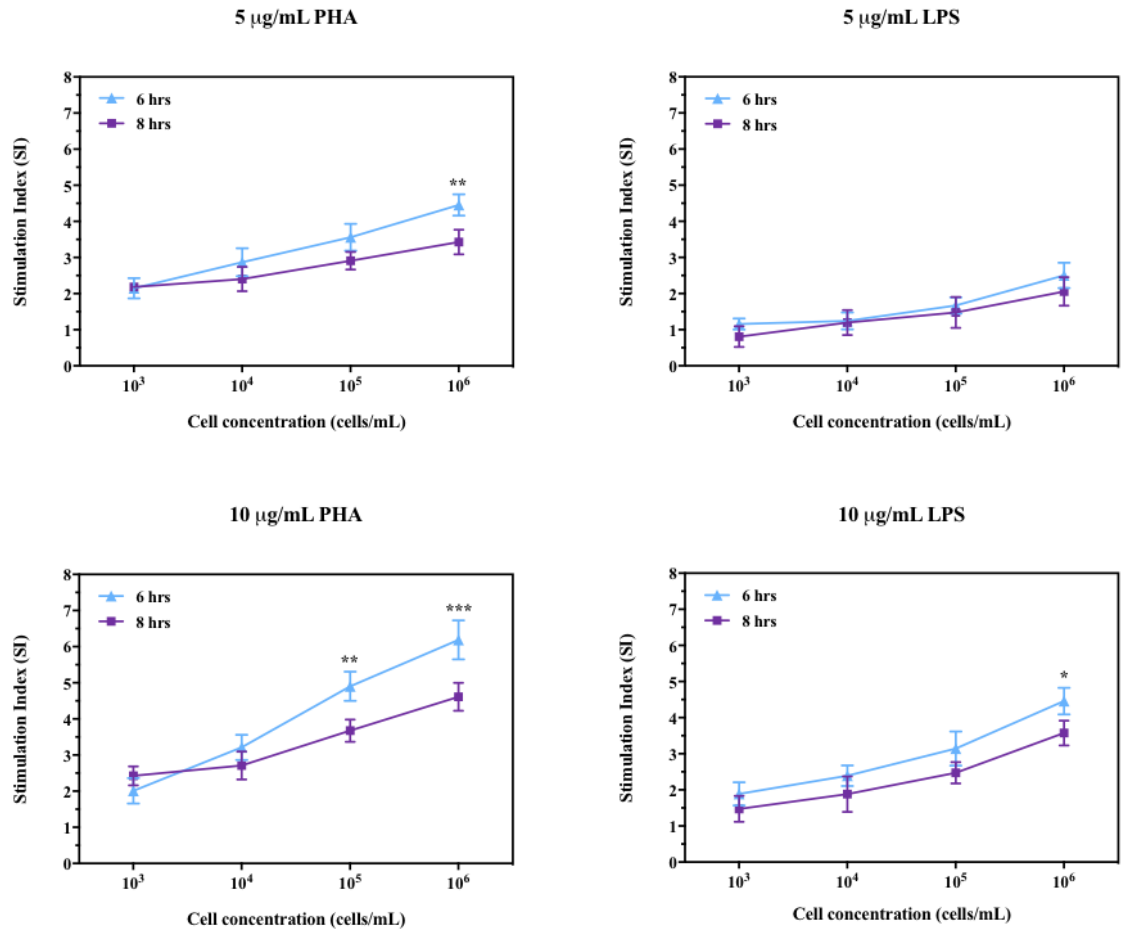


Figure 6.4. Comparison of MTT labelling time of 6 hr or 8 hr to maximise detection of proliferative responses (SI) of MT-4 cells to PHA and LPS stimulation. Values are the means \pm SD of three technical replicates. Significantly different at * $P \leq 0.05$, ** $P \leq 0.01$, *** $P \leq 0.001$.

A similar trend was seen with the BIA-ALCL cells and for cells stimulated with 10 µg/mL of LPS where significantly higher SI were obtained with MTT incubation of 6 hr, $P < 0.05$ (Figure 6.5).

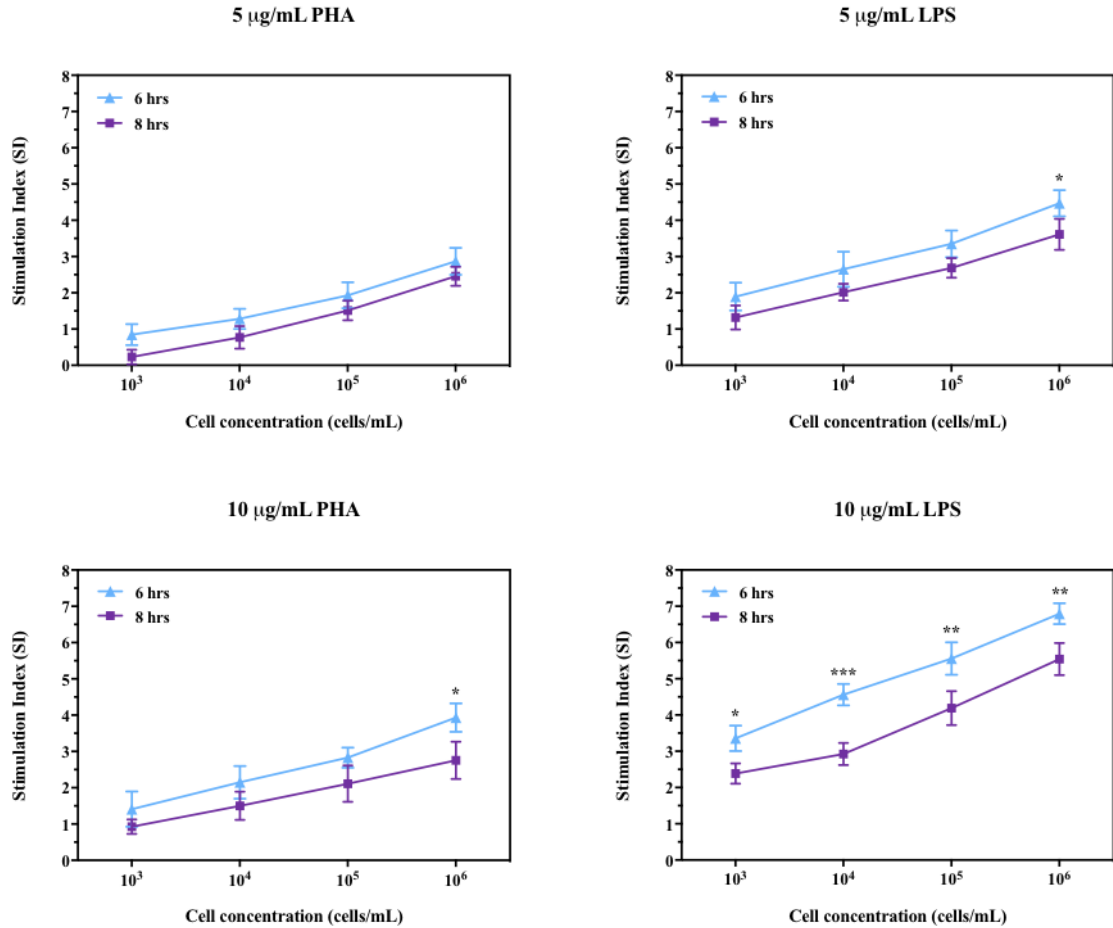


Figure 6.5. Comparison of MTT labelling time of 6 or 8 hr to maximise detection of proliferative responses (SI) of BIA-ALCL cells to PHA and LPS stimulation. Values are the means \pm SD of three technical replicates. Significantly different at $*P \leq 0.05$, $**P \leq 0.01$, $***P \leq 0.001$.

At 6 hr MTT incubation, both MT-4 cells and BIA-ALCL cells had significantly higher SI for cell concentration of 10^6 cells/mL when stimulated with PHA and LPS when compared to cell concentrations of 10^3 , 10^4 or 10^5 cells/mL, $P < 0.05$ (Figures 6.6 and 6.7). Similarly, MT-4 cells and BIA-ALCL cells at 10^5 cells/mL had significantly higher proliferative responses to 10 $\mu\text{g/mL}$ of PHA and LPS when compared to cell concentrations of 10^3 cells/mL, $P < 0.05$ (Figures 6.6 and 6.7).

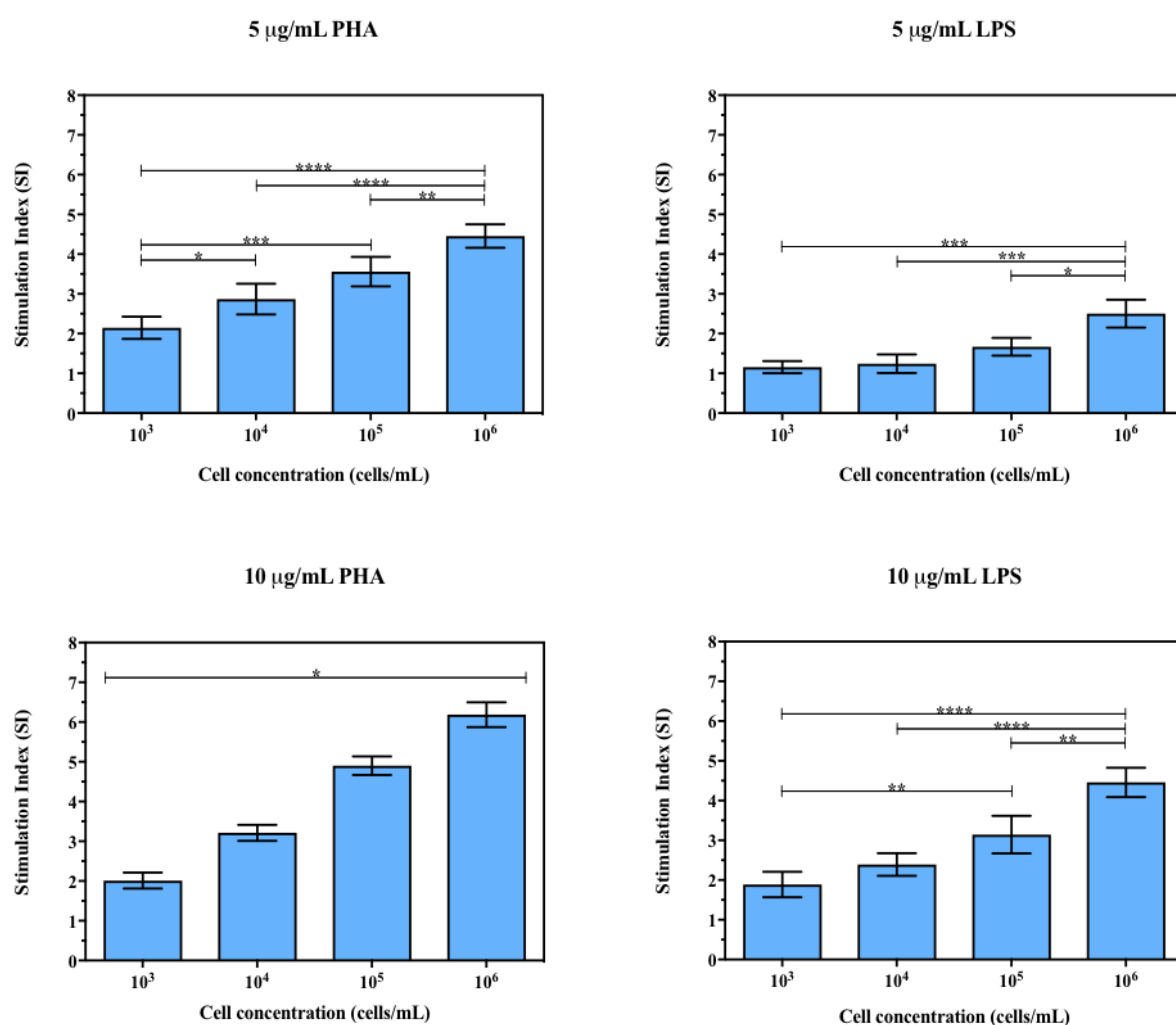


Figure 6.6. Proliferative response (SI) of MT-4 cells to PHA and LPS stimulation at MTT incubation of 6 hr. Values are the means \pm SD of three technical replicates. Significantly different at $*P \leq 0.05$, $**P \leq 0.01$, $***P \leq 0.001$, $****P \leq 0.0001$.

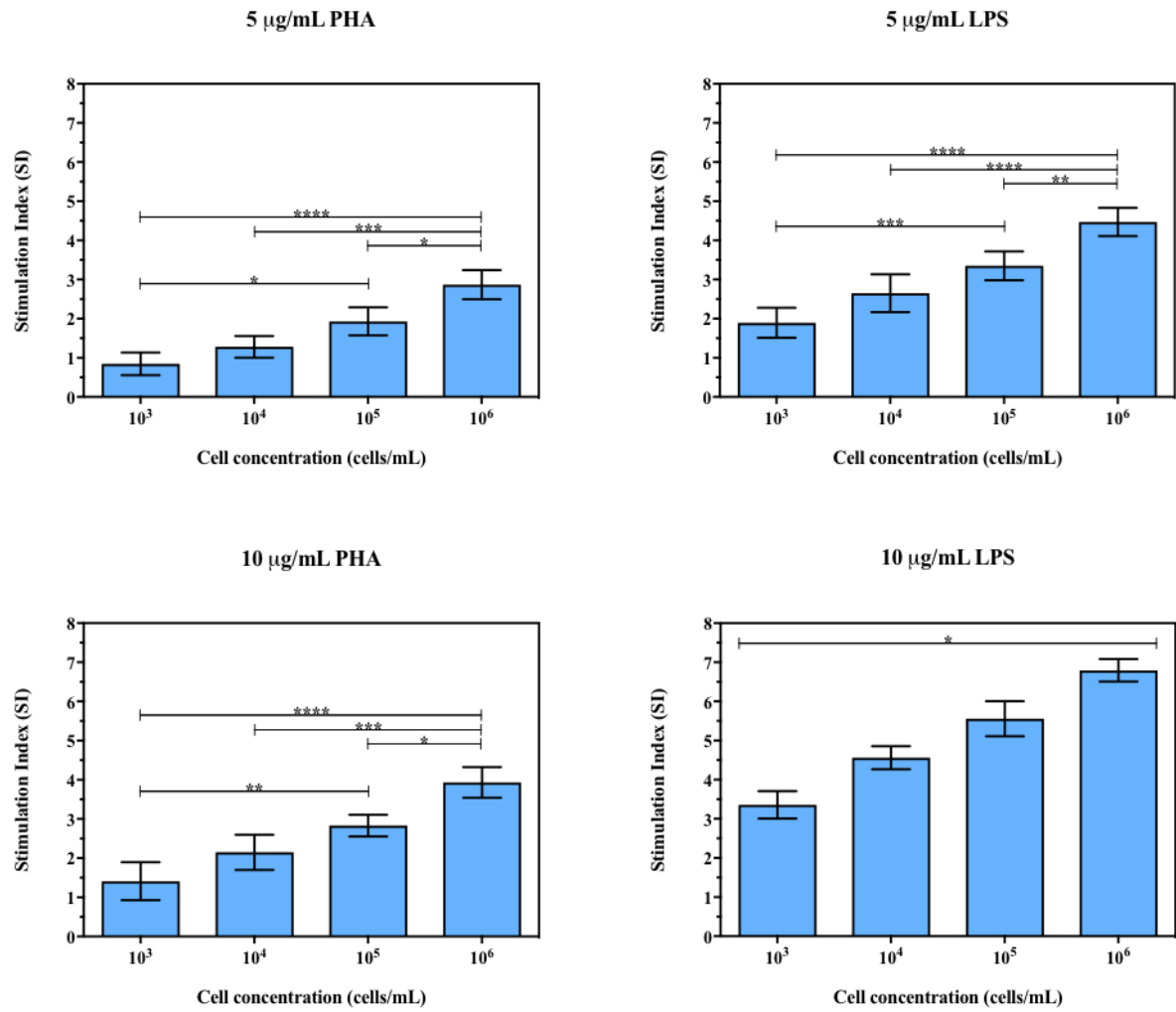


Figure 6.7. Proliferative response (SI) of BIA-ALCL cells to PHA and LPS stimulation at MTT incubation of 6 hr. Values are the means \pm SD of three technical replicates. Significantly different at $*P \leq 0.05$, $**P \leq 0.01$, $***P \leq 0.001$, $****P \leq 0.0001$.

To determine optimum cell concentration, we fitted a linear model using regression analysis for cell concentrations of 10^5 and 10^6 cells/mL stimulated with PHA and LPS and MTT incubation time of 6 hr. The goodness-of-fit test produced R square values ranging from 0.713 to 0.802 ($P < 0.05$).

Interpretation: We determined that 6 hr incubation with the MTT labelling reagent was optimum for these cell lines and used this for all subsequent experiments. We also deduced from the SI values and linear regression analysis of both cells that the optimum cell concentration for mitogen-induced cell proliferation was either 10^5 or 10^6 cells/mL.

6.2.2D. Stimulating cells with PHA to confirm optimum cell concentration

The aim of this experiment was to confirm that cell concentrations of 10^5 , $10^{5.5}$ and 10^6 cells/mL are optimum for mitogen-induced proliferation as shown in Section 6.2.2C.

Test conditions as per Section 6.2.2C. but using only PHA, the three cell concentrations and an MTT incubation of 6 hr.

Results

At MT-4 and BIA-ALCL cell concentrations of 10^5 , $10^{5.5}$ and 10^6 cells/mL significantly higher SI were obtained when stimulated with PHA, $P < 0.05$ (Figure 6.8) replicating our findings in Section 6.2.2C. Therefore, we have optimised a protocol for measuring the *in vitro* cell proliferation response of patient-derived BIA-ALCL tumour cells following mitogenic stimulation.

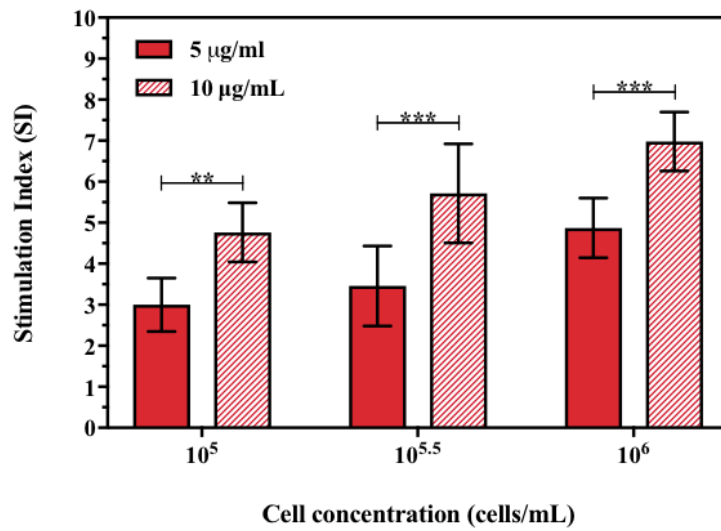
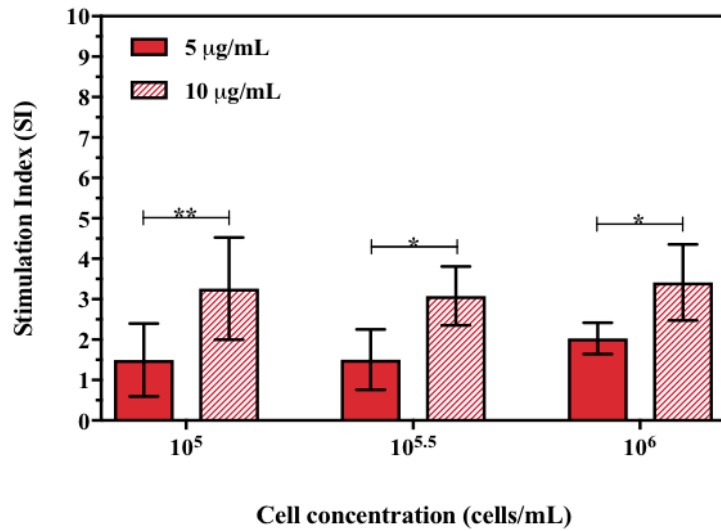
A**MT-4 cells****B****BIA-ALCL cells**

Figure 6.8. Proliferation response (SI) of (A) MT-4 cells and (B) BIA-ALCL cells to PHA. Values are the means \pm SD of three technical replicates. Significantly different at $*P \leq 0.05$, $**P \leq 0.01$, $***P \leq 0.001$.

6.3. Established *in vitro* cell proliferation assay

The established protocol for measuring the *in vitro* cell proliferation response of patient-derived BIA-ALCL tumour cells following mitogenic stimulation is shown in (Figure 6.9).

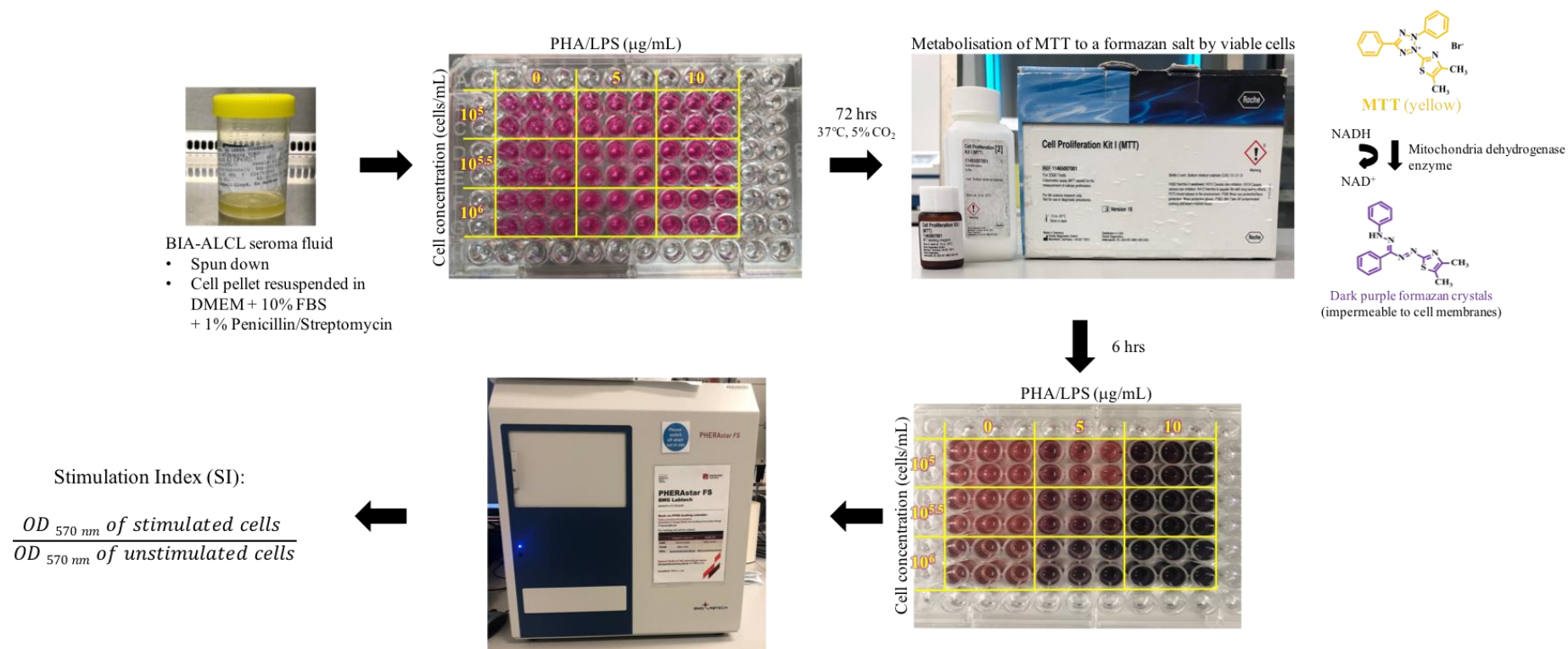


Figure 6.9. Established MTT colourimetric assay to determine cell proliferation.

Seroma fluid collected from BIA-ALCL patients was spun down and resuspended in DMEM + 10% FBS + 1% Penicillin/Streptomycin. Cells were seeded at a concentration of 10^5 , $10^{5.5}$ and 10^6 cells/mL in each well of a 96-well plate and stimulated to proliferate non-specifically with 20 µL of PHA or LPS at concentrations of 5 or 10 µg/mL. While some cells were not stimulated at all. The plate was incubated at 37 °C, 5% CO₂ for 72 hr. Cell proliferation was measured using an MTT colourimetric assay by incubating each well with 20 µL of MTT for 6 hr. The formed formazan crystals were then solubilised and quantified using a spectrophotometer. Cell proliferation was calculated as a stimulation index (SI) by dividing cells stimulated with mitogens by those not stimulated.

6.4. Part B: Response of patient-derived tumour cells and peripheral blood mononuclear cells to mitogenic stimulation

6.4.1. Introduction

We measured the cell proliferation response of nine patient-derived BIA-ALCL tumour cells, three BIA-ALCL cell lines (TLBR-1, TLBR-2, TLBR-3), two cutaneous-ALCL cell lines (MAC-1, MAC-2A), an MT-4 immortal human T-lymphotrophic virus-1 infected T-cell line, PBMC derived from BIA-ALCL patients, patients with CC and healthy controls undergoing primary breast augmentation to PHA and LPS for 72 hr at different cell concentrations.

6.4.2. Materials and Methods

6.4.2.1. Tumour cells/peripheral blood mononuclear cells/cell lines

BIA-ALCL tumour cells

Nine female patients from seven centres around Australia, presenting with Stage 1 BIA-ALCL disease participated in this study (Table 5.1, Section 5.3.1.). BIA-ALCL tumour cells were harvested fresh from the serous fluid and/or tumour mass as described in Section 2.5.1.

Three newly established BIA-ALCL cell lines, TLBR-1, -2 and -3, were also utilised (Table 2.2, Section 2.5.1.).

Cutaneous-ALCL cells

Two cutaneous-ALCL cell lines, MAC-1 and MAC-2A, were used (Section 2.5.1.).

MT-4 cells

MT-4 immortal T-cell line (ECACC 08081402) was utilised as detailed in Section 2.5.1.

Peripheral blood mononuclear cells

PBMC were purified from BIA-ALCL patients ($n = 5$), female patients having breast implants removed due to CC ($n = 3$) and healthy control patients without exposure to breast implants ($n = 3$) as detailed in Section 2.5.1.

6.4.2.2. *In vitro* cell proliferation assay

Cells were seeded at concentrations of 10^5 , $10^{5.5}$ and 10^6 cells/mL in a 96-well plate in six replicates and stimulated to proliferate non-specifically with 5 or 10 μ g/mL of PHA and LPS (Section 6.2.1.2.) while control or unstimulated wells, received 20 μ L of complete medium. Cells were incubated for 72 hr at 37°C, 5% CO₂. Cell proliferation was measured using the established protocol outlined in Section 6.3.

6.4.2.3. Statistical analysis

All statistical analyses were performed in GraphPad Prism 7.0. To test normality of data distribution, the Shapiro-Wilk test was used. The Kruskal Wallis test by ranks and the Mann-Whitney rank sum test was used to compare the age of patients and the time since implantation. Comparisons of the differences in proliferation responses, effects of cell and mitogen concentrations among the different cell culture types were analysed using one-way and two-way ANOVA. If significant differences were found, then Tukey's or Sidak's multiple comparisons post-hoc test were employed. All values are expressed as mean \pm standard error of the mean (SEM); P values less than or equal to 0.05 were considered statistically significant.

6.4.3. Results

6.4.3.1. Clinical features

Fourteen BIA-ALCL patients, including nine patient-derived tumour cells (patients 1610, 1612, 1618, 1626, 1627, 1701, 1713, 1714, 1715) and PBMC purified from five patients (1803, 1808, 1810, 1817, 1819), were included in this study (Table 5.1, Section 5.3.1.). The mean patient age was 43.4 years (range, 31 to 58 years) and the mean duration of time between insertion of implants and diagnosis of BIA-ALCL was 7.7 years (range, 4 to 14 years). In four patients, the indication for breast implants was postmastectomy reconstruction and in the remaining ten patients, the indication for implants was cosmetic augmentation. Thirteen patients (92.9%) presented with a unilateral malignant effusion, whereas patient 1627 (7.1%) presented with a tumour mass following infection. In two patients (1626 and 1714) the diagnosis of BIA-ALCL was preceded by CC. All patients were exposed to textured implants upon diagnosis. Silimed PU textured implants accounted for 57.1% of the implants used in this series, followed by salt-loss textures Allergan Biocell (28.6%) and Nagor (14.3%). All BIA-ALCL patients were treated with capsulectomy and removal of implants.

Among the controls, the three patients with CC (patients 1621, 1711, 1712) had a mean age of 54 years (range, 42 to 62 years) and a mean implantation time of 7.8 years (range, 3.5 to 15 years). While the three patients undergoing primary augmentation (patients 1630, 1705, 1710) had a mean age of 36.3 years (range, 35 to 37 years). There was no difference in the age of BIA-ALCL patients and non-tumour patients ($P = 0.0514$). There was also no significant difference in duration of implantation between the two groups ($P = 0.8456$).

6.4.3.2. Cell proliferation response following mitogenic stimulation

The BIA-ALCL tumour cells ($n = 9$) responded significantly more to stimulation with LPS when compared to PHA in higher cell concentrations and at both mitogen concentrations (5 and 10 $\mu\text{g/mL}$), $P < 0.05$ (Figure 6.10).

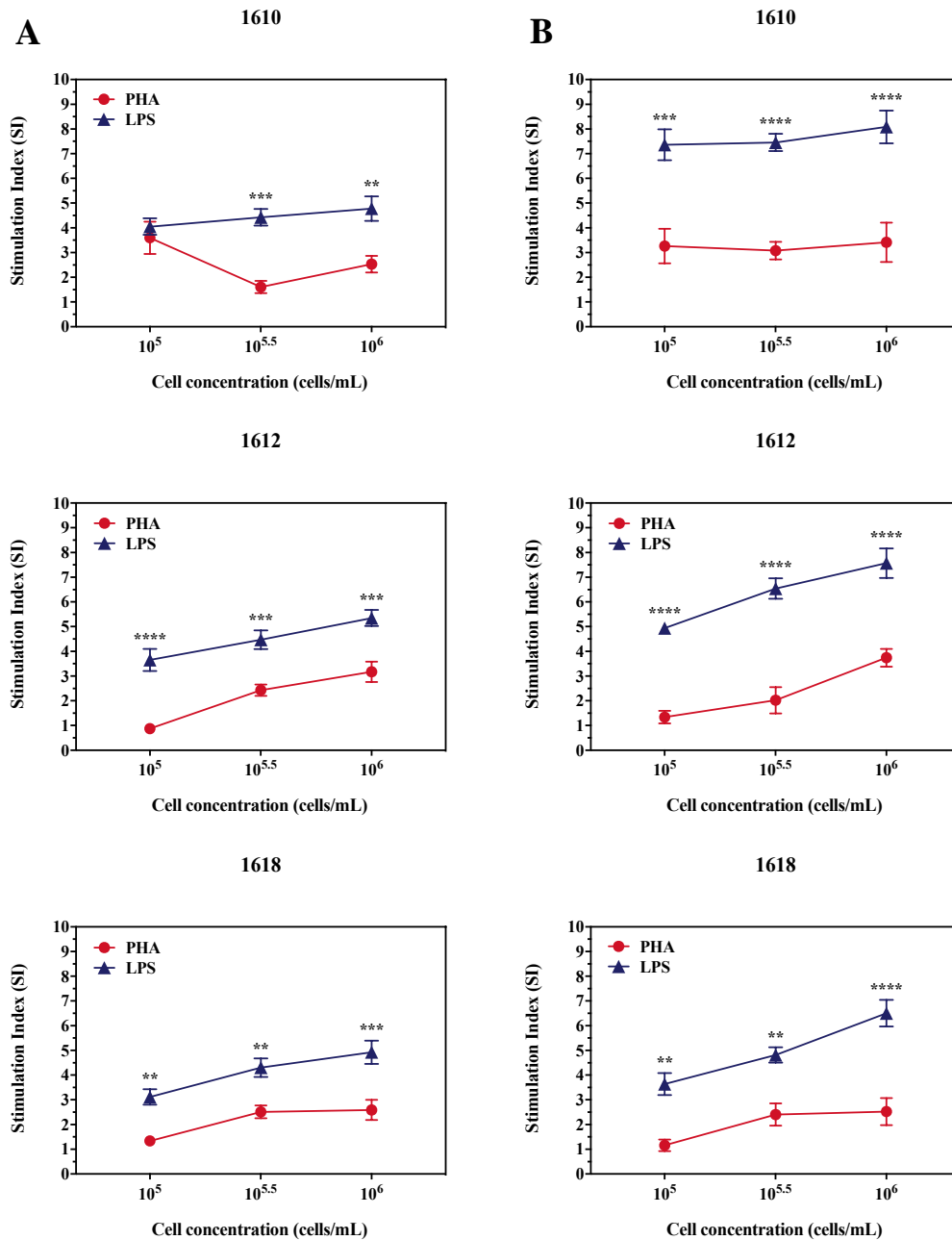


Figure 6.10. Proliferation response (SI) of the nine patient-derived BIA-ALCL tumour cells to (A) 5 and (B) 10 $\mu\text{g/mL}$ of PHA and LPS. Values are the means \pm SEM of six technical replicates. Significantly different at $*P \leq 0.05$, $**P \leq 0.01$, $***P \leq 0.001$, $****P \leq 0.0001$.

In patient 1627, who was the only patient in the cohort to present with a tumour mass, BIA-ALCL cells responded significantly to LPS in all cell concentrations at 10 μ g/mL but only at one cell concentration at 5 μ g/mL, $P < 0.05$ (Figure 6.10).

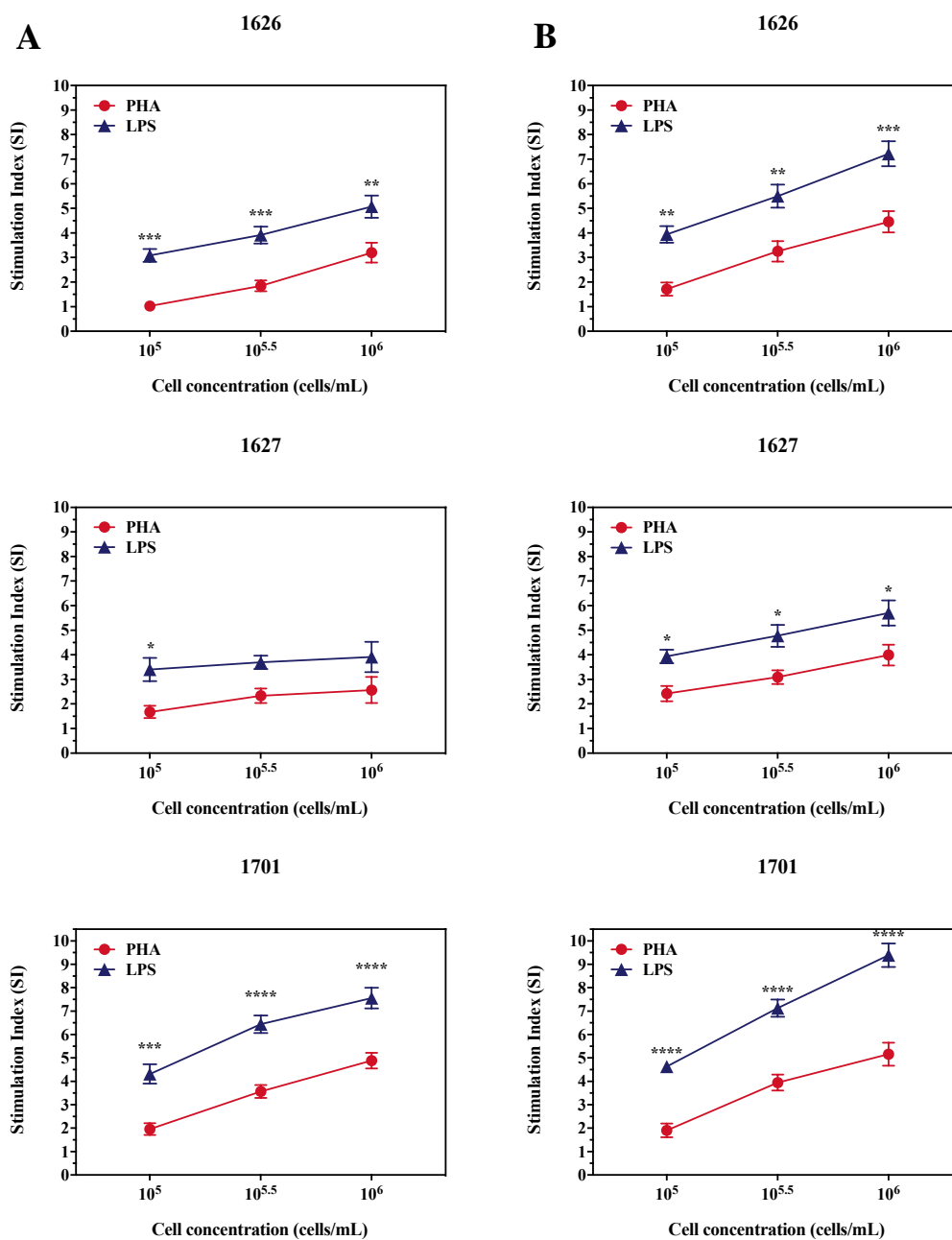


Figure 6.10. Continued.

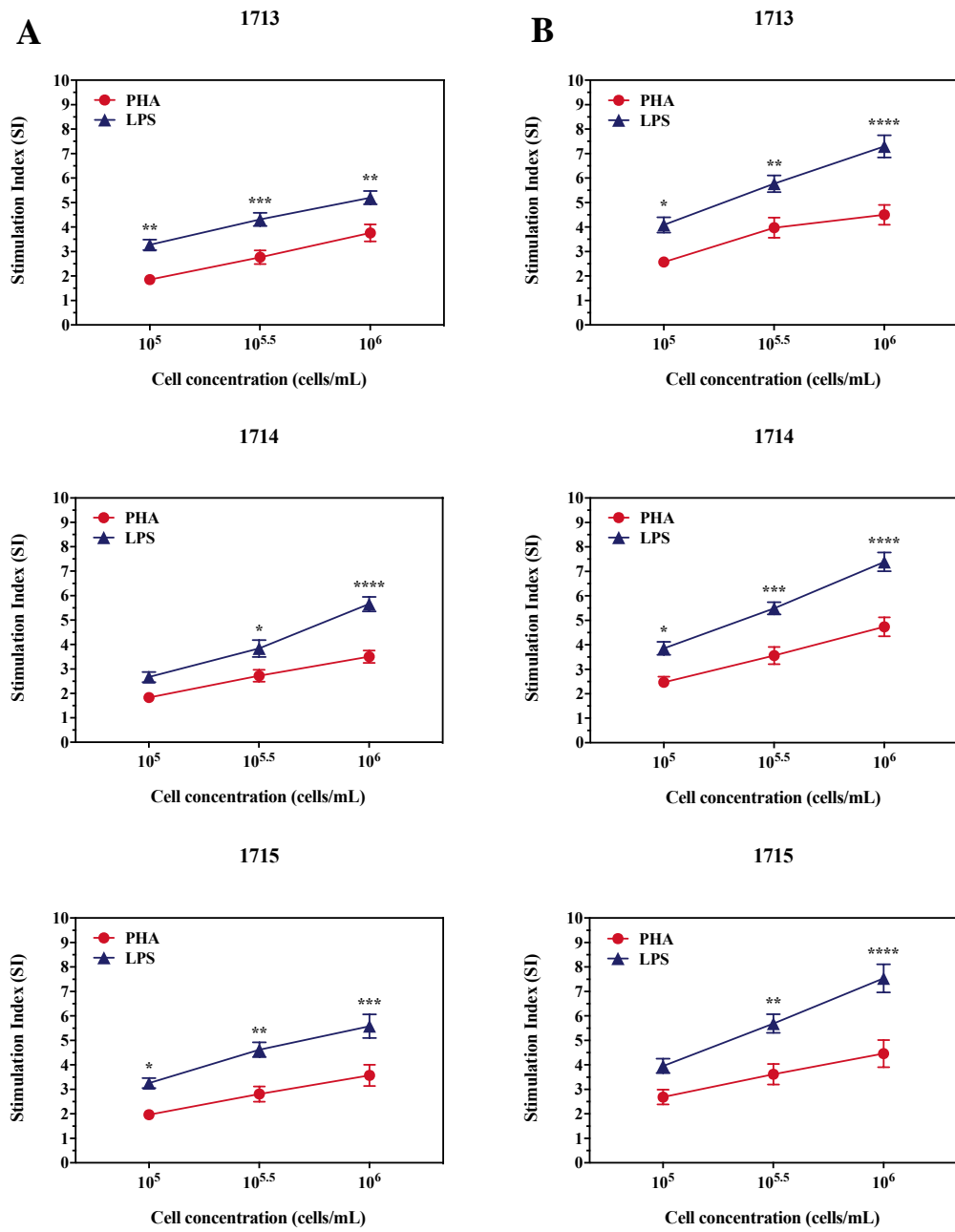


Figure 6.10. Continued.

A similar response was found in BIA-ALCL cell lines, TLBR-1, TLBR-2 and TLBR-3. We found significantly higher SI with LPS when compared with PHA at all cell concentrations at 10 $\mu\text{g/mL}$ ($P < 0.05$) and at higher cell concentrations tested at 5 $\mu\text{g/mL}$, $P < 0.001$ (Figure 6.11).

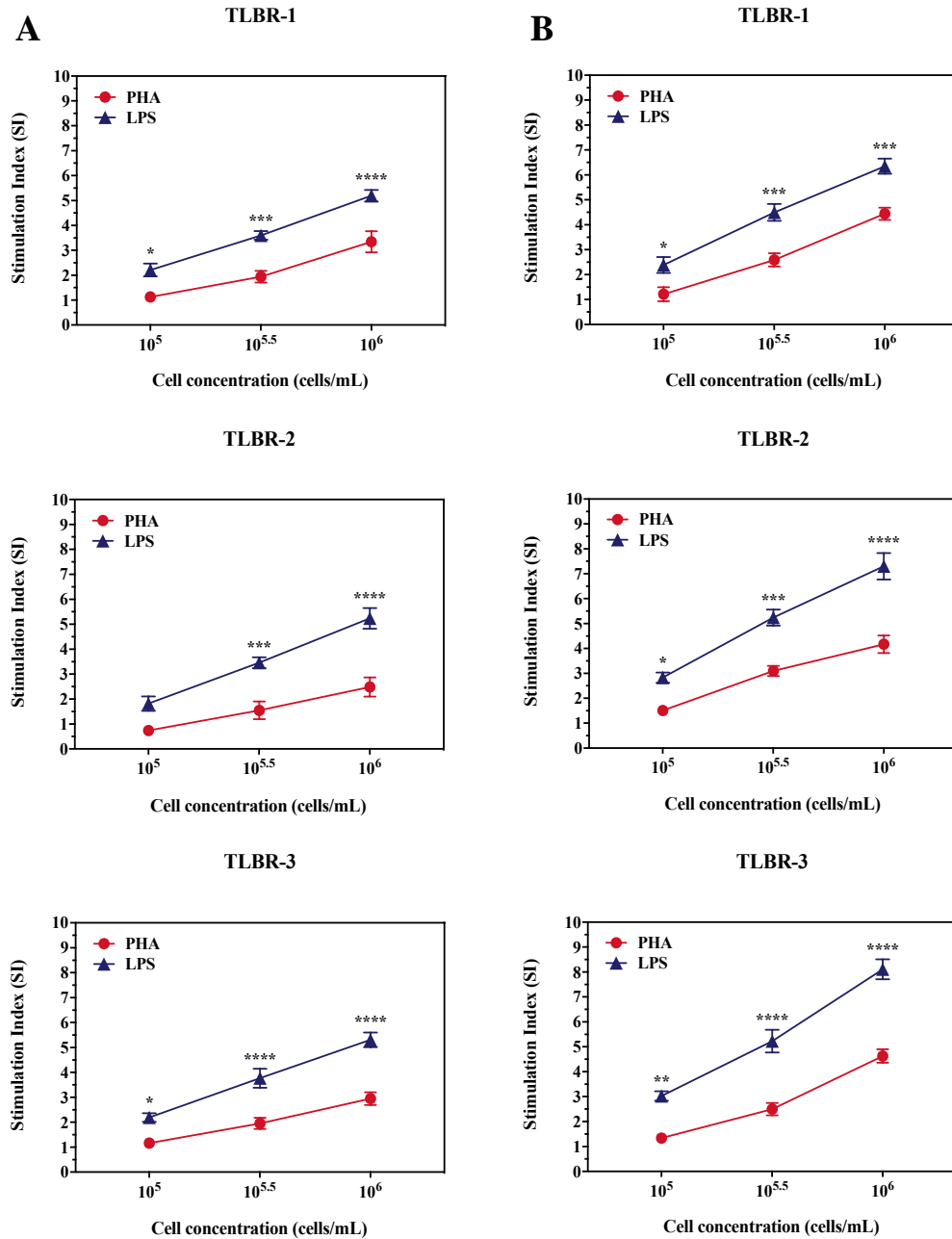


Figure 6.11. Proliferation response (SI) of the three BIA-ALCL cell lines, TLBR-1, TLBR-2 and TLBR-3, to (A) 5 and (B) 10 $\mu\text{g/mL}$ of PHA and LPS. Values are the means \pm SEM of six technical replicates. Significantly different at * $P \leq 0.05$, ** $P \leq 0.01$, *** $P \leq 0.001$, **** $P \leq 0.0001$.

In contrast to BIA-ALCL cells, cutaneous-ALCL cell lines, MAC-1, MAC-2A, had significantly higher proliferative responses to PHA-induced stimulation compared to LPS in all cell concentrations and at 5 and 10 $\mu\text{g/mL}$, $P < 0.05$ (Figure 6.12).

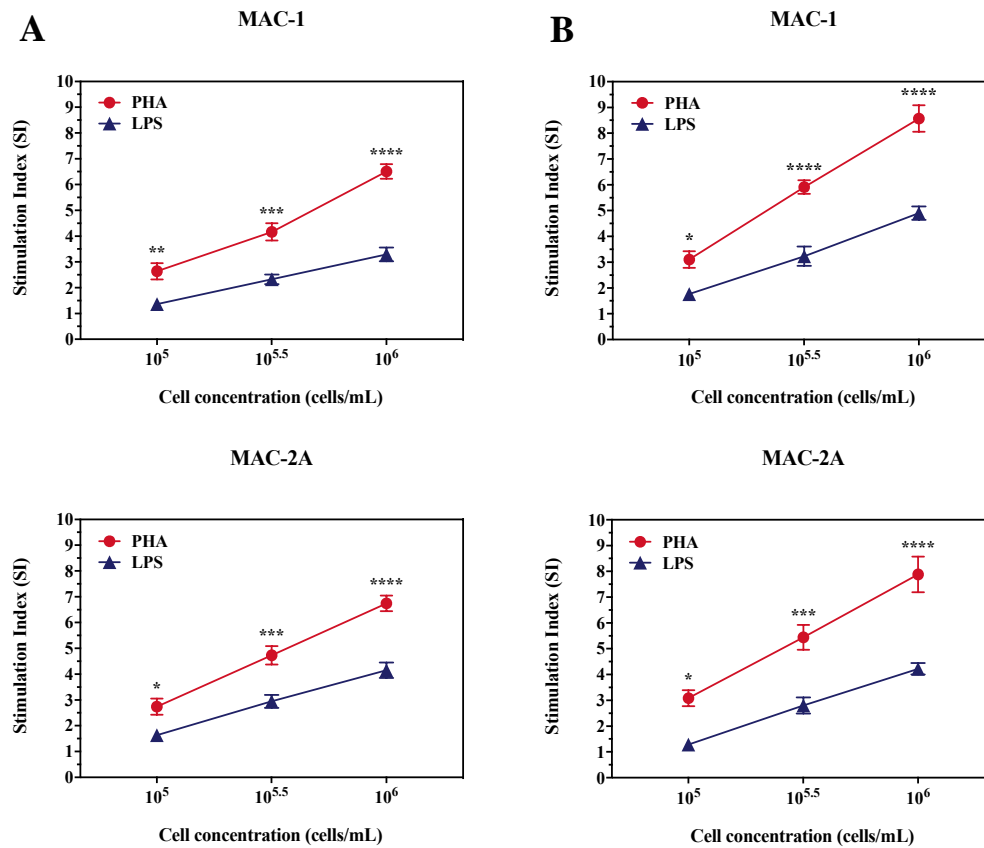


Figure 6.12. Proliferation response (SI) of the two cutaneous-ALCL cell lines, MAC-1 and MAC-2A, to (A) 5 and (B) 10 $\mu\text{g/mL}$ of PHA and LPS. Values are the means \pm SEM of six technical replicates. Significantly different at $*P \leq 0.05$, $**P \leq 0.01$, $***P \leq 0.001$, $****P \leq 0.0001$.

Similarly, MT-4 cells proliferated significantly more to PHA than LPS in all cell concentrations and at 5 and 10 $\mu\text{g/mL}$, $P < 0.05$ (Figure 6.13).

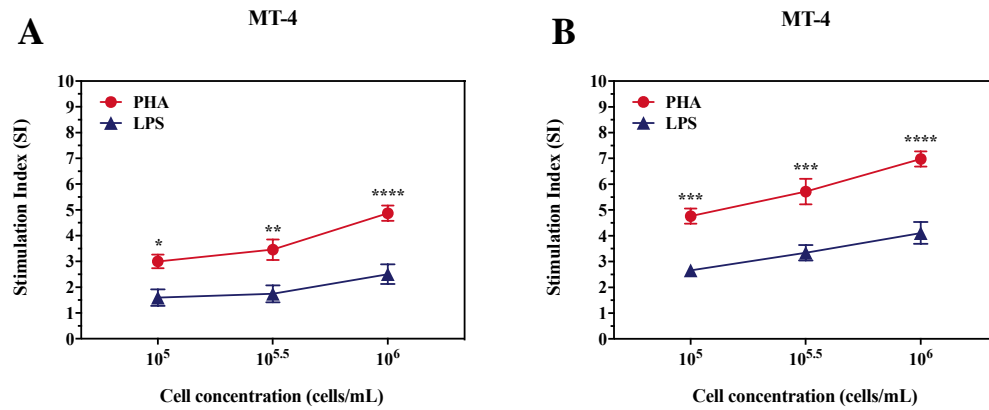


Figure 6.13. Proliferation response (SI) of the MT-4 immortal T-cell line to (A) 5 and (B) 10 $\mu\text{g/mL}$ of PHA and LPS. Values are the means \pm SEM of six technical replicates. Significantly different at $*P \leq 0.05$, $**P \leq 0.01$, $***P \leq 0.001$, $****P \leq 0.0001$.

PBMC collected from patients with contracture showed significantly more proliferation when stimulated with PHA compared to stimulation with LPS at all cell concentrations at 5 $\mu\text{g/mL}$ ($P < 0.05$) and at higher cell concentrations at 10 $\mu\text{g/mL}$, $P < 0.01$ (Figure 6.14).

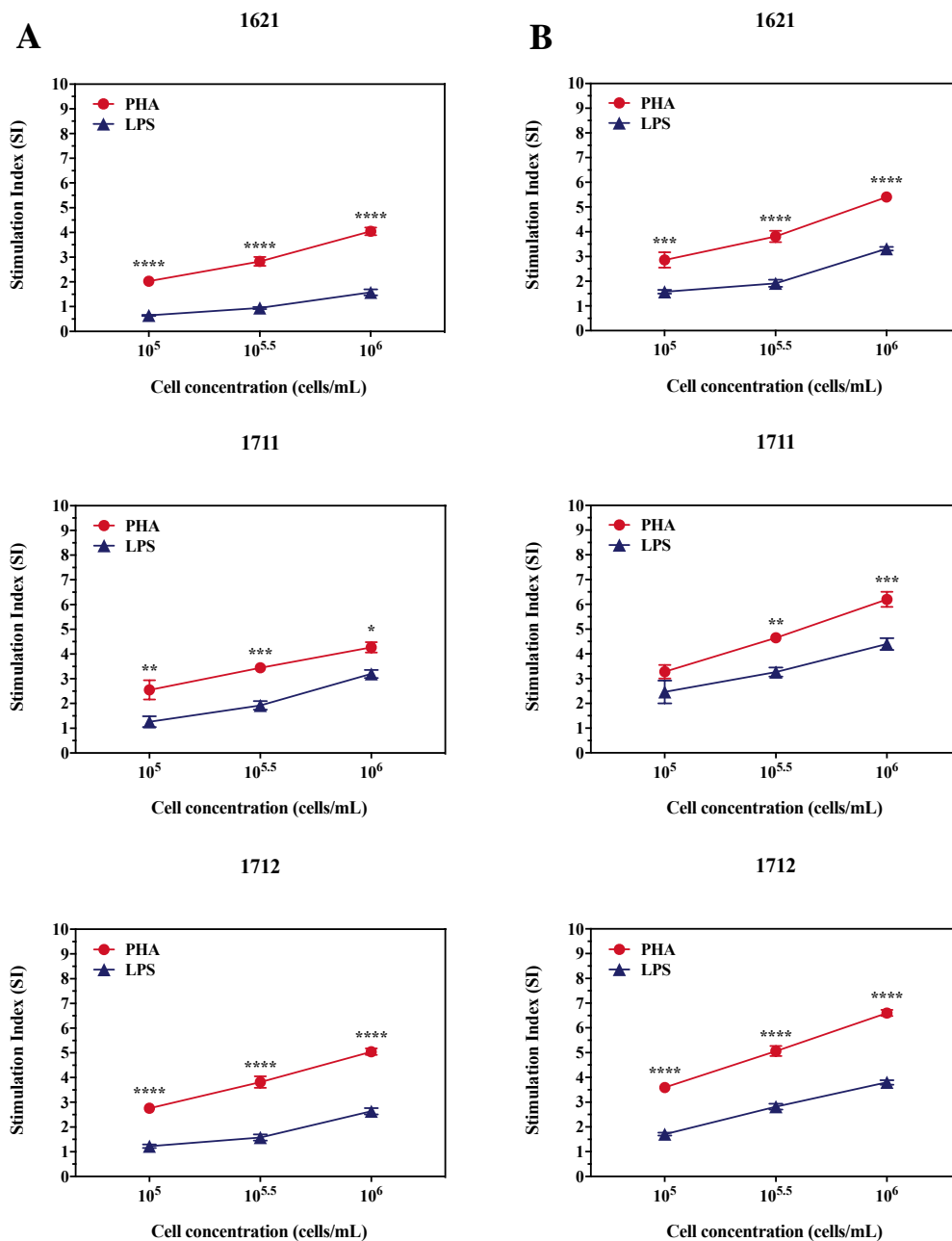


Figure 6.14. Proliferation response (SI) of the peripheral blood mononuclear cells purified from patients with capsular contracture to (A) 5 and (B) 10 $\mu\text{g/mL}$ of PHA and LPS. Values are the means \pm SEM of six technical replicates. Significantly different at * $P \leq 0.05$, ** $P \leq 0.01$, *** $P \leq 0.001$, **** $P \leq 0.0001$.

In patients undergoing primary breast augmentation and no previous exposure to breast implants, PHA produced the highest proliferative response in all cell concentrations and at both mitogen concentrations (5 and 10 $\mu\text{g/mL}$), $P < 0.0001$ (Figure 6.15).

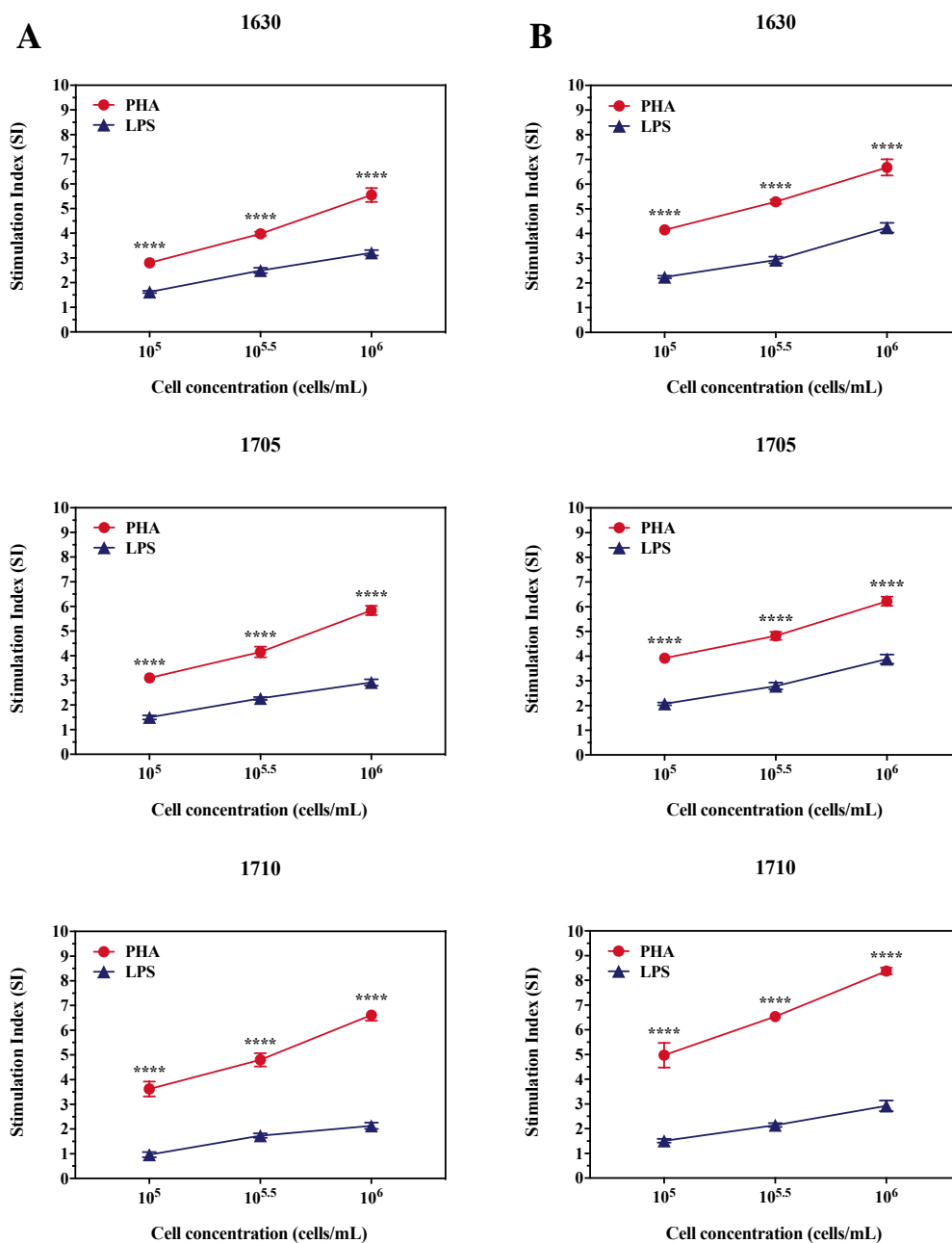


Figure 6.15. Proliferation response (SI) of the peripheral blood mononuclear cells purified from healthy patients undergoing primary breast augmentation to (A) 5 and (B) 10 $\mu\text{g/mL}$ of PHA and LPS. Values are the means \pm SEM of six technical replicates. Significantly different at **** $P \leq 0.0001$.

The PBMC from patients with BIA-ALCL did not demonstrate the LPS-induced proliferation and responded maximally to PHA at higher cell concentrations and when stimulated with 10 $\mu\text{g/mL}$, $P < 0.001$. A lower response was obtained with 5 $\mu\text{g/mL}$ of PHA compared to 5 $\mu\text{g/mL}$ of LPS but this was still significantly higher with the exception of patient 1817 ($P < 0.05$) (Figure 6.16).

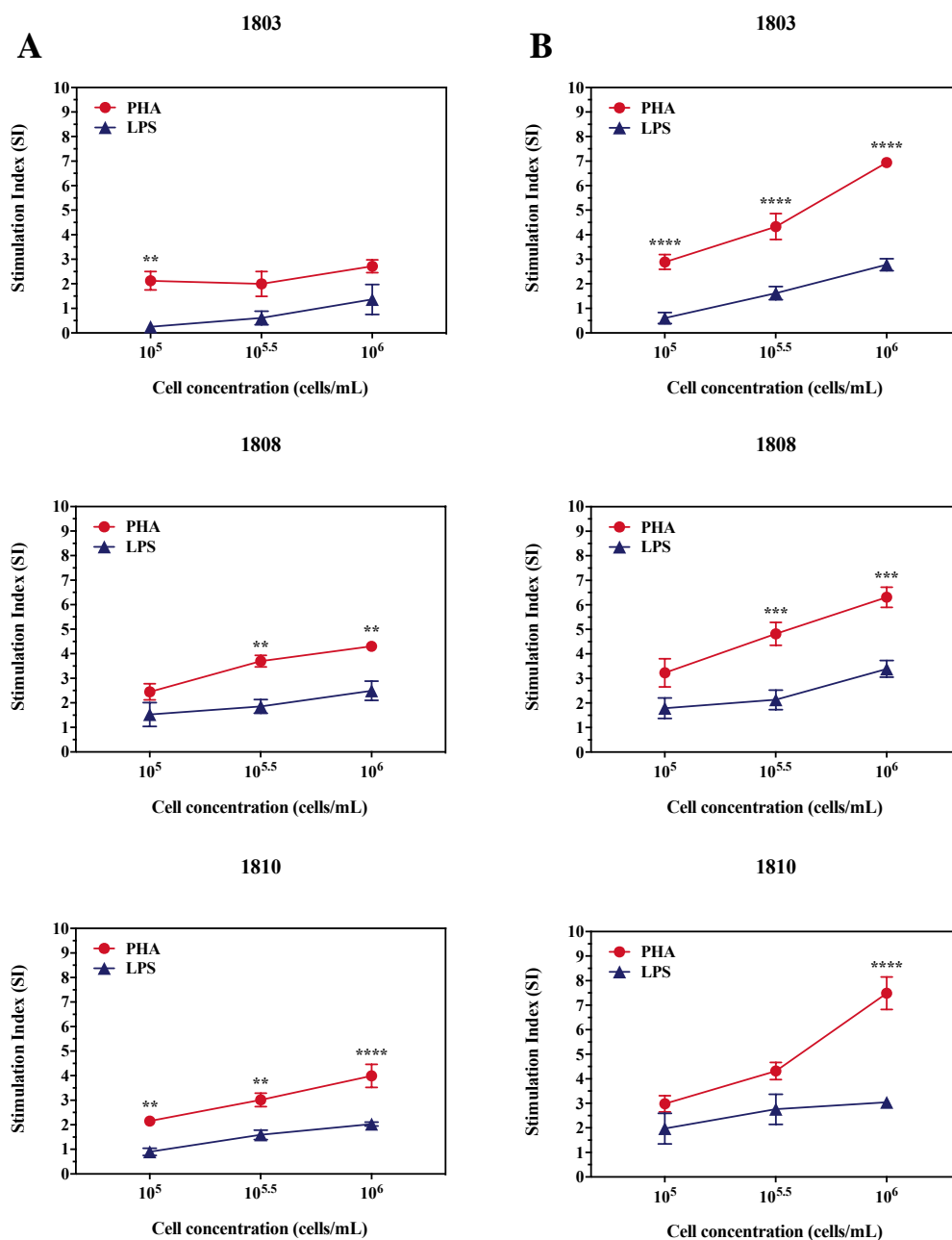


Figure 6.16. Proliferation response (SI) of the peripheral blood mononuclear cells purified from BIA-ALCL patients to (A) 5 and (B) 10 $\mu\text{g/mL}$ of PHA and LPS. Values are the means \pm SEM of six technical replicates. Significantly different at * $P \leq 0.05$, ** $P \leq 0.01$, *** $P \leq 0.001$, **** $P \leq 0.0001$.

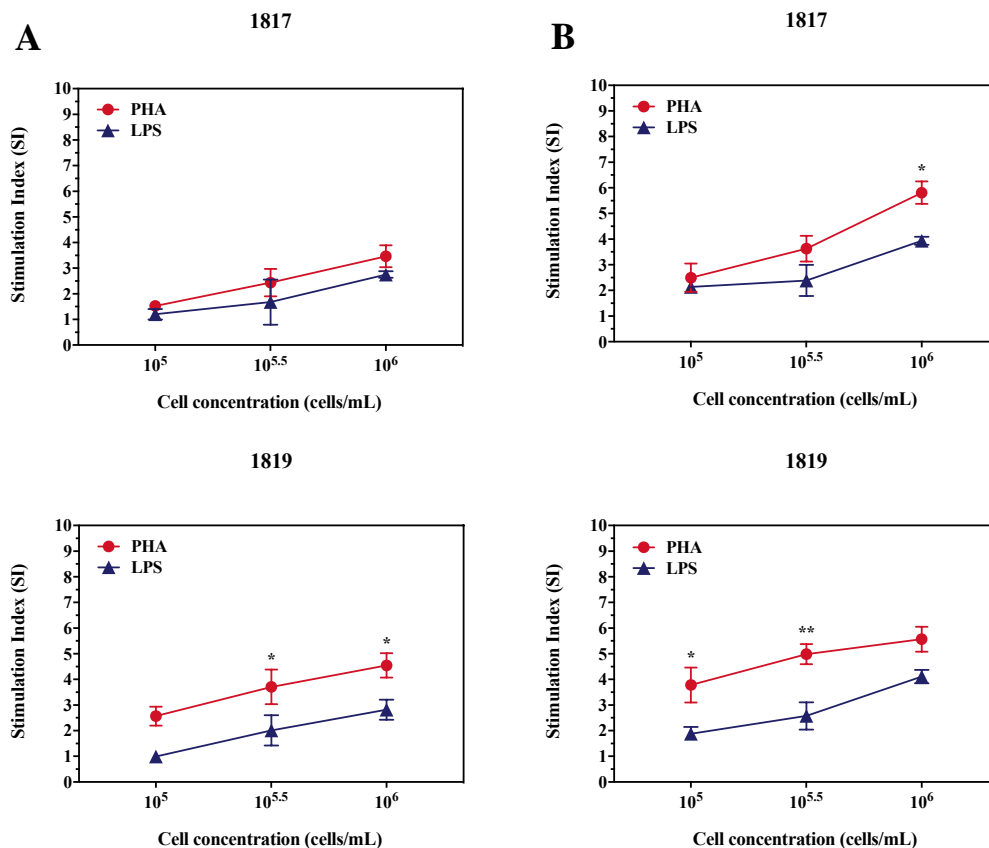


Figure 6.16. Continued.

Two-way ANOVA comparing the differences in proliferative responses (SI) among the different cells cultured showed that patient-derived BIA-ALCL tumour cells (SI: 4.4 (5 $\mu\text{g/mL}$), 5.9 (10 $\mu\text{g/mL}$)) had significantly higher responses when stimulated with LPS compared to proliferative responses achieved by cutaneous-ALCL (2.6 (5 $\mu\text{g/mL}$), 3.0 (10 $\mu\text{g/mL}$)) and MT-4 cell lines (2.0 (5 $\mu\text{g/mL}$), 3.4 (10 $\mu\text{g/mL}$)) ($P < 0.05$), and in PBMC purified from patients with CC (1.7 (5 $\mu\text{g/mL}$), 2.8 (10 $\mu\text{g/mL}$)), primary augmentation (2.1 (5 $\mu\text{g/mL}$), 2.8 (10 $\mu\text{g/mL}$)) and BIA-ALCL patients (1.6 (5 $\mu\text{g/mL}$), 2.5 (10 $\mu\text{g/mL}$)) ($P < 0.0001$) at 5 and 10 $\mu\text{g/mL}$ (Figure 6.17). Similarly, in BIA-ALCL (TLBR) cell lines (3.6 (5 $\mu\text{g/mL}$), 5.0 (10 $\mu\text{g/mL}$)) stimulated with LPS (5 and 10 $\mu\text{g/mL}$), significantly higher SI were obtained when compared to PBMC collected from contracture

patients ($P < 0.05$) and BIA-ALCL patients ($P < 0.01$). At 10 $\mu\text{g/mL}$, TLBR cells responded more to LPS than cutaneous-ALCL cells ($P = 0.0358$) and PBMC from healthy control patients ($P = 0.0020$) (Figure 6.17). There was no difference in proliferative responses to LPS-induced stimulation between BIA-ALCL tumour cells and TLBR cell lines at 5 and 10 $\mu\text{g/mL}$ ($P > 0.05$) (Figure 6.17).

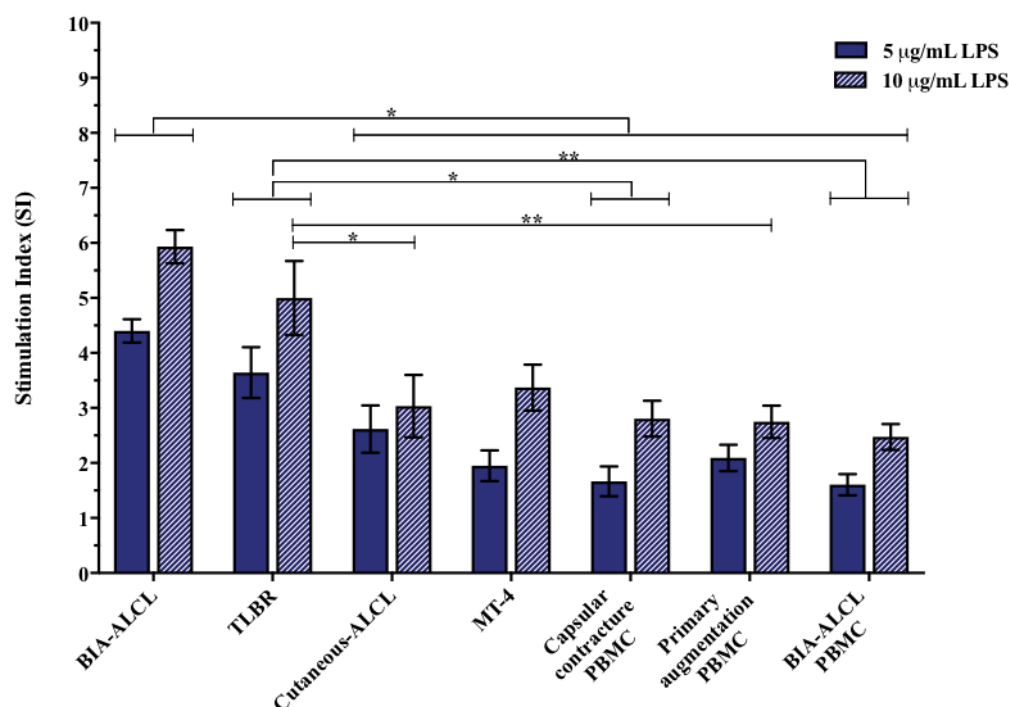


Figure 6.17. Summary of the proliferative response (SI) of the different cell types to 5 and 10 $\mu\text{g/mL}$ of LPS. Values are the means \pm SEM. Significantly different at $*P \leq 0.05$, $**P \leq 0.01$.

Conversely, PHA-induced stimulation (5 and 10 $\mu\text{g/mL}$) elicited significantly higher SI in cutaneous-ALCL cell lines (4.6 (5 $\mu\text{g/mL}$), 5.7 (10 $\mu\text{g/mL}$)) and in PBMC purified from primary augmentation patients (4.5 (5 $\mu\text{g/mL}$), 5.7 (10 $\mu\text{g/mL}$)) compared to BIA-ALCL tumour cells (2.5 (5 $\mu\text{g/mL}$), 3.2 (10 $\mu\text{g/mL}$)) and TLBR cell lines (1.9 (5 $\mu\text{g/mL}$), 2.8 (10 $\mu\text{g/mL}$)) ($P < 0.01$), which

had lower proliferative responses to PHA stimulation (Figure 6.18). At 10 $\mu\text{g/mL}$ of PHA, proliferative responses of BIA-ALCL cells were also lower than MT-4 cells (5.8) ($P < 0.01$), and PBMC from CC patients (4.6) ($P < 0.05$) and BIA-ALCL patients (4.6) ($P < 0.05$) (Figure 6.18). No difference in SI, following PHA-induced stimulation (5 and 10 $\mu\text{g/mL}$), was found between BIA-ALCL tumour cells and TLBR cell lines, and between cutaneous-ALCL and MT-4 cell lines (3.8 (5 $\mu\text{g/mL}$), 5.8 (10 $\mu\text{g/mL}$)) ($P > 0.05$). There was also no difference in proliferative responses to PHA among the PBMC purified from patients with BIA-ALCL (3.0 (5 $\mu\text{g/mL}$), 4.7 (10 $\mu\text{g/mL}$)), contracture (3.4 (5 $\mu\text{g/mL}$), 4.6 (10 $\mu\text{g/mL}$)) and healthy control patients ($P > 0.05$) (Figure 6.18).

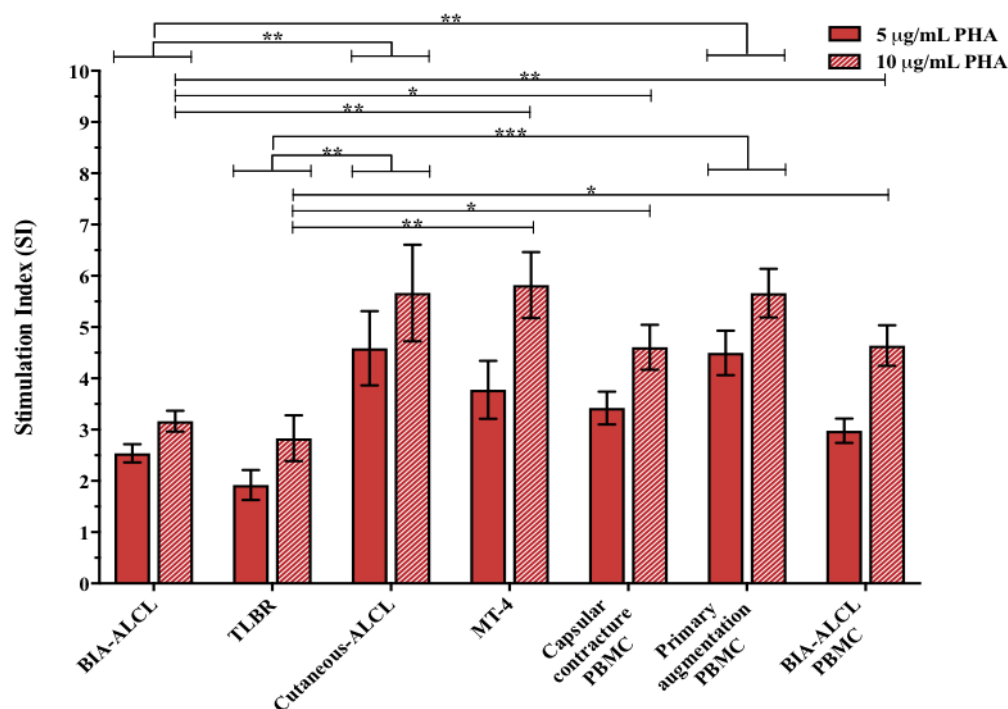


Figure 6.18. Summary of the proliferative response (SI) of the different cell types to 5 and 10 $\mu\text{g/mL}$ of PHA. Values are the means \pm SEM. Significantly different at $*P \leq 0.05$, $**P \leq 0.01$, $***P \leq 0.001$.

Figure 6.19 summarises the difference in the maximum significant SI obtained following stimulation with PHA and LPS for each individual BIA-ALCL patient (Tumour cells, $n = 9$; PBMC, $n = 3$), contracture patient ($n = 3$), healthy control patient ($n = 3$), and each cell line tested, TLBR ($n = 3$), cutaneous-ALCL ($n = 2$) and MT-4 cells. Overall, the maximum LPS response and the corresponding maximum PHA response occurred at the same cell concentration of 10^6 cells/mL and mitogen concentration of $10 \mu\text{g/mL}$.

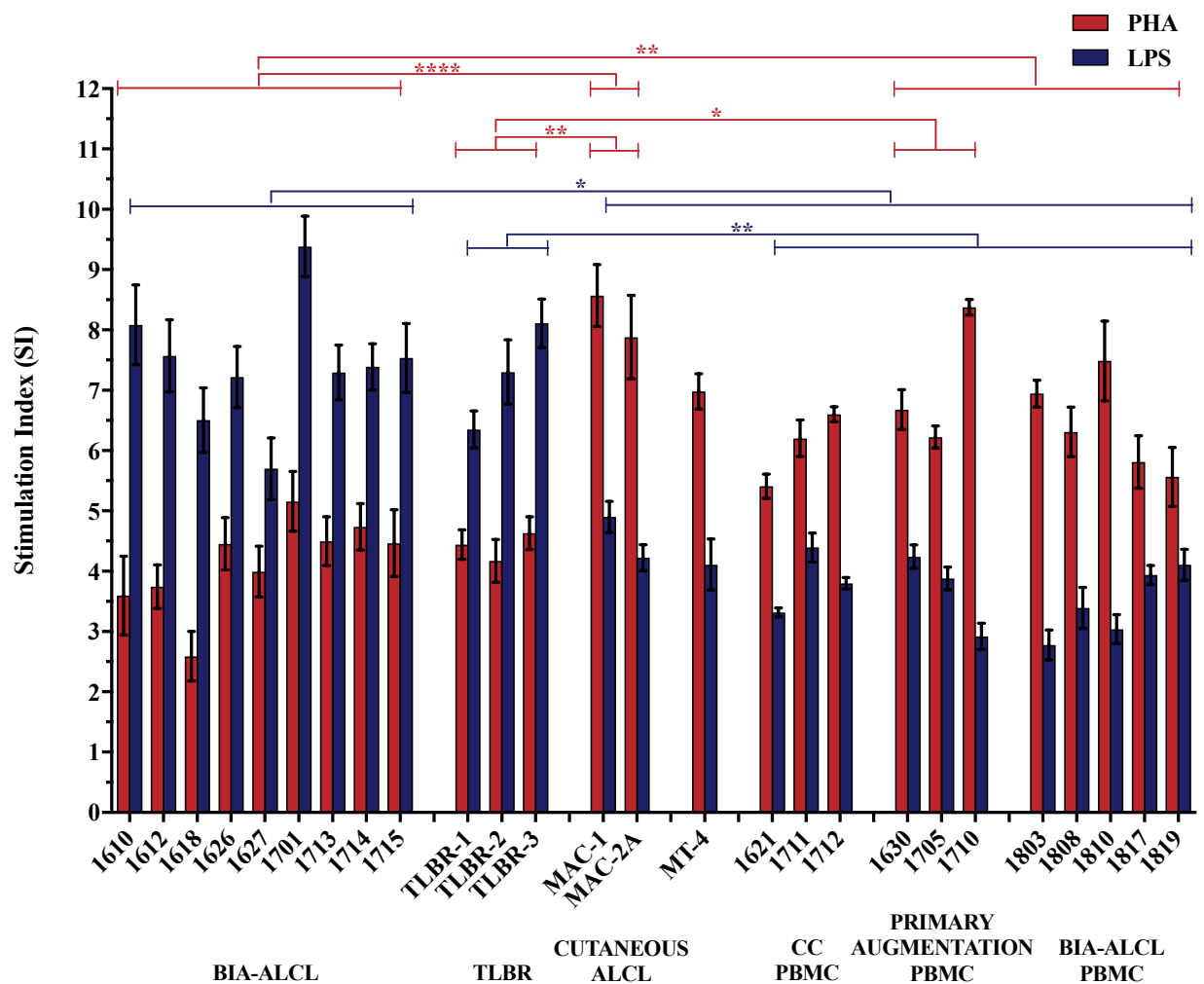


Figure 6.19. Maximum significant SI of the individual cell types tested following PHA and LPS stimulation. Values are the means \pm SEM of six technical replicates. Significantly different at * $P \leq 0.05$, ** $P \leq 0.01$, **** $P \leq 0.0001$.

The mean maximum response to LPS-induced stimulation was highest in patient-derived BIA-ALCL tumour cells (7.4) when compared to cutaneous-ALCL (4.6) and MT-4 cells lines (4.1), and PBMC purified from patients with CC (3.8), primary augmentation (3.7) and BIA-ALCL patients (3.4), $P < 0.05$. Among the BIA-ALCL patients, patient 1701 had the highest maximal stimulation to LPS (9.4) whilst patient 1627, the only patient who presented with a tumour mass, showed the lowest maximal response to LPS (5.7). In TLBR cell lines, the mean maximum response to LPS (7.3) was higher than the maximum responses produced by PBMC isolated from contracture, primary augmentation and BIA-ALCL patients ($P < 0.01$). No difference was found in the mean maximum SI to LPS between BIA-ALCL tumour cells and TLBR cell lines ($P > 0.05$).

Stimulation with PHA elicited the highest maximum SI in MAC-1 cutaneous-ALCL cell lines (8.6) followed by PBMC isolated from primary augmentation patient 1710 (8.4). While PBMC from BIA-ALCL patient 1810 had the highest maximum response to PHA (7.5) among its group. Overall, cutaneous-ALCL cells (8.2) and PBMC collected from primary augmentation (7.1) and BIA-ALCL patients (6.4) responded maximally to PHA when compared to BIA-ALCL tumour cells (4.1), $P < 0.01$. The mean maximum SI to stimulation with PHA was also higher in cutaneous-ALCL cells and PBMC from primary augmentation patients in comparison to TLBR cell lines (4.4), $P < 0.05$. There was no difference in the mean maximum SI to PHA among cutaneous-ALCL and MT-4 cell lines and purified PBMC ($P > 0.05$).

6.5. Discussion

In this Chapter we measured the response of primary BIA-ALCL tumour cells, tumour cell lines, an immortal T-cell line, and normal PBMC to stimulation with two non-specific mitogens, LPS, a cell wall polysaccharide derived from Gram-negative bacteria and PHA, a plant lectin T-cell mitogen.

Whilst all cells were able to respond significantly to both PHA and LPS, we identified a unique response to Gram-negative bacterial LPS for patient-derived BIA-ALCL tumour cells and BIA-ALCL (TLBR) cell lines. This is in contrast to tumour cells from the related cutaneous form of ALCL, a T-cell leukaemia cell line and PBMC derived from patients who have been diagnosed with CC and from those who have not been previously exposed to breast implants. Moreover, this response was absent in the PBMC from BIA-ALCL patients.

These findings are consistent with the growing body of evidence around the epidemiology of BIA-ALCL that bacterial presence acts as a significant proinflammatory transformative driver. The discovery of clusters of disease around a single surgeon experience and the higher risk associated in implants with a higher surface area and roughness reinforce the importance of bacterial contamination as a significant pathogenic mechanism.

It is important to note that the proliferative responses we demonstrated in BIA-ALCL tumour cells purified from the seroma of nine BIA-ALCL patients would also include responses from non-tumour cells. Haematological analysis of post-operative seroma fluid in BIA-ALCL patients has previously shown there is minimal contamination with whole blood, with mean values for haemoglobin concentration of 0.55 g/dL (range, 0.2 to 1.5), red blood cell count, $0.17 \times 10^{12}/L$ (range, 0.03 to 0.53), and leukocyte (white cell) count, $2.77 \times 10^9/L$ (range, 0.19 to 9.42) (McCaul et al., 2000). Moreover, analysis of 67 late breast implant seromas collected from 50 patients has shown the leukocytes are composed predominantly of T-lymphocytes or macrophages (63% of the

samples) with only sporadic granulocytes (37% of the samples) (Di Napoli et al., 2017). In the present study, we did not analyse the cell composition in the tumour cells we isolated from patient seroma fluid. Thus, the responses of the non-cancerous cells present in our patient-derived samples to LPS/PHA, which are likely to be very low to absent given that both mitogens induce strong stimulation of T-cells, would have been measured. This is in contrast to the MT-4, cutaneous-ALCL and BIA-ALCL cell lines we tested, which would only include proliferative responses from the cancer cells. Similarly, PBMC isolated from patients with contracture, primary augmentation and BIA-ALCL patients include lymphocytes (T-cells, B-cells and natural killer cells), monocytes and dendritic cells. The frequencies of these cell populations vary across individuals, but typically, lymphocytes are in the range of 70 to 90%, monocytes from 10 to 20%, while dendritic cells are rare, accounting for only 1 to 2% (Geissmann et al., 2003). The frequencies of cell types within the lymphocyte population include 70 to 85% CD3+ T-cells, 5 to 10% B-cells, and 5 to 20% natural killer cells (Geissmann et al., 2003). Thus, the proliferative responses we measured in the patient-derived PBMC would include all these cells. Nevertheless, we still identified high maximum responses to stimulation with PHA among the PBMC we purified. Additionally, the maximum significant SI to LPS-induced stimulation was highest in BIA-ALCL cells compared to all the other cell lines tested and is therefore, indicative of there being minimal non-transformed cells present in the seroma of BIA-ALCL patients.

In our cohort of BIA-ALCL patients, patient 1627 was the only patient that presented with an infection followed by incidental mass. Interestingly, tumour cells from this patient responded significantly to 10 µg/mL of LPS in all cell concentrations tested but only at 10⁵ cells/mL at 5 µg/mL. While overall it had the lowest maximum SI to stimulation with LPS in comparison to the rest of the patient cohort. A tumour mass associated with the fibrous breast capsule occurs less frequently in BIA-ALCL and patients are more likely to have a clinically aggressive disease. It is possible the differential response to LPS we identified in this patient could be due to the tumour

cells being purified from the mass rather than an effusion around the implant. Moreover, in this patient, the mass was preceded with an infection. Unfortunately, we did not have access to the clinical information as to whether this infection was from Gram-positive or Gram-negative bacteria. We suspect a Gram-positive infection since we cultured *S. aureus* from the capsule and implant of this patient (Chapter V), which could also explain the low responses to Gram-negative LPS stimulation. Nevertheless, our findings suggest that there is an observed difference between the LPS response for patients with mass disease versus seroma disease. Whilst the SI are low, it strengthens the hypothesis that seroma is probably reactive whilst mass disease is the true malignancy.

The high proliferative responses of BIA-ALCL cells to LPS-induced stimulation are somewhat surprising given responses to LPS are low to absent in many mammalian cells in comparison to the well-established effect of PHA on mitotic stimulation (Beinke et al., 2015). Bacterially derived LPS forms around 75% of the outer membrane of Gram-negative bacteria (Raetz and Whitfield, 2002). The structure of LPS consists of a hydrophobic lipid A domain, an oligosaccharide core and the outermost O-antigen (Raetz and Whitfield, 2002). Lipid A can be recognised by the innate immune system and produce macrophage activation and release of proinflammatory cytokines, with small doses capable of producing lethal shock (Raetz and Whitfield, 2002). The O-antigen, on the other hand, interacts with the adaptive immune system (Bryant et al., 2010). LPS is solubilised by LPS binding protein in the serum, the complex is then transferred to the Toll-like receptor 4 (TLR4) with the help of myeloid differentiating protein-2. This complex is then able to directly activate T-cells producing a powerful downregulation of the immune response as a means to increase survival of the bacteria (Feng et al., 2012). The role of LPS in both stimulating inflammation via the innate immunity pathway and turning down the host response via the adaptive immunity pathway is therefore unique and can both optimise bacterial survival and prolong host immune response and tissue damage (Ramachandran, 2014). Thus, the

presence of bacteria coupled with a likely genetic defect in the host, would explain the relatively uncommon incidence of BIA-ALCL as it requires both bacterial presence and genetic susceptibility (Blombery et al., 2016) to cause ongoing immune activation and malignant transformation in susceptible hosts overtime.

The findings from this Chapter that BIA-ALCL tumour cells respond strongest to stimulation with LPS compared to PHA further strengthens our hypothesis that bacteria are involved in the pathogenesis of BIA-ALCL and reinforces the importance of preventing bacterial contamination on breast implants at time of surgery.

Chapter VII.

Differential mitogenic response of Breast Implant-associated Anaplastic Large-cell Lymphoma to staphylococcal superantigens

7.1. Introduction

In Chapter VI we found that BIA-ALCL tumour cells display a unique response to LPS and this proliferative response was found to be absent in other non-Hodgkin's lymphomas (including cutaneous-ALCL), an immortal T-cell line, and normal PBMC harvested from patients exposed to breast implants *in vivo* and from healthy control patients.

In this Chapter we investigated whether Gram-positive bacterially derived antigenic drivers would interact differentially with BIA-ALCL tumour cells. We tested Gram-positive staphylococcal superantigens, staphylococcal enterotoxin A (SEA) and toxic shock syndrome toxin-1 (TSST-1), since their role and potential to restrict T-cell receptor expression has recently been reported (Kadin et al., 2016), and both *S. aureus* and coagulase negative staphylococci are frequently isolated from biofilms surrounding medical implants.

Superantigens are proteins produced by bacteria and viruses that can stimulate a large proportion of T-lymphocytes via interaction with the variable domain of the Beta chain of the T-cell antigen receptor (TCR-V β), causing cells to divide and differentiate into effector cells and release T-cell factors (IL-2, TNF- α and IL-1 β) (Balaban and Rasooly, 2000, McCormick et al., 2001).

SEA from *S. aureus* is a leading agent that causes food poisoning. It stimulates the cell proliferation of peripheral lymphocytes, induces the production of interferons and is important for

gut immunity against *S. aureus* infections (Emu et al., 2008, Pinchuk et al., 2010). TSST-1, responsible for toxic shock syndrome, is a toxin also secreted by *S. aureus* in response to environmental stress, such as low oxygen or low nutrient content in its surroundings (McCormick et al., 2001, Buonpane et al., 2005). It activates production of immune signalling molecules, such as TNF, IL-1, M protein and IFN- γ (Buonpane et al., 2005).

The aim of this Chapter was to measure the proliferation of primary BIA-ALCL tumour cells to staphylococcal superantigens (SEA and TSST-1) and compare BIA-ALCL cells response to PBMC purified from patients diagnosed with BIA-ALCL, cutaneous-ALCL cell lines, an immortal T-cell line, and control patients PBMC.

We also tested the effects of adding 1% penicillin/streptomycin solution (effective against most Gram-positive bacteria and Gram-negative bacteria, respectively) to the culture medium on mitogen-induced proliferation. This experiment was necessary because we found in the optimisation experiments of our bacterial biofilm and mammalian cells co-culture system (Section 8.4.4.) that the addition of these antibiotics in DMEM inhibited the growth of both Gram-positive and Gram-negative bacteria (Section 8.4.4.).

7.2. Materials and Methods

7.2.1. Tumour cells/cell lines

The same tumour cells/cell lines and PBMC were tested as per Section 6.4.2.1. This included, five patient-derived BIA-ALCL tumour cells, four presenting with seroma (patients 1618, 1701, 1713, 1714) and one presenting with a tumour mass (1627) (Table 5.1, Section 5.3.1.), three BIA-ALCL cell lines (TLBR-1, TLBR-2, TLBR-3) (Table 2.2, Section 2.5.1.), two cutaneous-ALCL cell lines (MAC-1, MAC-2A), an MT-4 immortal T-cell line, PBMC purified from patients diagnosed with CC (patients 1621, 1711, 1712), healthy controls undergoing primary

breast augmentation (patients 1630, 1705, 1710) and five BIA-ALCL patients (1803, 1808, 1810, 1817, 1819) (Table 5.1, Section 5.3.1.).

7.2.2. Preparation of staphylococcal superantigens

SEA and TSST-1 were prepared as described in Section 2.5.2. Concentrations of 5 and 10 µg/mL of SEA and TSST-1 prepared in RPMI 1640 medium were used for the cell proliferation assays.

7.2.3. *In vitro* cell proliferation assay

Cells were seeded at concentrations of 10^5 , $10^{5.5}$ and 10^6 cells/mL in a 96-well plate in six replicates and stimulated to proliferate non-specifically with 5 or 10 µg/mL of SEA and TSST-1, while control or unstimulated wells, received 20 µL of complete medium. Cells were incubated for 72 hr at 37°C, 5% CO₂. Cell proliferation was measured using the established protocol outlined in Section 6.3.

7.2.4. Testing the effects of 1% penicillin/streptomycin

BIA-ALCL tumour cells were seeded at 10^5 , $10^{5.5}$, 10^6 cells/mL in either DMEM containing 10% FBS and 1% penicillin/streptomycin solution or DMEM containing 10% FBS only into six replicate wells of a 96-well plate and stimulated to proliferate non-specifically with 5 or 10 µg/mL of SEA, TSST-1, PHA and LPS, while control wells, received 20 µL of test media. Cells were incubated for 72 hr at 37°C, 5% CO₂. Proliferation was measured using the established protocol (Section 6.3.).

7.2.5. Statistical analysis

All statistical analyses were performed in GraphPad Prism 7.0. To test normality of data distribution, the Shapiro-Wilk test was used. One-way and two-way ANOVA was used to evaluate the differences in proliferation responses, effects of cell and mitogen concentrations among the different cell culture types, and the effects of adding 1% penicillin/streptomycin in cultured medium. If significant differences were found, then Tukey's or Sidak's multiple comparisons post-hoc test were employed. All values are expressed as mean \pm SEM, *P* values less than or equal to 0.05 were considered statistically significant.

7.3. Results

7.3.1. Cell proliferation response following staphylococcal superantigen stimulation

Patient-derived BIA-ALCL tumour cells ($n = 5$; patients 1618, 1627, 1701, 1713, 1714) responded to both staphylococcal superantigens (SEA and TSST-1) with higher SI obtained with higher cell concentrations (Figure 7.1). We found higher SI were generally obtained with 10 $\mu\text{g/mL}$ when compared to responses at 5 $\mu\text{g/mL}$ for SEA whilst there was less of a difference for TSST-1 with some BIA-ALCL cells responding equally to 5 and 10 $\mu\text{g/mL}$ (patient 1701) (Figure 7.1). There was no significant difference in the maximum SI obtained in response to stimulation with SEA and TSST-1 for tumor cells sourced from four of the patients tested while patient's 1713 tumor cells responded significantly more to SEA ($P = 0.0007$) (Figure 7.1).

A similar response pattern was found in BIA-ALCL cell lines where TLBR-1 and TLBR-2 responded significantly more to stimulation with SEA when compared to TSST-1 and this was significantly different at higher cell concentrations and at both 5 and 10 $\mu\text{g/mL}$, $P < 0.05$ (Figure 7.2). In TLBR-3, higher SI were obtained with SEA at higher cell concentrations, although this was not significantly different to the response to TSST-1 ($P > 0.05$) (Figure 7.2).

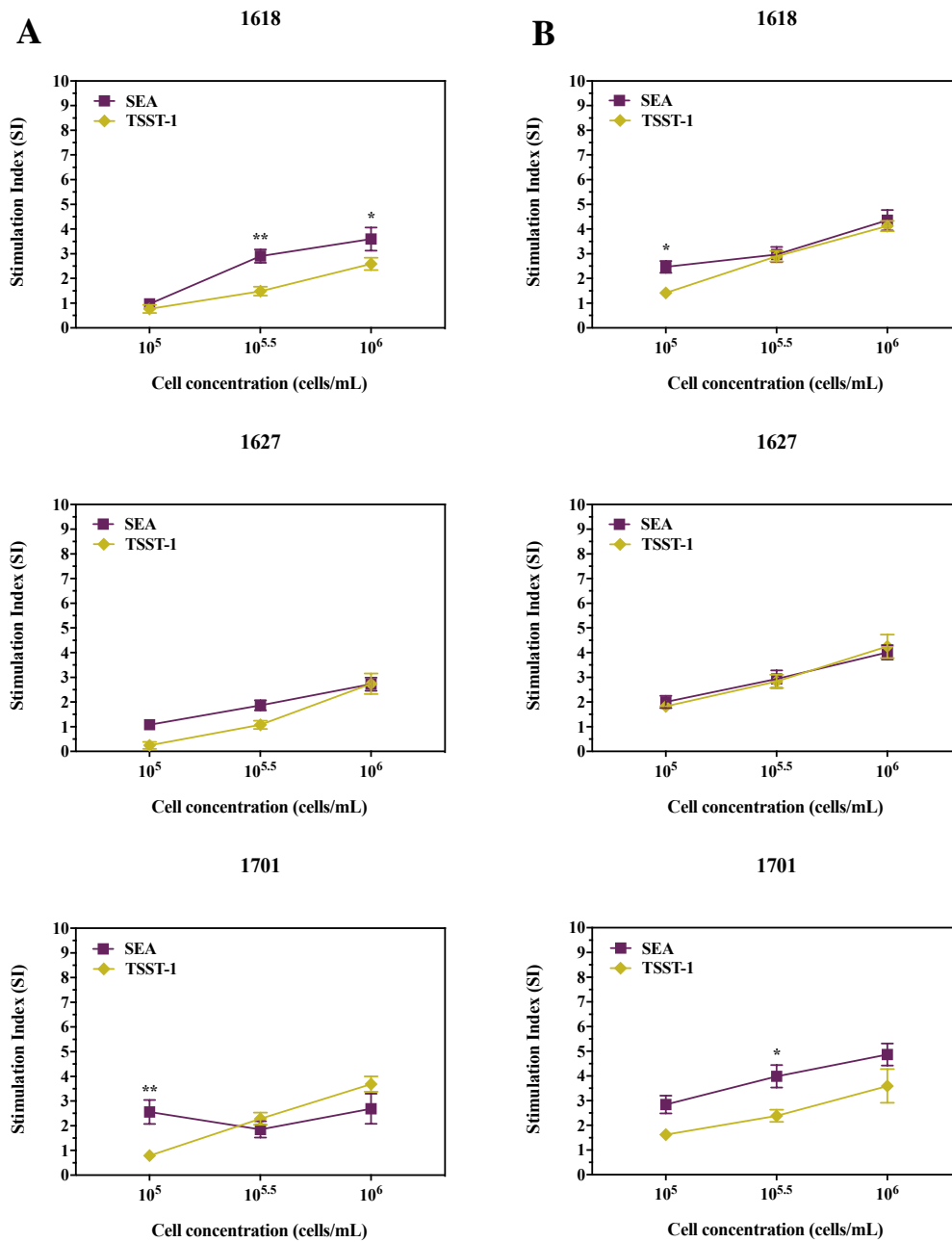


Figure 7.1. Proliferation response (SI) of the five patient-derived BIA-ALCL tumour cells to (A) 5 and (B) 10 $\mu\text{g/mL}$ of SEA and TSST-1. Values are the means \pm SEM of six technical replicates. Significantly different at $*P \leq 0.05$, $**P \leq 0.01$, $***P \leq 0.001$, $****P \leq 0.0001$.

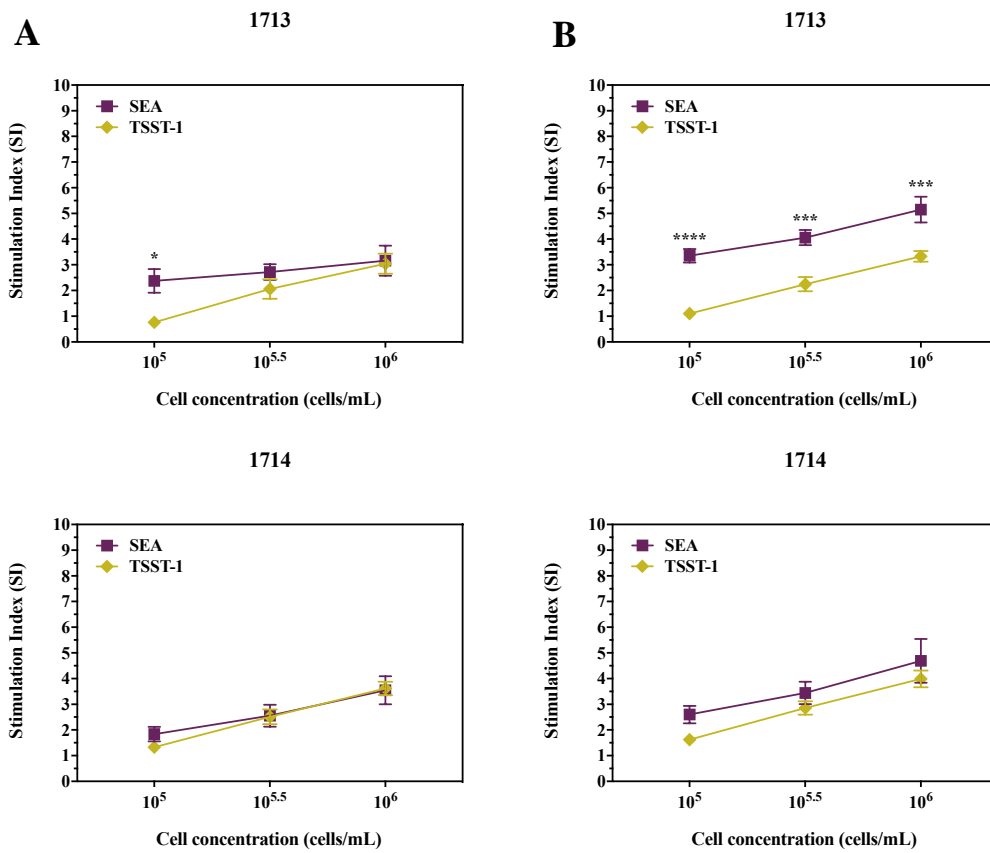


Figure 7.1. Continued.

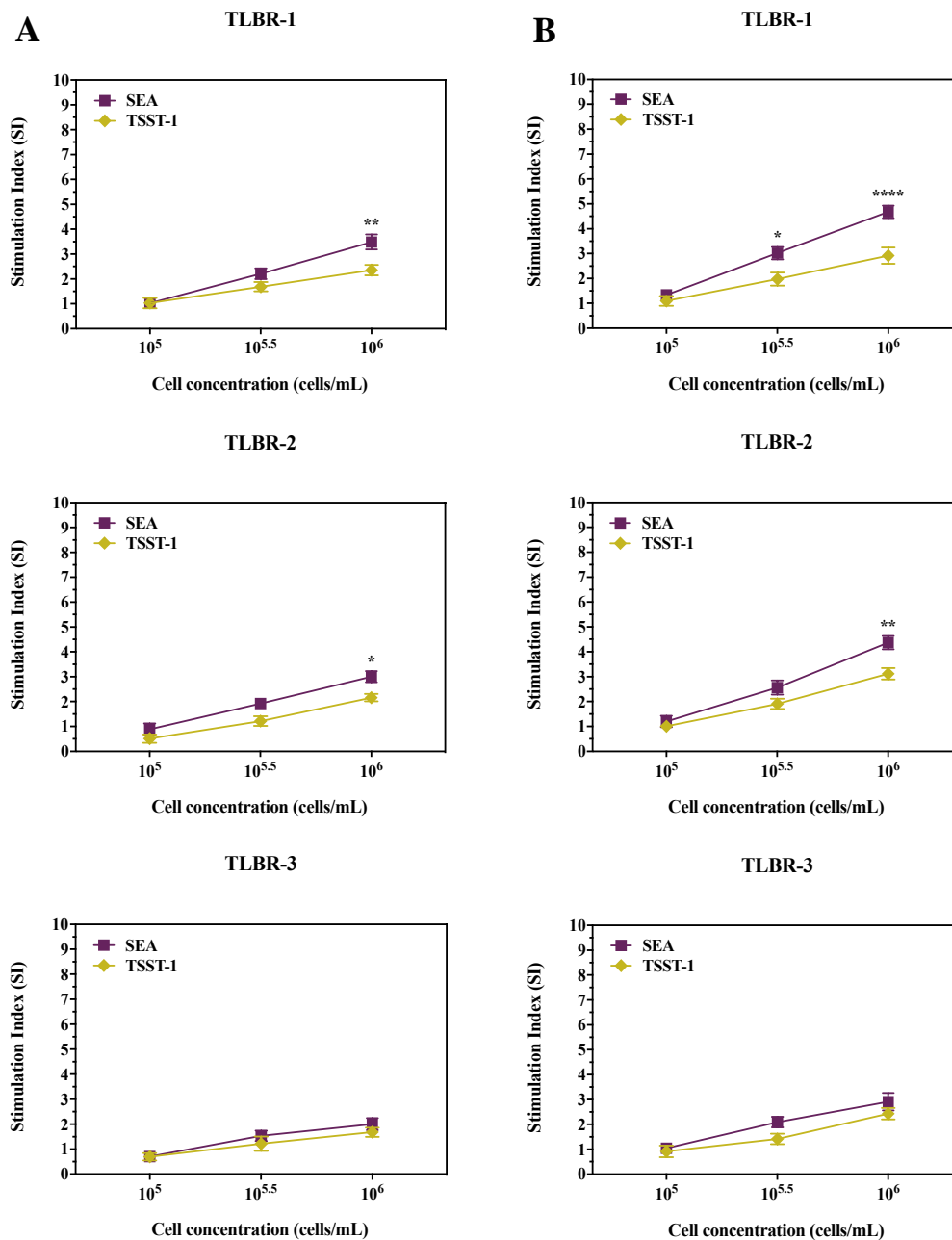


Figure 7.2. Proliferation response (SI) of the three BIA-ALCL cell lines, TLBR-1, TLBR-2 and TLBR-3, to (A) 5 and (B) 10 $\mu\text{g/mL}$ of SEA and TSST-1. Values are the means \pm SEM of six technical replicates. Significantly different at $*P \leq 0.05$, $**P \leq 0.01$, $****P \leq 0.0001$.

In contrast to BIA-ALCL cells, higher SI were obtained in cutaneous-ALCL cell lines, MAC-1 and MAC-2A, stimulated with TSST-1 compared to SEA and this was significant for MAC-1 cells at higher cell concentrations and at 5 and 10 $\mu\text{g/mL}$, $P < 0.0001$ (Figure 7.3).

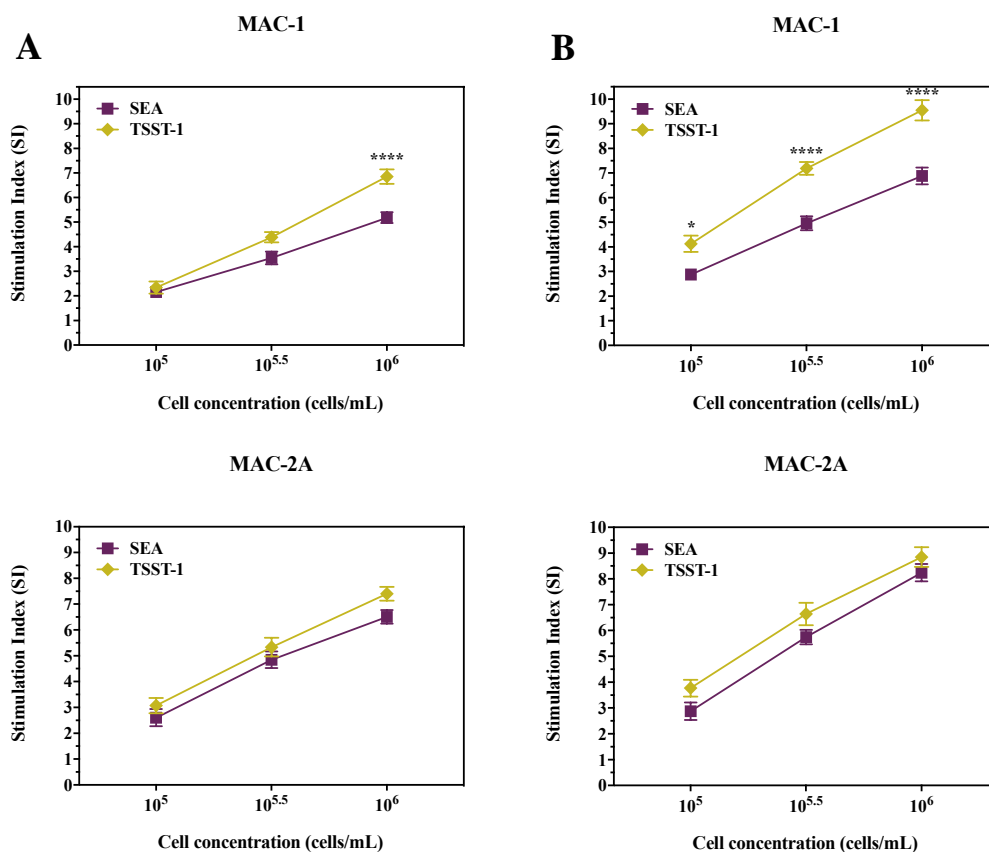


Figure 7.3. Proliferation response (SI) of the two cutaneous-ALCL cell lines, MAC-1 and MAC-2A, to (A) 5 and (B) 10 $\mu\text{g/mL}$ of SEA and TSST-1. Values are the means \pm SEM of six technical replicates. Significantly different at $*P \leq 0.05$, $****P \leq 0.0001$.

Higher SI were obtained when MT-4 cells were stimulated with SEA compared with TSST-1 (Figure 7.4).

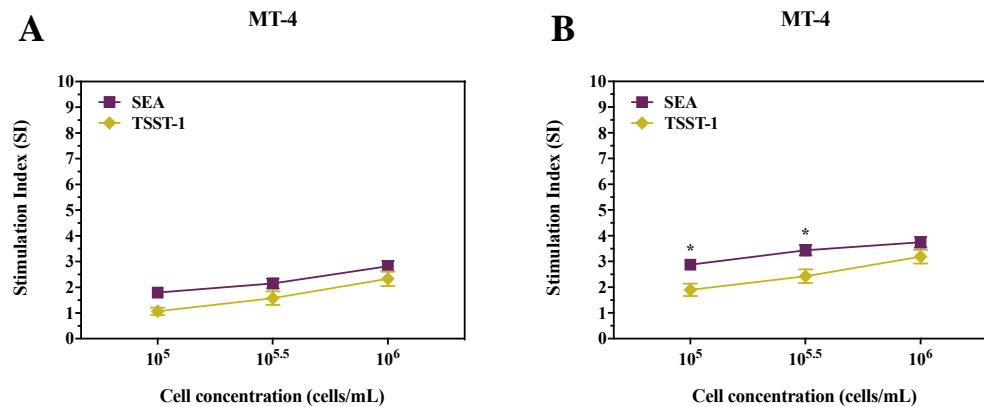


Figure 7.4. Proliferation response (SI) of the MT-4 immortal T-cell line to (A) 5 and (B) 10 µg/mL of SEA and TSST-1. Values are the means \pm SEM of six technical replicates. Significantly different at $*P \leq 0.05$.

The maximum SI obtained when PBMC purified from CC patients were stimulated with either TSST-1 or SEA were similar ($P > 0.05$), although there were significant differences in responses at differing cell and superantigen concentrations, e.g. the TSST-1 response was significantly higher at some cell concentrations in patients 1621 and 1712, $P < 0.05$ (Figure 7.5). While no differences in response between staphylococcal superantigens were found in patient 1711 irrespective of cell or mitogen concentration ($P > 0.05$) (Figure 7.5).

In primary breast augmentation patients with no previous exposure to breast implants, PBMC responded similarly (patient 1710) or significantly more to SEA when compared with TSST-1 (patients 1630 and 1705) in higher cell concentrations stimulated with 10 µg/mL and in lower cell concentrations at 5 µg/mL for patients 1630 and 1705, $P < 0.05$ (Figure 7.6). No differences in response between SEA and TSST-1 were found in 1710 ($P > 0.05$) (Figure 7.6).

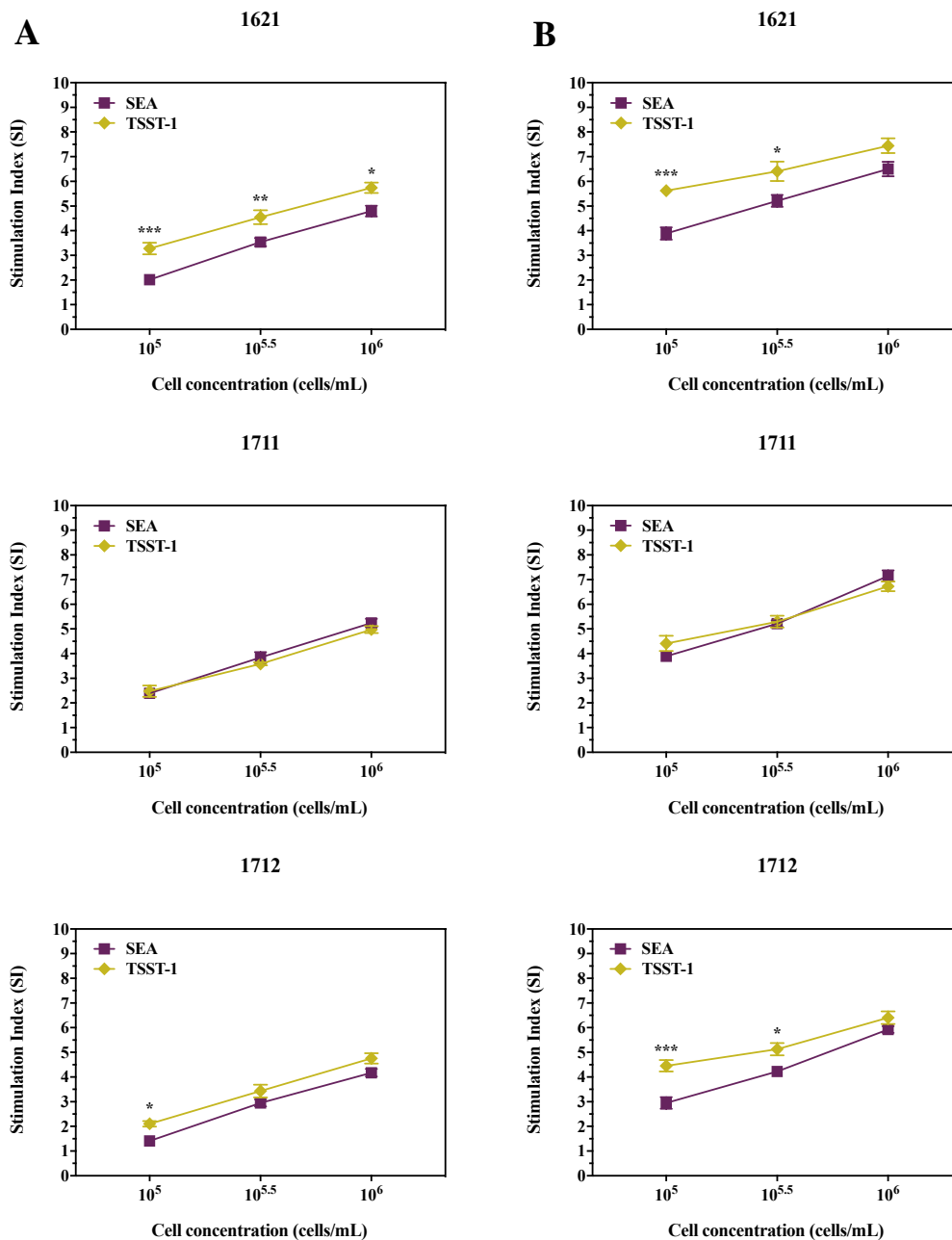


Figure 7.5. Proliferation response (SI) of the peripheral blood mononuclear cells purified from patients with capsular contracture to (A) 5 and (B) 10 $\mu\text{g/mL}$ of SEA and TSST-1. Values are the means \pm SEM of six technical replicates. Significantly different at $*P \leq 0.05$, $**P \leq 0.01$, $***P \leq 0.001$.

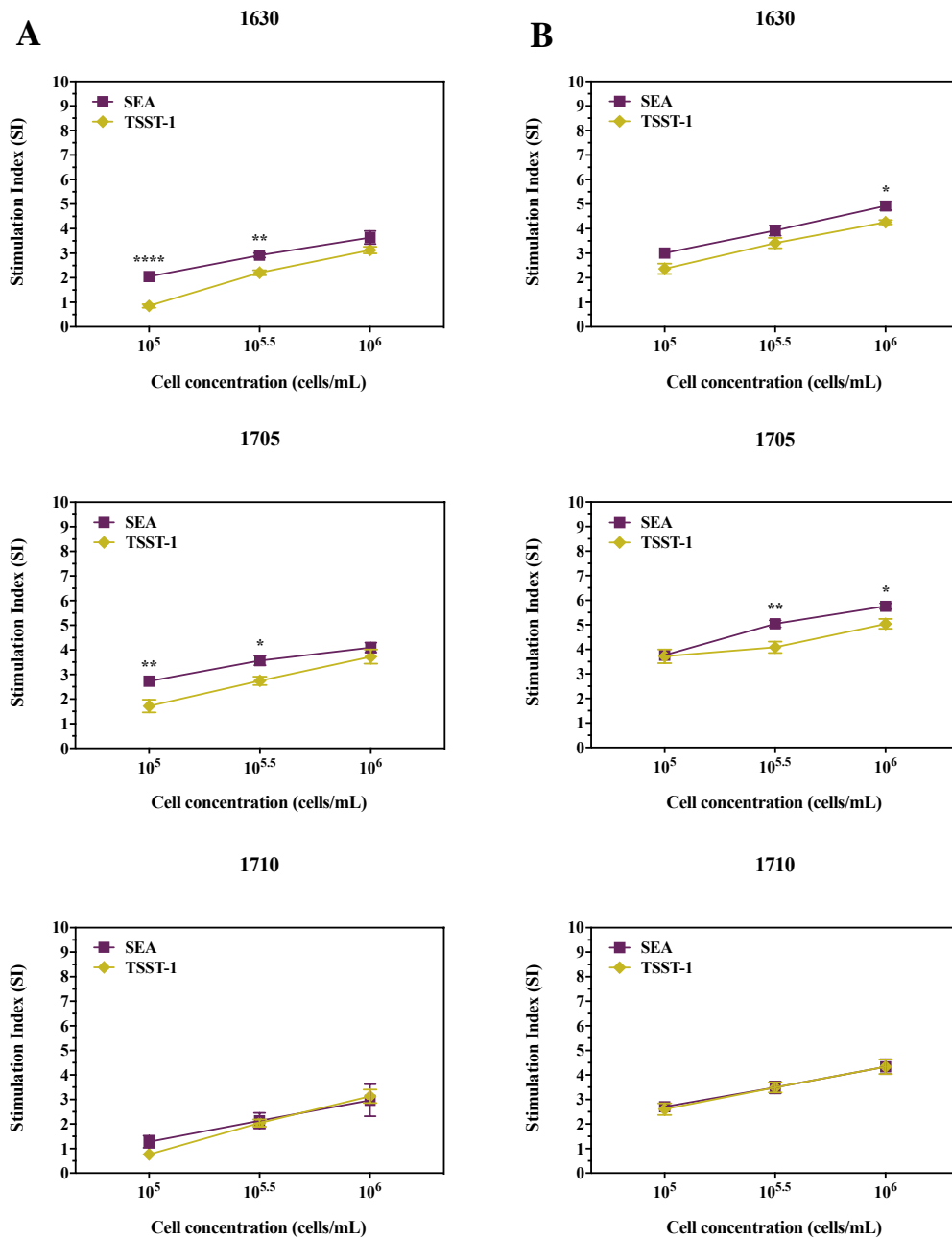


Figure 7.6. Proliferation response (SI) of the peripheral blood mononuclear cells purified from healthy patients undergoing primary breast augmentation to (A) 5 and (B) 10 $\mu\text{g/mL}$ of SEA and TSST-1. Values are the means \pm SEM of six technical replicates. Significantly different at $*P \leq 0.05$, $**P \leq 0.01$, $****P \leq 0.0001$.

The PBMC purified from BIA-ALCL patients showed responses to SEA were marginally higher at most cell and mitogen concentrations tested (Figure 7.7). For patient 1817, significantly higher SI were found following stimulation with 5 $\mu\text{g/mL}$ of SEA when compared to TSST-1 at all cell concentrations, $P < 0.05$. Similarly, at higher cell concentrations stimulated with 10 $\mu\text{g/mL}$, responses were stronger to SEA than TSST-1 for patients 1817 and 1819, $P < 0.05$ (Figure 7.7).

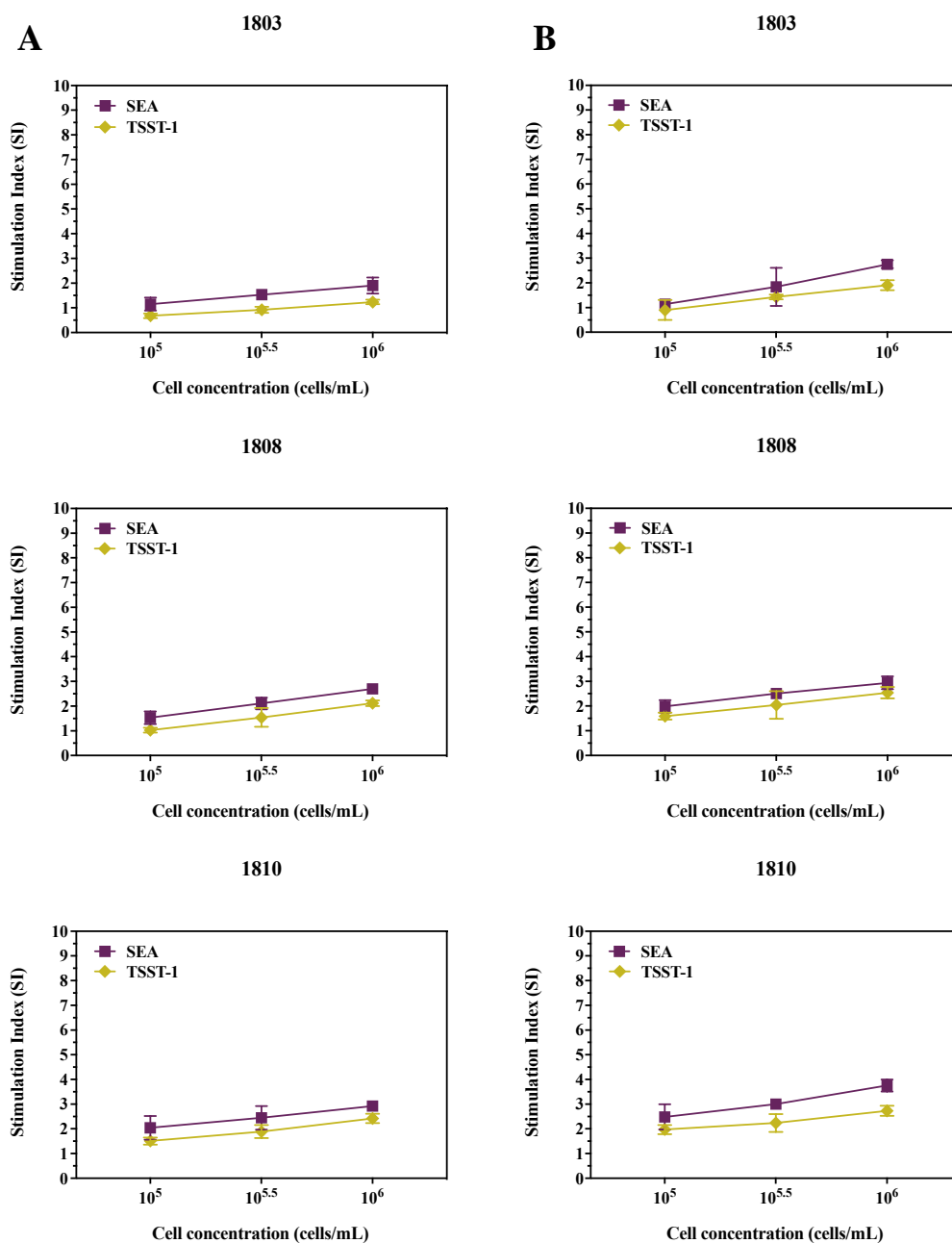


Figure 7.7. Proliferation response (SI) of the peripheral blood mononuclear cells purified from BIA-ALCL patients to (A) 5 and (B) 10 $\mu\text{g/mL}$ of SEA and TSST-1. Values are the means \pm SEM of six technical replicates. Significantly different at $*P \leq 0.05$, $**P \leq 0.01$.

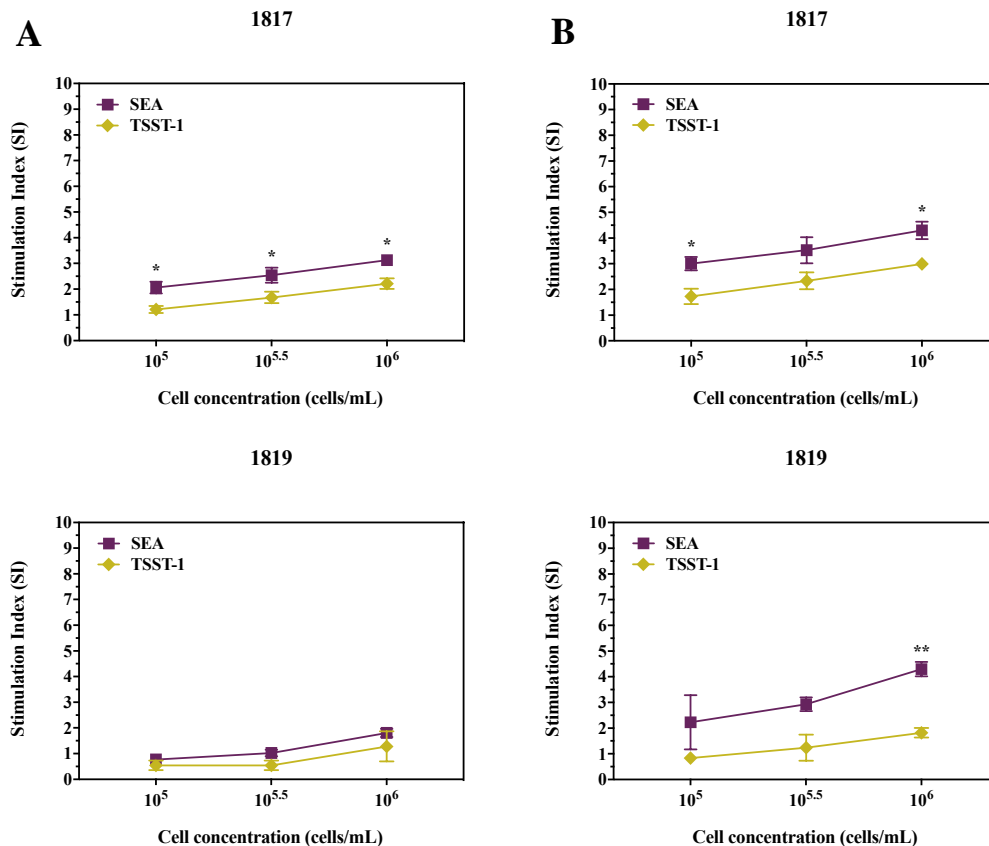


Figure 7.7. Continued.

A comparison of the differences in proliferative responses (SI) among the different cell culture types showed that stimulation with SEA elicited significantly higher responses in cutaneous-ALCL cell lines (MAC-1 and MAC-2A) (SI: 4.1 (5 $\mu\text{g/mL}$), 5.3 (10 $\mu\text{g/mL}$)) when compared to BIA-ALCL cells (BIA-ALCL: 2.4 (5 $\mu\text{g/mL}$), 3.6 (10 $\mu\text{g/mL}$); TLBR: 1.9 (5 $\mu\text{g/mL}$), 3.1 (10 $\mu\text{g/mL}$)) ($P < 0.05$) and PBMC purified from BIA-ALCL patients (2.0 (5 $\mu\text{g/mL}$), 2.9 (10 $\mu\text{g/mL}$)) ($P < 0.001$) at 5 and 10 $\mu\text{g/mL}$ (Figure 7.8). At 10 $\mu\text{g/mL}$ of SEA, significantly higher SI were obtained in PBMC from contracture patients (5.0) compared with BIA-ALCL (TLBR) cell lines ($P = 0.0068$) and BIA-ALCL patients' PBMC ($P = 0.0003$) (Figure 7.8). There was no difference in proliferative responses to SEA-induced stimulation between cutaneous-ALCL and

MT-4 cell lines (2.6 (5 $\mu\text{g/mL}$), 3.4 (10 $\mu\text{g/mL}$)) and PBMC from contracture patients (3.4 (5 $\mu\text{g/mL}$), 5.0 (10 $\mu\text{g/mL}$)), or between BIA-ALCL tumour cells and TLBR cell lines at 5 and 10 $\mu\text{g/mL}$ ($P > 0.05$) (Figure 7.8).

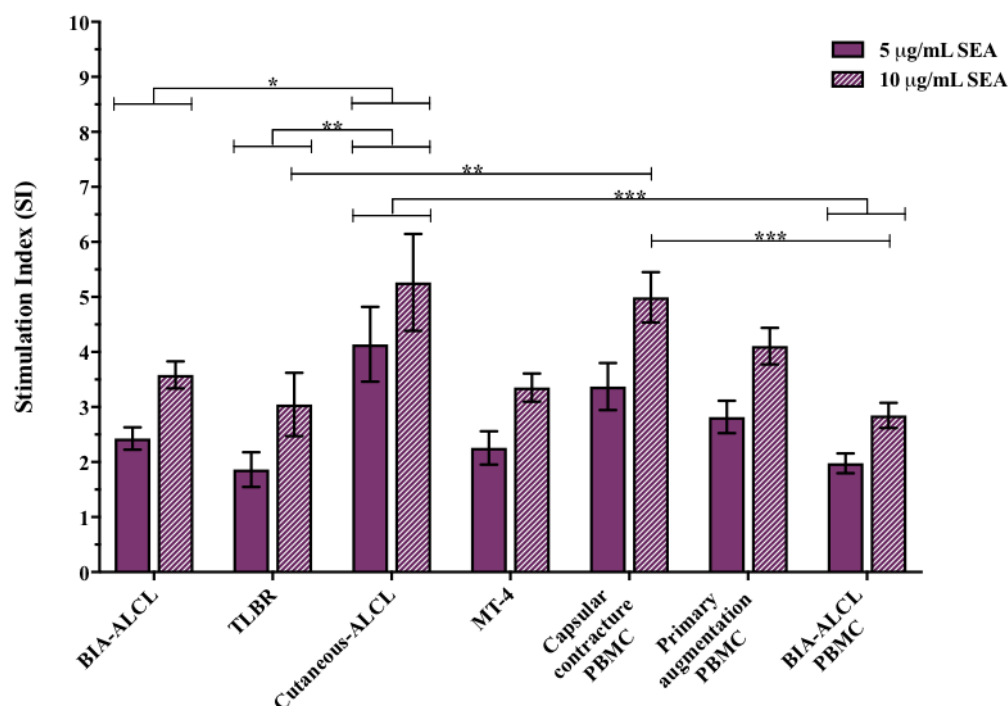


Figure 7.8. Summary of the proliferative response (SI) of the different cell types to 5 and 10 $\mu\text{g/mL}$ of SEA. Values are the means \pm SEM. Significantly different at $*P \leq 0.05$, $**P \leq 0.01$, $***P \leq 0.001$.

TSST-1-induced stimulation (5 and 10 $\mu\text{g/mL}$) led to significantly higher proliferative responses in cutaneous-ALCL cell lines (4.9 (5 $\mu\text{g/mL}$), 6.7 (10 $\mu\text{g/mL}$)) when compared to BIA-ALCL cells (BIA-ALCL: 1.9 (5 $\mu\text{g/mL}$), 2.7 (10 $\mu\text{g/mL}$); TLBR: 1.4 (5 $\mu\text{g/mL}$), 1.9 (10 $\mu\text{g/mL}$)) ($P < 0.0001$), MT-4 cells (1.7 (5 $\mu\text{g/mL}$), 2.5 (10 $\mu\text{g/mL}$)) ($P < 0.001$), and PBMC isolated from primary augmentation (2.3 (5 $\mu\text{g/mL}$), 3.7 (10 $\mu\text{g/mL}$)) ($P < 0.001$) and BIA-ALCL patients (1.4

(5 $\mu\text{g/mL}$), 1.9 (10 $\mu\text{g/mL}$)) ($P < 0.0001$) (Figure 7.9). Similarly, in contracture patients (3.9 (5 $\mu\text{g/mL}$), 5.8 (10 $\mu\text{g/mL}$)), significantly higher SI were obtained compared with BIA-ALCL cells ($P < 0.001$), MT-4 cells ($P < 0.05$), and PBMC from BIA-ALCL and healthy control patients ($P < 0.05$). At 10 $\mu\text{g/mL}$ of TSST-1, higher responses were found in PBMC from primary augmentation patients compared to TLBR cell lines ($P = 0.0073$) and PBMC from BIA-ALCL patients ($P = 0.0020$) (Figure 7.9). No difference in SI, following stimulation with TSST-1 (5 and 10 $\mu\text{g/mL}$), was found between cutaneous-ALCL and contracture patients' PBMC, and between BIA-ALCL tumour cells and TLBR cell lines ($P > 0.05$) (Figure 7.9).

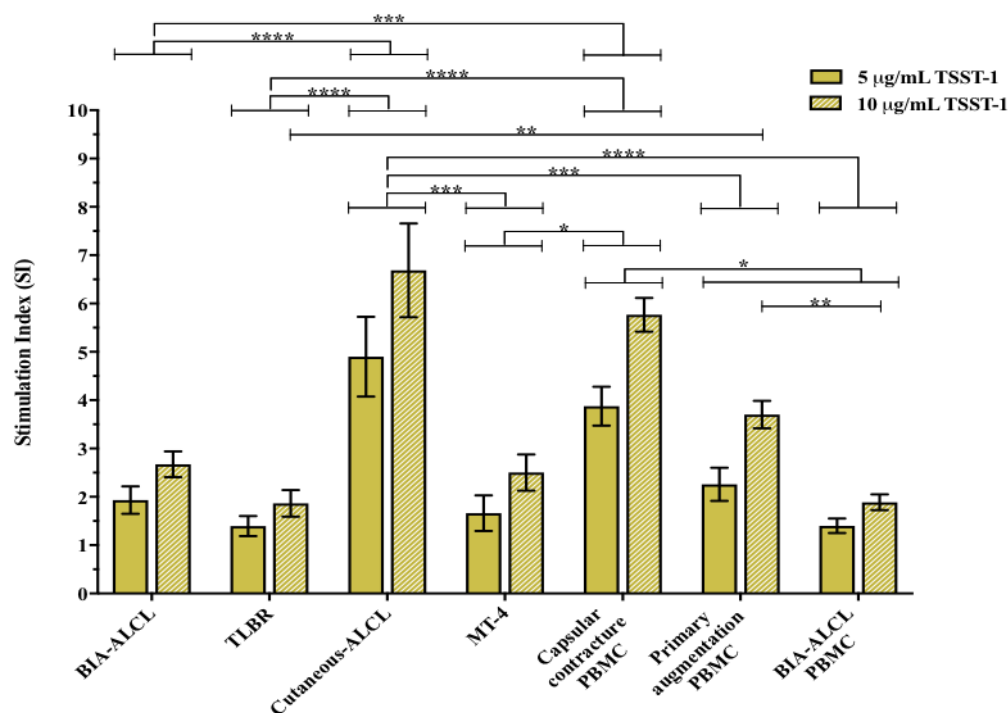


Figure 7.9. Summary of the proliferative response (SI) of the different cell types to 5 and 10 $\mu\text{g/mL}$ of TSST-1. Values are the means \pm SEM. Significantly different at $*P \leq 0.05$, $**P \leq 0.01$, $***P \leq 0.001$, $****P \leq 0.0001$.

The maximum significant SI following stimulation with staphylococcal superantigens, SEA and TSST-1, for each individual BIA-ALCL patient (Tumour cells, $n = 5$; PBMC, $n = 3$), contracture ($n = 3$) and primary augmentation patients ($n = 3$), and each cell line tested, TLBR ($n = 3$), cutaneous-ALCL ($n = 2$) and MT-4 cells, are shown in Figure 7.10. As with PHA and LPS, the maximum SEA and TSST-1 response occurred at the same cell concentration of 10^6 cells/mL and mitogen concentration of $10 \mu\text{g/mL}$.

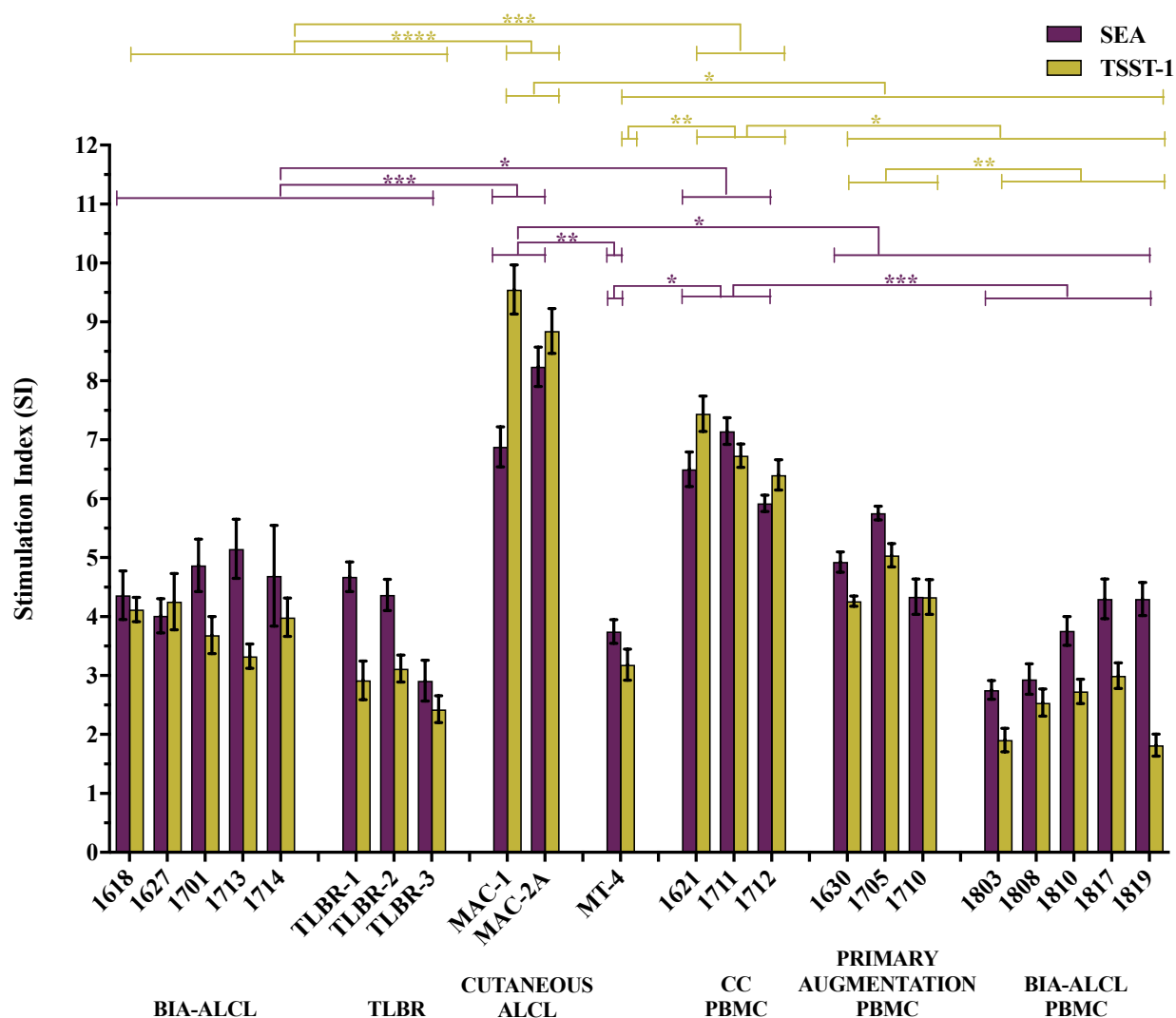


Figure 7.10. Maximum significant SI of the individual cell types tested following SEA and TSST-1 stimulation. Values are the means \pm SEM of six technical replicates. Significantly different at $*P \leq 0.05$, $**P \leq 0.01$, $***P \leq 0.001$, $****P \leq 0.0001$.

Overall, the mean maximum SI to SEA and TSST-1 was highest in cutaneous-ALCL cell lines (SEA, 7.6; TSST-1, 9.2). The maximum proliferative response of cutaneous-ALCL cells to SEA was significantly more than the maximum response produced by BIA-ALCL cells (BIA-ALCL, 4.6; TLBR cells, 4.0; $P < 0.001$), MT-4 cells (3.7, $P = 0.0038$), and PBMC isolated from primary augmentation (5.0) and BIA-ALCL patients (3.6) ($P < 0.05$). The mean maximum response to SEA was also higher in PBMC from CC patients (6.5) when compared to BIA-ALCL cells ($P < 0.05$), MT-4 cells ($P = 0.0416$) and BIA-ALCL patients' PBMC ($P = 0.0002$). We found no difference in the mean maximum SI to SEA between cutaneous-ALCL cells and contracture patients' PBMC, and between BIA-ALCL tumour cells and TLBR cell lines ($P > 0.05$).

Stimulation with TSST-1 produced the highest mean maximum SI in cutaneous-ALCL cell lines (9.2) than any other cell type tested ($P < 0.05$). The mean maximum response to TSST-1 was also higher in PBMC from contracture patients (6.9) when compared to BIA-ALCL cells (BIA-ALCL, 3.9; TLBR cells, 2.8; $P < 0.001$), MT-4 cells (3.2, $P = 0.0030$), and PBMC from primary augmentation (4.5) and BIA-ALCL (2.4) patients ($P < 0.05$). Moreover, PBMC from healthy control patients had higher mean maximum SI to TSST-1 in comparison to BIA-ALCL patients' PBMC ($P = 0.0070$). No difference in the mean maximum response to TSST-1 was found between BIA-ALCL tumour cells and TLBR cell lines ($P > 0.05$).

7.3.2. Differential response to SEA, TSST-1, PHA and LPS

Figure 7.11 summarises the mean maximum significant SI for each cell type tested. In both patient-derived BIA-ALCL tumour cells and TLBR cell lines, LPS-induced stimulation (BIA-ALCL, 7.41; TLBR, 7.25) elicited the highest maximum proliferative response compared with both staphylococcal superantigens (SEA: 4.62 (BIA-ALCL), 3.99 (TLBR); TSST-1: 3.88 (BIA-ALCL), 2.82 (TLBR)) ($P < 0.001$) and PHA (BIA-ALCL, 4.14; TLBR, 4.41) ($P < 0.01$). This is in contrast

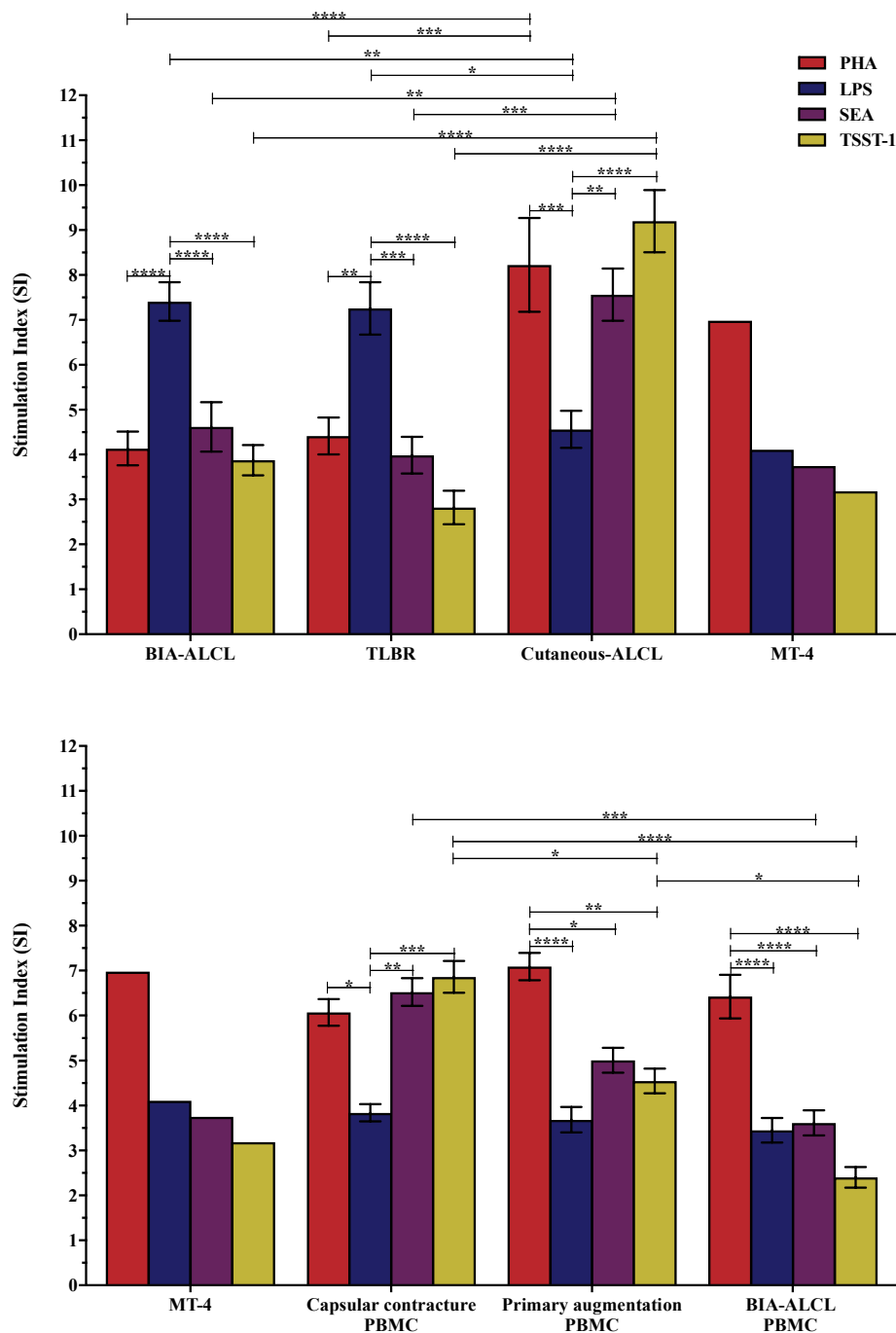


Figure 7.11. Mean maximum proliferative response (SI) of primary BIA-ALCL tumour cells (PHA/LPS, $n = 9$; SEA/TSST-1, $n = 5$), TLBR ($n = 3$), cutaneous-ALCL ($n = 2$) and MT-4 ($n = 1$) cell lines, and PBMC purified from patients with contracture ($n = 3$), primary augmentation ($n = 3$) and BIA-ALCL patients ($n = 5$), following stimulation with SEA, TSST-1, PHA and LPS. Values are the means \pm SEM. Significantly different at $*P \leq 0.05$, $**P \leq 0.01$, $***P \leq 0.001$, $****P \leq 0.0001$.

to the related cutaneous form of ALCL, which had higher maximum SI to PHA (8.22), SEA (7.56) and TSST-1 (9.20) than stimulation with LPS (4.56) ($P < 0.01$). However, we found no difference in the cell proliferation induced by PHA and staphylococcal superantigens in cutaneous-ALCL cell lines ($P > 0.05$). A similar pattern was also observed in PBMC purified from contracture patients, with higher maximum SI to PHA (6.07) and staphylococcal superantigens (SEA, 6.52; TSST-1, 6.86) than LPS (3.84) ($P < 0.05$). Again, no difference was found in proliferative responses to PHA and the Gram-positive superantigens tested ($P > 0.05$). While PBMC purified from BIA-ALCL and healthy control patients, responded maximally to PHA (BIA-ALCL, 6.42; Primary augmentation, 7.09) compared with LPS (BIA-ALCL, 3.45; Primary augmentation, 3.68), SEA (BIA-ALCL, 3.61; Primary augmentation, 5.01) and TSST-1 (BIA-ALCL, 2.40; Primary augmentation, 4.55) ($P < 0.05$). No statistical comparisons were made for MT-4 cells given that there was only one result from this cell line but from this result it is clear the mean maximum SI to PHA (6.98) is higher than the other mitogens (LPS, 4.11; SEA, 3.75; TSST-1, 3.19).

7.3.3. Effects of penicillin/streptomycin antibiotics

The addition of penicillin/streptomycin in the cell culture medium was found to have no effect on cell proliferation. There was no significant difference in the proliferation response (SI) of BIA-ALCL tumour cells cultured in DMEM containing 10% FBS, 1% penicillin/streptomycin and DMEM containing 10% FBS for all cell concentrations and at 5 and 10 $\mu\text{g/mL}$ of SEA, LPS and PHA ($P > 0.05$) (Figure 7.12). For TSST-1, in the absence of penicillin/streptomycin significantly higher SI were obtained at the lowest concentration of 10^5 cells/mL and at both 5 and 10 $\mu\text{g/mL}$, $P < 0.01$ (Figure 7.12). However, given the low proliferative responses of BIA-ALCL cells to TSST-1 stimulation (Figure 7.9), it is likely that at low cell concentrations the effect of penicillin/streptomycin would be negligible.

A

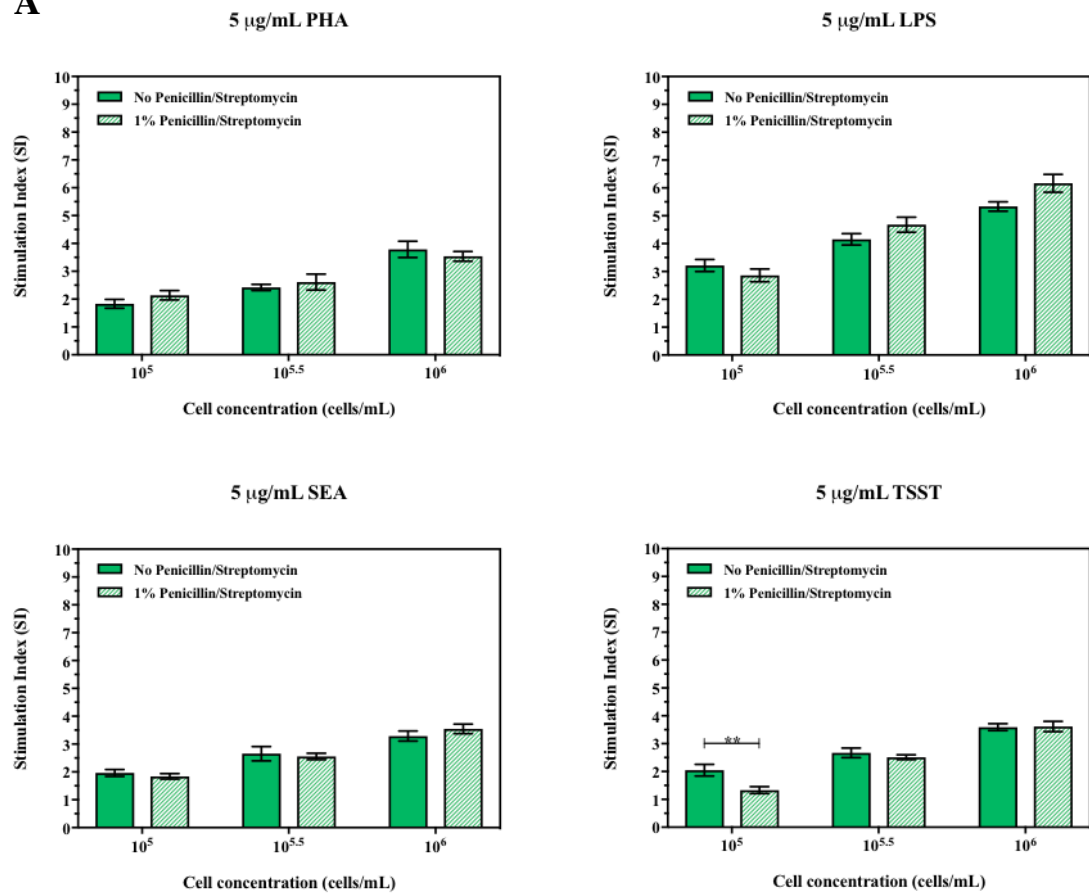


Figure 7.12. Comparison of the proliferation responses (SI) of BIA-ALCL tumour cells to non-specific mitogens at (A) 5 and (B) 10 µg/mL cultured in media with or without 1% penicillin/streptomycin. Values are the means \pm SEM of six technical replicates. Significantly different at $**P \leq 0.01$, $**P \leq 0.01$.

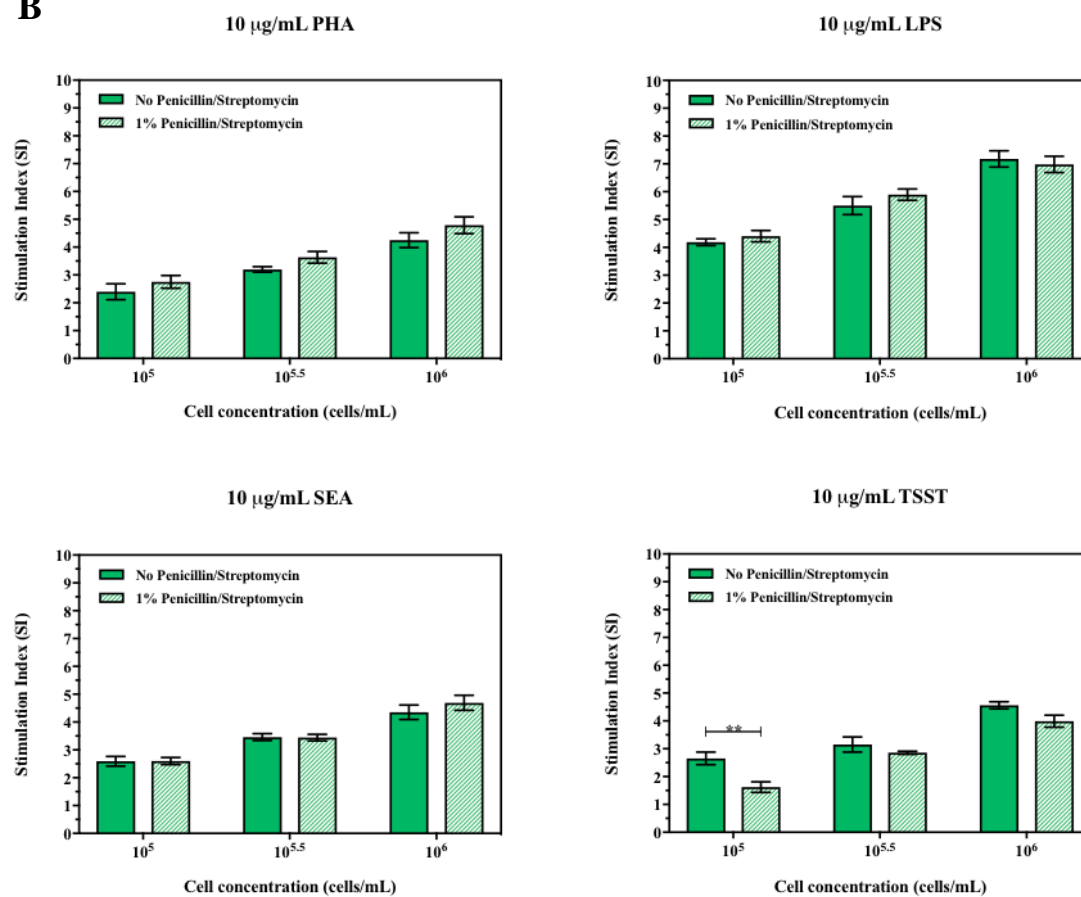
B

Figure 7.12. Continued.

7.4. Discussion

In this Chapter we measured the proliferative response of primary BIA-ALCL tumour cells, tumour cell lines, an immortal T-cell line, and normal PBMC to Gram-positive staphylococcal superantigens, SEA and TSST-1. We then compared these results to the proliferative responses to Gram-negative bacterial LPS and the plant lectin T-cell mitogen, PHA (Chapter VI).

Whilst all cells were able to respond to both SEA and TSST-1, we have shown patient-derived BIA-ALCL tumour cells and BIA-ALCL (TLBR) cell lines respond maximally to LPS. With similar proliferative responses to SEA, TSST-1 and PHA observed. In contrast, in tumour cells from the related cutaneous-ALCL, we identified equal responses to PHA, SEA and TSST-1, and these responses were stronger than those to LPS. We observed the same pattern in PBMC purified from contracture patients, which responded equally to PHA, SEA and TSST-1. While in MT-4 cells, there was a maximum response to PHA and this was also the case in PBMC collected from BIA-ALCL patients and healthy control patients with no prior exposure to breast implants.

These findings point to an underlying bacterial infection, most likely from Gram-negative bacteria, as a contributing factor to the transformation of inflammatory T-cells into malignant lymphoma in BIA-ALCL. It is probable that the presence of multiple bacterial species within bacterial biofilm in BIA-ALCL specimens (Hu et al., 2016) is composed of different proportions of Gram-negatives to Gram-positives, whose compositions are different because they contain different proteins in their cell walls. In Gram-positive bacteria the cell wall is primarily composed of peptidoglycan while in Gram-negative bacteria the cell wall contain three main components, LPS, lipoproteins and peptidoglycan (Aderem and Ulevitch, 2000). Depending on the proportion of these bacterial species different bacterial antigens will be released, which can further potentiate T-cell differentiation, proliferation and malignant transformation.

In BIA-ALCL tumour cells from the single patient to present with a tumour mass (patient 1627), proliferation responses to SEA (mean, 4.0) and TSST-1 (mean, 4.3) were equal to those to LPS (mean, 5.7) and PHA (mean, 4.0). It was predicted that stronger responses to staphylococcal superantigens would occur given that we cultured *S. aureus* from the patients' capsule and implant (Chapter V). However, we were unable to show this, which suggests that there is a difference between the mitogenic responses of the tumour cells isolated from patients with mass disease and seroma disease, and further strengthens the hypothesis that seroma is likely reactive to the presence of bacterial antigens.

Tumour cells from the related cutaneous form of ALCL showed more proliferation to SEA, TSST-1 and PHA. The pathogenesis of cutaneous-ALCL is only partially understood. It has been previously reported that certain human leukocyte antigen class II alleles were associated with cutaneous-ALCL (Linnemann et al., 2004). This suggests that one of the molecular pathogenesis mechanisms may involve inappropriate T-cell activation via antigen presentation followed by an accumulation of neoplastic memory T-cells (Linnemann et al., 2004). *S. aureus* has been suggested as one of the potential triggers/promoters of cutaneous-ALCL (Abrams et al., 2001, Mirvish et al., 2011). Willerslev-Olsen et al. (2016) recently showed that SEA was present in the cutaneous-ALCL skin isolates, which could explain the stronger proliferation observed in these cell lines to staphylococcal superantigens. It is believed that SEA impacts malignant T-cells indirectly by activating infiltrating bystander non-malignant T-cells, which in response to this stimulus produce IL-2 and other regulatory cytokines (Willerslev-Olsen et al., 2016). These cytokines signal in a paracrine fashion and stimulate nearby malignant T-cells to upregulate JAK3/STAT3 signalling, which leads to IL-17 upregulation (Willerslev-Olsen et al., 2016). Thus, the potential for SEA to activate STAT3 oncogene signalling and promote cancer progression and IL-17 secretion in cutaneous-ALCL, is further evidence for the role of bacterial antigens in malignant lymphomas.

Interestingly, in patients with contracture we also found higher proliferative responses in their PBMC to SEA and TSST-1 superantigen-induced stimulation. This is in line with the fact that *Staphylococcus* spp. are associated with 70% of contracted breasts and are frequently implicated in causing implant-related infections (Arciola et al., 2012, Ribeiro et al., 2012, Deva et al., 2013). Staphylococcal superantigens have the ability to bypass the normal rules of antigen presentation by binding (without prior cellular processing) to the outside of the antigen-binding cleft of major histocompatibility complex (MHC) class II molecules of antigen-presenting cells and to specific variable regions of the β -chain of the TCR (Balaban and Rasooly, 2000). This binding results in activation of up to 40% of the naïve T-cell population, which in turn leads to a massive release of proinflammatory cytokines (Darenberg et al., 2004). In contracture patients, the degree of CC seems to be associated with a prolonged or accelerated inflammatory process (Pittet et al., 2005, Khan, 2010). In our cohort of CC patients ($n = 3$), the mean implantation time was 7.8 years and ranged from 3.5 to 15 years, it is likely the exaggerated responses in the inflammatory process observed in some patients may be due to local factors including bacterial infection, which can further increase the degree of inflammation, finally leading to fibrosis. Thus, future studies analysing the cytokine profiles of PBMC in CC and BIA-ALCL patients could prove useful.

In this Chapter we also tested the effects of penicillin/streptomycin on mitogen-induced cell proliferation to ensure the presence of these antibiotics did not dampen the responses we observed. Penicillin/streptomycin solution is used to prevent bacterial contamination of cell cultures. Penicillin (Penicillin G) is a beta-lactam antibiotic from *Penicillium chrysogenum*. It is predominantly active against Gram-positive bacteria by inhibiting peptidoglycan synthesis whilst Gram-negative bacteria are resistant due to the LPS and protein layer that surrounds the peptidoglycan layer of their cell wall (Olson et al., 2002). Streptomycin is an aminoglycoside antibiotic derived from *Streptomyces griseus*. It is predominantly active against Gram-negative bacteria and inhibits protein synthesis (Olson et al., 2002). We cultured BIA-ALCL tumour cells

in either DMEM with or without the addition of penicillin/streptomycin and found these antibiotics had no effect on the proliferative responses of BIA-ALCL tumour cells. Thus, the SI values we obtained for all the cells we tested following stimulation with staphylococcal superantigens, LPS and PHA, are indeed reflective of their true proliferative responses.

The findings from this Chapter show differential responsiveness of BIA-ALCL tumour cells to Gram-negative bacterial LPS and suggests a potential pathway for bacterial LPS to trigger proliferation and differentiation of T-cells and supports our hypothesis of a bacterial antigenic trigger of the tumour.

Chapter VIII.

The development of a co-culture system of mammalian cells and biofilm composed of different bacterial species

8.1. Introduction

The unifying hypothesis for BIA-ALCL pathogenesis proposes a combination of bacterial contamination, high surface area textured implants, genetic susceptibility and time of exposure to implants that pushes T-lymphocytes to transform into BIA-ALCL (Loch-Wilkinson et al., 2017). The role of bacteria as one of the likely four main factors is particularly relevant. In Chapter V we showed that BIA-ALCL specimens demonstrate a high level of bacterial contamination, although given the relative rarity of this disease and hence small sample size we found this was no different to the levels in CC. In Hu et al.'s (2016) study, which had a larger sample size ($n = 26$), they found a high level of bacterial contamination that was analogous to the levels seen in CC. A further and unexpected finding from this study was that the microbiome in BIA-ALCL was shifted significantly toward Gram-negative bacteria (*R. pickettii*) as compared with the usual Gram-positive microbiome (*Staphylococcus spp.*) in contracture (Hu et al., 2016). Interestingly, recent literature suggest that local microbiomes may play a role in both initiating and potentiating other malignancies including breast, gastric and oral cancers (Wang and Ganly, 2014, Kwa et al., 2016, Yang et al., 2017).

In Chapter VI we showed that BIA-ALCL tumour cells have a unique proliferative response to LPS from Gram-negative bacteria and in Chapter VII we showed that this strong response is absent with Gram-positive staphylococcal superantigens. This is in contrast to tumour cells from

the related CD30+ ALK- cutaneous form of ALCL and PBMC derived from patients with BIA-ALCL, contracture patients and from healthy controls. These findings suggest a potential pathway for bacterial LPS to trigger proliferation and differentiation of T-cells and provides support to our hypothesis of a bacterial antigenic trigger to malignant transformation.

In this Chapter we further investigated the differential response of BIA-ALCL tumour cells to bacterial biofilm infection composed of different pathogen species, including Gram-negative bacteria, *R. pickettii* and *P. aeruginosa*, and compared these responses to Gram-positive bacteria, *S. aureus*, *S. epidermidis* and methicillin-resistant *S. aureus* (MRSA). With the aim to develop a co-culture of biofilm and mammalian cells and to measure the proliferation response of BIA-ALCL tumour cells to biofilm infection composed of the aforementioned bacterial species.

8.2. Part A: Optimisation of bacterial biofilm formation assays

To address our study aim to develop a co-culture model of mammalian cells and bacterial biofilm, we performed a series of optimisation experiments with *S. aureus* since they are often implicated in implant-related infections (Arciola et al., 2012, Ribeiro et al., 2012, Deva et al., 2013).

8.2.1. Optimisation methods

8.2.1.1. Bacterial strains and culture conditions

S. aureus strain ATCC 25923 was used for the co-culture assays and prepared as detailed in Section 2.1.2.

8.2.1.2. Biofilm formation assays

Approximately 10^8 bacterial cells/mL was diluted 1:10 in PBS to give roughly 10^7 cells/mL. For the *in vitro* bacterial attachment assays, this concentration was further diluted 1:100 in either

DMEM or RPMI 1640 medium to give approximately 10^5 cells/mL. One mL of which was added in triplicate wells of a flat-bottom 12-well cell culture plate (Corning; Sigma-Aldrich). Control wells were filled with 1 mL of media only (Figure 8.1). Replicate plates were set-up to separately assess biofilm biomass and biofilm viability. All plates were incubated at 37°C in a 5% CO₂ incubator for the appropriate test incubation time.

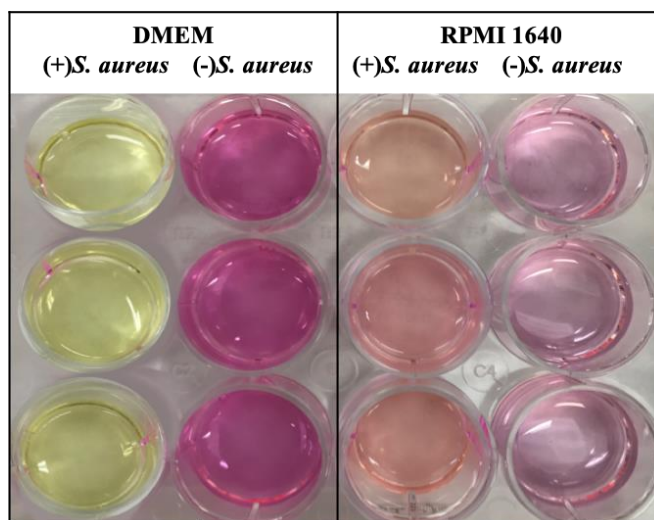


Figure 8.1. *S. aureus* biofilm formation for 24 hr in the wells of a cell culture plate containing DMEM and RPMI 1640 medium.

Following biofilm formation, the supernatant containing planktonic cells was removed from the wells and transferred to a new 12-well plate and assayed for planktonic growth by measuring absorbance at OD 600 nm using a plate reader. The test medium was used as a blank. The wells containing formed biofilm were then washed by adding 1 mL of PBS to the wells and gently swirling the plate around to remove loosely adhered bacteria. The PBS was removed and discarded. This was repeated three times.

8.2.1.3. Biofilm quantification

Biofilm mass was determined using CV staining as per Section 2.2.2. and the number of viable cells (CFU counts) was also measured (Section 2.2.2.).

8.2.1.4. Statistical analysis

All statistical analyses were performed with GraphPad Prism 7.0. The data were tested for normality of distribution by the D'Agostino and Pearson or Shapiro-Wilk normality test. To determine the differences in bacterial attachment, we used one-way and two-way ANOVA with Tukey's or Sidak's multiple comparisons post-hoc tests for normally distributed data. A one-way ANOVA with Tukey's multiple comparisons post-hoc test were used to look for differences in proliferative responses after co-culture with biofilms composed of different bacterial species. For data that were not normally distributed, the Kruskal-Wallis non-parametric ANOVA followed by Dunn's multiple comparisons post-hoc test was used. *P* values less than or equal to 0.05 were considered statistically significant. Values are expressed as mean log 10 CFU/mL \pm SD.

8.2.2. Testing the growth of bacteria in cell culture media and biofilm formation in a cell culture plate

The aim of this experiment was to grow *S. aureus* biofilm in cell culture media that (i) would attach to the bottom of the wells of a cell culture plate, (ii) remain viable, and (iii) would not release too many planktonic cells in culture and hence trigger an acute infection of mammalian cells. The formation of *S. aureus* biofilm was determined following 24 or 48 hr incubation in triplicate as described in Sections 8.2.1.1 to 8.2.1.3.

Results

Based on CV staining, we found *S. aureus* formed significantly more biofilm at 24 and 48 hr when grown in DMEM (OD₆₀₀: 1.24 (24 hr), 1.29 (48 hr)) when compared to RPMI 1640 medium (0.20 (24 hr), 0.12 (48 hr)), *P* < 0.0001 (Figure 8.2A). No difference in biofilm mass was observed

between *S. aureus* grown in DMEM at 24 and 48 hr, $P = 0.9982$ (Figure 8.2A). CFU counts showed DMEM (7.23 log₁₀ CFU/mL) had significantly higher numbers of bacteria attached to the wells at 48 hr compared with RPMI 1640 medium (5.83), $P = 0.0479$ (Figure 8.2B).

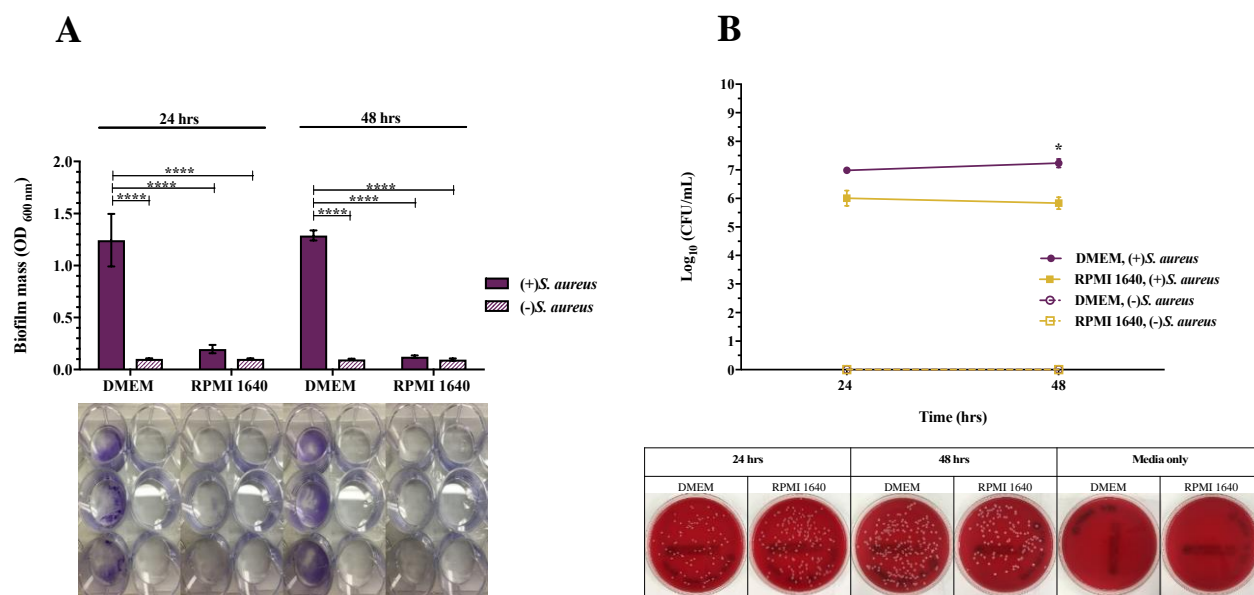


Figure 8.2. Quantification of *S. aureus* biofilm biomass and viability after 24 and 48 hr culture in DMEM and RPMI.

10^5 cells/mL of *S. aureus* was grown in triplicate in either DMEM or RPMI 1640 medium in a 12-well plate to form either a 24 or 48 hr biofilm. Biofilm formation and viability was quantified by (A) crystal violet staining and (B) viability CFU counts. Values are the means \pm SD. Significantly different at $*P \leq 0.05$, $****P \leq 0.0001$.

There was no significant difference in the numbers of planktonic bacteria between the two types of media after 24 (DMEM, 0.39; RPMI, 0.35) and 48 hr (DMEM, 0.33; RPMI, 0.35) suggesting that neither media was toxic to the bacteria and both supported bacterial growth, $P > 0.05$ (Figure 8.3).

Interpretation: *S. aureus* biofilm develops better in DMEM compared to RPMI 1640 medium based on CV staining and CFU counts (Figure 8.2). Thus, DMEM was the preferred culture medium in all subsequent experiments.

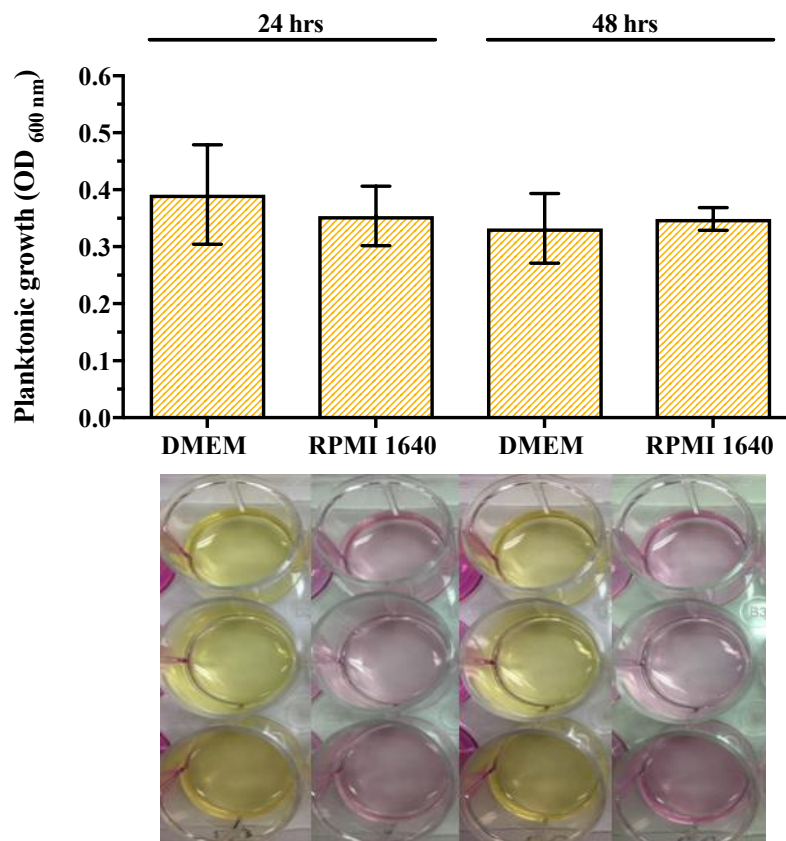


Figure 8.3. Mean absorbance of culture supernatant from triplicate *S. aureus* planktonic growth in DMEM and RPMI 1640 medium after 24 and 48 hr. Values are the means \pm SD.

8.2.3. Growing *S. aureus* biofilm over five days, changing the media every 24 hr

The aim of this experiment was to grow *S. aureus* biofilm over five days, with and without daily media changes, as we planned on growing the biofilm for two days and then culturing it with mammalian cells for at least three days. Ideally, we wanted to see if the biofilm remains viable after five days so that when they are cultured with mammalian cells they can elicit an immune response.

S. aureus (10^5 cells) was grown in triplicate in 1 mL DMEM for 24 hr after which time the media was either changed every 24 hr for the next five days or not at all. Removed media was

assayed for planktonic growth at all time points. On day six, the plate was assayed for biofilm formation and planktonic growth as described in Section 8.2.1.3.

Results

S. aureus failed to form biofilms when the media was changed every 24 hr (OD_{600} 0.28) (Figure 8.4). However, when the media was not changed over the five days culture, *S. aureus* formed biofilms (OD_{600} 1.34, $7.19 \log_{10}$ CFU/mL), $P < 0.0001$ (Figure 8.4). There were significantly more planktonic cells when the media was not changed from days two to five of the culture when compared to daily media changes ($P < 0.05$) (Figure 8.5).

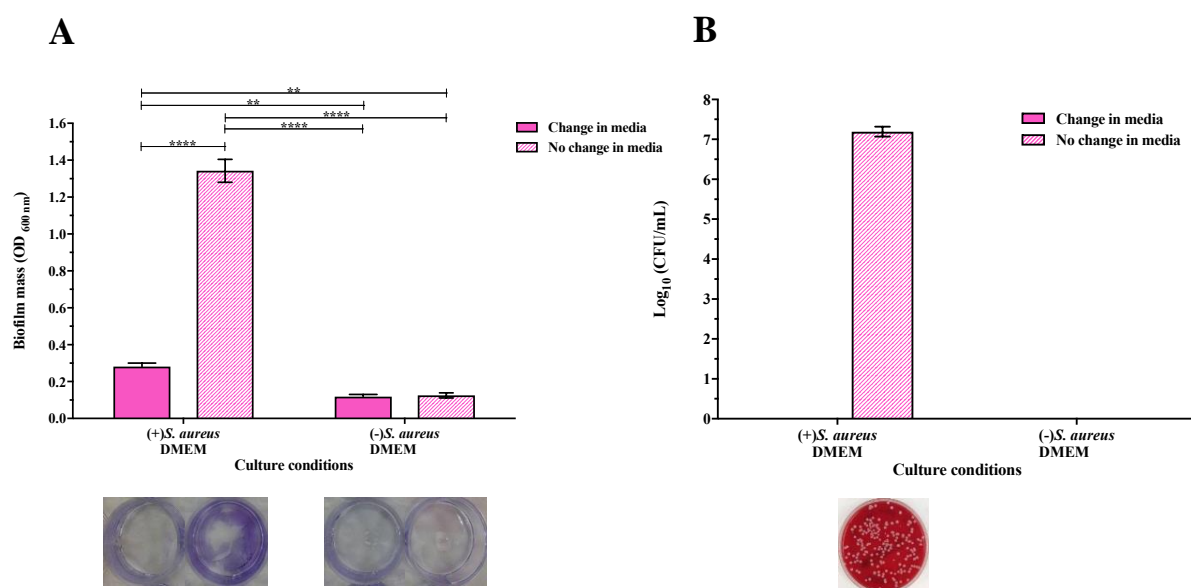


Figure 8.4. *S. aureus* biofilm (A) biomass and (B) viability after five days in culture with daily media changes or no change in media. Values are the means \pm SD of three technical replicates. Significantly different at $**P \leq 0.01$, $****P \leq 0.0001$.

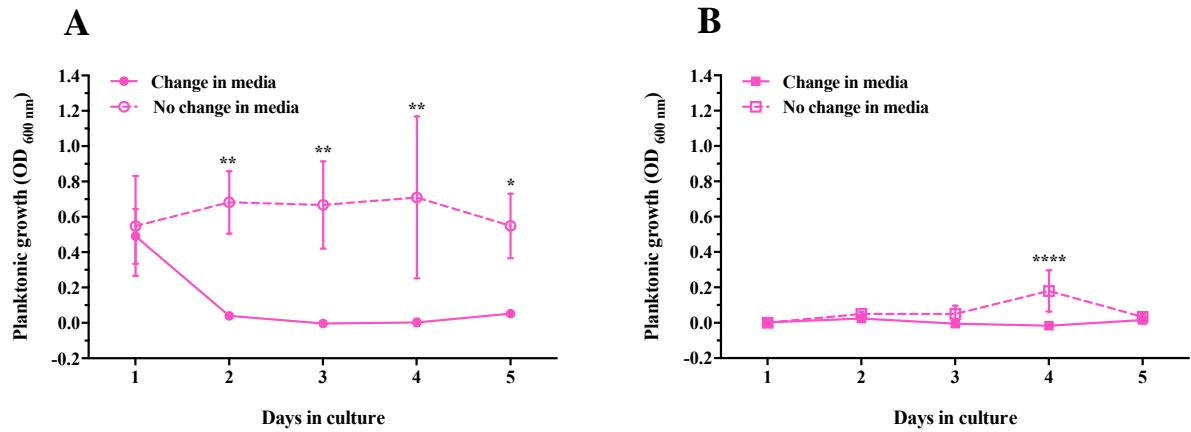


Figure 8.5. Mean absorbance of culture supernatant from (A) *S. aureus* planktonic growth and (B) DMEM only after five days in culture with daily media changes or no change in media. Values are the means \pm SD of three technical replicates. Significantly different at $*P \leq 0.05$, $**P \leq 0.01$, $****P \leq 0.0001$.

Interpretation: Because our main aim is to culture bacterial biofilm with mammalian cells, it is necessary to change the media to remove non-adhered planktonic cells, otherwise they will continue to multiply and kill the lymphocytes we add to the co-culture. In this experiment, the first media change occurred after 24 hr, and hence *S. aureus* was given 24 hr to form a biofilm. Although in the previous experiment we found no difference in biofilm mass between 24 and 48 hr, it is possible that the 24 hr biofilm may not have been attached as well as the 48 hr biofilm, and so when the media was changed it detached. Alternatively, the issue could be due to the constituents of the media (e.g. cations), which may have had an effect on biofilm EPS stabilisation. Thus, the EPS of a 24 hr biofilm would not be as stable as the EPS of a 48 hr biofilm. In the next section we tried growing biofilm for longer in its preferred medium, TSB on the surface of polycarbonate coupons.

8.2.4. *S. aureus* biofilm formation on polycarbonate coupons and transfer to tissue culture plates

The aim of this experiment was to grow *S. aureus* in TSB, since it is the preferred medium for biofilm growth, to form biofilm on the surface of polycarbonate coupons.

Biofilm formation assays

S. aureus was diluted to give approximately 10^5 cells/mL in 1 mL of either DMEM, 10% or 20% TSB and seeded in triplicate wells of a 12-well plate. Sterile polycarbonate coupons (13 mm diameter) (Biosurface Technologies Corp., Bozeman, Montana, USA) were added into each well and the plate incubated at 37°C for 48 hr (Figure 8.6). After which, the coupons were washed three times with PBS to remove any non-adhered planktonic cells and then carefully transferred into the wells of a new 12-well plate containing 1 mL of DMEM per well, and incubated at 37°C, 5% CO₂. After 24 hr, the media was removed and 1 mL of fresh DMEM added. This process was repeated following a further 24 and 48 hr (3 days in total) (Figure 8.6). The coupons were then washed three times with PBS, transferred to a new 12-well plate containing 1 mL PBS per well and viability counts conducted as described in Section 8.2.1.3.

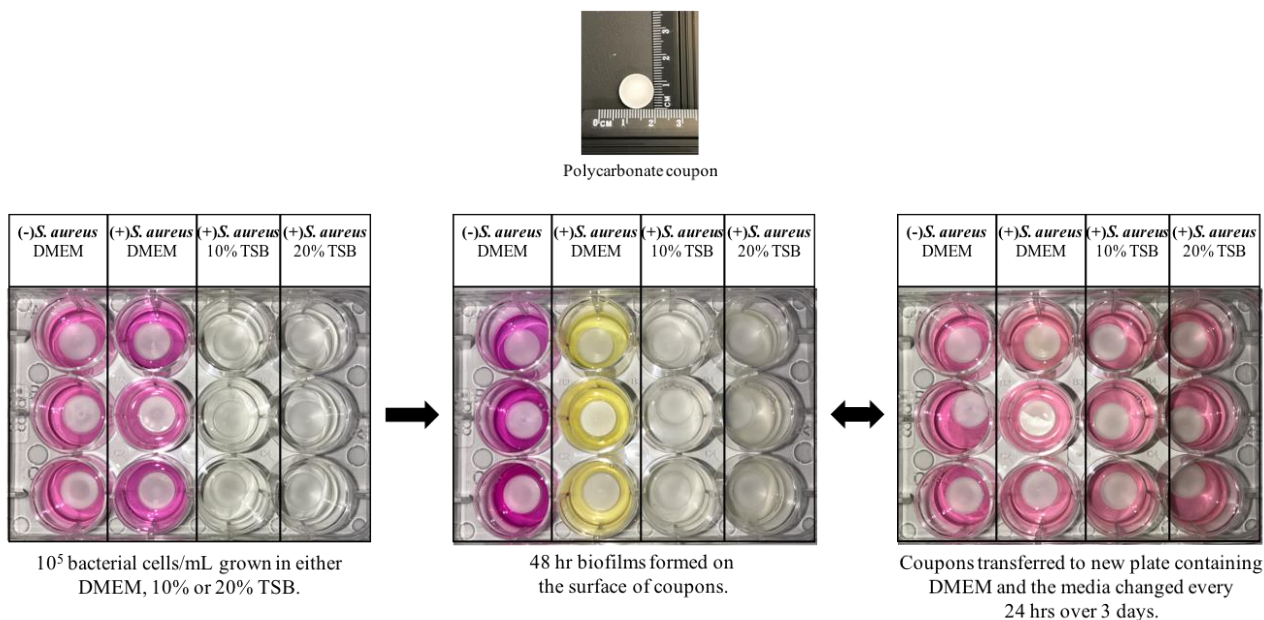


Figure 8.6. Process for growing *S. aureus* biofilm on polycarbonate coupons in DMEM, 10% TSB or 20% TSB for 48 hr and then in DMEM with daily media changes for three days.

Results

There was no significant difference in the number of bacteria attached to the coupons when *S. aureus* was initially grown in DMEM (5.14), 10% (6.07) or 20% TSB (5.82) ($P > 0.05$) (Figure 8.7). However, the standard deviation obtained in CFU/mL was large for all conditions tested (SD: 0.6739 (DMEM), 1.402 (10% TSB), 0.3539 (20% TSB)) and thus not suitable for use in the co-culture assay (Figure 8.7).

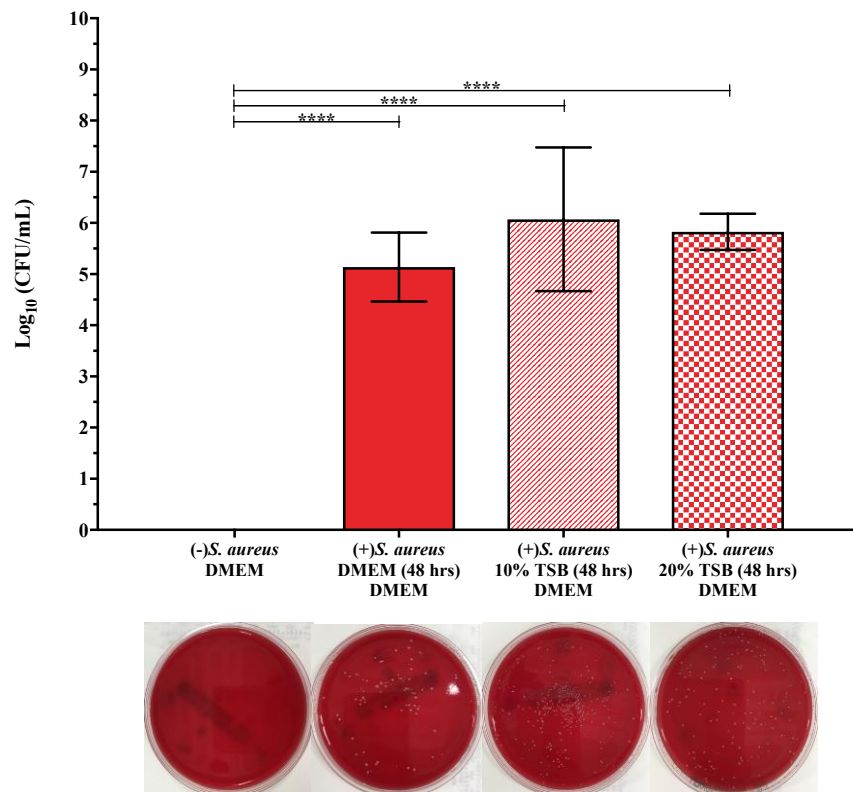


Figure 8.7. *S. aureus* biofilm formed in triplicate in DMEM, 10% TSB or 20% TSB on polycarbonate coupons for 48 hr and then transferred to DMEM with daily media changes for three days. Values are the means \pm SD. Significantly different at **** $P \leq 0.0001$.

8.2.5. Growing *S. aureus* biofilm on breast implants over seven days

The aim of this experiment was to repeat the experiment outlined in Section 8.2.4. only this time we grew biofilm on textured breast implants. Because we want to measure the immune

response of lymphocytes from BIA-ALCL patients to biofilm infection, it was more relevant to use breast implants, particularly textured, for our biofilm formation assays given the high association of textured surface implants with BIA-ALCL (Loch-Wilkinson et al., 2017). In addition, we used the same implants as described in the *in vitro* bacterial attachment assays (Section 2.7.), which have smaller dimensions compared to the polycarbonate coupons and hence would require a lower volume of mammalian cells to be added to the co-culture.

Preparation of breast implants

Motiva SilkSurface and Motiva VelvetSurface textured breast implants (Motiva, Alajuela, Costa Rica) (Table 2.3, Section 2.6.1.3.) were tested and prepared as described in Section 2.7.

Biofilm formation assays

S. aureus biofilm was grown in either DMEM, 10% or 20% TSB in replicate wells of a 24-well plate to form a 48 hr biofilm on the surface of 5 mm diameter Motiva SilkSurface and VelvetSurface textured breast implants. After which, the implants were washed three time with PBS and transferred to a new plate with the wells containing 500 μ L of DMEM and the media changed every 24 hr for five days (Figure 8.8). Biofilm formation on the implants was quantified by CFU counts and planktonic growth was assayed after each media change (Section 8.2.1.3.).

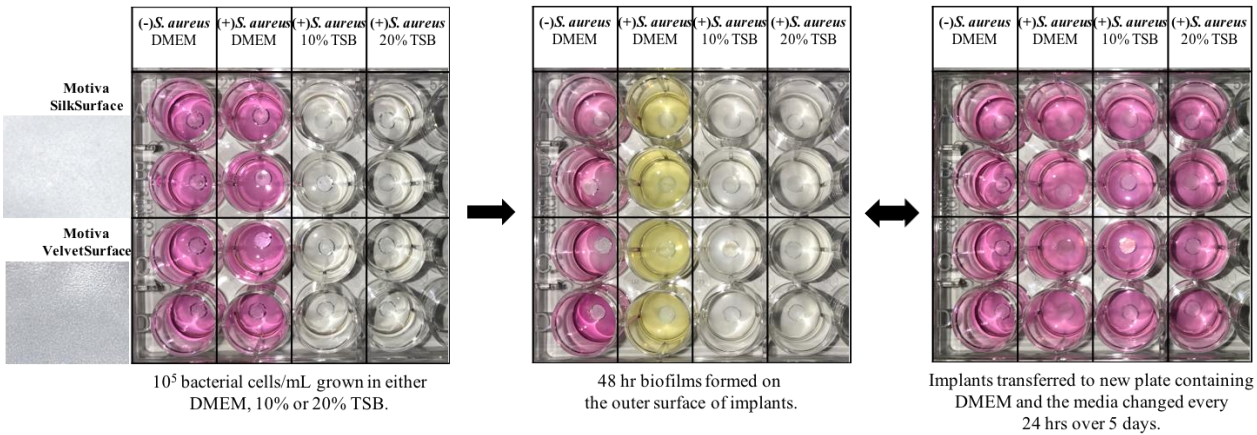


Figure 8.8. Process for growing *S. aureus* biofilm on replicate Motiva SilkSurface and Motiva VelvetSurface textured implants in DMEM, 10% TSB or 20% TSB for 48 hr and then in DMEM with daily media changes for five days.

Results

When *S. aureus* was initially grown in DMEM, significantly more bacteria were attached to Motiva SilkSurface (5.75) compared with Motiva VelvetSurface (5.15) implants after five days, $P = 0.0196$ (Figure 8.9). In addition, significantly higher numbers of *S. aureus* were attached to Motiva implants initially cultured in 20% TSB (SilkSurface, 5.78; VelvetSurface, 5.94) when compared to Motiva VelvetSurface implants initially grown in DMEM, $P < 0.05$ (Figure 8.9). There was no difference in the number of bacteria attached between Motiva VelvetSurface and Motiva SilkSurface implants in the different media conditions tested after the seven days in culture, $P = 0.8913$.

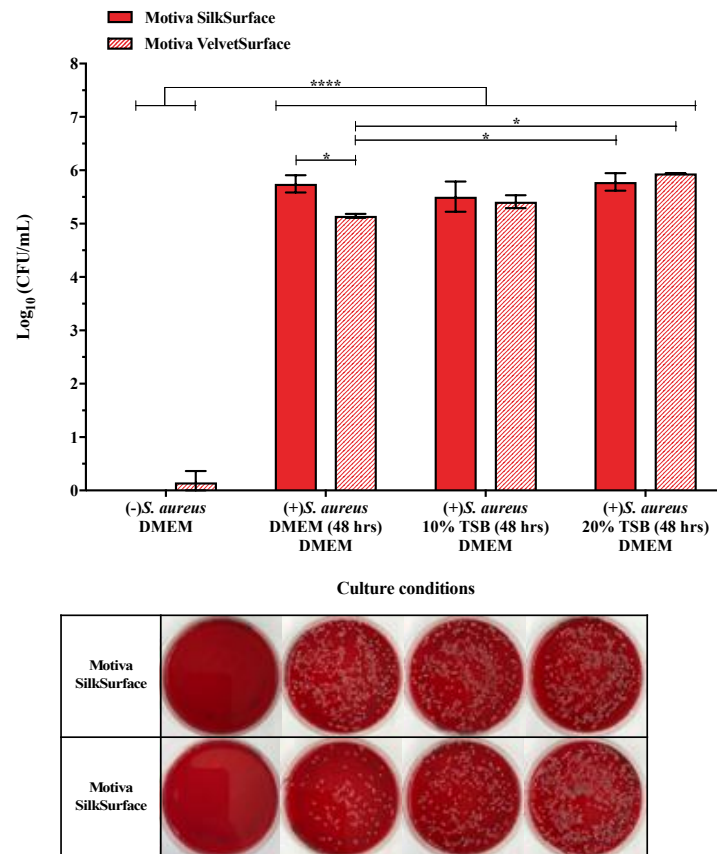


Figure 8.9. Quantification of *S. aureus* biofilm formed in DMEM, 10% TSB or 20% TSB on the surface of replicate textured breast implants for 48 hr and then transferred to DMEM with daily media changes for five days. Values are the means \pm SD. Significantly different at $*P \leq 0.05$, $****P \leq 0.0001$.

We also assayed planktonic growth after daily media changes over the five days in culture and found significantly higher planktonic growth when *S. aureus* was initially grown in DMEM compared with when initially grown in 10% or 20% TSB, $P < 0.05$ (Figure 8.10). No significant difference in planktonic growth was found between 10% or 20% TSB in both textured implant types ($P > 0.05$) (Figure 8.10).

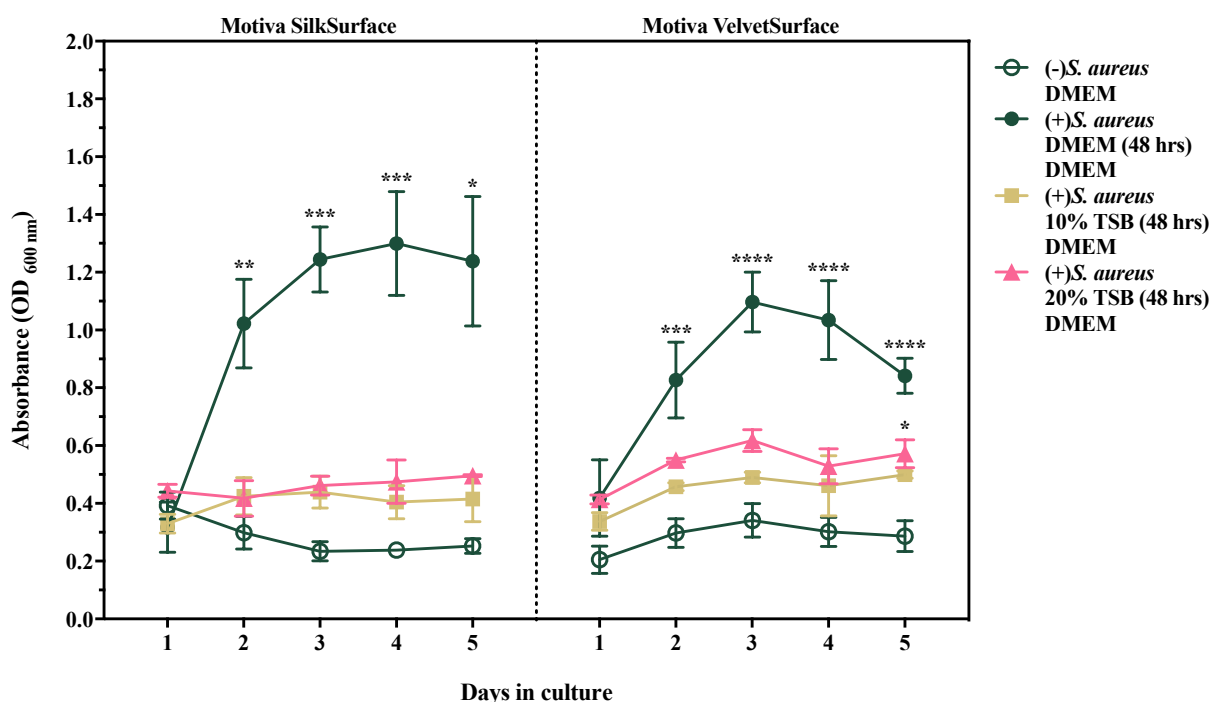


Figure 8.10. Mean absorbance of culture supernatant from replicate *S. aureus* planktonic growth after five days in culture with daily media changes. Values are the means \pm SEM. Significantly different at $*P \leq 0.05$, $**P \leq 0.01$, $***P \leq 0.001$, $****P \leq 0.0001$.

Interpretation: We found no significant difference in bacterial attachment between the two textured implant types utilised. This is consistent with our findings from Chapter III. where we determined the 3D surface area for Motiva VelvetSurface and Motiva SilkSurface implants to be 4.3mm^2 and 3.9mm^2 , respectively, classifying them as minimal surface area implants using our proposed breast

implant surface classification. Thus, in subsequent experiments we tested only one implant type. The higher planktonic growth observed in wells initially grown in DMEM but not TSB suggests that DMEM may supply more nutrients to *S. aureus* during the first 48 hr so perhaps these bacteria are more metabolically active and replicate more quickly, and thus can release more planktonic organisms.

8.2.6. Growing *S. epidermidis*, *P. aeruginosa* and *R. pickettii* biofilm on breast implants over seven days

S. epidermidis, *P. aeruginosa* and *R. pickettii* biofilm was grown on textured breast implants. Test conditions as per Section 8.2.5. but using only Motiva VelvetSurface implants.

Bacterial strains and culture conditions

S. epidermidis (ATCC 35984), *P. aeruginosa* (ATCC 25619) and *R. pickettii* (ATCC 27511) were cultured as per Section 2.1.2. The overnight bacteria culture was diluted to approximately 10^5 cells/mL for *S. epidermidis*, *R. pickettii*, and approximately 10^4 cells/mL for *P. aeruginosa* in 500 μ L of either DMEM, 10% or 20% TSB and the biofilm formation assays conducted in replicate as outlined in Section 8.2.5.

Results

Higher numbers of *S. epidermidis* (5.34), *P. aeruginosa* (7.36) and *R. pickettii* (4.44) were attached to implants when initially cultured in 20% TSB when compared to 10% TSB (*S. epidermidis*, 5.21; *P. aeruginosa*, 6.44; *R. pickettii*, 4.13) and DMEM (*S. epidermidis*, 4.40; *P. aeruginosa*, 5.58; *R. pickettii*, 3.62), although this difference was not significant due to the low number of replicate test samples (Figure 8.11). The lower numbers of *R. pickettii* attached to implants, although not significant, could be because these bacterial species replicate at a slower rate compared to the *P. aeruginosa* and the *S. epidermidis*.

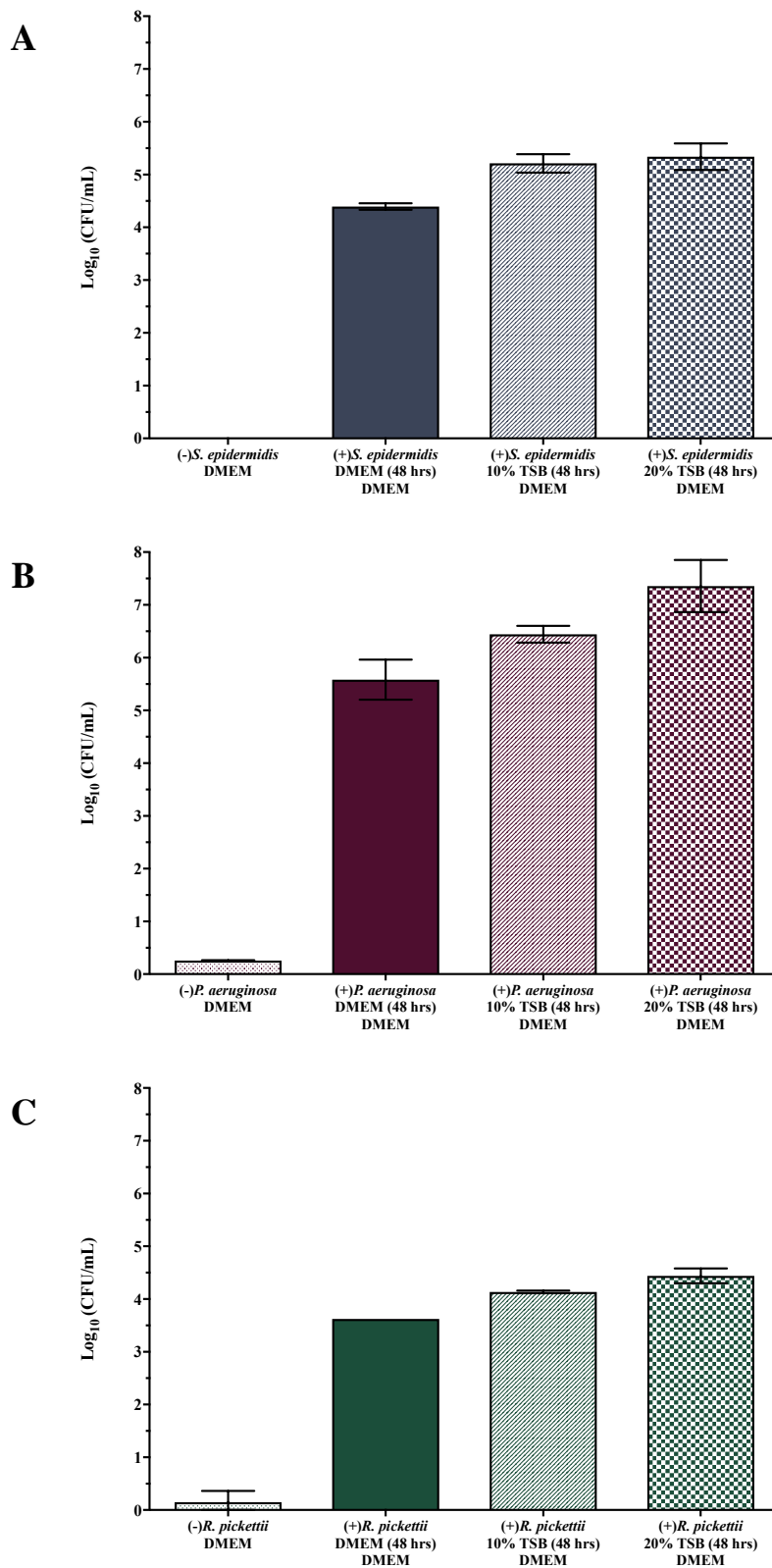


Figure 8.11. (A) *S. epidermidis* (B) *P. aeruginosa* and (C) *R. pickettii* biofilm formed in DMEM, 10% TSB or 20% TSB on replicate textured breast implants for 48 hr and then transferred to DMEM with daily media changes for five days. Values are the means \pm SD.

We also assayed planktonic growth for *S. epidermidis*, *P. aeruginosa* and *R. pickettii* after five days in culture with daily media changes and found as with *S. aureus*, 48 hr biofilm formation in DMEM results in significantly higher planktonic growth compared to 10% or 20% TSB, $P < 0.05$ (Figure 8.12).

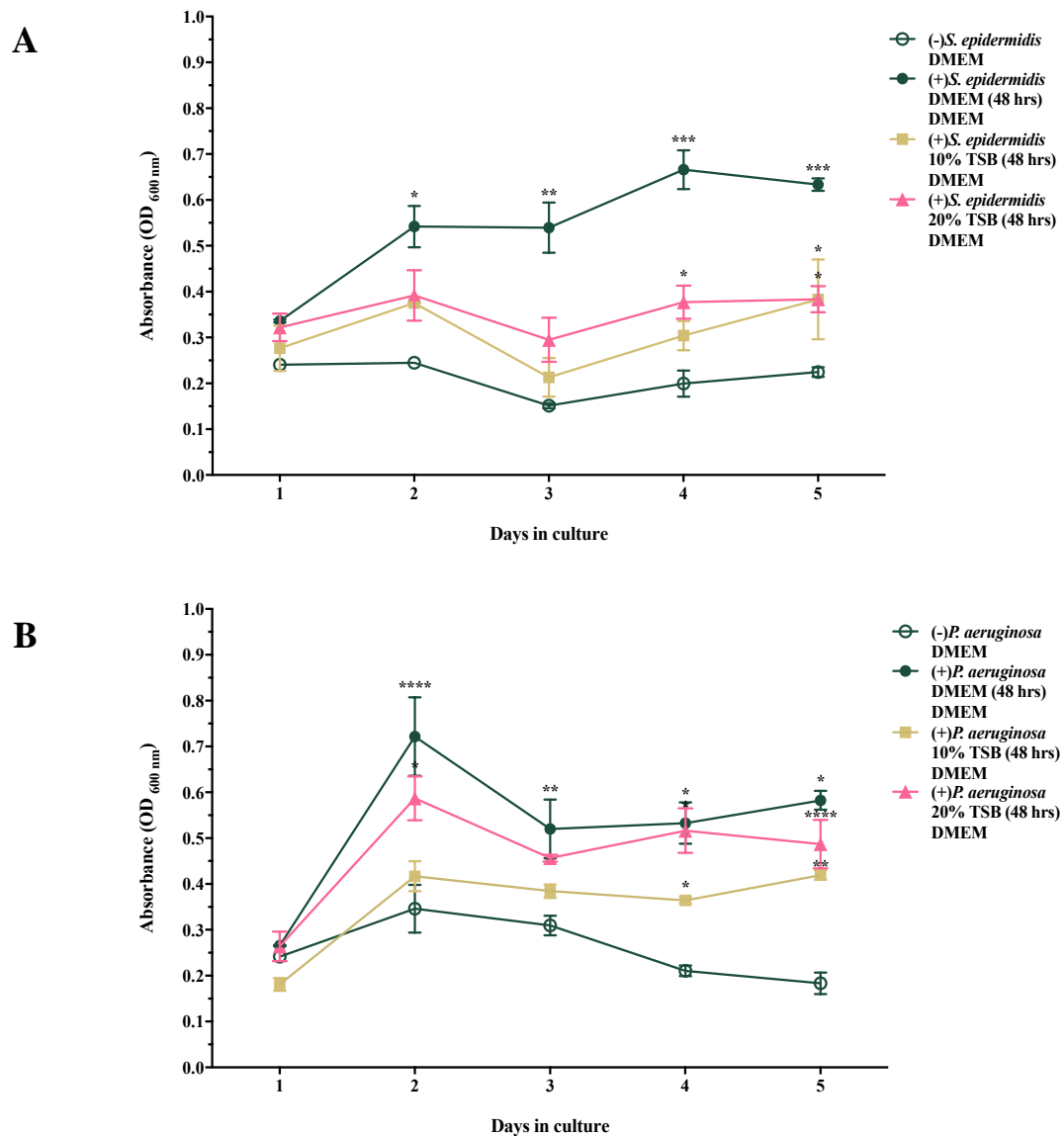


Figure 8.12. Mean absorbance of culture supernatant from replicate (A) *S. epidermidis*, (B) *P. aeruginosa* and (C) *R. pickettii* planktonic growth after five days in culture with daily media changes. Values are the means \pm SEM. Significantly different at $*P \leq 0.05$, $**P \leq 0.01$, $***P \leq 0.001$, $****P \leq 0.0001$.

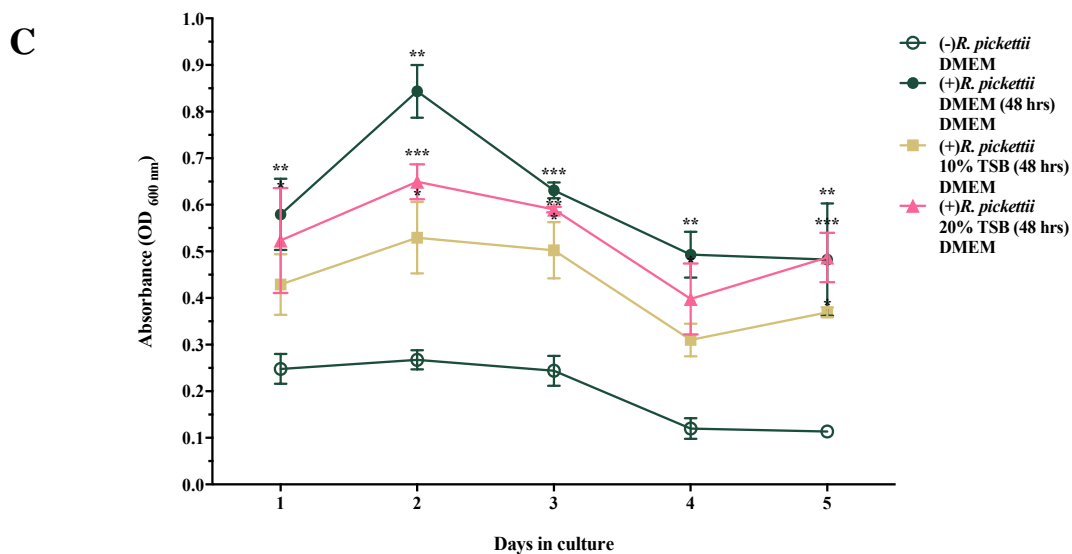


Figure 8.12. Continued.

Therefore, because we wanted minimal planktonic growth in culture, in future experiments we used TSB to initially grow 48 hr biofilms on textured breast implants, 10% TSB for *S. aureus*, *S. epidermidis* and *P. aeruginosa*, and 20 % TSB for *R. pickettii*.

8.3. Established bacterial biofilm formation assay

The established protocol for growing viable *S. aureus*, *S. epidermidis*, *P. aeruginosa* and *R. pickettii* biofilm on textured breast implants is shown in Figure 8.13.

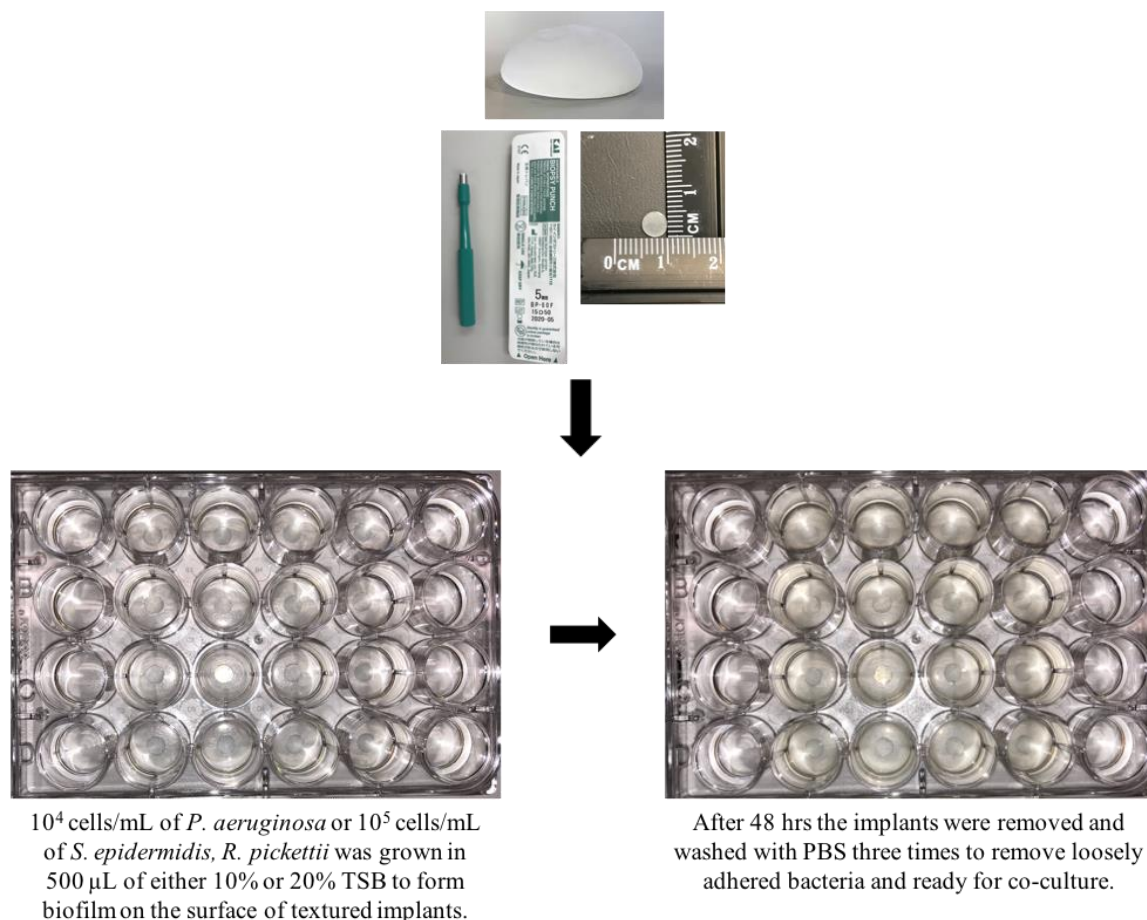


Figure 8.13. Established bacterial biofilm formation assay using textured breast implants.

8.4. Part B: Optimisation of mammalian cells and bacterial biofilm co-culture assays

In these series of optimisation experiments we cultured bacterial biofilm with BIA-ALCL tumour cells and aimed to measure the cell proliferation reaction to living biofilm as opposed to subunits of bacterial cell wall.

8.4.1. Optimisation methods

8.4.1.1. Biofilm formation assays

We grew 48 hr *P. aeruginosa*, *S. epidermidis* or *R. pickettii* biofilms on Motiva VelvetSurface textured implants using the established protocol outlined in Section 8.3.

8.4.1.2. Preparation of tumour cells

BIA-ALCL tumour cells from patient 1713 (Table 5.1, Section 5.3.1.) were prepared as detailed in Section 2.5.1. BIA-ALCL cells were harvested by centrifugation (753 x g, 5 min at 22°C) and resuspended in complete DMEM. For the initial co-culture optimisation experiments, cells were seeded at either 10^5 or $10^{5.5}$ cells/mL into replicate wells of a 24-well plate for 1 hr in 37°C, 5% CO₂ prior to co-culture with bacterial biofilm.

8.4.1.3. Tumour cells and biofilm co-culture

The implants with formed biofilm were washed three times with PBS and then carefully transferred into the wells containing the 10^5 or $10^{5.5}$ BIA-ALCL cells/mL and the plate incubated at 37°C, 5% CO₂ for three days.

The following conditions were tested: (i) BIA-ALCL cells only, (ii) BIA-ALCL cells + implant only, (iii) BIA-ALCL cells + biofilm, (iv) BIA-ALCL cells + biofilm + 5 µg/mL of gentamicin (50 µL/well, Sigma-Aldrich) (active against Gram-negative bacteria, particularly strains of *Pseudomonas*), and (v) BIA-ALCL cells + 10 µg/mL of LPS (50 µL/well)

8.4.1.4. MTT colourimetric assay to determine cell proliferation response to biofilm

The co-culture supernatant (100 µL) was transferred to a 96-well plate and cell proliferation was measured using the protocol outlined in Section 6.3.

8.4.1.5. Biofilm quantification

After the three days co-culture the implants were assayed for viable biofilm formation by washing the implants three times with PBS and viability counts conducted as described in Section 8.2.1.3.

8.4.2. Co-culture of BIA-ALCL tumour cells with *P. aeruginosa* biofilm

The aim of this experiment was to culture BIA-ALCL tumour cells with *P. aeruginosa* biofilm for three days and measure the proliferation response. The response of BIA-ALCL cells to

P. aeruginosa biofilm infection was determined in replicate as described in Sections 8.4.1.1. to 8.4.1.5.

Results

Overall, cell proliferation (SI) for all conditions tested was higher with the higher cell concentration (Figure 8.14). We found BIA-ALCL tumour cells had high proliferative responses to *P. aeruginosa* biofilm at both cell concentrations (SI: 6.8 (10^5 cells/mL), 8.9 ($10^{5.5}$ cells/mL)). Co-culture of $10^{5.5}$ BIA-ALCL cells/mL with biofilm produced significantly higher SI compared to stimulation with LPS in both cell concentrations (10^5 cells/mL, 4.0; $10^{5.5}$ cells/mL, 4.9) $P < 0.05$ (Figure 8.14). The addition of gentamicin appeared to have no effect on proliferation with strong responses observed at 10^5 (6.3) and $10^{5.5}$ cells/mL (7.8) and this was not significantly different to biofilm stimulation when gentamicin is absent ($P > 0.05$) (Figure 8.14). The SI we found in patient 1713 following LPS stimulation (10^5 cells/mL, 4.0; $10^{5.5}$ cells/mL, 4.9) was consistent with our findings from Chapter 6.4.3.2. (10^5 cells/mL, 4.1; $10^{5.5}$ cells/mL, 5.8). Co-culture of 10^5 and $10^{5.5}$ BIA-ALCL cells/mL with implant only (10^5 cells/mL, 2.2; $10^{5.5}$ cells/mL, 3.1) showed significantly lower SI when compared to co-culture of $10^{5.5}$ BIA-ALCL cells/mL with biofilm in the presence and absence of gentamicin, $P < 0.05$ (Figure 8.14). Moreover, these responses were no different to the SI of control, unstimulated BIA-ALCL cells (1.0) at both 10^5 ($P = 0.5150$) and $10^{5.5}$ cells/mL ($P = 0.1034$), which shows the implant itself has no effect on cell proliferation.

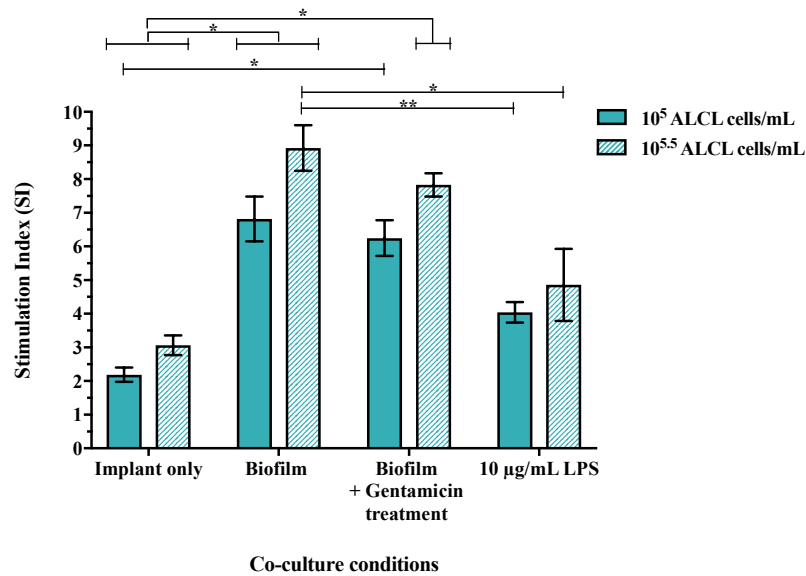


Figure 8.14. Co-culture of BIA-ALCL tumour cells with *P. aeruginosa* biofilm.

*Proliferation response (SI) of BIA-ALCL cells to biofilm infection, LPS stimulation and textured implants after three days in culture. Values are the means \pm SEM of replicates. Significantly different at $*P \leq 0.05$, $**P \leq 0.01$.*

In this co-culture system *P. aeruginosa* biofilm remained viable and attached to implants with a mean of 4.35 log₁₀ CFU/mL for implants cultured without gentamicin, which was not significantly different from the mean of 3.67 log₁₀ CFU/mL for implants cultured with gentamicin (Figure 8.15).

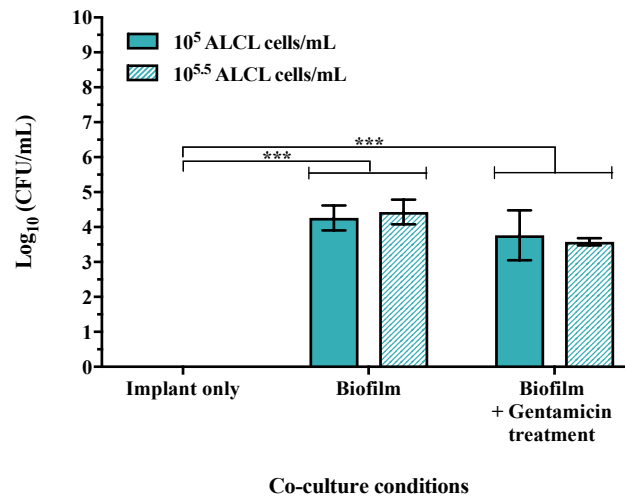


Figure 8.15. Viability of the biofilm formed on replicate implants after three days in culture. Values are the means \pm SD. Significantly different at $***P \leq 0.001$.

8.4.3. Co-culture of BIA-ALCL tumour cells with *S. epidermidis* and *R. pickettii* biofilms

The aim of this experiment was to measure the proliferation response of BIA-ALCL tumour cells to *S. epidermidis* and *R. pickettii* biofilms. The response of BIA-ALCL cells to biofilm infection was determined as described in Sections 8.4.1.1. to 8.4.1.4. but in triplicate and using a cell concentration of $10^{5.5}$ BIA-ALCL cells/mL.

Results

As expected, BIA-ALCL tumour cells responded significantly more to *S. epidermidis* biofilm (4.7) and LPS stimulation (5.6) than cells cultured with the textured implants only (1.5), $P < 0.001$ (Figure 8.16). Although no significant difference in proliferative responses were found between co-culture of BIA-ALCL cells with *S. epidermidis* biofilm and stimulation of cancerous cells with LPS ($P > 0.05$) (Figure 8.16). Exposure of the BIA-ALCL cells to the implant only had no effect on cell proliferation with no difference in SI between implant only and control, unstimulated BIA-ALCL cells (1.0) ($P = 0.3765$). No antibiotic for Gram-positive *S. epidermidis* was tested.

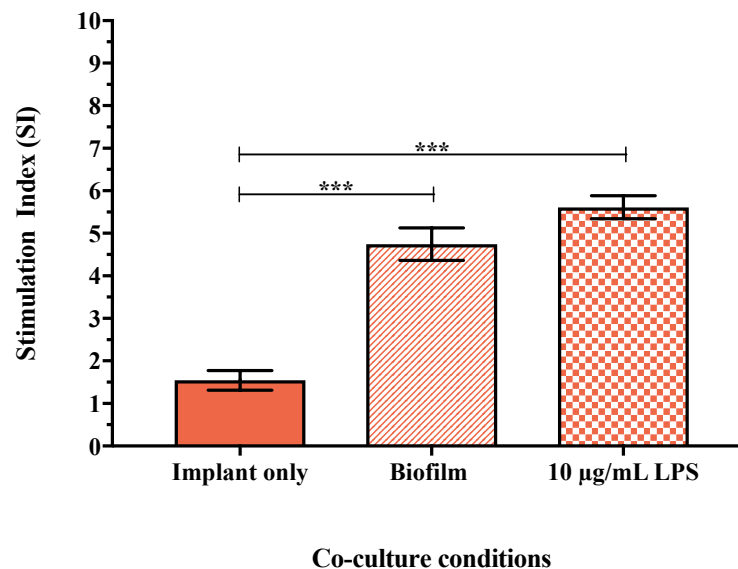


Figure 8.16. Proliferation response (SI) of BIA-ALCL tumour cells to *S. epidermidis* biofilm, LPS stimulation and textured implants after three days in culture. Values are the means \pm SEM of three replicates. Significantly different at *** $P \leq 0.001$.

Similarly, we found significantly higher proliferative responses in BIA-ALCL tumour cells to *R. pickettii* biofilm (with gentamicin, 5.3; without gentamicin, 6.6) and to LPS stimulation (5.6) when compared to BIA-ALCL cells cultured with textured implants only (1.5), $P < 0.0001$ (Figure 8.17). In contrast to *P. aeruginosa*, the addition of gentamicin had an effect on proliferative responses with BIA-ALCL cells responding significantly more to *R. pickettii* biofilm when the antibiotic is absent compared with when it is added, $P = 0.0378$ (Figure 8.17). The presence of implant shell alone had no effect on cell proliferation with no difference in SI between implant only and control, unstimulated BIA-ALCL cells (1.0), $P = 0.4099$.

Assessment of the viability of *S. epidermidis* and *R. pickettii* biofilms formed on the textured implants after the three days co-culture yielded unexpected findings. We found low numbers of *S. epidermidis* ($2.04 \log_{10}$ CFU/mL) and *R. pickettii* ($2.93 \log_{10}$ CFU/mL) attached to the implants cultured with BIA-ALCL cells, which were not significantly different ($P > 0.05$). While we were unable to culture bacteria from *R. picketti* biofilm cultured with BIA-ALCL cells and gentamcin.

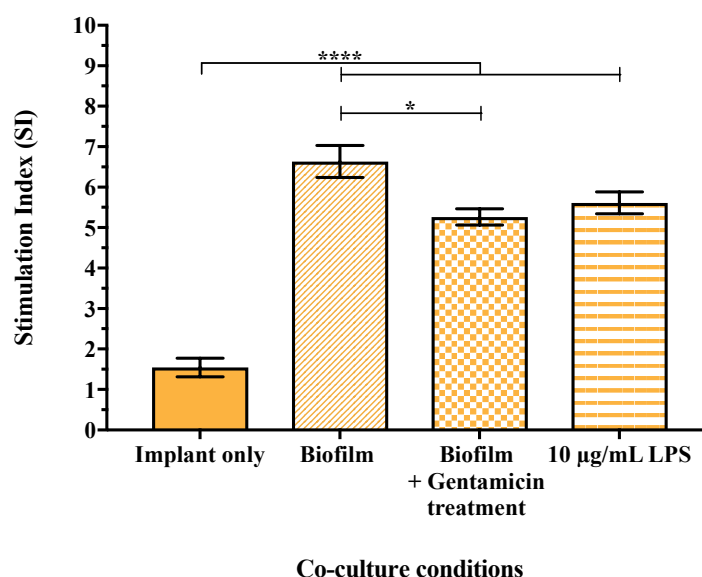


Figure 8.17. Proliferation response (SI) of BIA-ALCL tumour cells to *R. pickettii* biofilm, LPS stimulation and textured implants after three days in culture. Values are the means \pm SEM of three replicates. Significantly different at $*P \leq 0.05$, $****P \leq 0.0001$.

Interpretation: The low CFU counts obtained for *S. epidermidis* and *R. pickettii* biofilms following three days of co-culture in the absence of antibiotic suggested that they could either be detaching from the surface of the implant and thus removed during media changes. Our inability to demonstrate any live bacteria in the *R. pickettii* co-cultures treated with gentamicin suggests that the biofilm was being killed. Since our aim was to measure the proliferation response of cancerous cells to different bacterial species biofilm, to ensure viable biofilms we opted not to add gentamicin to our co-cultures in all subsequent experiments. Furthermore, because the MTT assay is a measure of metabolic cell viability, the high SI values to biofilm infection we detected for *S. epidermidis* (Figure 8.16), *R. pickettii* (Figure 8.17) and *P. aeruginosa* (Figure 8.14) could include bacteria if they were detaching from the implant. In the next experiment, we investigated if this was the case.

8.4.4. Testing the culture medium to determine if bacteria detach from biofilm formed on implants

The aims of this experiment were to:

1. determine whether planktonic bacteria from the biofilm formed on the surface of implants were detaching or being killed by the addition of penicillin/streptomycin to the culture medium and
2. determine if the planktonic bacteria were contributing significantly to the SI obtained.

We grew 48 hr *P. aeruginosa*, *R. pickettii* and *S. epidermidis* biofilms on textured breast implants in triplicates as per Section 8.3. The implants were then washed three times with PBS and transferred to the wells of a new 24-well plate containing 500 μ L of either DMEM supplemented with 10% FBS and 1% penicillin/streptomycin solution or DMEM supplemented with 10% FBS, and incubated at 37°C, 5% CO₂ for three days. After which, the culture supernatant was assayed for bacteria by culture onto HBA and MTT assay (Section 6.3.). The implants were also assayed for viable biofilm by CFU counts (Section 8.4.1.5.).

Results

We found bacteria detach from the surface of implants during culture after plating of culture supernatants onto HBA grew viable *P. aeruginosa*, *R. pickettii* and *S. epidermidis* (Figure 8.18).

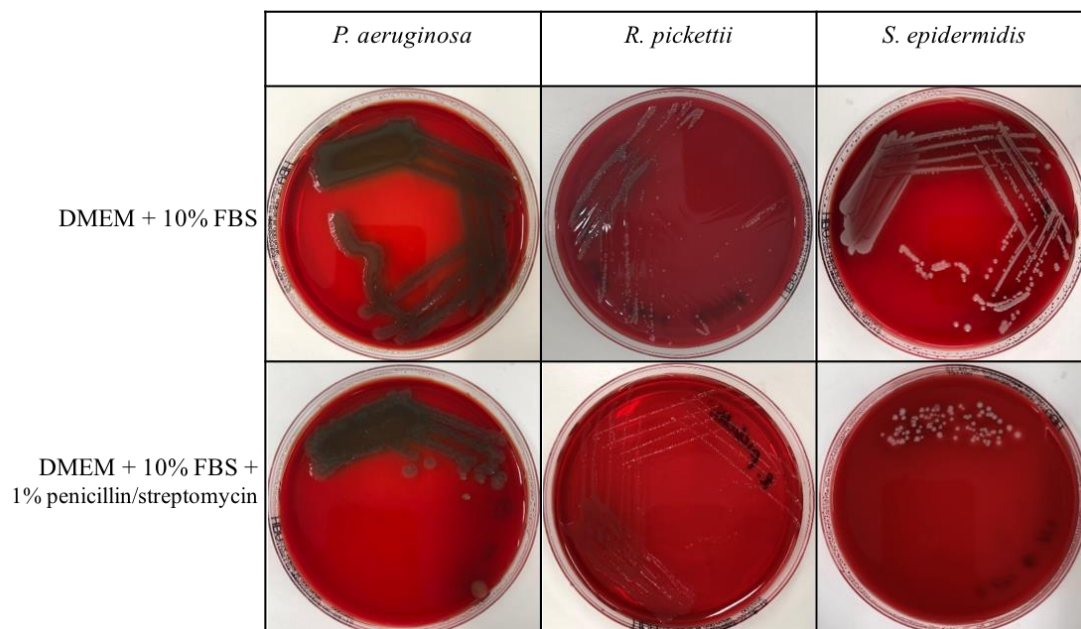


Figure 8.18. Testing the culture medium by standard plate culture to determine if bacteria detach from biofilm formed on implants.

In addition, MTT analysis of the culture supernatant showed significantly higher SI in DMEM containing 10% FBS (*P. aeruginosa*, 11.3; *R. pickettii*, 9.2; *S. epidermidis*, 9.5) when compared to DMEM supplemented with 10% FBS and 1% penicillin/streptomycin (*P. aeruginosa*, 2.4; *R. pickettii*, 1.7; *S. epidermidis*, 1.5), $P < 0.0001$ (Figure 8.19). There was also higher SI in *P. aeruginosa* compared with *R. pickettii* when cultured in DMEM without any antibiotics, $P = 0.0380$ (Figure 8.19).

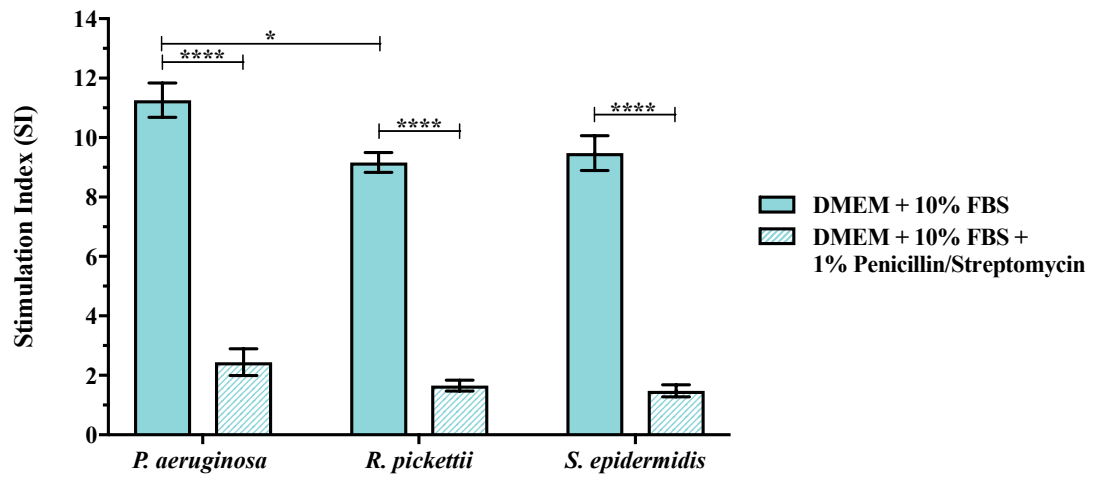


Figure 8.19. Stimulation index obtained by detached biofilm bacteria during three days of co-culture with BIA-ALCL cells as measured by MTT assay. Values are the means \pm SEM of three replicates. Significantly different at $*P \leq 0.05$, $****P \leq 0.0001$.

CFU counts on the viability of the biofilms formed on implants cultured in DMEM + 10% FBS + 1% penicillin/streptomycin for three days showed there were still bacteria attached (Figure 8.20). Although there were significantly lower numbers of bacteria attached when compared to the starting bacterial numbers ($P < 0.05$), where the log reduction of bacteria attached to the implant before and after co-culture was highest for *P. aeruginosa* (7.12), followed by *S. epidermidis* (6.39) and *R. pickettii* (5.49). CFU counts on the culture supernatant showed the presence of bacteria (*P. aeruginosa*, 4.21; *R. pickettii*, 3.34; *S. epidermidis*, 1.55) but these were significantly lower compared with the numbers attached to the implant for *P. aeruginosa* (5.06) and *S. epidermidis* (3.51) (Figure 8.20). Overall, *P. aeruginosa* had higher bacterial numbers attached to the implant and in the culture supernatant when compared to *R. pickettii* and *S. epidermidis* ($P < 0.05$), reflecting the fast growth rates of *P. aeruginosa* (Figure 8.20).

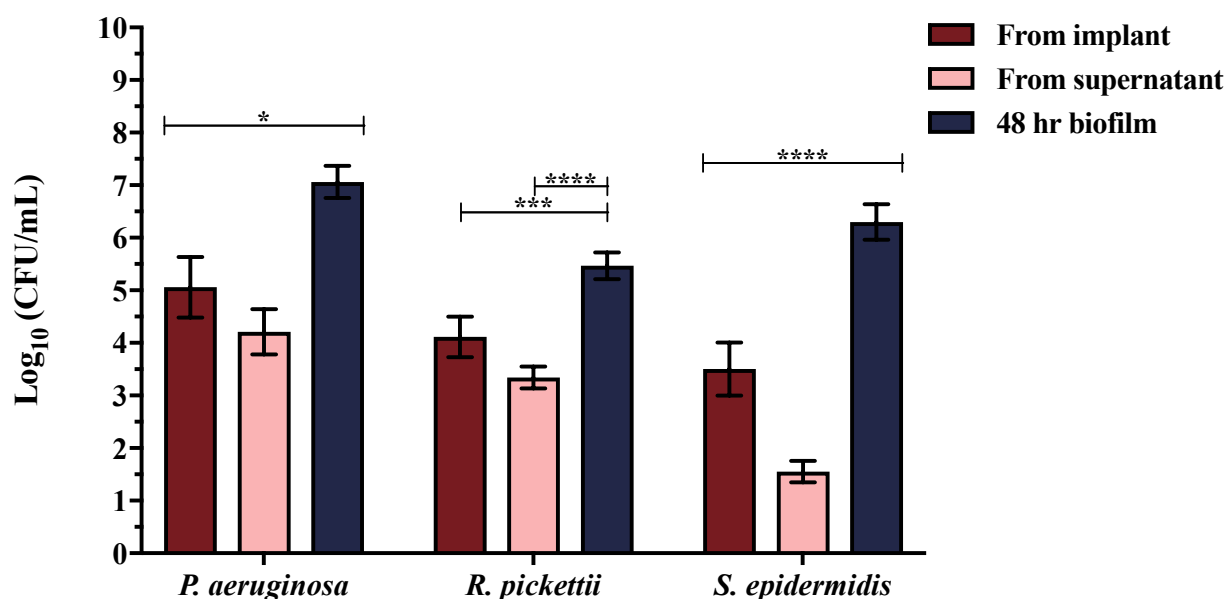


Figure 8.20. Quantification of biofilm formed on triplicate implants before and after co-culture and in co-culture supernatant after three days in co-culture with BIA-ALCL tumour cells. Values are the means \pm SD. Significantly different at $*P \leq 0.05$, $***P \leq 0.001$, $****P \leq 0.0001$.

Interpretation: These findings confirm that bacteria indeed come off the implants into the culture and can contribute to the MTT assay, reducing its accuracy as a measure of BIA-ALCL proliferation. To address this issue, we aimed to develop a method that accounted for the bacterial contribution to the SI.

8.5. Part C: Co-culture of BIA-ALCL tumour cells and biofilm composed of different bacterial species

8.5.1. Introduction

BIA-ALCL tumour cells were cultured with biofilm composed of *P. aeruginosa*, *R. pickettii*, *S. epidermidis* and MRSA. To account for the bacteria that detach from the biofilm formed on

implants we concurrently cultured bacterial biofilm with DMEM only. Proliferative responses from the biofilm/media co-culture were then subtracted from the responses obtained from the co-culture of biofilm with BIA-ALCL cells.

8.5.2. Materials and Methods

8.5.2.1. Preparation of breast implants

Motiva VelvetSurface textured breast implants (Table 2.3, Section 2.6.1.3.) were prepared as described in Section 2.7.

8.5.2.2. Bacterial strains and culture conditions

P. aeruginosa (ATCC 25619), *R. pickettii* (ATCC 27511), *S. epidermidis* (ATCC 35984) and MRSA (ATCC 43300) were used for the co-culture assays and prepared as detailed in Section 2.1.2. MRSA was included given the inhibitory effects of penicillin/streptomycin on *S. epidermidis* growth.

8.5.2.3. Biofilm formation assays

Forty-eight hour *P. aeruginosa*, *R. pickettii* and *S. epidermidis* biofilms were grown on the surface of textured implant outer shells using the established protocol outlined in Section 8.3. MRSA (10^5 cells/mL) was grown in 10% TSB in a 24-well plate to form a 48 hr biofilm on the implants (Section 8.3.).

8.5.2.4. Preparation of tumour cells

Tumour cells were recovered from malignant effusion from a single BIA-ALCL patient, patient 1714 (Table 5.1, Section 5.3.1.), and were prepared as detailed in Section 2.5.1. BIA-ALCL cells were harvested by centrifugation (753 x g, 5 min at 22°C) and resuspended in DMEM supplemented with 10% FBS and 1% penicillin/streptomycin. Cells were seeded at $10^{5.5}$ cells/mL

(500 µL) into six replicate wells of a 24-well plate for 1 hr in 37°C, 5% CO₂ prior to co-culture with bacterial biofilm.

8.5.2.5. Co-culture of BIA-ALCL tumour cells with bacterial biofilm

The implants with formed biofilm were washed three times with PBS and then carefully transferred into wells containing either 10^{5.5} BIA-ALCL cells/mL or 500 µL of complete DMEM. The following conditions were tested: (i) BIA-ALCL cells only, (ii) BIA-ALCL cells + implant only, (iii) BIA-ALCL cells + biofilm, (iv) BIA-ALCL cells + 10 µg/mL of LPS (50 µL/well), and (v) biofilm + media. Plates were incubated at 37°C, 5% CO₂ for three days.

8.5.2.6. MTT colourimetric assay to determine cell proliferation response to biofilm

The co-culture supernatant (100 µL) was transferred to a 96-well plate and cell proliferation was measured using the protocol outlined in Section 6.3.

To measure the proliferation response of the BIA-ALCL cells to biofilm infection, we subtracted the SI obtained from the culture of biofilm with DMEM from the SI of the culture of biofilm with BIA-ALCL cells, as follows:

Proliferation response (SI) =

$$SI_{\text{Biofilm/BIA-ALCL}} \left(\frac{\text{Stimulated BIA-ALCL cells}}{\text{Unstimulated BIA-ALCL cells}} \right) - SI_{\text{Biofilm/DMEM}} \left(\frac{\text{Stimulated DMEM}}{\text{Unstimulated DMEM}} \right)$$

8.5.2.7. Biofilm quantification

After the three days co-culture the implants were washed three times with PBS and assayed for viable biofilm formation by viability counts as described in Section 8.2.1.3.

8.5.3. Results

8.5.3.1. Cell proliferation response following bacterial biofilm infection

The presence of LPS (SI: 6.8), MRSA (5.1), *R. pickettii* (5.4) and *P. aeruginosa* (7.6) biofilms in co-culture with BIA-ALCL tumour cells and textured implants produced significant potentiation of tumour cell growth after three days when compared with exposure of the tumour cells to the implant shell alone (1.2), $P < 0.01$ (Figure 8.21). The SI obtained by stimulating BIA-ALCL cells with LPS, MRSA, *R. pickettii* and *P. aeruginosa* biofilms in co-culture were not significantly different ($P > 0.05$) (Figure 8.21). Among the four bacterial species, *P. aeruginosa* had the highest proliferation response followed by *R. pickettii* and MRSA. In contrast, the response of BIA-ALCL cells to *S. epidermidis* (1.2) was significantly lower when compared to *R. pickettii*, *P. aeruginosa* and LPS stimulation ($P < 0.05$) and was not significantly different from the implant only condition (Figure 8.21). While exposure of the BIA-ALCL cells to the implant only showed significantly higher SI when compared to the control, unstimulated BIA-ALCL cells (1.0), $P = 0.0427$.

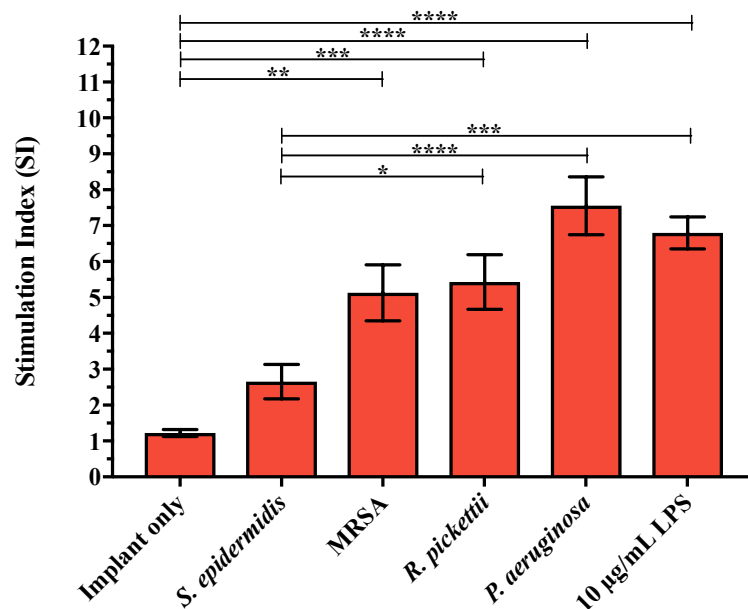


Figure 8.21. Proliferation response (SI) of BIA-ALCL tumour cells to biofilm composed of different bacterial species, LPS stimulation and textured implants. Values are the means \pm SEM of six replicates. Significantly different at $*P \leq 0.05$, $**P \leq 0.01$, $***P \leq 0.001$, $****P \leq 0.0001$.

MTT analysis of the co-culture supernatant showed that more bacteria detached from *P. aeruginosa* biofilm (2.6) in comparison to the other species (*S. epidermidis*, 1.4; MRSA, 1.6; *R. pickettii*, 2.1) and this was significant for MRSA ($P = 0.0178$) and *S. epidermidis* ($P = 0.0033$) (Figure 8.22).

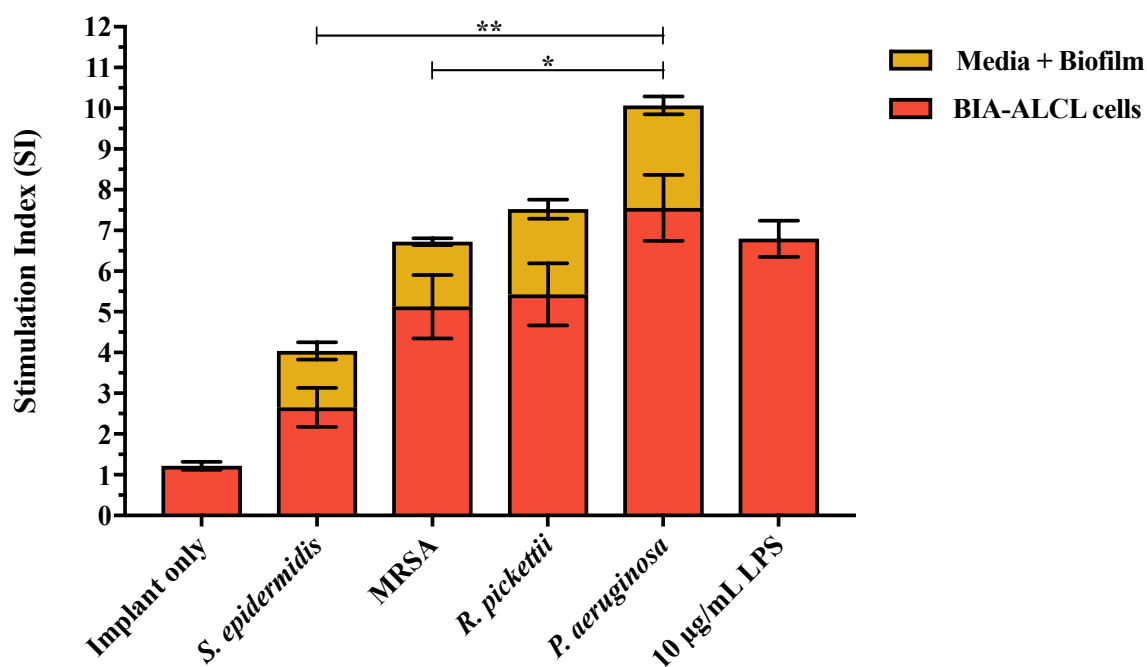


Figure 8.22. Stimulation index from co-culture of media only to biofilm composed of different bacterial species, LPS stimulation and textured implants. Values are the means \pm SEM of six replicates. Significantly different at $*P \leq 0.05$, $**P \leq 0.01$.

8.5.3.2. Bacterial numbers attached to the implant before and after co-culture and in the co-culture supernatant

Biofilm/BIA-ALCL tumour cells co-culture

Assessment of the viability of the biofilms formed on the implants following three days co-culture showed that there were significantly lower numbers of *S. epidermidis*, MRSA and *P. aeruginosa* attached when compared to the starting bacterial numbers, $P < 0.01$ (Figure 8.23). The log reduction of bacteria attached to the implant before and after co-culture was equal for all species,

S. epidermidis (6.40), MRSA (6.47), *R. pickettii* (6.61) and *P. aeruginosa* (6.91). Moreover, the co-culture supernatant had significantly less bacteria when compared to the numbers attached to the implant before and after co-culture for MRSA (from supernatant, 2.39; 48 hr biofilm, 5.72; from implant, 3.26), *R. pickettii* (from supernatant, 2.75; 48 hr biofilm, 4.57; from implant, 3.93) and *P. aeruginosa* (from supernatant, 2.98; 48 hr biofilm, 6.90; from implant, 4.82), $P < 0.01$ (Figure 8.23). Among the four species, *P. aeruginosa* had the highest number of bacteria attached before and after co-culture ($P < 0.05$), and in the co-culture supernatant when compared to *S. epidermidis* (from implant, 2.58; from supernatant, 2.08; 48 hr biofilm, 5.83), $P = 0.0193$ (Figure 8.23). These findings show that we have not optimised the starting number of bacteria attached to the implant, which should be the same for each of the species, and as a result no interspecies statistical comparisons were made.

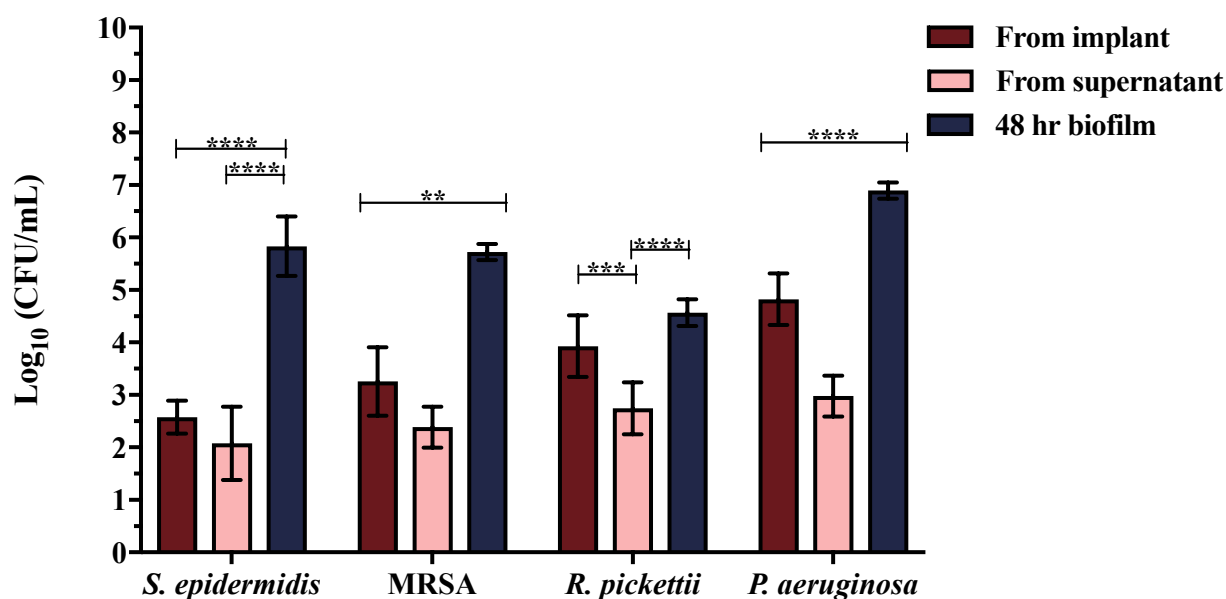


Figure 8.23. Biofilm bacterial numbers formed on six replicate implants before and after co-culture and in co-culture supernatant after three days in co-culture with BIA-ALCL tumour cells. Values are the means \pm SD. Significantly different at $*P \leq 0.05$, $**P \leq 0.01$, $****P \leq 0.0001$.

Biofilm/media co-culture

CFU counts on the viability of the implants with formed biofilms in co-culture with DMEM only showed that bacterial numbers were highest before co-culture, while the co-culture supernatant had the lowest number of bacteria, $P < 0.05$ (Figure 8.24). As with the BIA-ALCL cells co-culture, *P. aeruginosa* was found to have significantly more bacteria attached to implants before and after co-culture (48 hr biofilm, 6.90; from implant, 4.66) than any other species ($P < 0.05$), as well as in the supernatant (2.88) when compared to MRSA (48 hr biofilm, 5.72; from implant, 3.59; from supernatant, 2.13) and *S. epidermidis* (48 hr biofilm, 5.83; from implant, 2.93; from supernatant, 1.85), $P < 0.05$ (Figure 8.24). *P. aeruginosa* and *S. epidermidis* had the highest log reduction before and after co-culture with 6.91 and 6.09, respectively. While a 5.74 log reduction in MRSA and 4.57 in *R. pickettii* attached to the implant before and after co-culture was found.

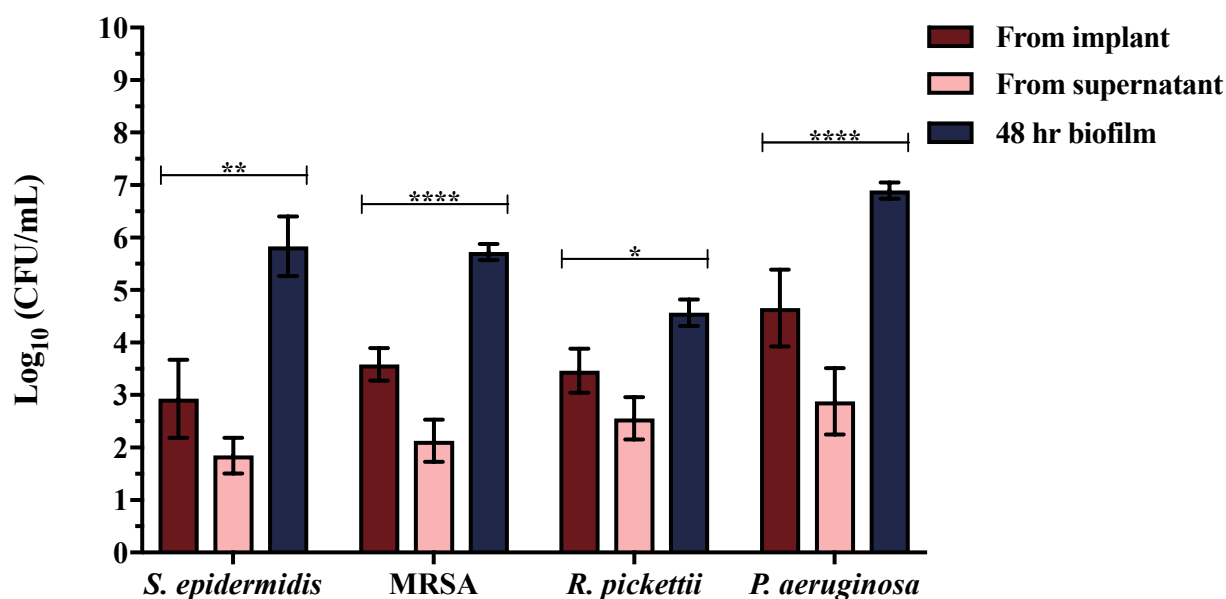


Figure 8.24. Quantification of biofilm formed on six replicate implants before and after co-culture and in co-culture supernatant after three days in co-culture with media only. Values are the means \pm SD. Significantly different at $*P \leq 0.05$, $**P \leq 0.01$, $****P \leq 0.0001$.

8.6. Discussion

In this Chapter we aimed to develop a co-culture assay of BIA-ALCL tumour cells with a number of bacterial species in the presence of textured breast implant shells to determine the likely interactions.

We found the presence of *P. aeruginosa*, *R. pickettii* and MRSA in co-culture with BIA-ALCL tumour cells and textured implant outer shell produced significant potentiation of tumour cell growth when compared to exposure of BIA-ALCL cells to implant shell alone. Moreover, the potentiation of tumour cell growth was similar to the proliferation induced by LPS alone. Among the four species of bacteria, we found Gram-negative *P. aeruginosa* had the highest response, followed by Gram-negative *R. pickettii* and Gram-positive MRSA. Gram-positive *S. epidermidis* showed the lowest response and was even lower than proliferation responses to LPS alone. This was surprising given that the BIA-ALCL tumour cells were derived from patient 1714 whose explanted specimens were culture positive for *S. epidermis* (Chapter V). However, the log reduction of *S. epidermidis* attached to the implant before and after co-culture was high, even in the absence of BIA-ALCL cells (average log reduction = 6.25), which suggests that the number of bacteria attached to the implant is important.

The co-culture of bacterial species with BIA-ALCL tumour cells are consistent with our findings from Chapter VI and has further reinforced the importance of Gram-negative bacterial growth in the stimulation and proliferation of BIA-ALCL tumour cells. The presence of textured implant shell alone did not produce a significant proliferative response each time and when it did, it was a low amount of proliferation. This suggests that it is likely that the breast implant shell acts as a passive carrier for the growth of bacteria rather than acting as a proinflammatory stimulant as has been previously reported (Bizjak et al., 2015, Evren et al., 2017). However, more research is needed to determine whether the implant shell is a factor or not.

The co-culture of BIA-ALCL tumour cells with different bacterial species was subject to a number of limitations. The difficulties associated in achieving a stable balance of the BIA-ALCL tumour cells and the bacterial population is that both cell types are in competition for nutrients from the growth medium, available surface space, and in driving the pH value towards their favoured regimen (Vasilev et al., 2009). More acidic and basic pH values are favourable for *S. epidermidis* and *P. aeruginosa*, respectively, while mammalian cells prefer neutral or slightly basic pH values (Zaatreh et al., 2016). Pathogenic bacteria are more capable of driving the pH value in their favour, as mammalian cells rely on other support (e.g. bloodstream) to maintain a favourable pH environment (Störmer et al., 2008). Future studies to control for this could include adding supportive components of the immune system or other antibiotics to counterbalance the bacterial growth and pathogenicity. Alternatively, we could perform the co-culture assays using transwell inserts. The transwell system consists of a transwell insert, which contains a microporous membrane that comes in different sizes, and a transwell plate to which the inserts go into. BIA-ALCL tumour cells can be seeded in the transwell insert (upper compartment of transwell system) while bacteria can be grown in the lower compartment of the transwell plate. However, a limitation of this system is that the BIA-ALCL cells and the bacteria are separated with no direct cell contact between the cell types. Thus, we can only determine the effect of bacterial biofilm on mammalian cells via metabolic products or released products. As an alternative, we could culture the BIA-ALCL tumour cells with conditioned media from biofilm cultures, which have been described in studies measuring the immune response of human epithelial keratinocytes exposed to biofilm conditioned media (Secor et al., 2011, Tankersley et al., 2014).

During co-culture we discovered that bacteria detach from the implant shell during culture with the cancerous cells. Since MTT reduction is a marker reflecting viable cell metabolism, the high responses we found in our co-culture supernatants would therefore include lymphocytes as well as bacteria. Although we found the addition of penicillin/streptomycin solution in our culture

medium appeared to limit the growth of bacteria that do detach from the implant shell into the culture, it almost completely inhibited Gram-positive *S. epidermidis* both from the implant and any that detached from it. At present, we have been unable to overcome the issue of bacteria detaching from the implant shell during co-culture. Therefore, to address this issue in the short-term, we instead cultured 48 hr biofilms with BIA-ALCL tumour cells as well as with culture media only. To measure the proliferation response of the BIA-ALCL cells to bacterial biofilm infection we subtracted the SI of biofilm/media co-culture from the SI of biofilm/BIA-ALCL cells co-culture. Thus, effectively treating the bacteria that detach from the implant shell as background. This method has potentially compounding effects as there is no way to control the rate of biofilm growth on the implant shell initially and once in culture with the tumour cells/media for each of the bacterial species tested. Although we had six replicates for each condition, this would invariably be a limitation of using this method.

There have been other studies that have cultured bacterial biofilm with other mammalian cells, utilising similar methods to investigate implant-associated infections. A study by Chandra et al. (2007) employed a catheter-based *in vitro* model (Chandra et al., 2001) that involved growing *Candida albicans* biofilm on silicone elastomer discs in a 12-well tissue culture plate for 90 min. The discs were then incubated with 2×10^6 cells/mL of adherent PBMC for 48 hr and the cytokine profiles of PBMC following co-culture were compared to those of PBMC cultured with planktonic *C. albicans* (Chandra et al., 2001). Similarly, approximately 10^3 cells/mL of *S. epidermidis* was grown on test sample discs made of polystyrene, titanium alloy and bone cement, and then directly cultured with human primary osteoblasts over a period of two and seven days (Zaatreh et al., 2016). Both studies reported no issues with bacterial attachment as well as no loss of functionality in the mammalian cells following co-culture. The latter study also found the medium had no detrimental effects on bacterial growth, despite containing potentially interfering components (Zaatreh et al., 2016).

Bacterial biofilms have been shown to have an immunoprotective effect in the presence of mammalian cells. In Gram-negative *P. aeruginosa* the exopolysaccharide alginate protects the biofilm bacteria from IFN- γ -mediated macrophage killing (Leid et al., 2005). While in an earlier study, Jesaitis et al. (2003) showed that host defence mechanisms are compromised in the presence of *P. aeruginosa* biofilms. In Gram-positive *S. epidermidis* polysaccharide intercellular adhesion protects against phagocytosis and killing by human polymorphonuclear leukocytes and major antibacterial peptides of the skin (Vuong et al., 2004). Alternatively, immune cells have also been shown to produce components that inhibit biofilm formation. For example, lactoferrin, a common secretory component of human neutrophils, has been shown to inhibit *P. aeruginosa* biofilm production (Singh et al., 2002), which is thought to be modulated by scavenging and protease- or oxygen radical-mediated degradation by *P. aeruginosa* (Wilderman et al., 2001). In the present study, we did not screen for any loss of functionality exhibited by the BIA-ALCL tumour cells in the presence of bacterial biofilm. However, given the significant potentiation of BIA-ALCL cell growth following co-culture with bacterial biofilm in comparison to controls, the immunosuppressive effect of biofilms did not likely alter their functionality. It is also possible that the BIA-ALCL cells were able to phagocytose the bacterial cells detaching from the biofilm.

Future studies are needed to further investigate the effects of experimental parameters, including co-culture incubation time, initial number of BIA-ALCL tumour cells and bacteria, and different textured implant surface types. However, whether bacterial detachment from the implant shell is inevitable with our co-culture system, we could therefore investigate what effect, if any, the detached planktonic bacteria have on the mammalian cells. Ultimately, we want to compare the interactions of BIA-ALCL cells co-cultured with biofilm to those of other cell lines and normal cells co-cultured with biofilm to gain insight into the immune response to biofilm-related infections and elucidate their role in the pathogenesis of BIA-ALCL.

Chapter IX.

Effect of TLR4 on LPS stimulation of BIA-ALCL tumour cells

9.1. Introduction

In Chapter VI and VIII we identified strong proliferative responses to LPS stimulation in patient-derived BIA-ALCL tumour cells and established BIA-ALCL cell lines. The mechanism by which this response is occurring we postulate is likely through Toll-like receptor 4 (TLR4). TLRs are pattern recognition receptors in mammals that recognise damage-associated molecular patterns and pathogen-associated molecular patterns, including LPS (Akira et al., 2001, Nagai et al., 2002, Yamamoto et al., 2003, Lucas and Maes, 2013).

TLR4 is part of the innate immune system. The mechanism by which LPS triggers TLR4 is a complex process, which in turn triggers both Myeloid differentiation factor 88 (MyD88)-dependent and MyD88-independent or TIR domain-containing adaptor inducing IFN-beta (TRIF)-dependent pathways (Figure 9.1) (Akira et al., 2001, Lucas and Maes, 2013). Signalling through the MyD88-dependent pathway via Toll/interleukin-1 receptor (TIR) domain-containing adaptor protein (TIRAP) is responsible for early phase transcription factor nuclear factor kappa-light-chain enhancer of activated B-cells (NF- κ B) and mitogen-activated protein kinase (MAPK) activation that facilitates the induction of proinflammatory cytokines, including IL-6 and TNF- α (Lucas and Maes, 2013) (Figure 9.1). Alternatively, the TRIF-dependent pathway via TIR domain-containing adaptor inducing IFN-beta-related adaptor molecule (TRAM) and TRIF activates interferon

regulatory factor 3, which culminates in the induction of type 1 interferons (IFN- β - and IFN-inducible genes) (Figure 9.1) (Lucas and Maes, 2013).

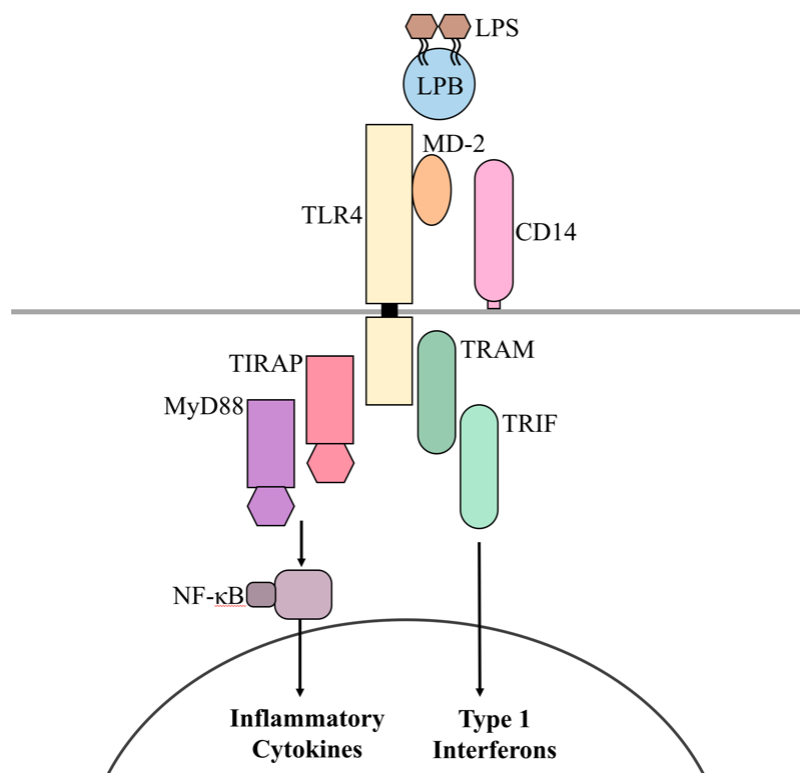


Figure 9.1. Overview of TLR4 signalling.

TLR activation occurs through receptor dimerisation where TLR4 builds homodimers. TLR4 activation ensues when LPS binds to LPS-binding protein (LBP). CD14 and myeloid differentiation factor-2 (MD-2) are required for TLR4 dimerisation. TLR4 signalling can follow two different intracellular pathways: (i) MyD88-dependent pathway via TIRAP induces the transcription factor NF- κ B resulting in the release of inflammatory cytokines and (ii) MyD88-independent pathway via TRAM and TRIF leads to the release of type 1 interferons.

The aim of this Chapter was to investigate whether LPS stimulation is mediated by TLR4 in BIA-ALCL tumour cells. We inhibited TLR4 signalling using a TLR4 inhibitor peptide kit that contains a TLR4 inhibitory peptide consisting of an 11 amino acid inhibitory sequence, KYSFKLILAEY (Novus Biologicals; In Vitro Technologies). The peptide binds to TLR4 and its cytoplasmic adaptors, TIRAP and TRAM, interfering with TLR4-TIRAP and TLR4-TRAM interactions (Lysakova-Devine et al., 2010). Specifically, it is thought that the TLR4 inhibitor binds

to the TIR domains of the receptor and adaptor proteins. However, the exact binding sites and inhibitory mechanism remain to be fully elucidated (Lin et al., 2012, Piao et al., 2013).

9.2. Optimisation of TLR4 inhibitor peptide

The aim of this optimisation experiment was to determine the optimum concentration of the TLR4 inhibitor peptide by titration assay.

9.2.1. Preparation of TLR4 inhibitory peptide

The TLR4 inhibitor peptide kit contains a viral inhibitor peptide of TLR4 (VIPER; molecular weight, 2780.3) and a control peptide or CP7 (control sequence – RNTISGNIYSA; molecular weight, 2601.0). Both peptides were brought to RT and centrifuged briefly (753 x g, 2 min at RT) prior to opening the lids. 5 mM stock solutions of VIPER and CP7 were prepared by adding 72 µL and 76 µL of sterile water to the tube of peptide, respectively, according to the manufacturer's instructions. For the titration assays, these stock solutions were diluted further in DMEM to make working solutions ranging from zero to 30 µM.

9.2.2. TLR4 inhibition assay on BIA-ALCL tumour cells

BIA-ALCL tumour cells were harvested by centrifugation at 753 x g for 5 min at 22°C and resuspended in complete DMEM at a concentration of $10^{5.5}$ cells/mL and seeded into triplicates wells (100 µL/well) of a 96-well plate prefilled with 10 µL of TLR4 inhibitor peptide or control peptide at concentrations, 0.5, 1.0, 2.5, 5.0, 7.5, 15.0 and 30.0 µM as shown in Table 9.1. The plate was incubated for 2 hr prior to TLR4 activation with LPS. We chose 2 hr preincubation with inhibitor and control peptides as previous studies showed this was sufficient for VIPER to potently inhibit TLR4-mediated responses in the human embryonic kidney cell line 293 and murine leukaemia monocyte-macrophage cell line RAW264.7 (Lysakova-Devine et al., 2010, Sahoo et al.,

2018). After which, either 10 µg/mL of LPS was added for test cells or 10 µL of complete DMEM was added for control, unstimulated cells and incubated a further 72 hr at 37°C, 5% CO₂.

Table 9.1. Titration assay to determine optimum TLR4 inhibitor concentration.

	1	2	3	4	5	6	7	8	9
LPS (10 µg/mL)	-	+	+	+	+	+	+	+	+
VIPER (µM)	0	0	0.5	1.0	2.5	5.0	7.5	15.0	30.0
CP7 (µM)	0	0	0.5	1.0	2.5	5.0	7.5	15.0	30.0

9.2.3. MTT assay to determine inhibition of LPS-induced TLR4 activation

The inhibition of LPS-induced TLR4 activation by VIPER was measured with MTT utilising the established protocol in Section 6.3.

Results

We found 30 µM of TLR4 inhibitor peptide/VIPER produced total inhibition of LPS-induced activation being greater than 50% reduction in SI values lower than 30 µM of control peptide, CP7 (SI: VIPER, 1.4; CP7, 3.9) (Figure 9.2). VIPER concentrations at 5.0 (3.8) (~10% reduction), 7.5 (3.3) (~20% reduction) and 15.0 µM (2.3) (~60% reduction) also showed some degree of inhibition (Figure 9.2).

Therefore, we established the optimum concentration of the TLR4 inhibitor peptide is 30 µM and used this concentration in all subsequent inhibition assays.

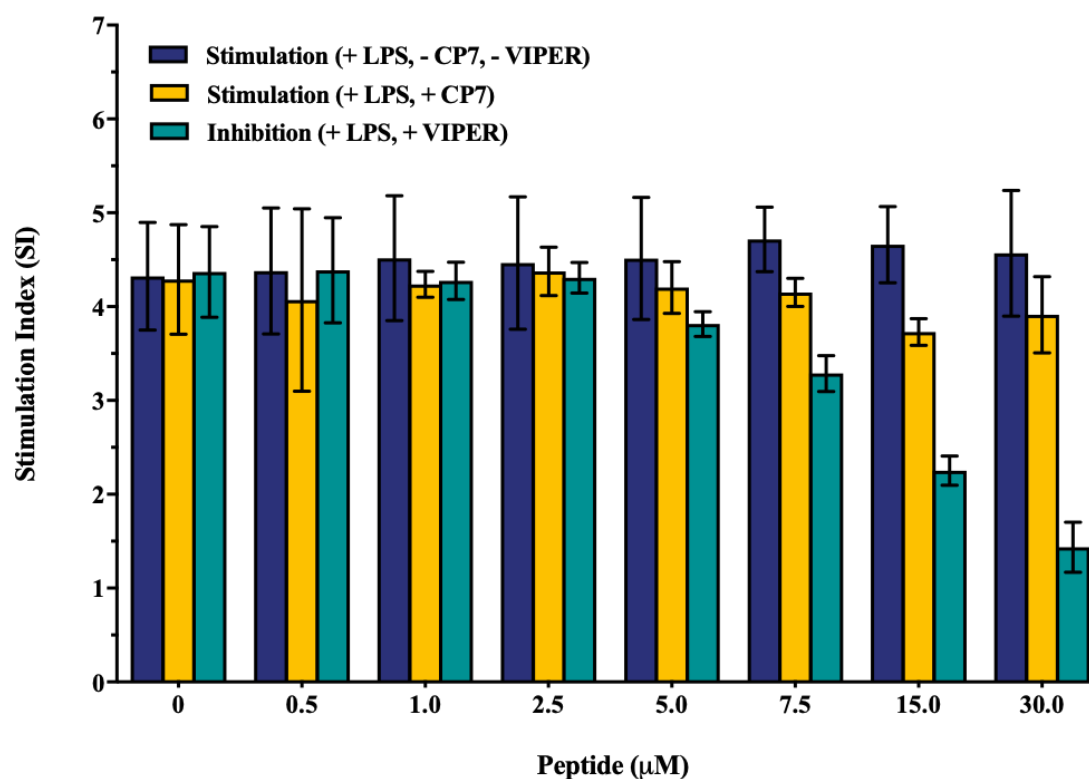


Figure 9.2. Titration assay to determine optimum TLR4 inhibitor concentration.

BIA-ALCL cells were incubated with or without TLR4 inhibitor peptide/VIPER or control peptide/CP7 at concentrations, 0.5, 1.0, 2.5, 5.0, 7.5, 15.0 and 30.0 μM, for 2 hr prior to TLR4 activation with 10 μg/mL LPS for 72 hr. Proliferation response (SI) was then measured by MTT. Values are the means \pm SEM of three technical replicates.

9.3. Materials and Methods

9.3.1. Tumour cells/cell lines

BIA-ALCL tumour cells

Seven female patients presenting with Stage 1 BIA-ALCL disease participated in this study (patients 1610, 1627, 1701, 1713, 1714, 1802, 1825) (Table 5.1, Section 5.3.1.). BIA-ALCL tumour cells were harvested fresh from the serous fluid and/or tumour mass as described in Section 2.5.1. Two of the BIA-ALCL cell lines, TLBR-2 and TLBR-3, were also utilised (Table 2.2, Section 2.5.1.).

Plasma

Plasma from peripheral blood of two BIA-ALCL patients (1714 and 1825; Table 5.1, Section 5.3.1.) were also analysed and isolated as detailed in Section 2.5.1.

9.3.2. TLR4 inhibition assays

BIA-ALCL cells were harvested by centrifugation ($753 \times g$ for 5 min at 22°C) and resuspended in complete DMEM at a concentration of $10^{5.5}$ cells/mL and seeded into triplicates wells (200 μL /well) of a 96-well plate prefilled with 20 μL of 30 μM TLR4 inhibitor peptide (VIPER) or control peptide (CP7). The plate was incubated for 2 hr prior to addition of 10 $\mu\text{g}/\text{mL}$ of LPS for test cells or 20 μL of complete DMEM for control, unstimulated cells. Cells were incubated for 72 hr at 37°C , 5% CO_2 . After which, the culture supernatants were collected to determine LPS-induced TNF- α production using an enzyme-linked immunosorbent assay (ELISA), and cell proliferation and viability by MTT.

9.3.3. Enzyme-linked immunosorbent assay for TNF- α

LPS-induced TNF- α production was measured by ELISA. ELISA kit for TNF- α (Novex®; Thermo Fisher Scientific) contained a 96-well microtitre plate precoated with immunoaffinity-purified anti-human TNF- α antibodies, and the assays were performed following the manufacturer's instructions. Standards and samples, 100 μL (diluted 2:3 in either incubation buffer (50 μL) for standards and plasma samples or standard diluent buffer (50 μL) for BIA-ALCL cells) were added to the wells of the plate and incubated for 2 hr at RT. The wells were aspirated and washed four times with wash buffer. 100 μL of Human TNF α Biotin Conjugate solution was then added to all wells and incubated for 1 hr at RT. The solution was aspirated and the wells washed four times with wash buffer and incubated for 30 min at RT with 100 μL of Streptavidin-horseradish peroxidase solution. After removal of non-bound horseradish peroxidase conjugate by

washing (four times with wash buffer), 100 μ L of stabilised Chromogen was added to all wells and incubated for 30 min at RT in the dark. The reaction was stopped by the addition of 100 μ L of Stop solution. The absorbency of the ELISA was read at 450 nm with a PHERAstar microplate reader. Stabilised Chromogen was used as a blank. Standard curves for the human TNF- α ranging from 0 to 1000 pg/mL were constructed by linear regression and plotted as a linear curve. TNF- α concentrations of experimental samples were calculated with Microsoft Excel (Version 16, Microsoft Corp., Redmond, Washington, USA).

9.3.4. *In vitro* cell proliferation assay

LPS-induced TNF- α production was also measured by MTT as outlined in Section 6.3.

9.3.5. Statistical analysis

All statistical analyses were performed in GraphPad Prism 7.0. To test normality of data distribution, the Shapiro-Wilk test was used. Differences in LPS-induced TNF- α production and proliferation responses following stimulation, inhibition or no stimulation of BIA-ALCL cells with LPS were analysed using two-way ANOVA. If significant differences were found, then Tukey's multiple comparisons post-hoc test were employed. *P* values less than or equal to 0.05 were considered statistically significant.

9.4. Results

9.4.1. Clinical features

Seven BIA-ALCL patients, including patient-derived tumour cells from six patients (85.7%) presenting with a unilateral malignant effusion (patients 1610, 1701, 1713, 1714, 1802, 1825), and from one patient (14.2%) who presented with a tumour mass following infection (patient

1627), were included in this study (Table 5.1, Section 5.3.1.). In addition, PBMC purified from two BIA-ALCL patients (1714, 1825) were also tested (Table 5.1, Section 5.3.1.). The mean patient age was 44.7 years (range, 33 to 58 years) and the mean duration of time between insertion of implants and diagnosis of BIA-ALCL was 7.87 years (range, 3.5 to 13 years). In two patients, the indication for breast implants was postmastectomy reconstruction and in the remaining five patients, the indication for implants was cosmetic augmentation. In one patient the diagnosis of BIA-ALCL was preceded by CC. All patients were exposed to textured implants upon diagnosis. Silimed PU textured implants accounted for 57.1% and Allergan Biocell accounted for 42.9% of the implants used in this series. All BIA-ALCL patients were treated with capsulectomy and removal of implants.

9.4.2. Standard curve for TNF- α ELISA

The concentration of TNF- α in the BIA-ALCL cells and plasma was calculated from the standard curve, which was constructed using the relative absorbance from solutions of human TNF- α with known concentrations (Figure 9.3) The equation of the line from the standard curve was determined to be $y = 291.72x - 43.355$ with a coefficient of determination (R^2) of 0.9939. This line equation was used to calculate the concentration of TNF- α in the stimulated, inhibited and unstimulated BIA-ALCL cells.

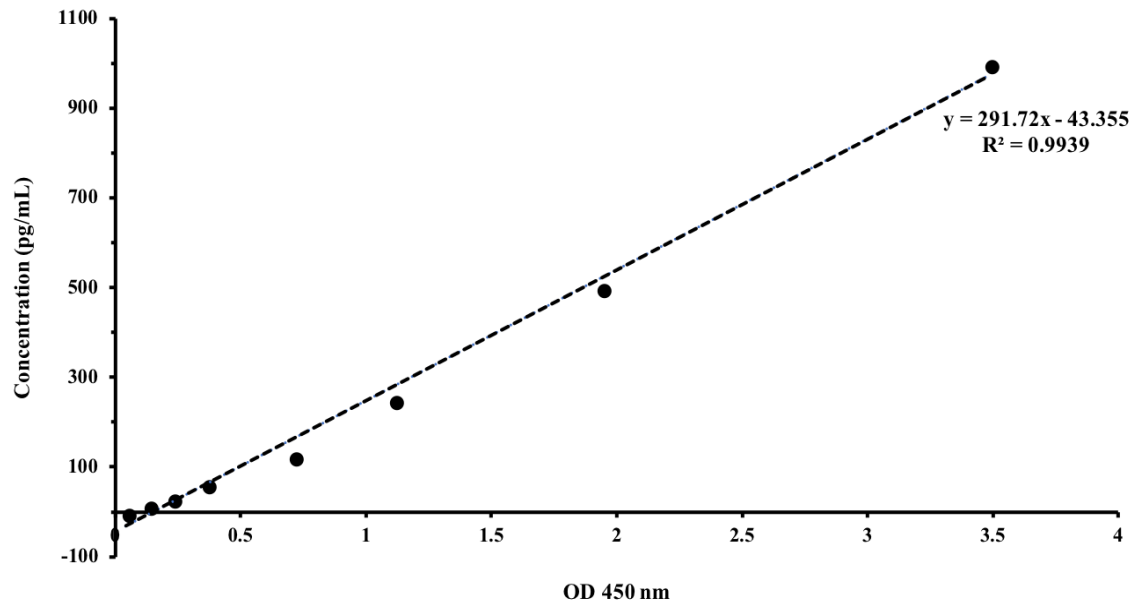


Figure 9.3. Standard curve generated for human TNF- α ELISA.

Standards ranged from 1000, 500, 250, 125, 62.5, 31.2, 15.6, and 0 pg/mL human TNF- α and absorbance was measured at an optical density of 450 nm wavelength. The equation of the line from the standard curve was determined to be $y = 291.72x - 43.355$ with a R-squared of 99.39%.

9.4.3. TLR4 inhibition

BIA-ALCL tumour cells were pretreated with 30 μ M of TLR4 inhibitor peptide or control peptide prior to stimulation with 10 μ g/mL of LPS for 72 hr. After which, supernatants were harvested and measured by ELISA for TNF- α and for cell viability by MTT.

TNF- α ELISA

The TLR4 inhibitor peptide but not the CP7 control peptide inhibited LPS-induced TNF- α production in all BIA-ALCL tumour cells (pg/mL: 80.82 (1610), 47.66 (1627), 125.45 (1701), 141.69 (1714), 110.97 (1825), 87.63 (TLBR-3)) and reached significance in the majority of cells ($P < 0.05$), except TLBR-2 (62.15) ($P = 0.0857$) and patients 1713 (68.86) ($P = 0.4746$) and 1802 (18.20) ($P = 0.1432$) (Figure 9.4). While unstimulated BIA-ALCL cells (76.83 (1610), 58.46 (1627), 94.05 (1701), 41.34 (1713), 116.90 (1714), 92.10 (1825), 45.81 (TLBR-2), 65.06 (TLBR-3)) had significantly less TNF- α than the LPS-stimulated cells inhibited with control peptide

(181.95 (1610), 91.52 (1627), 193.72 (1701), 83.83 (1713), 234.75 (1714), 186.91 (1825), 89.86 (TLBR-2), 125.94 (TLBR-3)) ($P < 0.05$), except patient 1802 (no stimulation, 25.69; stimulation, 42.70), $P = 0.3837$ (Figure 9.4). The mean amount of TNF- α in the plasma of the two BIA-ALCL patients was 85.48 pg/mL (patient 1714) and 73.19 pg/mL (patient 1825) (Figure 9.4). This is higher than the TNF- α plasma concentration reported in a healthy control population (8.7 pg/mL) and in patients with chronic lymphocytic leukemia (16.4 pg/mL), aged between 13 to 80 years (Ferrajoli et al., 2002).

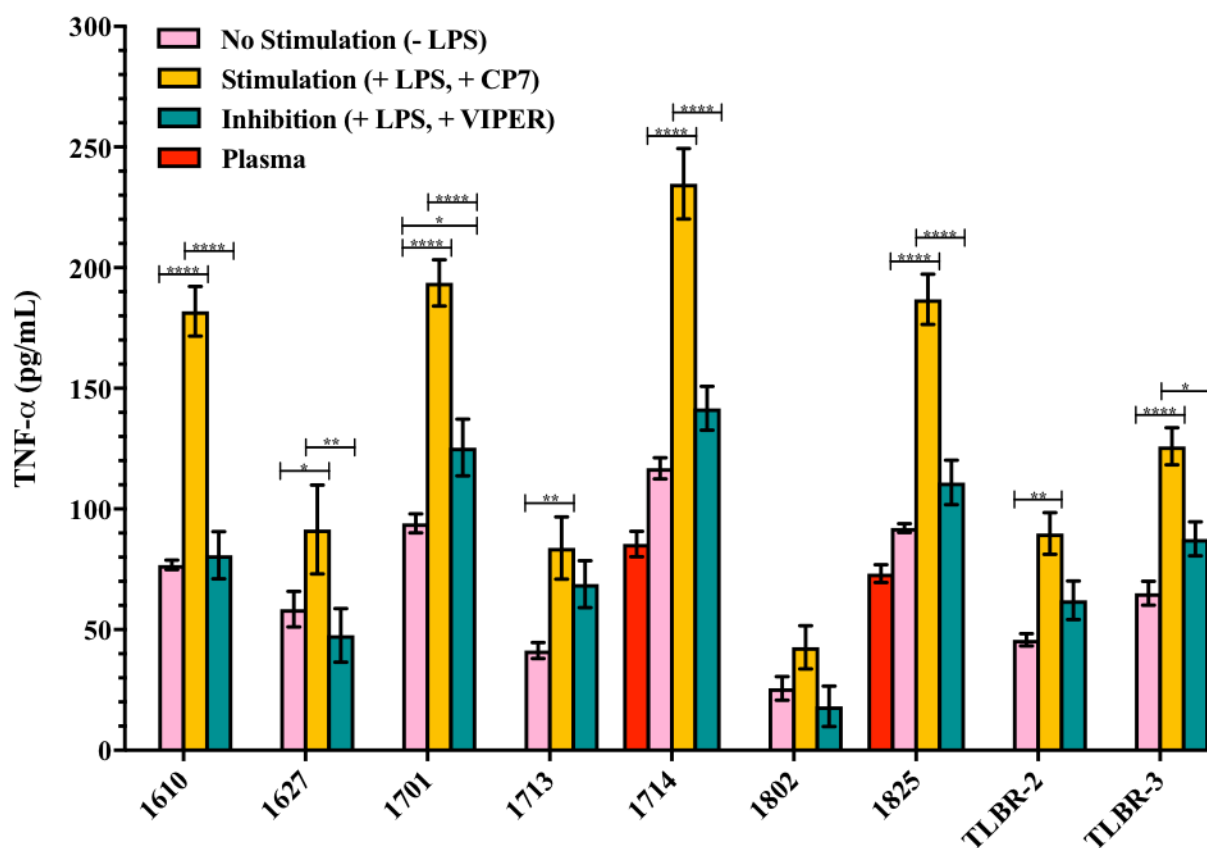


Figure 9.4. Inhibitory effect of the TLR4 inhibitor peptide on LPS-mediated TLR4 activation in BIA-ALCL cells as measured by ELISA. Values are the means \pm SEM of three technical replicates. Significantly different at $*P \leq 0.05$, $**P \leq 0.01$, $***P \leq 0.0001$.

Cell proliferation response following stimulation, inhibition and no stimulation

The addition of TLR4 inhibitor peptide (SI: 5.3 (1610), 2.5 (1627), 4.6 (1701), 4.9 (1714), 5.2 (1825), 3.5 (TLBR-2), 5.1 (TLBR-3)) resulted in lower proliferative responses than the CP7 control peptide (9.6 (1610), 5.1 (1627), 8.6 (1701), 10.4 (1714), 9.0 (1825), 6.4 (TLBR-2), 8.6 (TLBR-3)) in all BIA-ALCL cells stimulated with LPS and this was significant in the majority of cells ($P < 0.05$), except for patients 1713 (inhibition, 3.7; stimulation, 5.4) ($P = 0.4253$) and 1802 (inhibition, 2.9; stimulation, 4.7) ($P = 0.2546$) (Figure 9.5).

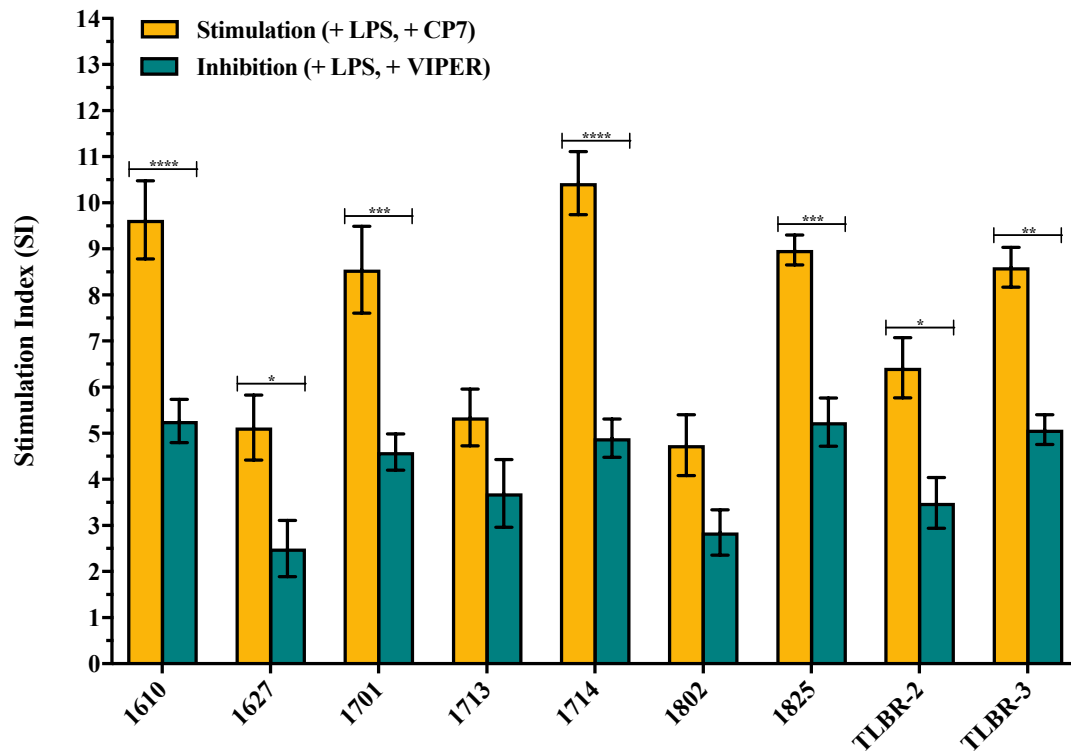


Figure 9.5. Inhibitory effect (SI) of the TLR4 inhibitor peptide on LPS-mediated TLR4 activation in BIA-ALCL cells as measured by MTT. Values are the means \pm SEM of three technical replicates. Significantly different at $*P \leq 0.05$, $**P \leq 0.01$, $***P \leq 0.001$, $****P \leq 0.0001$.

9.5. Discussion

In this Chapter we sought to investigate whether the observed proliferative response to stimulation by LPS occurs through TLR4. We utilised a chemical inhibitor of the TLR4 pathway to determine if this was the likely pathway for bacterial interaction with BIA-ALCL tumour cells.

We identified a consistent inhibition of both the production of TNF- α and the proliferation response by both patient-derived BIA-ALCL tumour cells and established BIA-ALCL cell lines with the addition of the TLR4 inhibitor VIPER. These findings suggest that there is an interaction via TLR4 that directly pushes tumour cells to proliferate and survive in BIA-ALCL.

It is important to note that we still observed high SI values (mean = 4.18) for the inhibited LPS-induced BIA-ALCL cells (+ LPS, + VIPER). Thus, it is probable that the LPS is stimulating the lymphoma cells in a secondary manner. Another possible explanation is that the concentration of the TLR4 inhibitor peptide used was too low to effectively produce total inhibition.

The TLRs are a family of transmembrane receptors that recognise specific molecular patterns associated with a variety of microbial pathogens (Akira et al., 2006, Kawai and Akira, 2010). TLR4 functions as the primary signalling receptor for Gram-negative bacterial LPS (Akira et al., 2006). However, we found that responses to LPS are just dampened and are not completely blocked given that the BIA-ALCL cells are still responding to LPS, which are unlikely to be occurring through TLR4. It is possible that another TLR may also be involved. TLR2 expression is critical for the recognition of many diverse microbial structures. TLR2 responds to lipoproteins derived from Gram-negative and Gram-positive bacteria, viruses, fungi and parasites (Ishii et al., 2008). One of the reasons TLR2 can recognise so many diverse ligands is that it can associate with TLR1 and TLR6 to form a heterodimeric receptor complex on the cell surface (Hajjar et al., 2001). While it is well established that TLR4 is the primary receptor through which LPS is detected, there are some studies to the contrary. For example, it has been shown that TLR2 rather than TLR4

recognise LPS or lipid A from *Leptospira interrogans* (Nahori et al., 2005). This was attributed to the structural differences between this LPS molecule and those of most Gram-negative bacteria, such as enteropathogens (Nahori et al., 2005). Such that, lipid A structures that are unable to signal through TLR4 are able to signal through TLR2, and those of other TLR ligands could compensate for a relative lack of TLR4 signalling (Girard et al., 2003, Smith et al., 2003). Thus, it could be that our BIA-ALCL cell lines have more robust signalling through other innate immune receptor pathways. Moreover, it is reasonable to assume that full resistance to Gram-negative bacterial infections requires integration of information from a variety of innate immune receptors (Miller et al., 2005). This is supported by findings from mutant mice that show TLR2-deficient macrophages produced IL-6 and TNF- α in response to LPS or lipid A to the same extent as wild-type macrophages (Akira et al., 2001). In contrast, TLR4-deficient macrophages did not produce any detectable levels of IL-6 or TNF- α (Akira et al., 2001), which suggests that the TLR4 pathway may therefore be the most important for Gram-negative bacteria. Variation in lipid A may be only one strategy bacteria use to escape recognition by the innate immune system. It is probable that the structures of other bacterial ligands, such as lipopeptides and flagellins also vary between species (Miller et al., 2005).

Further studies investigating the expression of TLR2 and TLR4 and their associated accessory proteins in BIA-ALCL cells are needed. In addition, we need to perform the same TLR4 inhibition assays on the cutaneous-ALCL cells, MT-4 cells and normal PBMC to show that the inhibitor peptide prevents LPS proliferation in these cells. Moreover, gene expression studies in BIA-ALCL cells and normal cells will prove useful if it can show the TLR4 expression is just being upregulated in BIA-ALCL cells and hence explain the increased SI under normal cellular proliferation. This work will be important to elucidate the role of Gram-negative bacteria in the pathogenesis of BIA-ALCL.

Chapter X.

General Discussion

BIA-ALCL is a recently recognised and distinct malignancy of T-lymphocytes exclusively associated with textured breast implants used for both aesthetic and reconstructive surgery (Clemens and Miranda, 2015, Doren et al., 2017, Loch-Wilkinson et al., 2017, Srinivasa et al., 2017). A unifying hypothesis has been put forward implicating a combination of high surface area textured implants, bacterial contamination, genetic susceptibility and time of exposure to explain pathogenesis (Loch-Wilkinson et al., 2017). To date, the two most frequently implicated aetiological contributors appear to be the use of textured implants and chronic bacterial stimulation. In this thesis, we investigated the role of implant textures of varying morphology, the interaction of their surface with bacteria and the potential role of chronic bacterial antigen stimulation in the aetiopathogenesis of this disease.

It is postulated that the surface area of the texture provides bacteria with a better substrate on which to proliferate with the complexity of the surface also preventing access of host cells to mount an effective immune response (Loch-Wilkinson et al., 2017). Previous studies have shown textured implants promote higher bacterial growth compared to smooth implants *in vitro* (Jacombs et al., 2014) and in implants removed from patients with chronic implant infection (Hu et al., 2015). However, these studies utilised implants that were either experimental and hence not directly comparable to clinical implants or were obtained clinically but were not representative of all implant types. In Chapter III, we developed an *in vitro* bacterial attachment protocol and utilised

micro CT analysis to further characterise the surface texture of 11 available commercial implant types and their capacity to support bacterial growth. The use of surface and three-dimensional scanning allowed a more accurate morphological assessment of the different implants based on the direct measurement of their surface area and roughness without loss of resolution in higher thickness implant textures. Using this information we were able to group implant surfaces into four categories – high, intermediate, low and minimal, which correlated with bacteria growth. We found that increasing surface area and surface roughness was associated with significant potentiation of bacterial attachment and growth for both Gram-positive (*S. aureus* and *S. epidermidis*) and Gram-negative (*P. aeruginosa* and *R. pickettii*) organisms. As predicted, the high surface area Silimed PU textured implants grew significantly more bacteria whilst the minimal surface area implants grew significantly less bacteria for all species at 24 hr. The intermediate surface area implants, including Polytech Mesmo and the salt-loss produced implants, Eurosilicone and Allergan Biocell, also correlated with bacterial attachment and growth but we found this did not differ from the high surface PU implants for *S. epidermidis* and *P. aeruginosa*, which likely reached maximal growth capacity earlier than the other species. The correlation of surface area/roughness with propensity for bacterial growth links our proposed classification of implant outer shells (high, intermediate, low and minimal) to a functional outcome. The application of which will be a valid tool to help surgeons select the optimal implant surface for breast augmentation and reconstruction patients.

In Chapter IV, we investigated the influence of two textured miniature implants, type A (manufactured through a proprietary process) and type B (salt-loss produced), on bacterial attachment in an *in vivo* porcine model (Tamboto et al., 2010). Following deliberate inoculation of pig breast pockets with human *S. epidermidis*, we found the type B implant had significantly more bacteria attached than the type A implant after being left *in situ* for 11 weeks. Micro CT analysis confirmed the type B implant had a higher surface area and surface roughness in comparison to the minimal surface area type A implant. Thus, we demonstrated both *in vivo* and *in vitro* that greater

surface area textured implants provide a more ideal surface that promotes higher attachment and growth of bacteria. Moreover, the analysis of lymphocytes in both capsules and on the surface of implants contaminated with *S. epidermidis* showed that there is a strong T-cell response. Interestingly, the higher surface area/roughness type B inoculated implants had an increased lymphocytic infiltrate compared with the inoculated type A implants. The higher bacterial load on type B implants may explain the observed higher lymphocyte numbers and predominantly T-cell hyperplasia. This response was likely due to the presence of bacteria and not innate physiological defences considering there was a significant linear correlation between the number of T-cells and the number of bacteria.

The findings from this Chapter also highlight the challenge associated with breast implants in that they are placed into a potentially contaminated pocket, with high levels of bacteria present in breast ducts and tissue. This was evident in the low levels of *S. epidermidis* detected in all inoculated implants and the consistent culture of endogenous porcine *Staphylococcus* from explanted control implants. Therefore, it is most likely the biofilm we confirmed visually were composed mainly of natural pig flora rather than the human *Staphylococcus* inoculum. While contamination of the implants with endogenous pig *Staphylococcus* was the likely source of the biofilm observed on non-inoculated specimens. Nevertheless, whether bacterial contamination in prosthetic implants is deliberate or by chance, they will form biofilm once they come into contact with the implant surface. Over time, this biofilm will reach a critical mass that induces a host inflammatory reaction and can lead to ultimate failure of the implant. This is why it is important for anti-infective strategies to be used during surgery to minimise the bacterial load in the first place so that biofilm contamination remains below the threshold for host response.

The higher bacterial growth in higher surface area textured implants *in vitro* and *in vivo* and the predominantly T-cell lymphocytic infiltrate produced from this association in pigs adds weight to the theory that BIA-ALCL are being caused by bacterial contamination on the surface of the

implant. In Australia and New Zealand, women with Allergan Biocell textured implants are up to 14 times more likely to develop BIA-ALCL compared with low surface area Mentor Siltex textured implants (Loch-Wilkinson et al., 2017). Similarly, the high surface area Silimed PU texture is associated with a 10 times higher risk of BIA-ALCL but is likely to be an underestimate given they have been available for a shorter time in Australia (Loch-Wilkinson et al., 2017). Moreover, Hu et al. (2015) have shown a linear relationship between bacterial biofilm load and the number of CD4+ T-lymphocytes in human specimens recovered from patients with chronic implant infection. In Chapter V, we investigated new cases of BIA-ALCL to determine the bacterial load and host response in fresh specimens. In our cohort of patients, all were exposed to textured implants with Silimed PU and Allergan Biocell accounting for over 80% of implants followed by Nagor textured implants. It is postulated that these high surface area textured implants act as a passive conduit for the growth and proliferation of bacteria, which, once they reach a threshold, promotes inflammation that causes ongoing immune activation and malignant transformation in susceptible hosts over time (Doren et al., 2017, Loch-Wilkinson et al., 2017). Indeed, we identified a high bacterial load, present as a biofilm, in explanted implants and capsules from BIA-ALCL patients. However, we found this was no different to the number of bacteria present in contralateral non-ALCL breast samples and samples taken from non-tumour contracture patients. There was also no difference in the number of bacteria attached to the different textured implant types between BIA-ALCL breasts and contralateral normal breasts. Moreover, we found no correlation between increasing numbers of bacteria and the number of lymphocytes. Malignant T-cells are commonly CD4 positive but we detected low numbers of these cells in BIA-ALCL capsules when compared to non-tumour capsules. Indeed, late onset seroma and peri-prosthetic effusion is the most common presentation, and few patients present with a firm mass. We sampled BIA-ALCL capsules in ten patients with late seroma. In these patients, the malignant cells are restricted to the seroma and there is no evidence of tumour evasion into the capsule (Clemens et al., 2016). This might explain the low

CD4+ T-cell count we obtained. While the only patient in the cohort to present with a tumour mass (patient 1627) showed an increasingly high number of CD4+ T-cells in their capsule compared to their non-ALCL normal breast capsule. Further studies measuring the levels of T- and B-lymphocytes in the seroma fluid of BIA-ALCL patients would provide a more accurate analysis. Future studies should also include determination of the microbiome in additional BIA-ALCL and non-tumour contracted cases to shed more light on which bacterial strains could be driving cancer development.

It has previously been shown that the microbiome of BIA-ALCL specimens contain significantly more Gram-negative bacteria of some species than the microbiome surrounding non-tumour implant capsules, which contain significantly more Gram-positive *Staphylococcus* (Hu et al., 2016). In Chapters VI and VII, we therefore evaluated the role of Gram-negative and Gram-positive bacteria, respectively, in the aetiopathogenesis of BIA-ALCL. Specifically, we investigated whether bacterially derived antigenic drivers (LPS, SEA and TSST-1) would interact differentially with BIA-ALCL tumour cells as compared with tumour cells derived from the related cutaneous form of ALCL, an MT-4 immortal T-cell leukaemia cell line, and with PBMC harvested from BIA-ALCL patients, individuals exposed to breast implants *in vivo* and patients undergoing primary augmentation. We also compared the proliferative responses of these cells to bacterial antigens with their responses to the plant mitogen, PHA. We found that BIA-ALCL tumour cells display a unique response to Gram-negative bacterial LPS. This proliferative response was absent in all the other cell lines tested including the cutaneous form of ALCL and PBMC purified from BIA-ALCL patients. Whilst the BIA-ALCL tumour cells responded equally to the Gram-positive staphylococcal superantigens, SEA and TSST-1, and to PHA stimulation, these responses were significantly lower than those observed for LPS. In contrast, the cutaneous-ALCL cells and the PBMC derived from contracture patients responded maximally to both staphylococcal superantigens (SEA and TSST-1) and to PHA stimulation. While a more predictable higher

response to PHA by the MT-4 cell line and PBMC purified from BIA-ALCL patients and normal healthy controls was also shown. Interestingly, patient 1627 (tumour mass presentation) had the lowest maximum SI to LPS-induced stimulation in the cohort and also had low maximal responses to staphylococcal superantigens. Although we predicted stronger responses to Gram-positive antigens since the mass was preceded with an infection, which was most likely *Staphylococcus* spp. based on culture results. The differential response to LPS could be because we analysed tumour cells purified from the mass rather than an effusion around the implant. This suggests that there is an observed difference between the LPS response for patients with mass disease versus seroma disease, strengthening the hypothesis that seroma is likely reactive to the presence of bacterial antigens whilst mass disease is the true malignancy.

In Chapter VIII, we further subjected the BIA-ALCL cells to co-culture with live bacterial biofilm and textured implant shells. We showed in the presence of *P. aeruginosa*, *R. pickettii* and MRSA biofilms and textured implant outer shells, there is significant potentiation of BIA-ALCL tumour cell growth compared with the exposure of BIA-ALCL cells to the implant shell alone. These findings reinforce the importance of bacteria in the stimulation and proliferation of BIA-ALCL cells. The presence of the textured breast implant shell alone demonstrated low proliferative responses, which supports the view that implants act as a passive conduit for the growth and proliferation of bacteria instead of acting as an inflammatory stimulant (Bizjak et al., 2015, Evren et al., 2017). Co-culture of BIA-ALCL cells with *P. aeruginosa* showed the strongest proliferative response, followed by *R. pickettii* and MRSA. We also showed these responses were equal to the proliferation induced by LPS only. The augmented proliferative response seen by co-culture of *P. aeruginosa* species with tumour cells has further reinforced the importance of Gram-negative bacterial growth in the stimulation and proliferation of BIA-ALCL cells. In contrast, in the presence of *S. epidermidis*, the proliferation response of BIA-ALCL cells was considerably lower than the other bacterial species and those induced following stimulation with LPS. This was unexpected

considering that we utilised BIA-ALCL tumour cells from patient 1714 whose explanted specimens were culture positive for *S. epidermidis*. It was likely that there was an insufficient number of bacteria attached to the implant surface to begin with, given that we found the log reduction of *S. epidermidis* attached to the implant before and after co-culture was high, even in the absence of BIA-ALCL cells. Further studies are needed to ensure that the starting number of bacteria attached to the implant are optimal and more importantly, are the same for each of the species to allow for statistical comparisons to be made. The application of our co-culture system of BIA-ALCL tumour cells and bacterial biofilm is not yet refined and further work is ongoing to achieve a stable balance of the cancerous cells and biofilm.

The significant potentiation of BIA-ALCL tumour cell growth to LPS stimulation and in co-culture with *P. aeruginosa*, *R. pickettii* and MRSA biofilm are consistent with the growing body of evidence around the epidemiology of BIA-ALCL that bacterial presence acts as a significant proinflammatory transformative driver in this lymphoma. The detection of a Gram-negative shift in the microbiome of BIA-ALLC tumour cells (Hu et al., 2016) is also consistent with our results. The reporting of clusters of disease around a single surgeon experience (Hu et al., 2015, Loch-Wilkinson et al., 2017) and the higher risk demonstrated for implants with a high surface area/roughness (Loch-Wilkinson et al., 2017), reinforce the importance of bacterial contamination as a significant pathogenetic mechanism.

The role of chronic bacterial infection driving malignant transformation into lymphoma have been clearly established for *H. pylori* and gastric mucosal associated lymphoid tissue (MALT) lymphoma (Parsonnet and Isaacson, 2004). The eventual evidence for pathogenesis came when six patients with proven gastric MALT lymphoma regressed completely following eradication of *H. pylori* after antibiotic treatment (Miura et al., 1996). Our findings in BIA-ALCL are beginning to mirror the early evidence that eventually proved bacterial pathogenicity of MALT lymphomas. However, in the case of BIA-ALCL, the infectious load is likely to be low grade, indolent and may

well be polymicrobial with the release of both Gram-negative and Gram-positive bacterial antigens into the peri-implant milieu. Depending on the proportion and/or species of Gram-negative bacteria to Gram-positive bacteria different bacterial antigens will be released, which promotes a different sort of immune response that leads to malignant transformation. Because infected breast implants cannot be treated successfully by antibiotic therapy, surgical removal can be seen as the equivalent anti-microbial therapy. The complete regression for patients with early stage disease by surgical implant removal supports the hypothesis that removal of bacterial antigenic drivers can effectively treat the tumour. This may also explain the absence of an observed increase in advanced cases of BIA-ALCL prior to its recognition as the early stage lymphoma was effectively treated by implant exchange alone.

A number of other bacterial pathogens are now also being linked to lymphoma. *Chlamydia psittaci* has been reported in ocular adnexal MALT lymphomas with regression of the tumour reported following anti-microbial therapy (Ferrerri et al., 2004, Ferreri et al., 2005, Ferreri et al., 2008). Potentiation of cutaneous T-cell lymphomas have also been linked to bacterial infection/antigen exposure (Woetmann et al., 2007). More relevant to BIA-ALCL, a patient with cutaneous-ALCL has been shown to have infection with *C. pneumoniae* and herpes virus 8 (Borghi et al., 2013). Their disease regressed with a combination of surgical treatment and antibiotic treatment (Caselli et al., 2016). Detection of *C. pneumoniae* DNA/RNA sequences in Sézary syndrome (a precursor of T-cell cutaneous lymphoma) has also been described (Abrams et al., 2001). Furthermore, bacterial antigens were present and potentiated activation and transformation of this early form of lymphoproliferation into clonal expansion indicating a path toward T-cell transformation (Abrams et al., 2001).

The underlying mechanisms for bacterially driven mutagenesis in BIA-ALCL are most likely multifactorial and include other proinflammatory mechanisms through both the innate and adaptive immune systems. These include the production of reactive oxygen species and

accumulation of mutational load (Arabski et al., 2005), the production of direct lymphomagenic and oncogenic factors (Ando et al., 2002), e.g. CagA from *H. pylori* (Wroblewski et al., 2010, Chaturvedi et al., 2012) and antigen restriction of T-cell receptor expression selecting out clonal responses of lymphocytes (Irwin et al., 1992, Irwin et al., 1993, Kadin et al., 2016). In Chapter IX, we investigated whether the likely pathway for the unique response of BIA-ALCL cells to LPS stimulation both directly in the proliferation assays and in co-culture with textured implants occurs through TLR4. Using a TLR4 inhibitor peptide we identified a consistent inhibition of TNF- α production and reduced cell proliferation by BIA-ALCL tumour cells. These findings are consistent with the previously described mechanism of interaction of LPS with TLR4 (Akira et al., 2001, Lucas and Maes, 2013) and suggest that interaction via TLR4 directly pushes tumour cells to proliferate and survive in BIA-ALCL. However, we speculate that LPS stimulation may also be occurring in a secondary manner given the TLR4 inhibited, LPS-induced BIA-ALCL cells still produced moderate SI values. It is possible other TLRs are involved, such as TLR2, which have been implicated in the recognition of LPS from Gram-negative bacteria containing structural variations in the lipid A region of LPS (Miller et al., 2005, Nahori et al., 2005). Therefore, more studies are needed to confirm TLR as a mechanism for tumourgenesis and to examine the potential for TLR blocking agents to potentially minimise the risk of the development of BIA-ALCL.

The interaction of bacterial antigens with BIA-ALCL tumour cells, creation of an immune synapse (mediated by antigen presenting cells, MHC class I/II, cytokine milieu), can then progress to effect multi-step T-cell differentiation (Matis et al., 1983, Pontzer et al., 1992). The T-lymphocyte is a principal player in the adaptive immune response and is pushed from a naïve state to differentiate into multiple effector pathways by antigenic stimulation (Pennock et al., 2013). The cell of origin for BIA-ALCL remains unclear. It may result from either a CD4 derived Th1, Th17 or perhaps a more primordial progenitor innate lymphoid cell (Turner, 2017). Th1/Th17 cells are antigen driven memory T-cells and so if antigen activated T-cell precursors of BIA-ALCL cells

mimic polarisation and maturation of non-malignant Th memory T-cells, their phenotype may determine the time required to initiate BIA-ALCL (Kadin et al., 2016). The late onset of BIA-ALCL (around seven to ten years) after initial implantation is consistent with these findings. Moreover, exposure to bacterial pathogens via the T-cell receptor and/or TLR can preferentially push T-cell into a Th17 phenotype (Tan et al., 2016). The Th17 phenotype supports the contention that BIA-ALCL may arise from a chronic inflammatory process and that possibly chronic bacterial stimulation is essential for the initiation and progression of the disease.

The role of bacteria, biological pathways and host predisposition to track antigenic stimulation and transformation of T-cells into lymphoma is a novel and previously unexplored area of research. This has important implications, where in the short term this will translate into greater ability to risk stratify BIA-ALCL patients presenting with seroma if such bacteria or bacterial antigens are found in the seroma fluid. In addition, antimicrobials targeting the offending bacteria can be bound to implants thus preventing biofilm and resulting chronic inflammation. The wider implications is that the bacterial microbiome is being increasingly recognised as a potential cause of common cancers, including breast (Urbaniak et al., 2014, Chan et al., 2016, Kwa et al., 2016, Yang et al., 2017), colorectal (Buc et al., 2013, Sears and Garrett, 2014), gastric (Noto and Peek Jr, 2017) and oral cancers (Wang and Ganly, 2014). Indeed, 30% of BIA-ALCL patients have had a prior history of breast cancer that required reconstructive surgery (Loch-Wilkinson et al., 2017). Thus, the mechanism(s) whereby shift in bacterial populations that we carry on our skin, breast, gut, oral cavity and medical prosthetics influence the genesis of malignancy may provide us with a greater opportunity for prevention and treatment of cancer in the future.

Conclusion

The incidence of BIA-ALCL is increasing worldwide and heightened awareness of this disease is required to recognise it early and ensure early removal of the breast implant. The studies

presented in this thesis provide important new insights into the biology of BIA-ALCL, likely due to the use of higher surface area/roughness textured implants and chronic bacterial antigen stimulation. The differential proliferative response of BIA-ALCL tumour cells to LPS, and to Gram-negative and Gram-positive bacteria in co-culture, support the hypothesis that bacterial antigens are critical in the pathogenesis of BIA-ALCL. Cell proliferation is likely mediated via the TLR4 receptor and represents another pathway for bacteria to drive the genesis of malignancy. Further studies are needed to elucidate the role of TLR as a mechanism for tumourgenesis and to examine the potential for TLR blocking agents to potentially minimise the risk of the development of BIA-ALCL. For now, the prevention of bacterial infection on breast implants should be an important goal for surgeons utilising these implants in both aesthetic and reconstructive surgery.

Appendices

Appendix 1. Human ethics approval

Appendix 2. Participant information and consent forms

Appendix 3. BIA-ALCL proforma

Appendix 4. Animal ethics approval

Appendix 5. Animal ethics approval letter

Appendix 6. Permission for reproduction of material from Oxford University Press

Office of the Deputy Vice-Chancellor
(Research)

Research Office
Research Hub, Building C5C East
Macquarie University
NSW 2109 Australia
T: +61 (2) 9850 4459
<http://www.research.mq.edu.au/>
ABN 90 952 801 237



1 September 2016

Dear Professor Deva

Reference No: 5201600427

Title: *Breast implant related infection, biofilm, capsular contracture, cancer*

Thank you for submitting the above application for ethical and scientific review. Your application was considered by the Macquarie University Human Research Ethics Committee (HREC (Medical Sciences)).

I am pleased to advise that ethical and scientific approval has been granted for this project to be conducted at:

- Macquarie University

This research meets the requirements set out in the *National Statement on Ethical Conduct in Human Research* (2007 – Updated May 2015) (the *National Statement*).

Standard Conditions of Approval:

1. Continuing compliance with the requirements of the *National Statement*, which is available at the following website:

<http://www.nhmrc.gov.au/book/national-statement-ethical-conduct-human-research>

2. This approval is valid for five (5) years, subject to the submission of annual reports. Please submit your reports on the anniversary of the approval for this protocol.

3. All adverse events, including events which might affect the continued ethical and scientific acceptability of the project, must be reported to the HREC within 72 hours.

4. Proposed changes to the protocol and associated documents must be submitted to the Committee for approval before implementation.

It is the responsibility of the Chief investigator to retain a copy of all documentation related to this project and to forward a copy of this approval letter to all personnel listed on the project.

Should you have any queries regarding your project, please contact the Ethics Secretariat on

9850 4194 or by email ethics.secretariat@mq.edu.au

The HREC (Medical Sciences) Terms of Reference and Standard Operating Procedures are available from the Research Office website at:

http://www.research.mq.edu.au/for/researchers/how_to_obtain_ethics_approval/human_research_ethics

The HREC (Medical Sciences) wishes you every success in your research.

Yours sincerely

A handwritten signature in black ink, appearing to read 'Tony Eyers', with a stylized flourish at the end.

Professor Tony Eyers

Chair, Macquarie University Human Research Ethics Committee (Medical Sciences)

This HREC is constituted and operates in accordance with the National Health and Medical Research Council's (NHMRC) *National Statement on Ethical Conduct in Human Research* (2007) and the *CPMP/ICH Note for Guidance on Good Clinical Practice*.

Details of this approval are as follows:

Approval Date: 25 August 2016

The following documentation has been reviewed and approved by the HREC (Medical Sciences):

***If the document has no version date listed one will be created for you. Please ensure the footer of these documents are updated to include this version date to ensure ongoing version control.**

Department of Biomedical Sciences
Faculty of Medicine and Health Sciences
MACQUARIE UNIVERSITY NSW 2109



Phone: +61 (0)98502773 / 0422256323
Fax: +61 (0)98123610
Email: karen.vickery@mq.edu.au
Email: anand.deva@mq.edu.au

Chief Investigator's / Supervisor's Name & Title: **A/Professor Karen Vickery and A/Professor Anand Deva**

Participant Information and Consent Form

Name of Project: Breast implant related infection, biofilm, capsular contracture and cancer

You are invited to participate in a study of the biological and immunological causes associated with breast implant capsular contracture (constriction of tissue around the breast implant) and cancer. The purpose of the study is to better understand the causes of these complications.

The study is being conducted by Associate Professor Karen Vickery and Associate Professor Anand Deva of the Faculty of Medicine and Health Sciences. Contact either Karen Vickery on Ph 98502773 / 0422256323, email karen.vickery@mq.edu.au or Anand Deva on Ph 98123890, email anand.deva@mq.edu.au.

If you decide to participate, you will be donating part of the tissue capsule around the breast implant that is to be removed at the time of your surgery. If you are patient with breast cancer, or patient with breast augmentation, 5 ml of peripheral blood maybe taken at the time of surgery when you have IV access, so no additional harm or discomfort should be experienced. Blood samples will be used to look at lymphocytes, proteins and other immunological characteristics.

We will look for evidence of bacteria or the chemicals and cells involved in the immune response to the breast contraction or cancer. There will be no surgery or procedure additional to the operation that has been recommended by your surgeon. Also there will be no additional cost to you. This tissue is normally removed and would be thrown away.

We will be collecting your general medical information and age for comparison between patients and for data analysis. Any information or personal details gathered in the course of the study are confidential. No individual will be identified in any publication of the results. All the data will be kept securely in a locked filing cabinet in a locked room at Faculty of Medicine and Health Sciences, Macquarie University. Only study personnel will have access to the data. A summary of the results of the data can be made available to you on request by contacting either Associate Professor Karen Vickery or Associate Professor Anand Deva, Faculty of Medicine and Health Sciences, 2 Technology Place, Macquarie University 2109.

Participation in this study is entirely voluntary: you are not obliged to participate and if you decide to participate, you are free to withdraw at any time without having to give a reason and without consequence.

I, _____ (*participant's name*) have read (*or, where appropriate, have had read to me*) and understand the information above and any questions I have asked have been answered to my satisfaction. I agree to participate in this research, knowing that I can withdraw from further participation in the research at any time without consequence. I have been given a copy of this form to keep.

Participant's Name: _____
(Block letters)

Participant's Signature: _____ Date: _____

Investigator's Name: _____
(Block letters)

Investigator's Signature: _____ Date: _____

The ethical aspects of this study have been approved by the Macquarie University Human Research Ethics Committee. If you have any complaints or reservations about any ethical aspect of your participation in this research, you may contact the Committee through the Director, Research Ethics & Integrity (telephone (02) 9850 7854; email ethics@mq.edu.au). Any complaint you make will be treated in confidence and investigated, and you will be informed of the outcome.

(INVESTIGATOR'S [OR PARTICIPANT'S] COPY)

Department of Biomedical Sciences
Faculty of Medicine and Health Sciences
MACQUARIE UNIVERSITY NSW 2109



Phone: +61 (0)98502773 / 0422256323

Fax: +61 (0)98123610

Email: karen.vickery@mq.edu.au

Email: anand.deva@mq.edu.au

Chief Investigator's / Supervisor's Name & Title: A/Professor Karen Vickery and A/Professor Anand Deva

Participant Information and Consent Form

Name of Project: Breast implant related infection, biofilm, capsular contracture and cancer

We would like to invite you as a healthy person receiving breast implants to participate in an investigation into breast augmentation complications by donating a small amount of blood. As a patient without any complications we will compare the proteins and cells in your blood against the proteins and cells in blood obtained from patients with breast implant related complications. Your blood will act as a normal control. In this way we hope to better understand the biological and immunological causes associated with breast implant capsular contracture (constriction of tissue around the breast implant) and cancer.

The study is being conducted by Associate Professor Karen Vickery and Associate Professor Anand Deva of the Faculty of Medicine and Health Sciences. Contact either Karen Vickery on Ph 98502773 / 0422256323, email karen.vickery@mq.edu.au or Anand Deva on Ph 98123890, email anand.deva@mq.edu.au.

If you decide to participate, you will be donating 5ml of peripheral blood at the time of surgery when you have IV access, so no additional harm or discomfort should be experienced. There will be no surgery or procedure additional to the operation that has been recommended by your surgeon. Also there will be no additional cost to you.

We will be collecting your general medical information and age for comparison between patients and data analysis. Any information or personal details gathered in the course of the study are confidential. No individual will be identified in any publication of the results. All the data will be kept securely in a locked filing cabinet in a locked room at Faculty of Medicine and Health Sciences, Macquarie University. Only study personnel will have access to the data. A summary of the results of the data can be made available to you on request by contacting either Associate Professor Karen Vickery or Associate Professor Anand Deva, Faculty of Medicine and Health Sciences, 2 Technology Place, Macquarie University 2109.

Participation in this study is entirely voluntary: you are not obliged to participate and if you decide to participate, you are free to withdraw at any time without having to give a reason and without consequence.

I, _____ (*participant's name*) have read (*or, where appropriate, have had read to me*) and understand the information above and any questions I have asked have been answered to my satisfaction. I agree to participate in this research, knowing that I can withdraw from further participation in the research at any time without consequence. I have been given a copy of this form to keep.

Participant's Name: _____
(Block letters)

Participant's Signature: _____ Date: _____

Investigator's Name: _____
(Block letters)

Investigator's Signature: _____ Date: _____

The ethical aspects of this study have been approved by the Macquarie University Human Research Ethics Committee. If you have any complaints or reservations about any ethical aspect of your participation in this research, you may contact the Committee through the Director, Research Ethics & Integrity (telephone (02) 9850 7854; email ethics@mq.edu.au). Any complaint you make will be treated in confidence and investigated, and you will be informed of the outcome.

(INVESTIGATOR'S [OR PARTICIPANT'S] COPY)

BIA - ALCL notification form

REPORTER INFORMATION			
Reporter Name		Signature of reporter	
Date report made			
Does reporter wish for their details to remain confidential		YES <input type="checkbox"/> NO <input type="checkbox"/>	
Name Facility Patient Implanted		Name Facility ALCL Diagnosed	
Suburb or postcode		Suburb or postcode	
Address		Address	
Primary ALCL Contact for further information		Phone Number ()	
Specialty (<i>please tick</i>)		Email	
Plastic/Reconstructive <input type="checkbox"/> Breast/Endocrine <input type="checkbox"/> General <input type="checkbox"/> Other <input type="checkbox"/> <i>Specify</i>			
PATIENT DEMOGRAPHIC INFORMATION			
Patient Medicare number		Date of Birth	
Patient initials		City	State
		Country	Postcode
Patient Gender FEMALE <input type="checkbox"/> MALE <input type="checkbox"/> TRANSGENDER <input type="checkbox"/>			
PAST AND CURRENT MEDICAL HISTORY FORM			
COMORBIDITY INFORMATION			
Does the patient have a history of breast cancer? YES <input type="checkbox"/> NO <input type="checkbox"/> UNKNOWN <input type="checkbox"/>			
<i>If yes, please answer the following questions:</i> Breast Cancer Diagnosis Date _____			
Which breast was affected? RIGHT <input type="checkbox"/> LEFT <input type="checkbox"/> BILATERAL <input type="checkbox"/> NOT REPORTED <input type="checkbox"/>			
Co-morbidities:			
Auto-immune disease <input type="checkbox"/> <i>Specify</i> _____ Coeliac disease <input type="checkbox"/>			
Other malignancy <input type="checkbox"/> <i>Specify</i> _____			
Other <input type="checkbox"/> <i>Specify</i> _____			
IMPLANT/DEVICE INFORMATION FORM			
HISTORY OF BREAST SURGERY			
Please list all breast surgical procedures (e.g. Breast Augmentation, Tissue Expander Placement, Biopsy, Breast Cancer) that the patient had prior to ALCL diagnosis, including dates:			
Procedure 1		DATE	
Procedure 2		DATE	
Procedure 3		DATE	
Procedure 4		DATE	
HISTORY OF PRIOR IMPLANT			
Did the patient have previous implants? YES <input type="checkbox"/> NO <input type="checkbox"/> UNKNOWN <input type="checkbox"/>			
Previous Implant History dates		Time having any implant (<i>years</i>)	
Did the patient have previous expanders? YES <input type="checkbox"/> NO <input type="checkbox"/> UNKNOWN <input type="checkbox"/>			
Previous Expander Dates			
IMPLANT PROCEDURE INFORMATION & DEVICE DETAILS			
Date Implanted	Date Explanted	Time having current implant (<i>years</i>)	
Number of Implants (<i>please tick</i>) UNILATERAL-LEFT <input type="checkbox"/> UNILATERAL-RIGHT <input type="checkbox"/> BILATERAL <input type="checkbox"/> UNKNOWN <input type="checkbox"/>			
	<u>LEFT</u>	<u>RIGHT</u>	<u>BOTH</u>
Plane of Implant placement (<i>please tick</i>)	Sub-glandular/Sub-fascial <input type="checkbox"/>	Sub-glandular/Sub-fascial <input type="checkbox"/>	Sub-glandular/Sub-fascial <input type="checkbox"/>
	Sub-pectoral <input type="checkbox"/>	Sub-pectoral <input type="checkbox"/>	Sub-pectoral <input type="checkbox"/>
	Sub-flap <input type="checkbox"/>	Sub-flap <input type="checkbox"/>	Sub-flap <input type="checkbox"/>
	Not Reported <input type="checkbox"/>	Not Reported <input type="checkbox"/>	Not Reported <input type="checkbox"/>
Manufacturer name			
Supplier name			
Brand/Trade name			
Implant Surface Type			
Implant fill type (saline, silicone gel)			
Implant Model Number			
Implant Catalog Number			

Implant Serial Number			
Implant Lot Number			
Implant Batch Number			
Style of Implant/Description			
Size of Implant/Actual Filler Volume			
Indication for Initial Implant: COSMETIC AUGMENTATION <input type="checkbox"/> RECONSTRUCTION-post cancer <input type="checkbox"/> RECONSTRUCTION-benign/prophylactic <input type="checkbox"/> REVISION <input type="checkbox"/> NOT REPORTED <input type="checkbox"/>			
Did the patient have fat grafting performed?	YES <input type="checkbox"/>	NO <input type="checkbox"/>	UNKNOWN <input type="checkbox"/>
Did the patient have ADM or mesh inserted?	YES <input type="checkbox"/>	NO <input type="checkbox"/>	UNKNOWN <input type="checkbox"/>
If yes, please specify type/manufacturer: _____			
IMPLANT RUPTURE INFORMATION			
Did the Implant Rupture?	YES <input type="checkbox"/>	NO <input type="checkbox"/>	UNKNOWN <input type="checkbox"/>
INITIAL CLINICAL PRESENTATION FORM			
Description of Case Presentation (ie: Seroma, delamination if PU, precautionary implant removal, previous breast cancer history)			
Was there capsular involvement?	YES <input type="checkbox"/>	NO <input type="checkbox"/>	UNKNOWN <input type="checkbox"/>
Invasion beyond the fibrous capsule into breast parenchyma?	YES <input type="checkbox"/>	NO <input type="checkbox"/>	UNKNOWN <input type="checkbox"/>
ALCL DIAGNOSTIC INFORMATION FORM			
ALCL DIAGNOSTIC INFORMATION			
Date of ALCL Diagnosis	Age at ALCL Diagnosis	ALCL Anatomic Site	
ALCL Primary to Other Site	YES <input type="checkbox"/>	NO <input type="checkbox"/>	UNKNOWN <input type="checkbox"/>
ALCL Secondary to Other Site	YES <input type="checkbox"/>	NO <input type="checkbox"/>	UNKNOWN <input type="checkbox"/>
ALCL Affected Breast	UNILATERAL-LEFT <input type="checkbox"/> UNILATERAL-RIGHT <input type="checkbox"/>	BILATERAL <input type="checkbox"/>	UNKNOWN <input type="checkbox"/>
Was the diagnosis made prior to taking the patient to the Operating Room?	YES <input type="checkbox"/>	NO <input type="checkbox"/>	UNKNOWN <input type="checkbox"/>
ALCL PATHOLOGIC INFORMATION			
Primary Diagnosis of ALCL?	YES <input type="checkbox"/>	NO <input type="checkbox"/>	UNKNOWN <input type="checkbox"/>
Suspected Case of ALCL without Pathologic Confirmation?	YES <input type="checkbox"/>	NO <input type="checkbox"/>	UNKNOWN <input type="checkbox"/>
Pathologically Confirmed?	YES <input type="checkbox"/>	NO <input type="checkbox"/>	UNKNOWN <input type="checkbox"/>
	CD30+ YES <input type="checkbox"/>	NO <input type="checkbox"/>	
	ALK- YES <input type="checkbox"/>	NO <input type="checkbox"/>	
Please document which of the following reports have been provided:			
Pathology Report	YES <input type="checkbox"/>	NO <input type="checkbox"/>	UNKNOWN <input type="checkbox"/>
Immunohistochemical stain results	YES <input type="checkbox"/>	NO <input type="checkbox"/>	UNKNOWN <input type="checkbox"/>
ALCL Diagnostic Procedure (Select all)	ASPIRATION CYTOLOGY <input type="checkbox"/> CAPSULE BIOLOGY <input type="checkbox"/>	UNKNOWN <input type="checkbox"/>	
	OTHER <input type="checkbox"/> Specify _____		
ALCL Distant Involvement?	REGIONAL NODES <input type="checkbox"/> DISTANT SITES <input type="checkbox"/>	DISSEMINATED <input type="checkbox"/>	UNKNOWN <input type="checkbox"/>

A copy of this approval letter must be kept in the facility where your animals are housed.

Tuesday, 20 June 2017

Dr Gregory Michael Cronin
Veterinary Science; Faculty of Science
The University of Sydney
Email: greg.cronin@sydney.edu.au

Dear Dr Cronin

I am pleased to inform you that the University of Sydney Animal Ethics Committee (AEC) has approved your project entitled **"Investigation of implant surface modification on prevention of biofilm development."**

Details of the approval are as follows:

Project Number: 2017/1193
Project Type: Experimental (non-wildlife)
Project Duration: 08/06/2017 – 08/06/2020
Approval Period: 08/06/2017 – 08/06/2018
Annual Report Due: 08/06/2018

In compliance with Section 27 of the NSW *Animal Research Act 1985*, this Animal Research Authority (ARA) remains in force for a period of 12 months from the date of issue, unless cancelled sooner.

Renewal of the ARA is conditional upon submission of a satisfactory annual report to the AEC in accordance with the *Australian code for the care and use of animals for scientific purposes 8th Edition 2013*.

Authorised Personnel: Cronin Gregory Michael (CI); Mohler Virginia; Macnamara Gregory; Macnamara Benjamin; Palmer David; Toribio Nobel; Clark Joshua; Vickery Karen; Hu Honghua; Deva Anand; Rahman Arifur; Aljohani Khalid; Mempin Maria;

Project Description:

Bacteria live either as free floating individuals or as groups of organisms attached to a surface called biofilm. Bacteria in biofilm are surrounded by material that they release called EPS or slime. The EPS helps protect the bacteria from antibiotics. It also prevents the host immune cells eg white blood cells from penetrating the biofilm and killing the bacteria. Biofilm infections therefore, are very hard to treat and often require the infection to be cut out surgically.

Biofilm infection around human breast implants is a significant cause of capsular contracture or implant failure. Lately, there has been an increase in a breast implant-associated cancer called anaplastic large cell lymphoma (BIA-ALCL). This is a T cell (one of the white blood cells called a lymphocyte normally found in the blood) derived cancer within the Non-Hodgkin lymphoma group and recent evidence suggests a role for biofilm infection and implant surface morphology. This proposal aims to use the pig-breast implant model to investigate if chronic bacterial biofilm infection can promote excess T cell multiplication (hyperplasia), as a possible prelude to cancer formation on medical implants over time.

When medical implants are inserted into a human the human tissue attaches to the implant and keeps it in place. The effect of biofilm infection on how well the host tissue attaches to the implant or

integrates with the medical implant will be determined. We will also determine if the surface profile of the implant ie if it is smooth or rough (textured) affects tissue integration and biofilm infection. We will also investigate how the host defends the body against biofilm by measuring the immune response to the biofilm. We will measure cell mediated immune response (especially the T lymphocytes) to biofilm infection in the laboratory by culturing pig lymphocytes with different compounds that cause lymphocytes to multiply. Compounds commonly used to stimulate lymphocytes to multiply includes mitogens which are compounds derived from plants and bacteria. We will also see if bacteria can cause the pig lymphocytes to multiply. We will obtain the pig lymphocytes from around the mini-breast implants and from the pig's blood. The project will also determine if all lymphocytes (multiclonal) or only some lymphocytes (clonal) respond to the biofilm by looking at the lymphocytes genetics and markers. We will also determine if proteins from the biofilm leave the biofilm and enter the host circulation.

Documents Approved:

05/05/2017	Monitoring Sheet	Anaesthesia Record Monitoring Sheet
05/05/2017	Other	Flow chart
05/05/2017	Monitoring Sheet	Housing monitoring sheet for sows
24/05/2017	Other	Photos of surgical procedure on a sow udder
24/05/2017	Monitoring Sheet	Post-surgery monitoring form

Animals Approved:

Please refer to the document at the end of this letter, which details your approved animal usage and location(s).

Conditions of Approval

1. This project must be conducted according to the approved project including continuing compliance with the conditions outlined in this ARA and with the *Animal Research Act 1985*, *Animal Research Regulation 2010*, the *Australian code for the care and use of animals for scientific purposes 8th edition 2013* (the Code) and all other relevant legislation.
2. Any changes to the project must be approved by the AEC prior to their implementation. This includes notifying the AEC of any changes to named personnel, source of animals, animal numbers, location of animals and experimental procedures.
3. An annual progress report or completion report must be submitted on or before the anniversary of approval of the project.
4. All unexpected adverse events that may impact on the wellbeing of an animal must be reported to the AEC within 48 hours, as per Clause 2.1.5 [v] [d] and 2.4.34 [ii] in the Code. Please refer to the Animal Ethics website and log into IRMA to complete an Adverse Event form.
5. The AEC must be notified if rodents are required to be singly housed.
6. All animal enclosures (e.g. pens, cages and containers) must be clearly identified with chief investigator name, number of animals, DOB if provided and date of arrival, sex and strain.
7. The following documentation must be kept in the facility where your animals are housed or with you when undertaking fieldwork:
 - A copy of this ARA
 - Emergency contact details in case of an animal emergency
 - Approved monitoring records
8. Personnel working on this project must be sufficiently qualified by education, training and experience for their role, or adequately supervised.
All new investigators must successfully complete the Introduction to Animal Research (ITAR) course.

9. Data must be retained and stored in accordance with the relevant legislation and University guidelines.
10. The AEC will make regular announced inspections of all animal facilities and/or specific research projects. The Animal Welfare Veterinarian will be conducting unannounced inspections of all animal facilities and/or specific research projects.
11. Any drugs to be used for procedures involving animals must within date (not expired) and stored appropriately as per the manufacturer's recommendations. It is the responsibility of the Chief Investigator to ensure that all relevant and current authority for the use of restricted drugs is obtained.

Please do not hesitate to contact the Ethics Office at animal.ethics@sydney.edu.au should you require further information or clarification.

Yours sincerely



Dr Lois Cavanagh
Chair
Animal Ethics Committee

The AEC is constituted and operates in accordance with the NSW Animal Research Act 1985 and its associated Regulations, the Australian code for the care and use of animals for scientific purposes 8th Edition 2013 and the Australian Code for the Responsible Conduct of Research 2007. All personnel named on the project should be conversant with these documents.



RESEARCH INTEGRITY &
ETHICS ADMINISTRATION

Animal Research Authority

A copy of this approval letter must be kept in the facility where your animals are housed.

Animals Approved:

Country	State	Invasiveness	Location	Classification one	Classification two	Common/strain name	Approved	Total used to date
Australia	NSW	4. Minor surgery with recovery	Camden Mayfarm (C03)	Domestic mammals	Pigs	Crossbred Large White Landrace	6	0

Dear: Associate Professor Vickery,

Your notification of collaboration for the following project was considered and noted by the Animal Ethics Committee at the meeting of 21 June 2018.

0783 - 5201807831104 - Vickery - "Investigation of implant surface modification on prevention of biofilm development."

Decision:

The Committee noted the collaborative report.

This email serves as official notification of the AEC decision. Please keep a copy for your records. Should you have any queries or require clarification, please contact the AEC Secretariat.

Regards,

Animal Ethics

Research Services | C5C-17 Wallys Walk L3,
Macquarie University | NSW | 2109 | Australia

T: +61 2 9850 7758 (*Animal Welfare Officer*)

T: +61 2 9850 4457 (*Animal Ethics Administration*)

T: +61 2 9850 4456 (*Animal Ethics Secretariat*)

E: animal.ethics@mq.edu.au

W: <http://www.mq.edu.au/research>

**OXFORD UNIVERSITY PRESS LICENSE
TERMS AND CONDITIONS**

Aug 01, 2018

This Agreement between Macquarie University -- Maria Mempin ("You") and Oxford University Press ("Oxford University Press") consists of your license details and the terms and conditions provided by Oxford University Press and Copyright Clearance Center.

License Number 4400220574054

License date Aug 01, 2018

Licensed content publisher Oxford University Press

Licensed content publication Aesthetic Surgery Journal

Licensed content title Bacterial Biofilms: A Cause for Accelerated Capsular Contracture?

Licensed content author Deva, Anand K.; Chang, Lionel C.

Licensed content date Mar 1, 1999

Type of Use Thesis/Dissertation

Institution name

Title of your work Miss

Publisher of your work Macquarie University

Expected publication date Aug 2018

Permissions cost 0.00 AUD

Value added tax 0.00 AUD

Total 0.00 AUD

Title Miss

Instructor name A/Prof Karen Vickery

Institution name Macquarie University

Expected presentation date Aug 2018

Portions Figure 1. Appearance of inflamed and contracted left breast before removal of implant

Requestor Location Macquarie University
Luxottica Building
Desk 22, Level 1, 75 Talavera Rd

Macquarie Park, New South Wales 2109
Australia
Attn: Maria

Publisher Tax ID GB125506730

Billing Type Invoice

Billing Address Macquarie University
Luxottica Building
Desk 22, Level 1, 75 Talavera Rd

Macquarie Park, Australia 2109
Attn: Maria

Total 0.00 AUD

Terms and Conditions

STANDARD TERMS AND CONDITIONS FOR REPRODUCTION OF MATERIAL FROM AN OXFORD UNIVERSITY PRESS JOURNAL

1. Use of the material is restricted to the type of use specified in your order details.
2. This permission covers the use of the material in the English language in the following territory: world. If you have requested additional permission to translate this material, the terms and conditions of this reuse will be set out in clause 12.
3. This permission is limited to the particular use authorized in (1) above and does not allow you to sanction its use elsewhere in any other format other than specified above, nor does it apply to quotations, images, artistic works etc that have been reproduced from other sources which may be part of the material to be used.
4. No alteration, omission or addition is made to the material without our written consent. Permission must be re-cleared with Oxford University Press if/when you decide to reprint.
5. The following credit line appears wherever the material is used: author, title, journal, year, volume, issue number, pagination, by permission of Oxford University Press or the sponsoring society if the journal is a society journal. Where a journal is being published on behalf of a learned society, the details of that society must be included in the credit line.
6. For the reproduction of a full article from an Oxford University Press journal for whatever purpose, the corresponding author of the material concerned should be informed of the proposed use. Contact details for the corresponding authors of all Oxford University Press journal contact can be found alongside either the abstract or full text of the article concerned, accessible from www.oxfordjournals.org Should there be a problem clearing these rights, please contact journals.permissions@oup.com
7. If the credit line or acknowledgement in our publication indicates that any of the figures, images or photos was reproduced, drawn or modified from an earlier source it will be necessary for you to clear this permission with the original publisher as well. If this permission has not been obtained, please note that this material cannot be included in your publication/photocopies.
8. While you may exercise the rights licensed immediately upon issuance of the license at the end of the licensing process for the transaction, provided that you have disclosed complete and accurate details of your proposed use, no license is finally effective unless and until full payment is received from you (either by Oxford University Press or by Copyright Clearance Center (CCC)) as provided in CCC's Billing and Payment terms and conditions. If full payment is not received on a timely basis, then any license preliminarily granted shall be deemed automatically revoked and shall be void as if never granted. Further, in the event that you breach any of these terms and conditions or any of CCC's Billing and Payment terms and

conditions, the license is automatically revoked and shall be void as if never granted. Use of materials as described in a revoked license, as well as any use of the materials beyond the scope of an unrevoked license, may constitute copyright infringement and Oxford University Press reserves the right to take any and all action to protect its copyright in the materials.

9. This license is personal to you and may not be sublicensed, assigned or transferred by you to any other person without Oxford University Press's written permission.

10. Oxford University Press reserves all rights not specifically granted in the combination of (i) the license details provided by you and accepted in the course of this licensing transaction, (ii) these terms and conditions and (iii) CCC's Billing and Payment terms and conditions.

11. You hereby indemnify and agree to hold harmless Oxford University Press and CCC, and their respective officers, directors, employs and agents, from and against any and all claims arising out of your use of the licensed material other than as specifically authorized pursuant to this license.

12. Other Terms and Conditions:

v1.4

Questions? customer care@copyright.com or +1-855-239-3415 (toll free in the US) or +1-978-646-2777.

References

- ABRAMS, J. T., BALIN, B. J. & VONDERHEID, E. C. 2001. Sezary T Cell Activating Factor is a Chlamydia pneumoniae Associated Protein. *Annals of the New York Academy of Sciences*, 941, 69.
- ADAMS JR, W. P. 2009. Capsular contracture: What is it? What causes it? How can it be prevented and managed? *Clinics in Plastic Surgery*, 36, 119-126.
- ADAMS JR, W. P., CONNER, W. C. H., BARTON JR, F. E. & ROHRICH, R. J. 2000. Optimizing breast pocket irrigation: an in vitro study and clinical implications. *Plastic and Reconstructive Surgery*, 105, 334-338.
- ADAMS JR, W. P., CONNER, W. C. H., BARTON JR, F. E. & ROHRICH, R. J. 2001. Optimizing breast - pocket irrigation: the post - betadine era. *Plastic and Reconstructive Surgery*, 107, 1596-1601.
- ADAMS JR, W. P., HAYDON, M. S., RANIERE JR, J., TROTT, S., MARQUES, M., FELICIANO, M., ROBINSON JR, J. B., TANG, L. & BROWN, S. A. 2006a. A rabbit model for capsular contracture: development and clinical implications. *Plastic and Reconstructive Surgery*, 117, 1214-1219.
- ADAMS JR, W. P., RIOS, J. L. & SMITH, S. J. 2006b. Enhancing patient outcomes in aesthetic and reconstructive breast surgery using triple antibiotic breast irrigation: six - year prospective clinical study. *Plastic and Reconstructive Surgery*, 117, 30-36.
- ADEREM, A. & ULEVITCH, R. J. 2000. Toll-like receptors in the induction of the innate immune response. *Nature*, 406, 782.
- AHN, C. Y., KO, C. Y., WAGAR, E. A., WONG, R. S. & SHAW, W. W. 1996. Microbial evaluation: 139 implants removed from symptomatic patients. *Plastic and Reconstructive Surgery*, 98, 1225-9.
- AJDIC, D., ZOGHBI, Y., GERTH, D., PANTHAKI, Z. J. & THALLER, S. 2016. The relationship of bacterial biofilms and capsular contracture in breast implants. *Aesthetic Surgery Journal*, 36, 297-309.

- AKIRA, S., TAKEDA, K. & KAISHO, T. 2001. Toll - like receptors: critical proteins linking innate and acquired immunity. *Nature Immunology*, 2, 675-680.
- AKIRA, S., UEMATSU, S. & TAKEUCHI, O. 2006. Pathogen recognition and innate immunity. *Cell*, 124, 783-801.
- ALADILY, T. N., MEDEIROS, L. J., AMIN, M. B., HAIDERI, N., YE, D., AZEVEDO, S. J., JORGENSEN, J. L., DE PERALTA-VENTURINA, M., MUSTAFA, E. B. & YOUNG, K. H. 2012. Anaplastic large cell lymphoma associated with breast implants: a report of 13 cases. *The American Journal of Surgical Pathology*, 36, 1000-1008.
- ALBORNOZ, C. R., BACH, P. B., MEHRARA, B. J., DISA, J. J., PUSIC, A. L., MCCARTHY, C. M., CORDEIRO, P. G. & MATROS, E. 2013. A paradigm shift in US Breast reconstruction: increasing implant rates. *Plastic and Reconstructive Surgery*, 131, 15-23.
- ALEXANDER, D. D., MINK, P. J., ADAMI, H. O., CHANG, E. T., COLE, P., MANDEL, J. S. & TRICHOPOULOS, D. 2007. The non - Hodgkin lymphomas: A review of the epidemiologic literature. *International Journal of Cancer*, 120, 1-39.
- ALHEDE, M., BJARNSHOLT, T., JENSEN, P. Ø., PHIPPS, R. K., MOSER, C., CHRISTOPHERSEN, L., CHRISTENSEN, L. D., VAN GENNIP, M., PARSEK, M. & HØIBY, N. 2009. Pseudomonas aeruginosa recognizes and responds aggressively to the presence of polymorphonuclear leukocytes. *Microbiology*, 155, 3500-3508.
- ALLESEN - HOLM, M., BARKEN, K. B., YANG, L., KLAUSEN, M., WEBB, J. S., KJELLEBERG, S., MOLIN, S., GIVSKOV, M. & TOLKER - NIELSEN, T. 2006. A characterization of DNA release in Pseudomonas aeruginosa cultures and biofilms. *Molecular Microbiology*, 59, 1114-1128.
- ALLISON, D. G. 2003. The biofilm matrix. *Biofouling*, 19, 139-150.
- ALOBID, B., SEVILLA, D. W., EL-TAMER, M. B., MURTY, V. V., SAVAGE, D. G. & BHAGAT, G. 2009. Aggressive presentation of breast implant - associated ALK - 1 negative anaplastic large cell lymphoma with bilateral axillary lymph node involvement. *Leukemia & Lymphoma*, 50, 831-833.
- ANDERSON, G. & O'TOOLE, G. 2008. Innate and induced resistance mechanisms of bacterial biofilms. *Bacterial Biofilms*. Springer.

- ANDO, T., WASSENAAR, T. M., PEEK, R. M., ARAS, R. A., TSCHUMI, A. I., VAN DOORN, L.-J., KUSUGAMI, K. & BLASER, M. J. 2002. A *Helicobacter pylori* restriction endonuclease-replacing gene, *hrgA*, is associated with gastric cancer in Asian strains. *Cancer Research*, 62, 2385-2389.
- ANGELL, M. 1996. Evaluating the health risks of breast implants: the interplay of medical science, the law, and public opinion. *New England Journal of Medicine*, 334, 1513-1518.
- ARABSKI, M., KLUPINSKA, G., CHOJNACKI, J., KAZMIERCZAK, P., WISNIEWSKA-JAROSINSKA, M., DRZEWOSKI, J. & BLASIAK, J. 2005. DNA damage and repair in *Helicobacter pylori*-infected gastric mucosa cells. *Mutation Research/Fundamental and Molecular Mechanisms of Mutagenesis*, 570, 129-135.
- ARACO, A., CARUSO, R., ARACO, F., OVERTON, J. & GRAVANTE, G. 2009. Capsular contractures: a systematic review. *Plastic and Reconstructive Surgery*, 124, 1808-19.
- ARCIOLA, C. R., CAMPOCCIA, D., SPEZIALE, P., MONTANARO, L. & COSTERTON, J. W. 2012. Biofilm formation in *Staphylococcus* implant infections. A review of molecular mechanisms and implications for biofilm - resistant materials. *Biomaterials*, 33, 5967-5982.
- ARION, H. G. 1965. Presentation d'une prothese retra mammaire. *Journal of the Society for Gynecologic (French)*, 2, 5.
- ASHLEY, F. L. 1970. A new type of breast prosthesis. Preliminary report. *Plastic and Reconstructive Surgery*, 45, 421-4.
- ASHLEY, F. L. 1972. Further studies on the natural - Y breast prosthesis. *Plastic and Reconstructive Surgery*, 49, 414-9.
- ASPLUND, O., GYLBERT, L., JURELL, G. & WARD, C. 1996. Textured or smooth implants for submuscular breast augmentation: a controlled study. *Plastic and Reconstructive Surgery*, 97, 1200-1206.
- ASPS 2015. ASPS Plastic Surgery Statistics Report. Available online: www.plasticsurgery.org (accessed on 1 February 2016).
- ATLAN, M., BIGERELLE, M., LARRETA-GARDE, V., HINDIÉ, M. & HEDÉN, P. 2016. Characterization of breast implant surfaces, shapes, and biomechanics: a comparison of high cohesive anatomically shaped textured silicone, breast implants from three different manufacturers. *Aesthetic Plastic Surgery*, 40, 89-97.

- AWASTHI, A., MURUGAIYAN, G. & KUCHROO, V. K. 2008. Interplay between effector Th17 and regulatory T cells. *Journal of Clinical Immunology*, 28, 660.
- AZAROVA, A. M., GAUTAM, G. & GEORGE, R. E. 2011. Emerging importance of ALK in neuroblastoma. *Seminars in Cancer Biology*, 21, 267-275.
- BABU, S. S., MÖHWALD, H. & NAKANISHI, T. 2010. Recent progress in morphology control of supramolecular fullerene assemblies and its applications. *Chemical Society Reviews*, 39, 4021-4035.
- BAEKE, J. L. 2002. Breast deformity caused by anatomical or teardrop implant rotation. *Plastic and Reconstructive Surgery*, 109, 2555-64; discussion 2568-9.
- BAKER, J. J. L. Classification of spherical contractures. Scottsdale, Arizona: Presented at the Aesthetic Breast Symposium, 1964.
- BALABAN, N. & RASOOLY, A. 2000. Staphylococcal enterotoxins. *International Journal of Food Microbiology*, 61, 1-10.
- BARNSLEY, G. P., SIGURDSON, L. J. & BARNSLEY, S. E. 2006. Textured surface breast implants in the prevention of capsular contracture among breast augmentation patients: a meta-analysis of randomized controlled trials. *Plastic and Reconstructive Surgery*, 117, 2182-2190.
- BARONE, F. E., PERRY, L., KELLER, T. & MAXWELL, G. P. 1992. The biomechanical and histopathologic effects of surface texturing with silicone and polyurethane in tissue implantation and expansion. *Plastic and Reconstructive Surgery*, 90, 77-86.
- BARR, S. & BAYAT, A. 2011. Breast implant surface development: perspectives on development and manufacture. *Aesthetic Surgery Journal*, 31, 56-67.
- BARR, S., HILL, E. & BAYAT, A. 2009. Current implant surface technology: an examination of their nanostructure and their influence on fibroblast alignment and biocompatibility. *Eplasty*, 9, e22.
- BARR, S., HILL, E. & BAYAT, A. 2017. Functional biocompatibility testing of silicone breast implants and a novel classification system based on surface roughness. *Journal of the Mechanical Behavior of Biomedical Materials*, 75, 75-81.

- BARTSICH, S., ASCHERMAN, J. A., WHITTIER, S., YAO, C. A. & ROHDE, C. 2011. The breast: a clean - contaminated surgical site. *Aesthetic Surgery Journal*, 31, 802-6.
- BATRA, M., BERNARD, S. & PICHA, G. 1995. Histologic comparison of breast implant shells with smooth, foam, and pillar microstructuring in a rat model from 1 day to 6 months. *Plastic Reconstructive Surgery*, 95, 354-63.
- BAUMGAERTNER, I., COPIE-BERGMAN, C., LEVY, M., HAIOUN, C., CHARACHON, A., BAIA, M., SOBHANI, I. & DELCHIER, J. C. 2009. Complete remission of gastric Burkitt's lymphoma after eradication of *Helicobacter pylori*. *World Journal of Gastroenterology: WJG*, 15, 5746.
- BEINKE, C., PORT, M., LAMKOWSKI, A. & ABEND, M. 2015. Comparing seven mitogens with PHA - M for improved lymphocyte stimulation in dicentric chromosome analysis for biodosimetry. *Radiation Protection Dosimetry*, 168, 235-241.
- BELL, M. S. & MCKEE, D. 2009. An illuminating no - touch device for breast augmentation. *The Canadian Journal of Plastic Surgery*, 17, 30.
- BENGTSON, B. P., VAN NATTA, B. W., MURPHY, D. K., SLICTON, A., MAXWELL, G. P. & GROUP, S. U. C. C. S. 2007. Style 410 highly cohesive silicone breast implant core study results at 3 years. *Plastic and Reconstructive Surgery*, 120, 40S-48S.
- BERRIDGE, M. V., HERST, P. M. & TAN, A. S. 2005. Tetrazolium dyes as tools in cell biology: new insights into their cellular reduction. *Biotechnology Annual Review*, 11, 127-152.
- BERRY, M., CUCCHIARA, V. & DAVIES, D. 2010. Breast augmentation: part II – adverse capsular contracture. *Journal of Plastic, Reconstructive and Aesthetic Surgery*, 63, 2098-2107.
- BERTONI, F., COIFFIER, B., STATHIS, A., TRAVERSE-GLEHEN, A. & ZUCCA, E. 2011. MALT lymphomas: pathogenesis can drive treatment. *Oncology*, 25, 1134.
- BISHARA, M. R., ROSS, C. & SUR, M. 2009. Primary anaplastic large cell lymphoma of the breast arising in reconstruction mammoplasty capsule of saline filled breast implant after radical mastectomy for breast cancer: an unusual case presentation. *Diagnostic Pathology*, 4, 11.

- BIZJAK, M., SELMI, C., PRAPROTNIK, S., BRUCK, O., PERRICONE, C., EHRENFELD, M. & SHOENFELD, Y. 2015. Silicone implants and lymphoma: the role of inflammation. *Journal of Autoimmunity*, 65, 64-73.
- BJARNSHOLT, T., JENSEN, P. Ø., BURMØLLE, M., HENTZER, M., HAAGENSEN, J. A., HOUGEN, H. P., CALUM, H., MADSEN, K. G., MOSER, C. & MOLIN, S. 2005. *Pseudomonas aeruginosa* tolerance to tobramycin, hydrogen peroxide and polymorphonuclear leukocytes is quorum - sensing dependent. *Microbiology*, 151, 373-383.
- BLOMBERG, P., THOMPSON, E. R., JONES, K., ARNAU, G. M., LADE, S., MARKHAM, J. F., LI, J., DEVA, A., JOHNSTONE, R. W. & KHOT, A. 2016. Whole exome sequencing reveals activating JAK1 and STAT3 mutations in breast implant - associated anaplastic large cell lymphoma anaplastic large cell lymphoma. *Haematologica*, 101, e387-e390.
- BLOUNT, A. L., MARTIN, M. D., LINEBERRY, K. D., KETTANEH, N. & ALFONSO, D. R. 2013. Capsular contracture rate in a low - risk population after primary augmentation mammoplasty. *Aesthetic Surgery Journal*, 33, 516-521.
- BOGETTI, P., BOLTRI, M., BALOCCO, P. & AL., E. 2000. Augmentation mammoplasty with a new cohesive gel prosthesis. *Aesthetic Plastic Surgery*, 24, 440.
- BOLES, B. R. & HORSWILL, A. R. 2008. Agr-mediated dispersal of *Staphylococcus aureus* biofilms. *PLOS Pathogens*, 4, e1000052.
- BOLES, B. R., THOENDEL, M., ROTH, A. J. & HORSWILL, A. R. 2010. Identification of genes involved in polysaccharide-independent *Staphylococcus aureus* biofilm formation. *PLOS One*, 5, e10146.
- BOREYKO, J. B., BAKER, C. H., POLEY, C. R. & CHEN, C. H. 2011. Wetting and dewetting transitions on hierarchical superhydrophobic surfaces. *Langmuir*, 27, 7502-7509.
- BORGHI, A., CASELLI, E., DI LUCA, D., SEBASTIANI, A., PERRI, P., SERACENI, S., CONTINI, C. & VIRGILI, A. 2013. Detection of *Chlamydia pneumoniae* and human herpesvirus 8 in primary cutaneous anaplastic large-cell lymphoma: a case report. *Infectious Agents and Cancer*, 8, 41.
- BRINTON, L. A. & BROWN, S. L. 1997. Breast implants and cancer. *Journal of the National Cancer Institute*, 89, 1341-1349.

- BRITEZ, M. E. M., LLANO, C. C. & CHAUX, A. 2012. Periprosthetic breast capsules and immunophenotypes of inflammatory cells. *European Journal of Plastic Surgery*, 35, 647-651.
- BRODY, G., DEAPEN, D., GILL, P., EPSTEIN, A., MARTIN, S. & ELATRA, W. T cell non - Hodgkin's anaplastic lymphoma associated with one style of breast implants. San Antonio, Texas: American Society of Plastic Surgeons Annual Conference, 2010.
- BRODY, G. S. 2012. Brief recommendations for dealing with a new case of anaplastic large T - cell lymphoma. *Plastic and Reconstructive Surgery*, 129, 871e-2e.
- BRONZ, G. 2002. A comparison of naturally shaped and round implants. *Aesthetic Surgery Journal*, 22, 238-46.
- BROWN, M. H., SHENKER, R. & SILVER, S. A. 2005. Cohesive silicone gel breast implants in aesthetic and reconstructive breast surgery. *Plastic and Reconstructive Surgery*, 116, 768.
- BRYANT, C. E., SPRING, D. R., GANGLOFF, M. & GAY, N. J. 2010. The molecular basis of the host response to lipopolysaccharide. *Nature Reviews Microbiology*, 8, 8.
- BRYERS, J. D. 2008. Medical biofilms. *Biotechnology and Bioengineering*, 100, 1-18.
- BUC, E., DUBOIS, D., SAUVANET, P., RAISCH, J., DELMAS, J., DARFEUILLE-MICHAUD, A., PEZET, D. & BONNET, R. 2013. High prevalence of mucosa - associated E. coli producing cyclomodulin and genotoxin in colon cancer. *PLOS One*, 8, e56964.
- BUONPANE, R. A., MOZA, B., SUNDBERG, E. J. & KRANZ, D. M. 2005. Characterization of T cell receptors engineered for high affinity against toxic shock syndrome toxin - 1. *Journal of Molecular Biology*, 353, 308-321.
- BURKHARDT, B. R. 1988. Capsular contracture: hard breasts, soft data. *Clinics in Plastic Surgery*, 15, 521-532.
- BURKHARDT, B. R. & DEMAS, C. P. 1994. The effect of Siltex texturing and povidone - iodine irrigation on capsular contracture around saline inflatable breast implants. *Plastic and Reconstructive Surgery*, 93, 123-8; discussion 129-30.
- BURKHARDT, B. R. & EADES, E. 1995. The effect of Biocell texturing and povidone - iodine irrigation on capsular contracture around saline - inflatable breast implants. *Plastic and Reconstructive Surgery*, 96, 1317-25.

- BURKHARDT, B. R., FRIED, M., SCHNUR, P. L. & TOFIELD, J. J. 1981. Capsules, infection, and intraluminal antibiotics. *Plastic and Reconstructive Surgery*, 68, 43-47.
- CALOBRACE, M. B. & CAPIZZI, P. J. 2014. The biology and evolution of cohesive gel and shaped implants. *Plastic and Reconstructive Surgery*, 134, 6S-11S.
- CALOBRACE, M. B. & HAMMOND, D. 2014. Anatomic gel implants: from concept to device. *Plastic and Reconstructive Surgery*, 134, 4S-9S.
- CAMILI, A. & BASSLER, B. L. 2006. Bacterial small-molecule signaling pathways. *Science*, 311, 1113-1116.
- CAMPOCCIA, D., MONTANARO, L. & ARCIOLA, C. R. 2006. The significance of infection related to orthopedic devices and issues of antibiotic resistance. *Biomaterials*, 27, 2331-2339.
- CAO, Q., LIU, F., LI, S., LIU, N., LI, L., LI, C. & PENG, T. 2016. Primary rare anaplastic large cell lymphoma, ALK positive in small intestine: case report and review of the literature. *Diagnostic Pathology*, 11, 83.
- CAPLIN, D. A. 2014. Indications for the use of MemoryShape breast implants in aesthetic and reconstructive breast surgery: long-term clinical outcomes of shaped versus round silicone breast implants. *Plastic and Reconstructive Surgery*, 134, 27S-37S.
- CAPOZZI, A. & PENNISI, V. R. 1981. Clinical experience with polyurethane-covered gel-filled mammary prostheses. *Plastic and Reconstructive Surgery*, 68, 512-20.
- CASELLI, E., BORGHI, A., MARITATI, M., GAFÀ, R., LANZA, G., DI LUCA, D., VIRGILI, A. & CONTINI, C. 2016. Relapses of primary cutaneous anaplastic large - cell lymphoma in a female immunocompetent patient with persistent chlamydia pneumoniae and human herpesvirus 8 infection. *Infectious Agents and Cancer*, 11, 31.
- CASH, T. F., DUEL, L. A., PERKINS, L. L. & SARWER, D. B. 2002. Women's psychosocial outcomes of breast augmentation with silicone gel - filled implants: a 2-year prospective study. *Plastic and Reconstructive Surgery*, 109, 2.
- CASTELLI, P., CARONNO, R., FERRARESE, S., MANTOVANI, V., PIFFARETTI, G., TOZZI, M., LOMAZZI, C., RIVOLTA, N. & SALA, A. 2006. New trends in prosthesis infection in cardiovascular surgery. *Surgical Infections*, 7, s-45-s-47.

- CERAVOLO, M. P. & DEL VESCOVO, A. 1993. Another look at steroids: Intraluminal methylprednisolone in retropectoral augmentation mammoplasty. *Aesthetic Plastic Surgery*, 17.
- CERCA, N., PIER, G. B., VILANOVA, M., OLIVEIRA, R. & AZEREDO, J. 2005. Quantitative analysis of adhesion and biofilm formation on hydrophilic and hydrophobic surfaces of clinical isolates of *Staphylococcus epidermidis*. *Research in Microbiology*, 156, 506.
- CHAMBLESS, J. D. & STEWART, P. S. 2007. A three - dimensional computer model analysis of three hypothetical biofilm detachment mechanisms. *Biotechnology and Bioengineering*, 97, 1573-1584.
- CHAN, A. A., BASHIR, M., RIVAS, M. N., DUVALL, K., SIELING, P. A., PIEBER, T. R., VAISHAMPAYAN, P. A., LOVE, S. M. & LEE, D. J. 2016. Characterization of the microbiome of nipple aspirate fluid of breast cancer survivors. *Scientific Reports*, 6, 28061.
- CHAN, S. C., BIRDSELL, D. C. & GRADEEN, C. Y. 1991a. Detection of toluenediamines in the urine of a patient with polyurethane - covered breast implants. *Clinical Chemistry*, 37, 756-758.
- CHAN, S. C., BIRDSELL, D. C. & GRADEEN, C. Y. 1991b. Urinary excretion of free toluenediamines in a patient with polyurethane-covered breast implants. *Clinical Chemistry*, 37, 2143-5.
- CHANDRA, J., KUHN, D. M., MUKHERJEE, P. K., HOYER, L. L., MCCORMICK, T. & GHANNOUM, M. A. 2001. Biofilm formation by the fungal pathogen *Candida albicans*: development, architecture, and drug resistance. *Journal of Bacteriology*, 183, 5385-5394.
- CHANG, J. & LEE, G. W. 2011. Late hematogenous bacterial infections of breast implants: two case reports of unique bacterial infections. *Annals of Plastic Surgery*, 67, 14-16.
- CHANG, L., CALDWELL, E., READING, G. & AL., E. 1992. A comparison of conventional and low-bleed implants in augmentation mammoplasty. *Plastic and Reconstructive Surgery*, 89, 79.
- CHATURVEDI, R., DE SABLET, T., PEEK JR, R. M. & WILSON, K. T. 2012. Spermine oxidase, a polyamine catabolic enzyme that links *Helicobacter pylori* CagA and gastric cancer risk. *Gut Microbes*, 3, 48-56.

- CHOKR, A., WATIER, D., ELEAUME, H., PANGON, B., GHNASSIA, J. C., MACK, D. & JABBOURI, S. 2006. Correlation between biofilm formation and production of polysaccharide intercellular adhesin in clinical isolates of coagulase - negative staphylococci. *International Journal of Medical Microbiology*, 296, 381-388.
- CHONG, S. J. & DEVA, A. K. 2015. Understanding the etiology and prevention of capsular contracture. *Clinics in Plastic Surgery*, 42, 427-36.
- CHOTT, A., VONDERHEID, E. C., OLBRICHT, S., MIAO, N. N., BALK, S. P. & KADIN, M. E. 1996. The same dominant T cell clone is present in multiple regressing skin lesions and associated T cell lymphomas of patients with lymphomatoid papulosis. *Journal of Investigative Dermatology*, 106, 696-700.
- CHOWDARY VENIGALLA, R. K., TRETTER, T., KRIENKE, S., MAX, R., ECKSTEIN, V., BLANK, N., FIEHN, C., DICK HO, A. & LORENZ, H. M. 2008. Reduced CD4+, CD25– T cell sensitivity to the suppressive function of CD4+, CD25high, CD127–/low regulatory T cells in patients with active systemic lupus erythematosus. *Arthritis and Rheumatology*, 58, 2120-2130.
- CHUNG, K. K., SCHUMACHER, J. F., SAMPSON, E. M., BURNE, R. A., ANTONELLI, P. J. & BRENNAN, A. B. 2007. Impact of engineered surface microtopography on biofilm formation of *Staphylococcus aureus*. *Biointerphases*, 2, 89-94.
- CLEMENS, M. W., MEDEIROS, L. J., BUTLER, C. E., HUNT, K. K., FANALE, M. A., HORWITZ, S., WEISENBURGER, D. D., LIU, J., MORGAN, E. A. & KANAGAL-SHAMANNA, R. 2016. Complete surgical excision is essential for the management of patients with breast implant – associated anaplastic large-cell lymphoma. *Journal of Clinical Oncology*, 34, 160.
- CLEMENS, M. W. & MIRANDA, R. N. 2015. Coming of Age: Breast Implant – Associated Anaplastic Large Cell Lymphoma After 18 Years of Investigation. *Clinics in Plastic Surgery*, 42, 605-613.
- CLOUTIER, M., MANTOVANI, D. & ROSEI, F. 2015. Antibacterial coatings: challenges, perspectives, and opportunities. *Trends in Biotechnology*, 33, 637-652.
- CODNER, M. A., MEJIA, J. D., LOCKE, M. B., MAHONEY, A., THIELS, C., NAHAI, F. R., HESTER, T. R. & NAHAI, F. 2011. A 15 - year experience with primary breast augmentation. *Plastic and Reconstructive Surgery*, 127, 1300-1310.

- COHEN, P. L. & BROOKS, J. J. 1991. Lymphomas of the breast. A clinicopathologic and immunohistochemical study of primary and secondary cases. *Cancer*, 67, 1359-1369.
- COLEMAN, D. J., FOO, I. T. & SHARPE, D. T. 1991. Textured or smooth implants for breast augmentation? A prospective controlled trial. *British Journal of Plastic Surgery*, 44, 444-8.
- COLLIS, N., COLEMAN, D., FOO, I. T. & SHARPE, D. T. 2000. Ten - year review of a prospective randomized controlled trial of textured versus smooth subglandular silicone gel breast implants. *Plastic and Reconstructive Surgery*, 106, 786-791.
- COLVIN, K. M., IRIE, Y., TART, C. S., URBANO, R., WHITNEY, J. C., RYDER, C., HOWELL, P. L., WOZNIAK, D. J. & PARSEK, M. R. 2012. The Pel and Psl polysaccharides provide *Pseudomonas aeruginosa* structural redundancy within the biofilm matrix. *Environmental Microbiology*, 14, 1913-1928.
- COOK, P. D., OSBORNE, B. M., CONNOR, R. L. & STRAUSS, J. F. 1995. Follicular lymphoma adjacent to foreign body granulomatous inflammation and fibrosis surrounding silicone breast prosthesis. *The American Journal of Surgical Pathology*, 19, 712-717.
- COSTA, F., CARVALHO, I. F., MONTELARO, R. C., GOMES, P. & MARTINS, M. C. L. 2011. Covalent immobilization of antimicrobial peptides (AMPs) onto biomaterial surfaces. *Acta Biomaterialia*, 7, 1431-1440.
- COSTERTON, J. W. 2005. Biofilm theory can guide the treatment of device - related orthopaedic infections. *Clinical Orthopaedics and Related Research*, 437, 7-11.
- COSTERTON, J. W., STEWART, P. S. & GREENBERG, E. P. 1999. Bacterial biofilms: a common cause of persistent infections. *Science*, 284, 1318-22.
- COURTISS, E. H., GOLDWYN, R. M. & ANASTASI, G. W. 1979. The fate of breast implants with infections around them. *Plastic and Reconstructive Surgery*, 63, 812-6.
- CRAWFORD, R. J., WEBB, H. K., TRUONG, V. K., HASAN, J. & IVANOVA, E. P. 2012. Surface topographical factors influencing bacterial attachment. *Advances in Colloid and Interface Science*, 179, 142-149.

- CRESCENZO, R., ABATE, F., LASORSA, E., GAUDIANO, M., CHIESA, N., DI GIACOMO, F., SPACCAROTELLA, E., BARBAROSSA, L., ERCOLE, E. & TODARO, M. 2015. Convergent mutations and kinase fusions lead to oncogenic STAT3 activation in anaplastic large cell lymphoma. *Cancer Cell*, 27, 516-532.
- CRICK, C. R., ISMAIL, S., PRATTEN, J. & PARKIN, I. P. 2011. An investigation into bacterial attachment to an elastomeric superhydrophobic surface prepared via aerosol assisted deposition. *Thin Solid Films*, 519, 3722-3727.
- CROME, S., WANG, A. & LEVINGS, M. 2010. Translational Mini - Review Series on Th17 Cells: Function and regulation of human T helper 17 cells in health and disease. *Clinical and Experimental Immunology*, 159, 109-119.
- CRONIN, T. D. & GEROW, F. J. Augmentation mammoplasty: a new "natural feel" prosthesis. Amsterdam, Netherlands: Transactions of the Third International Congress of Plastic and Reconstructive Surgery Excerpta Medica, 1964.
- CUNNINGHAM, B. 2007. The Mentor study on contour profile gel silicone MemoryGel breast implants. *Plastic and Reconstructive Surgery*, 120, 33S.
- CUNNINGHAM, B. L., LOKEH, A. & GUTOWSKI, K. A. 2000. Saline-filled breast implant safety and efficacy: a multicenter retrospective review. *Plastic and Reconstructive Surgery*, 105, 2143-9; discussion 2150-1.
- DALBY, M. J., YARWOOD, S. J., RIEHLE, M. O., JOHNSTONE, H. J., AFFROSSMAN, S. & CURTIS, A. S. 2002. Increasing fibroblast response to materials using nanotopography: morphological and genetic measurements of cell response to 13-nm-high polymer demixed islands. *Experimental Cell Research*, 276, 1-9.
- DANINO, A. M., BASMACIOGLU, P., SAITO, S., ROCHER, F., BLANCHET-BARDON, C., REVOL, M. & SERVANT, J. M. 2001. Comparison of the capsular response to the Biocell RTV and Mentor 1600 Siltex breast implant surface texturing: a scanning electron microscopic study. *Plastic and Reconstructive Surgery*, 108, 2047-2052.
- DARENBERG, J., SÖDERQUIST, B., HENRIQUES NORMARK, B. & NORRBY-TEGLUND, A. 2004. Differences in potency of intravenous polyspecific immunoglobulin G against streptococcal and staphylococcal superantigens: implications for therapy of toxic shock syndrome. *Clinical Infectious Diseases*, 38, 836-842.
- DAROUICHE, R. O. 1998. Medical implant having a durable, resilient and effective antimicrobial coating. Google Patents.

- DE BOER, M., VAN LEEUWEN, F. E., HAUPTMANN, M., OVERBEEK, L. I., DE BOER, J. P., HIJMERING, N. J., SERNEE, A., KLAZEN, C. A., LOBBES, M. B. & VAN DER HULST, R. R. 2018. Breast implants and the risk of anaplastic large - cell lymphoma in the breast. *JAMA Oncology*, 4, 335-341.
- DE JONG, D., VASMEL, W. L., DE BOER, J. P., VERHAVE, G., BARBE, E., CASPARIE, M. K. & VAN LEEUWEN, F. E. 2008. Anaplastic large - cell lymphoma in women with breast implants. *JAMA*, 300, 2030-5.
- DE KIEVIT, T. 2009. Quorum sensing in *Pseudomonas aeruginosa* biofilms. *Environmental Microbiology*, 11, 279-288.
- DEL POZO, J. & PATEL, R. 2007. The challenge of treating biofilm - associated bacterial infections. *Clinical Pharmacology and Therapeutics*, 82, 204-209.
- DEL POZO, J. L., TRAN, N. V., PETTY, P. M., JOHNSON, C. H., WALSH, M. F., BITE, U., CLAY, R. P., MANDREKAR, J. N., PIPER, K. E. & STECKELBERG, J. M. 2009. Pilot study of association of bacteria on breast implants with capsular contracture. *Journal of Clinical Microbiology*, 47, 1333-1337.
- DEN BRABER, E., DE RUIJTER, J., GINSEL, L., VON RECUM, A. & JANSEN, J. 1998. Orientation of ECM protein deposition, fibroblast cytoskeleton, and attachment complex components on silicone microgrooved surfaces. *Journal of Biomedical Materials Research: an Official Journal of the Society for Biomaterials, the Japanese Society for Biomaterials, and the Australian Society for Biomaterials*, 40, 291-300.
- DEVA, A. K., ADAMS, W. P., JR. & VICKERY, K. 2013. The role of bacterial biofilms in device-associated infection. *Plastic and Reconstructive Surgery*, 132, 1319-28.
- DEVA, A. K. & CHANG, L. C. 1999. Bacterial biofilms: a cause for accelerated capsular contracture? *Aesthetic Surgery Journal*, 19, 130-133.
- DI NAPOLI, A., PEPE, G., GIARNIERI, E., CIPPITELLI, C., BONIFACINO, A., MATTEI, M., MARTELLI, M., FALASCA, C., COX, M. C. & SANTINO, I. 2017. Cytological diagnostic features of late breast implant seromas: From reactive to anaplastic large cell lymphoma. *PLOS One*, 12, e0181097.
- DIAMANTIDIS, M. D. & MYROU, A. D. 2011. Perils and pitfalls regarding differential diagnosis and treatment of primary cutaneous anaplastic large - cell lymphoma. *The Scientific World Journal*, 11, 1048-1055.

- DIAMANTIDIS, M. D., PAPADOPOULOS, A., KAIAFA, G., NTAIOS, G., KARAYANNOPOULOU, G., KOSTOPOULOS, I., GIRTOVITIS, F., SAOULI, Z., KONTONINAS, Z. & RAPTIS, I. D. 2009. Differential diagnosis and treatment of primary, cutaneous, anaplastic large cell lymphoma: not always an easy task. *International Journal of Hematology*, 90, 226-229.
- DIEHN, M., ALIZADEH, A. A., RANDO, O. J., LIU, C. L., STANKUNAS, K., BOTSTEIN, D., CRABTREE, G. R. & BROWN, P. O. 2002. Genomic expression programs and the integration of the CD28 costimulatory signal in T cell activation. *Proceedings of the National Academy of Sciences*, 99, 11796-11801.
- DOBKE, M. K., GRZYBOWSKI, J., STEIN, P., LANDON, B. N., DOBAK, J. & PARSONS, C. L. 1994. Fibroblast behavior in vitro is unaltered by products of staphylococci cultured from silicone implants. *Annals of Plastic Surgery*, 32, 118-125.
- DOBKE, M. K., SVAHN, J. K., VASTINE, V. L., LANDON, B. N., STEIN, P. C. & PARSONS, C. L. 1995. Characterization of microbial presence at the surface of silicone mammary implants. *Annals of Plastic Surgery*, 34, 563-571.
- DONLAN, R. M. 2001. Biofilm formation: a clinically relevant microbiological process. *Clinical Infectious Diseases*, 33, 1387-1392.
- DONLAN, R. M. & COSTERTON, J. W. 2002. Biofilms: survival mechanisms of clinically relevant microorganisms. *Clinical Microbiology Reviews*, 15, 167-193.
- DOREN, E. L., MIRANDA, R. N., SELBER, J. C., GARVEY, P. B., LIU, J., MEDEIROS, L. J., BUTLER, C. E. & CLEMENS, M. W. 2017. US Epidemiology of Breast Implant – Associated Anaplastic Large Cell Lymphoma. *Plastic and Reconstructive Surgery*, 139, 1042-1050.
- DREXLER, H., GIGNAC, S., VON WASIELEWSKI, R., WERNER, M. & DIRKS, W. 2000. Pathobiology of NPM - ALK and variant fusion genes in anaplastic large cell lymphoma and other lymphomas. *Leukemia*, 14, 1533.
- DUVIC, M., MOORE, D., MENTER, A. & VONDERHEID, E. C. 1995. Cutaneous T - cell lymphoma in association with silicone breast implants. *Journal of the American Academy of Dermatology*, 32, 939-942.
- EDMISTON, C. E., MCBAIN, A. J., ROBERTS, C. & LEAPER, D. 2015. Clinical and microbiological aspects of biofilm - associated surgical site infections. *Biofilm - Based Healthcare - Associated Infections*, 830, 47-67.

- EHRENTAUT, S., NAGEL, S., SCHERR, M. E., SCHNEIDER, B., QUENTMEIER, H., GEFFERS, R., KAUFMANN, M., MEYER, C., PROCHOREC-SOBIESZEK, M. & KETTERLING, R. P. 2013. t (8; 9)(p22; p24)/PCM1-JAK2 Activates SOCS2 and SOCS3 via STAT5. *PLOS One*, 8, e53767.
- EHRlich, G. D., AHMED, A., EARL, J., HILLER, N. L., COSTERTON, J. W., STOODLEY, P., POST, J. C., DEMEO, P. & HU, F. Z. 2010. The distributed genome hypothesis as a rubric for understanding evolution in situ during chronic bacterial biofilm infectious processes. *FEMS Immunology and Medical Microbiology*, 59, 269-279.
- EL-SHEIKH, Y., TUTINO, R., KNIGHT, C., FARROKHVAR, F. & HYNES, N. 2008. Incidence of capsular contracture in silicone versus saline cosmetic augmentation mammoplasty: A meta - analysis. *Canadian Journal of Plastic Surgery*, 16, 211-215.
- EMU, B., SINCLAIR, E., HATANO, H., FERRE, A., SHACKLETT, B., MARTIN, J. N., MCCUNE, J. & DEEKS, S. G. 2008. HLA class I - restricted T - cell responses may contribute to the control of human immunodeficiency virus infection, but such responses are not always necessary for long - term virus control. *Journal of Virology*, 82, 5398-5407.
- EPSTEIN, A. L. & KAPLAN, H. S. 1979. Feeder layer and nutritional requirements for the establishment and cloning of human malignant lymphoma cell lines. *Cancer Research*, 39, 1748-1759.
- ERDMAN, S. E., RAO, V. P., OLIPITZ, W., TAYLOR, C. L., JACKSON, E. A., LEVKOVICH, T., LEE, C. W., HORWITZ, B. H., FOX, J. G. & GE, Z. 2010. Unifying roles for regulatory T cells and inflammation in cancer. *International Journal of Cancer*, 126, 1651-1665.
- ERSEK, R. A. & SALISBURY, A. V. 1997. Textured surface, nonsili - cone gel breast implants: Four years' clinical outcome. *Plastic and Reconstructive Surgery*, 100.
- EVREN, S., KHOURY, T., NEPPALLI, V., CAPPUCCINO, H., HERNANDEZ-ILIZALITURRI, F. J. & KUMAR, P. 2017. Breast Implant - Associated Anaplastic Large Cell Lymphoma (ALCL): A Case Report. *The American Journal of Case Reports*, 18, 605.
- FADEEVA, E., TRUONG, V. K., STIESCH, M., CHICHKOV, B. N., CRAWFORD, R. J., WANG, J. & IVANOVA, E. P. 2011. Bacterial retention on superhydrophobic titanium surfaces fabricated by femtosecond laser ablation. *Langmuir*, 27, 3012-3019.
- FAGRELL, D., BERGGREN, A. & TARPILA, E. 2001. Capsular contracture around saline-filled fine textured and smooth mammary implants: a prospective 7.5 - year follow - up. *Plastic and Reconstructive Surgery*, 108, 2108-12; discussion 2113.

- FALINI, B. & MARTELLI, M. P. 2009. Anaplastic large cell lymphoma: changes in the World Health Organization classification and perspectives for targeted therapy. *Haematologica*, 94, 897-900.
- FALINI, B., PILERI, S., ZINZANI, P. L., CARBONE, A., ZAGONEL, V., WOLF-PEETERS, C., VERHOEF, G., MENESTRINA, F., TODESCHINI, G. & PAULLI, M. 1999. ALK+ lymphoma: clinico-pathological findings and outcome. *Blood*, 93, 2697-2706.
- FDA 2013. Update on the Safety of Silicone Gel-Filled Breast Implants.
- FDA 2018. Breast Implant-Associated Anaplastic Large Cell Lymphoma (BIA-ALCL).
- FDA 2011. Anaplastic large cell lymphoma (ALCL) in women with breast implants: Preliminary FDA findings and analyses. *Center for Devices and Radiological Health Silver Spring*.
- FELGAR, R. E., SALHANY, K. E., MACON, W. R., PIETRA, G. G. & KINNEY, M. C. 1999. The expression of TIA - 1+ cytolytic - type granules and other cytolytic lymphocyte-associated markers in CD30+ anaplastic large cell lymphomas (ALCL): correlation with morphology, immunophenotype, ultrastructure, and clinical features. *Human Pathology*, 30, 228-236.
- FENG, C., STAMATOS, N. M., DRAGAN, A. I., MEDVEDEV, A., WHITFORD, M., ZHANG, L., SONG, C., RALLABHANDI, P., COLE, L. & NHU, Q. M. 2012. Sialyl residues modulate LPS - mediated signaling through the Toll - like receptor 4 complex. *PLOS One*, 7, e32359.
- FERRAJOLI, A., KEATING, M. J., MANSHOURI, T., GILES, F. J., DEY, A., ESTROV, Z., KOLLER, C. A., KURZROCK, R., THOMAS, D. A. & FADERL, S. 2002. The clinical significance of tumor necrosis factor - α plasma level in patients having chronic lymphocytic leukemia. *Blood*, 100, 1215-1219.
- FERRANDO, A. A. & LOOK, A. T, 2003. Gene expression profiling in T - cell acute lymphoblastic leukemia. *Seminars in Hematology*, 40, 274-280.
- FERRERI, A., DOGNINI, G., PONZONI, M., PECCIARINI, L., CANGI, M., SANTAMBROGIO, G., RESTI, A., DE CONCILIIS, C., MAGNINO, S. & PASINI, E. 2008. Chlamydia psittaci - eradicating antibiotic therapy in patients with advanced-stage ocular adnexal MALT lymphoma. *Annals of Oncology*, 19, 194-195.

- FERRERI, A. J., GOVI, S., PILERI, S. A. & SAVAGE, K. J. 2012. Anaplastic large cell lymphoma, ALK-positive. *Critical Reviews in Oncology/Hematology*, 83, 293-302.
- FERRERI, A. J., GUIDOBONI, M., PONZONI, M., DE CONCILIIS, C., DELL'ORO, S., FLEISCHHAUER, K., CAGGIARI, L., LETTINI, A. A., DAL CIN, E. & IERI, R. 2004. Evidence for an association between *Chlamydia psittaci* and ocular adnexal lymphomas. *Journal of the National Cancer Institute*, 96, 586-594.
- FERRERI, A. J., PONZONI, M., GUIDOBONI, M., DE CONCILIIS, C., RESTI, A. G., MAZZI, B., LETTINI, A. A., DEMETER, J., DELL'ORO, S. & DOGLIONI, C. 2005. Regression of ocular adnexal lymphoma after *Chlamydia psittaci* - eradicating antibiotic therapy. *Journal of Clinical Oncology*, 23, 5067-5073.
- FEY, P. D. & OLSON, M. E. 2010. Current concepts in biofilm formation of *Staphylococcus epidermidis*. *Future Microbiology*, 5, 917-933.
- FLEMMING, H. C. & WINGENDER, J. 2010. The biofilm matrix. *Nature Reviews Microbiology*, 8, 623.
- FOSS, H. D., ANAGNOSTOPOULOS, I., ARAUJO, I., ASSAF, C., DEMEL, G., KUMMER, J., HUMMEL, M. & STEIN, H. 1996. Anaplastic large - cell lymphomas of T - cell and null - cell phenotype express cytotoxic molecules. *Blood*, 88, 4005-4011.
- FRANCI, G., FALANGA, A., GALDIERO, S., PALOMBA, L., RAI, M., MORELLI, G. & GALDIERO, M. 2015. Silver nanoparticles as potential antibacterial agents. *Molecules*, 20, 8856-8874.
- FRANCOLINI, I. & DONELLI, G. 2010. Prevention and control of biofilm - based medical - device - related infections. *FEMS Immunology and Medical Microbiology*, 59, 227-238.
- FREEDMAN, A. & JACKSON, I. 1989. Infections in breast implants. *Infectious Disease Clinics of North America*, 3, 275-287.
- FRITZSCHE, F. R., PAHL, S., PETERSEN, I., BURKHARDT, M., DANKOF, A., DIETEL, M. & KRISTIANSEN, G. 2006. Anaplastic large - cell non - Hodgkin's lymphoma of the breast in periprosthetic localisation 32 years after treatment for primary breast cancer — a case report. *Virchows Archiv*, 449, 561-564.

- FRÖJD, V., LINDERBÄCK, P., WENNERBERG, A., DE PAZ, L. C., SVENSÄTER, G. & DAVIES, J. R. 2011. Effect of nanoporous TiO₂ coating and anodized Ca²⁺ modification of titanium surfaces on early microbial biofilm formation. *BMC Oral Health*, 11, 8.
- FUX, C., WILSON, S. & STOODLEY, P. 2004. Detachment characteristics and oxacillin resistance of *Staphylococcus aureus* biofilm emboli in an in vitro catheter infection model. *Journal of Bacteriology*, 186, 4486-4491.
- GABRIEL, S. E., WOODS, J. E., O'FALLON, W. M., BEARD, C. M., KURLAND, L. T. & MELTON, L. J., 3RD 1997. Complications leading to surgery after breast implantation. *The New England Journal of Medicine*, 336, 677-82.
- GALKIN, A. V., MELNICK, J. S., KIM, S., HOOD, T. L., LI, N., LI, L., XIA, G., STEENSMA, R., CHOPIUK, G. & JIANG, J. 2007. Identification of NVP - TAE684, a potent, selective, and efficacious inhibitor of NPM-ALK. *Proceedings of the National Academy of Sciences*, 104, 270-275.
- GANG, S. G., KIM, J. K., WEE, S. Y., KIM, C. H. & TARK, M. S. 2012. Peptococcus infection after breast augmentation using autologous fat injection. *Archives of Plastic Surgery*, 39, 669.
- GAUDET, G., FRIEDBERG, J. W., WENG, A., PINKUS, G. S. & FREEDMAN, A. S. 2002. Breast lymphoma associated with breast implants: two case - reports and a review of the literature. *Leukemia and Lymphoma*, 43, 115-119.
- GEISSMANN, F., JUNG, S. & LITTMAN, D. R. 2003. Blood monocytes consist of two principal subsets with distinct migratory properties. *Immunity*, 19, 71-82.
- GELLATLY, S. L. & HANCOCK, R. E. 2013. *Pseudomonas aeruginosa*: new insights into pathogenesis and host defenses. *Pathogens and Disease*, 67, 159-173.
- GEORGE, E. V., PHARM, J., HOUSTON, C., AL - QURAN, S., BRIAN, G., DONG, H., HAI, W., REEVES, W. & YANG, L. J. 2013. Breast implant - associated ALK - negative anaplastic large cell lymphoma: a case report and discussion of possible pathogenesis. *International Journal of Clinical and Experimental Pathology*, 6, 1631-42.
- GERFEN, C. R. & SAWCHENKO, P. E. 1984. An anterograde neuroanatomical tracing method that shows the detailed morphology of neurons, their axons and terminals: immunohistochemical localization of an axonally transported plant lectin, Phaseolus vulgaris leucoagglutinin (PHA - L). *Brain Research*, 290, 219-238.

- GIDENGIL, C. A., PREDMORE, Z., MATTKE, S., VAN BUSUM, K. & KIM, B. 2015. Breast implant-associated anaplastic large cell lymphoma: a systematic review. *Plastic and Reconstructive Surgery*, 135, 713-720.
- GIORDANO, S., PELTONIEMI, H., LILIUS, P. & SALMI, A. 2013. Povidone - iodine combined with antibiotic topical irrigation to reduce capsular contracture in cosmetic breast augmentation: a comparative study. *Aesthetic Surgery Journal*, 33, 675-680.
- GIRARD, R., PEDRON, T., UEMATSU, S., BALLOY, V., CHIGNARD, M., AKIRA, S. & CHABY, R. 2003. Lipopolysaccharides from *Legionella* and *Rhizobium* stimulate mouse bone marrow granulocytes via Toll - like receptor 2. *Journal of Cell Science*, 116, 293-302.
- GRIVENNIKOV, S. & KARIN, M. 2008. Autocrine IL - 6 signaling: a key event in tumorigenesis? *Cancer Cell*, 13, 7-9.
- GUALCO, G., CHIOATO, L., HARRINGTON JR, W. J., WEISS, L. M. & BACCHI, C. E. 2009. Primary and secondary T-cell lymphomas of the breast: clinico-pathologic features of 11 cases. *Applied immunohistochemistry & molecular morphology: AIMM/official publication of the Society for Applied Immunohistochemistry*, 17, 301.
- GUILHEN, C., FORESTIER, C. & BALESTRINO, D. 2017. Biofilm dispersal: multiple elaborate strategies for dissemination of bacteria with unique properties. *Molecular Microbiology*, 105, 188-210.
- GÜNTHER, F., WABNITZ, G. H., STROH, P., PRIOR, B., OBST, U., SAMSTAG, Y., WAGNER, C. & HÄNSCH, G. M. 2009. Host defence against *Staphylococcus aureus* biofilms infection: phagocytosis of biofilms by polymorphonuclear neutrophils (PMN). *Molecular Immunology*, 46, 1805-1813.
- HAJJAR, A. M., O'MAHONY, D. S., OZINSKY, A., UNDERHILL, D. M., ADEREM, A., KLEBANOFF, S. J. & WILSON, C. B. 2001. Cutting edge: functional interactions between toll-like receptor (TLR) 2 and TLR1 or TLR6 in response to phenol - soluble modulin. *The Journal of Immunology*, 166, 15-19.
- HAKELIUS, L. & OHLSEN, L. 1992. A clinical comparison of the tendency to capsular contracture between smooth and textured gel - filled silicone mammary implants. *Plastic Reconstructive Surgery*, 90, 247-54.
- HAKELIUS, L. & OHLSEN, L. 1997. Tendency to capsular contracture around smooth and textured gel-filled silicone mammary implants: a five - year follow - up. *Plastic and Reconstructive Surgery*, 100, 1566-9.

- HAKELIUS, L. & OHLSÉN, L. 1992. A clinical comparison of the tendency to capsular contracture between smooth and textured gel - filled silicone mammary implants. *Plastic and Reconstructive Surgery*, 90, 247-254.
- HALL-STOODLEY, L., COSTERTON, J. W. & STOODLEY, P. 2004. Bacterial biofilms: from the natural environment to infectious diseases. *Nature Reviews Microbiology*, 2, 95-108.
- HALLBERG, B. & PALMER, R. H. 2013. Mechanistic insight into ALK receptor tyrosine kinase in human cancer biology. *Nature Reviews Cancer*, 13, 685.
- HANDEL, N., CORDRAY, T., GUTIERREZ, J. & AL., E. 2006. A long - term study of outcomes, complications, and patient satisfaction with breast implants. *Plastic Reconstructive Surgery*, 117, 757.
- HANKE, M. L., HEIM, C. E., ANGLE, A., SANDERSON, S. D. & KIELIAN, T. 2013. Targeting macrophage activation for the prevention and treatment of Staphylococcus aureus biofilm infections. *The Journal of Immunology*, 190, 2159-2168.
- HANKE, M. L. & KIELIAN, T. 2012. Deciphering mechanisms of staphylococcal biofilm evasion of host immunity. *Frontiers in Cellular and Infection Microbiology*, 2, 62.
- HARRIS, L. G. & RICHARDS, R. G. 2006. Staphylococci and implant surfaces: a review. *Injury*, 37, S3-S14.
- HEADON, H., KASEM, A. & MOKBEL, K. 2015. Capsular Contracture after Breast Augmentation: An Update for Clinical Practice. *Archives of Plastic Surgery*, 42, 532-43.
- HEDEN, P., JERNBECK, J. & HOBER, M. 2001. Breast augmentation with anatomical cohesive gel implants: the world's largest current experience. *Clinics in Plastic Surgery*, 28, 531-52.
- HENDERSON, P. W., NASH, D., LASKOWSKI, M. & GRANT, R. T. 2015. Objective Comparison of Commercially Available Breast Implant Devices. *Aesthetic Plastic Surgery*, 39, 724-32.
- HENRIKSEN, T. F., FRYZEK, J. P., HOLMICH, L. R. & AL., E. 2005. Reconstructive breast implantation after mastectomy for breast cancer: clinical outcomes in a nationwide prospective cohort study. *The Archives of Surgery*, 140, 1152.

- HESTER JR, T. R., GHAZI, B. H., MOYER, H. R., NAHAI, F. R., WILTON, M. & STOKES, L. 2012. Use of dermal matrix to prevent capsular contracture in aesthetic breast surgery. *Plastic and Reconstructive Surgery*, 130, 126S-136S.
- HESTER, T. R. & CUKIC, J. 1990. Use of stacked polyurethane - covered mammary implants in aesthetic and reconstructive breast surgery. *Plastic Reconstructive Surgery*, 10, 503.
- HESTER, T. R., JR., TEBBETTS, J. B. & MAXWELL, G. P. 2001. The polyurethane - covered mammary prosthesis: facts and fiction (II): a look back and a "peek" ahead. *Clinics in Plastic Surgery*, 28, 579-86.
- HEYDARKHAN-HAGVALL, S., CHOI, C. H., DUNN, J. & AL., E. 2007. Influence of systematically varied nano - scale topography on cell morphology and adhesion. *Cell Communication and Adhesion*, 14, 14.
- HØGDALL, D., HVOLRIS, J. J. & CHRISTENSEN, L. 2010. Improved detection methods for infected hip joint prostheses. *APMIS*, 118, 815-823.
- HØIBY, N., BJARNSHOLT, T., GIVSKOV, M., MOLIN, S. & CIOFU, O. 2010. Antibiotic resistance of bacterial biofilms. *International Journal of Antimicrobial Agents*, 35, 322-332.
- HORI, K. & MATSUMOTO, S. 2010. Bacterial adhesion: from mechanism to control. *Biochemical Engineering Journal*, 48, 424-434.
- HOU, S., GU, H., SMITH, C. & REN, D. 2011. Microtopographic patterns affect Escherichia coli biofilm formation on poly (dimethylsiloxane) surfaces. *Langmuir*, 27, 2686-2691.
- HU, H., JACOMBS, A., VICKERY, K., MERTEN, S. L., PENNINGTON, D. G. & DEVA, A. K. 2015. Chronic biofilm infection in breast implants is associated with an increased T - cell lymphocytic infiltrate: implications for breast implant-associated lymphoma. *Plastic and Reconstructive Surgery*, 135, 319-29.
- HU, H., JOHANI, K., ALMATROUDI, A., VICKERY, K., VAN NATTA, B., KADIN, M. E., BRODY, G., CLEMENS, M., CHEAH, C. Y., LADE, S., JOSHI, P. A., PRINCE, H. M. & DEVA, A. K. 2016. Bacterial Biofilm Infection Detected in Breast Implant - Associated Anaplastic Large-Cell Lymphoma. *Plastic and Reconstructive Surgery*, 137, 1659-69.
- IRWIN, M. J., HUDSON, K. R., FRASER, J. D. & GASCOIGNE, N. R. 1992. Enterotoxin residues determining T-cell receptor V β binding specificity. *Nature*, 359, 841.

- IRWIN, M. J., HUDSON, K. R., AMES, K. T., FRASER, J. D. & GASCOIGNE, N. 1993. T-cell receptor beta-chain binding to enterotoxin superantigens. *Immunological Reviews*, 131, 61-78.
- ISAPS 2018. ISAPS International Survey on Aesthetic/Cosmetic. Available online: www.isaps.org (accessed on 28 December 2018).
- ISHII, K. J., KOYAMA, S., NAKAGAWA, A., COBAN, C. & AKIRA, S. 2008. Host innate immune receptors and beyond: making sense of microbial infections. *Cell Host and Microbe*, 3, 352-363.
- ISHITSUKA, K. & TAMURA, K. 2014. Human T - cell leukaemia virus type I and adult T-cell leukaemia-lymphoma. *The Lancet Oncology*, 15, e517-e526.
- ISLANDER, U., ANDERSSON, A., LINDBERG, E., ADLERBERTH, I., WOLD, A. E. & RUDIN, A. 2010. Superantigenic *Staphylococcus aureus* stimulates production of interleukin - 17 from memory but not naive T cells. *Infection and Immunity*, 78, 381-386.
- JACOMBS, A., ALLAN, J., HU, H., VALENTE, P. M., WESSELS, W. L., DEVA, A. K. & VICKERY, K. 2012. Prevention of biofilm - induced capsular contracture with antibiotic - impregnated mesh in a porcine model. *Aesthetic Surgery Journal*, 32, 886-891.
- JACOMBS, A., TAHIR, S., HU, H., DEVA, A. K., ALMATROUDI, A., WESSELS, W. L., BRADSHAW, D. A. & VICKERY, K. 2014. In vitro and in vivo investigation of the influence of implant surface on the formation of bacterial biofilm in mammary implants. *Plastic and Reconstructive Surgery*, 133, 471e-80e.
- JANOWSKY, E. C., KUPPER, L. L. & HULKA, B. S. 2000. Meta - analyses of the relation between silicone breast implants and the risk of connective - tissue diseases. *The New England Journal of Medicine*, 342, 781-790.
- JEANNERET-SOZZI, W., TAGHIAN, A., EPELBAUM, R., POORTMANS, P., ZWAHLEN, D., AMSLER, B., VILLETTE, S., BELKACÉMI, Y., NGUYEN, T. & SCALLIET, P. 2008. Primary breast lymphoma: patient profile, outcome and prognostic factors. A multicentre Rare Cancer Network study. *BMC Cancer*, 8, 86.
- JEFFERSON, K. K. 2004. What drives bacteria to produce a biofilm? *FEMS Microbiology Letters*, 236, 163-173.

- JENSEN, P. Ø., GIVSKOV, M., BJARNSHOLT, T. & MOSER, C. 2010. The immune system vs. *Pseudomonas aeruginosa* biofilms. *FEMS Immunology and Medical Microbiology*, 59, 292-305.
- JESAITIS, A. J., FRANKLIN, M. J., BERGLUND, D., SASAKI, M., LORD, C. I., BLEAZARD, J. B., DUFFY, J. E., BEYENAL, H. & LEWANDOWSKI, Z. 2003. Compromised host defense on *Pseudomonas aeruginosa* biofilms: characterization of neutrophil and biofilm interactions. *The Journal of Immunology*, 171, 4329-4339.
- JEWELL, M., SPEAR, S. L., LARGENT, J., OEFELEIN, M. G. & ADAMS JR, W. P. 2011. Anaplastic large T - cell lymphoma and breast implants: a review of the literature. *Plastic and Reconstructive Surgery*, 128, 651-661.
- JOKS, M., MYŚLIWIEC, K. & LEWANDOWSKI, K. 2011. Primary breast lymphoma – a review of the literature and report of three cases. *Archives of Medical Science: AMS*, 7, 27.
- JONULEIT, H., SCHMITT, E., STASSEN, M., TUETTENBERG, A., KNOP, J. & ENK, A. H. 2001. Identification and functional characterization of human CD4⁺ CD25⁺ T cells with regulatory properties isolated from peripheral blood. *Journal of Experimental Medicine*, 193, 1285-1294.
- JUNDT, F., ANAGNOSTOPOULOS, I., FÖRSTER, R., MATHAS, S., STEIN, H. & DÖRKEN, B. 2002. Activated Notch1 signaling promotes tumor cell proliferation and survival in Hodgkin and anaplastic large cell lymphoma. *Blood*, 99, 3398-3403.
- KADIN, M. E., CAVAILLE-COLL, M. W., GERTZ, R., MASSAGUE, J., CHEIFETZ, S. & GEORGE, D. 1994. Loss of receptors for transforming growth factor beta in human T - cell malignancies. *Proceedings of the National Academy of Sciences*, 91, 6002-6006.
- KADIN, M. E., DEVA, A., XU, H., MORGAN, J., KHARE, P., MACLEOD, R. A., VAN NATTA, B. W., ADAMS, W. P., JR., BRODY, G. S. & EPSTEIN, A. L. 2016. Biomarkers Provide Clues to Early Events in the Pathogenesis of Breast Implant-Associated Anaplastic Large Cell Lymphoma. *Aesthetic Surgery Journal*, 36, 773-781.
- KALIA, V. C. 2013. Quorum sensing inhibitors: an overview. *Biotechnology Advances*, 31, 224-245.
- KAMEL, M., PROTZNER, K., FORNASIER, V., PETERS, W., SMITH, D. & IBANEZ, D. 2001. The peri - implant breast capsule: An immunophenotypic study of capsules taken at explantation surgery. *Journal of Biomedical Materials Research Part A*, 58, 88-96.

- KARATAN, E. & WATNICK, P. 2009. Signals, regulatory networks, and materials that build and break bacterial biofilms. *Microbiology and Molecular Biology Reviews*, 73, 310-347.
- KATSIKOIANNI, M. & MISSIRLIS, Y. 2004. Concise review of mechanisms of bacterial adhesion to biomaterials and of techniques used in estimating bacteria - material interactions. *European Cells and Materials Journal*, 8, 37-57.
- KAWAI, T. & AKIRA, S. 2010. The role of pattern - recognition receptors in innate immunity: update on Toll - like receptors. *Nature Immunology*, 11, 373-384.
- KEECH, J. A., JR. & CREECH, B. J. 1997. Anaplastic T - cell lymphoma in proximity to a saline - filled breast implant. *Plastic and Reconstructive Surgery*, 100, 554-5.
- KELLOGG, B. C., HIRO, M. E. & PAYNE, W. G. 2014. Implant - associated anaplastic large cell lymphoma: beyond breast prostheses. *Annals of Plastic Surgery*, 73, 461-464.
- KEMPF, W. 2006. CD30+ lymphoproliferative disorders: histopathology, differential diagnosis, new variants, and simulators. *Journal of Cutaneous Pathology*, 33, 58-70.
- KEMPF, W., PFALTZ, K., VERMEER, M. H., COZZIO, A., ORTIZ-ROMERO, P. L., BAGOT, M., OLSEN, E., KIM, Y. H., DUMMER, R. & PIMPINELLI, N. 2011. EORTC, ISCL, and USCLC consensus recommendations for the treatment of primary cutaneous CD30 - positive lymphoproliferative disorders: lymphomatoid papulosis and primary cutaneous anaplastic large - cell lymphoma. *Blood*, 118, 4024-4035.
- KHAN, U. D. 2010. Breast augmentation, antibiotic prophylaxis, and infection: comparative analysis of 1,628 primary augmentation mammoplasties assessing the role and efficacy of antibiotics prophylaxis duration. *Aesthetic Plastic Surgery*, 34, 42-47.
- KIM, K. H., AKASE, Z., SUZUKI, T. & SHINDO, D. 2010. Charging effects on SEM/SIM contrast of metal/insulator system in various metallic coating conditions. *Materials transactions*, 51, 1080-1083.
- KINNEY, M. C. & JONES, D. 2007. Cutaneous T - cell and NK - cell lymphomas: the WHO - EORTC classification and the increasing recognition of specialized tumor types. *American Journal of Clinical Pathology*, 127, 670-686.
- KJØLLER, K., HOLMICH, L. R., JACOBSEN, P. H. & AL., E. 2002. Epidemiological investigation of local complications after cosmetic breast implant surgery in Denmark. *Annals of Plastic Surgery*, 48, 229.

- KLOOS, W. E. & MUSSELWHITE, M. S. 1975. Distribution and persistence of *Staphylococcus* and *Micrococcus* species and other aerobic bacteria on human skin. *Applied Microbiology*, 30, 381-395.
- KNIGHT, R., LOCH-WILKINSON, A. M., WESSELS, W., PAPADOPOULOS, T., MAGNUSSON, M., LOFTS, J., CONNELL, T., HOPPER, I., BEATH, K. & LADE, S. 2016. Epidemiology and risk factors for Breast implant-associated anaplastic large cell lymphoma (BIA - ALCL) in Australia & New Zealand. *Plastic and Reconstructive Surgery Global Open*, 4, 94-95.
- KORN, T., BETTELLI, E., OUKKA, M. & KUCHROO, V. K. 2009. IL - 17 and Th17 Cells. *Annual Review of immunology*, 27, 485-517.
- KRAEMER, D. M., TONY, H.-P., GATTENLOHNER, S. & MULLER, J. 2003. Lymphoplasmacytic lymphoma in a patient with leaking silicone implant. *Haematologica*, 88, ELT30.
- KREJSGAARD, T., LITVINOV, I. V., WANG, Y., XIA, L., WILLERSLEV-OLSEN, A., KORALOV, S. B., KOPP, K. L., BONEFELD, C. M., WASIK, M. A. & GEISLER, C. 2013. Elucidating the role of interleukin - 17F in cutaneous T - cell lymphoma. *Blood*, 122, 943-950.
- KRENACS, L., WELLMANN, A., SORBARA, L., HIMMELMANN, A. W., BAGDI, E., JAFFE, E. S. & RAFFELD, M. 1997. Cytotoxic cell antigen expression in anaplastic large cell lymphomas of T - and null - cell type and Hodgkin's disease: evidence for distinct cellular origin. *Blood*, 89, 980-989.
- KRITIKOS, A., PAGIN, M., BORENS, O., VOIDE, C. & ORASCH, C. 2015. Identification of *Propionibacterium avidum* from a breast abscess: an overlooked etiology of clinically significant infections. *New Microbes and New Infections*, 4, 9-10.
- KUEFER, M. U., LOOK, A. T., PULFORD, K., BEHM, F. G., PATTENGAL, P. K., MASON, D. Y. & MORRIS, S. W. 1997. Retrovirus - mediated gene transfer of NPM - ALK causes lymphoid malignancy in mice. *Blood*, 90, 2901-2910.
- KUMAR, D., PANIGRAHI, M. K., SURYAVANSHI, M., MEHTA, A. & SAIKIA, K. K. 2016. Quantification of DNA extracted from formalin fixed paraffin - embedded tissue comparison of three techniques: Effect on PCR efficiency. *Journal of Clinical and Diagnostic Research: JCDR*, 10, BC01.

- KUO, S. H. & CHENG, A. L. 2013. *Helicobacter pylori* and mucosa - associated lymphoid tissue: what's new. *ASH Education Program Book*, 2013, 109-117.
- KWA, M., PLOTTEL, C. S., BLASER, M. J. & ADAMS, S. 2016. The intestinal microbiome and estrogen receptor – positive female breast cancer. *JNCI: Journal of the National Cancer Institute*, 108.
- LAM, L. T., WRIGHT, G., DAVIS, R. E., LENZ, G., FARINHA, P., DANG, L., CHAN, J. W., ROSENWALD, A., GASCOYNE, R. D. & STAUDT, L. M. 2008. Cooperative signaling through the signal transducer and activator of transcription 3 and nuclear factor - κ B pathways in subtypes of diffuse large B - cell lymphoma. *Blood*, 111, 3701-3713.
- LAPID, O. 2011. Use of gentamicin collagen sponges for the treatment of periprosthetic breast implant infection. *Journal of Plastic, Reconstructive and Aesthetic Surgery*, 64, e313-e316.
- LASA, I. & PENADÉS, J. R. 2006. Bap: a family of surface proteins involved in biofilm formation. *Research in Microbiology*, 157, 99-107.
- LAZZERI, D., AGOSTINI, T., BOCCI, G., GIANNOTTI, G., FANELLI, G., NACCARATO, A. G., DANESI, R., TUCCORI, M., PANTALONI, M. & D'ANIELLO, C. 2011. ALK - 1 – negative anaplastic large cell lymphoma associated with breast implants: a new clinical entity. *Clinical Breast Cancer*, 11, 283-296.
- LECHNER, M. G., LADE, S., LIEBERTZ, D. J., PRINCE, H. M., BRODY, G. S., WEBSTER, H. R. & EPSTEIN, A. L. 2011. Breast implant - associated, ALK - negative, T - cell, anaplastic, large - cell lymphoma: establishment and characterization of a model cell line (TLBR - 1) for this newly emerging clinical entity. *Cancer*, 117, 1478-89.
- LECHNER, M. G., LIEBERTZ, D. J. & EPSTEIN, A. L. 2010. Characterization of cytokine - induced myeloid - derived suppressor cells from normal human peripheral blood mononuclear cells. *The Journal of Immunology*, 185, 2273-2284.
- LECHNER, M. G., MEGIEL, C., CHURCH, C. H., ANGELL, T. E., RUSSELL, S. M., SEVELL, R. B., JANG, J. K., BRODY, G. S. & EPSTEIN, A. L. 2012. Survival signals and targets for therapy in breast implant - associated ALK - anaplastic large cell lymphoma. *Clinical Cancer Research*, 18, 4549-4559.
- LEID, J. G., WILLSON, C. J., SHIRTLIFF, M. E., HASSETT, D. J., PARSEK, M. R. & JEFFERS, A. K. 2005. The exopolysaccharide alginate protects *Pseudomonas aeruginosa* biofilm bacteria from IFN - γ - mediated macrophage killing. *The Journal of Immunology*, 175, 7512-7518.

- LEMAITRE, F., STEIN, A., RAOULT, D. & DRANCOURT, M. 2011. Pseudoclavibacter - like subcutaneous infection: a case report. *Journal of Medical Case Reports*, 5, 468.
- LEMPERLE, G. & EXNER, K. 1993. Effect of cortisone on capsular contracture in double-lumen breast implants: ten years' experience. *Aesthetic Plastic Surgery*, 17, 317-323.
- LEVIN, B., FOO, H., LEE, A. & GOTTLIEB, T. 2008. Propionibacterium avidum as the cause of severe breast infection following reduction mammoplasty. *ANZ Journal of Surgery*, 78, 318-319.
- LEWIS, K. 2010. Persister cells. *Annual Review of Microbiology*, 64, 357-372.
- LIN, Z., LU, J., ZHOU, W. & SHEN, Y. 2012. Structural insights into TIR domain specificity of the bridging adaptor Mal in TLR4 signaling. *PLOS One*, 7, e34202.
- LINNEMANN, T., GELLRICH, S., LUKOWSKY, A., MIELKE, A., AUDRING, H., STERRY, W. & WALDEN, P. 2004. Polyclonal expansion of T cells with the TCR V β type of the tumour cell in lesions of cutaneous T - cell lymphoma: evidence for possible superantigen involvement. *British Journal of Dermatology*, 150, 1013-1017.
- LIU, X., ZHOU, L., PAN, F., GAO, Y., YUAN, X. & FAN, D. 2015. Comparison of the postoperative incidence rate of capsular contracture among different breast implants: a cumulative meta - analysis. *PLOS One*, 10, e0116071.
- LOCH-WILKINSON, A., BEATH, K. J., KNIGHT, R. J. W., WESSELS, W. L. F., MAGNUSSON, M., PAPADOPOULOS, T., CONNELL, T., LOFTS, J., LOCKE, M. & HOPPER, I. 2017. Breast implant – associated anaplastic large cell lymphoma in Australia and New Zealand: High - surface - area textured implants are associated with increased risk. *Plastic and Reconstructive Surgery*, 140, 645-654.
- LÓPEZ, D., VLAMAKIS, H. & KOLTER, R. 2010. Biofilms. *Cold Spring Harbor Perspectives in Biology*, 2, a000398.
- LUCAS, K. & MAES, M. 2013. Role of the Toll Like receptor (TLR) radical cycle in chronic inflammation: possible treatments targeting the TLR4 pathway. *Molecular Neurobiology*, 48, 190-204.
- LUNDBERG, D. S., YOURSTONE, S., MIECZKOWSKI, P., JONES, C. D. & DANGL, J. L. 2013. Practical innovations for high-throughput amplicon sequencing. *Nature Methods*, 10, 999.

- LYSAKOVA-DEVINE, T., KEOGH, B., HARRINGTON, B., NAGPAL, K., HALLE, A., GOLENBOCK, D. T., MONIE, T. & BOWIE, A. G. 2010. Viral inhibitory peptide of TLR4, a peptide derived from vaccinia protein A46, specifically inhibits TLR4 by directly targeting MyD88 adaptor - like and TRIF - related adaptor molecule. *The Journal of Immunology*, 185, 4261-4271.
- MA, J., SUN, Y., GLEICHAUF, K., LOU, J. & LI, Q. 2011. Nanostructure on taro leaves resists fouling by colloids and bacteria under submerged conditions. *Langmuir*, 27, 10035-10040.
- MACADAM, S. A., HO, A. L., LENNOX, P. A. & PUSIC, A. L. 2013. Patient - reported satisfaction and health-related quality of life following breast reconstruction: a comparison of shaped cohesive gel and round cohesive gel implant recipients. *Plastic Reconstructive Surgery*, 131, 431-41.
- MAH, T.-F. C. & O'TOOLE, G. A. 2001. Mechanisms of biofilm resistance to antimicrobial agents. *Trends in Microbiology*, 9, 34-39.
- MALATA, C. M., FELDBERG, L., COLEMAN, D. J., FOO, I. T. & SHARPE, D. T. 1997. Textured or smooth implants for breast augmentation? Three year follow - up of a prospective randomised controlled trial. *British Journal of Plastic Surgery*, 50, 99-105.
- MARQUES, M., BROWN, S. A., CORDEIRO, N. D., RODRIGUES-PEREIRA, P., COBRADO, M. L., MORALES-HELGUERA, A., QUEIRÓS, L., LUÍS, A., FREITAS, R. & GONÇALVES-RODRIGUES, A. 2011. Effects of coagulase - negative staphylococci and fibrin on breast capsule formation in a rabbit model. *Aesthetic Surgery Journal*, 31, 420-428.
- MATHAS, S., HINZ, M., ANAGNOSTOPOULOS, I., KRAPPMANN, D., LIETZ, A., JUNDT, F., BOMMERT, K., MECHTA-GRIGORIOU, F., STEIN, H. & DÖRKEN, B. 2002. Aberrantly expressed c - Jun and JunB are a hallmark of Hodgkin lymphoma cells, stimulate proliferation and synergize with NF - κ B. *The EMBO Journal*, 21, 4104-4113.
- MATIS, L. A., GLIMCHER, L. H., PAUL, W. E. & SCHWARTZ, R. H. 1983. Magnitude of response of histocompatibility - restricted T - cell clones is a function of the product of the concentrations of antigen and Ia molecules. *Proceedings of the National Academy of Sciences*, 80, 6019-6023.
- MATZ, C. & KJELLEBERG, S. 2005. Off the hook – how bacteria survive protozoan grazing. *Trends in Microbiology*, 13, 302-307.

- MAXWELL, G. P. & GABRIEL, A. 2009. The evolution of breast implants. *Clinics in Plastic Surgery*, 36, 1-13.
- MAXWELL, G. P. & GABRIEL, A. 2014. The evolution of breast implants. *Plastic and Reconstructive Surgery*, 134, 12S-17S.
- MCALEER, J. P. & VELLA, A. T. 2008. Understanding how lipopolysaccharide impacts CD4 T - cell immunity. *Critical Reviews in Immunology*, 28, 281-299.
- MCCARTHY, C. M., KLASSEN, A. F., CANO, S. J., SCOTT, A., VANLAEKEN, N., LENNOX, P. A., ALDERMAN, A. K., MEHRARA, B. J., DISA, J. J., CORDEIRO, P. G. & PUSIC, A. L. 2010. Patient satisfaction with postmastectomy breast reconstruction: a comparison of saline and silicone implants. *Cancer*, 116, 5584-91.
- MCCAUL, J., ASLAAM, A., SPOONER, R., LOUDEN, I., CAVANAGH, T. & PURUSHOTHAM, A. 2000. Aetiology of seroma formation in patients undergoing surgery for breast cancer. *The Breast*, 9, 144-148.
- MCCORMICK, J. K., YARWOOD, J. M. & SCHLIEVERT, P. M. 2001. Toxic shock syndrome and bacterial superantigens: an update. *Annual Reviews in Microbiology*, 55, 77-104.
- MCLAUGHLIN, J. K., LIPWORTH, L., MURPHY, D. K. & AL., E. 2007. The safety of silicone gel-filled breast implants: a review of the epidemiologic evidence. *Annals of Plastic Surgery*, 59, 569.
- MEDILANSKI, E., KAUFMANN, K., WICK, L. Y., WANNER, O. & HARMS, H. 2002. Influence of the surface topography of stainless steel on bacterial adhesion. *Biofouling*, 18, 193-203.
- MEYLE, E., STROH, P., GÜNTHER, F., HOPPY-TICHY, T., WAGNER, C. & HÄNSCH, G. M. 2010. Destruction of bacterial biofilms by polymorphonuclear neutrophils: relative contribution of phagocytosis, DNA release, and degranulation. *The International Journal of Artificial Organs*, 33, 608-620.
- MILLER, S. I., ERNST, R. K. & BADER, M. W. 2005. LPS, TLR4 and infectious disease diversity. *Nature Reviews Microbiology*, 3, 36-46.
- MIRVISH, E. D., POMERANTZ, R. G. & GESKIN, L. J. 2011. Infectious agents in cutaneous T - cell lymphoma. *Journal of the American Academy of Dermatology*, 64, 423-431.

- MIRZABEIGI, M. N., SBITANY, H., JANDALI, S. & SERLETTI, J. M. 2011. The role of postoperative antibiotics in reducing biofilm - related capsular contracture in augmentation mammoplasty. *Plastic and Reconstructive Surgery*, 128, 34e-35e.
- MITIK-DINEVA, N., WANG, J., TRUONG, V., STODDART, P., ALEXANDER, M., ALBUTT, D., FLUKE, C., CRAWFORD, R. & IVANOVA, E. 2010. Bacterial attachment on optical fibre surfaces. *Biofouling*, 26, 461-470.
- MITIK-DINEVA, N., WANG, J., TRUONG, V. K., STODDART, P., MALHERBE, F., CRAWFORD, R. J. & IVANOVA, E. P. 2009. Escherichia coli, Pseudomonas aeruginosa, and Staphylococcus aureus attachment patterns on glass surfaces with nanoscale roughness. *Current Microbiology*, 58, 268-273.
- MIURA, N., HAMAMOTO, T., OKADA, K., NOGUCHI, N., MITSUDA, A., KITAOKA, S., UMEKI, K., KITANO, M., MATSUNO, M. & SUOU, T. 1996. Regression of primary low - grade B - cell gastric lymphoma of mucosa-associated lymphoid tissue type after eradication of Helicobacter pylori. *Gastroenterological Endoscopy*, 38, 1068-1072.
- MIYOSHI, I. 1982. Type C - virus producing cell lines derived from adult T cell leukemia. *Gann Monograph on Cancer Research*, 28, 219-228.
- MLADICK, R. A. 1993. "No - touch" submuscular saline breast augmentation technique. *Aesthetic Plastic Surgery*, 17, 183-192.
- MORTON, L. M., WANG, S. S., DEVESA, S. S., HARTGE, P., WEISENBURGER, D. D. & LINET, M. S. 2006. Lymphoma incidence patterns by WHO subtype in the United States, 1992-2001. *Blood*, 107, 265-276.
- MOSCOSO, M., GARCÍA, E. & LÓPEZ, R. 2006. Biofilm formation by Streptococcus pneumoniae: role of choline, extracellular DNA, and capsular polysaccharide in microbial accretion. *Journal of Bacteriology*, 188, 7785-7795.
- MUKHTAR, R. A., THROCKMORTON, A. D., ALVARADO, M. D., EWING, C. A., ESSERMAN, L. J., CHIU, C. & HWANG, E. S. 2009. Bacteriologic features of surgical site infections following breast surgery. *The American Journal of Surgery*, 198, 529-531.
- MURANSKI, P., BORMAN, Z. A., KERKAR, S. P., KLEBANOFF, C. A., JI, Y., SANCHEZ-PEREZ, L., SUKUMAR, M., REGER, R. N., YU, Z. & KERN, S. J. 2011. Th17 cells are long lived and retain a stem cell - like molecular signature. *Immunity*, 35, 972-985.

- MUSSOLIN, L., DAMM-WELK, C., PILLON, M., ZIMMERMANN, M., FRANCESCHETTO, G., PULFORD, K., REITER, A., ROSOLEN, A. & WOESSMANN, W. 2013. Use of minimal disseminated disease and immunity to NPM-ALK antigen to stratify ALK - positive ALCL patients with different prognosis. *Leukemia*, 27, 416.
- MUZZAFAR, T., WEI, E. X., LIN, P., MEDEIROS, L. J. & JORGENSEN, J. L. 2009. Flow cytometric immunophenotyping of anaplastic large cell lymphoma. *Archives of Pathology and Laboratory Medicine*, 133, 49-56.
- NAGAI, Y., AKASHI, S., NAGAFUKU, M., OGATA, M., IWAKURA, Y., AKIRA, S., KITAMURA, T., KOSUGI, A., KIMOTO, M. & MIYAKE, K. 2002. Essential role of MD - 2 in LPS responsiveness and TLR4 distribution. *Nature Immunology*, 3, 667.
- NAHABEDIAN, M. Y. 2014. Shaped versus Round Implants for Breast Reconstruction: Indications and Outcomes. *Plastic and Reconstructive Surgery - Global Open*, 2, e116.
- NAHORI, M.-A., FOURNIÉ-AMAZOUZ, E., QUE-GEWIRTH, N. S., BALLOY, V., CHIGNARD, M., RAETZ, C. R., SAINT GIRON, I. & WERTS, C. 2005. Differential TLR recognition of leptospiral lipid A and lipopolysaccharide in murine and human cells. *The Journal of Immunology*, 175, 6022-6031.
- NAMNOUM, J. D., LARGENT, J., KAPLAN, H. M., OEFELEIN, M. G. & BROWN, M. H. 2013. Primary breast augmentation clinical trial outcomes stratified by surgical incision, anatomical placement and implant device type. *Journal of Plastic, Reconstructive and Aesthetic Surgery*, 66, 1165-72.
- NEMECEK, J. A. & YOUNG, V. L. 1993. How safe are silicone breast implants? *Southern Medical Journal*, 86, 932-944.
- NETSCHER, D. T. 2004. Subclinical infection in breast capsules. *Plastic and Reconstructive Surgery*, 114, 818-20.
- NETSCHER, D. T., WEIZER, G., WIGODA, P., WALKER, L. E., THORNBY, J. & BOWEN, D. 1995. Clinical relevance of positive breast periprosthetic cultures without overt infection. *Plastic and Reconstructive Surgery*, 96, 1125-1129.
- NEWMAN, M. K., ZEMMEL, N. J., BANDAK, A. Z. & KAPLAN, B. J. 2008. Primary breast lymphoma in a patient with silicone breast implants: a case report and review of the literature. *Journal of Plastic, Reconstructive and Aesthetic Surgery*, 61, 822-825.

- NICHTER, L. S., HARDESTY, R. A. & ANIGIAN, G. M. 2018. IDEAL IMPLANT® Structured Breast Implants: Core Study Results at 6 Years. *Plastic and Reconstructive Surgery*, 142, 66-75.
- NOTO, J. M. & PEEK JR, R. M. 2017. The gastric microbiome, its interaction with *Helicobacter pylori*, and its potential role in the progression to stomach cancer. *PLOS Pathogens*, 13, e1006573.
- NURYASTUTI, T., KROM, B. P., AMAN, A. T., BUSSCHER, H. J. & VAN DER MEI, H. C. 2011. Ica - expression and gentamicin susceptibility of *Staphylococcus epidermidis* biofilm on orthopedic implant biomaterials. *Journal of Biomedical Materials Research Part A*, 96, 365-371.
- O'GARA, J. P. 2007. Ica and beyond: biofilm mechanisms and regulation in *Staphylococcus epidermidis* and *Staphylococcus aureus*. *FEMS Microbiology Letters*, 270, 179-188.
- O'GARA, J. P. & HUMPHREYS, H. 2001. *Staphylococcus epidermidis* biofilms: importance and implications. *Journal of Medical Microbiology*, 50, 582-587.
- O'SHAUGHNESSY, K. 2015. Evolution and update on current devices for prosthetic breast reconstruction. *Gland Surgery*, 4, 97-110.
- OLSEN, M. A., LEFTA, M., DIETZ, J. R., BRANDT, K. E., AFT, R., MATTHEWS, R., MAYFIELD, J. & FRASER, V. J. 2008. Risk factors for surgical site infection after major breast operation. *Journal of the American College of Surgeons*, 207, 326-335.
- OLSON, M. E., CERI, H., MORCK, D. W., BURET, A. G. & READ, R. R. 2002. Biofilm bacteria: formation and comparative susceptibility to antibiotics. *Canadian Journal of Veterinary Research*, 66, 86.
- ØRUM, H., NIELSEN, P. E., EGHOLM, M., BERG, R. H., BUCHARDT, O. & STANLEY, C. 1993. Single base pair mutation analysis by PNA directed PCR clamping. *Nucleic Acids Research*, 21, 5332-5336.
- OTTO, M. 2008. Staphylococcal biofilms. *Microbiology and Immunology*, 332, 207-228.
- PAJKOS, A., DEVA, A. K., VICKERY, K., COPE, C., CHANG, L. & COSSART, Y. E. 2003. Detection of subclinical infection in significant breast implant capsules. *Plastic and Reconstructive Surgery*, 111, 1605-1611.

- PAMP, S. J., GJERMANSEN, M., JOHANSEN, H. K. & TOLKER - NIELSEN, T. 2008. Tolerance to the antimicrobial peptide colistin in *Pseudomonas aeruginosa* biofilms is linked to metabolically active cells, and depends on the *pmr* and *mexAB - oprM* genes. *Molecular Microbiology*, 68, 223-240.
- PANNECOUQUE, C., DAELEMANS, D. & DE CLERCQ, E. 2008. Tetrazolium - based colorimetric assay for the detection of HIV replication inhibitors: revisited 20 years later. *Nature Protocols*, 3, 427.
- PARK, B. Y., LEE, D. H., LIM, S. Y., PYON, J. K., MUN, G. H., OH, K. S. & BANG, S. I. 2014. Is late seroma a phenomenon related to textured implants? A report of rare complications and a literature review. *Aesthetic Plastic Surgery*, 38, 139-145.
- PARSEK, M. R. & FUQUA, C. 2004. Biofilms 2003: emerging themes and challenges in studies of surface-associated microbial life. *Journal of Bacteriology*, 186, 4427-4440.
- PARSEK, M. R. & SINGH, P. K. 2003. Bacterial biofilms: an emerging link to disease pathogenesis. *Annual Reviews in Microbiology*, 57, 677-701.
- PARSONNET, J., HANSEN, S., RODRIGUEZ, L., GELB, A. B., WARNKE, R. A., JELLUM, E., ORENTREICH, N., VOGELMAN, J. H. & FRIEDMAN, G. D. 1994. *Helicobacter pylori* infection and gastric lymphoma. *The New England Journal of Medicine*, 330, 1267-1271.
- PARSONNET, J. & ISAACSON, P. G. 2004. Bacterial infection and MALT lymphoma. *The New England Journal of Medicine*, 350, 213-215.
- PASMORE, M., TODD, P., SMITH, S., BAKER, D., SILVERSTEIN, J., COONS, D. & BOWMAN, C. N. 2001. Effects of ultrafiltration membrane surface properties on *Pseudomonas aeruginosa* biofilm initiation for the purpose of reducing biofouling. *Journal of Membrane Science*, 194, 15-32.
- PASSOS, S. T., SILVER, J. S., O'HARA, A. C., SEHY, D., STUMHOFFER, J. S. & HUNTER, C. A. 2010. IL - 6 promotes NK cell production of IL - 17 during toxoplasmosis. *The Journal of Immunology*, 184, 1776-1783.
- PASTORELLO, R. G., COSTA, F. D. A., OSÓRIO, C. A., MAKDISSI, F. B., BEZERRA, S. M., DE BROT, M., CAMPOS, A. H. J., SOARES, F. A. & VASSALLO, J. 2018. Breast implant-associated anaplastic large cell lymphoma in a Li-FRAUMENI patient: a case report. *Diagnostic pathology*, 13, 10.

- PAVITHRA, D. & DOBLE, M. 2008. Biofilm formation, bacterial adhesion and host response on polymeric implants — issues and prevention. *Biomedical Materials*, 3, 034003.
- PAWSON, R., SCHULZ, T., MATUTES, E. & CATOVSKY, D. 1997. The human T - cell lymphotropic viruses types I/II are not involved in T prolymphocytic leukemia and large granular lymphocytic leukemia. *Leukemia*, 11, 1305-1311.
- PAYDAS, S. 2015. Hepatitis C virus and lymphoma. *Critical Reviews in Oncology/Hematology*, 93, 246-256.
- PEARSON, J. D., LEE, J. K., BACANI, J. T., LAI, R. & INGHAM, R. J. 2012. NPM-ALK: the prototypic member of a family of oncogenic fusion tyrosine kinases. *Journal of Signal Transduction*, 2012.
- PEEK, R. M., JR. & KUIPERS, E. J. 2012. Gained in translation: the importance of biologically relevant models of *Helicobacter pylori* - induced gastric cancer. *Gut*, 61, 2-3.
- PENNOCK, N. D., WHITE, J. T., CROSS, E. W., CHENEY, E. E., TAMBURINI, B. A. & KEDL, R. M. 2013. T cell responses: naive to memory and everything in between. *Advances in Physiology Education*, 37, 273-283.
- PERCIVAL, S. L., SULEMAN, L., VUOTTO, C. & DONELLI, G. 2015. Healthcare - associated infections, medical devices and biofilms: risk, tolerance and control. *Journal of Medical Microbiology*, 64, 323-334.
- PERIASAMY, S., JOO, H. S., DUONG, A. C., BACH, T. H. L., TAN, V. Y., CHATTERJEE, S. S., CHEUNG, G. Y. & OTTO, M. 2012. How *Staphylococcus aureus* biofilms develop their characteristic structure. *Proceedings of the National Academy of Sciences*, 109, 1281-1286.
- PFAFFL, M. W., HORGAN, G. W. & DEMPFL, L. 2002. Relative expression software tool (REST©) for group-wise comparison and statistical analysis of relative expression results in real-time PCR. *Nucleic Acids Research*, 30, e36-e36.
- PFOERTNER, S., JERON, A., PROBST-KEPPER, M., GUZMAN, C. A., HANSEN, W., WESTENDORF, A. M., TOEPFER, T., SCHRADER, A. J., FRANZKE, A. & BUER, J. 2006. Signatures of human regulatory T cells: an encounter with old friends and new players. *Genome Biology*, 7, R54.

- PIAO, W., RU, L. W., PIEPENBRINK, K. H., SUNDBERG, E. J., VOGEL, S. N. & TOSHCHAKOV, V. Y. 2013. Recruitment of TLR adapter TRIF to TLR4 signaling complex is mediated by the second helical region of TRIF TIR domain. *Proceedings of the National Academy of Sciences*, 110, 19036-19041.
- PIER, G. B., COLEMAN, F., GROUT, M., FRANKLIN, M. & OHMAN, D. E. 2001. Role of alginate O acetylation in resistance of mucoid *Pseudomonas aeruginosa* to opsonic phagocytosis. *Infection and Immunity*, 69, 1895-1901.
- PINCHUK, I. V., BESWICK, E. J. & REYES, V. E. 2010. Staphylococcal enterotoxins. *Toxins*, 2, 2177-2197.
- PITTET, B., MONTANDON, D. & PITTET, D. 2005. Infection in breast implants. *The Lancet Infectious Diseases*, 5, 94-106.
- POEPPL, N., SCHREML, S., LICHTENEGGER, F., LENICH, A., EISENMANN-KLEIN, M. & PRANTL, L. 2007. Does the surface structure of implants have an impact on the formation of a capsular contracture? *Aesthetic Plastic Surgery*, 31, 133-139.
- POLLOCK, H. 1993. Breast capsular contracture: a retrospective study of textured versus smooth silicone implants. *Plastic and Reconstructive Surgery*, 91, 404.
- PONTZER, C. H., IRWIN, M. J., GASCOIGNE, N. & JOHNSON, H. M. 1992. T - cell antigen receptor binding sites for the microbial superantigen staphylococcal enterotoxin A. *Proceedings of the National Academy of Sciences*, 89, 7727-7731.
- PUCKETT, S. D., TAYLOR, E., RAIMONDO, T. & WEBSTER, T. J. 2010. The relationship between the nanostructure of titanium surfaces and bacterial attachment. *Biomaterials*, 31, 706-713.
- PULFORD, K., LAMANT, L., MORRIS, S. W., BUTLER, L. H., WOOD, K. M., STROUD, D., DELSOL, G. & MASON, D. Y. 1997. Detection of anaplastic lymphoma kinase (ALK) and nucleolar protein nucleophosmin (NPM) - ALK proteins in normal and neoplastic cells with the monoclonal antibody ALK1. *Blood*, 89, 1394-1404.
- RAETZ, C. R. & WHITFIELD, C. 2002. Lipopolysaccharide endotoxins. *Annual Review of Biochemistry*, 71, 635-700.
- RAMACHANDRAN, G. 2014. Gram - positive and gram - negative bacterial toxins in sepsis: a brief review. *Virulence*, 5, 213-218.

- RANSJÖ, U., ASPLUND, O., GYLBERT, L. & JURELL, G. 1985. Bacteria in the female breast. *Scandinavian Journal of Plastic and Reconstructive Surgery*, 19, 87-89.
- RIBEIRO, M., MONTEIRO, F. J. & FERRAZ, M. P. 2012. Infection of orthopedic implants with emphasis on bacterial adhesion process and techniques used in studying bacterial - material interactions. *Biomatter*, 2, 176-194.
- RICE, S. A., TAN, C. H., MIKKELSEN, P. J., KUNG, V., WOO, J., TAY, M., HAUSER, A., MCDOUGALD, D., WEBB, J. S. & KJELLEBERG, S. 2009. The biofilm life cycle and virulence of *Pseudomonas aeruginosa* are dependent on a filamentous prophage. *The ISME Journal*, 3, 271.
- RIEGER, U., MESINA, J., KALBERMATTEN, D., HAUG, M., FREY, H., PICO, R., FREI, R., PIERER, G., LÜSCHER, N. & TRAMPUZ, A. 2013. Bacterial biofilms and capsular contracture in patients with breast implants. *British Journal of Surgery*, 100, 768-774.
- RIEGER, U. M., RASCHKE, G. F., FREI, R., DJEDOVIC, G., PIERER, G. & TRAMPUZ, A. 2014. Role of bacterial biofilms in patients after reconstructive and aesthetic breast implant surgery. *Journal of Long Term Effects of Medical Implants*, 24, 131-8.
- RIERA, L., LASORSA, E., AMBROGIO, C., SURRENTI, N., VOENA, C. & CHIARLE, R. 2010. Involvement of GRB2 adaptor protein in nucleophosmin - anaplastic lymphoma kinase (NPM - ALK) mediated signaling and anaplastic large cell lymphoma growth. *Journal of Biological Chemistry*, 285, 26441-26450.
- RODEN, A. C., MACON, W. R., KEENEY, G. L., MYERS, J. L., FELDMAN, A. L. & DOGAN, A. 2008. Seroma - associated primary anaplastic large - cell lymphoma adjacent to breast implants: an indolent T-cell lymphoproliferative disorder. *Modern Pathology*, 21, 455-463.
- ROHDE, H., BURANDT, E. C., SIEMSEN, N., FROMMELT, L., BURDELSKI, C., WURSTER, S., SCHERPE, S., DAVIES, A. P., HARRIS, L. G. & HORSTKOTTE, M. A. 2007. Polysaccharide intercellular adhesin or protein factors in biofilm accumulation of *Staphylococcus epidermidis* and *Staphylococcus aureus* isolated from prosthetic hip and knee joint infections. *Biomaterials*, 28, 1711-1720.
- ROHDE, H., FRANKENBERGER, S., ZÄHRINGER, U. & MACK, D. 2010. Structure, function and contribution of polysaccharide intercellular adhesin (PIA) to *Staphylococcus epidermidis* biofilm formation and pathogenesis of biomaterial-associated infections. *European Journal of Cell Biology*, 89, 103-111.

- ROHRICH, R. J. 2000. The FDA approves saline - filled breast implants: what does this mean for our patients? *Plastic Reconstructive Surgery*, 106, 903-5.
- ROSEN, S. T. & QUERFELD, C. 2006. Primary cutaneous T-cell lymphomas. *ASH Education Program Book*, 2006, 323-330.
- ROWAN, B., WHEELER, M. A. & CROOKS, R. M. 2002. Patterning bacteria within hyperbranched polymer film templates. *Langmuir*, 18, 9914-9917.
- ROWLINSON, M.-C., LEBOURGEOIS, P., WARD, K., SONG, Y., FINEGOLD, S. M. & BRUCKNER, D. A. 2006. Isolation of a strictly anaerobic strain of *Staphylococcus epidermidis*. *Journal of Clinical Microbiology*, 44, 857-860.
- ROZHOK, S., FAN, Z., NYAMJAV, D., LIU, C., MIRKIN, C. A. & HOLZ, R. C. 2006. Attachment of motile bacterial cells to prealigned holed microarrays. *Langmuir*, 22, 11251-11254.
- RUPANI, A., FRAME, J. D. & KAMEL, D. 2015. Lymphomas Associated with Breast Implants: A Review of the Literature. *Aesthetic Surgery Journal*, 35, 533-44.
- RUTHERFORD, S. T. & BASSLER, B. L. 2012. Bacterial quorum sensing: its role in virulence and possibilities for its control. *Cold Spring Harbor Perspectives in Medicine*, 2, a012427.
- RYAN, G., MARTINELLI, G., KUPER-HOMMEL, M., TSANG, R., PRUNERI, G., YUEN, K., ROOS, D., LENNARD, A., DEVIZZI, L. & CRABB, S. 2007. Primary diffuse large B - cell lymphoma of the breast: prognostic factors and outcomes of a study by the International Extranodal Lymphoma Study Group. *Annals of Oncology*, 19, 233-241.
- RYAN, M. P. & ADLEY, C. C. 2013. The antibiotic susceptibility of water - based bacteria *Ralstonia pickettii* and *Ralstonia insidiosa*. *Journal of Medical Microbiology*, 62, 1025-1031.
- RYAN, M. P. & ADLEY, C. C. 2014. *Ralstonia* spp.: emerging global opportunistic pathogens. *European Journal of Clinical Microbiology and Infectious Diseases*, 33, 291-304.
- RYDER, C., BYRD, M. & WOZNIAK, D. J. 2007. Role of polysaccharides in *Pseudomonas aeruginosa* biofilm development. *Current Opinion in Microbiology*, 10, 644-648.

- SAHOO, S., ROSEN, P. P., FEDDERSEN, R. M., VISWANATHA, D. S., CLARK, D. A. & CHADBURN, A. 2003. Anaplastic large cell lymphoma arising in a silicone breast implant capsule: a case report and review of the literature. *Archives of Pathology and Laboratory Medicine*, 127, e115-e118.
- SAHOO, S. S., PRATHEEK, B. M., MEENA, V. S., NAYAK, T. K., KUMAR, P. S., BANDYOPADHYAY, S., MAITI, P. K. & CHATTOPADHYAY, S. 2018. VIPER regulates naive T cell activation and effector responses: Implication in TLR4 associated acute stage T cell responses. *Scientific Reports*, 8, 7118.
- SAID, J. W., TASAKA, T., TAKEUCHI, S., ASOU, H., DE VOS, S., CESARMAN, E., KNOWLES, D. & KOEFFLER, H. 1996. Primary effusion lymphoma in women: report of two cases of Kaposi's sarcoma herpes virus - associated effusion - based lymphoma in human immunodeficiency virus - negative women. *Blood*, 88, 3124-3128.
- SAKURAGI, Y. & KOLTER, R. 2007. Quorum - sensing regulation of the biofilm matrix genes (pel) of *Pseudomonas aeruginosa*. *Journal of Bacteriology*, 189, 5383-5386.
- SALTA, M., WHARTON, J. A., STOODLEY, P., DENNINGTON, S. P., GOODES, L. R., WERWINSKI, S., MART, U., WOOD, R. J. & STOKES, K. R. 2010. Designing biomimetic antifouling surfaces. *Philosophical Transactions of the Royal Society of London A: Mathematical, Physical and Engineering Sciences*, 368, 4729-4754.
- SAUER, K., CAMPER, A. K., EHRLICH, G. D., COSTERTON, J. W. & DAVIES, D. G. 2002. *Pseudomonas aeruginosa* displays multiple phenotypes during development as a biofilm. *Journal of Bacteriology*, 184, 1140-1154.
- SAVAGE, K., CHHANABHAI, M., GASCOYNE, R. & CONNORS, J. 2004. Characterization of peripheral T - cell lymphomas in a single North American institution by the WHO classification. *Annals of Oncology*, 15, 1467-1475.
- SAVAGE, K. J., HARRIS, N. L., VOSE, J. M., ULLRICH, F., JAFFE, E. S., CONNORS, J. M., RIMSZA, L., PILERI, S. A., CHHANABHAI, M. & GASCOYNE, R. D. 2008. ALK – anaplastic large - cell lymphoma is clinically and immunophenotypically different from both ALK+ ALCL and peripheral T - cell lymphoma, not otherwise specified: report from the International Peripheral T - Cell Lymphoma Project. *Blood*, 111, 5496-5504.
- SCHAUB, T. A., AHMAD, J. & ROHRICH, R. J. 2010. Capsular contracture with breast implants in the cosmetic patient: saline versus silicone – a systematic review of the literature. *Plastic and Reconstructive Surgery*, 126, 2140-2149.

- SCHEUERMAN, T. R., CAMPER, A. K. & HAMILTON, M. A. 1998. Effects of substratum topography on bacterial adhesion. *Journal of Colloid and Interface Science*, 208, 23-33.
- SCHINDELIN, J., ARGANDA-CARRERAS, I., FRISE, E., KAYNIG, V., LONGAIR, M., PIETZSCH, T., PREIBISCH, S., RUEDEN, C., SAALFELD, S. & SCHMID, B. 2012. Fiji: an open - source platform for biological - image analysis. *Nature Methods*, 9, 676.
- SCHOGGINS, J. W., WILSON, S. J., PANIS, M., MURPHY, M. Y., JONES, C. T., BIENIASZ, P. & RICE, C. M. 2011. A diverse range of gene products are effectors of the type I interferon antiviral response. *Nature*, 472, 481.
- SCHREML, S., HEINE, N., EISENMANN-KLEIN, M. & PRANTL, L. 2007. Bacterial colonization is of major relevance for high - grade capsular contracture after augmentation mammaplasty. *Annals of Plastic Surgery*, 59, 126-130.
- SCUTO, A., KUJAWSKI, M., KOWOLIK, C., KRYMSKAYA, L., WANG, L., WEISS, L. M., DIGIUSTO, D., YU, H., FORMAN, S. & JOVE, R. 2011. STAT3 inhibition is a therapeutic strategy for ABC - like diffuse large B - cell lymphoma. *Cancer Research*, 71, 3182-3188.
- SEARS, C. L. & GARRETT, W. S. 2014. Microbes, microbiota, and colon cancer. *Cell Host and Microbe*, 15, 317-328.
- SECOR, P. R., JAMES, G. A., FLECKMAN, P., OLERUD, J. E., MCINNERNEY, K. & STEWART, P. S. 2011. Staphylococcus aureus Biofilm and Planktonic cultures differentially impact gene expression, mapk phosphorylation, and cytokine production in human keratinocytes. *BMC Microbiology*, 11, 143.
- SFORZA, M., ZACCHEDDU, R., ALLERUZZO, A., SENO, A., MILETO, D., PAGANELLI, A., SULAIMAN, H., PAYNE, M. & MAUROVICH-HORVAT, L. 2017. Preliminary 3 - Year Evaluation of Experience With SilkSurface and VelvetSurface Motiva Silicone Breast Implants: A Single - Center Experience With 5813 Consecutive Breast Augmentation Cases. *Aesthetic Surgery Journal*, 38, S62-S73 .
- SHAH, Z., LEHMAN JR, J. A. & TAN, J. 1981. Does Infection Play a Role in Breast Capsular Contracture? *Plastic and Reconstructive Surgery*, 68, 34-38.
- SIBON, D., FOURNIER, M., BRIÈRE, J., LAMANT, L., HAIOUN, C., COIFFIER, B., BOLOGNA, S., MOREL, P., GABARRE, J. & HERMINE, O. 2012. Long - term outcome of adults with systemic anaplastic large - cell lymphoma treated within the Groupe d'Etude des Lymphomes de l'Adulte trials. *Journal of Clinical Oncology*, 30, 3939-3946.

- SILVESTRI, L., VAN SAENE, H. K. & PARODI, P. C. 2011. Decolonization strategies to control *Staphylococcus aureus* infections in breast implant surgery. *Plastic and Reconstructive Surgery*, 128, 328-329.
- SIMOES, M., SIMOES, L. C. & VIEIRA, M. J. 2010. A review of current and emergent biofilm control strategies. *LWT - Food Science and Technology*, 43, 573-583.
- SINCLAIR, T. M., KERRIGAN, C. L. & BUNTIC, R. 1993. Biodegradation of the polyurethane foam covering of breast implants. *Plastic and Reconstructive Surgery*, 92, 1003-13; discussion 1014.
- SINGH, P. K., PARSEK, M. R., GREENBERG, E. P. & WELSH, M. J. 2002. A component of innate immunity prevents bacterial biofilm development. *Nature*, 417, 552.
- SKINNIDER, B. F. & MAK, T. W. 2002. The role of cytokines in classical Hodgkin lymphoma. *Blood*, 99, 4283-4297.
- SMITH, C. A., GRUSS, H.-J., DAVIS, T., ANDERSON, D., FARRAH, T., BAKER, E., SUTHERLAND, G. R., BRANNAN, C. I., COPELAND, N. G. & JENKINS, N. A. 1993. CD30 antigen, a marker for Hodgkin's lymphoma, is a receptor whose ligand defines an emerging family of cytokines with homology to TNF. *Cell*, 73, 1349-1360.
- SMITH, M. F., MITCHELL, A., LI, G., DING, S., FITZMAURICE, A. M., RYAN, K., CROWE, S. & GOLDBERG, J. B. 2003. Toll - like receptor (TLR) 2 and TLR5, but not TLR4, are required for *Helicobacter pylori* - induced NF - κ B activation and chemokine expression by epithelial cells. *Journal of Biological Chemistry*, 278, 32552-32560.
- SMITH, R. S. & IGLEWSKI, B. H. 2003. *P. aeruginosa* quorum - sensing systems and virulence. *Current Opinion in Microbiology*, 6, 56-60.
- SPEAR, S. L. & BAKER, J. L., JR. 1995. Classification of capsular contracture after prosthetic breast reconstruction. *Plastic and Reconstructive Surgery*, 96, 1119-23; discussion 1124.
- SPEAR, S. L., ELMARAGHY, M. & HESS, C. 2000. Textured - surface saline - filled silicone breast implants for augmentation mammoplasty. *Plastic and Reconstructive Surgery*, 105.
- SPEAR, S. L. & MARDINI, S. 2001. Alternative filler materials and new implant designs: what's available and what's on the horizon? *Clinics in Plastic Surgery*, 28, 435-43.

- SPEAR, S. L., MURPHY, D. K. & ALLERGAN SILICONE BREAST IMPLANT, U. S. C. C. S. G. 2014. Natrelle round silicone breast implants: Core Study results at 10 years. *Plastic and Reconstructive Surgery*, 133, 1354-61.
- SRINIVASA, D. R., MIRANDA, R. N., KAURA, A., FRANCIS, A. M., CAMPANALE, A., BOLDRINI, R., ALEXANDER, J., DEVA, A. K., GRAVINA, P. R. & MEDEIROS, L. J. 2017. Global Adverse Event Reports of Breast Implant – Associated ALCL: An International Review of 40 Government Authority Databases. *Plastic and Reconstructive Surgery*, 139, 1029-1039.
- STAPPER, A. P., NARASIMHAN, G., OHMAN, D. E., BARAKAT, J., HENTZER, M., MOLIN, S., KHARAZMI, A., HØIBY, N. & MATHEE, K. 2004. Alginate production affects *Pseudomonas aeruginosa* biofilm development and architecture, but is not essential for biofilm formation. *Journal of Medical Microbiology*, 53, 679-690.
- STEIN, H., FOSS, H. D., DÜRKOP, H., MARAFIOTI, T., DELSOL, G., PULFORD, K., PILERI, S. & FALINI, B. 2000. CD30+ anaplastic large cell lymphoma: a review of its histopathologic, genetic, and clinical features. *Blood*, 96, 3681-3695.
- STEVENS, W. G., HIRSCH, E. M., TENENBAUM, M. J. & ACEVEDO, M. 2010. A prospective study of 708 form - stable silicone gel breast implants. *Aesthetic Surgery Journal*, 30, 693-701.
- STEVENS, W. G., NAHABEDIAN, M. Y., CALOBRACE, M. B., HARRINGTON, J. L., CAPIZZI, P. J., COHEN, R., D'INCELLI, R. C. & BECKSTRAND, M. 2013. Risk factor analysis for capsular contracture: a 5 - year Sientra study analysis using round, smooth, and textured implants for breast augmentation. *Plastic and Reconstructive Surgery*, 132, 1115-23.
- STEWART, T. J. & SMYTH, M. J. 2011. Improving cancer immunotherapy by targeting tumor-induced immune suppression. *Cancer and Metastasis Reviews*, 30, 125-140.
- STÖRMER, M., KLEESIEK, K. & DREIER, J. 2008. pH value promotes growth of *Staphylococcus epidermidis* in platelet concentrates. *Transfusion*, 48, 836-846.
- SUEN, J. L., LI, H. T., JONG, Y. J., CHIANG, B. L. & YEN, J. H. 2009. Altered homeostasis of CD4+ FoxP3+ regulatory T - cell subpopulations in systemic lupus erythematosus. *Immunology*, 127, 196-205.

- SUGIMOTO, S., IWAMOTO, T., TAKADA, K., OKUDA, K.-I., TAJIMA, A., IWASE, T. & MIZUNOE, Y. 2013. Staphylococcus epidermidis Esp degrades specific proteins associated with Staphylococcus aureus biofilm formation and host - pathogen interaction. *Journal of Bacteriology*, 195, 1645-1655.
- SUTHERLAND, I. W. 2001. Biofilm exopolysaccharides: a strong and sticky framework. *Microbiology*, 147, 3-9.
- SUZUKI, R., KAGAMI, Y., TAKEUCHI, K., KAMI, M., OKAMOTO, M., ICHINOHASAMA, R., MORI, N., KOJIMA, M., YOSHINO, T. & YAMABE, H. 2000. Prognostic significance of CD56 expression for ALK - positive and ALK - negative anaplastic large - cell lymphoma of T/null cell phenotype. *Blood*, 96, 2993-3000.
- SWERDLOW, S. H. 2008. WHO classification of tumours of haematopoietic and lymphoid tissues. *WHO Classification of Tumours*, 22008, 439.
- SWERDLOW, S. H., CAMPO, E., PILERI, S. A., HARRIS, N. L., STEIN, H., SIEBERT, R., ADVANI, R., GHIELMINI, M., SALLES, G. A. & ZELENETZ, A. D. 2016. The 2016 revision of the World Health Organization classification of lymphoid neoplasms. *Blood*, 127, 2375-2390.
- TALAGAS, M., UGUEN, A., CHARLES-PETILLON, F., CONAN-CHARLET, V., MARION, V., HU, W., AMICE, J. & DE BRAEKELEER, M. 2014. Breast implant - associated anaplastic large - cell lymphoma can be a diagnostic challenge for pathologists. *Acta cytologica*, 58, 103-107.
- TALMADGE, J. E., DONKOR, M. & SCHOLAR, E. 2007. Inflammatory cell infiltration of tumors: Jekyll or Hyde. *Cancer and Metastasis Reviews*, 26, 373-400.
- TALPUR, R., BASSETT, R. & DUVIC, M. 2008. Prevalence and treatment of Staphylococcus aureus colonization in patients with mycosis fungoides and Sézary syndrome. *British Journal of Dermatology*, 159, 105-112.
- TAMBOTO, H., VICKERY, K. & DEVA, A. K. 2010. Subclinical (biofilm) infection causes capsular contracture in a porcine model following augmentation mammoplasty. *Plastic and Reconstructive Surgery*, 126, 835-42.
- TAN, T. G., SEFIK, E., GEVA-ZATORSKY, N., KUA, L., NASKAR, D., TENG, F., PASMAN, L., ORTIZ-LOPEZ, A., JUPP, R. & WU, H.-J. J. 2016. Identifying species of symbiont bacteria from the human gut that, alone, can induce intestinal Th17 cells in mice. *Proceedings of the National Academy of Sciences*, 113, E8141-E8150.

- TANKERSLEY, A., FRANK, M. B., BEBAK, M. & BRENNAN, R. 2014. Early effects of *Staphylococcus aureus* biofilm secreted products on inflammatory responses of human epithelial keratinocytes. *Journal of Inflammation*, 11, 17.
- TARPILA, E., GHASSEMIFAR, R., FAGRELL, D. & AL., E. 1997a. Capsular contracture with textured versus smooth saline-filled implants for breast augmentation: a prospective clinical study. *Plastic and Reconstructive Surgery*, 99, 1934.
- TARPILA, E., GHASSEMIFAR, R., FAGRELL, D. & BERGGREN, A. 1997b. Capsular contracture with textured versus smooth saline-filled implants for breast augmentation: A prospective clinical study. *Plastic and Reconstructive Surgery*, 99, 1934-1939.
- TART, A. & WOZNIAK, D. J. 2008. Shifting paradigms in *Pseudomonas aeruginosa* biofilm research. *Microbiology and Immunology*, 322, 193-206.
- TATEDA, K., ISHII, Y., HORIKAWA, M., MATSUMOTO, T., MIYAIRI, S., PECHERE, J. C., STANDIFORD, T. J., ISHIGURO, M. & YAMAGUCHI, K. 2003. The *Pseudomonas aeruginosa* autoinducer N - 3 - oxododecanoyl homoserine lactone accelerates apoptosis in macrophages and neutrophils. *Infection and Immunity*, 71, 5785-5793.
- TAYLOR, C. R., SIDDIQI, I. N. & BRODY, G. S. 2013. Anaplastic large cell lymphoma occurring in association with breast implants: review of pathologic and immunohistochemical features in 103 cases. *Applied Immunohistochemistry & Molecular Morphology*, 21, 13-20.
- TEUGHEL, W., VAN ASSCHE, N., SLIEPEN, I. & QUIRYNEN, M. 2006. Effect of material characteristics and/or surface topography on biofilm development. *Clinical Oral Implants Research*, 17, 68-81.
- TGA 2018. Breast implants and anaplastic large cell lymphoma. Update - additional confirmed cases of anaplastic large cell lymphoma.
- THOMPSON, P. A., LADE, S., WEBSTER, H., RYAN, G. & PRINCE, H. M. 2010. Effusion - associated anaplastic large cell lymphoma of the breast: time for it to be defined as a distinct clinico - pathological entity. *Haematologica*, 95, 1977-1979.
- THORNTON, J. W., ARGENTA, L. C., MCCLATCHEY, K. D. & MARKS, M. W. 1988. Studies on the endogenous flora of the human breast. *Annals of Plastic Surgery*, 20, 39-42.

- TIELKER, D., HACKER, S., LORIS, R., STRATHMANN, M., WINGENDER, J., WILHELM, S., ROSENAU, F. & JAEGER, K. E. 2005. *Pseudomonas aeruginosa* lectin LecB is located in the outer membrane and is involved in biofilm formation. *Microbiology*, 151, 1313-1323.
- TRICKETT, A. & KWAN, Y. L. 2003. T cell stimulation and expansion using anti-CD3/CD28 beads. *Journal of Immunological Methods*, 275, 251-255.
- TRUONG, V. K., LAPOVOK, R., ESTRIN, Y. S., RUNDELL, S., WANG, J. Y., FLUKE, C. J., CRAWFORD, R. J. & IVANOVA, E. P. 2010a. The influence of nano - scale surface roughness on bacterial adhesion to ultrafine-grained titanium. *Biomaterials*, 31, 3674-3683.
- TRUONG, V. K., RUNDELL, S., LAPOVOK, R., ESTRIN, Y., WANG, J. Y., BERNDT, C. C., BARNES, D. G., FLUKE, C. J., CRAWFORD, R. J. & IVANOVA, E. P. 2009. Effect of ultrafine - grained titanium surfaces on adhesion of bacteria. *Applied Microbiology and Biotechnology*, 83, 925-937.
- TRUONG, V. K., WANG, J., LAPOVOK, R., ESTRIN, Y., MALHERBE, F., BERNDT, C., CRAWFORD, R. & IVANOVA, E. 2010b. Bacterial attachment response on titanium surfaces with nanometric topographic features. *Trends in Colloid and Interface Science XXIII*. Springer.
- TUNNEY, M., DUNNE, N., EINARSSON, G., MCDOWELL, A., KERR, A. & PATRICK, S. 2007. Biofilm formation by bacteria isolated from retrieved failed prosthetic hip implants in an in vitro model of hip arthroplasty antibiotic prophylaxis. *Journal of Orthopaedic Research*, 25, 2-10.
- TURNER, S. D. 2017. An Exploration into the Origins and Pathogenesis of Anaplastic Large Cell Lymphoma, Anaplastic Lymphoma Kinase (ALK) - Positive. *Cancers*, 9, 141.
- URBANIAK, C., CUMMIN, J., BRACKSTONE, M., MACKLAIM, J. M., GLOOR, G. B., BABAN, C. K., SCOTT, L., O'HANLON, D. M., BURTON, J. P. & FRANCIS, K. P. 2014. Bacterial microbiota of human breast tissue. *Applied and Environmental Microbiology*, 80, 3007-3014.
- VALENCIA-LAZCANO, A. A., ALONSO-RASGADO, T. & BAYAT, A. 2013. Characterisation of breast implant surfaces and correlation with fibroblast adhesion. *Journal of the Mechanical Behavior of Biomedical Materials*, 21, 133-148.
- VAN HEERDEN, J., TURNER, M., HOFFMANN, D. & MOOLMAN, J. 2009. Antimicrobial coating agents: can biofilm formation on a breast implant be prevented? *Journal of Plastic, Reconstructive and Aesthetic Surgery*, 62, 610-617.

- VASILEV, K., COOK, J. & GRIESSER, H. J. 2009. Antibacterial surfaces for biomedical devices. *Expert Review of Medical Devices*, 6, 553-567.
- VAZQUEZ, B., GIVEN, K. S. & COURTNEY, H. G. 1987. Breast augmentation: a review of subglandular and submuscular implantation. *Aesthetic Plastic Surgery*, 11, 6.
- VEERACHAMY, S., YARLAGADDA, T., MANIVASAGAM, G. & YARLAGADDA, P. K. 2014. Bacterial adherence and biofilm formation on medical implants: a review. *Proceedings of the Institution of Mechanical Engineers, Part H: Journal of Engineering in Medicine*, 228, 1083-1099.
- VENARD, V., CARRET, A., PASCAL, N., RIHN, B., BORDIGONI, P. & LE FAOU, A. 2000. A convenient semi-quantitative method for the diagnosis of Epstein - Barr virus reactivation. *Archives of Virology*, 145, 2211-2216.
- VERGIER, B., BEYLOT-BARRY, M., PULFORD, K., MICHEL, P., BOSQ, J., DE MURET, A., BEYLOT, C., DELAUNAY, M., AVRIL, M. & DALAC, S. 1998. Statistical evaluation of diagnostic and prognostic features of CD30+ cutaneous lymphoproliferative disorders: a clinicopathologic study of 65 cases. *The American Journal of Surgical Pathology*, 22, 1192-1202.
- VICKERY, K., PAJKOS, A. & COSSART, Y. 1995. In vitro response to mitogens by duck splenic mononuclear cells. *Research in Veterinary Science*, 59, 242-246.
- VINH, D. C. & EMBIL, J. M. 2005. Device - related infections: a review. *Journal of Long Term Effects of Medical Implants*, 15, 467-488.
- VIRDEN, C. P., DOBKE, M. K., STEIN, P., PARSONS, C. L. & FRANK, D. H. 1992. Subclinical infection of the silicone breast implant surface as a possible cause of capsular contracture. *Aesthetic Plastic Surgery*, 16, 173-179.
- VOCKERODT, M., YAP, L. F., SHANNON - LOWE, C., CURLEY, H., WEI, W., VRZALIKOVA, K. & MURRAY, P. G. 2015. The Epstein – Barr virus and the pathogenesis of lymphoma. *The Journal of Pathology*, 235, 312-322.
- VON OHLE, C., GIESEKE, A., NISTICO, L., DECKER, E. M. & STOODLEY, P. 2010. Real - time microsensor measurement of local metabolic activities in ex vivo dental biofilms exposed to sucrose and treated with chlorhexidine. *Applied and Environmental Microbiology*, 76, 2326-2334.

- VUONG, C., KOCIANOVA, S., VOYICH, J. M., YAO, Y., FISCHER, E. R., DELEO, F. R. & OTTO, M. 2004. A crucial role for exopolysaccharide modification in bacterial biofilm formation, immune evasion, and virulence. *Journal of Biological Chemistry*, 279, 54881-54886.
- WALKER, P. S., WALLS, B. & MURPHY, D. K. 2009. Natrelle saline - filled breast implants: a prospective 10 - year study. *Aesthetic Surgery Journal*, 29, 19-25.
- WANG, F., MENG, W., WANG, B. & QIAO, L. 2014a. Helicobacter pylori - induced gastric inflammation and gastric cancer. *Cancer Letters*, 345, 196-202.
- WANG, H. P., ZHU, Y. L. & SHAO, W. 2013. Role of Helicobacter pylori virulence factor cytotoxin - associated gene A in gastric mucosa - associated lymphoid tissue lymphoma. *World Journal of Gastroenterology*, 19, 8219.
- WANG, L. & GANLY, I. 2014. The oral microbiome and oral cancer. *Clinics in Laboratory Medicine*, 34, 711-719.
- WANG, Y., GU, X., ZHANG, G., WANG, L., WANG, T., ZHAO, Y., ZHANG, X., ZHOU, Y., KADIN, M. & TU, P. 2014b. SATB1 overexpression promotes malignant T - cell proliferation in cutaneous CD30+ lymphoproliferative disease by repressing p21. *Blood*, 123, 3452-3461.
- WATANABE, M., SASAKI, M., ITOH, K., HIGASHIHARA, M., UMEZAWA, K., KADIN, M. E., ABRAHAM, L. J., WATANABE, T. & HORIE, R. 2005. JunB Induced by Constitutive CD30 – Extracellular Signal - Regulated Kinase 1/2 Mitogen - Activated Protein Kinase Signaling Activates the CD30 Promoter in Anaplastic Large Cell Lymphoma and Reed - Sternberg Cells of Hodgkin Lymphoma. *Cancer Research*, 65, 7628-7634.
- WEATHERS, W. M., WOLFSWINKEL, E. M., HATEF, D. A., LEE, E. I., HOLLIER, L. H. & BROWN, R. H. 2013. Implant - associated anaplastic large cell lymphoma of the breast: Insight into a poorly understood disease. *Canadian Journal of Plastic Surgery*, 21, 95-98.
- WEE, A. T., MORREY, B. F. & SANCHEZ-SOTELO, J. 2013. The fate of elbows with unexpected positive intraoperative cultures during revision elbow arthroplasty. *JBJS*, 95, 109-116.
- WELLMANN, A., DOSEEVA, V., BUTSCHER, W., RAFFELD, M., FUKUSHIMA, P., STETLER-STEVENSON, M. & GARDNER, K. 1997. The activated anaplastic lymphoma kinase increases cellular proliferation and oncogene up - regulation in rat 1a fibroblasts. *The FASEB Journal*, 11, 965-972.

- WHITCHURCH, C. B., TOLKER-NIELSEN, T., RAGAS, P. C. & MATTICK, J. S. 2002. Extracellular DNA required for bacterial biofilm formation. *Science*, 295, 1487-1487.
- WHITEHEAD, K. A., COLLIGON, J. & VERRAN, J. 2005. Retention of microbial cells in substratum surface features of micrometer and sub - micrometer dimensions. *Colloids and Surfaces B: Biointerfaces*, 41, 129-138.
- WIENER, T. C. 2007. The role of betadine irrigation in breast augmentation. *Plastic and Reconstructive Surgery*, 119, 12-15.
- WIENER, T. C. 2008. Relationship of incision choice to capsular contracture. *Aesthetic Plastic Surgery*, 32, 303-306.
- WIENER, T. C. 2012. Minimizing Capsular Contracture in a “Clean - Contaminated Site”. *Aesthetic Surgery Journal*, 32, 352-353.
- WILCZYNSKI, J. R., RADWAN, M. & KALINKA, J. 2008. The characterization and role of regulatory T cells in immune reactions. *Frontiers in Bioscience*, 13, 2266-2274.
- WILDERMAN, P. J., VASIL, A. I., JOHNSON, Z., WILSON, M. J., CUNLIFFE, H. E., LAMONT, I. L. & VASIL, M. L. 2001. Characterization of an endoprotease (PrpL) encoded by a PvdS - regulated gene in *Pseudomonas aeruginosa*. *Infection and immunity*, 69, 5385-5394.
- WILLEMZE, R., KERL, H., STERRY, W., BERTI, E., CERRONI, L., CHIMENTI, S., DIAZ-PEREZ, J., GEERTS, M., GOOS, M. & KNOBLER, R. 1997. EORTC classification for primary cutaneous lymphomas: a proposal from the Cutaneous Lymphoma Study Group of the European Organization for Research and Treatment of Cancer. *Blood*, 90, 354-371.
- WILLERSLEV-OLSEN, A., KREJSGAARD, T., LINDAHL, L. M., LITVINOV, I. V., FREDHOLM, S., PETERSEN, D. L., NASTASI, C., GNIADECKI, R., MONGAN, N. P. & SASSEVILLE, D. 2016. Staphylococcal enterotoxin A (SEA) stimulates STAT3 activation and IL - 17 expression in cutaneous T-cell lymphoma. *Blood*, 127, 1287-1296.
- WILLIAMS, P. & CÁMARA, M. 2009. Quorum sensing and environmental adaptation in *Pseudomonas aeruginosa*: a tale of regulatory networks and multifunctional signal molecules. *Current Opinion in Microbiology*, 12, 182-191.

- WIXTROM, R. N., STUTMAN, R. L., BURKE, R. M., MAHONEY, A. K. & CODNER, M. A. 2012. Risk of breast implant bacterial contamination from endogenous breast flora, prevention with nipple shields, and implications for biofilm formation. *Aesthetic Surgery Journal*, 32, 956-963.
- WOETMANN, A., LOVATO, P., ERIKSEN, K. W., KREJSGAARD, T., LABUDA, T., ZHANG, Q., MATHIESEN, A.-M., GEISLER, C., SVEJGAARD, A. & WASIK, M. A. 2007. Nonmalignant T cells stimulate growth of T - cell lymphoma cells in the presence of bacterial toxins. *Blood*, 109, 3325-3332.
- WOLFRAM, D., RABENSTEINER, E., GRUNDTMAN, C., BOCK, G., MAYERL, C., PARSON, W., ALMANZAR, G., HASENOHRL, C., PIZA-KATZER, H. & WICK, G. 2012. T regulatory cells and TH17 cells in peri - silicone implant capsular fibrosis. *Plastic and Reconstructive Surgery*, 129, 327e-337e.
- WONG, A. K., LOPATEGUI, J., CLANCY, S., KULBER, D. & BOSE, S. 2008. Anaplastic large cell lymphoma associated with a breast implant capsule: a case report and review of the literature. *The American Journal of Surgical Pathology*, 32, 1265-1268.
- WONG, C. H., SAMUEL, M., TAN, B. K. & SONG, C. 2006. Capsular contracture in subglandular breast augmentation with textured versus smooth breast implants: a systematic review. *Plastic and Reconstructive Surgery*, 118, 1224-1236.
- WROBLEWSKI, L. E., PEEK, R. M. & WILSON, K. T. 2010. Helicobacter pylori and gastric cancer: factors that modulate disease risk. *Clinical microbiology reviews*, 23, 713-739.
- WU, L., ESTRADA, O., ZABORINA, O., BAINS, M., SHEN, L., KOHLER, J. E., PATEL, N., MUSCH, M. W., CHANG, E. B. & FU, Y. X. 2005. Recognition of host immune activation by Pseudomonas aeruginosa. *Science*, 309, 774-777.
- WÜNDISCH, T., DIECKHOFF, P., GREENE, B., THIEDE, C., WILHELM, C., STOLTE, M. & NEUBAUER, A. 2012. Second cancers and residual disease in patients treated for gastric mucosa - associated lymphoid tissue lymphoma by Helicobacter pylori eradication and followed for 10 years. *Gastroenterology*, 143, 936-942.
- XU, L. C. & SIEDLECKI, C. A. 2012. Submicron - textured biomaterial surface reduces staphylococcal bacterial adhesion and biofilm formation. *Acta biomaterialia*, 8, 72-81.
- YAMAMOTO, M., SATO, S., HEMMI, H., HOSHINO, K., KAISHO, T., SANJO, H., TAKEUCHI, O., SUGIYAMA, M., OKABE, M. & TAKEDA, K. 2003. Role of adaptor TRIF in the MyD88 - independent toll - like receptor signaling pathway. *Science*, 301, 640-643.

- YAMAOKA, Y. 2010. Mechanisms of disease: *Helicobacter pylori* virulence factors. *Nature Reviews Gastroenterology and Hepatology*, 7, 629.
- YAN, Y. Y., GAO, N. & BARTHLOTT, W. 2011. Mimicking natural superhydrophobic surfaces and grasping the wetting process: A review on recent progress in preparing superhydrophobic surfaces. *Advances in Colloid and Interface Science*, 169, 80-105.
- YANG, J., TAN, Q., FU, Q., ZHOU, Y., HU, Y., TANG, S., ZHOU, Y., ZHANG, J., QIU, J. & LV, Q. 2017. Gastrointestinal microbiome and breast cancer: correlations, mechanisms and potential clinical implications. *Breast Cancer*, 24, 220-228.
- YANG, L., BARKEN, K. B., SKINDERSON, M. E., CHRISTENSEN, A. B., GIVSKOV, M. & TOLKER-NIELSEN, T. 2007. Effects of iron on DNA release and biofilm development by *Pseudomonas aeruginosa*. *Microbiology*, 153, 1318-1328.
- YANG, X. O., NURIEVA, R., MARTINEZ, G. J., KANG, H. S., CHUNG, Y., PAPPU, B. P., SHAH, B., CHANG, S. H., SCHLUNS, K. S. & WATOWICH, S. S. 2008. Molecular antagonism and plasticity of regulatory and inflammatory T cell programs. *Immunity*, 29, 44-56.
- YAO, Z., PAINTER, S. L., FANSLOW, W. C., ULRICH, D., MACDUFF, B. M., SPRIGGS, M. K. & ARMITAGE, R. J. 1995. Human IL - 17: a novel cytokine derived from T cells. *The Journal of Immunology*, 155, 5483-5486.
- YARWOOD, J. M., BARTELS, D. J., VOLPER, E. M. & GREENBERG, E. P. 2004. Quorum sensing in *Staphylococcus aureus* biofilms. *Journal of Bacteriology*, 186, 1838-1850.
- YOUNG, V. L., HERTL, M. C., MURRAY, P. R., JENSEN, J., WITT, H. & SCHORR, M. W. 1997. Microbial growth inside saline - filled breast implants. *Plastic and Reconstructive Surgery*, 100, 182-196.
- ZAATREH, S., WEGNER, K., STRAUS, M., PASOLD, J., MITTELMEIER, W., PODBIELSKI, A., KREIKEMEYER, B. & BADER, R. 2016. Co - culture of *S. epidermidis* and human osteoblasts on implant surfaces: An advanced in vitro model for implant - associated infections. *PLOS One*, 11, e0151534.
- ZHANG, B. G., MYERS, D. E., WALLACE, G. G., BRANDT, M. & CHOONG, P. F. 2014. Bioactive coatings for orthopaedic implants — recent trends in development of implant coatings. *International Journal of Molecular Sciences*, 15, 11878-11921.

ZHANG, J., SHI, J., ILIC, S., JUN XUE, S. & KAKUDA, Y. 2008. Biological properties and characterization of lectin from red kidney bean (*Phaseolus vulgaris*). *Food Reviews International*, 25, 12-27.

